
Science
AAAS

Volume 322, Issue 5898

COVER

Ordovician sedimentary rocks at Presqu'île de Crozon, Brittany, France. These rocks show high-frequency cycles of less than 500,000 years between bay and open marine conditions. This and similar records allow reconstruction of global sea level from 550 to 250 million years ago. The pink boulder at the bottom is about 15 centimeters across. See page 64.

Photo: Bilal U. Haq

DEPARTMENTS

EDITORIAL

NEWS OF THE WEEK

NEWS FOCUS

LETTERS

BOOKS *ET AL.*

47

POLICY FORUM

PERSPECTIVES

CONTENTS continued >>

Published by AAAS

SCIENCE EXPRESS

www.sciencexpress.org

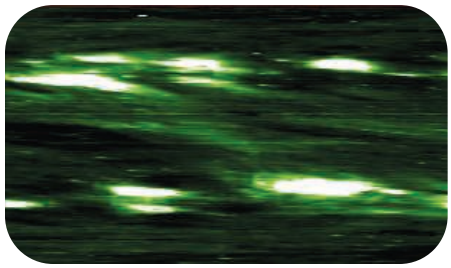

REVIEW

BREVIA

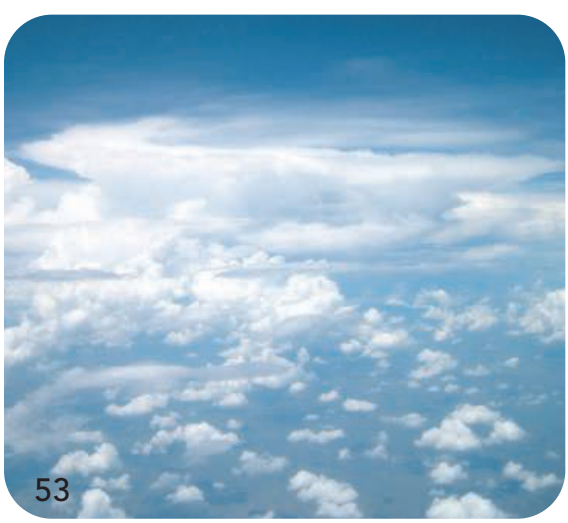

RESEARCH ARTICLE

REPORTS

CONTENTS continued >>

REPORTS *CONTINUED...*

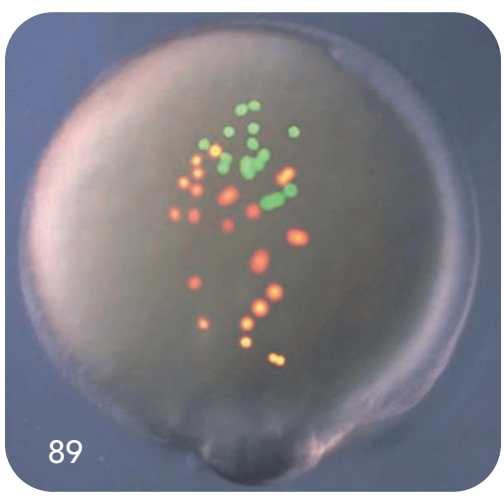

AAAS
ADVANCING SCIENCE, SERVING SOCIETY

SCIENCE (ISSN 0036-8075) is published weekly on Friday, except the last week in December, by the American Association for the Advancement of Science, 1200 New York Avenue, NW, Washington, DC 20005. Periodicals Mail postage (publication No. 484460) paid at Washington, DC, and additional mailing offices. Domestic individual membership and subscription (51 issues): $144 ($74 allocated to subscription). Domestic institutional subscription (51 issues): $770; Foreign postage extra: Mexico, Caribbean (surface mail) $55; other countries (air assist delivery) $85. First class, airmail, student, and emeritus rates on request. Canadian rates with GST available upon request, GST #1254 88122. Publications Mail Agreement Number 1069624. SCIENCE is printed on 30 percent post-consumer recycled paper. **Printed in the U.S.A.**

Change of address: Allow 4 weeks, giving old and new addresses and 8-digit account number. **Postmaster:** Send change of address to AAAS, P.O. Box 96178, Washington, DC 20090–6178. **Single-copy sales:** $10.00 current issue, $15.00 back issue prepaid includes surface postage; bulk rates on request. The identification code for *Science* is 0036-8075. *Science* is indexed in the *Reader's Guide to Periodical Literature* and in several specialized indexes.

Printed on 30% post-consumer recycled paper.

CONTENTS continued **>>**

Dangerous diet.

SCIENCE**NOW**

www.sciencenow.org

HIGHLIGHTS FROM OUR DAILY NEWS COVERAGE

How to Eat a Nasty Ant
Gobs of mucus help lizards turn a dangerous insect into a delicacy.

Bells Ring for First U.S. Carbon Auction
Plan puts price tag on pollution from power industry.

Flowing Toward Oblivion?
Something invisible is pulling on thousands of galaxies.

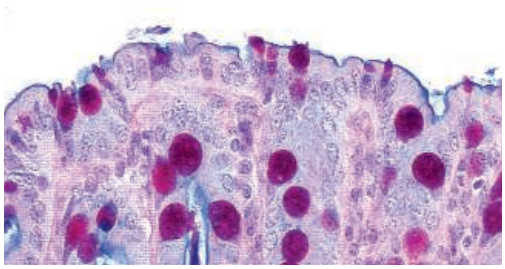

Purinergic receptor antagonists inhibit inflammation.

SCIENCE **SIGNALING**

www.sciencesignaling.org

THE SIGNAL TRANSDUCTION KNOWLEDGE ENVIRONMENT

RESEARCH ARTICLE: Purinergic Control of T Cell Activation by ATP Released Through Pannexin-1 Hemichannels
U. Schenk, A. M. Westendorf, E. Radaelli, A. Casati, M. Ferro, M. Fumagalli, C. Verderio, J. Buer, E. Scanziani, F. Grassi
Pannexin hemichannel-mediated release of ATP provides an autocrine, costimulatory signal for T cell activation.

RESEARCH ARTICLE: Kinome siRNA Screen Identifies Regulators of Ciliogenesis and Hedgehog Signal Transduction
M. Evangelista, T. Y. Lim, J. Lee, L. Parker, A. Ashique, A. S. Peterson, W. Ye, D. P. Davis, F. J. de Sauvage
Cdc2l1 is a component of the Hh signaling pathway and opposes the activity of the negative regulator Sufu.

PERSPECTIVE: A Wnt-fall for Gene Regulation—Repression
N. P. Hoverter and M. L. Waterman
Recognition of a nonclassical Wnt-response element by the transcription factor TCF results in β-catenin acting as a transcriptional repressor of certain Wnt target genes.

PRESENTATION: Somatic Cell Genetics for the Study of NF-κB Signaling in Innate Immunity
R. Krumbach, S. Bloor, G. Ryzhakov, F. Randow
A forward genetic screen in immortalized cells identifies NF-κB signaling components required to transduce signals from Toll-like receptors.

Help climbing out of a rut.

SCIENCE **CAREERS**

www.sciencecareers.org/career_development

FREE CAREER RESOURCES FOR SCIENTISTS

Mind Matters: Getting Out of a Rut
I. S. Levine
If you are bored at work, talk to people and try something new.

Taken for Granted: A Big Idea About Fostering Innovation
B. L. Benderly
An unorthodox program helps young innovators turn inspiration into reality.

In Person: Ich bin Postdoctorin in Berlin
V. Maneeratana
The biggest challenges in moving abroad are not always scientific.

October 2008 Funding News
J. Fernández
Learn about the latest in research funding, scholarships, fellowships, and internships.

SCIENCE**PODCAST**

www.sciencemag.org/multimedia/podcast

FREE WEEKLY SHOW

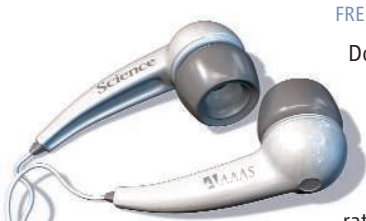

Download the 3 October *Science* Podcast to hear about illusory pattern perception, trans-Atlantic bluefin tuna movements, relieving malnutrition with high-calorie rations, and more.

Separate individual or institutional subscriptions to these products may be required for full-text access.

EDITED BY STELLA HURTLEY

A Matter of Faith?

The intersection, if any, between science and religion is a hot-button issue guaranteed to inflame scientists and nonscientists alike. **Norenzayan and Shariff** (p. 58) review recent empirical approaches in social psychology, experimental economics, and evolutionary anthropology primarily aimed at studying prosocial behavior among humans past and present. A synthesis of these findings highlights issues that are being tackled in the current wave of experimental studies and the interdisciplinary interest in religion as a force for cooperative and altruistic human interactions.

Ups and Downs

Most of the geological history of the Paleozoic Era (542 to 251 million years ago) remains opaque, largely due to the difficulty of constructing records from such old and sparse remains. In particular, the history of sea level during the Paleozoic has remained piecemeal. **Haq and Schutter** (p. 64, cover) integrated published accounts of sea-level changes to reconstruct the history of sea-level fluctuations for the entire Paleozoic. One hundred seventy-two individual events were recorded, each lasting typically between half a million and three million years and varying in magnitude from a few tens to ~125 meters. Most events were not caused by glaciations, however, leaving unanswered the question of what caused more than half of these changes in Paleozoic sea level.

Temperature-Sensitive Water Layers

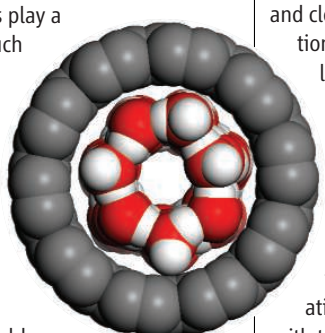

Water layers that interact with hydrophobic properties play a key role in processes such as protein folding and membrane transport, but their properties can be difficult to determine because they are themselves in contact with bulk water. The interior of single-walled carbon nanotubes (SWNTs) would be expected to be hydrophobic, and water will absorb in their interior. **Wang *et al.*** (p. 80) used a gentle method to open SWNTs with diameters of 1.4 nanometers and studied their absorption and nuclear magnetic resonance (NMR) properties over a range of different temperatures. The water actually underwent a transition from appearing to be in a hydrophobic environment at 22°C to appearing to be in a hydrophilic environment at 8°C.

Mighty Wheat >>

All over the world, wheat is one of the most important food crops, but due to its large and complex genome it has been deemed an impossible genome to sequence. Now Paux *et al.* (p. 101) have tackled the first task needed to get at the full genome by constructing a physical map of the largest wheat chromosome, chromosome 3B. At 1 gigabase, this chromosome alone is larger than all of the rice and human genomes. This feat demonstrates that, in the relatively near future, it should be possible to develop a physical map of large polyploid plant genomes (17 gigabases) using a chromosome-based strategy.

Back to the Future for Negative Refraction

Waves refract, changing their angle of propagation when going from one medium to another. The extent of refraction depends on the relative refractive indices of the media. In nature, all materials are run-of-the-mill positively refracting. However, recent work has demonstrated materials with a negative refractive index. The ability to manipulate electromagnetic radiation with such materials can lead to perfect lensing and cloaking. However, limitations on the fabrication of these metamaterials inevitably lead to losses, which can severely limit their implementation. Linking time-reversal processes with negative refraction, **Pendry** (p. 71, published online 28 August) discusses an alternate route that may overcome these limiting losses. Optically active materials, with the correct nonlinear optical properties, may be able to be made to mimic negative refraction without the losses associated with true negative refractive materials.

Lending an Electron

Catalysts for the preparation of chirally pure organic compounds tend to operate through paired electron mechanisms involving charged or highly polarized intermediates. Generation of an intermediate with an unpaired electron (a radical) can open other reaction pathways, favoring different products while avoiding undesirable competing reactions. In this vein, **Nicewicz and MacMillan** (p. 77, published online 4 September; see the Perspective by **Renaud and Leong**) demonstrate the utility of a photo-excitable ruthenium complex for shuttling single electrons to induce otherwise intractable reactions. The complex was combined with a chiral amine established for catalyzing a range of aldehyde transformations. Upon visible light irradiation, electron transfer to and from the Ru co-catalyst facilitates a radical mechanism for efficient asymmetric alkylation of the aldehydes, avoiding an aldehyde self-coupling reaction.

Gas from the Past

Carbon dioxide is the atmospheric trace gas with the largest influence on climate. Because the carbon cycle and climate are coupled so intimately, with CO_2 variations both causing and being caused by climate change, knowing how climate and atmospheric CO_2 have varied in the past is central to a better understanding of climate dynamics. **Ahn and Brook** (p. 83, published online 11 September) compare records of atmospheric CO_2 concentrations, Antarctic surface air temperatures, and Greenland climate during a relatively under-studied period: the last ice age, from 90,000 to 20,000 years ago.

CREDITS (TOP TO BOTTOM): CATHERINE FEUILLET; WANG *ET AL.*

Published by AAAS

Life History Matters

In plants, changes in life history traits have been suggested to be correlated with their rate of evolution, but previous analyses have yielded conflicting results. In order to investigate whether the rate of molecular evolution correlates with life history traits, **Smith and Donoghue** (p. 86) tested the evolutionary rates across five groups of flowering plants. The rates of molecular evolution were generally low in trees and shrubs with long generation times in comparison to the relatively high rates of molecular evolution in related herbaceous plants, which have shorter generation times. Thus, evolutionary rates can indeed differ among closely related species, depending on their life history traits.

Getting to Grips with Gastrulation

Gastrulation involves the coordinated movements of germ layers to form the body axis. **Nair and Schilling** (p. 89, published online 21 August) studied chemokine regulation of endodermal morphogenesis and the positioning of the liver and pancreas in developing zebrafish. During development the endoderm normally migrates together with mesoderm, but the two germ layers could be physically separated by disrupting chemokine signaling, due to a loss of integrin-dependent adhesion to fibronectin. A chemokine-mediated adhesive interaction may thus normally tether endodermal cells to their mesodermal neighbors, providing a mechanism by which chemokines regulate embryonic cell movements distinct from their roles as classical chemoattractants.

Homing In on the Hub

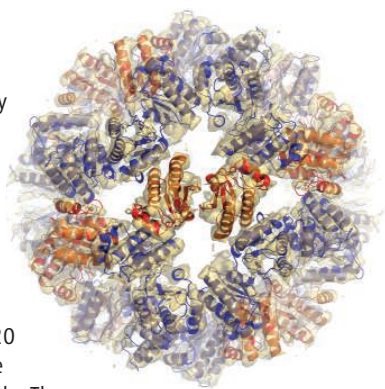

Microorganisms respond to a variety of environmental stresses by up-regulating stress-response genes. In many cases the response is coordinated by a multiprotein signaling hub, the stressosome, which integrates multiple inputs to affect a single outcome. **Marles-Wright *et al.*** (p. 92) have fitted high-resolution structures of the stressosome components into an electron microscopy structure to determine a pseudo-atomic resolution structure of the stressosome from *Bacillus subtilis*. The complex has an icosohedral virus-capsid-like core with 20 protruding turrets. Sequences comprising the turrets are variable, perhaps allowing them to sense different signals. The conserved domains of the core may integrate these signals to give a single signaling outcome.

Homer-ing In on Memories

The neural correlates of remembering can only be studied with complete confidence in humans, because the subjects can verbally report their internal experience. Brain surgery in which therapeutic electrodes are implanted in the brain of patients with intractable epilepsy provides an opportunity for doing such studies. **Gelbard-Sagiv *et al.*** (p. 93, published online 4 September; see 5 September news story by **Miller**) report that neurons in and near the hippocampus of these patients showed specific patterns of activation for each episode of the television show *The Simpsons*. Later, when these same episodes were brought to mind by free recollection, the same pattern of neural activity was seen, demonstrating that, at least in the hippocampus, recall of a stimulus is accompanied by activation of the same neurons that were activated during the initial experience.

Controlling Conspiracy Theories

Believing oneself to be in control is a well-established and remarkably effective route to reduced anxiety and stress; conversely, being placed in an out-of-control situation activates behaviors aimed at regaining secure ground. **Whitson and Galinsky** (p. 115) show that the need for control is sufficiently strong as to influence perception to the extent of seeing patterns where they do not exist. In a series of studies, subjects were provided with feedback unrelated to their performance. Doing so increased their reported need for personal structure, increased the likelihood that they would see patterns in random visual static, and led them to see conspiracies where there were none. Allowing subjects to combat their anxiety through self-affirmation exercises brought their illusory perceptions under control.

CREDIT: MARLES-WRIGHT *ET AL.*

Jim Wells is a professor in the departments of Pharmaceutical Chemistry and Cellular and Molecular Pharmacology at the University of California at San Francisco.

Mary Woolley is president and chief executive officer of Research!America in Alexandria, VA.

A Populist Movement for Health?

ONE OF THE MOST EFFECTIVE SCIENCE-BASED MOVEMENTS TO RAISE PUBLIC AWARENESS OF a global problem has been Al Gore's efforts, complementing the science-based work of the Intergovernmental Panel on Climate Change, to expose the perils of global warming. Through decades of commitment, Gore and his team have laid out the science and consequences of unmitigated consumption of fossil fuels and the irredeemable impact this will have on the planet if unchecked. More than ever, this message is now resonating with the public.

Human health presents a similarly massive global problem. Globalization is accelerating the spread of AIDS, drug-resistant forms of tuberculosis, and other infectious agents. Industrialization, with its accompanying sedentary life-styles and extended life spans, is creating new epidemics of obesity, diabetes, cancer, and heart disease, among others. When a life-altering medical condition is diagnosed, too often even the best in the medical community have few clues as to the molecular mechanism at work, far less the ability to produce a cure or prevent others from experiencing a similar fate. Despite increased attention to health promotion, we focus on crisis and symptom management, as opposed to prevention and cure, reflecting a limited understanding of the molecular basis for disease.

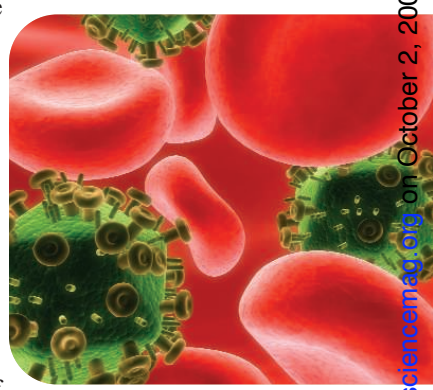

Consider this: We now know that we are encoded by about 25,000 human genes and their products, many of which represent potential new drug targets. Yet we have drugs for fewer than 200 of these gene products. Moreover, of the approximately 20 to 30 new drug entities that the U.S. Food and Drug Administration has been approving each year, only 3 to 5 address a new molecular target or novel mechanism. At this rate, it will require hundreds of years to fully exploit our knowledge of human biology to develop robust medical treatments. Despite the tools and technologies of modern medical science, we are still in the Dark Ages of understanding our own biology and discovering agents that can provide cures.

How can we stimulate innovation and enlightened public policy? Is a Gore-like populist movement possible for global health? Although the science community has advocated more funding to support the basic science that is crucial to understand disease and develop cures, recent efforts have had little impact. In part, the science community is responsible because we have not effectively helped the public realize that without a higher national and international priority for basic research, a crisis in human health is not far off.

It is time for the scientific community to launch a bold combination strategy, the most important element of which is to identify the "Al Gore(s)" of basic science. This requires increased efforts and funding from scientific societies and advocacy organizations that are empowered to deliver compelling messages to media and elected officials and can identify and provide financial support for communicators for basic science. The research community needs champions who can articulate a compelling long-term vision for research that can accelerate the needed transition from a crisis/symptom mode to a prevention/cure mode of health care.

The second part of the strategy involves scientists' own time and, yes, money, to support such advocacy groups. Both are scarce resources, but if scientists want to spur basic science that underlies improving society, they must take personal responsibility to make it happen. Championing research in situations such as social gatherings does not come easily to many researchers, who may feel that their area of science is too complex for nonscientists to understand (or frankly don't feel a need to help them understand). Many community events and meetings now include discussions of carbon footprints and alternative energy. Scientists need to take or create more occasions to explain to the public how far we are from really understanding the basis of disease and our consequent vulnerability.

Now is the time to take bold actions both personally and through advocacy groups to accelerate public awareness in support of basic research. By failing to do so, we consign ourselves and future generations to a world with little hope for dramatically improving human health and well-being.

– Jim Wells and Mary Woolley

10.1126/science.1163960

Published by AAAS

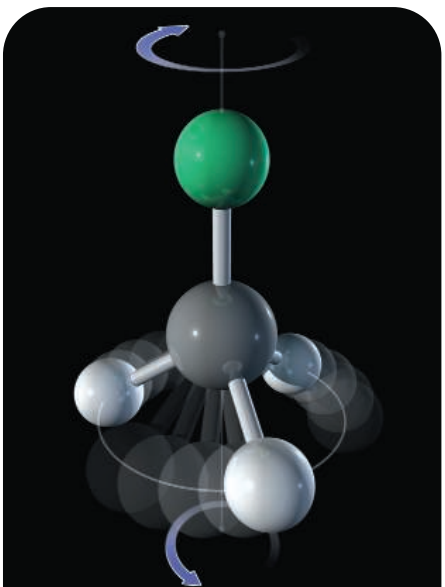

CHEMISTRY

Spinning in Place

Unlike macroscopic objects, molecules vibrate and rotate in discrete increments. To uncover the underlying quantum-mechanical restrictions governing such behavior, spectroscopists induce specific patterns of motion through light absorption. Thus, the molecules under study must be free to move about, but unless they are to some degree restricted, the flurry of different movements can be hard to disentangle. A promising compromise is the use of *para* hydrogen (p-H_2) matrices. When p-H_2 (H_2 with oppositely oriented nuclear spins) is cooled to low temperature, it forms an unusual medium, termed a quantum solid, in which the nuclei delocalize in space. Consequently, guest molecules embedded in a matrix of this solid retain a certain amount of flexibility. Lee *et al.* show through infrared absorption spectroscopy that CH_3F molecules can rotate about the C-F axis in such a matrix, but are restricted from tumbling in orthogonal directions. The study bolsters the utility of p-H_2 matrices for precise spectral characterization of small molecules. — JSY

J. Chem. Phys. **129**, 104502 (2008).

*Helen Pickersgill is a locum editor in *Science*'s editorial department.

MICROBIOLOGY

Adapting to Drug Resistance

Developing a new therapy for drug-resistant infections is an expensive and arduous process that may give relief for less time that it takes to develop the agent. Hence, delaying the onset of resistance by administering drugs in combination is a currently favored strategy, but two groups show this may not be quite so simple to implement wisely. By experimentation and modeling, Hegreness *et al.* made the counterintuitive discovery that synergistically acting drug pairs, such as doxycycline and erythromycin, may actually accelerate the evolution of resistance. In fact, antagonistic drug pairs are more effective at forestalling resistance emergence because as one drug becomes ineffective, its suppressive effect on the other diminishes and unmasks the potency of the second drug. Of course, the precise outcome depends on the drug ratios, doses, pharmacokinetics, and modes of action.

Developing policies for the implementation of drug combinations requires population modeling. Boni *et al.* compared the consequences of the standard wait-and-switch global deployment of drugs for malaria control with the simultaneous deployment of multiple drugs. Their model shows that if three different drugs are offered for use at the same time within a malarious population, the clinical burden is reduced, the emergence of resistance is delayed by two- to fourfold, and the number of failed treatments is almost halved. — CA

Proc. Natl. Acad. Sci. U.S.A. **105**, 13977, 14216 (2008).

DEVELOPMENT

Signal Stability

Chordin and BMP signaling develop opposing trends across the *Xenopus* embryo, defining between them the axis from dorsal to ventral and destinations in between. The interactions between these and other factors involve complex regulatory interactions, including both negative and positive feedback loops. Although predictions from some combinations of the known regulatory loops might suggest that axis establishment is rather tenuous, instead, observations of real embryos indicate that dorsal-ventral axis establishment in *Xenopus* is robust to perturbation. Inomata *et al.* identify the protein ONT1 as a stabilizing factor in the signaling networks defining the dorsal-ventral axis. The protein is expressed first in late blastula stages and is generally found in the more dorsal regions as the embryo develops; diminished ONT1 function results in dorsalization of the embryo. ONT1 binds to chordin and also to a protease known to degrade chordin, and seems to function as a scaffold enticing chordin to its demise. The biphasic outcome of this interaction ensures that enough, but not too much, chordin survives to define the developing dorsal axis. — PJH

Cell **134**, 854 (2008).

CELL BIOLOGY

Transcription Without Borders

In bacteria, genes encoding functionally related proteins are often grouped into coordinately regulated modules, one notable instance being the lactose operon. In mammals, the regulation of gene expression is thought to be controlled on an individual basis, such that specific proteins or RNAs bind to the regulatory elements of a single gene and activate or repress its transcription directly.

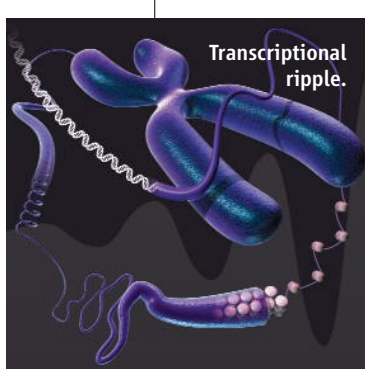

Using growth factors to induce transcription of immediate early genes (IEGs) in mammalian cells, Ebisuya *et al.* find that a gene that is being transcribed can incidentally activate the transcription of neighboring genes, enabling the coordinated expression of clusters of genes. Activation occurred via a ripple, which traveled both upstream and downstream from the IEG, and also passed through intergenic (non–protein coding) chromatin, resulting in the transcription of noncoding RNAs. Although protein-coding genes account for only 1.5% of the human genome, more than 70% of the DNA is

CREDITS (TOP TO BOTTOM): CHRIS BICKEL/*SCIENCE*

transcribed. These results provide a potential explanation for this pervasive transcription, which may serve to propagate transcriptional activation into neighboring genes. — HP*

Nat. Cell Biol. **10**, 1106 (2008).

BIOCHEMISTRY

Breaking the Back of BCR-ABL

One of the advances in the war on cancer has been the development of small molecules that target protein tyrosine kinases; one such drug, imatinib, is used to inhibit the BCR-ABL kinase in the treatment of chronic myelogenous leukemia. Nevertheless, elation has been tempered by the realization that resistance to imatinib can arise via mutation of a gatekeeper amino acid (threonine 315) to the bulkier and more hydrophobic isoleucine, which hinders access of the drug to its binding site. Similar resistance-mediating mutations have been observed for other drug–tyrosine kinase pairs in solid tumors. Not only do the mutations block drug binding, but they also tilt the kinase structure toward constitutively active conformations. Azam *et al.* have analyzed a series of mutations in a series of tyrosine kinases and find that the critical threonine sits atop a spine of hydrophobic residues linked to the activation loop. Replacing the threonine with isoleucine stabilizes and stiffens the spine and also enhances the coordination of ATP, thereby stimulating kinase activity. They used this insight to refine the inhibitor PD166326 into a candidate drug called compound 14, which packs neatly against the disrupted spine and inhibits the BCR-ABL variant T315I at 0.6 μM versus the lack of effect of PD166326 at 10 μM. — GJC

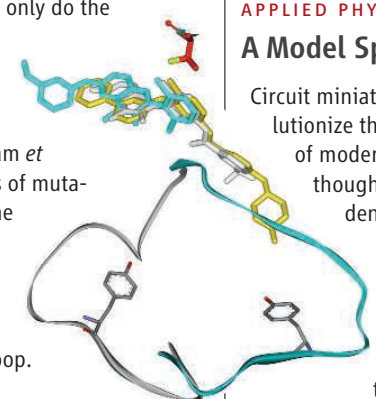

Interaction of PD166326 (blue), imatinib (yellow), and compound 14 (gray) with the activation loop (blue, gray) and the gatekeeper threonine (red).

CREDIT: AZAM *ET AL.*, *NAT. STRUCT. MOL. BIOL.* **15**, 10.1038/NSMB.1486 (2008)

Nat. Struct. Mol. Biol. **15**, 10.1038/nsmb.1486 (2008).

EVOLUTION

Neutral Plantings

The transcriptome of an organism encompasses all of its gene transcripts at a specific time and changes with the individual's environment and developmental stage. These changes either could be guided by adaptive selection or, like the neutral theory of gene evolution, may result from random events not under selection. Taking advantage of the genomic database of the plant *Arabidopsis*, Broadley *et al.* examined more than 18,000 gene transcripts in leaves of 14 taxa from the cabbage family. They found differences in the expression of a gene among taxa, suggesting that there was plasticity in expression in the most recent common ancestor or that the founder effect of a small population may have resulted in differential changes in gene expression among descendant taxa, but that the changes observed do not reflect functional adaptation. These findings show that appropriate null models are required when comparing transcriptomes in both time and space, and that modeling of transcriptome networks should take evolutionary effects into account. — LMZ

New Phytol. **180**, 10.1111/j.1469-8137.2008.02640.x (2008).

APPLIED PHYSICS

A Model Spin Amplifier

Circuit miniaturization has continued to revolutionize the speed and diverse capabilities of modern electronic systems. At present, though, the increase in device-packing density onto microelectronics chips and the associated problem of managing heat dissipation is becoming an issue in limiting performance. Using the spin of the electrons in place of traditional charge flow is therefore being explored as a possible route to circumvent that performance roadblock. The transistor is the present building block of microelectronics. However, the equivalent spin amplifier, or spin transistor, would require a room-temperature magnetic semiconductor. Because all the true magnetic semiconductors to date have been limited to cryogenic temperatures, the prospect of developing a practical spin transistor seems some way off. Breaking the process down into three stages—spin detection, signal amplification, and spin filtering of that amplified signal—Acremann *et al.* suggest an alternative method that may provide a spin amplifier using a sequence of electrical and magnetic field pulses to manipulate the magnetization of a patterned ferromagnetic layer. Such an engineered spin amplifier using presently available materials may bring forward the development of spintronics, and with it the additional functionality of having sensing, memory storage, and logical operation in a single device. — ISO

Appl. Phys. Lett. **93**, 102513 (2008).

Published by AAAS

www.sciencemag.org

Science

1200 New York Avenue, NW
Washington, DC 20005
Editorial: 202-326-6550, FAX 202-289-7562
News: 202-326-6581, FAX 202-371-9227
Bateman House, 82-88 Hills Road
Cambridge, UK CB2 1LQ
+44 (0) 1223 326500, FAX +44 (0) 1223 326501

Subscription Services For change of address, missing issues, new orders and renewals, and payment questions: 866-434-AAAS (2227) or 202-326-6417, FAX 202-842-1065. Mailing addresses: AAAS, P.O. Box 96178, Washington, DC 20090-6178 or AAAS Member Services, 1200 New York Avenue, NW, Washington, DC 20005

Institutional Site Licenses please call 202-326-6755 for any questions or information

Reprints: Author Inquiries 800-635-7181
Commercial Inquiries 803-359-4578

Permissions 202-326-7074, FAX 202-682-0816

Member Benefits AAAS/Barnes&Noble.com bookstore www.aaas.org/bn; AAAS Online Store http://www.apisource.com/aaas/ code MKB6; AAAS Travels: Betchart Expeditions 800-252-4910; Apple Store www.apple/eppstore/aaas; Bank of America MasterCard 1-800-833-6262 priority code FAA3YU; Cold Spring Harbor Laboratory Press Publications www.cshlpress.com/affiliates/aaas.htm; GEICO Auto Insurance www.geico.com/landingpage/go51.htm?logo=17624; Hertz 800-654-2200 CDP#343457; Office Depot https://bsd.officedepot.com/portalLogin.do; Seabury & Smith Life Insurance 800-424-9883; Subaru VIP Program 202-326-6417; VIP Moving Services http://www.vipmayflower.com/domestic/index.html; Other Benefits: AAAS Member Services 202-326-6417 or www.aaasmember.org.

science_editors@aaas.org	(for general editorial queries)
science_letters@aaas.org	(for queries about letters)
science_reviews@aaas.org	(for returning manuscript reviews)
science_bookrevs@aaas.org	(for book review queries)

Published by the American Association for the Advancement of Science (AAAS), *Science* serves its readers as a forum for the presentation and discussion of important issues related to the advancement of science, including the presentation of minority or conflicting points of view, rather than by publishing only material on which a consensus has been reached. Accordingly, all articles published in *Science*—including editorials, news and comment, and book reviews—are signed and reflect the individual views of the authors and not official points of view adopted by AAAS or the institutions with which the authors are affiliated.

AAAS was founded in 1848 and incorporated in 1874. Its mission is to advance science, engineering, and innovation throughout the world for the benefit of all people. The goals of the association are to: enhance communication among scientists, engineers, and the public; promote and defend the integrity of science and its use; strengthen support for the science and technology enterprise; provide a voice for science on societal issues; promote the responsible use of science in public policy; strengthen and diversify the science and technology workforce; foster education in science and technology for everyone; increase public engagement with science and technology; and advance international cooperation in science.

Information for Authors
See pages 634 and 635 of the 1 February 2008 issue or access www.sciencemag.org/about/authors

Inside Story

A dead boar in all its complexity is revealed in this photograph by Swedish physician Anders Persson, winner of this year's Lennart Nilsson Award for photography. Persson, director of the Center for Medical Image Science and Visualization at Linköping University, has combined magnetic resonance, ultrasound, and positron emission tomography to get 3D images from inside the body. Particularly useful for autopsies, his photos have been featured on the forensics TV show *CSI*.

Napoleon: Case Closed

Historians have long speculated about what killed Napoleon, who died in exile at 52 on the isle of St. Helena in 1821. His doctor said it was stomach cancer, but analysis of some hairs and accounts of his symptoms raised the notion that he was poisoned with arsenic.

Now the Italian National Institute of Nuclear Physics says it has ruled out homicide. Scientists analyzed several preserved samples of Napoleon's hairs, one from when he was only a year old and others cut a few days before his death, along with hairs from his son, his wife Josephine, and 10 other people living at the same time.

The hairs, placed in a nuclear reactor and bombarded with neutrons to determine their composition, were all found to be "extremely toxic," says institute director Ettore Fiorini and colleagues, with arsenic levels more than 100 times what would be found today. Napoleon's arsenic load registered 8.3 parts per million as an infant and 18.9 ppm when he died, the researchers report in the bulletin of the Italian Physical Society, *Il Nuovo Saggiatore.*

Fiorini notes that at the time, arsenic was everywhere–in paints, drugs, tapestries, and preserved food. Angela Santagostino, a toxicologist in the Department of Environmental Sciences at the University of Milan-Bicocca, says the scientists have finally come up with conclusive proof that there was "not an intentional poisoning."

THE BATTERED BRAIN

Last June, pro wrestler Chris Benoit strangled his family and hanged himself at age 37. Benoit had suffered various blows to his head in the course of his career. When neurosurgeon Julian Bailes of West Virginia University, Morgantown, examined the brain at the request of the Sports Legacy Institute, he found damage similar to that of advanced dementia.

Now scientists at Boston University are hoping to get a better fix on what happens to banged-up brains with the establishment of a new Center for the Study of Traumatic Encephalopathy. Twelve athletes, including six retired NFL football players, have announced they will be donating their brains to aid studies of what happens after severe concussions. Big names include former New England Patriots linebacker Ted Johnson and former Olympic soccer champ Cindy Parlow.

Researchers have long suspected a link between athletes' head injuries and chronic traumatic encephalopathy (CTE). With donated brains, they'll be able to look for biomarkers of CTE, which can cause dementia-like symptoms and personality changes in patients, says neurologist Robert Stern, the center's co-director. Preliminary work suggests that CTE causes a buildup of tau protein, also implicated in Alzheimer's disease. Research also points to a genetic component. "We really need to understand this disease better—we're still in the infancy there," says co-director Ann McKee, a neuropathologist. McKee says she's most interested in learning how brain trauma in young adults can trigger brain damage that, as is possible in Benoit's case, surfaces many years later.

Little Gray Cells Add Up

To succeed in science, it helps to be very smart. But being very, *very* smart is even better.

That's what researchers at Vanderbilt University conclude from a longitudinal study begun at Johns Hopkins University in 1972. The Study of Mathematically Precocious Youth tracks the careers of students who were in the top 1% of scorers in the math portion of the SAT at the age of 13. Twenty-five years later, the crème de la crème within this elite group have produced the most publications and patents, psychologist David Lubinski and colleagues report. "Measures with high ceilings are needed" to reveal such distinctions, the authors say. For example, 28% of those with science doctorates had authored a peer-reviewed publication, but the probability rose with their SAT-M scores (see chart, above), according to a paper in the October issue of *Psychological Science*.

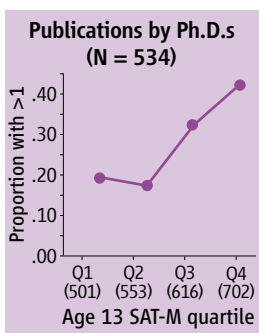

Psychologist Diane Halpern of Claremont McKenna College in California says the data are valid as far as they go. But "the flip side of this question" is how many top scientists "would score among the top 1% of the population on a math test. … I don't know what proportion of Nobel Prize–winners have IQs above 140 or 145, which would be predicted from the points made in this paper. "

CREDITS (LEFT TO RIGHT): SUSANA VERA/REUTERS; ANDERS PERSSON; SOURCE: PARK *ET AL.*, *PSYCHOLOGICAL SCIENCE*, VOL 19, NO 10, 2008

Three Q's >>

Fredy Peccerelli and his family fled Guatemala for New York City in 1980 after his father received death threats. He returned as a forensic anthropologist and since 1995 has helped identify some 5000 Guatemalan men, women, and children massacred during the country's 36-year armed conflict. In September, Peccerelli and imprisoned Cuban physician Oscar Elías Biscet received the New York Academy of Sciences' Heinz R. Pagels Human Rights of Scientists award.

Q: Why dig up a very painful past?
Our work provides evidence to back up the testimonies of individuals who lost their loved ones so that there can be an attempt to bring the killers to justice. It allows us to see the brutalities involved in the killings—for example, 25% of the bodies we have exhumed were children.

Q: How do you go about your work?
We meet up with family members of victims. We locate the graves and take the bodies to the lab to identify victims and determine the cause of death. We ultimately hand over our findings to the government prosecutor. We are launching our own DNA lab to strengthen the identification process.

Q: There have been only a handful of trials so far. What keeps you going?
I'm optimistic that there will be more attempts at justice—either in Guatemala or in international courts. I feel very lucky to have escaped the conflict. … [W]hile I was watching a Yankees game in New York, my fellow citizens were getting massacred. I want to repay the country by documenting the truth about these killings.

CREDITS (TOP TO BOTTOM): FAFG; IMAGE COURTESY OF ROYAL SOCIETY OF CHEMISTRY; INSET: SOURCE: R. LIU; SOURCE: COMMITTEE ON SCIENCE AND TECHNOLOGY/U.S. HOUSE OF REPRESENTATIVES

AWARDS

BRINGING HONOR. Anthropologist Stephen Houston, who has spent his career deciphering the Mayan glyph system, is one of 25 winners of this year's "genius grants" from the John D. and Catherine T. MacArthur Foundation. "There can be no rational sense of deserving" the 5-year, $500,000 prize, says Houston, a professor at Brown University, who combines linguistics, history, and ethnography to understand the classic Mesoamerican society. Houston compares the impact of deciphering Mayan writings on scholars to the effect decoding hieroglyphs had on Egyptologists. He plans to use the prize money to examine how Mayans viewed their bodies and which actions brought "honor or dishonor" to one's physical self.

A complete list of this year's winners is at www.macfound.org.

TWO CULTURES

SURF'S UP! So much for slogging through organic chemistry in some dank basement lab. University of Hawaii, Honolulu, chemist Robert Liu and colleagues have taken their synthetic chemistry to the beach. Liu, who specializes in photochemical reactions triggered by sunlight, developed a magazine-sized reactor that uses the sun's rays to produce variants of vitamin A. The reactions normally generate excess heat that must be dissipated using cold water. But in a report published online last month in *Green Chemistry*, Liu's team described how they built their reactor into a boogie board, which radiates unwanted heat into the Pacific Ocean as researchers ride the waves. Cowabunga, dude! The only problem: Good luck getting students back into the lab.

Got a tip for this page? E-mail people@aaas.org

<< Politics

LOCKED OUT. In a move that has sparked bipartisan outrage in Congress, officials at the U.S. Department of Veterans Affairs (VA) have barred a former VA microbiologist from entering one of its hospitals in Pittsburgh, Pennsylvania. The banishment came 2 days after microbiologist Janet Stout testified before the House Science Committee about a controversial VA decision to destroy her large collection of *Legionella* bacteria in 2006. At the hearing, committee members were harshly critical of that step, which Stout says followed a clash with VA officials over her lab's research priorities.

The move "appears to be punishment for Dr. Stout's appearance," representatives Brad Miller (D–NC) and Dana Rohrabacher (R–CA) wrote in a 19 September letter to VA officials. They want the agency to hand over all records relating to an 11 September e-mail from Terry Wolf, director of the VA Pittsburgh Health System, that orders the staff to block Stout's access "without prior approval of my office." Stout left the VA last year, but Wolf writes that she "has been seen on VA premises" and "still receives mail here. Both practices must be terminated immediately."

Stout, who now runs the private Special Pathogens Laboratory in Pittsburgh, says she is mystified by the effort to bar her from a public hospital "where people come and go freely." She periodically visits the building to consult with former colleagues on projects but hasn't yet tested the ban. "I don't know if they are trying to intimidate me or create fear among my former colleagues," she says. VA officials didn't return calls from *Science*.

Zerhouni bows out
30

Phoenix sees what it was looking for
32

INFECTIOUS DISEASE

New Malaria Plan Called Ambitious By Some, Unrealistic by Others

It was standing room only last week at U.N. headquarters in New York City when a star-studded cast, including philanthropist Bill Gates, U2 rocker Bono, and British Prime Minister Gordon Brown, kicked off the latest in a string of grand plans to conquer malaria, the mosquito-transmitted scourge that kills some 1 million people a year, mostly African children.

Big guns. Celebrities and dignitaries, including U2 lead singer Bono, helped launch the Global Malaria Action Plan.

GOOD INTENTIONS

WHEN?	WHO?	GOAL?	WHAT HAPPENED?
1955	World Health Organization	Eradicate malaria	Campaign broke down in 1960s
1998	Roll Back Malaria partnership	Reduce cases and deaths by 50% by 2010	Little progress so far
2000	African heads of state (Abuja Declaration)	Reduce African malaria deaths by 50% by 2010	Little progress so far
2001	United Nations (Millennium Development Goals, MDG)	"Have halted by 2015 and begun to reverse the incidence of malaria and other major diseases"	Appears feasible
2005	MDG Working Group on Malaria	Reduce cases and deaths by 75% by 2015	Too early to tell

The goals of the Global Malaria Action Plan (GMAP) are stunningly ambitious: Reduce malaria deaths to near zero by 2015, then progressively eliminate the disease from countries and regions until it is eradicated from the planet. That will take mosquito- and parasite-foiling technologies that have yet to be invented, along with billions of new dollars a year that the plan's architects hope generous donors will provide. GMAP, assembled over the past year with input from more than 250 experts, is the creation of the Roll Back Malaria (RBM) partnership, a coalition of international agencies, public and private donors, and malaria-affected countries.

Regina Rabinovich, head of infectious diseases at the Bill and Melinda Gates Foundation and one of the key forces behind the plan, calls the goals "ambitious but achievable." But many malaria experts say it's unlikely that GMAP will meet its targets—even with abundant funding—although they applaud the renewed commitment. Several also caution that donors and agencies should be careful in what they promise, given the humbling outcomes of previous grand plans (see table, above).

Scientists and the World Health Organization (WHO) also exuded confidence in the 1950s when they vowed to eradicate malaria, for instance. After that initiative's spectacular demise in the 1960s, malaria cases surged worldwide, and support for malaria control and research essentially dried up.

After a long hiatus, international health and development agencies reentered the fight against malaria in the late 1990s, setting a series of increasingly ambitious targets. They culminated in Bill and Melinda Gates' unexpected call last year to again attempt to eradicate the disease, a word that hadn't been uttered in the context of malaria for some 40 years (*Science*, 7 December 2007, p. 1544).

"We set year after year new goals and never meet any of them," says Christian Lengeler, a malaria researcher at the Swiss Tropical Institute. Lengeler, who has worked extensively in Tanzania, calls GMAP's 2015 target of zero deaths "totally unrealistic." "Silly," says another scientist. As for the eventual eradication of malaria, "maybe, but not in my lifetime," seems to be the general consensus.

This time it is different, insist Rabinovich and Awa Marie Coll-Seck, executive director of RBM. For one, coffers are flush. Thanks to contributions from the Gates Foundation, the Global Fund to Fight AIDS, Tuberculosis and Malaria, the World Bank, the President's Malaria Initiative, and others, international funding for malaria control jumped from $51 million in 2003 to an estimated $1.1 billion in 2008. Last week, the Global Fund announced that it will award $1.62 billion over the next 2 years to help poor countries fight malaria, and the World Bank pledged $1.1 billion to expand its Malaria Booster Program. These and other smaller contributions unveiled last week still fall significantly short of the $5 billion or $6 billion a year GMAP says is needed.

Also in the past few years, malaria interventions, such as long-lasting insecticide-treated bed nets and a new class of drugs known as artemisinin-based combination therapies (ACTs), have proved their mettle (*Science*, 26 October 2007, p. 556). A half-dozen African countries with committed leadership and a lot of outside support have scaled up these interventions rapidly—Ethiopia, for instance, distributed 20 million bed nets in just 18 months. A few of these countries or areas, those with small populations and high access to prevention and treatment, have seen roughly a 50% decline in malaria cases and deaths since 2000, WHO notes in its 2008 World Malaria Report. Ensuring universal access to these and other tools such as indoor insecticide spraying and preventive treatments in pregnant women can halve deaths by 2010, says GMAP, and then reduce them to near zero 5 years out. ▶

PHOTO CREDIT: KATHY WILLENS/AP PHOTO

Peanut paste on trial in Niger
36

Computing corn genetics
40

But none of the countries has reached the target of 80% coverage with existing interventions, set just a few years ago, much less the 90% called for by GMAP. Across the continent, just 23% of children slept under a bed net in 2006, and only 3% of patients were treated with ACTs, according to WHO estimates.

The challenges facing big countries like the Democratic Republic of the Congo (DRC) and Nigeria are especially daunting. They account for about 20% to 25% of malaria deaths, although hard data are scarce, and are plagued by civil unrest and weak health systems. "That it can be done in Zambia, with a population of 10 million and a dynamic minister of health, does not say a thing about what to do in DRC," agrees Rabinovich.

To develop the radical types of new vaccines, drugs, and insecticides needed for the toughest areas—as well as for eradication many decades from now—GMAP calls for pumping $750 million to $900 million a year into research. A working group is already hammering out a detailed research and development plan, which Rabinovich says should be ready in 15 months.

To prime the pump, Gates announced $168 million for research on the next generation of malaria vaccines. The award is going to the Bethesda, Maryland–based PATH Malaria Vaccine Initiative, which will try to build off the experience gained from vaccine candidates already in the pipeline, says MVI Director Christian Loucq. GlaxoSmithKline's RTS,S, which targets the malaria parasite form that infects the liver, for instance, is about to enter phase III trials—the first malaria vaccine candidate to get that far. MVI is investigating additional antigens that target different stages in the parasite's life cycle that could be used in combination, as well as novel adjuvants to boost vaccine power. Although expected to be significantly more efficacious, such second-generation vaccines won't be available until well after 2015 and, like RTS,S, will still be only partially protective.

Another intriguing possibility is a transmission-blocking vaccine that would be administered to humans but that would target the parasite after it is taken up by the mosquito in her blood meal. Loucq calls the approach "elegant," the equivalent of an "immunological bed net," but cautions that it is early days.

Whether the exact targets are met is beside the point, says RBM leader Coll-Seck. "I am a glass-half-full person," she says. If GMAP leads to a significant reduction in malaria cases and deaths—even if the plan promised much more—who would call that a failure, she asks.

–LESLIE ROBERTS

ANTHRAX INVESTIGATION

NAS Study May Fail to Settle Anthrax Case

The Federal Bureau of Investigation (FBI) has provided the U.S. National Academy of Sciences (NAS) with a list of 15 questions that it wants the academy to consider in its review of the scientific evidence in the FBI's case against Bruce Ivins, the Army microbiologist implicated in the anthrax letter attacks of 2001. Besides asking whether the genomic analysis carried out to trace the source of the anthrax was valid, the questions address aspects such as the source of silicon found in the spores and whether the attacker needed specialized equipment to grind the spores into an easily dispersible powder.

But even before the academy frames the scope of the study and seeks approval from its governing board, members of Congress and bioterrorism experts are voicing concerns that a purely scientific review won't counter skepticism that Ivins, working solo, was the perpetrator of the attacks. One expert calls the FBI's request "a nice little jujitsu move" to deflect attention from nonscientific questions about the investigation, such as how the FBI ruled out all the other individuals who had access to RMR-1029, the flask of anthrax under Ivins's control. Last week, those concerns prompted Representative Rush Holt (D–NJ) to introduce legislation proposing a commission—similar to the one that investigated the 11 September 2001 terrorist strikes—that would review all the evidence in the case.

Since Ivins committed suicide on 29 July, FBI officials have unsealed court documents that detail part of the scientific evidence linking the anthrax in the letters to the flask under Ivins's control at the U.S. Army Medical Research Institute of Infectious Diseases at Fort Detrick, Maryland. By requesting the NAS study, the FBI is essentially subjecting that evidence to peer review in lieu of a jury trial. The last question on the FBI's 15 September list is whether "testimony regarding the methods used to link the mailed anthrax to RMR 1029" would meet evidentiary standards in a court of law.

Closed. FBI boss Robert Mueller hopes the study will wrap up the case.

CREDIT: SUSAN WALSH/AP PHOTO

Gregory Koblentz, a biodefense researcher at George Mason University in Fairfax, Virginia, says even for a scientific review, the questions posed by the FBI don't go far enough. He and Alan Pearson of the Center for Arms Control and Non-Proliferation in Washington, D.C., want the academy to ask more probing questions about the science as well as undertake a broader investigation; they are submitting their suggestions to NAS. For example, says Pearson, referring to a question on the FBI's list, it isn't pertinent to ask whether "*Bacillus anthracis* samples dried with a rudimentary methodology can pose an inhalation hazard resulting in pulmonary anthrax. Of course they can. The question is whether [this method] can produce anthrax like that found in the letter."

"Our aim here is to lay out the facts gathered in this investigation and be as transparent as we can," says FBI spokesperson Paul Bresson. "That is all we can do and all we can control. As we have stated previously, we would have preferred to have brought this case to trial."

–YUDHIJIT BHATTACHARJEE

Published by AAAS

ASTROPARTICLE PHYSICS

Europeans Think Big For Particle Detectors

Looking up. The MAGIC telescopes helped demonstrate gamma ray detection.

CREDIT: ASPERA/R. WAGNER, MPI FOR PHYSICS, MUNICH

European physicists who study particles from outer space made a pitch this week for the ambitious and costly experiments they want to build over the next decade. "We've worked hard to get the tools; now we need to move to large-scale detectors," says Christian Spiering of DESY, Germany's particle physics lab in Hamburg.

Astroparticle physicists aim to snare the likes of cosmic rays, neutrinos, gravitational waves, and dark matter particles as they pass by or through Earth. To better capture these elusive cosmic signals, ASPERA, a network of astroparticle physicists funded by the European Union, this week released a road map for future projects, along with a pitch to funding agencies to double the current €70 million annual spending on astroparticle physics over the next 8 to 10 years—a tall order in what's expected to be a tough funding climate.

Researchers have been detecting particles from space for decades, but so far the scientific breakthroughs from their sensors have been few. But this groundwork will soon pay off, says Spiering, who chairs ASPERA's road map committee. The road map, released on 29 September, divides the field into seven areas and identifies a key instrument in each.

Three of those instruments rely on tested technology, and construction could begin on them soon. First, the proposed Pierre Auger Observatory North, a vast array of detectors that would look for ultrahigh-energy cosmic rays, would likely be a bigger Northern Hemisphere version of the existing Auger array in Argentina. Second, the Cerenkov Telescope Array would look for incoming high-energy gamma rays, following the detection strategy of existing telescopes such as MAGIC in the Canary Islands. And the recently completed ANTARES, a neutrino observatory on the Mediterranean seabed, is the prototype for the third, KM3NeT, which would use a cubic kilometer of seawater as its detector. For these three proposals, "we have the technology; now we have to find the money," says ASPERA coordinator Stavros Katsanevas of France's CNRS research agency.

The road map doesn't detail the detector of choice for two other subfields, spotting dark matter and measuring neutrino mass from a phenomenon called double beta decay; the outcomes of ongoing experiments using a variety of techniques will inform those decisions. ASPERA's lineup finishes with two mammoth projects: an underground neutrino observatory called LAGUNA with a detector made from a million tons of either water or liquid argon, and a next-generation gravitational-wave antenna dubbed the Einstein Telescope. Both require more design work, and results from the Large Hadron Collider and current gravitational-wave detectors could change the specifications. "By mid next decade, we can launch these ambitious projects," says Katsanevas.

Metallurgist John Wood of Imperial College London, who headed a European Union–sponsored effort to identify research infrastructure projects, is skeptical of ASPERA's call for funding increases. "In the current climate, their chances are pretty slim," he says. "Politically, it's a very difficult time." But Katsanevas says, "I'm not afraid of that." The needed doubling of funding assumed that all of the road map's projects remained European-led, whereas he expects many will become collaborations with North America or Asia or both. In fact, French officials have asked the Organisation for Economic Co-operation and Development in Paris to act as a coordinating body, comparing regional road maps to find openings for collaboration. **–DANIEL CLERY**

Protection for Researchers

A California measure signed into law this week aims to protect researchers from harassment and attacks by animal-rights extremists. Publishing information about researchers that is likely to incite threats or acts of violence or trespassing on a researcher's property with the intent of interfering with his or her academic work is now a misdemeanor. Police hope arrests made for these infractions will yield evidence on shadowy extremist groups. Several university researchers have been targeted in recent attacks (*Science*, 8 August, p. 755). **–GREG MILLER**

Hubble Trouble … Again

The failure of a critical device that formats data aboard the orbiting Hubble Space Telescope has delayed this month's long-planned shuttle rescue mission until at least February. Agency officials say it will take several months to prepare the spare data system, which they want to send up because relying on a redundant component would leave the telescope without a backup. Changing out the component will add to the list of fixes, says John Shannon, shuttle program manager. But NASA science chief Edward Weiler says, "Hubble has a habit of coming back." **–ANDREW LAWLER**

Making Space Reservations

NASA will be allowed to buy seats through 2016 aboard the Russian Soyuz spacecraft, which ferries passengers to and from the space station, as part of a stopgap funding measure passed this week. The U.S. government slapped sanctions on Russia for alleged sales of nuclear material to Iran, which prohibited NASA from dealing with the Russian space industry. A waiver that allowed the space agency to carry out such spending was set to expire in 2011. Soyuz needs to be booked well in advance, however, and a failure to extend the waiver this year would leave Americans without a way to get into space if the shuttle, as planned, is taken out of service in 2010. **–ANDREW LAWLER**

Not Those Stock Analysts

The United States faces a shortfall of Ph.D.s to help analyze the status of its fisheries, according to a joint report by the departments of Commerce and Education. The report estimates that the National Oceanic and Atmospheric Administration (NOAA) alone will need to hire 150% more stock-assessment scientists (it now has 90) over the next decade, and universities are expected to confer about half the degrees needed each year. **–ERIK STOKSTAD**

Published by AAAS

NATIONAL INSTITUTES OF HEALTH

Adding a Turn to the Roadmap, Zerhouni to Step Down

Without saying much about his next move, Elias Zerhouni announced last week that he is resigning from the U.S. National Institutes of Health (NIH). He will step down by the end of October after more than 6 years as director. During that time, he tried to break down institutional and scientific barriers at the $29 billion agency and push discoveries into medicine. Those efforts won praise from Congress and leaders in the research community. But he also had to deal with a string of ethics controversies, and it was a tough time for rank-and-file scientists, who were squeezed by 5 years of flat budgets.

Transition. Elias Zerhouni explains NIH's mission to lawmakers, seated with his deputy director, Raynard Kington (*left*).

Rumors have swirled since January that Zerhouni might replace Johns Hopkins University President William Brody, who is retiring at the end of this year. When reporters asked Zerhouni about this last week, he responded: "That's not been decided by me at all." Instead, he said he plans to "take some time out" and do some writing. He chose to depart before the 4 November presidential election, he said, so that the next Administration will "focus on NIH as early and as soon as possible."

As for why he's leaving at all, Zerhouni saw his departure as following "the natural cycle of tenures for this position," about 6 years. A look back at the previous eight directors shows that their terms varied in length; two stayed longer than 6 years: James Shannon (13 years) and James Wyngaarden (9 years).

Zerhouni, 57, an Algerian-born radiologist who invented several new imaging techniques, was an administrator at Johns Hopkins before he took the helm of NIH in May 2002. Zerhouni's background set him apart from his predecessor, the basic biologist Harold Varmus. Many observers say Zerhouni's management experience made him the right person for a time of belt-tightening. A 5-year doubling of NIH's budget from 1998 to 2003 was coming to an end, and Varmus and some other scientific leaders were concerned about NIH's unchecked administrative growth, including the creation in 2000 of an institute focused on imaging.

In response, Zerhouni created a formal plan called the NIH Roadmap, a set of initiatives aimed at moving basic discoveries to the bedside, funded at first by taxing each of NIH's institutes. But just as these new programs were taking off, NIH's budget stopped growing, sending success rates for research grants crashing from about 30% to 20% this year. Some members of the community blamed Zerhouni and his Roadmap. Defenders say, however, that the plan was useful as a selling point for biomedical research in Congress.

Although Congress has recently given NIH tiny budget boosts, some say it has significantly elevated the NIH director. It passed a 2006 law capping the number of institutes and centers at 27, giving the NIH director more control over NIH's portfolio, and creating a permanent fund for Roadmap-like projects. That pot of money had risen to $496 million, as large as many of smaller institutes. Varmus says the NIH director's new powers will make the position "a lot more interesting."

At the same time, some Roadmap components remain just experiments. A program to bring industry-style molecular screening to academia is beset by skeptics. And the new Clinical and Translational Science Awards, which are forcing medical schools to integrate clinical science programs, have been criticized as inadequate.

Zerhouni has been credited widely for trying to promote novel research and young investigators, including most recently for creating the "transformative" R01 award for risky projects. Although the total number of these awards so far is modest, "the important thing was that Zerhouni recognized" the need for them, says cell biologist Keith Yamamoto of the University of California, San Francisco, who also helped plan a major overhaul of peer review.

Zerhouni may have reaped more than the usual share of controversy. He defended sexual research grants to a Republican-led Congress and departed from the Bush Administration's tough line against human embryonic stem cell research. Addressing an uproar over industry consulting by NIH scientists, he banned such outside activities.

President George W. Bush has not yet named an acting NIH director, but Zerhouni has recommended current NIH Deputy Director Raynard Kington for the post. An M.D. and Ph.D. in health policy and economics who studied health disparities before coming to NIH, Kington is not well-known to the extramural biomedical research community. As deputy, much of his time has been taken up with dealing with the intramural ethics controversy.

The acting director will face a number of immediate challenges. One is deciding how to allocate the pain of a budget freeze through March, just approved by Congress in a continuing resolution (*Science*NOW, 29 September). Typically, NIH deals with such uncertainty by funding ongoing grants at the 80% level and funding fewer new awards until the next budget is approved. That will increase stress on investigators. In the short term, leading NIH "is going to be an even tougher job," says Howard Garrison, public affairs director of the Federation of American Societies for Experimental Biology in Bethesda, Maryland. Also requiring quick attention is a call from Senate investigators for a review of conflict-of-interest rules for extramural researchers. Given such pressures, many NIH watchers hope a new director will be in place before next spring.

–JOCELYN KAISER

CREDIT: UPI PHOTO/LANDOV

Published by AAAS

NOAA

U.S. Oceans Chief Leaves a Mixed Legacy in His 7-Year Wake

For 7 years, former Navy Vice Adm. Conrad Lautenbacher has preached his mantra of "one NOAA" as a way to unify the hydra-headed National Oceanic and Atmospheric Administration (NOAA). Congress has rewarded his management prowess with larger budgets, allowing the agency to expand its efforts on everything from tracking wildfires to monitoring tsunamis. Last week, Lautenbacher announced he is leaving, and scientists say the spry technocrat leaves a reorganized and stronger NOAA research program—as well as some big headaches for the next U.S. oceans skipper.

Tucked into the Commerce Department, NOAA has responsibility for myriad activities in the air, at sea, and in space. "When I came to NOAA, I saw it as a holding company of six or seven multidisciplinary, very fine scientific enterprises," says Lautenbacher. "[But] it was too compartmentalized."

Lautenbacher sought to break down agency stovepipes with 44 programs that cut across issues such as aquaculture, environmental modeling, and geodesy. He also combined six agency labs in Boulder, Colorado, to create the Earth System Research Laboratory (ESRL). "He's done a good job of knitting the pieces of NOAA together," says marine geologist Rodey Batiza, a program manager at the U.S. National Science Foundation who has served as an outside reviewer for the agency. Congress apparently agreed: Legislators hiked the agency's budget from $3.1 billion to $4.2 billion during Lautenbacher's tenure, although they also pumped hundreds of millions of dollars into pet projects.

CREDIT: NOAA

Making waves. This spring, NOAA's Conrad Lautenbacher unveiled a management plan to preserve a fragile marine sanctuary in Hawaii.

The improved cooperation helped bolster tsunami monitoring efforts, says geophysicist Costas Synolakis of the University of Southern California in Los Angeles. Since the Sumatra tsunami of December 2004, NOAA's Pacific Marine Environmental Laboratory (PMEL) in Seattle, Washington, has collaborated with the National Weather Service on 33 new advanced undersea pressure gauges that have improved the service's predictive accuracy. The weather service is also installing new tsunami-modeling software developed by PMEL's scientists. By the same token, former NOAA advisory board chair Leonard Pietrafesa, a fluid physicist at North Carolina State University in Raleigh, says that ESRL has paved the way for better predictions of hurricane intensity.

While Lautenbacher was making it easier for NOAA's scientists to talk to one another, the agency itself was having trouble communicating with two other federal agencies on one of its most important programs, the National Polar-Orbiting Operational Environmental Satellite System. Delays and cost overruns in the $14 billion Earth-monitoring program, which NOAA manages with NASA and the Pentagon, triggered a 2006 Pentagon review that stripped from the system five climate sensors. A report that year by the Department of Commerce inspector general faulted NOAA leadership's "poor management oversight" of the program, and the three agencies are still trying to agree on a budget for it.

Lautenbacher says he did his best to manage the "poorly conceived" program, which was created in 1994. "I don't regret how NOAA managed it," he says. He reassures climate scientists that making precise climate data "operational" will be a priority for a "National Climate Service," a new entity that his deputies are proposing for the next Administration.

Lautenbacher, who will step down next month, plans to move to Atlanta, Georgia, to chart his future. Deputy NOAA Administrator William Brennan will serve as acting director.

–ELI KINTISCH

Italy Restricts Academic Hires

An attempt to address Italy's economic woes appears to place tough restrictions on academic hiring. An amendment to a newly enacted financial law restricts institutions to replacing at most 20% of the jobs lost through retirement and other reasons. "We cannot [hire] anyone until 2013, as there is nobody who is going to retire for the next few years," says physicist Stefano Fantoni, head of SISSA, the prestigious postgraduate science school in Trieste.

Italian scientists are also wary about a provision that authorizes public universities to look for sponsors and become private foundations. The new law comes on top of a proposed 10% cut in university funding by 2010. "In Italy, pure research is always the first sector in science to suffer," says Giancarlo Ruocco, head of the physics department at the University of Rome La Sapienza. **–LAURA MARGOTTINI**

Going Green Once, Twice …

North America's first carbon-emissions auction went smoothly last week. Organized by a consortium of 10 Northeast and Mid-Atlantic states aiming for a 10% reduction in carbon emissions from their power companies by 2018, the Regional Greenhouse Gas Initiative auction closed at a price of $3.07 per ton. Jim Rubens, an energy policy adviser with the Union of Concerned Scientists, called the price a "Goldilocks" figure: It's enough to impact carbon emissions from utilities in participating states without destabilizing the economy.

–RACHEL ZELKOWITZ

A Rewarmed Climate Report

In a surprising twist, White House officials plan to rework a draft report on climate change because of complaints that it hypes—not underplays—the threat of global warming. The Unified Synthesis Product, released in July, was meant to summarize the 21 previous federal Climate Change Science Program (CCSP) reports. But statements like "The future is in our hands" and "the choice is ours" have enraged critics such as Roger A. Pielke Sr. of the University of Colorado, Boulder. Pielke says the draft "promotes a particular narrow perspective."

CCSP staffer Chad McNutt says the report was released before it was ready because "we wanted to do this fast." Now editors are sifting through 500 pages of comments. One editor, Jerry Melillo of Woods Hole Oceanographic Institution in Massachusetts, doesn't think that the July version was overly politicized. But he says some points "could have been stated more clearly." **–ELI KINTISCH**

Published by AAAS

PLANETARY SCIENCE

Minerals Suggest Water Once Flowed on Mars—But Where?

Scientists on the Phoenix mission to the high arctic of Mars announced this week that the rover had found some long-sought soil minerals. "These [minerals] are indicators of liquid water in the past," Phoenix principal investigator Peter Smith of the University of Arizona (UA), Tucson, said at a bicoastal press conference on 29 September. The minerals are exactly what Phoenix was sent to look for in the high-latitude soil just centimeters above the frozen water suspected from orbital data.

The catch is that from Phoenix observations so far, team members can't say for certain when or where the water was liquid: recently, where Phoenix found the minerals, or long ago, somewhere else on the planet. The minerals might have blown in from ancient deposits formed in the atmosphere. And time is running out for Phoenix to find answers. The gathering gloom of martian winter means it has only a couple of months to live.

The discoveries come from two Phoenix instruments. The Thermal and Evolved Gas Analyzer (TEGA) recorded the release of water when it heated a soil sample to high temperature, most likely when water was driven off from clay, said TEGA lead scientist William Boynton of UA. TEGA also detected carbon dioxide being driven off at high temperature—a clear sign that calcium carbonate was breaking down, Boynton said. The Microscopy, Electrochemistry, and Conductivity Analyzer confirmed the presence of calcium carbonate, said MECA lead scientist Michael Hecht of the Jet Propulsion Laboratory in Pasadena, California. It measured a stable pH of 8.3 in a soil slurry even after Phoenix added acid, evidence that calcium carbonate was buffering the pH. MECA detected calcium ions in solution as well.

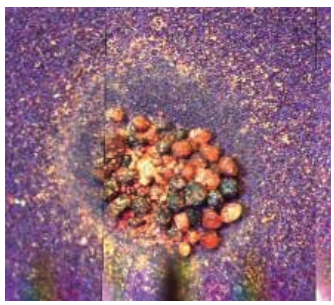

Dirt. Martian soil harbors minerals formed from wet rock.

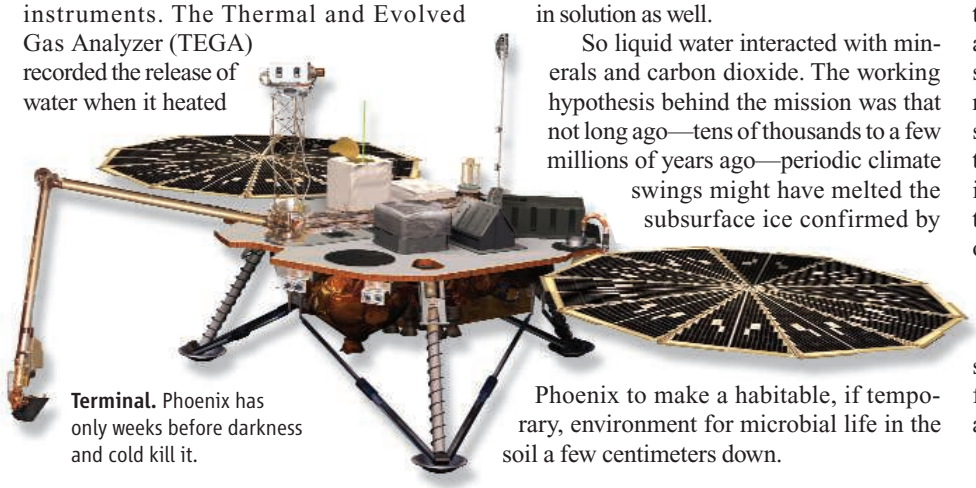

Terminal. Phoenix has only weeks before darkness and cold kill it.

So liquid water interacted with minerals and carbon dioxide. The working hypothesis behind the mission was that not long ago—tens of thousands to a few millions of years ago—periodic climate swings might have melted the subsurface ice confirmed by Phoenix to make a habitable, if temporary, environment for microbial life in the soil a few centimeters down.

That scenario could still hold, says geochemist Nicholas Tosca of Harvard University. "Liquid water is required to form these minerals," he says. "How much liquid water could be debated. A thin film could do it." That would be enough for microbes too. But scientists cannot yet show that the minerals formed where Phoenix found them. They may have formed billions of years ago where massive deposits of clay are found today. Also, carbonates reported in martian dust may have formed in the atmosphere and could have been blown to the Phoenix site, although Smith sees few signs of such transport. "I'm not sure what they could do to test that," says Tosca.

Now that Phoenix has completed its 90-day nominal mission and a 30-day extended mission, it's living on borrowed time. Martian winter is coming on, with the sun spending more and more time each day below the horizon, starving the spacecraft's solar panels. Mission managers are rushing to fill TEGA's last four sample cells before power levels fall too low for the sampling arm to operate. "We have not finished," declares Smith. Near the top of the team's remaining to-do list will be looking for organic matter possibly lingering from past life. "If there's any there, it's not very much," said Boynton, but "we are still looking."

By late November, the crushing cold should shut down the lander as carbon dioxide frost begins to encase it. Water-ice snow is already beginning to fall from passing clouds.

–RICHARD A. KERR

CRYPTOGRAPHY

Quantum Network Set to Send Uncrackable Secrets

Next week in Vienna, European scientists and engineers will put the bizarre and abstruse laws of quantum mechanics to a practical, everyday use. Researchers will demonstrate a network for transmitting uncrackable encoded messages in quantum-mechanical packets of light. Such quantum networks could soon link banks or government offices, some researchers say. "This is a moment when research turns into technology," says Chip Elliott, a network engineer at BBN Technologies in Cambridge, Massachusetts, who 5 years ago led efforts to build the more primitive DARPA network. Still, he cautions, "it's too early to say whether there are customers for this."

The product of a 4-year, €11.4 million collaboration funded by the European Union, the network will connect six sites across the city through eight existing fiber-optic links, all belonging to industrial giant Siemens. It will distribute the numerical "keys" for scrambling secret messages.

A message can be encrypted by converting it into a string of 0s and 1s and scrambling those bits by compounding them with a key, a random string of 0s and 1s. If only the sender, Alice, and the receiver, Bob, know the key, then only they can read the message. The trick is to transmit the key without its being seen by an eavesdropper, Eve. So-called quantum key distribution exploits the fact that it's impossible to measure a photon without also altering it.

For example, Alice can send Bob individual photons polarized horizontally to signify 0 or vertically to signify 1. Thanks to quantum weirdness, she can also send photons polarized both ways at the same time. If Eve tries to

Published by AAAS

Too much. Ice coming off Jakobshavn Isbræ glacier surged after warm ocean water arrived.

GLACIOLOGY

Winds, Not Just Global Warming, Eating Away at the Ice Sheets

The surge of glaciers draining both the Greenland and West Antarctic ice sheets has alarmed scientists and the public alike. Global warming appeared to be taking an early toll on the planet's largest stores of ice while accelerating the rise of sea level. But two new studies point to random, wind-induced circulation changes in the ocean—not global warming—as the dominant cause of the recent ice losses through those glaciers. In Greenland, at least, "you're going to have trouble blaming this on global warming," says glaciologist Richard Alley of Pennsylvania State University in State College. But he says the results underscore the threat of global warming by showing how warmth can "hit ice sheets where it hurts," as glaciologist Robert Bindschadler of NASA's Goddard Space Flight Center in Greenbelt, Maryland, puts it.

The losses long puzzled glaciologists because the atmosphere over the glaciers didn't seem to have warmed enough to trigger them. Meltwater didn't lubricate glacial flow enough to explain the losses either (*Science*, 18 April, p. 301). Could the culprit be ocean waters? They can carry lots of heat to glaciers that float out onto coastal waters, but oceanographers had not been taking the ocean's temperature off the ice sheets.

So physical oceanographer David Holland of New York University and his colleagues turned to scientists of a different stripe: fisheries researchers. They had recorded bottom temperatures off southwest Greenland while surveying shrimp populations from 1991 to 2006. Holland and colleagues reported online this week in *Nature Geoscience* that an influx of warmer, saltier water in 1997 "coincided precisely" with the rapid thinning and subsequent acceleration of Jakobshavn Isbræ glacier, Greenland's most prolific outlet for ice. The warm water must have melted the glacier's exposed underside and weakened it, they say, leading to the breakup of the ice shelf that had been bracing the glacier against the shore and helping to hold it back. "I think it's fantastic," says Bindschadler. They've "got this nailed in Greenland."

Holland and colleagues traced the influx of ocean warmth back to the atmosphere over the North Atlantic. An abrupt weakening of winds due to a natural atmospheric phenomenon called the North Atlantic Oscillation drove more waters from the Irminger Sea near Iceland around the tip of Greenland, up onto the shelf, and under the ice.

A similar natural process may have been at work in recent heightened ice losses off West Antarctica, researchers reported in the 18 September *Geophysical Research Letters*. Glacier modelers Malte Thoma of the Alfred Wegener Institute for Polar and Marine Research in Bremerhaven, Germany, and colleagues, including Holland, had no water temperature data there, but they did have wind observations. When they plugged those numbers into an ocean-ice model, the shifting winds drew deeper, warmer offshore waters in the model up onto the continental shelf and under the ice at the same time in the mid-1990s that the real glaciers draining the West Antarctic Ice Sheet sped up. The wind shift may have been natural or caused by global warming, says co-author Adrian Jenkins of the British Antarctic Survey in Cambridge, U.K. Therefore, "whether we're going to see a continuation of [those losses] is not clear."

The vagaries of the atmosphere may be sending some confusing signals about global warming, researchers say, but that's no reason to stop worrying about the ice. "The really important thing is," says Alley, "when you look at [climate] projections, you have warming around Greenland." And that warmth now has an obvious way to get at the ice.

–RICHARD A. KERR

measure the light particles, that very act will "collapse" the two-way-at-once photons into either vertical or horizontal ones. Bob and Alice can detect that by comparing some randomly chosen bits.

A few companies make quantum systems to connect two users through a single link. The Vienna project weaves six disparate systems into an automated network. "You just make a connection to one node and can connect to any other user," says Andreas Poppe, a physicist at the Austrian Research Centers in Vienna.

In fact, the network will not be a fully quantum network, which would let Alice pass photons to Bob across any number of nodes. That would require devices called "quantum repeaters" that are at least a few years away. In the Vienna network, each user generates a key that is stored as classical (nonquantum) 0s and 1s in the node he or she links to. Those classical bits flow from node to node as needed, quantum mechanically encrypted as they cross each link. "What our network assumes is that you can trust each of the intermediate nodes," says Andrew Shields, a physicist with Toshiba Research Europe in Cambridge, U.K.

Nobody will be invited to try to hack the network, either. That's because hackers would likely ignore the quantum mechanics and attack the system's conventional parts, which wouldn't test the new concept, Poppe says.

Still, researchers hope the demonstration will signal the emergence of the new technology, especially for private networks. Some experts are skeptical. "I think the impact on the actual practice of cryptography is likely to be small," says Ronald Rivest, a computer scientist at the Massachusetts Institute of Technology in Cambridge. Current techniques, which rely not on shared secret keys but on mathematical manipulations that are practically impossible to work backward, already work well, says Rivest, who predicts that the niche for the quantum systems will be small.

Network developers hope for more. "I think, on our scale of things, it will be a historic day," says physicist Nicolas Gisin of the University of Geneva, Switzerland. The question is, will technologists and market analysts see it that way, too?

–ADRIAN CHO

CREDIT: BOB STRONG/REUTERS

Published by AAAS

RESEARCH FOUNDATIONS

Biochemist Robert Tjian Named President of Hughes Institute

The Howard Hughes Medical Institute (HHMI), the largest private funder of biomedical research in the United States, has chosen a new president. He is University of California, Berkeley, biochemist Robert Tjian, a longtime Hughes investigator known as a driven researcher and devoted mentor. On 1 April, Tjian will replace Thomas Cech, who will return to research at the University of Colorado, Boulder.

The Chevy Chase, Maryland–based HHMI, which has an endowment of $17.5 billion and spent $685 million last year, supports more than 350 investigators at universities and funds education programs and scientists abroad. Tjian said "there are many reasons" why he accepted an offer from the Hughes board of trustees, which based its search on nominations. The main one, he says, is "to give back" to the institution that has funded him for 22 years. Moreover, Hughes "has a huge impact," and "I think it's a fantastic opportunity to try to help scientific research and science education in the United States and internationally," Tjian says.

Tjian, 59, studies the biochemistry of gene transcription. At Berkeley, he has been heavily involved in recruiting new faculty, reshaping its research and education programs, and directing its nearly decade-old health sciences initiative, which promotes interdisciplinary research. He also co-founded Tularik, a biotech company that was sold to Amgen in 2004 for $1.3 billion.

Multitasker. Biochemist Robert Tjian's broad experiences likely helped win him the job of HHMI president.

HHMI board of trustees member Joseph Goldstein says this range of experiences made Tjian "exactly right" for a job that has become "more complicated" in the past few years, as Cech began new programs and oversaw the creation of HHMI's first research campus, Janelia Farm, in Loudoun County, Virginia. Tjian is "an outstanding scientist, he's an excellent mentor to students and postdoctoral fellows, he's interested in education, he has a reputation for being very organized, and he has a broad view of biology and medicine," says Goldstein, a Nobel Prize–winning biochemist at the University of Texas Southwestern Medical Center in Dallas, who has known Tjian for more than 20 years.

As Cech did during his 8 years at HHMI, Tjian plans to keep his Berkeley lab—he says he wouldn't have taken the job otherwise—but will spend no more than 1 day a week there and at Janelia Farm. He has also agreed to give up his position on the boards of several biotech companies by April.

Tjian says that he has no specific new programs in mind coming in: "I need to go in there and take a look." For now, he plans to continue HHMI's aim of funding the "right people." He doesn't expect to tinker with Janelia Farm, which he considers an ongoing "experiment." He expects to visit Hughes in the coming months while Cech is still there to "learn the ropes." **–JOCELYN KAISER**

FELLOWSHIPS

An International Plan to Hatch Scientist-Entrepreneurs

TIANJIN, CHINA—Who said science and business don't mix? Last week, more than 100 young researchers from 60 countries were special guests at the summer meeting of the World Economic Forum (WEF), held near Tianjin, China's third biggest urban area. While corporate titans anguished over the U.S. bank bailout, young scientists and entrepreneurs explored how to forge new links.

To ease neophytes into the world of dealmaking, the InterAcademy Panel (IAP), a network that sponsors science-in-society programs on behalf of 100 national science academies, plans to award five $10,000 seed grants to the most compelling joint R&D proposals arising from interactions at the meeting between scientists and business leaders. "The idea is to nurture new linkages," says IAP co-chair Howard Alper, a chemist and chair of Canada's Science, Technology and Innovation Council. "Companies need not put in a cent at the beginning." Alper expects many academies to provide matching grants. The effort is timely, says Padmasree Warrior, chief technology officer at the California computer firm, Cisco Systems. "The lines are blurring between breakthrough, start-up, and scale-up," she says.

Top scientists are no strangers to WEF, famed for its winter meetings in Davos, Switzerland. Klaus Schwab, WEF's founder and executive chair, says he has long sought "to integrate technology even more into WEF activities." Last spring, Alper and fellow IAP co-chair Chen Zhu, China's health minister, persuaded Schwab to expand WEF's science program and invite young scientists. "We want to create a sustained integration of S&T [science and technology] in the forum," says Alper.

As a result, WEF's second annual "New Champions" meeting featured workshops on managing science and frontier science, and plenary sessions on nanotechnology and life sciences. "The academics seemed to embrace the idea that they needed to engage with the business community in language that the latter could understand," says Tom Ilube, chief executive officer of Garlik, a company based in Richmond, U.K., that specializes in protecting consumers against identify theft.

Guruprasad Madhavan cottoned on quickly. At the meeting, the S&T policy fellow at the National Academies in Washington, D.C., forged a partnership with entrepreneurs who will help him develop a low-cost medical device business model for poor villages in Tamil Nadu, his home state in southern India. With such tangible outcomes, Alper and others hope scientists have earned a permanent place at the WEF table.

–RICHARD STONE

CREDIT: BARBARA RIES/HHMI, 2008

Published by AAAS

The Peanut Butter Debate

A new type of ready-to-use food is changing the way severe malnutrition is treated. But questions remain about how far to push its introduction—and science has a hard time providing the answer

SAE SABOUA, NIGER—On a scorching hot day in this dusty, dry corner of the Sahel, mothers carrying babies and small children line up outside a couple of big tents. Some of the infants look healthy but others are shockingly thin, their arms like broomsticks. They're waiting to enter a "therapeutic feeding center" operated by the French section of Médecins Sans Frontières (MSF). Once inside, the children are measured and weighed and receive a quick health checkup. If they're found to be severely malnourished, they immediately receive a silvery sachet containing a new type of food that might just save their lives.

Open and squeeze the sachet and out pour 92 grams of a brown paste that looks like dark peanut butter. It's called Plumpy'nut, and one serving has 500 calories and plenty of proteins, vitamins, and minerals. Aid organizations like MSF say the paste, a so-called ready-to-use therapeutic food (RUTF), has revolutionized care for malnourished children. Plumpy'nut has a long shelf life, it does not need to be mixed with water—a major risk with standard treatments based on milk powder—and it is simple for mothers to give to their children at home. Perhaps best of all, children love the sweet, sticky stuff.

Online
sciencemag.org
Podcast interview with the author of this article.

But the nutrition world is divided on just how far the introduction of these products should go. MSF wants to move beyond treating severe malnutrition and introduce peanut butter–like pastes to *prevent* that condition, which occurs in some 20 million children in Africa and South Asia every year. In one district in Niger, MSF has started giving the product to as many as 80,000 children between 6 and 36 months, in what's called "blanket distribution." MSF likens the move to the large-scale introduction of antiretroviral drugs in Africa, which it helped pioneer.

But others ask: Where's the science to support such a plan? Few dispute the power of RUTFs in treating severely wasted children. But there's little evidence that such products work equally well in preventing malnutrition. And besides, skeptics say, adding them to the regular diet of millions of children is too complicated and too costly—MSF's program cost more than $55 per child in 2007—to keep up in the long run. "For prevention, we need other products," says André Briend, a nutrition expert at the World Health Organization (WHO) in Geneva, Switzerland, who helped invent Plumpy'nut while working as a French government researcher.

The issue has pitted those who want to see solid evidence before embarking on a major aid program against those—impatient with talk about *P*-values, cost-effectiveness, and sustainability—who want to act now. "Thousands of kids are dying," says Milton Tectonidis, a former MSF nutrition expert and a vocal advocate of a massive introduction of RUTFs. "We have enough data now. Do something!"

A new approach

Part Sahara, part Sahel, Niger is one of the poorest countries in the world. More than 70% of the population is illiterate. Malnutrition is

CREDIT: M. ENSERINK/*SCIENCE*

Published by AAAS

Sweet fix. Malnourished children receive sachets of Plumpy'nut at an MSF feeding center in Maradi province, Niger.

pervasive, especially during the so-called hunger gap—the 5 or 6 months before the annual harvest, when the previous year's supplies of sorghum and millet are running out. Protracted dry spells periodically lead to severe food crises, but even in good years, the essentially vegan diet doesn't always provide enough nutrition for fast-growing children younger than 3, says Susan Shepherd, a medical adviser at MSF in Geneva.

Until a few years ago, the standard treatment for severe malnutrition was F100, a milk powder fortified with dozens of vitamins and minerals. F100 was developed in the 1980s by veteran nutrition scientist Michael Golden, now a professor emeritus at the University of Aberdeen, U.K. It needs to be reconstituted with clean drinking water and consumed almost immediately. Left unrefrigerated for a few hours, it turns into a bacterial soup that can cause infectious diseases. That's why F100 is administered only in special nutrition "hospitals" where children often stay as long as 4 weeks with a caretaker, usually their mother.

Those are serious drawbacks. A mother who leaves home and work may put other children or the harvest at risk. Hospital capacities are limited, forcing governments and aid organizations to turn away patients. During a 2002 famine in Angola, MSF treated 8000 children in in-patient centers, Shepherd says, far short of what was needed. Crowded hospitals also help spread infectious diseases. Studies have shown that only between 25% and 45% of patients make a full recovery—and as many as one in five dies.

Golden and others started looking for alternatives to F100 in the 1990s. In 1997, Briend, then at the Institute of Research for Development in Paris, teamed up with Michel Lescanne, the director of Nutriset, a food company in Normandy. Lescanne had experimented with Mars-like bars that had almost the same composition as F100; the problem was that they melted easily. Briend found his inspiration in a jar of Nutella, a hazelnut spread that his children loved; the duo developed a paste consisting of roasted, ground peanuts combined with vegetable oil, milk powder, sugar, and a mix of minerals and vitamins.

Plumpy'nut, as they called it, is less than 2% water, which makes it a hostile environment for microbes. Suspended in a fatty environment, the vitamins and minerals are very stable. Plumpy'nut can last for up to 2 years without refrigeration and does not spoil even after the package is opened.

Mark Manary, a nutrition scientist at Washington University in St. Louis, Missouri, was the first to test the product in clinical trials, in Malawi. Two studies published in 2004 showed that it was "really a breath of fresh air," Manary says: Almost 80% of severely malnourished children recovered. And the home-based treatment regimen proved easy to organize on a large scale.

Experiences elsewhere were similar. Steve Collins, who leads an Irish relief organization called Valid International, saw high recovery rates in Ethiopia, Malawi, and Sudan. MSF was sold on Plumpy'nut after it was able to treat as many as 60,000 children during a severe food crisis in Niger in 2005, says Shepherd—a vast improvement from the Angolan experience. In June of 2007, four United Nations agencies, including WHO and UNICEF, issued a joint statement advocating home treatment with RUTFs for severely malnourished children who don't have other illnesses.

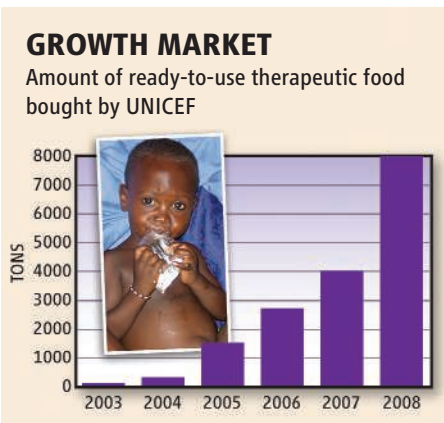

As a result, demand and production have exploded. Nutriset is the biggest producer by far, making more than 15,000 tons in 2008. Although some are dismayed by Nutriset's patents on Plumpy'nut (see sidebar, p. 38), other companies are entering the market as well. In Malawi, Manary set up a Nutriset franchise that churns out 500 tons of Plumpy'nut a year. UNICEF, the biggest RUTF buyer in the world, may purchase as many as 8000 tons in 2008 and expects global production to grow to at least 50,000 tons by 2011.

Given that success, many were surprised when a series of major papers on malnutrition published in *The Lancet* earlier this year offered only lukewarm support for RUTFs. In a vociferous statement, MSF accused the authors of "undermining the support for this lifesaving intervention," which led to a rift with the journal (*Science*, 1 February, p. 555). WHO's Briend was dismayed as well. But the authors of the series have since said that they were misunderstood and that they do in fact support the use of RUTFs to treat severe malnutrition.

Daunting studies

Although there's consensus about treatment, prevention is a very different matter. MSF and some other nongovernmental organizations are now proposing giving peanut paste as a supplement to children who are moderately malnourished or just at risk of severe malnutrition. Every case of severe malnutrition starts as a milder one, says Shepherd—so why wait until a child is emaciated? "After 2005 we said, 'Hell, let's try to expand it.'"

Many alternatives haven't worked, experts agree. Severe malnutrition is the result of a downward spiral of poor-quality food, weak immunity, infections and diarrhea, loss of energy and appetite, and so on. Many approaches have been tried to stop that cycle: Children have been given an inexpensive, fortified blend of corn and soy flour, or tablets with specific micronutrients such as vitamin A or zinc. Mothers have been taught to breastfeed longer, cook better meals, or wash their hands to avoid infections. But nothing has really proven adequate.

Whether peanut pastes will do better is far from certain. When MSF's program started, only two studies had looked at their ability to prevent severe malnutrition, both by Manary's team in Malawi. They found that moderately malnourished children given RUTFs gained weight faster than those who received corn-soy flour, "but it wasn't a knockout," Manary says.

MSF was not deterred: The fact that it worked so well as a therapy was reason enough to believe it would work in prevention, too, says Shepherd. In 2006, MSF gave Plumpy'nut to all moderately malnourished children in its centers in one district, Guidan Roumdji. But simply identifying those children and supplying them with the peanut butter proved a huge logistical challenge; so in 2007, the agency decided to switch to mass distribution to all children between 6 and 36 months of age. Instead of Plumpy'nut, it used Plumpy'doz, a Nutriset product that comes in big jars. Mothers are supposed to give their children just three spoonfuls of Plumpy'doz per day; that way, children get only a quarter of the calories, but their intake of micronutrients stays about the same.

Nutrition science is difficult enough in Western countries; clinical trials to evaluate a food program in a country like Niger are an even bigger challenge, says Rebecca Freeman-Grais, a researcher at Epicentre, MSF's epidemiology division. The study population is hard to reach, and communication is difficult. Randomizing children to two different regimes within a village would have met with resistance, she says, so the

CREDIT: M. ENSERINK/*SCIENCE*; SOURCE: UNICEF

Published by AAAS

Homemade. STA, in the Nigerien capital Niamey, is one of four Nutriset franchises that produce Plumpy'nut in the developing world.

PATENTS: A RECIPE FOR PROBLEMS?

NIAMEY, NIGER—A giant peanut roaster and grinder, a mixing and filling machine—it doesn't take all that much to produce the new ready-to-use therapeutic foods (RUTFs). A factory barely larger than a house in the quiet outskirts of Niger's capital produces some 500 tons of Plumpy'nut annually. But it can't do so on its own: The company, STA, is a franchise of Nutriset, a company in France that together with the French government owns the patent to Plumpy'nut and similar pastes.

As the market for RUTFs is booming, that situation has come under scrutiny. Aid organizations say there should be no patents on key humanitarian nutrition products, and some worry that Nutriset, a small family-run business, won't be able to meet the soaring demand. "That is absolutely becoming a problem," says Ellen 't Hoen of the Access to Medicine Campaign at Médecins Sans Frontières (MSF), one of Nutriset's main clients.

Most past inventions in humanitarian nutrition, such as a widely used fortified milk powder called F100, weren't patented; nor was oral rehydration therapy, a lifesaver for diarrhea patients. But Nutriset and the French Institute of Research for Development obtained patents for Plumpy'nut that last until 2018 and are valid in Europe, North America, and about 30 African countries. Nutriset has threatened lawsuits to keep others—including Compact in Norway and MSI in Germany—from selling similar pastes.

Nutriset's Adeline Lescanne says the company is rapidly boosting its own production capacity and at the same time taking the technology to the developing world, where it helps to stimulate the local economy. It has set up four franchises—in Niger, Malawi, Ethiopia, and the Dominican Republic—that have received equipment and training and now produce Plumpy'nut on a small scale. It has also signed a licensing deal that lets Valid International, an Irish charity, produce its own product under a different name.

MSF and UNICEF, another big buyer, acknowledge that so far there have been no shortages nor evidence of price gouging. Nor is the patent valid in many malnutrition hot spots, including India, where Compact is building a factory and several other companies are interested as well. Still, MSF and UNICEF don't like to be dependent on one major producer for delivering what is becoming an essential product to a large chunk of Africa. MSF says Nutriset and other companies entering the RUTF market should forgo patents—or at least be generous in cutting licensing deals.

It's unclear, meanwhile, whether the patent would withstand a challenge by a competitor. It covers not just Plumpy'nut but also, 't Hoen says, "pretty much any nut paste with milk powder, oil, and micronutrients." Other companies could market a similar product and see what happens in court if sued, she says—but neither Compact nor MSI have been willing to take that risk. Michael Golden, who formulated F100, believes the pressure should not be on Nutriset but on the French government; he hopes that France's foreign minister, Bernard Kouchner, a physician who helped found MSF in 1971, will intervene. **–M.E.**

researchers compared entire villages to which Plumpy'nut was given with others to which it was not—but of course, no two villages are exactly the same. MSF's decision to move to blanket distribution of Plumpy'doz interrupted the trial, which was supposed to last for 18 months, and forced the researchers to choose a different design that compared the two products. Other aid organizations distributed food in the area as well, introducing more possible confounders.

The data, which are now under review at *The Journal of the American Medical Association*, show that Plumpy'nut does lead to a substantial decrease in the incidence of severe malnutrition, says Philippe Guérin, Epicentre's medical director. But Plumpy'doz—although designed with prevention in mind—appears to be much less effective. That may be because children get fewer calories, but there may be other factors, says Guérin. A survey suggested that rather than giving a little bit every day, some mothers let their children eat it all early on. Plumpy'doz may also be more likely to be shared between the children in a household than the single-dose Plumpy'nut packages.

Epicentre's conclusion was not welcome news to MSF. MSF's Shepherd says it's important that the researchers analyze their data independently—but says she does not agree with Epicentre's analysis. Tectonidis, who believes Plumpy'doz works in prevention and has no faith in the Epicentre study, went further: In September 2007, while working at the MSF office in Rome, he visited the project in Niger and obtained a copy of the study's database. He then asked Golden, who was not previously involved in the study, to analyze it. Golden's unpublished manuscript says the Plumpy'doz intervention had a "dramatic effect." Guérin says he has not seen Golden's paper and declined to comment on it.

Is it practical?

Nutrition science aside, there are other questions. Even if Plumpy'nut or similar products work well for prevention, with their hefty price tag, are they the most cost-effective way? How long does the intervention go on, who pays for it, and doesn't it make a population dependent on foreign aid? "When you're going to tell the world what to do about hundreds of millions of children, it also has to work in practice," Manary says.

One solution may be to make peanut butters cheaper—for instance, by replacing all or part of the powdered milk, the most expensive ingredient, with soy. Perhaps that approach should be combined with very good infection control, says Manary. Many other ideas were on the agenda at a closed expert meeting at WHO headquarters this week, which participants said promised to be lively.

But for the moment, the debate is moot in the Guidan Roumdji district. In a spat unrelated to the scientific debate, the government of Niger accused MSF France of violating several rules and suspended all of its activities on 29 July. Negotiations are ongoing, but for now, both the treatment programs for severely malnourished children and the Plumpy'doz distribution to more than 80,000 children have come to an abrupt halt.

–MARTIN ENSERINK

CREDIT: M. ENSERINK/*SCIENCE*

Published by AAAS

PLANETARY SCIENCE

Culture Wars Over How to Find an Ancient Niche for Life on Mars

Researchers seeking the next Mars rover landing site disagree about what makes for the most promising possibility: lots of water-altered minerals or familiar water-shaped terrain

MONROVIA, CALIFORNIA—"This is not a contest," the workshop's organizers kept insisting, but it sure sounded like one. At the end of 3 days of sales pitches, cross examinations, and warm debate, more than 100 planetary scientists gathered* in a hotel ballroom here cast their ballots for the most scientifically inviting spot to send the $1.9 billion Mars Science Laboratory (MSL) in early 2010.

"Everyone wants to maximize the science," says planetary geologist James Rice of Arizona State University in Tempe. In deciding how to do that, most attendees aligned themselves with one of two parties. Spectroscopists, who find martian minerals from orbit by their distinctive spectral colors, tended to favor sites that beam strong spectral signatures of rock altered by water. Geologists, by contrast, preferred sites whose geological forms speak most eloquently of past water pooling on the surface.

Water is key because, as the official mission fact sheet puts it, NASA intends MSL to assess "whether the landing area ever had or still has environmental conditions favorable to microbial life." With that theme in mind, a lineup of paleontologists, geochemists, and geologists opened the workshop by explaining the most promising circumstances on ancient Earth for preserving evidence of habitability and traces of past life, such as river deltas that trap and preserve fossils and organic matter.

Then the wrangling began. Leading spectroscopists had proposed two of the seven landing sites still in the running (*Science*, 9 November 2007, p. 908) because the sites simply screamed "water!" to them. Jean-Pierre Bibring of the University of Paris, Orsay, is principal investigator of the OMEGA spectrometer onboard the Mars Express orbiter. To follow the water, he has argued, you should follow the clays. That's because clays form only after rock comes into prolonged contact with lots of water under mild conditions favorable for life. Microbes could draw energy and nutrients from the weathering rock, while the resulting clay would be ideal for preserving organic matter.

Bibring advocated landing on the highlands above Mawrth Vallis, a site blazing with the spectral colors of water-related minerals. Clays make up more than 50% of the surface there, Bibring reported—more abundant than anywhere else on Mars. The diversity of minerals—a half-dozen different clays plus a couple of other hydrated minerals—speaks of a changing environment as a layer cake of rock was altered. For similar reasons, John Mustard of Brown University and colleagues argued for landing in Nili Fossae, a great crack in the martian crust from which MSL could drive into a side canyon where many of the half-dozen aqueous minerals of the region outcrop.

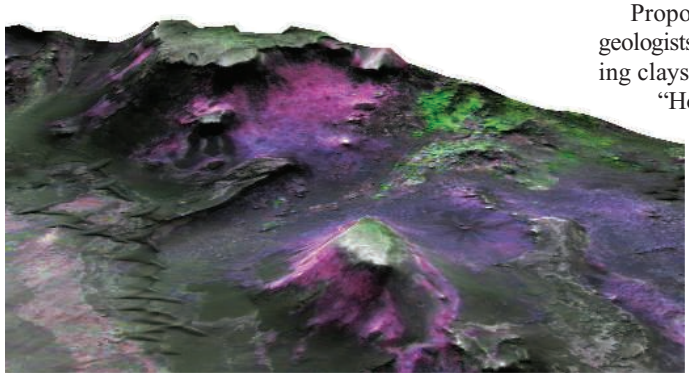

Go for color. Near the proposed Nili Fossae landing site, erosion of 600-meter-high mesas reveals the spectral blue and magenta of much-sought clays.

CREDIT: NASA/JPL/JHU APL/UNIVERSITY OF ARIZONA/BROWN UNIVERSITY (B. EHLMANN, J. MUSTARD)

Geologists weren't sold on either Mawrth or Nili. The spectroscopists "argue that there's such [spectral] diversity, there must be something of interest there," says Horton Newsom of the University of New Mexico in Albuquerque, "but there's no geological evidence. It's essential to have both—a geological story with the spectra to back it up."

In the case of Mawrth, was the source of the clays sediment that washed into a lake? Was it volcanic ash that fell from the sky? Was it crustal rock altered by hot springs? "How is a story going to come out of this?" demanded geologist Linda Kah of the University of Tennessee, Knoxville. Figuring it out once the rover got there, as Bibring suggested, was too risky an option for geologists still smarting from having landed the Spirit rover on an apparent lakebed that turned out to be a barren lava plain.

To avoid disappointment next time, many geologists favored landing in 67-kilometer-wide Eberswalde Crater. "It's the natural place to go," says Rice, who led the pitch for the crater site. "It's the best delta on Mars," meaning a river must have flowed into a lake in Eberswalde, dropping its load of sediment on entering the still water. Several different clays appear in the beautifully layered delta deposits exposed by wind erosion. Eberswalde "would make it a lot of fun," said Kah. Other favorites of geologists were Holden Crater, another likely crater lake with layered, clay-bearing deposits but no true delta, and Gale Crater, whose 5-kilometer-high mound of layered deposits boasts a variety of water-related minerals, although the origin of the mound is uncertain.

Proponents of Nili and Mawrth took the geologists' point about the advantages of studying clays laid down in quiet standing water.

"Holden is a very interesting site," says Mustard, but there are shortcomings. Gale Mound lacks a single strong geological story, he notes, and Eberswalde could prove to be a "one-trick pony" if organic matter doesn't turn up there.

After 2.5 days of consideration, more than 100 attendees voted on how mineralogically and geologically diverse each site is, how good a geologic story each is telling, how good the prospects for habitability are, and how good the chances for preservation are. Two sites that had neither a strong geological story nor good spectral diversity—Miyamoto Crater and southern Meridiani—came in dead last. Nili and Mawrth did considerably better but still trailed the three craters with layered deposits, Eberswalde leading them all.

The outcome didn't surprise Mustard. Nili, at least, "kind of scares people," he says. "It's hard to fit into a geological scenario." But it's not over for Nili or Mawrth. Mission managers together with a landing-site steering committee will decide within a month or so which three sites will receive further study. Engineering considerations—such as too much cold at far-southern Holden and Eberswalde—might clear the way for a brightly colored site. Then another open workshop next spring will recommend a single site.

–RICHARD A. KERR

*Third MSL Landing Site Workshop, 15–17 September, sponsored by the NASA-appointed Mars Landing Site Steering Committee and the MSL Project.

Published by AAAS

PROFILE: EDWARD BUCKLER

Romping Through Maize Diversity

A computer whiz turned geneticist borrows tactics from Wal-Mart and cattle breeders to manage what may be the world's largest genetic analysis

ITHACA, NEW YORK—On a steamy July morning, Edward Buckler and a crew of technicians, graduate students, postdocs, and a visiting professor from Mexico have fanned out among the 2-meter stalks in a large field of corn here. Bar-code readers in hand, they snip, stretch, or poke individual plants in order to track dozens of traits important to the crop's growth and vitality. Each week, they record the height of every stalk; in early summer, they counted leaves, assessed surface "hairiness," and took small samples of tissue to freeze-dry and send to Germany.

Welcome to the Nested Association Mapping (NAM) project, arguably the world's largest controlled genetic study. It encompasses more than 1000 genetic markers in each of 5000 lines of maize in an effort to elucidate the relationship between genes and physical traits in plants. "It's basically the maize analog of the human HapMap Project, but it is much more powerful and cost-effective," says population geneticist Magnus Nordborg of the University of Southern California in Los Angeles.

Buckler, the 38-year-old plant geneticist running the show, doesn't believe in thinking small. If he gets his way, plane flights will one day monitor tens of thousands of plants daily. "I'd like to know what goes on every hour of every day," says Buckler, a U.S. Department of Agriculture (USDA) researcher based at Cornell University here.

Buckler has capitalized on his combination of computer and biology expertise to develop methods to find genes faster. He and his colleagues have also used existing maize variants to boost the vitamin A content of corn. "Ed seems equally at home in the field pollinating maize as in the lab or developing software or doing theory," says plant geneticist J. Antoni Rafalski of E. I. du Pont de Nemours & Co. (Inc.) in Wilmington, Delaware. Adds James Holland of USDA at North Carolina State University (NCSU) in Raleigh, "He has single-handedly influenced the plant genetics community to a remarkable extent."

The goal of the massive NAM study is two-pronged. Maize is the number-one crop produced around the world, and NAM will help breeders to exploit its natural variation to improve yields and nutritional value. In addition, Buckler expects to answer a fundamental question: Do a few genes underlie each complex trait, or is there a bewildering array, with each having a minor influence? The answer will not only help plant breeders, but it may also aid biomedical researchers trying to understand the genetics of diabetes, heart disease, and other disorders. "I expect we will learn a lot about quantitative genetics from the maize work, and this will, of course, help us to understand human variation as well," says Nordborg.

So far, its looks like more than a few genes control most traits. That realization will complicate attempts to pin down the genetic basis of disease. But with maize, even a 1% improvement in yield translates into millions more tons of food for people and animals, so genes of small effect can make a significant difference. Thanks in large part to Buckler's efforts, "people have changed their thinking, and companies are much more focused on natural diversity" as opposed to adding new genes to improve crops, says USDA plant geneticist Michael McMullen of the University of Missouri, Columbia.

Ed Buckler

CREDIT: E. PENNISI/*SCIENCE*

Genetics by second nature

Growing up in Arlington, Virginia, Buckler had unlimited access to a personal computer, on which he designed his own games. To him, genetics is basically life's equivalent of computer programming. "There are not many rules: You get to recombine and to mutate, but you can make incredibly complex things." Buckler laughs, giving his boyish smile: "And it's more rewarding to do genetics than programming."

After high school, he left for the University of Virginia, Charlottesville. He studied early American cultures and became both fascinated with the domestication of maize and appalled at how inefficient agriculture was. "I decided that if I wanted to do something worthwhile, plant genetics was the way to go," he says. With a Ph.D. from the University of Missouri, Columbia, and postdoc experience in statistical genetics at NCSU, Buckler joined USDA in 1998 to work on the Maize Diversity Project, part of the Plant Genome Initiative (*Science*, 23 October 1998, p. 652). Now poised for its second renewal, the project has morphed over time from an emphasis on genome evolution to a massive effort to conquer the genetics of complex traits, with NAM as a key component.

As the Maize Diversity Project matured, Buckler and his colleagues came up with a more efficient way to find genes that influence traits. Researchers typically take two approaches to this task. In one, linkage analysis, they use families—which in corn means plants that can be traced back to the same set of parents. The other approach, association studies, relies on unrelated individuals, be they corn seedlings or people. "What we've been doing is blending the lines between the two" approaches, Buckler explains.

Published by AAAS

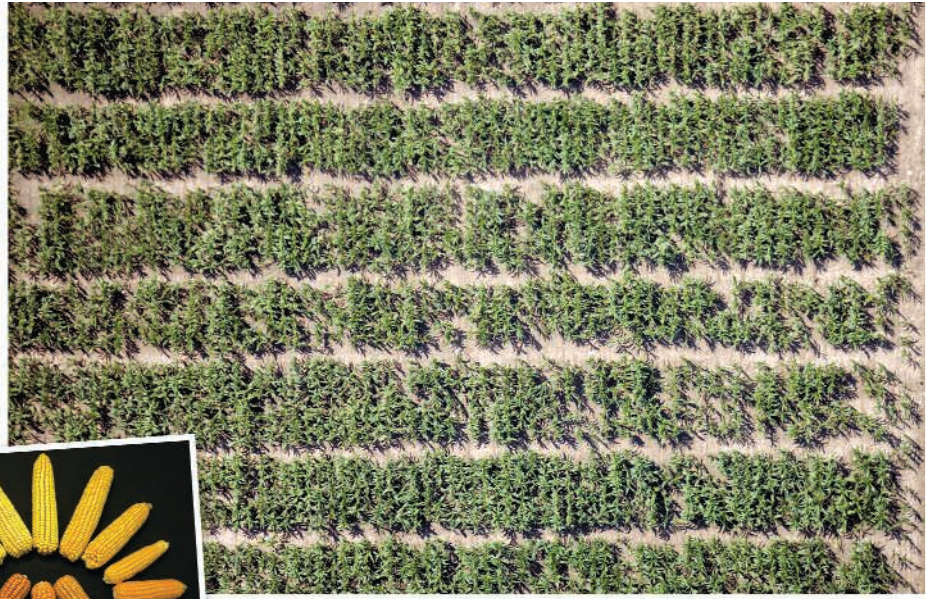

Maize maze. This experimental cornfield in upstate New York will help researchers pin down the genetic basis of traits such as kernel color (*inset*).

CREDIT: JON REIS; INSET: TORBERT ROCHEFORD AND CATHERINE BERMUDEZ KANDIANIS

In association studies, researchers often look for gene variants that co-occur with a trait, such as golden rather than yellow kernels. But many of the variants they find are false positives, for example, having no effect on kernel color at all. The number of such false positives can be influenced by kinship among individuals and by evolutionary history. For example, when two populations are isolated from each other, their genomes can diverge in such a way that a particular variant might seem to be associated with kernel color, even though it isn't. "That's really a complicated and difficult problem," says John Doebley, a plant geneticist at the University of Wisconsin, Madison. Likewise, when two individual plants are closely related, their kinship can skew any associations detected.

With Jianming Yu, now at Kansas State University in Manhattan, Buckler has found ways to incorporate both history and kinship into his analyses, eliminating many false associations. For example, to take account of how closely individual plants are related, Yu, Buckler, and their colleagues used genetic markers to assess kinship, then borrowed mathematical tricks used by cattle breeders to analyze giant pedigree matrices. The resulting "unified mixed model" method greatly reduced the number of false positives, they reported in the February 2006 issue of *Nature Genetics*. Buckler estimates, for example, that about 9 million DNA variants, or SNPS, would show up as linked to flowering time using the old approach. The new method narrows that to only a few thousand.

The method has also yielded natural gene variants that enrich maize in vitamin A. Buckler, Torbert Rocheford of the University of Illinois, Urbana-Champaign, and their colleagues measured the amount of the vitamin in hundreds of lines of corn that vary in kernel color—the more orange, the more vitamin A. Using association studies, they pinned down the gene variants responsible for producing more vitamin A precursors (*Science*, 18 January, p. 330). Without this method, "we would have had a lot more junk to deal with," says Buckler. Now researchers with HarvestPlus for Africa and elsewhere are using Buckler's genetic markers to breed those variants into maize varieties, thus boosting vitamin A without introducing foreign genes.

Bigger is better

Once Buckler started doing association studies, he hungered to make them more powerful. For NAM, he and his colleagues picked 25 unrelated "parent" lines of maize, including popcorn, sweet corn, tropical and temperate varieties, plus long-used commercial strains, representing the full range of diversity in this species. Buckler, Cornell colleague Stephen Kresovich, Holland, and, later, McMullen bred each line with the much-studied (and now draft-sequenced) B73 maize. From each "parent," they created a "family" of 200 new lines, for a total of 5000 lines. Thus this single study includes "families" available for linkage analysis, as well as a large, diverse population of 5000 lines for association studies. The next biggest genetic study involves mice, uses just eight strains, and has the ultimate goal of creating 1000 new strains (*Science*, 25 July 2003, p. 456).

NAM also presented an enormous data-crunching challenge. At the time, "it was not obvious to me how gene-phenotype association information could be jointly analyzed across the 25 cross-populations," Holland recalls. "Ed conceived of the analysis that would efficiently achieve that." Nor was Buckler daunted by the challenge of generating thousands of new maize lines and recording how individual plants grew. His response to his colleagues' concerns: Borrow methods from an operation that daily tracks tens of thousands of items—Wal-Mart. He outfitted his team with the same portable bar-code scanners that Wal-Mart uses for taking inventory and had them tag each plant.

Now that the hard work is done, anyone can grow out the seeds of the NAM lines or traipse through the project's fields to measure variation in their favorite trait, such as starch content. Then, using the project's analytical tools, they can home in on the genes affecting that trait.

Buckler calls the NAM project a "field of dreams," and, as in the movie of the same name, it's attracting attention and copycats. Dozens of private and academic researchers have ordered NAM seeds from USDA to start their own fields. Cornell's Rebecca Nelson and graduate student Jesse Poland are assessing the genetic basis of disease resistance in a NAM field next to Buckler's. Says Poland: "It's an incredible resource."

Yet even in the dream fields, pinning down genes will not be easy. "Association mapping is not without its problems," says Rafalski. Human geneticists have millions of markers to help navigate the human genome, and they still struggle to find gene variants connected to disease; maize researchers have only about 1100 markers. And picking out which associated variants are the most promising is always a challenge, he adds.

However, Buckler is still thinking big. He has $1 million from the U.S. National Science Foundation to partially sequence each parent NAM maize strain, which will yield many more markers. He has also set his sights beyond cornfields: He wants to apply genomics to USDA's vast archive of germ plasm—seeds and other tissues from all plants. Breeders can order any of some 600,000 crop varieties from USDA, but it's often hard to know which varieties will improve a crop the most. To begin to find out, Buckler is starting with the grape germ plasm on file, assessing 10,000 SNPs and, to a limited extent, their association to relevant traits. He's hopeful money will come through next year to assess the SNPs in the entire USDA collection. "That Ed is an idea person is as much of an understatement as you can say," says McMullen. "He's always proposing new ideas, and even before we can do the experiment, [the project] will be bigger."

–ELIZABETH PENNISI

Published by AAAS

LETTERS

edited by Jennifer Sills

Keeping an Eye on the Prize

I WAS VERY DISAPPOINTED TO FIND OUT ("Fame inflation," Newsmakers, 1 February, p. 553) that I, like Steven Running, am not a Nobel laureate. According to the "Dear colleagues" letter I received from Ogunlade Davidson and Bert Metz on behalf of the IPCC, I am indeed a Nobel laureate, albeit perhaps along with many, many others. The letter says, "You no doubt have heard about the award of the Nobel Peace Prize to the IPCC, jointly with Al Gore of the USA. This makes all of you a Nobel laureate and we, as co-chairs, want to congratulate you wholeheartedly with this exceptional recognition." Additionally, a beautiful Nobel Peace Prize certificate with my name on it now adorns my wall. Although the financial remuneration has not yet arrived, I have enjoyed the celebrity status associated with the honor. **ROGER A. SEDJO**

Resources for the Future, Washington, DC 20036–1400, USA. E-mail: sedjo@rff.org

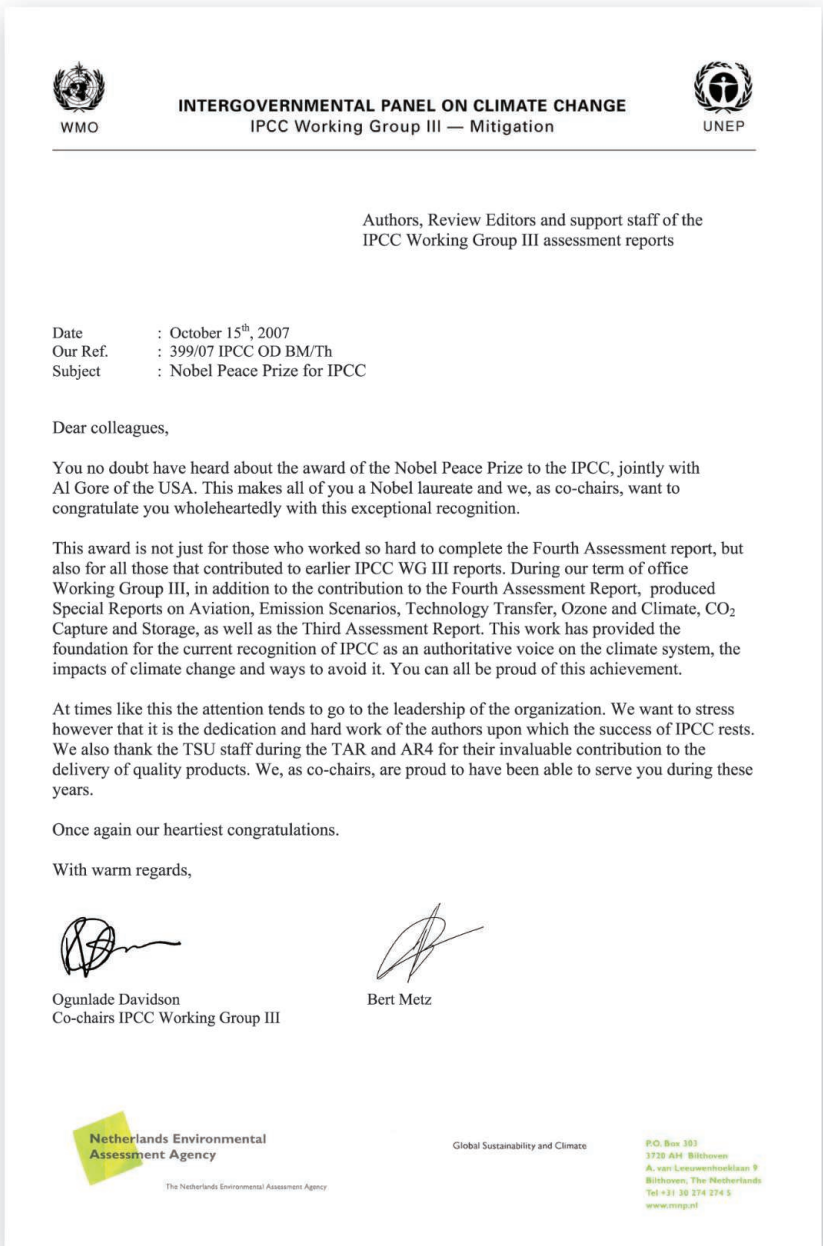

WMO

INTERGOVERNMENTAL PANEL ON CLIMATE CHANGE
IPCC Working Group III — Mitigation

UNEP

Authors, Review Editors and support staff of the
IPCC Working Group III assessment reports

Date : October 15th, 2007
Our Ref. : 399/07 IPCC OD BM/Th
Subject : Nobel Peace Prize for IPCC

Dear colleagues,

You no doubt have heard about the award of the Nobel Peace Prize to the IPCC, jointly with Al Gore of the USA. This makes all of you a Nobel laureate and we, as co-chairs, want to congratulate you wholeheartedly with this exceptional recognition.

This award is not just for those who worked so hard to complete the Fourth Assessment report, but also for all those that contributed to earlier IPCC WG III reports. During our term of office Working Group III, in addition to the contribution to the Fourth Assessment Report, produced Special Reports on Aviation, Emission Scenarios, Technology Transfer, Ozone and Climate, CO_2 Capture and Storage, as well as the Third Assessment Report. This work has provided the foundation for the current recognition of IPCC as an authoritative voice on the climate system, the impacts of climate change and ways to avoid it. You can all be proud of this achievement.

At times like this the attention tends to go to the leadership of the organization. We want to stress however that it is the dedication and hard work of the authors upon which the success of IPCC rests. We also thank the TSU staff during the TAR and AR4 for their invaluable contribution to the delivery of quality products. We, as co-chairs, are proud to have been able to serve you during these years.

Once again our heartiest congratulations.

With warm regards,

Ogunlade Davidson
Co-chairs IPCC Working Group III

Bert Metz

Netherlands Environmental Assessment Agency
The Netherlands Environmental Assessment Agency

Global Sustainability and Climate

P.O. Box 303
3720 AH Bilthoven
A. van Leeuwenhoeklaan 9
Bilthoven, The Netherlands
Tel +31 30 274 274 5
www.mnp.nl

Epigenomics: A Roadmap, But to Where?

RECENTLY, THE DIRECTOR OF THE NATIONAL Institutes of Health (NIH) allocated $190 million for an "Epigenomics" Roadmap initiative (*1*). As investigators in this area, we endorse the idea that chromatin biology is an appropriate, if not essential, area for the NIH to support, not only for its fundamental biological significance but also its relevance to human disease. Nonetheless, we believe that this initiative, at least in its current form, will not yield significant benefits. If the use of the term "epigenome" is intended to equate the value of this Roadmap initiative with the Human Genome Project, it fails on several grounds.

First, it does not consider our current understanding of the roles of sequence-specific DNA recognition events and transcriptional networks in controlling epigenetic changes. A multifaceted effort that elucidates transcriptional circuits that tell us where and when signal-responsive, sequence-specific regulators function would be more useful for understanding cell type programming. Second, merely cataloging modification patterns offers comparatively little new or useful information. We already know that most genes are associated with one of a few patterns of chromatin modifications and that the patterns themselves do not tell us how that gene is regulated or how its expression state is inher-

Published by AAAS

ited. Most histone modifications are highly dynamic and change rapidly in response to changes in signals that turn genes on or off.

This initiative will divert substantial resources, enough to fund 200 multiyear individual grants. There is a notion favored by some that individual scientists need to be corralled to work together under a more rigid, directed framework to solve important problems. We disagree. Real innovation comes from the bottom up, and good science policy requires promoting the free market of ideas rather than central planning (*2*).

HITEN D. MADHANI,[1]* NICOLE J. FRANCIS,[2] ROBERT E. KINGSTON,[3] ROGER D. KORNBERG,[4] DANESH MOAZED,[5] GEETA J. NARLIKAR,[1] BARBARA PANNING,[1] KEVIN STRUHL[6]

[1]Department of Biochemistry and Biophysics, University of California, San Francisco, CA 94158, USA. [2]Department of Molecular, Cellular, and Developmental Biology, Harvard University, Cambridge, MA 02138, USA. [3]Department of Molecular Biology, Massachusetts General Hospital, Boston, MA 02114, USA. [4]Department of Structural Biology, Stanford University School of Medicine, Stanford, CA 94305, USA. [5]Department of Cell Biology, Harvard Medical School, Boston, MA 02115, USA. [6]Department of Biological Chemistry and Molecular Pharmacology, Harvard Medical School, Boston, MA 02115, USA.

*To whom correspondence should be addressed. E-mail: hiten@biochem.ucsf.edu

References and Notes

1. NIH Roadmap for Medical Research (http://nihroadmap.nih.gov/epigenomics/).
2. Links to a full version of this letter and petition for readers to sign can be found at http://madhanilab.ucsf.edu/epigenomics/.

Protecting Aggregate Genomic Data

A PAPER PUBLISHED RECENTLY IN *PLOS Genetics* (*1*) describes a statistical method for resolving individual genotypes within a mix of DNA samples or data sets containing aggregate single-nucleotide polymorphism data. This scientific advance may have important implications for forensics and for genome-wide association studies (GWAS). It has also changed our understanding of the risks of making aggregate genomic data publicly available. While we assess the broader scientific, ethical, and policy implications of this development, NIH has moved swiftly to remove aggregate genomic data from our publicly available Web sites. Further information about changes in NIH open-access policies for GWAS is available on the NIH's GWAS Web site (*2*).

The paper by Homer *et al*. showed that a new statistical technique applied to aggregate data can determine whether a specific individual's genomic data are part of a given data set, including whether they are in the control group or the case (affected) group. It may also be possible to statistically infer whether a relative of the individual is a member of the case or control groups. The method requires having an individual's high-density genotype data in hand from another source. Though the specific identity of the individual who was the source of the data could only be determined if that source were known through other means or reference data, this discovery nonetheless has implications for how these summary data should be protected. As a result, NIH has removed from open-access databases the aggregate results (including *P* values and genotype counts) for all the GWAS that had been available on NIH sites (such as dbGaP and CGEMS). NIH intends to move the aggregate genotype data to the controlled-access database, where there is a firewall as well as protections and policies in place for appropriate data access, including review and approval of data access requests. The new finding does not have the same implications for data available through controlled access, and NIH access policies for individual-level genotype and phenotype data have not changed.

Sharing genomic data and, particularly, allele frequencies has become common practice, if not an imperative, in science. Yet, the protection of participant privacy and the confidentiality of their data are of paramount importance. These new statistical approaches have implications far beyond NIH data-sharing policies, as aggregate GWAS data have been provided in publicly available form in many other ways, including other research databases and Web sites, journal articles and other publications, and scientific presentations. NIH urges the scientific community to consider carefully how these data are shared and take appropriate precautions to secure aggregate GWAS data in order to protect participant privacy and data confidentiality.

In short order and over the coming months, NIH will work with our advisory groups and the wide range of stakeholders related to GWAS to further explore and address the policy implications of this finding. We call on our colleagues in the scientific community to join us in these important deliberations.

ELIAS A. ZERHOUNI[1] AND ELIZABETH G. NABEL[2]

[1]Director, National Institutes of Health, Bethesda, MD 20892, USA. [2]Co-Chair, Senior Oversight Committee, NIH Policy for Sharing GWAS Data, and Director, National Heart, Lung, and Blood Institute, Bethesda, MD 20892, USA.

References

1. N. Homer *et al*., *PLoS Genet.* **4**, e1000167 (2008).
2. NIH Genome-wide Association Studies Web site: http://grants.nih.gov/grants/gwas/.

Closing a Loophole in the FDA Amendments Act

IN THEIR POLICY FORUM "MOVING TOWARD transparency of clinical trials" (7 March, p. 1340), D. A. Zarin and T. Tse caution that "FDAAA 801 still leaves areas of 'opacity.'" We would like to point out another loophole: FDAAA 801 will only cover future drugs. The thousands of drugs on the market today, including the controversial examples cited by Zarin and Tse, will be grandfathered in and not covered.

Whether this matters to public health depends on whether today's uncovered drugs will soon become obsolete. To address this

Letters to the Editor

Letters (~300 words) discuss material published in *Science* in the previous 3 months or issues of general interest. They can be submitted through the Web (www.submit2science.org) or by regular mail (1200 New York Ave., NW, Washington, DC 20005, USA). Letters are not acknowledged upon receipt, nor are authors generally consulted before publication. Whether published in full or in part, letters are subject to editing for clarity and space.

CORRECTIONS AND CLARIFICATIONS

Reports: "Cell identity mediates the response of *Arabidopsis* roots to abiotic stress" by J. R. Dinneny *et al*. (16 May, p. 942). On page 945, the URL for the supporting online material was incorrect. The correct URL is www.sciencemag.org/cgi/content/full/1153795/DC1.

Books *et al*.: "The social origin of mind" by A. Jolly (7 September 2007, page 1326). The caption to the photograph should have read "Chacma baboons (*Papio hamadryas ursinus*) in the Okavango Delta, Botswana."

Reports: "The FERONIA receptor-like kinase mediates male-female interactions during pollen tube reception" by J.-M. Escobar-Restrepo *et al.* (3 August 2007, p. 656). On page 657, second column, second paragraph, the sentence "The *FER* open reading frame contains a single 175-bp intron in the 5′ untranslated region and produces a transcript of 2682 bp, which encodes a putative receptor-like serine-threonine kinase (RLK) (Fig. 1F)" contains two errors. It should read, "The FER primary transcript contains a single 175-bp intron in the 5′ untranslated region and produces an open reading frame of 2682 bp, which encodes a putative receptor-like serine-threonine kinase (RLK) (Fig. 1F)."

Reports: "Virus-enabled synthesis and assembly of nanowires for lithium ion battery electrodes" by K. T. Nam *et al*. (12 May 2006, p. 885). Reference 28 should be D. Guy, B. Lestriez, D. Guyomard, *Adv. Mater*. **16**, 553 (2004).

Published by AAAS

question, we examined prescribing trends over the past 8 years for three drug classes cited by Zarin and Tse. From listings of the top 200 drugs (*1*) for the years 2000 through 2007, we extracted the numbers of prescriptions dispensed in U.S. retail pharmacies. Within these three drug classes, we totaled the annual number of prescriptions of brand and generic drugs that had been first marketed in the United States within the past 20 years.

We found that oral drugs for diabetes, including Avandia (*2*, *3*), are (as of 2007) being prescribed 265,000 times each day; their prescribing rate has been increasing 8% annually. Cholesterol-lowering drugs, including Zetia (*4*) and Baycol (*5*), are now being prescribed 528,000 times each day; this rate has been increasing 10% annually. Finally, antidepressants (*6*) are being prescribed 673,000 times each day; this rate has been increasing 22% annually.

These data indicate, in our opinion, that these drugs—none of which will be covered by FDAAA 801—are widely prescribed and unlikely to disappear soon from the U.S. market. It is unfortunate that FDAAA 801 grandfathers in currently marketed drugs. While this act provides for a registry and results database that is prospective, we need one that is also retrospective. Such a database has in fact existed for decades at the FDA (*7*). If we can make better use of it, a solution to this area of "opacity" lies readily within our grasp.

ERICK H. TURNER,[1,2]* NORWAN J. MOALEJI,[3] BETH L. ARNOLD[4]

[1]Portland Veterans Affairs Medical Center, Portland, OR 97239, USA. [2]Oregon Health and Science University, Department of Psychiatry, Portland, OR 97239, USA. [3]Loma Linda Veterans Affairs Medical Center, Loma Linda, CA 92357, USA. [4]Fircrest School RHC, Shoreline, WA 98155, USA.

*To whom correspondence should be addressed. E-mail: turnere@ohsu.edu

References

1. *Drug Topics*, "Top 200 Drugs" (http://drugtopics.modernmedicine.com/Top+200+Drugs).
2. S. E. Nissen, K. Wolski, *N. Engl. J. Med.* **356**, 2457 (2007).
3. B. M. Psaty, C. D. Furberg, *N. Engl. J. Med.* **357**, 67 (2007).
4. K. Suckling, *Expert Opin. Pharmacother.* **9**, 1067 (2008).
5. B. M. Psaty, C. D. Furberg, W. A. Ray, N. S. Weiss, *JAMA* **292**, 2622 (2004).
6. E. H. Turner, A. M. Matthews, E. Linardatos, R. A. Tell, R. Rosenthal, *N. Engl. J. Med.* **358**, 252 (2008).
7. E. H. Turner, *PLoS Med.* **1**, e60 (2004); http://dx.doi.org/10.1371/journal.pmed.0010060.

Response

TURNER AND COLLEAGUES ARE CORRECT THAT the "basic results" provisions of Section 801 of the FDA Amendments Act (FDAAA 801) will not apply to trials that were completed prior to 27 September 2007. Thus, the body of data that was used to support approval for products currently on the market will not necessarily be made public under this provision. As all of the top 20 brand drugs by total U.S. prescriptions in 2007 (*1*) were approved prior to 2005, based on Initial Year of Original FDA Approval data listed in Drugs@FDA (*2*), it is readily apparent that much of the data underlying current medical decisions are unlikely to be submitted to ClinicalTrials.gov. The scope of the law is determined by the timing of the trial, however, not the date of approval of the drug; therefore, non–phase I trials of these approved products initiated after or ongoing as of late 2007 would meet the time criterion for applicability under FDAAA 801 and be required to report results.

Turner calls for public access to FDA reviews contained in all approved NDAs (*3*). In addition to this possibility, FDAAA 801

includes a provision whereby the Secretary of Health and Human Services may require registration and results reporting for certain clinical trials of FDA-approved drugs, biologics, and devices retrospectively to protect public health (trials completed up to 10 years prior to enactment of the act, i.e., September 27, 1997). Finally, FDAAA 801 explicitly provides for consideration, during the 3-year rule-making process, of mandatory results reporting from certain clinical trials of drugs, biologics, and devices not approved by the FDA. Such a policy would substantially broaden the evidence base available to the public.

DEBORAH A. ZARIN AND TONY TSE*

National Library of Medicine, National Institutes of Health, Department of Health and Human Services, Bethesda, MD 20894, USA.

*To whom correspondence should be addressed. E-mail: atse@mail.nih.gov

References

1. Verispan VONA. *Top 200 Brand Drugs by Units in 2007* (2008); http://drugtopics.modernmedicine.com/drugtopics/data/articlestandard//drugtopics/072008/491207/article.pdf.
2. Food and Drug Administration. Drugs@FDA (www.accessdata.fda.gov/Scripts/cder/DrugsatFDA/).
3. E. H. Turner, *PLoS Med*. **1**, e60 (2004); http://dx.doi.org/10.1371/journal.pmed.0010060.

Big Payoffs Possible for Small-Molecule Screening

IN THE NEWS FOCUS "INDUSTRIAL-STYLE screening meets academic biology" (8 August, p. 764), J. Kaiser presents the discovery of several potential small-molecule therapeutics and probes for cellular function along with skeptical views from industrial scientists questioning "whether this massive effort is worth the time and money." The goals of the pharmaceutical industry and academia are very different. Industry scientists are focused on discovering a highly specific and potent compound that can benefit human health. Academic scientists focus on finding compounds that can reveal novel cellular mechanisms, a basic tenet in chemical biology (*1*). It is this pursuit that allows the academician to foster student learning and interdisciplinary collaborations with faculty that could lead to a novel biological probe or a potential therapeutic. The current $100 million-per-year funding from the NIH Molecular Libraries Initiative (MLI) is a wise investment in the training of future scientists and teachers. Students working with faculty mentors on these screening efforts learn how to solve problems across all areas of science and mathematics; indeed, the "challenge of merging two cultures—biologists and chemists" is an opportunity for a better education (*2*). Such an interdisciplinary approach to science education is timely, given the recently passed Public Law 110-69, "America Competes Act," which includes appropriation of $896 million for "education and human resources" (*3*) that will promote the training of future science and mathematics teachers. Regardless of the skepticism, I believe that the NIH MLI could "pay it forward" to our society in many ways.

JEFFREY H. TONEY

College of Natural, Applied and Health Sciences, Kean University, Union, NJ 07083, USA. E-mail: jetoney@kean.edu

References

1. S. L. Schreiber, *Nat. Chem. Biol*. **1**, 64 (2005).
2. R. L. Stein, *J. Biomol. Screen*. **8**, 615 (2003).
3. Public Law 110-69 (H.R. 2272), sec. 7002, fiscal year 2008.

EVOLUTION

A Challenge Standing on Shaky Clay

Michael Ruse

There were a number of ironies about the 2005 trial in Dover, Pennsylvania, in which a judge ruled that the local school board should not insist on the introduction of so-called intelligent design theory (IDT) into the curricula of state-supported biology classes. Most obvious was the fact that the judge who made the ruling was appointed by none other than President George W. Bush. Others included that both sides used philosophers as expert witnesses and that two scholars involved—against IDT, Robert Pennock of Michigan State University, and for IDT, Steve Fuller of the University of Warwick in England—were graduates of the same program at the University of Pittsburgh and their time there had even overlapped. Fuller has already written an account of the trial (*1*), and now in *Dissent over Descent* he gives his background thinking about the issues.

Dissent over Descent
Intelligent Design's Challenge to Darwinism
by Steve Fuller
Icon Books, Cambridge, 2008. 278 pp. £12.99, C$26. ISBN 9781840468045.

One certainly cannot critique Fuller for being less than forthright in his feelings and judgments. Early on we learn of the "deep and largely pernicious influence" of Thomas Kuhn's thinking on the general public and on some scientists. Then we are told how out of touch with the general scientific community are the London Royal Society and the American National Academy of Sciences, with the implication that their opposition to IDT should count for little. Charles Darwin, it appears, were he living today, would be in favor of IDT. The well-known geneticist (and former president of AAAS) Francisco Ayala is a Catholic, theistic evolutionist. Fuller holds that Richard Dawkins "arguably owes more to 18th-century secular theodicy than to Darwin's own 19th-century anti-theodicy." Thus it is not surprising to find him insisting a "literal reading of the Bible has done more to help than hurt science over the centuries."

I sense that these outrageous obiter dicta are intentional. The average reader, especially the average science reader, will be so incensed that he or she will fail to spot the underlying argument that Fuller wants to make. Fuller will get away with things by default. However, I too am a philosopher and, although not a Pittsburgh graduate, I know the tricks of the trade. More amused than cross, let me go to the heart of Fuller's case against Darwinian evolutionary theory and for IDT—for his is as much a negative critique of the opposition as a positive defense of his own beliefs. Fuller feels that Charles Darwin failed to make the case for his mechanism of natural selection. Darwin did not give a cause for evolution. He certainly did not unify the field. At most he gave lists of facts. Moreover, today if we feel that advance has been made, it is primarily in the molecular field, and this owes little or nothing to traditional evolutionary thought. At best Darwinism is a kind of tarted-up natural theology and, this being so, why not IDT?

CREDIT: JOE SUTLIFF

The important thing is that all of this is completely wrong and is backed by no sound scholarship whatsoever. In at least one case, Fuller makes his case by an egregious misreading—of something I wrote about the role of genetic drift in Sewall Wright's shifting balance theory (*2*). For the record, Charles Darwin set out to provide a cause, what he called—following his mentors like William Whewell (who in turn referred back to Newton)—a true cause or *vera causa*. Darwin felt, and historians and philosophers of science as well as practicing evolutionary biologists still feel, that he succeeded, for two reasons. First, he showed how organisms can be changed by human picking or selecting. Although Fuller repeatedly claims that Darwin intended no analogy here, that is simply not true. In the face of virtually everybody—including Alfred Russel Wallace, who (in the manuscript he sent to Darwin in 1858) explicitly denied a link between artificial and natural selection (*3*)—Darwin insisted that we can gain confidence about selection in nature from what happens when humans are active. Second, Darwin brought everything together in a "consilience of inductions." He argued that if you take selection as the causal mechanism, then you can explain instinct, the fossil record, geographical distributions of organisms, anatomy, systematics, and embryology. In turn, the success of these explanations feeds back to support the belief in selection. About as unifying a setup as it is possible to imagine.

One can go on to look at things today. It is ludicrous to claim that modern evolutionary biology is not integrated with molecular biology. Motoo Kimura's neutral theory (*4*) depends crucially on the claim that selection has little or no effect on processes down at the molecular level. Genetic fingerprinting has proved absolutely vital for observational and experimental studies of evolution. Someone like British ornithologist Nicholas Davies, working out the relationships among individual dunnocks (*Prunella modularis*) (*5*), would have been powerless without the technique. And in evolutionary developmental biology (evo-devo), currently the hottest area of evolutionary research (*6*), how does one speak of genetic homologies between fruitflies and humans without talking about molecules?

At Dover, the author supported the wrong side. Intelligent design theory is a form of Christianity made up to look like science. The judge correctly ruled that it has no place in science classrooms. Reading *Dissent over Descent* should not change anyone's verdict. As a historian and philosopher of science, I can only hope that the science community does not judge us all by Fuller's example.

The reviewer is at the Department of Philosophy, Florida State University, Tallahassee, FL 32306–1500, USA. E-mail: mruse@fsu.edu

References

1. S. Fuller, *Science vs. Religion? Intelligent Design and the Problem of Evolution* (Polity, Cambridge, 2007).
2. M. Ruse, *Mystery of Mysteries: Is Evolution a Social Construction?* (Harvard Univ. Press, Cambridge, MA, 1999); reviewed by D. L. Hull, *Science* **284**, 1131 (1999).
3. A. R. Wallace, *J. Proc. Linn. Soc. Zool.* **3**, 53 (1858).
4. M. Kimura, *The Neutral Theory of Molecular Evolution*

Published by AAAS

(Cambridge Univ. Press, Cambridge, 1983); reviewed by J. H. Gillespie, *Science* **224**, 732 (1984).
5. N. B. Davies, *Dunnock Behaviour and Social Evolution* (Oxford Univ. Press, Oxford, 1992).
6. S. B. Carroll, *Endless Forms Most Beautiful: The New Science of Evo Devo and the Making of the Animal Kingdom* (Norton, New York, 2005); reviewed by D. Duboule, *Science* **308**, 955 (2005).

10.1126/science.1164798

PHYSICS

Some Science for Today's Electorate

Kenneth R. Foster

In *Physics for Future Presidents*, Richard Muller, a physics professor at the University of California, Berkeley, comments on the science that constrains potential solutions to a variety of issues: energy, terrorism, nuclear power, space exploration, global warming. The fine book is not a policy manual for candidates in the current U.S. election but rather a popularized version of Muller's science-and-society course for non–science majors (*1*).

Through his clear and entertaining text, Muller presents essentially quantitative arguments to nontechnical readers in simple and graphic ways. The level of writing roughly compares to that of the science coverage in major U.S. newspapers. Muller uses only elementary physics concepts, which he carefully explains to his readers.

Physics for Future Presidents
The Science Behind the Headlines
by Richard A. Muller
Norton, New York, 2008. 380 pp. $26.95, C$29.50, £15.99, €21. ISBN 9780393066272.

The author notes, for example, that the cost of energy varies tremendously depending on source, from less than one U.S. cent per kilowatt hour in generation costs from burning coal to $1000 per kilowatt hour for energy drawn from disposable AAA batteries. Owners of hybrid automobiles, he cautions, should not be too smug about the money they are saving in gasoline until they consider the costs of the inevitable replacement of the batteries in their car.

He explains that the low cost of generating electricity from coal and the plentiful supplies of this fuel are important factors in the issue of global climate change: "Coal produces more carbon dioxide per kilowatt-hour of energy than virtually any other source." But China builds an average of over 1 gigawatt of coal-fired generating capacity every week and has enough coal "to meet the worst scenarios of the global-warming models."

Muller offers readers "physics by total immersion" and stays "away from issues in politics, business, and diplomacy." But he often reaches beyond technical facts and sometimes expresses views that, undoubtedly, are widely shared by the scientific community even if he does not argue them out very carefully.

For example, Muller views alternative energy sources such as fusion and solar power, as well as recycling, hydrogen as fuel, and the Kyoto Protocol, as "nonsolutions" to the problem of global warming. He says that the low-hanging fruit lies in conservation.

Carrying a current. Muller performs an electrical demonstration for his students.

As another example, Muller is skeptical about the value of putting humans in space. He writes that the space shuttle "is the dream of man in space. … But it is not safe, it cannot be made safe, and it is not done for science." In his view, although space offers an excellent platform for some things—spying, gathering weather imagery, global positioning, satellite communications, and important scientific endeavors (such as the Hubble Space Telescope)—"these are best done with robotics." Muller recommends reducing the priority given to putting humans in space and making "science truly the primary [goal] of the government science program."

Many readers will be confused by Muller's chapters on climate change, in which he takes on former Vice President Al Gore and his 2006 film *An Inconvenient Truth* (*2*). Muller gives Gore credit for alerting the public to the dangers of carbon dioxide and global warming, a problem that Muller acknowledges is real and serious. But he complains that Gore accomplished this "through a combination of artistry, powerful writing, and exaggeration, mixed with some degree of distortion and a large amount of cherry picking" (i.e., selective quotation of data).

Muller discusses the famous comparison of plots of the variations in atmospheric carbon dioxide and in global temperatures over the past 600,000 years. Gore used the close tracking of the two graphs to bolster the claim that carbon dioxide drives global temperature. Muller claims that many climate scientists think the increases in atmospheric carbon dioxide are the result of increasing global temperatures, not the other way around. He cautions that when the public finds out "Gore has exaggerated the case, [it] may reject the truly scientific case for fossil fuel–induced global warming" and "throw out the baby with the dirty bathwater."

Muller himself may be guilty of a biased presentation here. Although for most of the past 600,000 years the global temperature increases preceded rises in atmospheric carbon dioxide, in modern times the order of the changes has reversed. Gore's presentation has been praised by climate change experts for its "striking clarity" (*3*). A more balanced discussion might have noted some of the other, worse distortions we have seen in the climate change debates. And if Gore has exaggerated or selectively represented data to further an agenda, that is a common problem in public life that cannot be remedied by a book such as Muller's.

Despite this mild caveat, *Physics for Future Presidents* is an outstanding example of public communication of science, and it would be a great holiday present even for people who might not end up in the White House.

The reviewer is in the Department of Bioengineering, University of Pennsylvania, Philadelphia, PA 19104–6392, USA. E-mail: kfoster@seas.upenn.edu

References and Notes

1. Videos of Muller's lectures from this and past semesters are available through links from http://muller.lbl.gov/teaching/Physics10/PffP.html.
2. Reviewed by R. Holt, *Science* **317**, 198 (2007).
3. J. Hansen, *N. Y. Rev. Books* **53** (12), 12 (13 July 2006).

10.1126/science.1165024

AGRICULTURE

Sustainable Biofuels Redux

Science-based policy is essential for guiding an environmentally sustainable approach to cellulosic biofuels.

G. Philip Robertson,[1*] Virginia H. Dale,[2] Otto C. Doering,[3] Steven P. Hamburg,[4] Jerry M. Melillo,[5] Michele M. Wander,[6] William J. Parton,[7] Paul R. Adler,[8] Jacob N. Barney,[9] Richard M. Cruse,[10] Clifford S. Duke,[11] Philip M. Fearnside,[12] Ronald F. Follett,[13] Holly K. Gibbs,[14] Jose Goldemberg,[15] David J. Mladenoff,[16] Dennis Ojima,[17] Michael W. Palmer,[18] Andrew Sharpley,[19] Linda Wallace,[20] Kathleen C. Weathers,[21] John A. Wiens,[22] Wallace W. Wilhelm[23]

CREDIT: ERIK SANDBERG/BERNSTEIN & ANDRIULLI

Last May's passage of the 2008 Farm Bill raises the stakes for biofuel sustainability: A substantial subsidy for the production of cellulosic ethanol starts the United States again down a path with uncertain environmental consequences. This time, however, the subsidy is for both the refiners ($1.01 per gallon) and the growers ($45 per ton of biomass), which will rapidly accelerate adoption and place hard-to-manage pressures on efforts to design and implement sustainable production practices—as will a 2007 legislative mandate for 16 billion gallons of cellulosic ethanol per year by 2022. Similar directives elsewhere, e.g., the European Union's mandate that 10% of all transport fuel in Europe be from renewable sources by 2020, make this a global issue. The European Union's current reconsideration of this target places even more emphasis on cellulosic feedstocks (*1*). The need for knowledge- and science-based policy is urgent.

Biofuel sustainability has environmental, economic, and social facets that all interconnect. Tradeoffs among them vary widely by types of fuels and where they are grown and, thus, need to be explicitly considered by using a framework that allows the outcomes of alternative systems to be consistently evaluated and compared. A cellulosic biofuels industry could have many positive social and environmental attributes, but it could also suffer from many of the sustainability issues that hobble grain-based biofuels, if not implemented the right way.

Although many questions about biofuel sustainability remain unanswered—indeed, some remain unasked—what we now know with reasonable certainty can be readily summarized. First, we know that grain-based biofuel cropping systems as currently managed cause environmental harm. In addition to questions of carbon debt created by land cleared elsewhere to replace displaced food production (*2*–*4*), farming our existing landscapes more intensively, with even greater quantities of biomass extracted, can easily exacerbate existing environmental problems. The effects of more intense agriculture are well documented: increased soil erosion, greater nitrate and phosphorus loss, and a decline in biodiversity, with concomitant impacts on ground and surface water quality, air quality, and biodiversity-based services such as pest suppression and wildlife amenities. Business as usual writ larger is not an environmentally welcome outcome.

Second, because grain-based ethanol will likely remain in the nation's energy portfolio, it is important to understand that appropriate practices can soften its environmental impact.

[1]W. K. Kellogg Biological Station and Department of Crop and Soil Sciences, Michigan State University, Hickory Corners, MI 49060, USA. [2]Environmental Sciences Division, Oak Ridge National Laboratory, Oak Ridge, TN 37831–6036, USA. [3]Department of Agricultural Economics, Purdue University, West Lafayette, IN 47907, USA. [4]Center for Environmental Studies, Brown University, Providence, RI 02906, and Environmental Defense Fund, Boston, MA 01028, USA. [5]The Ecosystems Center, Marine Biological Laboratory, Woods Hole, MA 02543, USA. [6]Natural Resources and Environmental Sciences, University of Illinois, Urbana, IL 61801, USA. [7]Natural Resource Ecology Laboratory, Colorado State University, Fort Collins, CO 80523–1499, USA. [8]Pasture Systems and Watershed Management Research Unit, U.S. Department of Agriculture–Agricultural Research Service (USDA-ARS), University Park, PA 16802, USA. [9]Department of Plant Sciences, University of California, Davis, CA 95616, USA. [10]Department of Agronomy, Iowa State University, Ames, IA 50011, USA. [11]Ecological Society of America, Washington, DC 20036, USA. [12]National Institute for Research in the Amazon (INPA), Manaus, Amazonas, CEP 69011-970, Brazil. [13]Soil Plant Nutrient Research, USDA–ARS, Fort Collins, CO 80526–8119, USA. [14]Center for Sustainability and the Global Environment (SAGE), Nelson Institute for Environmental Studies, University of Wisconsin–Madison, Madison, WI 53726, USA. [15]Instituto de Eletrotécnica e Energia, University of São Paulo, São Paulo, Brazil. [16]Department of Forest and Wildlife Ecology, University of Wisconsin, Madison, WI 53706, USA. [17]The H. John Heinz Center for Science, Economics, and the Environment, Washington, DC 20006, USA. [18]Department of Botany, Oklahoma State University, Stillwater, OK 74078, USA. [19]Department of Crop, Soil and Environmental Sciences, University of Arkansas, Fayetteville, AR 72701, USA. [20]Department of Botany and Microbiology, University of Oklahoma, Norman, OK 73019, USA. [21]Cary Institute of Ecosystem Studies, Millbrook, NY 12545, USA. [22]PRBO Conservation Science, Petaluma, CA 94954, USA. [23]USDA–ARS, University of Nebraska, Lincoln, NE 68583, USA.

*Author for correspondence. E-mail: robertson@kbs.msu.edu

Published by AAAS

Although the price of cellulosic feedstocks will likely remain lower than that of grain, the added costs of pretreatment and enzymes for cellulosic biomass refining will likely continue to make grain competitive with cellulosic feedstocks for the foreseeable future, even considering cheaper cellulosic biomass. There are many factors affecting the relative prices of ethanol derived from different feedstocks, but with the current infrastructure investment in grain ethanol refineries, it seems likely that grain ethanol will continue to consume a substantial proportion of U.S. corn production—25% in 2007, >30% in 2008—for at least the next decade. Thus, it makes sense to consider ways to minimize the environmental costs of additional intensive grain production.

We know, for example, that no-till farming can slow erosion and build soil organic matter where residue inputs are sufficient; that advanced fertilizer technologies can improve crop nitrogen capture and reduce nitrous oxide fluxes; that cover crops and riparian plantings can sequester soil carbon and intercept nitrate leakage and phosphorus runoff; that rotational diversity and inclusion of unmanaged habitat can better support pollinators and other beneficial insects, as well as wildlife; and that crop genetic improvements can reduce the need for pesticides and can increase stress tolerance and water- and nutrient-use efficiency. But improved practices require incentives to ensure their adoption, and current adoption rates are slow or stalled. Significant mitigation of the adverse environmental consequences of more intensive grain production requires incentives that work.

Third, we know that the development of cellulosic feedstocks has substantial promise for avoiding many of the environmental challenges that face grain-based biofuels. In the long term, most cellulosic feedstocks are expected to be generated from perennial crops grown specifically for that purpose. Perenniality eliminates the need for most chemical inputs and tillage after an establishment phase and lessens the need for nitrogen fertilizer. Further, cellulosic crops can be grown as more complex species mixes, including native polycultures (*5*) grown for additional conservation benefits. Moreover, the cultivation of cellulosic crops has the potential to promote soil carbon sequestration, reduce nitrous oxide emissions, provide to ecosystems in the surrounding landscape biodiversity-based services such as pollination and pest suppression, and afford much higher rates of energy return than grain-based systems.

But however promising, these environmental benefits are by no means given. Whether they are realized will depend on which, where, and how cellulosic biofuels are produced. And tradeoffs are unavoidable. Siting cellulosic biofuel crops on marginal lands, rather than on our most productive croplands, could mean preventing competition with food production and concomitant effects on commodity prices, as well as minimizing or even avoiding the carbon debt associated with land clearing. However, marginal lands can also be rich in biodiversity, may require sizable inputs of nutrients and water to make production economically viable, and may carry the opportunity cost (*6*) of forgone future carbon sequestration.

Management practices, including crop choice, intensity of inputs, and harvesting strategy, also will have a strong influence on the sustainability of cellulosic biofuels. For example, extensive monocultures may be economically favorable relative to polycultures but may reduce landscape diversity and the ecosystem services that more-diverse landscapes provide. Some proposed biofuels crops are exotic (*7*) and others are known to be invasive (*8*), which can have further negative influences on local-to-regional biodiversity. Other cellulosic crops may require substantial chemical inputs and irrigation, with the potential for water pollution, nitrous oxide emissions, and, in arid regions, further competition for water. In addition, excessive removal of "waste" residue from annual cropping systems will rob the soil of carbon (*9*), increase erosion (*10*), and reduce soil fertility. Also, excessive forest thinning will reduce long-term forest productivity and wildlife habitat. In sum, the potential benefits of cellulosic crops could too readily be negated by inattention to choices of location and management practices.

Globally, to produce an important amount of energy with biofuels will require a large amount of land—perhaps as much as is in row-crop agriculture today. This will change the landscape of Earth, not just the United States, in a significant way. To avoid perverse outcomes, such as U.S. policies that cause carbon debt elsewhere, we also need to keep a global perspective that recognizes effects of U.S. decisions on both the magnitude and direction of land-use change elsewhere.

The identification of unintended consequences early in the development of alternative fuel strategies will help to avoid costly mistakes and regrets about the effects on the environment. Policies that support long-term sustainability of both our landscapes and our atmosphere are essential if we are to chart a low-carbon economy that is substantially better than business as usual.

Getting to such an economy will also require a more comprehensive and collaborative research agenda than what has been undertaken to date. In particular, there is an urgent need for research that emphasizes:

(i) a systems approach to assess the energy yield, carbon implications, and the full impact of biofuel production on downstream and downwind ecosystems, however distant from the point of production;

(ii) a focus on ecosystem services—including those that are biodiversity-based—to provide the information necessary for the development and implementation of land-management approaches that meet multiple needs; and

(iii) an understanding of the implications of policy and management practices at different spatial scales—from farm and forest to landscapes, watersheds, food-sheds, and the globe—and an assessment of alternative cost-effective policies designed to meet sustainability goals.

Decision-makers at all levels need to understand that applying best available practices to biofuel crop production will have positive impacts both on the sustainability of our working lands and on providing a long-term place for biofuels in our renewable energy portfolio—and that the policies necessary to ensure this outcome are not currently in place. Legislated environmental performance standards for cellulosic ethanol production could, for example, go far toward promoting sustainable outcomes. Such standards could range from a prohibition of specific practices, such as growing invasive species for feedstock or removing excessive annual crop residue, to the provision of incentive payments based on avoided greenhouse gas emissions, both direct and indirect. We know enough today to begin formulating these standards, and both the industry and the environment will benefit from their early identification and refinement.

Sustainable biofuel production systems could play a highly positive role in mitigating climate change, enhancing environmental quality, and strengthening the global economy, but it will take sound, science-based policy and additional research effort to make this so.

References

1. J. Kanter, *New York Times*, 12 September 2008; www.nytimes.com/2008/09/12/business/worldbusiness/12biofuels.html.
2. J. Fargione, J. Hill, D. Tilman, S. Polasky, P. Hawthorne, *Science* **319**, 1235 (2008).
3. T. Searchinger *et al.*, *Science* **319**, 1238 (2008).
4. K. L. Kline, V. H. Dale, *Science* **321**, 199 (2008).
5. D. Tilman, J. Hill, C. Lehman, *Science* **314**, 1598 (2006).
6. C. B. Field, J. E. Campbell, D. B. Lobell, *Trends Ecol. Evol.* **23**, 65 (2008).
7. E. Heaton, F. Dohleman, S. Long, *Glob. Change Biol.* **14**, 2000 (2008).
8. J. Barney, J. DiTomaso, *Bioscience* **58**, 64 (2008).
9. W. W. Wilhelm, J. M. F. Johnson, D. L. Karlen, D. T. Lightle, *Agron. J.* **99**, 1665 (2007).
10. R. L. Graham, R. Nelson, J. Sheehan, R. D. Perlack, L. L. Wright, *Agron. J.* **99**, 1 (2007).

10.1126/science.1161525

Published by AAAS

ASTRONOMY

The Shining Make-Up of Our Star

A revision to the chemical composition of the Sun based on models of its outer atmosphere is at odds with our understanding of its inner workings.

Martin Asplund

The content of chemical elements in the Sun functions as an astronomical yardstick against which the compositions of all other stars, gas clouds, and galaxies in the cosmos are referenced. Rather than being constant, as any good ruler should be, however, this elemental abundance scale has in the past few years undergone a substantial revision based on improved modeling of the solar surface layers and the emitted solar spectrum (*1*, *2*). Although this adjustment has been welcomed by most in the astronomy community, there is concern that it seems incompatible with our understanding of the solar interior.

The chemical composition of a star like the Sun is inferred from its spectrum, which provides the elemental fingerprint in the form of absorption lines. To convert the strength of a spectral line to an elemental abundance requires detailed modeling of the stellar atmosphere and the processes between atoms and radiation that shape the emergent solar spectrum. A major complication here comes from convection, which reaches up to the surface in the Sun and thereby modifies the atmospheric structure and spectrum formation. Instead of the traditional one-dimensional (1D) and hydrostatic modeling, the new analyses (*1*–*3*) use a 3D and hydrodynamical solar model in which the convective energy transport is realistically treated together with the interaction between the radiation field and the gas. Also, nonequilibrium atomic processes are considered when computing the emergent solar spectrum, and new input data for the spectral lines are used.

Together, these improved ingredients add up to almost half the derived solar abundances of carbon, nitrogen, oxygen, and neon compared with the canonical values from a decade ago (*2*, *4*). This revision is particularly noteworthy given that these are the four most abundant elements next to hydrogen and helium. The results seem highly robust as molecular lines and atomic transitions arising from excitation levels having vastly different sensitivities to the atmospheric conditions point to the same abundances.

One long-standing conundrum has been why the Sun that was born 4.5 billion years ago contained much more heavy elements

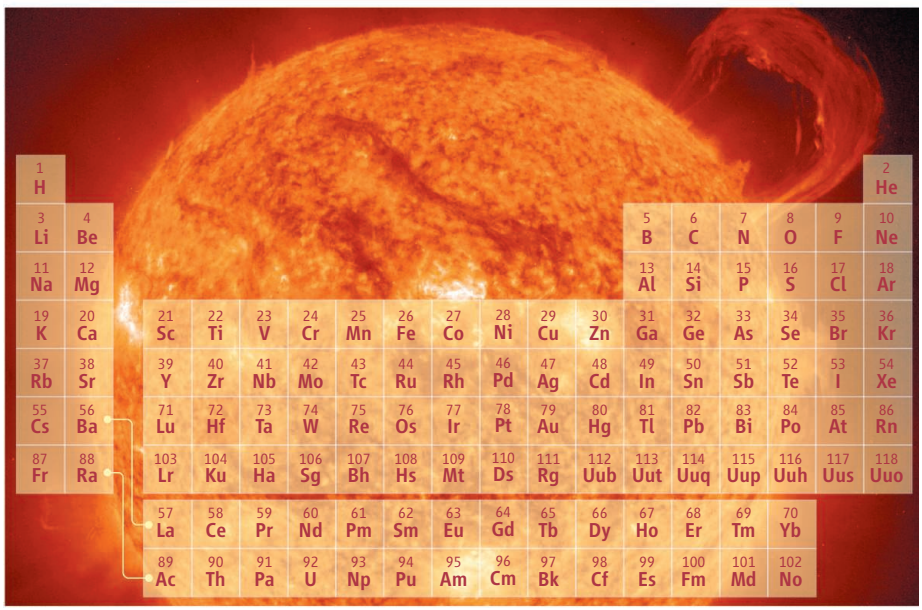

PHOTO CREDIT: ESA/NASA/SOHO

than the present-day interstellar medium and young, massive stars in the Galactic neighborhood. The overall content of heavy elements in the Milky Way should steadily increase with time as stars die and spew out their nuclear-processed ashes from which subsequent stellar generations are formed (*5*). The revised lower solar content of C, N, and O has finally brought the Sun into line with its surroundings (*6*).

Modelers of the solar interior have been less enthusiastic (*7*). The lower content of heavy elements reduces the opacity, thus requiring changes to the computed temperature and density as a function of depth in the solar models. This would not have been such a serious problem had it not been for helioseismology, a technique that has been used to provide a window to peer into the solar interior. Sound waves generated by the convective motions in the outer ~30% of the Sun cause it to ring like a bell with a dominant period of about 5 min. Helioseismology maps the variation of sound speed with depth from measuring the exact frequencies of the different oscillation modes. Unfortunately, the inferred sound speed is inconsistent with the predicted values from interior models constructed with the new solar chemical composition. The irony is that solar-interior models based on the old abundances gave strikingly good agreement.

Ever since this "solar model problem" was first realized, much work has been devoted to identifying a solution. The most straightforward explanation would be that the opacity in the solar interior has been underestimated, requiring an increase by 10 to 20% throughout an extended region below the convection zone where the temperatures are 2 to 5×10^6 K (*7*). Subsequent studies have failed to identify such a shortcoming in existing atomic calculations, although a minor part of the missing opacity could well be forthcoming (*8*). Another way of compensating for the diminished opacity from the lower O abundance is to substantially increase the content of other elements such as Ne, which can only be indirectly inferred in the Sun. After receiving some initial support (*9*), this idea now appears inconsistent with the evidence from other nearby solar-like stars. Other hypotheses, such as a much higher metal content in the interior than in the solar atmosphere due to underestimated diffusion, have similarly been ruled out. Perhaps the only proposal still standing is internal gravity waves, which both induce mixing below the convection zone and enhance the effective opacity in the region with the largest helioseismology discrepancies (*10*, *11*). Although the expected effect goes in the right direction, unfortunately no detailed quantitative estimate of the impact on sound speed has appeared yet for this promising premise.

With the steady elimination of suggestions aimed at the solar interior modeling, the focus

Max Planck Institut für Astrophysik, Garching, Germany. E-mail: masplund@mpa-garching.mpg.de

Published by AAAS

has partly shifted to confirming or refuting the new solar abundances of references *1–3*. Despite the more sophisticated modeling of the atmosphere and spectrum, could it be that the revised values are in fact underestimated and the real abundances closer to the old ones? Recently, independent analyses based on different 3D solar atmosphere models have appeared, which tend to find intermediate values (*12–15*). Unfortunately, these latest studies have been restricted to only oxygen and without considering the molecular transitions; hence, it remains to be shown that all available abundance indicators will yield consistent results. Reassuringly, the particular choice of 3D model turns out to be relatively unimportant. Instead, the main differences come from subtleties in the computations of the solar spectrum, especially how possible blending lines from other elements and collisional cross sections for the nonequilibrium spectral line calculations are treated, and how the strengths of the spectral lines are measured. However, the jury is still out on whether these alternative choices are preferable to those in the original 3D-based analyses that sparked the whole solar modeling problem. If true, these intermediate oxygen abundance results would alleviate but not remove the discrepancy with helioseismology. Another explanation working in concert would then still be required, presumably related to refinements in the solar interior modeling or opacity calculations.

Perhaps an amicable resolution to the solar modeling problem is possible after all through compromises by both the solar atmosphere and interior camps. Regardless of how the final blame is apportioned, studies of the Sun as well as other stars will then be on a much firmer footing. With stars as widely used cosmic probes, this will directly translate to a better understanding of the universe as a whole.

References

1. M. Asplund *et al.*, *Astron. Astrophys.* **417**, 751 (2004).
2. M. Asplund, N. Grevesse, A. J. Sauval, *ASP Conf. Ser.* **336**, 25 (2005).
3. C. Allende Prieto, D. L. Lambert, M. Asplund, *Astrophys. J. Lett.* **556**, L63 (2001).
4. E. Anders, N. Grevesse, *Geochim. Cosmochim. Acta* **53**, 197 (1989).
5. C. Chiappini, D. Romano, F. Matteucci, *Mon. Not. R. Astron. Soc.* **339**, 63 (2003).
6. N. Przybilla *et al.*, *Astron. Astrophys.*, available at http://arXiv.org/abs/0809.2403 (2008).
7. S. Basu, H. M. Antia, *Phys. Rep.* **457**, 217 (2008).
8. N. R. Badnell *et al.*, *Mon. Not. R. Astron. Soc.* **360**, 458 (2005).
9. J. J. Drake, P. Testa, *Nature* **436**, 525 (2005).
10. W. Press, G. B. Rybicki, *Astrophys. J.* **248**, 751 (1981).
11. D. Arnett, C. Meakin, P. A. Young, *ASP Conf. Ser.* **336**, 235 (2005).
12. E. Caffau *et al.*, *Astron. Astrophys.* **488**, 1031 (2008).
13. T. R. Ayres, *Astrophys. J.* **686**, 731 (2008).
14. R. Centeno, H. Socas-Navarro, *Astrophys. J. Lett.* **682**, L61 (2008).
15. J. Melendez, M. Asplund, *Astron. Astrophys.*, available at http://arXiv.org/abs/0808.2796 (2008).

10.1126/science.1148787

ECOLOGY

Bugs' Bugs

Evaluation of the chemical relationship between a beetle and its microbial associates shows that microbial ecology can lead to potential drugs.

May R. Berenbaum[1] and Thomas Eisner[2]

Although scientific progress leads to constant reevaluation and revision of concepts and ideas, one observation that has remained robust in the face of accumulating evidence across the centuries is that there are a lot of insects in the world. In 1758, in his profoundly influential book *Systema Naturae*, Carolus Linnaeus (*1*) described all animal species known at the time; of the 4203 species of animals he named, 2102—more than half—were insects. Linnaeus also provided a flexible binomial framework for naming and classifying organisms; species descriptions of all kinds have accumulated apace, but since Linnaeus began this effort they have accumulated fastest for insects. Between 1758 and 1800, close to 60,000 insect species were described; from 1800 to 1850, about 360,000 additional species were identified. Today, about 950,000 species of insects have been described.

A robust corollary of the observation that there are a lot of insects in the world is that the greatest proportion of all insect species belongs to the order Coleoptera—more than one-third of all known species are beetles. Today, more than 300,000 species of beetles have been described. Erwin and Scott (*2*), in a 1-year study of only 19 individuals of a single tree species (*Luehea seemannii*) in Panama, found more than 950 species of beetles, many of them new discoveries (that count did not even include weevils, the largest family of beetles). How many beetles remain undescribed is anyone's guess, but some experts estimate that it is between 5 and 8 million species.

Focused on only a single (but well-known) species of beetle, *Dendroctonus frontalis*, Scott *et al*. on page 63 of this issue (*3*) dramatically illustrate that, as numerous as they may be, beetles may represent just the tip of the biodiversity iceberg. A single beetle species itself can house an entire community of associated species. *D. frontalis* infests pine trees but is dependent on two symbiotic fungi—*Entomocorticum* sp. A, and to a lesser extent, *Ceratocystiopsis ranaculosus*—which both grow in the vascular system of the tree and provide food for the beetle larvae. Another fungus, *Ophiostoma minus*, can be a symbiont that assists the beetle in overcoming the defenses of the host tree, but it can also inhibit growth of the principal

Medicinal sources? Microbes (by the thousands) associated with insects remain to be discovered and tested for chemicals. Shown is a *Camponotus* ant infested with a *Cordyceps* fungus, which is related to the beetle-killing fungus that produces cyclosporin, the well-known immunesuppressive drug. The pharmacological properties of the ant-infesting fungus have yet to be investigated.

CREDIT: THOMAS EISNER/CORNELL UNIVERSITY

[1]Department of Entomology, University of Illinois, Urbana, IL 61801, USA. [2]Department of Neurobiology and Behavior, Cornell University, Ithaca, NY 14853, USA. E-mail: maybe@life.uiuc.edu; te14@cornell.edu

Entomocorticum fungal food source. The beetle deals with the aggressive fungus by harboring yet another species—an actinomycete bacterium—that secretes antibiotics to kill *O. minus*.

This coleopteran complexity eluded detection until now, even though *D. frontalis*, first described 140 years ago (*4*), is a widespread pest and arguably the most economically important pest of southern pine plantations in the United States. And it is by no means unique in harboring a complex microcosm of interacting species. *Acromyrmex* leaf-cutting ants associate with two very specialized symbiotic basidiomycete fungi that grow in underground gardens as food. At the same time, these ants maintain actinomycete *Pseudonocardia* bacteria on their cuticle to manufacture antibiotics that inhibit the growth of an unwelcome associate—*Escovopsis*, a parasitic fungus that attacks the food-source fungal garden (*5*). As Scott *et al*. suggest, in view of the enormous selection pressure that pathogens can exert, protective associations with antibiotic-producing bacteria may be a ubiquitous feature of insect-fungus partnerships. Given that more than 300,000 species of beetles are currently known, the number of partnerships, fungal associates, and bacterial symbionts yet to be elucidated is daunting.

According to May (*6*), the reasons for cataloging biodiversity are the "same reasons that compel us to reach out toward understanding the origins and eventual fate of the universe, or the structure of the elementary particles that it is built from." May also reminds us that Earth's biodiversity is declining at an unprecedented rate, due in large part to anthropogenic changes in land use, climate, soil, and water and air quality. How many beetles, with their communities of associates, will have ceased to exist before Scott *et al*. and other investigators can work out the details of their interrelationships is anyone's guess. According to the Red List of Threatened Species provided by the International Union for Conservation of Nature (*7*)—an authoritative accounting of rare, threatened, and endangered species—fewer than 800 of the 950,000 or so species of insects that have been described (~0.1%) have been evaluated as to their status. Moreover, of the insect species that have been evaluated, almost three-fourths are threatened. The powerful antibiotic chemistry exploited by the southern pine beetle that allows it to go about its business attacking trees is just one example of a more tangible benefit of examining terrestrial interactions than simply gaining insights into the cosmos.

There is no limit to what remains to be discovered in that interactive zone between macroorganism and microbe, where so many biological mutualisms and antagonisms play out. Microbes blanket the planet, and in their infinite variety they must be involved in infinite interactions. Deciphering these could lead to a vast increase in ecological knowledge, as well as to the isolation of natural products of unforeseen function. The latter possibility, clearly envisioned by Scott *et al*., is one that we take to be of particular importance. Chemical prospecting—the search for chemicals of use from nature, including medicinals—has been relegated to low priority by industry nowadays, in the belief that nature has already been exhaustively screened for such compounds. Scott *et al*. provide proof that such belief is unjustified, that the microbial world has been all but thoroughly explored (see the figure). Sure enough, microbes have been screened for some types of biotic and antibiotic action, but the bulk of their chemical capabilities remain to be uncovered. As demonstrated by Scott *et al*., even the least wanted among species can be the source of useful leads. A concerted effort to look into the more subtle aspects of microbial chemistry is therefore very much in order. The fact is that we don't even know the microbes themselves that inhabit our planet, let alone the molecules they need to secure their survival. Microbial ecology is still very much a part of the great frontier.

References

1. C. Linnaeus, *Systema Naturae per Regna Tria Naturae, Secundum Classes, Ordines, Genera, Species, cum Characteribus, Differentiis, Synonymis, Locis. Tomus I. Editio Decima, Reformata* [Laurentii Salvii, Holmiae (Stockholm), 1758].
2. T. L. Erwin, J. C. Scott, *Coleopt. Bull.* **34**, 305 (1980).
3. J. J. Scott *et al*., *Science* **322**, 63 (2008).
4. J. O. Zimmermann, *Trans. Am. Entomol. Soc.* **2**, 141 (1868).
5. C. R. Currie *et al*., *Science* **311**, 81 (2006).
6. R. M. May, *Philos. Trans. R. Soc. London Ser. B* **330**, 293 (1990).
7. www.iucnredlist.org

10.1126/science.1164873

ATMOSPHERIC SCIENCE

From Ocean to Stratosphere

Rising tropical sea surface temperatures alter atmospheric dynamics at heights of 16 kilometers or more.

Rudolf Deckert and Martin Dameris

The increasing burden of greenhouse gases from human activities, such as carbon dioxide, is warming the troposphere (the lowest part of Earth's atmosphere), whereas in the stratosphere (above the troposphere and extending from ~16 to 50 km), higher greenhouse gas concentrations cause a net radiative cooling that may delay ozone hole recovery in the Antarctic. But the picture is even more complex. Recent studies have shed light on how mass exchange between troposphere and stratosphere may be affected by tropical sea surface temperatures (SSTs) that are rising as a result of global warming.

The mass exchange between troposphere and stratosphere—the Brewer-Dobson circulation—is characterized by persistent upwelling of air in the tropics from the troposphere into the stratosphere. The air then downwells in the extratropics, mixing stratospheric air back into the troposphere, with a turnaround time of a few years (*1*). Some observational data indicate that the troposphere-stratosphere mass exchange is accelerating (*2*). Most numerical studies with coupled chemistry-climate models support this finding and relate it to the anthropogenic climate signal (*3*), but it is uncertain which mechanism communicates the anthropogenic climate signal to the mass exchange.

This mechanism needs to be pinpointed because the troposphere-stratosphere mass exchange affects the chemical composition and climate of Earth's atmosphere. The tropical upwelling branch of the Brewer-Dobson circulation lowers temperatures and ozone concentrations, especially in the lower stratosphere. The low temperatures in turn freeze-dry the upwelling tropospheric air. Furthermore, the upwelling controls the lifetime of anthropogenic ozone-depleting substances with sinks in the stratosphere. In the extratropical stratosphere, downwelling causes adiabatic warming and ozone accumulation until

Deutsches Zentrum für Luft- und Raumfahrt, Institut für Physik der Atmosphäre, Oberpfaffenhofen, 82234 Wessling, Germany. E-mail: rudolf.deckert@dlr.de

the air parcels return to the extratropical troposphere. This process contributes tropospheric ozone levels (*4*). Finally, changes in horizontal temperature gradients in the lower stratosphere cause remote shifts in surface weather and climate (*5*).

Evidence for a changing Brewer-Dobson circulation comes from satellite and radiosonde data, which indicate a reduction in temperatures and ozone and water vapor concentrations over the past four decades, particularly in the tropical lower stratosphere at all longitudes (*6*). This points to an accelerated tropical upwelling (*2*, *7*). Radiative changes as a result of anthropogenic ozone depletion might account for similar modifications (*8*), but cannot explain a sudden drop in tropical lower stratospheric temperatures in 2001 (*2*, *7*). Stratospheric mass transport trends derived from observations also tend to indicate accelerated upwelling but have large uncertainties (*7*, *9*).

Several independent studies with numerical global climate models confirm these observations (*3*, *10*–*13*). Consistently, the model studies find that lower temperatures and ozone concentrations occur in the tropical lower stratosphere as a result of a stronger tropical upwelling in a future warmer climate, although the high-latitude Brewer-Dobson response differs among the studies.

The model studies indicate that the upwelling intensification is mainly induced by a stronger driving from planetary waves; one to three troughs of these global-scale waves fit around a whole latitude circle. Planetary waves are produced in the troposphere by various processes, and can travel horizontally as well as vertically. Their life cycle usually ends when they disintegrate as a result of continuous damping or, more abruptly, due to wave breaking (like water waves approaching a beach). Some planetary waves can enter the stratosphere, where they usually vanish, conveying energy and momentum to the Brewer-Dobson circulation (*14*). During their life cycle, planetary waves are susceptible to SSTs, which affect location and intensity of their disintegration patterns.

Simulations show that there are various different latitudes where stratospheric wave disintegration responds to SST modifications (*10*, *12*). However, theoretical considerations imply that any year-round intensification in tropical upwelling requires enhanced stratospheric wave disintegration in the tropical/ subtropical region (*15*, *16*). The key question is how this low-latitude disintegration enhancement relates to higher tropical SSTs.

As an explanation, some model studies highlight the role of stronger zonal winds in the subtropical upper troposphere and lower stratosphere. These stronger winds are caused by the growing temperature contrast between the lower stratosphere, which cools, and the tropical upper troposphere, which warms, as a result of anthropogenic climate change. The altered zonal winds intensify planetary-wave disintegration in the stratosphere at low latitudes, thereby accelerating the tropical upwelling (*10*, *13*, *17*).

The warming of the tropical upper troposphere is mainly caused by higher tropical SSTs, which are part of global warming. The SST increase intensifies the activity of tropical thunderstorms (see the figure), which strengthens the associated latent-heat release, warms the tropical upper troposphere, and thus accelerates the zonal winds. However, it remains unclear whether altered wave generation or propagation dominate this SST-governed impact on the Brewer-Dobson circulation and whether waves generated in the tropics or extratropics are involved.

To address these open questions, an additional SST-related mechanism is being considered. The latent heat release from tropical thunderstorms causes pressure perturbations and hence generates tropical planetary waves, just like a stone hitting a water surface (*9*, *15*, *18*). The impact of this mechanism on the Brewer-Dobson circulation could strengthen as tropical SSTs rise and wave generation increases (*19*). In particular, observations show that SSTs in the western tropical Pacific Ocean—the highest SSTs on Earth—are anticorrelated with temperatures and ozone and water vapor concentrations in the tropical lower stratosphere (*2*). For example, high-SST anomalies coincide with low temperatures and ozone concentrations, and vice versa. The anticorrelation could be communicated via planetary-wave generation by tropical thunderstorms, as explained above (*6*).

Thus, heat and moisture at the sea surface affect not only tropospheric climate but also stratospheric dynamics. In particular, planetary waves appear to communicate modulations in tropical SSTs to the mass exchange between troposphere and stratosphere. This Brewer-Dobson circulation is likely to intensify in a future climate with higher tropical SSTs, with implications not only for the chemical composition and climate of the stratosphere but also at Earth's surface.

Tropical oceans and thunderstorms. Warmer tropical oceans intensify the activity of tropical thunderstorms, such as the "Hector" thunderstorm that develops nearly every year off the islands to the west of Darwin, Australia. As a result, the release of latent heat strengthens, affecting planetary waves and hence the mass exchange between troposphere and stratosphere.

CREDIT: HANS SCHLAGER/INSTITUT FÜR PHYSIK DER ATMOSPHÄRE, DEUTSCHES ZENTRUM FÜR LUFT- UND RAUMFAHRT, WESSLING, GERMANY

Published by AAAS

References and Notes

1. J. Austin, J. Wilson, F. Li, H. Vömel, *J. Atmos. Sci.* **64**, 905 (2007).
2. K. H. Rosenlof, G. C. Reid, *J. Geophys. Res.* **113**, D06107 (2008).
3. N. Butchart, *et al.*, *Clim. Dynam.* **27**, 727 (2006).
4. V. Grewe, *Atmos. Chem. Phys.* **6**, 1495 (2006).
5. N. Gillett, D. Thompson, *Science* **302**, 273 (2003).
6. D. W. J. Thompson, S. Solomon, *J. Climate* **18**, 4785 (2005).
7. W. J. Randel *et al.*, *J. Geophys. Res.* **111**, D12312 (2006).
8. P. M. Forster *et al.*, *Geophys. Res. Lett.* **34**, L23813 (2007).
9. W. J. Randel, R. R. Garcia, F. Wu, *J. Atmos. Sci.*, 10.1175/2008JAS2756.1 (2008).
10. M. A. Olsen, M. R. Schoeberl, J. E. Nielsen, *J. Geophys. Res.* **112**, D16104 (2007).
11. V. Eyring *et al.*, *J. Geophys. Res.* **112**, D16303 (2007).
12. V. I. Fomichev *et al.*, *J. Climate* **20**, 1121 (2007).
13. D. Rind, J. Lerner, J. Perlwitz, C. McLinden, M. Prather, *J. Geophys. Res.* **107**, 4800 (2002).
14. P. H. Haynes *et al.*, *J. Atmos. Sci.* **48**, 651 (1991).
15. A. M. Kerr-Munslow, W. A. Norton, *J. Atmos. Sci.* **63**, 1410 (2006).
16. R. A. Plumb, J. Eluszkiewicz, *J. Atmos. Sci.* **56**, 868 (1999).
17. R. R. Garcia, W. J. Randel, *J. Atmos. Sci.* **65**, 2731 (2008).
18. I. M. Dima, J. M. Wallace, *J. Atmos. Sci.* **64**, 2862 (2007).
19. R. Deckert, M. Dameris, *Geophys. Res. Lett.* **35**, L10813 (2008).

20. We thank H. Huntrieser for helpful comments. Further thanks go to R. Garcia, W. Randel, and F. Wu for sending their manuscripts.

10.1126/science.1163709

CHEMISTRY

A Light Touch Catalyzes Asymmetric Carbon-Carbon Bond Formation

The cooperation between a photoactivated catalyst and an organocatalyst enables a so far elusive stereoselective synthetic transformation.

Philippe Renaud and Paul Leong

One of the most formidable tasks in organic synthesis is the formation of carbon-carbon bonds, in part because the activation of the carbon atoms requires the control of highly reactive species. Not only must these reactions form the correct bond connectivity, but they usually need to produce one enantiomer (the left- or right-handed arrangement of functional groups around each carbon atom that acts as a stereogenic center). The α-alkylation of carbonyl compounds (those containing a C=O group) with alkyl halides is a classical method, but it works much better for ketones (two alkyl groups on the C=O) than for aldehydes (one alkyl and one H on the C=O) and often requires stoichiometric amounts of additional reagents to direct the handedness at the stereocenter. On page 77 of this issue, Nicewicz and MacMillan report a remarkable approach for the enantioselective α-alkylation of aldehydes that not only is catalytic but uses a photoredox cycle to control the formation of highly reactive intermediates (*1*).

Prior to this work, asymmetric versions of these α-alkylation reactions that yield preferentially one enantiomer relied heavily on the use of chiral auxiliaries, which help direct the stereochemistry of the product (*2*). However, chiral auxiliaries, in contrast to catalysts, are used in stoichiometric amounts, and additional steps are required for their attachment and removal. These considerations alone render the chiral auxiliary approach unsuitable for large-scale applications. Consequently, the development of catalytic systems that generate enantiomerically pure compounds by using a minimal amount of an environmentally friendly catalyst is a field of intensive research (*3*).

Given that aldehydes are among the most widely used building blocks in organic synthesis, α-alkylation reactions of aldehydes that are both catalytic and enantioselective would be highly desirable. Despite extensive efforts, such reactions have remained elusive until recently (*4*). The problem is that alkyl halides are only modestly reactive toward nucleophiles (reagents that form a new chemical bond by donating both bonding electrons), which necessitates the use of highly reactive aldehyde enolates. Because aldehyde enolates are difficult to prepare and are expected to react faster with the starting aldehydes than with an alkyl halide, a truly catalytic cycle is nearly impossible to achieve.

Nicewicz and MacMillan have proposed a solution to this challenging problem in which the difficult and slow ionic alkylation step (a two-electron process) has been replaced by rapid steps based on less stable open-shell molecules involving one-electron pathways. MacMillan's and Sibi's groups had already introduced the concept of organo-SOMO catalysis (one-electron processes that make use of SOMOs, singly occupied molecular orbitals) for enantioselective α-allylation (*5*, *6*), α-vinylation (*7*), and α-oxygenation (*8*) of aldehydes. However, a stoichiometric amount of oxidant is required to generate the

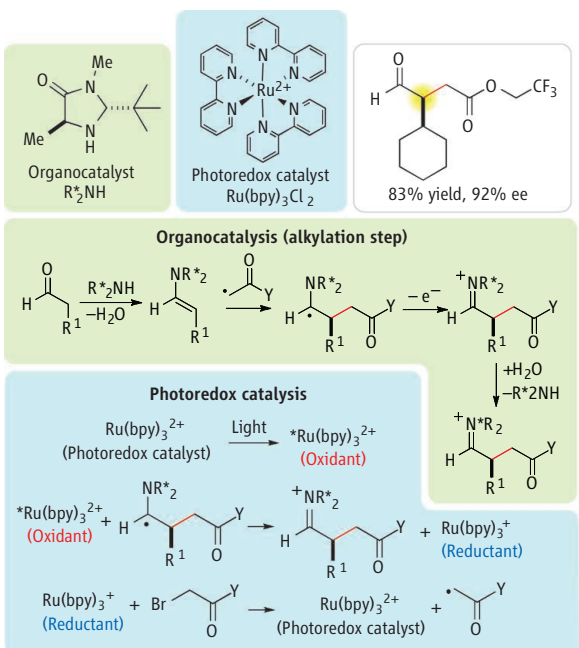

Asymmetric catalysis via one-electron steps. The steps of the organocatalytic reaction (green shading) are carefully intertwined with the photoredox cycle of $Ru(bpy)_3^{2+}$ (blue shading). The photoexcited state of $Ru(bpy)_3^{2+}$ readily oxidizes the radical resulting from the coupling of the activated alkyl halide and the enamine, which is generated by condensation of the aldehyde with the organocatalyst. The bulky chiral organocatalyst directs the approach of these reactants so that alkyl group R^1 has a preferred stereochemistry; hydrolysis recovers the final product. The photocatalyst, now $Ru(bpy)_3^{+}$, reduces the alkyl halide by one electron to create the radical (the activated species with an odd electron) as well as the initial $Ru(bpy)_3^{2+}$. (**Upper right**) A typical product, its yield, and enantiomeric excess (ee).

Department of Chemistry and Biochemistry, University of Berne, CH-3012 Berne, Switzerland. E-mail: philippe.renaud@ioc.unibe.ch; paul.leong@ioc.unibe.ch

Published by AAAS

radicals. This requirement represents a major drawback in terms of atom economy and waste production.

To address this limitation, Nicewicz and MacMillan have investigated ruthenium bipyridine complexes, which are well-established photoredox catalysts. Under irradiation with blue light, tris(bipyridine)ruthenium(II), $Ru(bpy)_3^{2+}$, forms a more reactive species, $*Ru(bpy)_3^{2+}$, an excited state in which an electron on the metal transfers to the bpy ligand, where it has enhanced oxidative and reducing power relative to the ground state (*9*).

Nicewicz and MacMillan elegantly combined this photoredox process (see the figure, blue shading) with organo-SOMO catalysis so that the desired transformation can occur in the correct sequence to generate enolate radicals by a reductive process, and, after coupling with the chiral enamine, oxidize the reaction product. Here, the radical needed in the organo-SOMO catalysis is obtained by a one-electron transfer that reduces an α-bromocarbonyl compound with a Ru(I) species, $Ru(bpy)_3^{+}$. The enolate radical possesses an electrophilic character and adds efficiently to the electron-rich chiral enamine (the aldehyde-organocatalyst condensation product) to form an intermediate 1-aminoalkyl radical. This radical is readily oxidized by the excited $*Ru(bpy)_3^{2+}$ back to the corresponding iminium ion, which upon hydrolysis yields the final product; the oxidation step also regenerates the $Ru(bpy)_3^{+}$ ion so that the photoredox catalytic cycle can begin again.

A key feature is that the alkylation step proceeds stereoselectively because of the presence of the chiral secondary amine organocatalyst, which, after condensation with the aldehyde, gives an enamine that helps direct the approach of the incoming radical. Despite the delicately intertwined organo-photoredox catalytic cycles, this reaction is technically simple. It can be performed even with a household 15-W fluorescent light, with no external heating or cooling of the reaction mixture. For example, typical reaction conditions use a relatively high organocatalyst loading (20 mol %) with a minute amount of the photoredox catalyst (0.5 mol %). Indeed, alkylation of a series of aliphatic aldehydes with bromomalonates, α-bromoesters, and α-bromo-β-ketoesters occurs in excellent yield (63 to 93%) and with high stereochemical control (enantiomeric excess up to 99%) in all cases, even where two stereocenters are created (see the figure, upper right panel).

The selectivities for one enantiomer rival those observed for the classical ionic and concerted reactions, dispelling the previous notion that the high reactivity of radicals precludes their use in catalytic asymmetric synthesis. The cooperation of organo-SOMO catalysis and photoredox catalysis offers many possibilities for asymmetric transformations. A burgeoning field of research is likely to emerge from this seminal work.

References

1. D. A. Nicewicz, D. W. C. MacMillan, *Science* **322**, 77 (2008); published online 4 September 2008 (10.1126/science.1161976).
2. S. Bräse, M. Christmann, Eds., *Asymmetric Synthesis—The Essentials* (Wiley-VCH, Weinheim, Germany, 2007).
3. E. N. Jacobsen, A. Pfaltz, H. Yamamoto, Eds., *Comprehensive Asymmetric Catalysis I–III with Supplements 1 and 2* (Springer, Berlin, 2004).
4. For an intramolecular alkylation reaction, see N. Vignola, B. List, *J. Am. Chem. Soc.* **126**, 450 (2004).
5. T. D. Beeson, A. Mastracchio, J.-B. Hong, K. Ashton, D. W. C. MacMillan, *Science* **316**, 582 (2007); published online 28 March 2007 (10.1126/science.1142696).
6. H. Y. Jang, J. B. Hong, D. W. MacMillan, *J. Am. Chem. Soc.* **129**, 7004 (2007).
7. H. Kim, D. W. MacMillan, *J. Am. Chem. Soc.* **130**, 398 (2008).
8. M. P. Sibi, M. Hasegawa, *J. Am. Chem. Soc.* **129**, 4124 (2007).
9. A. Juris *et al.*, *Coord. Chem. Rev.* **84**, 85 (1988).

10.1126/science.1164403

BIOCHEMISTRY

Not Comparable, But Complementary

New studies increase the number of protein-protein interactions but show little overlap. This is not a bad thing, though.

Lars Juhl Jensen[1,2] and Peer Bork[1,3]

It took many years between the introduction of DNA sequencing technologies in the mid-1970s and completion of the first genome sequences in the mid-1990s. Connecting the one-dimensional "parts lists" encoded within genomes—the proteins—into two-dimensional interaction maps is an even more daunting task, despite the introduction in the late 1980s of the yeast two-hybrid assay to identify protein–protein interactions (*1*) and high-throughput versions of this technology at the turn of the millennium (*2*, *3*). On page 104 in this issue, Yu *et al.* (*4*) identify 1809 interactions in the model organism budding yeast, of which more than 1500 are new relative to the early yeast two-hybrid studies (*2*, *3*). Together with the 2770 interactions recently determined by Tarassov *et al.* by a protein complementation assay (*5*), almost all of which are new, the number of binary interactions has more than tripled relative to earlier analyses (*2*, *3*). These studies bring us closer to a complete map of biophysical interactions in a single organism, and hence to the ultimate goal of functional understanding of the cellular machinery in space and time (*6*).

To document the quality of the identified interactions, the two groups performed extensive quality assessments, both on an absolute scale and relative to earlier large-scale studies. According to their estimates, only a few percent of the newly identified interactions are false-positives, which is more than an order of magnitude lower than suggested by previous quality assessments of large-scale yeast two-hybrid experiments (*7*, *8*). However, a direct comparison of those numbers is difficult and potentially confusing because each group used a different "gold standard" of known interacting and noninteracting protein pairs. Whereas Yu *et al.* take into account the genome-wide estimate for the number of interacting protein pairs relative to noninteracting ones, the standard used by Tarassov *et al.* is more than 40-fold enriched for interactions. This implicitly lowers the number of false-positives and hence inflates the estimated precision, which drops from 98.2% to around 50% if corrected for this bias. However, the latter value is overly pessimistic because the authors' reference set disfavors binary interaction assays.

A comparison of numbers becomes even more difficult when considering assays such as tandem affinity purification (*9*), which copurify proteins that are parts of the same complex. Four years after the first large-scale

[1]European Molecular Biology Laboratory, D-69117 Heidelberg, Germany. [2]The Novo Nordisk Foundation Centre for Protein Research, University of Copenhagen, DK-2200 Copenhagen, Denmark. [3]Max-Delbrück-Centre for Molecular Medicine, D-13092 Berlin, Germany. E-mail: peer.bork@embl.de

protein-protein interaction screens in 2002 (*10*, *11*), two genome-wide studies reported 491 and 547 protein complexes (containing more than two proteins) (*12*, *13*), respectively, and a total of 12,292 protein interactions can be inferred from the respective purifications. Yu *et al.* compared these inferred interactions and the nearly 3000 new and old interactions identified by the yeast two-hybrid assay (*2*–*4*) to their binary interaction gold standard and found the two-hybrid assay to be more precise than tandem affinity purification. Conversely, tandem affinity purification performs much better than the two-hybrid assay when using gold standards based on protein complexes (*4*, *5*, *7*, *8*). These results may seem contradictory, but as alluded to by Yu *et al.*, the approaches are in fact complementary: Binary interaction assays are better at identifying binary interactions, and complex purification assays are better at identifying co-complex interactions (all protein pairs that are part of the same complex) (*4*). The former provides evidence for direct interactions, whereas the latter allows the binary network to be subdivided into biologically relevant units (that is, complexes).

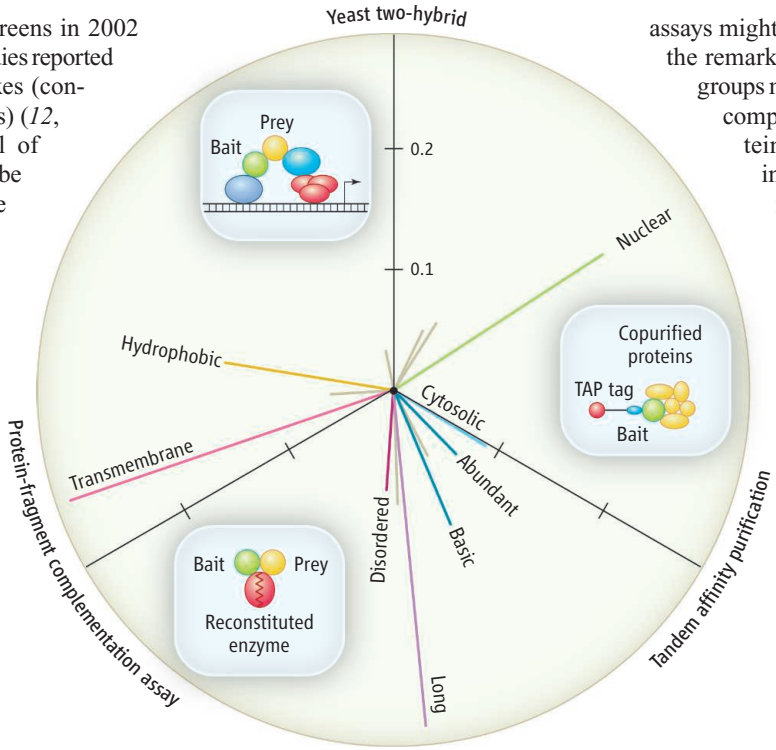

Protein preferences. The three methods shown for detecting protein interactions function in fundamentally different ways and hence have different physiochemical constraints. Of 15 protein features tested for biases between the sets of proteins for which interactions were identified by each assay, 8 differed significantly (false-positive rate of <0.001): presence of transmembrane helices, hydrophobicity, nuclear and cytosolic localization, abundance, predicted isoelectric point, length, and intrinsic disorder. The other seven protein features are shown in gray. The average normalized scores (*Z* scores) for each of these features are shown, projected onto a plane in which each axis corresponds to one of the three methods for detecting interactions. The length of each line thus represents the strength of the bias.

Although the conceptual difference might account for the poor agreement between the binary and the complex-purification methods, the only 63 interactions common between yeast two-hybrid (*2*–*4*) and protein complementation assay (*5*) screens likely reflect hidden physiochemical constraints inherent to each method. Thus, the different methods might simply capture interactions for different subsets of proteins. This complementation can be confirmed by biases in the types of proteins for which interactions were detected by each assay (see the figure). The most striking trend is that the protein complementation assay has been much better at detecting interactions for transmembrane (and thus hydrophobic) proteins than the other two assays, which Tarassov *et al.* highlight as one of its major strengths. Conversely, the yeast two-hybrid assay and tandem affinity purification both detect interactions for a higher proportion of nuclear proteins, which for the two-hybrid screen is to be expected, because the assay inherently functions inside the nucleus. Notably, interactions from low-throughput studies (*14*) are similarly biased toward nuclear proteins compared to all yeast proteins. Long proteins, unstructured proteins, and proteins with high isoelectric points are underrepresented among the interactions detected by the yeast two-hybrid assay, whereas tandem affinity purification shows a weak but statistically significant preference for abundant proteins and cytosolic proteins, as shown in the original studies (*12*, *13*), many of which form large stable complexes.

Because the tandem affinity purification approach is close to saturation in terms of protein coverage and, with the study by Yu *et al.*, most yeast proteins have now also been subjected to the two-hybrid assay, the apparent methodological complementation might suggest ways to improve the binary interaction map, because proteins amenable to a certain assay can be examined in greater depth. To improve coverage of interactions, numerous protein-specific optimizations of the existing assays might be necessary in the future, and the remarkable progress reported by both groups might be the last big step toward a complete catalog of all possible protein–protein interactions in budding yeast, which are estimated to number between 18,000 (*4*) and 30,000 (*7*, *8*).

Despite the challenging task of characterizing the complete binary "interactome," it is only a static, two-dimensional representation, because the interactions will never all happen at the same time in the same place. Spatial and temporal data will therefore be needed to decipher where and when an interaction takes place; for example, the interaction network changes considerably during the cell division cycle or other dynamic processes (*15*). Furthermore, interactions among proteins constitute only one part of the interactome, because associations to other biopolymers (including DNA and RNA), large lipids, and small molecules have to be considered. Finally, the directionality and functionality of the interactions need to be considered as observed, for example, in signaling networks. The growing high-quality interaction map of a model organism, highlighted by Yu *et al.* and Tarassov *et al.* provides the first layer of context to the "parts lists" and lays the foundation for integrating additional spatial, temporal, and functional dimensions necessary for a comprehensive understanding of the eukaryotic cell.

References

1. S. Fields, O. Song, *Nature* **340**, 245 (1989).
2. T. Ito *et al.*, *Proc. Natl. Acad. Sci. U.S.A.* **97**, 1143 (2000).
3. P. Uetz *et al.*, *Nature* **403**, 623 (2000).
4. H. Yu *et al.*, *Science* **322**, 104 (2008); published online 21 August 2008 (10.1126/science.1158684).
5. K. Tarassov *et al.*, *Science* **320**, 1465 (2008).
6. P. Bork, L. Serrano, *Cell* **121**, 507 (2005).
7. C. von Mering *et al.*, *Nature* **417**, 399 (2002).
8. J. S. Bader, A. Chaudhuri, J. M. Rothberg, J. Chant, *Nat. Biotechnol.* **22**, 78 (2004).
9. G. Rigaut *et al.*, *Nat. Biotechnol.* **17**, 1030 (1999).
10. A.-C. Gavin *et al.*, *Nature* **415**, 141 (2002).
11. Y. Ho *et al.*, *Nature* **415**, 180 (2002).
12. A.-C. Gavin *et al.*, *Nature* **440**, 631 (2006).
13. N. J. Krogan *et al.*, *Nature* **440**, 637 (2006).
14. T. Reguly *et al.*, *J. Biol.* **5**, 11 (2006).
15. U. de Lichtenberg, L. J. Jensen, S. Brunak, P. Bork, *Science* **307**, 724 (2005).

10.1126/science.1164801

The Origin and Evolution of Religious Prosociality
Ara Norenzayan, *et al.*
Science **322**, 58 (2008);
DOI: 10.1126/science.1158757

The Origin and Evolution of Religious Prosociality

Ara Norenzayan* and Azim F. Shariff

We examine empirical evidence for religious prosociality, the hypothesis that religions facilitate costly behaviors that benefit other people. Although sociological surveys reveal an association between self-reports of religiosity and prosociality, experiments measuring religiosity and actual prosocial behavior suggest that this association emerges primarily in contexts where reputational concerns are heightened. Experimentally induced religious thoughts reduce rates of cheating and increase altruistic behavior among anonymous strangers. Experiments demonstrate an association between apparent profession of religious devotion and greater trust. Cross-cultural evidence suggests an association between the cultural presence of morally concerned deities and large group size in humans. We synthesize converging evidence from various fields for religious prosociality, address its specific boundary conditions, and point to unresolved questions and novel predictions.

Religious prosociality, or the idea that religions facilitate acts that benefit others at a personal cost, has many proponents. Indeed, religious texts of all major religions explicitly encourage prosociality in their adherents (*1*, *2*). Social science theories have long pointed to religion as a cultural facilitator of social cohesion and ingroup solidarity (*3*, *4*), often at the expense of rival groups. However, opinion, rather than careful observation, has dominated the debate on religion's role in prosocial behavior. Recent years have seen new developments in evolutionary explanations of religion, bolstered by a small but growing empirical base that unites several academic disciplines. Here, we critically examine and synthesize evidence from anthropology, sociology, experimental psychology, and experimental economics for religious prosociality. We also address empirical inconsistencies found in studies examining the association between religion and prosociality, offer possible resolutions, and point to remaining issues and future directions.

Various evolutionary theories of religion all predict that religious beliefs and behaviors have facilitated human prosocial tendencies, but there is no scientific consensus yet as to exactly how this might have occurred. Some argue that at least certain religious beliefs and behaviors are evolutionary adaptations for group-living in large communities that have maximized genetic fitness (*5*), perhaps even by multilevel selection (*4*). However, these accounts have difficulty explaining the differential cultural distribution and cultural change over time of religious beliefs and behaviors. Two additional evolutionary accounts, however, are compatible with such cultural variability. One proposes that religious content itself is a cultural by-product of a suite of psychological tendencies evolved in the Pleistocene for other purposes, such as detecting and inferring the content of other minds and sensitivity to one's prosocial reputation in the group (*6*, *7*). Religious beliefs, to the extent that they were compatible with these psychological tendencies, could then culturally spread through social learning mechanisms and could solve adaptive problems, particularly the problem of cooperation in large groups. A third evolutionary perspective, known as cultural group selection (*8*), maintains that competition among social groups may favor the spread of fitness-enhancing cultural beliefs and costly practices, such as religious prosociality (*4*, *9*, *10*). This last-mentioned view takes as its starting point that religious beliefs are cultural by-products of evolved psychology, but argues that reputation-sensitivity, although important, is not sufficient to explain the features of strong prosocial tendencies such as the ones found in religious behavior.

Despite these important differences, large agreement is emerging that selective pressures over the course of human evolution can explain the wide cross-cultural reoccurrence, historical persistence, and predictable cognitive structure of religious beliefs and behaviors. The tendency to detect agency in nature likely supplied the cognitive template that supports the pervasive belief in supernatural agents (*6*, *7*, *11*). These agents are widely believed to transcend physical, biological, and psychological limitations (*6*, *7*). However, other important details are subject to cultural variation. Although in many societies supernatural agents are not directly concerned with human morality, in many others, morally concerned agents use their supernatural powers to observe and, in some cases, to punish and reward human social interactions. Examples include the God of Abrahamic religions and Viracocha, the Incan supreme God, but also many morally concerned deities found in traditional societies, such as the *adalo*, ancestral spirits of the Kwaio Solomon islanders (*7*). These beliefs are likely to spread culturally to the extent that they facilitate ingroup cooperation. This could occur by conforming to individual psychology that favors reputation-sensitive prosocial tendencies, as the by-product account holds; by competition among social groups, as the cultural group selection account would suggest; or possibly by some combination of the two. Religious behaviors and rituals, if more costly to cooperating group members than to freeloaders, may have reliably signaled the presence of devotion and, therefore, cooperative intention toward ingroup members, in turn, buffering religious groups against defection from freeloaders and reinforcing cooperative norms. Religious prosociality, thus, may have softened the limitations that kinship-based and (direct or indirect) reciprocity-based altruism place on group size. In this way, the cultural spread of religious prosociality may have facilitated the rise of stable, large, cooperative communities of genetically unrelated individuals.

The acute human sensitivity to prosocial reputation (*12*) is a psychological mechanism, originally unrelated to religion, that evolved to facilitate strong reciprocal cooperative bonds within groups (*13*). In an intensely social, gossiping species, reputational concerns likely contributed to the evolutionary stability of strong cooperation between strangers. Individuals known to be selfish could be detected, subsequently excluded from future interaction, and even actively punished (*13*, *14*). The threat of being found out, therefore, became a potent motivator for good behavior. Accordingly, studies have repeatedly shown that experimentally reducing the degree of anonymity in economic games increases the rate of prosocial behavior (*15*). Exposure to photographic and even schematic representations of human eyes increases prosocial behavior in economic games (*16*) and decreases cheating in naturalistic settings (*17*). We argue that religion's effect on prosocial tendencies similarly depends on such reputational sensitivity. The cognitive awareness of gods is likely to heighten prosocial reputational concerns among believers, just as the cognitive awareness of human watchers does among believers and nonbelievers alike (*18*). However, supernatural monitoring, to the degree that it is genuinely believed and cognitively salient, offers the powerful advantage that cooperative interactions can be observed even in the absence of social monitoring.

This line of reasoning accounts for a wide range of empirical evidence linking religion to prosocial tendencies and predicts that this association ought to be context-sensitive, with clear boundary conditions. First, religious devotion, insofar as it involves habitual worship of morally vigilant deities, is expected to be associated with greater prosocial reputational concern. Second, religious situations, such as religious ritual performance or being in religious

Department of Psychology, University of British Columbia, 2136 West Mall, Vancouver, BC V6T 1Z4, Canada.

*To whom correspondence should be addressed. E-mail: ara@psych.ubc.ca

surroundings, would, in societies with morally concerned deities, activate thoughts of these deities and habitually facilitate prosocial behavior. Therefore, experimentally inducing religious thoughts would also increase prosociality even when the situation is objectively anonymous. But this should be the case only when thoughts of morally concerned supernatural agents are cognitively accessible in the moment when prosocial decisions are called for. Third, religious behavior that signals genuine devotion would be expected to mobilize greater cooperation and trust, and when internal and external threats to group survival are high, religious groups would be expected to outlast secular ones. Fourth, large societies that have successfully stabilized high levels of cooperative norms would be more likely than smaller ones to espouse belief in morally concerned gods who actively monitor human interactions. In the remainder of this paper, we critically examine the available empirical evidence in light of these four predictions.

Self-Reports: Religiosity and Charitability

If religions centered around moralizing gods promote prosociality, it would be expected that individuals who report stronger belief in such gods would have stronger altruistic tendencies. Sociological surveys suggest that this is the case. Those who frequently pray and attend religious services reliably report more prosocial behavior, such as charitable donations and volunteerism (*1*, *19*). This "charity gap" is consistent across surveys and remains after controlling for income disparities, political orientation, marital status, education level, age, and gender. These findings have been much publicized as evidence that religious people are more prosocial than the nonreligious (*19*). However, it remains unresolved whether this charity gap persists beyond the ingroup boundaries of the religious groups (*1*). More importantly, these surveys are entirely based on self-reports of prosocial behavior. Psychologists have long known that self-reports of socially desirable behaviors (such as charitability) may not be accurate, reflecting instead impression management or self-deception (*20*). If, as we hypothesize, religious individuals are more motivated to maintain a prosocial reputation than the nonreligious, then the former may be more likely to engage in prosocial reputation management. Supporting this hypothesis, psychological research summarizing many studies has found that measures of religiosity are positively associated with tests of socially desirable responding, a common human tendency to project an overly positive image of oneself in evaluative contexts (*21*). This association raises questions about the validity of self-report measures of prosocial behavior. To address these methodological limitations, experiments with behavioral outcomes must be consulted.

Behavioral Evidence: In Search of the Good Samaritans

In several behavioral studies, researchers failed to find any reliable association between religiosity and prosocial tendencies. In the classic "Good Samaritan" experiment (*22*), for example, researchers staged an anonymous situation modeled after the Biblical parable—a man was lying on a sidewalk appearing to be sick and in need of assistance (Fig. 1). Participants varying in religiousness were led to pass by this victim (actually a research confederate) on their way to complete their participation in a study. Unobtrusively recorded offers of help showed no relation with religiosity in this anonymous context (*22*). Only a situational variable—whether participants were told to rush or take their time—produced differences in helping rates.

Fig. 1. In the parable of *The Good Samaritan* [painting by Jacopo Bassano, d. 1592, copyright 2006, The National Gallery, London], Christ preaches universal compassion and prosocial behavior. A similar message is found in many religions. Modern research from social psychology, experimental economics, and anthropology suggests, however, that religious prosociality is extended discriminately and only under specific conditions.

Other behavioral studies, however, have found reliable associations between religiosity and prosociality, but under limited conditions. In one study (*23*), researchers compared levels of cooperation and coordination between secular and religious kibbutzim in Israel. In this economic game, two members of the same kibbutz who remained anonymous to each other were given access to an envelope with a certain amount of money. Each participant simultaneously decided how much money to withdraw from the envelope and keep. Players only kept the money they requested if the sum of the requests did not exceed the total amount in the envelope. If it did, the players received nothing. The results showed that, controlling for relevant predictors, systematically less money was withdrawn in the religious kibbutzim than in the secular ones (*23*).

Thus, unlike studies such as the Good Samaritan, there were greater levels of prosociality among the religious in this study. One key difference is that reminders of God are likely to be chronically present in religious kibbutz, where religious prayer and attendance are a daily part of life. Another, is that prosociality in the religious kibbutz was clearly confined to the ingroup. In the kibbutzim study, highly religious men, who engaged in daily and communal prayer, took the least money, thereby showing the greatest amount of coordination and/or cooperation with ingroup members. It is also possible that regular, communal prayer involves public ritual participation, which, independent of religious devotion, might also encourage more prosociality.

Another approach to clarifying the nature and boundary conditions of religious prosociality is to investigate the altruistic or egoistic motivation underlying the prosocial act. One possibility holds that the greater prosociality of the religious is driven by an empathic motive to ameliorate the condition of others. Alternatively, prosocial behavior could be driven by egoistic motives, such as projecting a prosocial image or avoiding guilt (failing to live up to one's prosocial self-image). The preponderance of the evidence supports the latter explanation. Studies repeatedly indicate that the association between conventional religiosity and prosociality occurs primarily when a reputation-related egoistic motivation has been activated (*2*). In one experiment, for example, participants were given the option of volunteering to raise money for a sick child who could not pay his medical bills (*24*). Participants in one condition were led to believe that they would certainly be called upon if they volunteered. In

another, participants could volunteer although told that they were unlikely to be called upon. In the latter condition, participants could reap the social benefits of feeling (or appearing) helpful without the cost of the actual altruistic act. Only in the latter situation was a link between religiosity and volunteering evident. Many studies have corroborated that religiosity predicts prosocial behavior primarily when the prosocial act could promote a positive image for the participant, either in his or her own eyes or in the eyes of observers (*2*).

As insightful as these behavioral studies are, however, causal inference has been limited by their reliance on correlational designs. If religiosity is related to prosocial behavior under some contexts, it is possible that having a prosocial disposition causes one to be religious or that a third variable (such as dispositional empathy or being prone to guilt) causes both prosocial and religious tendencies. Recent controlled experiments have addressed this limitation by experimentally inducing thoughts of supernatural agents and then measuring prosocial behavior.

Experimental Evidence: When Gods Are on Our Minds

In one such experiment (*25*), university students who were randomly assigned to a condition in which they were casually told that the ghost of a dead student had been spotted in the experimental room, cheated less on a rigged computer task. A different study conceptually replicated this effect—temporary, unconscious activation of God concepts lowered rates of cheating (*26*). Moreover, among those in the control condition, religiosity as an individual difference measure did not predict levels of cheating. In another experiment, children were explicitly instructed not to look inside a box, and then left alone in the room with it (*25*). Those who were previously told that a fictional supernatural agent—Princess Alice—was watching were significantly less likely to peek inside the forbidden box.

We have proposed that the cultural spread of religious prosociality may have promoted stable levels of cooperation in large groups, where reputational and reciprocity incentives are insufficient. If so, then reminders of God may not only reduce cheating, but may also increase generosity toward strangers as much as reminders of secular institutions promoting prosocial behavior. These hypotheses were supported in two anonymous economic game experiments, one with a sample of university students and another with nonstudent adults (*27*) (Fig. 2).

Thoughts of God, activated without conscious awareness (*28*), thus caused greater generosity between anonymous strangers. One explanation for this finding is that the imagined presence of a morally concerned supernatural watcher reduced the anonymity of the situation and heightened prosocial reputational concerns, thereby increasing prosocial behavior. Alternatively, it is possible that thoughts of God and thoughts of charity or benevolence are cognitively associated; thus, priming the former concept increased behavioral tendencies consistent with the latter (*27*). This explanation, however, begs the question as to why God concepts are mentally associated with charity in the first place. These alternative explanations await further experimental investigation. In either case, the effect occurred only to the extent that thoughts of a morally concerned divine agent were activated in the moment of decision-making. Self-reported belief in God or self-reported religious devotion was, as has been found before, not a reliable predictor of generous behavior in anonymous settings.

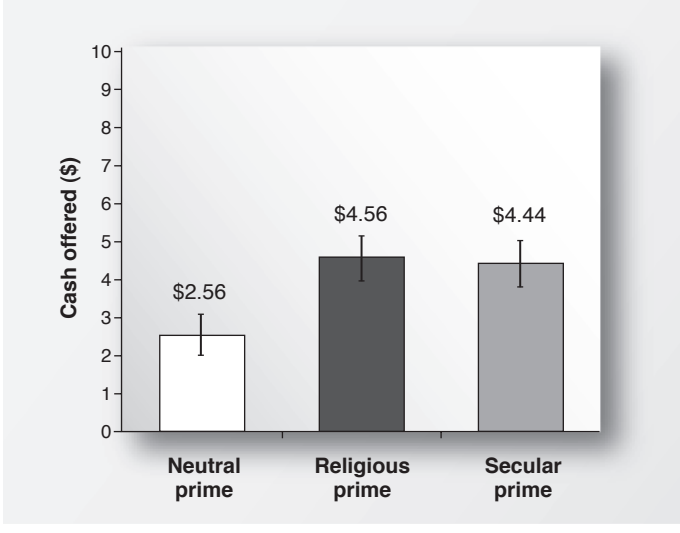

Fig. 2. Implicit activation of God concepts, relative to a neutral prime, increased offers in the one-shot, anonymous Dictator Game, $t(48) = 2.47$, $P = 0.02$, SE = 0.81, $d = 0.71$. (27). Priming secular concepts indicating moral authority had a similar effect, $t(48) = 2.29$, $P = 0.03$, SE = 0.82, $d = 0.67$. The results showed not only a quantitative increase in generosity, but also a qualitative shift in social norms. In the control group, the modal response was selfishness, a plurality of players pocketed all $10. In the God group, the mode shifted to fairness, a plurality of players split the money evenly ($N = 75$). It remains to be seen, however, whether these effects would occur if the recipient was clearly marked as an outgroup member.

Religious Prosociality, Costly Signaling, and Trust

In the absence of reputational information about a stranger's prosocial inclinations, outward evidence of sincere belief in the same or similar morally concerned gods may serve as a reliable cooperative signal. But a signal is only reliable to the extent that it is difficult to fake by potential freeloaders. Because professions of religious belief can be easily faked, theorists of religion have recognized that evolutionary pressures must have favored costly religious commitment, such as ritual participation and various restrictions on behavior, diet, and life-style, that validates the sincerity of otherwise unobservable religious belief (*5*, *29*). However, for costly signals to evolve as a stable strategy, religious behaviors ought to be more costly for cooperators than for freeloaders, and variation in costliness should predict degree of intragroup trust and cooperation. Mathematical models question the possibility that costly signaling as an individual fitness-maximizing strategy extends to nondyadic collective cooperation as in the case of religion (*9*, *10*), and models of costly signaling applied to religious behavior, with or without cultural group selection, are currently in their infancy (*30*). Nevertheless, qualitative and quantitative evidence is emerging, that, although not yet definitive, addresses parts of these predictions.

Attitudinal surveys show that religious individuals are perceived to be more trustworthy and more cooperative (*31*). From behavioral evidence, ethnographic examples such as the spread of Islam in Africa, which preceded the flourishing of wide-scale trade among Muslim converts (*32*), and the trade networks of Medieval Jewish Maghrebi merchants (*33*) are consistent with this idea. Costly commitment to the same supernatural deity may have lowered monitoring costs and fostered cooperation in communities spread across geographic and even ethnic boundaries. However, it is disputable whether membership in these religious groups was costlier than commitment to local deities or whether costliness was directly associated with greater intragroup trust; therefore, the ethnographic data are open to other interpretations, for example, that religious conversions led to greater access to preestablished trade networks along these religious lines.

To address these limitations, quantitative analyses are needed. Sociological analyses are consistent with the idea that religious groups imposing more costly requirements have members who are more committed. Controlling for relevant sociodemographic variables, "strict" Protestant (e.g., Mormon) and Jewish denominations (Orthodox) show higher levels of church and synagogue attendance and more monetary contributions to their religious communities (despite lower average income levels) than less strict ones (Methodist and Reform, respectively) (*30*). However, these findings do not demonstrate that strictness predicts community survival and growth. One systematic attempt to do so examined religious and secular communes in 19th-century America, whose survival de-

pended upon solving the collective action problem. Religious communes were found to outlast those motivated by secular ideologies, such as socialism (Fig. 3) (*29*). A further quantitative analysis of 83 of these religious and secular communes (*34*) for which more detailed records are available found that religious communes imposed more than twice as many costly requirements (including food taboos and fasts, constraints on material possessions, marriage, sex, and communication with the outside world) than secular ones. This difference emerged for each of the 22 categories of costly requirements examined. Importantly for costly religious signaling, the number of costly requirements predicted religious commune longevity (R^2 = 0.38) after the study controlled for population size and income and the year the commune was founded, although the number of costly requirements did not predict longevity for secular communes. Finally, religious ideology was no longer a predictor of commune longevity, once the number of costly requirements was statistically controlled, which suggests that the survival advantage of religious communes was due to the greater costly commitment of their members, rather than other aspects of religious ideology. However, these findings are correlational, making causal conclusions premature. They collectively imply, but do not definitively demonstrate, that the greater longevity of religious communes with costlier requirements was due to greater intragroup cooperation and trust levels, which have not been measured directly. These results also imply that greater costly commitment is at best a partial explanation as to why religious communes outlasted secular ones. Other aspects of religion that might promote greater community stability are open for investigation.

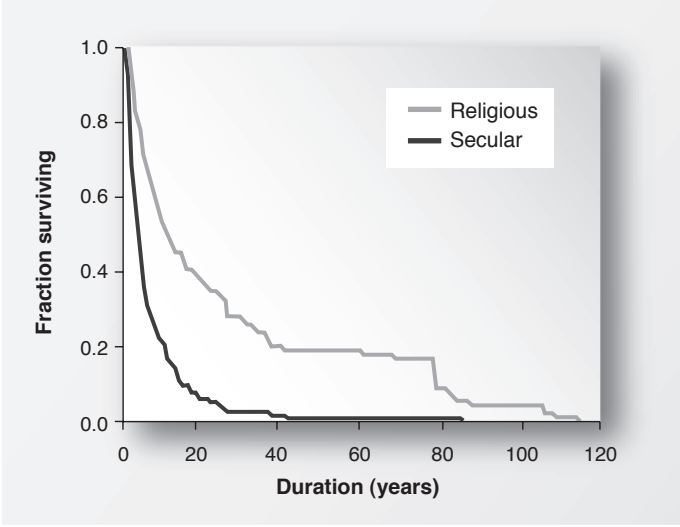

Fig. 3. Life expectancy of religious versus secular communes. An analysis of 200 religious and secular communes in 19th-century America (*29*), for every year of their life course, religious communes were about four times as likely to survive than their secular counterparts, log rank *T* statistic = 40.14, df = 1, $P < 0.00001$. This difference remained after statistically controlling for type of commune movement, year founded, and year at risk of dissolution (the last control assesses major historical trends that may independently impact commune dissolution). [Copyright 2003, reprinted from (*29*) with permission of Wiley-Liss, Inc., a subsidiary of John Wiley & Sons, Inc.]

The few relevant laboratory studies corroborate that there is an empirical association between religion and trusting behavior. Trust can be operationalized as a costly investment in a person or entity, with the future expectation of return. In one well-researched laboratory game of trust (*35*), participants were randomly assigned to be a proposer (truster) or a responder (trustee). In the first step, the proposer decides how much money to forward to the responder, which gets multiplied. In the second step, the responder decides how much money to send back to the proposer. By transferring money to the responder, the proposer stands to gain, but only if the responder can be trusted to reciprocate. In a variation of this trust experiment (*36*), researchers measured individual differences in the religiosity of the proposer and the responder. In addition, in some trials, proposers knew about the level of religiosity of the responder in an anonymous context. Results indicated that more money was forwarded to responders perceived to be religious, and this was particularly true for religious proposers. Furthermore, religious responders were more likely to reciprocate the proposer's offer than less religious responders. These findings are consistent with the idea that outward evidence of religious devotion may engender more trust, although two issues remain unresolved: They do not show that costly religious behavior elicits more trust and cooperation than less costly behavior under controlled conditions, as required by costly signaling explanations of religion; or that members of religious groups that impose more costly requirements are more trusting and less likely to take advantage of others, particularly ingroup members, as would be expected from cultural group selection accounts.

The relation between religion and trust is, therefore, an area ripe for more research. Experimental studies and alternative mathematical models of costly religious behavior (either as a stable strategy characteristic of individuals or as a stable strategy that takes into account intergroup social competition) will place these theoretical predictions on firmer empirical ground. The existing evidence, however, suggests the possibility that religious belief, to the extent that it could be advertised with sincerity, may enhance within-group interpersonal trust, lower monitoring costs, and so further reinforce intragroup prosocial tendencies. Belief in morally concerned gods may stabilize prosocial norms even in the absence of social monitoring mechanisms. This, in turn, would be expected to expand the reach of such norms, facilitating the emergence of larger cooperative communities which otherwise would be vulnerable to collapse. We examine this hypothesized association between moralizing gods and large group size next.

Big Groups, Big Gods: Cross-Cultural Evidence

From large village settlements at the dawn of agriculture to modern metropolises today, human beings are capable of living in extraordinarily large cooperative groups. However, extrapolating from cross-species comparisons of neocortex size, it has been estimated that human group sizes cannot exceed 150 individuals before groups divide or collapse (*37*). Although this specific number has been disputed (*38*), and whereas some Pleistocene foragers possibly lived in large villages, it is apparent that the size of human settlements since the end of the Pleistocene far exceed the limitations that kin-based and reciprocity-based altruism place on group size.

Cultural evolution, driven by between-group competition for resources and habitats, has favored large groups. However, large groups, which until recently lacked institutionalized social-monitoring mechanisms, are vulnerable to collapse because of high rates of freeloading (*13*). If unwavering and pervasive belief in moralizing gods buffered against such freeloading, then belief in such gods should be more likely in larger human groups where the threat of freeloading is most acute. Because there is considerable variability in the cultural distribution of morally concerned deities, researchers could measure whether this variability correlates with group size across cultures. In a quantitative cross-cultural analysis of the 186 societies in the Standard Cross-Cultural Sample, this prediction was confirmed. The larger the group size, the more likely the group culturally sanctioned deities who are directly concerned about human morality (*39*). Although most cultures in the world do not promote morally concerned deities, those that do tend to have disproportionately larger populations. As a consequence, the majority of religious adherents in the world worship moralizing gods.

One alternative explanation is that Christian and Muslim missionary activity may have caused both more belief in the moralizing Abrahamic God and may have favored larger group size. Another, is that because large societies are more socially stratified, belief in moralizing gods serves to preserve political and economic inequality. However, although missionized societies and caste-stratified societies were indeed more likely to endorse a moralizing God, the association between large group size and the prevalence of

moralizing Gods remained strong even after statistically controlling for missionary activity and for two indicators of societal inequality, as well as for population density and geographic region. Similarly, controlling for the cultural diffusion of moralizing Gods via Christian and Muslim missionary activity, society size, population size, and societal inequality, moralizing gods are more likely in societies with high water scarcity—where the threat to group survival, and the need to minimize freeloading, is also pronounced (*40*). The cross-cultural evidence suggests that moralizing gods are culturally stabilized when freeloading is more prevalent or particularly detrimental to group stability. However, further empirical research is needed to clarify causal direction and to distinguish between alternative explanations for these associations.

Conclusions, Outstanding Questions, and Future Directions

Many religious traditions around the world explicitly encourage the faithful to be unconditionally prosocial (*1*, *2*); yet, theoretical considerations and empirical evidence indicate that religiously socialized individuals should be, and are, much more discriminating in their prosociality (*2*). Although empathy and compassion as social-bonding emotions do exist and may play a role in prosocial acts of religious and nonreligious individuals some of the time (*41*), there is little direct evidence to date that such emotions are systematically implicated in religious prosociality.

The preponderance of the evidence points to religious prosociality being a bounded phenomenon. Religion's association with prosociality is most evident when the situation calls for maintaining a favorable social reputation within the ingroup. When thoughts of morally concerned deities are cognitively salient, an objectively anonymous situation becomes nonanonymous and, therefore, reputationally relevant, or alternatively, such thoughts activate prosocial tendencies because of a prior mental association. This could occur when such thoughts are induced experimentally or in naturalistic religious situations, such as when people attend religious services or engage in ritual performance. This explains why the religious situation is more important than the religious disposition in predicting prosocial behavior.

Although religions continue to be powerful facilitators of prosociality in large groups, they are not the only ones. The cultural spread of reliable secular institutions, such as courts, policing authorities, and effective contract-enforcing mechanisms, although historically recent, has changed the course of human prosociality. Consequently, active members of modern secular organizations are at least as likely to report donating to charity as active members of religious ones (*42*). Supporting this conclusion, experimentally induced reminders of secular moral authority had as much effect on generous behavior in an economic game as reminders of God (*27*), and there are many examples of modern, large, cooperative, and not very religious societies (such as those in Western and Northern Europe), that, nonetheless, retain a great degree of intragroup trust and cooperation (*43*).

Any one study we have discussed can be subject to alternative accounts; therefore, specific evidence should be interpreted with caution. Nevertheless, convergent evidence is emerging from several disciplines using different methods and procedures that supply different pieces of the religious prosociality puzzle. Despite the recent scientific progress in explaining the effects of religion on prosociality, open and important questions remain. In particular, more research is needed to address the costliness of religious and nonreligious rituals, and few studies have attempted to quantify these costs in relation to prosocial behavior. The finding that religiosity evokes greater trust underscores the need for more experimental and theoretical research, including mathematical modeling, to establish the specific conditions under which costly religious commitment could evolve as a stable individual strategy and whether these models need to take into account intergroup competition. More broadly, the extent to which religion is implicated in human cooperation, and the precise sequence of evolutionary developments in religious prosociality, remain open to lively scientific debate. Further progress on these issues will require concerted collaboration among historians, archaeologists, social scientists, and evolutionary biologists.

In recent years, moral psychology has received a great deal of scientific attention (*44*), and although most of the studies reviewed here concern behavioral outcomes, the relation between religious prosociality and moral intuitions and reasoning is ripe for further investigation. More direct research on the possible role of prosocial motivations, such as empathy and compassion, in religious prosociality are needed. Finally, we have seen that religious prosociality is not extended indiscriminately; the "dark side" of within-group cooperation is between-group competition and conflict (*45*). The same mechanisms involved in ingroup altruism may also facilitate outgroup antagonism. This is an area of no small debate, but scientific attention is needed to examine precisely how individuals and groups determine who are the beneficiaries of religious prosociality, and who its victims.

References and Notes

1. S. V. Monsma, *Interdiscipl. J. Res. Relat.* **3**, 3 (2007).
2. C. D. Batson, P. Schoenrade, W. L. Ventis, *Religion and the Individual* (Oxford Univ. Press, New York, 1993).
3. E. Durkheim, *The Elementary Forms of Religious Life* (Free Press, New York, 1995).
4. D. S. Wilson, *Darwin's Cathedral* (Univ. of Chicago Press, Chicago, 2002).
5. W. Irons, in *Evolution and the Capacity for Commitment*, R. Nesse, Ed. (Russell Sage Foundation, New York, 2001), pp. 292–309.
6. S. Atran, A. Norenzayan, *Behav. Brain Sci.* **27**, 713 (2004).
7. P. Boyer, *Religion Explained* (Basic Books, New York, 2001).
8. Cultural group selection is based on precise mathematical models and can overcome the theoretical and empirical difficulties often associated with arguments for genetic group selection, see (*9*, *10*).
9. R. Boyd, P. Richerson, *J. Theor. Biol.* **215**, 287 (2002).
10. N. S. Henrich, J. Henrich, *Why Humans Cooperate: A Cultural and Evolutionary Explanation* (Oxford Univ. Press, Oxford, 2007).
11. S. Guthrie, *Faces in the Clouds* (Oxford Univ. Press, Oxford, 1993).
12. E. Fehr, U. Fischbacher, *Nature* **425**, 785 (2003).
13. H. Gintis, S. Bowles, R. Boyd, E. Fehr, *Evol. Hum. Behav.* **24**, 153 (2003).
14. J. Henrich *et al.*, *Science* **312**, 1767 (2006).
15. E. Hoffman, K. McCabe, V. L. Smith, *Am. Econ. Rev.* **86**, 653 (1996).
16. K. J. Haley, D. M. T. Fessler, *Evol. Hum. Behav.* **26**, 245 (2005).
17. M. Bateson, D. Nettle, G. Roberts, *Biol. Lett.* **2**, 412 (2006).
18. D. Johnson, J. Bering, *Evol. Psychol.* **4**, 219 (2006).
19. A. Brooks, *Who Really Cares? The Surprising Truth About Compassionate Conservatism* (Basic Books, New York, 2006).
20. D. L. Paulhus, *J. Pers. Soc. Psychol.* **46**, 598 (1984).
21. D. E. Trimble, *Educ. Psychol. Meas.* **57**, 970 (1997).
22. J. Darley, C. D. Batson, *J. Pers. Soc. Psychol.* **27**, 100 (1973).
23. R. Sosis, B. Ruffle, *Curr. Anthropol.* **44**, 713 (2003).
24. C. D. Batson *et al.*, *J. Pers. Soc. Psychol.* **57**, 873 (1989).
25. J. M. Bering, *Behav. Brain Sci.* **29**, 453 (2006).
26. B. Randolph-Seng, M. E. Nielsen, *Int. J. Psychol. Rel.* **17**, 303 (2007).
27. A. F. Shariff, A. Norenzayan, *Psychol. Sci.* **18**, 803 (2007).
28. J. A. Bargh, T. L. Chartrand, *Am. Psychol.* **54**, 462 (1999).
29. R. Sosis, C. Alcorta, *Evol. Anthropol.* **12**, 264 (2003).
30. L. R. Iannaccone, *J. Polit. Econ.* **100**, 271 (1992).
31. P. Edgell, J. Gerteis, D. Hartmann, *Am. Sociol. Rev.* **71**, 211 (2006).
32. J. Ensminger, *J. Inst. Theor. Econ.* **153**, 4 (1997).
33. A. Greif, *Am. Econ. Rev.* **83**, 525 (1993).
34. R. Sosis, E. R. Bressler, *Cross-Cultural Res.* **37**, 211 (2003).
35. J. Berg, J. Dickhaut, K. McCabe, *Games Econ. Behav.* **10**, 122 (1995).
36. J. H. W. Tan, C. Vogel, *J. Econ. Psychol.*, in press.
37. R. I. M. Dunbar, *Annu. Rev. Anthropol.* **32**, 163 (2003).
38. R. J. Smith, *Curr. Anthropol.* **37**, 451 (2003).
39. F. L. Roes, M. Raymond, *Evol. Hum. Behav.* **24**, 126 (2003).
40. J. Snarey, *J. Sci. Study Relig.* **35**, 85 (1996).
41. D. Keltner, J. Haidt, in *Emotions: Current Issues and Future Directions*, T. Mayne, G. A. Bonanno, Eds. (Guildford Press, New York, 2001), pp. 192–213.
42. R. Putnam, *Bowling Alone: The Collapse and Revival of American Community* (Touchstone, New York, 2000).
43. B. Herrmann, C. Thöni, S. Gächter, *Science* **319**, 1362 (2008).
44. J. Haidt, *Science* **316**, 998 (2007).
45. J.-K. Choi, S. Bowles, *Science* **318**, 636 (2007).

46. We thank S. Atran, S. Heine, J. Henrich, M. Schaller, R. Sosis, and three anonymous reviewers for their comments and criticisms. The writing of this article was supported by a Social Sciences and Humanities Research Council of Canada grant (410-2007-0222) to the first author.

10.1126/science.1158757

Bacterial Protection of Beetle-Fungus Mutualism

Jarrod J. Scott,[1]* Dong-Chan Oh,[2]* M. Cetin Yuceer,[3] Kier D. Klepzig,[4] Jon Clardy,[2]† Cameron R. Currie[1]†

The pervasiveness of beneficial associations between symbiotic microbes and plants and animals in every ecosystem illustrates how the acquisition of a microbe's physiological capacity confers substantial fitness benefits to hosts (*1*). However, dependence on mutualistic microbes becomes a liability if antagonistic microbes attack or outcompete beneficial ones (*2*). Therefore, mechanisms to preserve beneficial microbes must be a widespread, although poorly understood, component of host-microbe mutualisms. We show that a beetle uses a bacterium to protect its fungal food source from a competitor fungus.

Southern pine beetles, *Dendroctonus frontalis*, engage in a beneficial symbiosis with the fungus *Entomocorticium* sp. A, which provides nourishment for their developing larvae. Adult beetles carry *Entomocorticium* sp. A in a specialized storage compartment called a mycangium (Fig. 1A), excavate ovipositional galleries within the inner bark and phloem of host pine trees, and inoculate these galleries with *Entomocorticium* sp. A (*3*, *4*). The success of the *D. frontalis*–*Entomocorticium* sp. A mutualism is challenged by an antagonistic fungus, *Ophiostoma minus*, which can outcompete *Entomocorticium* sp. A and thereby disrupt beetle larval development (*3*, *4*). Our results indicate that successful maintenance of the *D. frontalis*–*Entomocorticium* sp. A mutualism is likely mediated by an actinomycetous bacterium that produces antibiotics that selectively inhibit *O. minus*.

The presence of previously unknown actinomycetes within the *D. frontalis*–*Entomocorticium* sp. A mutualism was established by scanning electron microscopy (SEM) and enrichment culture isolations (*5*). SEM revealed unexpected and profuse growth of actinomycetes within the galleries of *D. frontalis*, as well as inside the mycangia (Fig. 1B and fig. S1A). Isolations from 110 beetle individuals yielded 846 colony-forming units (CFUs) of actinomycetes, including at least one CFU from each of 92 individuals. Out of 164 actinomycete CFUs selected to be transferred to pure culture, 99 isolates had a red morphotype, whereas 65 isolates had a white morphotype. DNA sequence analyses confirmed the visual morphotype distinction, and within each of the two morphotypes there was complete 16S rDNA sequence identity. The two morphotypes form a monophyletic clade closely related to *Streptomyces thermosacchari*. Furthermore, we also isolated the same red morphotype from 5 of 10 mycangia sampled.

We explored the potential role of the actinomycetes in mediating the *D. frontalis* fungal community by using symbiont pairing bioassays and chemical analyses. The bioassays, which crossed all possible combinations of the two actinomycete morphotypes with *Entomocorticium* sp. A and *O. minus*, revealed that isolates of the red morphotype produced a diffusible activity that inhibits the beetle's antagonistic fungus, *O. minus*, but only slightly affects the beneficial fungus, *Entomocorticium* sp. A (Fig. 1C and fig. S1, B and C). Extensive chemical and spectral analyses on strains of the red morphotype revealed the antifungal molecule responsible for selective inhibition to be a polyene peroxide, which we named mycangimycin. Mycangimycin ($C_{20}H_{24}O_4$), which has not been previously reported, is a linear 20-carbon carboxylic acid with an endoperoxide linking C-3 and C-5 to form a 1,2-dioxolane and a conjugated *cis*, *cis*, *trans*, *trans*, *cis*, *trans*-heptaene spanning C-7 to C-20 (Fig. 1D). Liquid culture antifungal assays using purified mycangimycin showed *O. minus* to be almost 20 times more susceptible [minimal inhibitory concentration (MIC) = 1.0 μM] than *Entomocorticium* sp. A (MIC = 19.0 μM) (fig. S1D). The identification of an actinomycete that is localized in the mycangium and galleries, which produces an antibiotic that selectively suppresses the antagonistic fungus, *O. minus*, indicates that *D. frontalis* engages in an additional mutualism with bacteria to regulate the *Entomocorticium* sp. A–*O. minus* fungal community. Because other bark-beetle species also depend on successfully maintaining beneficial fungi, tripartite beetle-fungus-bacterium mutualisms may be widespread.

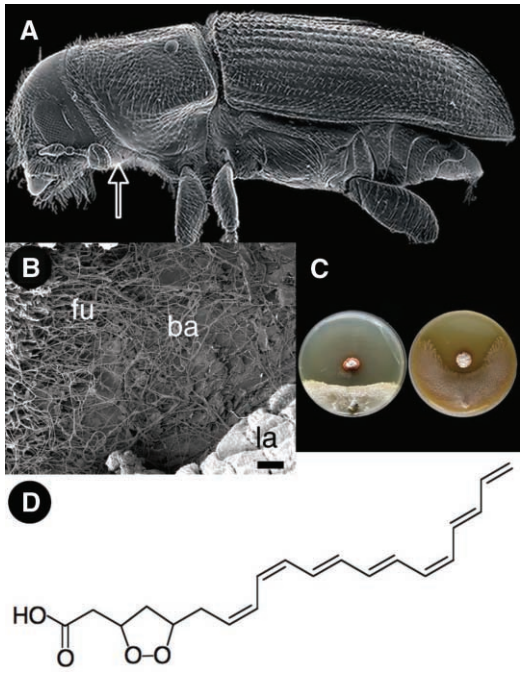

Fig. 1. (**A**) SEM micrograph of adult *D. frontalis* showing the location of a mycangium (arrow), which is used to transport *Entomocorticium* sp. A. (**B**) SEM micrograph from the *D. frontalis* gallery showing the actinomycetous bacterium (ba), fungus (fu), and beetle larva (la). (**C**) Representative examples of pairwise bioassay challenges illustrating inhibition of the fungal antagonist, *O. minus* (left), by a *D. frontalis* symbiotic actinomycete (strain SPB074). In contrast, the southern pine beetle's fungal mutualist, *Entomocorticium* sp. A, is relatively resistant (right) (see SOM for more details). (**D**) The structure of mycangimycin contains a seven-conjugated double bond chain and a five-membered endoperoxide ring.

Our study parallels earlier work on fungus-farming ants, which use actinomycetes to help protect their fungal gardens from pathogens (*6*). Taken together, these findings suggest that the use of antibiotic-producing actinomycetes may be a common method for maintaining beneficial microbes. Indeed, considering the importance of pathogens as a driving force in the evolution of all hosts, the benefit of such associations may extend to helping protect plants and animals from pathogens to which they themselves are susceptible (*7*, *8*). If, as seems likely, these associations are widespread, targeting them could be an effective strategy for locating novel biologically active natural products.

References and Notes

1. N. A. Moran, *Curr. Biol.* **16**, R866 (2006).
2. C. R. Currie, U. G. Mueller, D. Malloch, *Proc. Natl. Acad. Sci. U.S.A.* **96**, 7998 (1999).
3. K. D. Klepzig, R. T. Wilkens, *Appl. Environ. Microbiol.* **63**, 621 (1997).
4. R. W. Hofstetter *et al.*, *Oecologia* **147**, 679 (2006).
5. Materials and methods are available on *Science* Online.
6. C. R. Currie, J. A. Scott, R. C. Summerbell, D. Malloch, *Nature* **398**, 701 (1999).
7. M. Kaltenpoth, W. Gottler, G. Herzner, E. Strohm, *Curr. Biol.* **15**, 475 (2005).
8. J. T. Coombs, C. M. M. Franco, *Appl. Environ. Microbiol.* **69**, 5603 (2003).
9. We thank A. Adams, S. Adams, C. Booth, E. Caldera, J. Ensign, C. Hsu, Y. Kang, A. Lawrence, W. Monroe, P. Jeffreys, M. Palmisano, A. Pinto, M. Poulsen, K. Raffa, D. Stone, and E. Vallery for assistance. Support provided by the U.S. Department of Agriculture (C.R.C., K.D.K., and M.C.Y.), NIH (J.C.), and NSF (C.R.C.). We have a patent application submitted on mycangimycin.

Supporting Online Material

www.sciencemag.org/cgi/content/full/322/5898/63/DC1
Materials and Methods
Fig. S1
References

13 May 2008; accepted 12 June 2008
10.1126/science.1160423

[1]Department of Bacteriology, University of Wisconsin-Madison, WI 53706, USA. [2]Department of Biological Chemistry and Molecular Pharmacology, Harvard Medical School, Boston, MA 02115, USA. [3]Department of Forestry, Mississippi State University, Mississippi State, MS 39762, USA. [4]U.S. Department of Agriculture Forest Service, Southern Research Station, Pineville, LA 71360, USA.

*These authors contributed equally to this work.
†To whom correspondence should be addressed. E-mail: currie@bact.wisc.edu (C.R.C.); jon_clardy@hms.harvard.edu (J.C.)

A Chronology of Paleozoic Sea-Level Changes

Bilal U. Haq, *et al.*

Science **322**, 64 (2008);
DOI: 10.1126/science.1161648

A Chronology of Paleozoic Sea-Level Changes

Bilal U. Haq[1]* and Stephen R. Schutter[2]

Sea levels have been determined for most of the Paleozoic Era (542 to 251 million years ago), but an integrated history of sea levels has remained unrealized. We reconstructed a history of sea-level fluctuations for the entire Paleozoic by using stratigraphic sections from pericratonic and cratonic basins. Evaluation of the timing and amplitude of individual sea-level events reveals that the magnitude of change is the most problematic to estimate accurately. The long-term sea level shows a gradual rise through the Cambrian, reaching a zenith in the Late Ordovician, then a short-lived but prominent withdrawal in response to Hirnantian glaciation. Subsequent but decreasingly substantial eustatic highs occurred in the mid-Silurian, near the Middle/Late Devonian boundary, and in the latest Carboniferous. Eustatic lows are recorded in the early Devonian, near the Mississippian/Pennsylvanian boundary, and in the Late Permian. One hundred and seventy-two eustatic events are documented for the Paleozoic, varying in magnitude from a few tens of meters to ~125 meters.

Although there has been substantial progress in recent years in integrating the record of Mesozoic and Cenozoic eustatic fluctuations (*1*, *2*), relatively little attention has been paid to reevaluating or synthesizing Paleozoic sea-level data, the coverage of which has been largely piecemeal. The Paleozoic Era encompasses more than half of the Phanerozoic Eon, featuring some of the most intriguing unanswered questions in Earth history. Unexplored Paleozoic strata also are believed to contain important unrecovered hydrocarbons. A reevaluation of the eustatic history of this Era therefore would not only serve as a tool for exploration geology but hopefully also revive interest in Paleozoic Earth science.

Sea-level curves provide utilitarian predictive models of sedimentation and thus are invaluable in geologic exploration. These curves offer a working representation of the long-term trends of the base level along continental margins and the individual inundations and drainings/desiccations of interior seaways, and thus the migration of hydrocarbon reservoirs and source facies. Where local tectonic influences are minimal and have not deformed the stratigraphic record (or where tectonics can be corrected for), these curves also can aid in first-order correlations. The relative magnitude and frequency of sea-level highs and lows, the extent and nature of the transgressive condensed intervals on the shelf (when organic-rich sediments accumulate), and the duration of subaerial exposure and incision of the shelf are also important exploration criteria (*3*). Here we present an integrated semiquantitative model of the Paleozoic sea-level history. It is based on widely distributed sequence-stratigraphic data within the biochronostratigraphic constraints of varying quality and reliability for various Paleozoic periods.

Although previous reconstructions of regional sea-level histories have been limited to discrete slices of time, they provide a wealth of information on the long- and short-term trends and have been an invaluable resource for this synthesis [see the supporting online material (SOM) text]. Particularly, the studies from relatively stable pericratonic and cratonic basins of North American and Australian cratons have been indispensable. As discussed later, we have designated reference districts (RDs) for various time segments (largely from North America and Australia, but also from northern and southern Africa, northwestern Europe, and China). We interpret the sedimentary record in these districts as representing the modal mean of change in sea level during intervals of relative tectonic quiescence. The RDs were also compared with sections elsewhere around the world to ascertain the broad transgressive/regressive trends and individual variations of sea levels and provide corroborative data. Because of spatial constraints, in this article we only report a brief account of our main findings (see also SOM text).

Timing and magnitude of sea-level events in the Paleozoic. Obstacles encountered in resolving the timing and magnitude of individual sea level events based on a synthesis of worldwide data of varying quality and utility are not specific to the Paleozoic; they are also applicable to the younger eras. The Paleozoic, however, has a special suite of constraints that sets it apart. For example, most Paleozoic oceanic crust has been subducted (with the exception of a few obducted ophiolite mélanges), making it unfeasible to directly estimate the mean age of the oceanic crust for deciphering long-term eustatic trends. Paleozoic stratigraphy is also strongly biased toward epi- and pericratonic basins, characterized by their plentiful unconformities and endemic faunas. Nevertheless, these attributes make these basins natural places for the study of "unconformity-bounded" units (depositional sequences). The unconformity-bounded subdivision also makes the existing Paleozoic literature, spanning over a century of research, relevant and useful.

An accurate time scale is of crucial first-order importance for any global synthesis. Geological time scales have been improving and becoming better integrated in recent years. The Paleozoic time scale in particular has been in a considerable state of flux, with major recent changes to the ages of period and stage boundaries. The most up-to-date published time scale is that compiled by Gradstein *et al*. (*4*). Some parts of this chronostratigraphy have been updated recently (*5*), which we have adopted here. Ongoing attempts at astronomical tuning and recalibration of $^{40}Ar/^{39}Ar$ ages will probably lead to further refinements of the boundary ages (*6*). However, with the exception of a few radiometrically determined boundaries, all of the Paleozoic correlations are actually based on fossil biozonations. Thus, the duration of a biozone in question provides a minimum measure of uncertainty in the correlations of sequence boundaries.

The degree of precision of correlations from one basin to another depends on the biostratigraphic fossil assemblage used for such purposes. For the Paleozoic, biochronostratigraphy is traditionally based on several groups of commonly occurring fossils, the majority of which tend to be endemic and/or facies-controlled (*7*). This underscores the need to use multiple overlapping criteria (biozonal assignments based on several groups) where possible, to enhance the chronostratigraphic signal-to-noise ratio.

The second issue of importance for a reconstruction such as this concerns the uncertainty in estimating the magnitude of rises and falls in sea level. In the Paleozoic, the general lack of data on ice-volume proxies, such as oxygen isotopes (because of severe diagenetic alterations), limits us to relying on physical measures of sea-level changes from stratigraphic data. A fundamental limitation for accurate physical estimates stems from the lack of a universal reference point against which sea level changes can be computed. For convenience, we often compare past eustatic fluctuations with present-day (PD) shorelines, but over the longer periods this comparative reference point becomes less meaningful because continents have changed both by horizontal accretion/destruction and vertical motions. It is often possible to determine when the sea withdrew below the extant shelf edge, but it is challenging to accurately gauge the amount of

[1]National Science Foundation, Arlington, VA 22230, USA. [2]Murphy Oil International, Houston, TX 77094, USA.

*To whom correspondence should be addressed. E-mail: bhaq@nsf.gov

sea-level fall from stratigraphic data because of the unknown amount of erosion on the shelf. A rise in sea level is even more difficult to measure meaningfully because of the potentially less-than-complete filling of the accommodation space during the highstand or because of a subsequent fall in sea level that may erode part or much of the highstand systems tract. Thus, for practical purposes, all amplitude assessments from physical data must be considered relative rather than absolute.

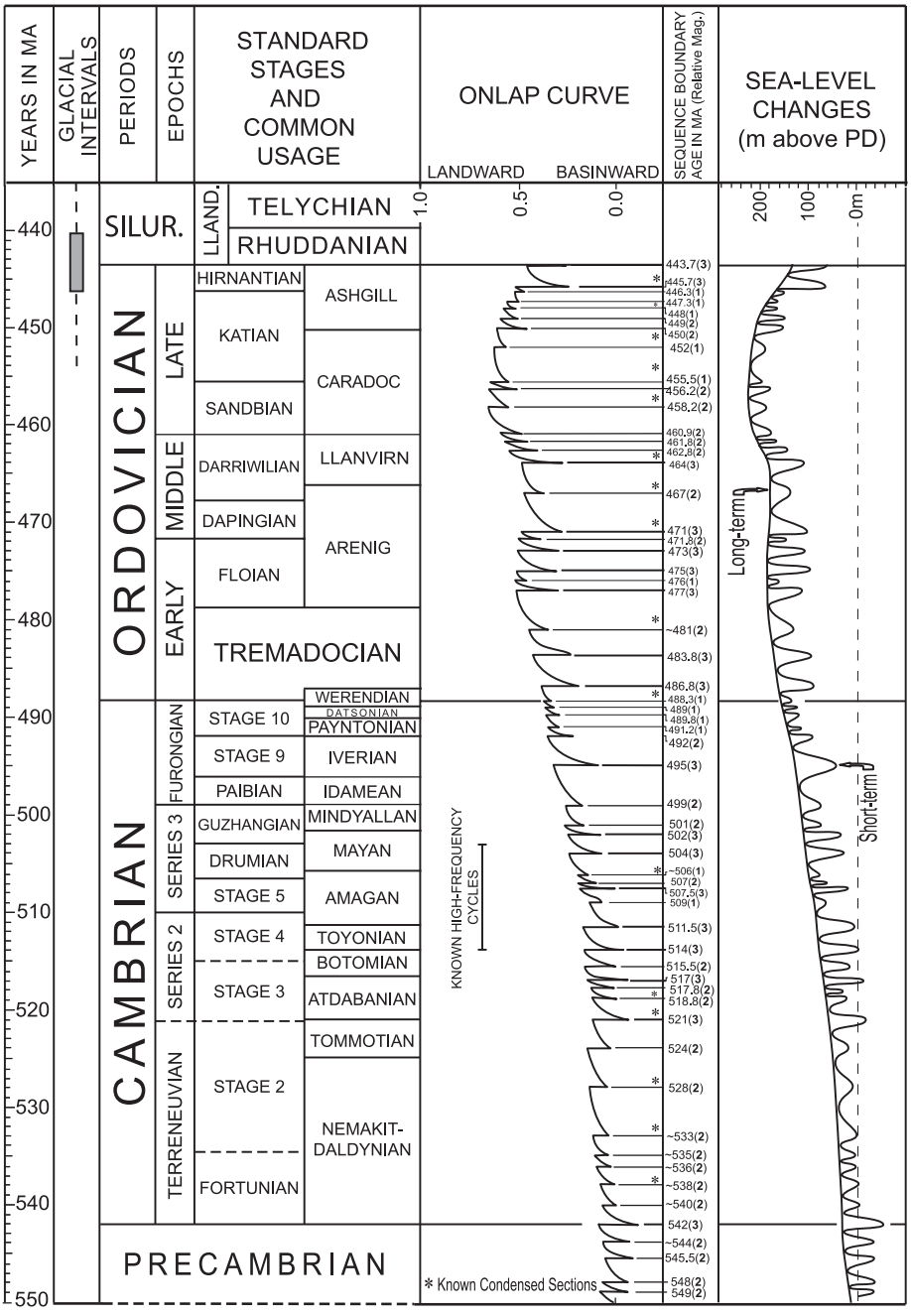

Fig. 1. Cambrian-Ordovician sea-level changes. The time scale and standard and regional stages are modeled after Gradstein *et al*. and Ogg *et al*. (*4*, *5*). The left half of Figs. 1 to 3 shows the stratigraphic subdivisions calibrated to the absolute time scale. Known intervals of continental glaciation (*26*–*28*) are indicated alongside the numerical time scale. The right half of each figure starts with an onlap curve, which is a measure of relative landward or basinward movement of the regional baseline as estimated in the RD sections. Sequences that are associated with known prominent condensed sections (indicated by asterisks) are also shown in this column. The biochronological ages of the sequence boundaries (estimated in the RDs and ancillary sections) are indicated in the next column. A semiquantitative measure of the relative magnitude of each short-term event is shown in parentheses [minor, **1** (<25 m); medium, **2** (25 to 75 m); and major, **3** (>75 m)]. Periods with known higher-frequency eustatic cycles and documented condensed sections are also indicated in this column, by vertical bars. This is followed to the right by the sea level curves, both the long-term envelope and the short-term curve of (third-order) fluctuations in the sea level (those suspected to be of fourth order are shown by dashed lines). The dashed vertical line in this column represents an approximation of the PD sea level. Long-term and short-term sea-level curves are calibrated to the PD sea level.

Backstripping can potentially refine such estimates through corrections for sediment loading and compaction and basin-floor subsidence (*8*, *9*). Nevertheless, considerable uncertainties remain in this approach because of long-ranging paleobathymetric indicators and the potential for differential subsidence. Corrections for the flexural response of a margin to the loading and unloading of water/ice and sediments are also not straightforward or precise and can bias the measurements in either direction. During this synthesis, the only meaningful approach we could adopt was to reproduce the magnitude estimates of rises and falls in sea level as gleaned from the RDs and ancillary sections (based variously on stratigraphic measures such as thickness of system tracts, bio- and lithofacies depth assessments, the depth of incision on shelves, and partial backstripping). We classified each event semiquantitatively (measured as a magnitude of fall from the previous highstand) as minor (<25 m), medium (25 to 75 m), or major (>75 m). From the worldwide data, it is apparent that although the overall long-term (cumulative) rise in sea level could be as much as 250 m, the individual third-order changes in sea level [that is, those occurring over ~0.5 to 6 million years (My)] rarely exceeded 150 m. Many of the higher-frequency (<0.5 My) variations are within the minor to medium range. These estimates will be subject to refinement in the future once various basins (in the RDs and elsewhere) have been effectively backstripped and when better paleobathymetric assessments are available.

Reconstruction of the Paleozoic sea-level history. Though Earth scientists have been interpreting changes in sea level based on stratigraphic data for over a century, the first attempt at an integrated history of the Paleozoic sea level was embedded in the broader presentation of seismic-stratigraphic methodology by Vail *et al*. (*10*). Hallam (*11*) also reviewed much of the Paleozoic sea level data accumulated up to the 1980s. More recently, Haq and Al-Qahtani (*12*) presented a regional history of the sea level in the Phanerozoic Arabian Platform and compared it with an updated eustatic sea level curve based on previous syntheses. However, the Paleozoic portions of those curves largely depicted second-order events, mostly cycles of >5 My duration.

The stratigraphic record is a composite of several orders of superimposed sedimentary cycles, depending on their causal mechanisms. They range from the high-frequency Milankovitch-scale climatic cycles (often 1 m to a few meters in thickness) to third-order (mostly 1 to 2 My in duration) and fourth-order (<0.5 My in duration)

eustatic cycles, and larger (several million years in duration) tectonic cycles. In practice, it is difficult to consistently separate third- and fourth-order cycles. Our ability to resolve the record chronostratigraphically in any given section depends on the thickness of the preserved section, the quality of the outcrop, the position of the section along the shelf-slope-basin profile, and the quality of biochronostratigraphic data. Here we have attempted to identify sequences at third-order resolution; however, a few fourth-order sedimentary cycles inevitably were also incorporated. Although the existence of higher-frequency cycles may be more widespread in the Paleozoic, some intervals more visibly preserve fourth-order (~400,000 years) cycles, such as the mid-Cambrian, mid-Devonian, mid- to late Carboniferous, and Permian (Figs. 1 to 3).

The Paleozoic sequence-stratigraphic data are derived entirely from public-domain outcrop sections (seismic data are generally lacking or spotty except for the late Paleozoic). The criteria for interpreting regional rises and falls in sea level from sequence-stratigraphic data and seismic data have been summarized elsewhere (*3*, *10*, *13*) and are not repeated here. In addition, several lithological features (condensed section deposits, transgressive coals, evaporites, carbonate megabreccias, and exposure-related and forced-regressive deposits) and paleontological attributes have also aided our interpretations in placing outcrop features within sequence-stratigraphic framework (see the description in the SOM text).

Reconstruction of the long-term envelope and the short-term history of changes in sea level requires differing approaches. The long-term changes are believed to be mostly driven by the slow tectonic processes that change the volumetric capacity of the ocean basins. Individually, each data set on which the long-term envelope can be based must be considered relative rather than absolute measures of eustatic trends. However, a long-term curve based on global continental flooding estimates (*14*–*17*), stacked regional sea-level data (evaluated by us), and modeling results for the mean age of the oceanic crust yields consistent results. Algeo and Seslavinsky (*17*) have presented an analysis of the flooding history and hypsometry of 13 Paleozoic landmasses and estimate that the long-term eustatic highs were 100 to 225 m above PD sea level. They also conclude that Paleozoic continents experienced an additional change of ±100 m in vertical movements because of epeirogeny. The upper limits of our estimates of long-term highs are influenced by this analysis.

More-recent modeling results of the Mesozoic-Cenozoic sea floor (*18*–*20*), although based on differing assumptions, consistently point to the mean age of the oceanic crust, rather than sea-floor spreading rates or ridge volume, as potential forcing for the long-term eustatic change. Cogné and Humler (*20*) have extrapolated their modeling results back to the Paleozoic, for which direct measurements of sea-floor isochrons are not possible because of subduction. Instead, they estimate land-ocean distributions from measurements of areas of continental landmasses based on paleomagnetic reconstructions. Their results show a credible agreement between periods of high fragmentation of the continents and high global sea levels through much of the Paleozoic. One recent aspect of the modeling efforts is the conclusion that continental margins could be subjected to a substantial degree of mantle flow–related vertical motions over relatively short geological intervals. This process causes changes in local dynamic topography, which may have led to an underestimation of changes in sea level from physical data in the past (*21*).

The shorter-term changes in sea level (third- and higher-order events) were more likely mostly driven by changes in the volume of water in the world ocean through glacial (and as yet unknown) processes. The short-term Paleozoic curve as portrayed here (Figs. 1 to 3) is based on the best of several sections in an area designated the RD, in which, according to our interpretations, tectonic influences were minimal and the eustatic signal is more likely to have been preserved. Sea level–change events identified in the RDs were then sought elsewhere worldwide (in the existing stratigraphic data) and documented in designated ancillary sections (SOM text).

The previous physically estimated magnitude of the shorter-term (third- and fourth-order) sea-

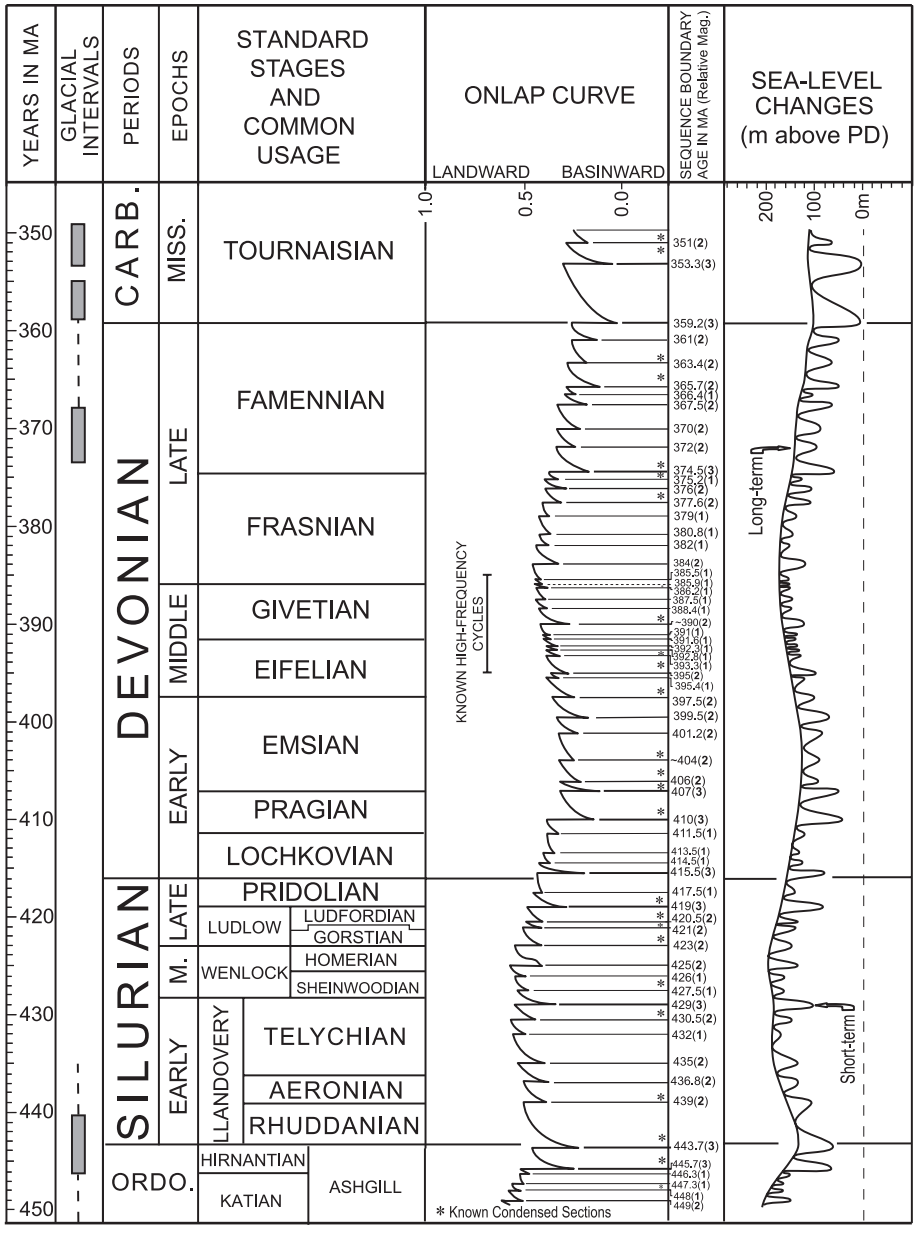

Fig. 2. Silurian-Devonian sea-level changes. See the caption of Fig. 1 for details.

level events in the Paleozoic range from a few tens of meters to ~250 m (*22*). A recent synthesis of the Carboniferous-Permian yielded fluctuations of a few tens of meters in the nonglacial intervals and changes of up to 120 m in the glacially dominated periods (*23*). Many of these regional estimates will be subject to refinement in the future, once the sections in question are rigorously backstripped.

Although we deem the long-term trends to be real, the difficulties in estimating meaningful measures of the magnitude of eustatic changes discussed above imply that the absolute global amplitude of both the long-term envelope and the short-term changes remain elusive. All such measures must be currently considered as approximate. These observations also caution us about the futility of generalizing the magnitude of individual sea-level events from one continental margin to represent worldwide eustatic values.

The concept of RDs [first proposed by M. E. Johnson (*24*)] implies that we consider the sections therein to be currently the best available representation of the modal mean for the time segment under consideration. Our criteria for inclusion of an area as a RD are as follows: (i) the time segment in question is represented by a period of tectonic quiescence locally (or is correctable for tectonic influences) and has suffered relatively little postdepositional deformation and is thus interpretable with sequence-stratigraphic methodologies; (ii) sections are relatively well-dated, preferably with multiple biostratigraphies (to enhance the chronostratigraphic signal-to-noise ratio); (iii) outcrops in the area have open public access; and (iv) the area will easily lend itself to geohistory analysis so that the relevant sections can be eventually backstripped (as well as corrected for local dynamic topographic changes over time) for more-refined estimates of the magnitude of changes in sea level. We list the selected RDs and ancillary sections in the SOM, along with background literature and ages assigned by us to the interpreted sequence boundaries.

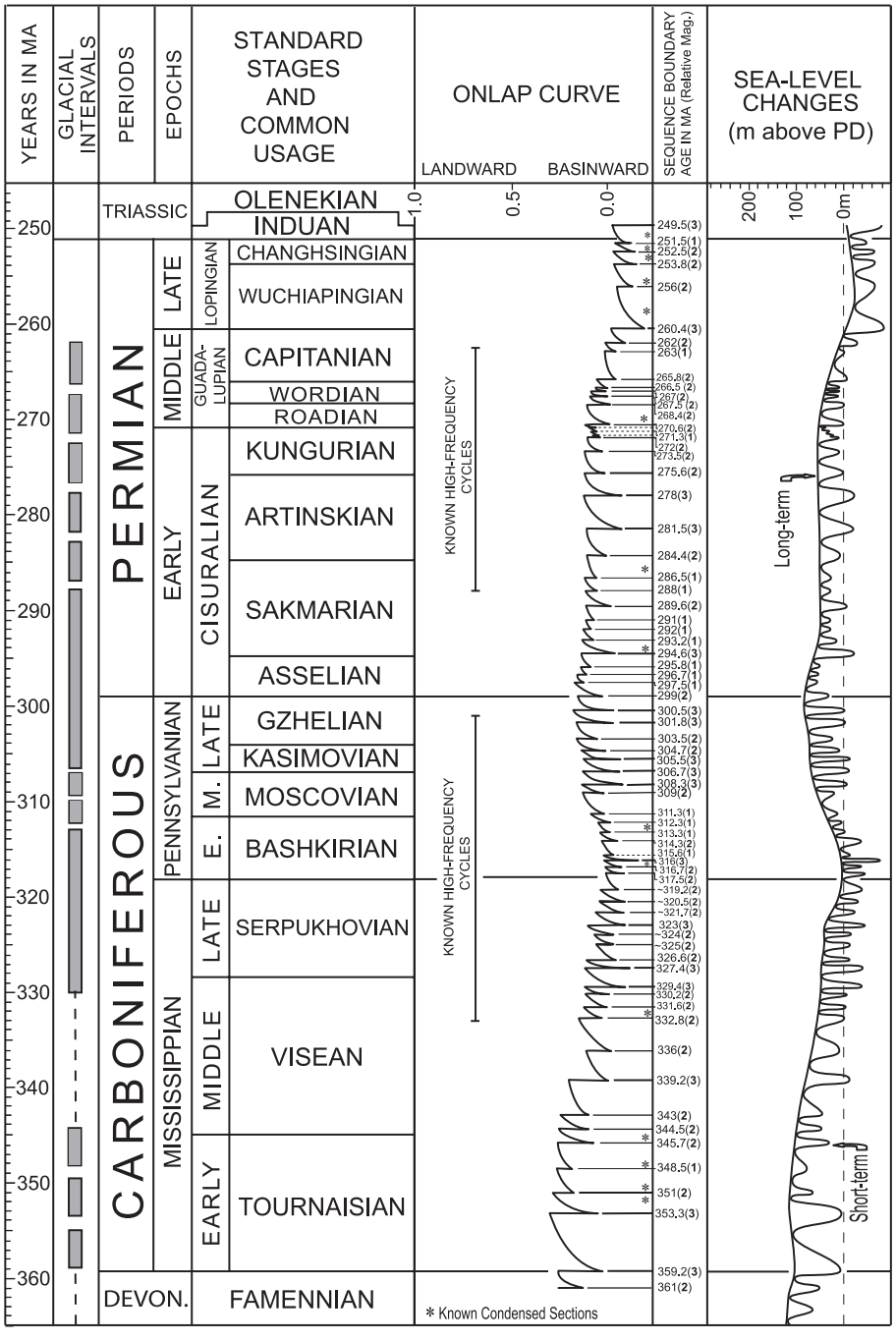

Fig. 3. Carboniferous-Permian sea-level changes. See the caption of Fig. 1 for details.

Results and conclusions. Here we offer (in our view) a robust working model of the history of the Paleozoic sea level that is, nevertheless, subject to refinement with better chonostratigraphies and when the sections are subjected to backstripping analyses. Our results show a long-term sea level curve, including a rising sea level during the Cambrian–through–Early Ordovician interval [see fig. S1 and explanation in (*25*)], a marked dip during the Middle Ordovician (the Dapingian to early Darriwilian) preceding a substantial rise entering the early Late Ordovician, and the highest sea levels of the Paleozoic during the early Katian (when the sea level is estimated to be ~225 m higher than at the PD). This was followed by a sharp fall during the latest Ordovician (late Katian to the Hirnantian) that continued into the earliest Silurian. The remainder of the Early Silurian saw the beginning of another long-term rise that culminated in a mid-Silurian (mid-Wenlock) high, followed by a decline that lasted from Late Silurian (Ludlow) through Early Devonian (Emsian). The Middle Devonian saw the beginning of yet another long-term rise, which reached its acme in the early Late Devonian (Frasnian). After a slight dip at the Frasnian/Famennian boundary and a recovery in the early Famennian, the long-term curve shows a gradual sea-level decline in the later Devonian (late Famennian) with a punctuated fall near the Devonian/Carboniferous boundary. After a short recovery, subsequent long-term decline began in the mid-Mississippian (mid Visean), reaching a low in the late Mississippian (near the Mississippian/Pennsylvanian boundary). The next long-term rise (though less pronounced than all previous rises) began in the mid-Pennsylvanian (Moscovian) and lasted only until the end of the Pennsylvanian (Gzhelian), followed by a slight fall thereafter in the earliest Permian (Asselian). The sea level stabilized at that level for the remainder

of the Early Permian. A sharp trend toward a declining sea level started in the mid-Permian (Roadian), culminating in the nadir of the sea level for the Paleozoic in the early Late Permian (Wuchiapingian). It began to recover in the latest Permian (Changhsingian), but the general low extended into the Early Triassic.

The shorter-term (third-order) base-level changes generally vary in duration from ~0.5 to 3.0 My (with the exception of Early-to-Middle Mississippian). One hundred seventy-two discrete third-order events (cycles) have been identified, with an average duration of ~1.7 My per cycle. In some intervals, the sections preferentially preserve fourth-order cycles, indicating a possible long-period orbital eccentricity control. Four such intervals have been identified so far: in the middle Cambrian (Toyonian to Mayan), middle Devonian (late Eifelian to Givetian), middle to late Carboniferous (late Visean to Kasimovian), and early to Middle Permian (Artinskian to Capitanian); however, fourth-order cycles may exist more widely. Whether this higher frequency is entirely due to higher sedimentation (a preservational effect) or the underlying signal (that is, long-term orbital forcing) is not always clear. The two younger intervals of higher-frequency cycles (in the Carboniferous and Permian) also coincide with periods of known glaciation, but for the two older intervals (the middle Cambrian and middle Devonian) no glaciation has been documented (*26*–*28*).

It should be noted that for the Early to middle Mississippian, the duration of most of the third-order cycles seem inordinately long (up to ~6.0 My). Although occasional long cycles (3 to 5 My) also occur at other times (for example, in the Cambrian through early Silurian), the consistent occurrence of long cycles in the Early to middle Mississippian may point to time-scale problems for this interval (the Tournaisian and Visean stages are also inordinately long, probably for the same reason).

We are unable to comment on all of the causes for shorter-term (third-order and fourth-order) eustatic changes in the Paleozoic. Although glaciation has been attributed to ~28% of the Paleozoic time (and suspected for another 10%), it has not been documented for the remainder of this era (*26*–*28*). Thus, waxing and waning ice sheets cannot be considered to be the only underlying cause for fluctuations in the Paleozoic sea level. Nevertheless, because the Paleozoic glacial record remains fragmentary, the question remains open. Conversely, there may be other, nonclimatic, causal mechanisms for short-term changes in sea level that still remain to be discovered.

References and Notes

1. J. Hardenbol *et al.*, *Soc. Econ. Paleontol. Mineral. Spec. Publ.* **60**, 3 (1998).
2. K. G. Miller *et al.*, *Science* **310**, 1293 (2005).
3. J. C. Van Wagoner, R. M. Mitchum, K. M. Campion, V. D. Rahmanian, *Am. Assoc. Petrol. Geol. Methods Explor. Ser.* **7**, 55 (1990).
4. *A Geologic Time Scale, 2004*, F. M. Gradstein, J. G. Ogg, A. G. Smith, Eds. (Cambridge Univ. Press, Cambridge, 2004), pp. 1–589.
5. J. G. Ogg, G. M. Ogg, F. M. Gradstein, *The Concise Geologic Time Scale* (Cambridge Univ. Press, Cambridge, 2008), pp. 1–178.
6. K. F. Kuiper *et al.*, *Science* **320**, 500 (2008).
7. Common Paleozoic biostratigraphic indicators include brachiopods, graptolites, chitinozoans, ammonoids, fusulinids, and conodonts. Brachiopods appear in the Early Cambrian and are common throughout the Paleozoic but tend to be provincial and facies-dependent, preferring shallow-water environments. Planktonic graptolites appear in the late Cambrian and persist through the early Devonian. They are particularly useful as index fossils in the Ordovician and Silurian, but they are more likely to occur in the basinal facies. Chitinozoa occur from Ordovician through Devonian and have been used successfully for the subdivision of this interval. Paleozoic ammonoids in general are common from the Devonian through the Permian and, although relatively widespread, they also show a considerable degree of provincialism or facies-dependence for some intervals. For example, the ammonoid *Goniatites,* preserved in Devonian-to-Permian strata, are strongly facies-controlled, preferring mostly the basinal environments of inland seas. Fusulinids have been used for biochronologic subdivision with varying degrees of success from the Late Mississippian through the Permian. Conodonts first appeared in the Cambrian and range through the Triassic. Their shallowest-water biofacies tend to be eurytopic, opportunistic, and long-ranging and thus only marginally useful for biostratigraphic resolution. But toward deeper waters they become more cosmopolitan and biostratigraphically meaningful. When deeper-water biofacies are present, conodonts are well suited for higher-resolution correlations from the Ordovician through the Permian interval.
8. W. A. van Sickel, M. A. Kominz, K. G. Miller, J. V. Browning, *Basin Res.* **16**, 451 (2004).
9. M. A. Kominz *et al.*, *Basin Res.* **20**, 211 (2008).
10. P. R. Vail, R. M. Mitchum, S. Thompson III, *Am. Assoc. Pet. Geol. Mem.* **26**, 63 (1977).
11. A. Hallam, in *Phanerozoic Sea-Level Changes* (Columbia Univ. Press, New York, 1992), p. 266.
12. B. U. Haq, A. M. Al-Qahtani, *GeoArabia* **10**, 127 (2005).
13. B. U. Haq, J. Hardenbol, P. R. Vail, *Soc. Econ. Paleontol. Mineral Spec. Publ.* **42**, 71 (1988).
14. D. U. Wise, in *The Geology of Continental Margin,* C. A. Burke, C. L. Drake, Eds. (Springer Verlag, New York, 1974), pp. 45–58.
15. *Phanerozoic History of Australia*, J. J. Veevers, Ed. (Clarendon Press, Oxford, 1984), pp. 1–418.
16. A. B. Ronov, *Am. J. Sci.* **294**, 777 (1994).
17. T. J. Algeo, K. B. Seslavinsky, in *Sequence Stratigraphy and Depositional Response to Eustatic, Tectonic and Climatic Forcing*, B. U. Haq, Ed. (Kluwer Academic, Dordrecht, The Netherlands, 1995), pp. 209–246.
18. M. Gurnis, *Nature* **344**, 754 (1990).
19. J. P. Cogné, E. Humler, V. Courtillot, *Earth Planet. Sci. Lett.* **245**, 115 (2006).
20. J. P. Cogné, E. Humler, *Earth Planet. Sci. Lett.* **273**, 251 (2008).
21. D. Müller, M. Sdrollias, C. Gaina, B. Steinberger, C. Heine, *Science* **319**, 1357 (2008).
22. For example, in the Middle and Late Cambrian, backstripped estimates from the Canadian Rockies yielded values of up to 250 m of change, whereas in Utah for strata of the same age, only ~100 m of change was estimated (*29*). In Iowa, nonbackstripped measurements from the Ordovician through Mississippian sequences provided estimates of a few tens of meters to ~100 m of change (*30*). Estimates from topographic relief of incised valleys in the Silurian yielded values of ~30 to >70 m of change worldwide (*24, 31, 32*). In the British Isles, a cumulative rise of 227 m in the Early Carboniferous and ~200 m in the mid-Carboniferous was indicated after partial backstripping, with the magnitude of individual third-order events ranging between 5 and 56 m (*33*). Estimates from the Late Mississippian yield magnitudes of 30 to 100 m of change in the Illinois Basin (*34*). Other estimates from North America in this glacially dominated interval imply minimum amplitudes of 80 m, reaching >100 m of change from preserved relief on subaerial exposure surfaces of large algal bioherms (*35*).
23. M. Rygel, C. R. Fielding, T. D. Frank, L. P. Birgenheier, *J. Sed. Res.* **78**, 500 (2008).
24. M. E. Johnson, J. Y. Rong, S. Kershaw, *N.Y. State Mus. Bull.* **491**, 3 (1998).
25. Because of scalar limitations, the Paleozoic cycle chart of sea level fluctuations is presented in three separate figures, each comprising two of the periods of the Paleozoic Era (Figs. 1 to 3). The SOM also includes a complete downloadable color PDF version (fig. S1) of the cycle chart with more details [for example, major orogenic and anoxic events, regional stratigraphic subdivisions and biozonations, and sequence nomenclature (*36*) and known carbonate megabreccias as they have been synthesized from the worldwide data. The latter tend to occur in the carbonate systems at major drawdowns of sea level].
26. M. V. Caputo, J. C. Crowell, *Geol. Soc. Am. Bull.* **96**, 1020 (1985).
27. N. Eyles, G. M. Young, in *Earth's Glacial Record,* M. Deynoux *et al.*, Eds. (Cambridge Univ. Press, Cambridge, 1994), p. 1.
28. J. L. Isbell, M. F. Miller, K. L. Wolfe, P. A. Lenaker, *Geol. Soc. Am. Spec. Pap.* **370**, 5 (2003).
29. G. C. Bond, M. A. Kominz, *Geol. Soc. Am. Bull.* **95**, 155 (1984).
30. B. J. Witzke, B. J. Bunker, *Geol. Soc. Am. Spec. Pap.* **306**, 307 (1996).
31. H. A. McClure, *Palaeogeogr. Palaeoclimatol. Palaeoecol.* **25**, 315 (1978).
32. D. Vaslet, *Episodes* **13**, 147 (1990).
33. W. H. C. Ramsbottom, *Proc. Yorkshire Geol. Soc.* **43**, 473 (1981).
34. L. A. Smith Jr., J. F. Read, *J. Sed. Res.* **71**, 985 (2001).
35. G. S. Soreghan, K. A. Giles, *Geology* **27**, 255 (1999).
36. L. L. Sloss, *Geol. Soc. Am. Bull.* **74**, 93 (1963).

37. Many regional experts, too numerous to name, both in the United States and abroad discussed the Paleozoic stratigraphic issues with us. Their insights were indispensable for our synthesis. B.U.H. acknowledges his release by NSF for a sabbatical during 2007 to complete this work. Much of that time was spent at the Institut Français de Recherche pour l'exploitation de la Mer, Brest, France. Their Marine Geosciences Department's (particularly S. Berne's) help in organizing the stay is gratefully acknowledged. S.R.S. in particular acknowledges P. Heckel for many valuable leads into Paleozoic eustasy and the state of Iowa for its amazing Paleozoic record. The authors also thank T. Algeo, A. Hallam, W. Hay, J. Ogg, and another anonymous reviewer for their comments and suggestions. We dedicate this work to our friends and colleagues Peter Vail, Jan Hardenbol, and Tony Hallam, pioneers in the study of sea-level changes of the past.

Supporting Online Material

www.sciencemag.org/cgi/content/full/322/5898/64/DC1
SOM Text
Fig. S1
References

11 June 2008; accepted 29 August 2008
10.1126/science.1161648

Ultrafast X-ray Thomson Scattering of Shock-Compressed Matter

Andrea L. Kritcher, *et al.*

Science **322**, 69 (2008);
DOI: 10.1126/science.1161466

Science (print ISSN 0036-8075; online ISSN 1095-9203) is published weekly, except the last week in December, by the American Association for the Advancement of Science, 1200 New York Avenue NW, Washington, DC 20005.

Ultrafast X-ray Thomson Scattering of Shock-Compressed Matter

Andrea L. Kritcher,[1,2]* Paul Neumayer,[2] John Castor,[2] Tilo Döppner,[2] Roger W. Falcone,[3] Otto L. Landen,[2] Hae Ja Lee,[3] Richard W. Lee,[2,3] Edward C. Morse,[1] Andrew Ng,[2] Steve Pollaine,[2] Dwight Price,[2] Siegfried H. Glenzer[2]

Spectrally resolved scattering of ultrafast K-α x-rays has provided experimental validation of the modeling of the compression and heating of shocked matter. The elastic scattering component has characterized the evolution and coalescence of two shocks launched by a nanosecond laser pulse into lithium hydride with an unprecedented temporal resolution of 10 picoseconds. At shock coalescence, we observed rapid heating to temperatures of 25,000 kelvin when the scattering spectra show the collective plasmon oscillations that indicate the transition to the dense metallic plasma state. The plasmon frequency determines the material compression, which is found to be a factor of 3, thereby reaching conditions in the laboratory relevant for studying the physics of planetary formation.

Shock wave heating is a key technique to produce matter at extreme conditions in the laboratory in which the physics of planetary formation (*1*) and modeling of planetary composition (*2*) can be tested. Contemporary experiments are designed to determine the equation of state (EOS) of light elements (*3*–*5*) or to measure effects of shock waves on matter, for example, to investigate effects by solar nebula shocks (*6*). In addition, the inertial confinement approach to controlled nuclear fusion (*7*) uses a deuterium-tritium–filled capsule that will be compressed to 1000 times solid density and heated to temperatures larger than the interior of the Sun by using a sequence of coalescing shock waves.

Previous shock wave experiments have been restricted to measuring particle and shock velocities (*4*). The experiments reported here directly measured the thermodynamic properties and dynamic structure factors of shocked matter. These experiments have become possible with the advent of penetrating powerful x-ray probes (*8*) produced by high-energy (300 J) petawatt-class ultrashort pulse lasers.

We shock-compressed lithium-hydride, LiH, with an energetic nanosecond laser and measured the conditions with spectrally resolved x-ray Thomson scattering (*9*). These pump-probe experiments show that efficient compression and heating occur at temperature and density conditions previously not accessible to quantitative in situ characterization. The experimental data show a factor of 3 compression with concomitant heating to T = 25,000 K = 2.2 eV, in broad agreement with radiation-hydrodynamic modeling. Although the range of temperatures traversed in phase space by shock compression agrees with calculations that use a quotidian (*10*) equation of state (QEOS), calculations with the Sesame (*11*) EOS tables provide a better match of the coalescence time.

In the schematic of the experiment shown together with a data record from the x-ray spectrometer (Fig. 1A), a 450-J laser beam (*12*) irradiates 300-μm-thick LiH (initial density of ρ_0 = 0.78 g cm^{-3}). The laser pulse was shaped in time (Fig. 1B) with a 4-ns-long foot at a laser intensity of 10^{13} W cm^{-2} followed by a 2-ns-long peak at 3 × 10^{13} W cm^{-2}. Radiation-hydrodynamic simulations (*13*) indicate that the two shock waves launched into the target compress the target to 2.2 g cm^{-3} and coalesce about 7 ns after the beginning of the laser drive (Fig. 1C).

An ultrashort pulse laser delayed from the nanosecond laser illuminates a titanium foil, producing a 10-ps-long K-α x-ray pulse (*14*) at an x-ray energy of E_0 = 4.51 keV that penetrates through the dense compressed LiH. By varying the delay between the nanosecond heater beam and the short pulse probe beam, we probed conditions before and during shock coalescence. The short pulse laser energy of 300 J is converted to Ti K-α with an efficiency of 5 × 10^{-5}, providing 10^{12} x-ray photons on target, sufficient for measurements of elastic and inelastic scattering components in a single shot.

The data record at shock coalescence shows features in the scattering spectrum resulting from interactions with the delocalized, that is, metallic, and bound electrons. The former undergo plasma (Langmuir wave) (*15*) oscillations at the plasma frequency that give rise to the inelastic plasmon scattering feature (*9*), whereas the latter give rise to elastic Rayleigh scattering.

The plasmon feature is downshifted from the incident 4.51-keV x-rays as determined by the Bohm Gross dispersion relation (*16*), with the leading term being the plasma frequency, ω_p =

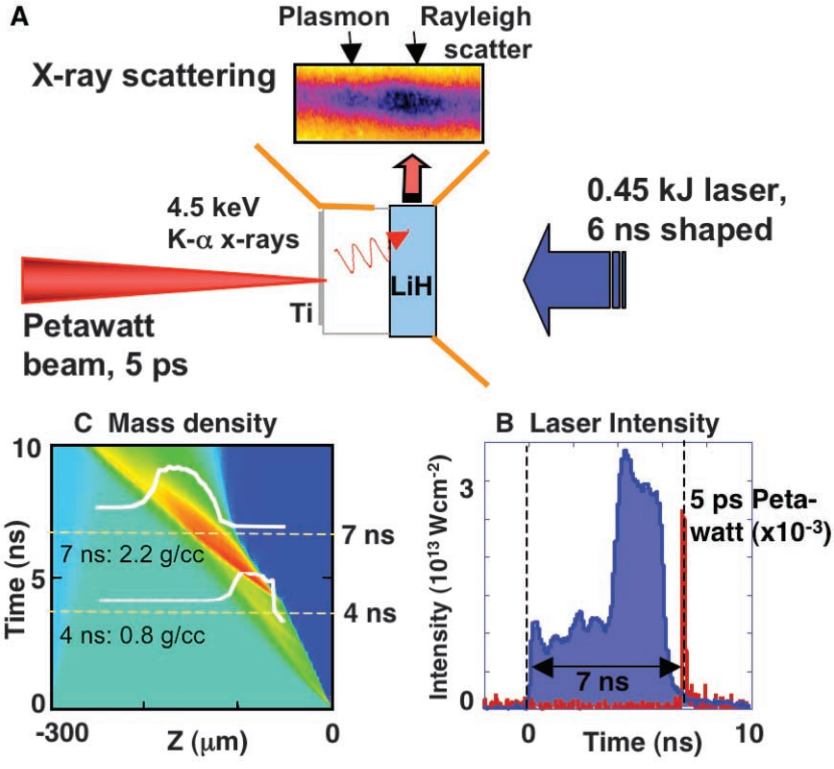

Fig. 1. (**A**) Schematic of the experimental setup. A short (10-ps), monoenergetic ($\Delta E/E$ < 0.5%), K-α x-ray probe is generated by ultrashort pulse laser irradiation of a titanium foil. The x-rays interact with matter compressed by a 6-ns-long shaped laser pulse. The x-ray Thomson scattering spectrum shows inelastic scattering on plasmons and elastic Rayleigh scattering features. (**B**) The evolution of the shocks is measured at various times by changing the delay between the ultrashort pulse laser and the long-pulse pump beam. (**C**) Radiation hydrodynamic modeling indicates coalescence of the shock waves at t = 7 ns.

[1]Nuclear Engineering Department, University of California Berkeley, Berkeley, CA 94709, USA. [2]Lawrence Livermore National Laboratory, Post Office Box 808, Livermore, CA 94551, USA. [3]Physics Department, University of California Berkeley, Berkeley, CA 94709, USA.

*To whom correspondence should be addressed. E-mail: kritcher@berkeley.edu

$(n_e e^2/\varepsilon_o m_e)^{1/2}$. Here, n_e is the electron density, ε_o the permittivity of free space, and e and m_e the electron charge and mass, respectively. Thermal corrections to the dispersion relation resulting from the propagation of the oscillations are small, whereas quantum diffraction is calculated from the Compton energy, $E_C = (h/2\pi)^2 k^2/2m_e$ = 9.3 eV. h is Planck's constant, and the magnitude of scattering vector k determines the scale length of electron density fluctuations probed in this experiment. The scattering vector depends only on the probe energy and scattering angle, $k = 4\pi(E_0/hc)\sin(\theta/2) = 1.6$ Å^{-1}. Thus, the downshift of the plasmon provides the electron density from its main dependence on the plasma frequency.

The strongly bound K-shell electrons of Li and H that interact with x-ray photons are not excited by the scattering process because their ionization potential is greater than the Compton energy, and therefore those electrons scatter elastically. The intensity of the elastic scattering feature is sensitive to the number of strongly bound electrons and the ion-ion structure factor; the latter is sensitive to the ion temperature. Hence, the temperature can be inferred from the elastic scattering strength.

The experimental scattering spectrum at shock coalescence, t = 7 ns, and at t = 4 ns, just before the second strong shock wave was launched, are shown in Fig. 2. These spectra are fit with calculated scattering profiles by using the theoretical dynamic form factor of (*17*). Also shown is a spectral profile of the Ti K-α source measured with the same spectrometer. In addition to the short probe pulse duration required to time-resolve the shock wave coalescence, this x-ray source exhibits no spectral features on the red wing of the K-α doublet, allowing accurate observations of inelastic scattering on plasmons.

The scattering signal at t = 4 ns shows only elastic scattering, indicating a lack of free electrons. The theoretical fit that takes into account contributions from bound and free electrons limits the degree of ionization to $Z^* < 0.1$. However, the intensity of the elastic scattering peak alone has increased by 40% ± 10% compared with scattering from cold samples, indicating a $T < 0.4$ eV.

In contrast, when the shock waves coalesce at t = 7 ns, strong plasmon oscillations give rise to inelastic scattering downshifted from the elastic peak by ΔE_{pl} = 24 eV. In this case, the elastic scattering signal has increased by 100% ± 10% compared with scattering from cold samples, indicating T = 2.2 eV. Compression and heating results in ionized material with Z^* = 1 for $Li^{(+)}H$ as determined from the shape of the scattering spectrum. An error bar of +2% and –10% is inferred from the minimum of the root mean square difference between the experimental data and the theoretical spectrum (*18*).

For the degenerate systems encountered here, the plasma screening length, λ_S = 0.57 Å, at which local electric fields are shielded by mobile charge carriers, approaches the Thomas-Fermi length (*17*). Therefore, scattering is collective with a scattering parameter (*19*) $\alpha = 1/k\lambda_S$ = 1.1, where the scattering scale length is on the order of the screening length required for the observation of plasmon oscillations.

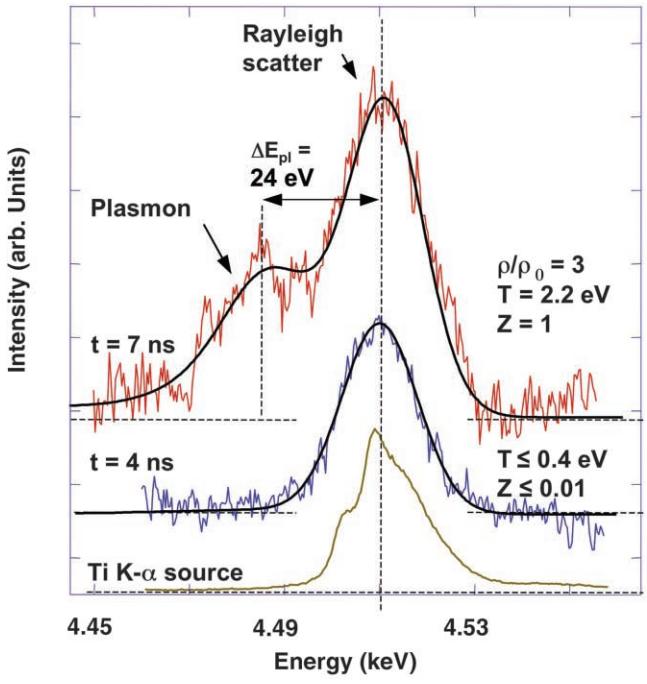

Fig. 2. X-ray scattering spectrum from shocked LiH, showing elastic Rayleigh scattering and inelastic plasmon scattering features. At t = 7 ns (top), the plasmon energy shift of 24 eV indicates 3× compression, whereas the intensity of the elastic scattering feature shows heating to temperatures of 2.2 eV. Earlier in time only elastic scattering is observed (middle) as demonstrated when compared with the K-α source spectrum (bottom). The observation of plasmons at t = 7 ns indicates the transition to the metallic free electron plasma in the solid phase.

The plasmon shift determined by the calculated spectra provides the electron density, $n_e = 1.7 \times 10^{23}$ cm^{-3}. The density is obtained with an error of 10% because of noise in these single-shot data. Accurate knowledge of the electron density further determines the absolute electron-electron structure factor (*20*). In the long-wavelength limit

$$S_{aa}(k) = k^2/[k^2 + (1/\lambda_S)^2] \quad (1)$$

with a indicating e or i for electron or ion, respectively. With λ_S for a partly degenerate electron fluid, we find $S_{ee}(k = 1.6$ Å$^{-1}) = 0.46$. This value, combined with the measured elastic and inelastic scattering amplitude, determines the absolute ion-ion structure factor, which yields the ion temperature from the ion Debye screening length. The spectral calculations and parameters of Fig. 2 include multiple-species ion-ion structure factors from one-component electron-ion interaction potentials (*17*) that have been shown to be consistent with previous experiments (*9*).

The evolution of the measured temperature as a function of time is shown (Fig. 3) along with results from radiation-hydrodynamic calculations using the code LASNEX (*18*). The strong rise at t = 7 ns indicates coalescence of the shock waves. The temperature has been inferred with an error of 10 to 20% because of noise. Partial scattering from uncompressed material has been accounted for, resulting in a correction of about 10%.

The simulation results shown in Fig. 3 are mainly dependent on the choice of the EOS and rather insensitive to details in radiation transport and heat conduction. The ranges of temperatures arise from variations in the amount of impurities and oxide layers consistent with target characterization. The QEOS, being the simpler model, includes a modified electronic Thomas-Fermi statistical model with ion thermal motion calculated beyond the Grüneisen EOS by including temperature-dependent corrections to the pressure. This model is consistent with the wide range of temperatures accessed in this experiment.

The Sesame EOS includes atomic structure based on solutions of the single-particle quantum levels in the self-consistent field of an atom (*21*). The peak temperature and the experimentally observed coalescence time are in excellent agreement with modeling that uses the Sesame EOS. However, early in time the agreement is less satisfactory, indicating that a future comparison with first-principle statistical models (*22*) will be of interest to understand these weakly shocked systems.

At peak temperature, the calculations indicate pressures in the range of P = 300 to 420 GPa. With Z^* = 1 and the electron density from the plasmon data, we find a density of $\rho = 2.25$ g cm^{-3}, corresponding to three times compressed LiH. This value is consistent with the EOS data obtained from density functional perturbation theory (*23*) and approaches conditions where a pressure-induced insulator-metal transition is predicted (*24*).

Our results demonstrate the capability to measure temperature and density in dense matter during shock compression with 10-ps temporal resolution. The experiments have shown the transition to a metallic plasma state in the solid phase, resulting in the observation of plas-

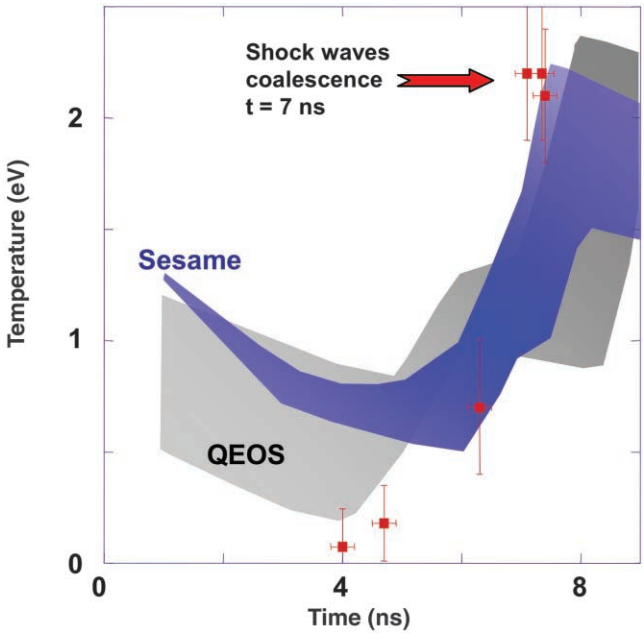

Fig. 3. The temperature of the shocked LiH as a function of time from x-ray Thomson scattering measurements and from radiation-hydrodynamic modeling using different EOS models. The range of temperatures for each model accounts for LiOH surface impurities (lower bounds) to no impurities (upper bounds). The experiments and calculations demonstrate efficient heating by shock coalescence, with small differences in shock timing resolved by the short K-α x-ray pulses. Error bars result mainly from noise in the experimental data.

mons. This feature has further allowed testing of radiation-hydrodynamic calculations with different EOS models for shock-compressed matter. This technique is opportune for inertial confinement fusion experiments that will achieve extreme densities, for example, on the National Ignition Facility (*25*).

Lastly, the K-α x-ray source used in this study provides the same number of x-ray photons on target as projected for future x-ray free electron laser facilities (*26*, *27*). This indicates that x-ray Thomson scattering experiments on dense matter will soon be accessible for high-repetition measurements of thermodynamic properties with 20- to 200-fs temporal resolution.

References and Notes

1. H. C. Connolly Jr., S. G. Love, *Science* **280**, 62 (1998).
2. T. Guillot, *Science* **286**, 72 (1999).
3. N. C. Holmes, M. Ross, W. J. Nellis, *Phys. Rev. B* **52**, 15835 (1995).
4. G. W. Collins *et al.*, *Science* **281**, 1178 (1998).
5. M. D. Knudson, D. L. Hanson, J. E. Bailey, C. A. Hall, J. R. Asay, *Phys. Rev. Lett.* **87**, 225501 (2001).
6. C. P. McKay, W. J. Borucki, *Science* **276**, 390 (1997).
7. J. D. Lindl *et al.*, *Phys. Plasmas* **11**, 339 (2004).
8. O. L. Landen *et al.*, *Rev. Sci. Instrum.* **72**, 627 (2001).
9. S. H. Glenzer *et al.*, *Phys. Rev. Lett.* **98**, 065002 (2007).
10. R. M. More, K. H. Warren, D. A. Young, G. B. Zimmerman, *Phys. Fluids* **31**, 3059 (1988).
11. S. Crockett, *Los Alamos National Laboratory Report No. LA-UR-06-8403* (Los Alamos National Laboratory, Los Alamos, NM, 2006).
12. B. C. Stuart *et al.*, in report no. UCRL-CONF-221530 (Conference on Lasers and Electro-Optics, IEEE/LEOS, Lasers and Electro-Optics Society and the Optical Society, Long Beach, CA, 21 to 26 May 2006), pp. 56–68.
13. J. J. MacFarlane, I. E. Golovkin, P. R. Woodruff, *J. Quant. Spectrosc. Radiat. Transfer* **99**, 381 (2006).
14. H. Chen *et al.*, *Phys. Rev. E* **76**, 056402 (2007).
15. L. Tonks, I. Langmuir, *Phys. Rev.* **33**, 195 (1929).
16. D. Bohm, E. P. Gross, *Phys. Rev.* **75**, 1851 (1949).
17. G. Gregori, A. Ravasio, A. Höll, S. H. Glenzer, S. J. Rose, *High Energy Density Phys.* **3**, 99 (2007).
18. Materials and methods are available as supporting material on *Science* Online.
19. J. Sheffield, *Plasma Scattering of Electromagnetic Radiation* (Academic Press, New York, 1975).
20. S. Ichimaru, *Rev. Mod. Phys.* **54**, 1017 (1982).
21. D. A. Lieberman, *Phys. Rev. B* **20**, 4798 (1979).
22. T. Ogitsu, E. Schwegler, F. Gygi, G. Galli, *Phys. Rev. Lett.* **91**, 175502 (2003).
23. W. Yu, C. Jin, A. Kohlmeyer, *J. Phys. Condens. Matter* **19**, 086209 (2007).
24. Y. Wang, R. Ahuja, B. Johansson, *Phys. Status Solidi* **235**, 470 (2003).
25. E. Moses, C. R. Wuest, *Fusion Sci. Tech. (Paris)* **47**, 314 (2005).
26. R. Akre *et al.*, *Phys. Rev. Spec. Top. Accelerators Beams* **11**, 030703 (2008).
27. W. Ackermann *et al.*, *Nat. Photonics* **1**, 336 (2007).

28. This work was performed under the auspices of the U.S. Department of Energy (DOE) by Lawrence Livermore National Laboratory under contract DE-AC52-07NA27344. This work was further supported by a DOE grant, the NA-16 Intermediate Facility Initiative, grant 08-ERI-002, grant 08-LW-004, and the Lawrence Scholar Program fellowship.

Supporting Online Material

www.sciencemag.org/cgi/content/full/322/5898/69/DC1
Materials and Methods
Figs. S1 to S4
References

6 June 2008; accepted 27 August 2008
10.1126/science.1161466

Time Reversal and Negative Refraction

J. B. Pendry

Time reversal and negative refraction have been shown to be intimately linked processes. We propose a scheme that exploits transitions between positive and negative frequencies to mimic negative refraction at an interface and hence to make a negatively refracting lens. The theory applies equally to electromagnetic and acoustic waves. We also propose an experimental realization, and under ideal circumstances this lens can exhibit subwavelength resolution, limited only by the strength of the time-reversed signal.

In a time-reversal experiment, a wave might strike a surface where it is reflected into a new state such that its phase evolves backward in time (*1*, *2*). As a result, a wave originally diverging from a source now converges back onto that source. In contrast, a wave striking a negatively refracting medium (*3*, *4*) is transmitted into the medium, where its phase evolves backward in space (Fig. 1), and the wave converges to a focus inside the medium. There is an appealing symmetry between the two processes, provoking a deeper inquiry into their relationship.

Let us examine the similarities between the two processes. Negative refraction implies that, as a pulse of waves moves forward, the phase evolves in the opposite direction. In other words, the group and phase velocities are oppositely directed

$$\frac{\omega}{k}\frac{d\omega}{dk} < 0 \qquad (1)$$

and hence moving into the negatively refracting medium begins the process of phase reversal (here, ω is the frequency and k is the wave vector).

Sometimes the same medium can host both positively and negatively refracting states. This may happen in certain chiral media (*5*), where the spin of the photon dictates positive or negative refraction, or in graphene (*6*, *7*), where the pseudospin of an electron close to the Fermi energy controls the phase evolution. Such media are designated as "self-conjugate."

Self conjugation forges the link between time reversal and negative refraction. Consider a wave of the form

$$\mathbf{E} = E_0\,\hat{\mathbf{e}}_0 \exp(i\mathbf{k}\cdot\mathbf{r} - i\omega t) \qquad (2)$$

where $\mathbf{E}$ is the electric component of the field, E_0 is a constant, $\hat{\mathbf{e}}_0$ is a unit vector defining the polarization, $\boldsymbol{r}$ is a position vector, and t is time. Now shift the frequency down by an amount $\delta\omega = 2\omega$ (here, $\mathbf{E}'$ is the shifted electric field)

$$\mathbf{E}' = E_0\,\hat{\mathbf{e}}_0 \exp(i\mathbf{k}\cdot\mathbf{r} + i\omega t) \qquad (3)$$

Reversing frequency has the same effect as reversing time (Fig. 2). The same figure shows that, if negative frequencies are included, any linearly dispersing medium can be regarded as self-

Department of Physics, The Blackett Laboratory, Imperial College London, London SW7 2AZ, UK. E-mail: j.pendry@imperial.ac.uk

Time Reversal and Negative Refraction

J. B. Pendry, *et al.*

Science **322**, 71 (2008);
DOI: 10.1126/science.1162087

Science (print ISSN 0036-8075; online ISSN 1095-9203) is published weekly, except the last week in December, by the American Association for the Advancement of Science, 1200 New York Avenue NW, Washington, DC 20005.

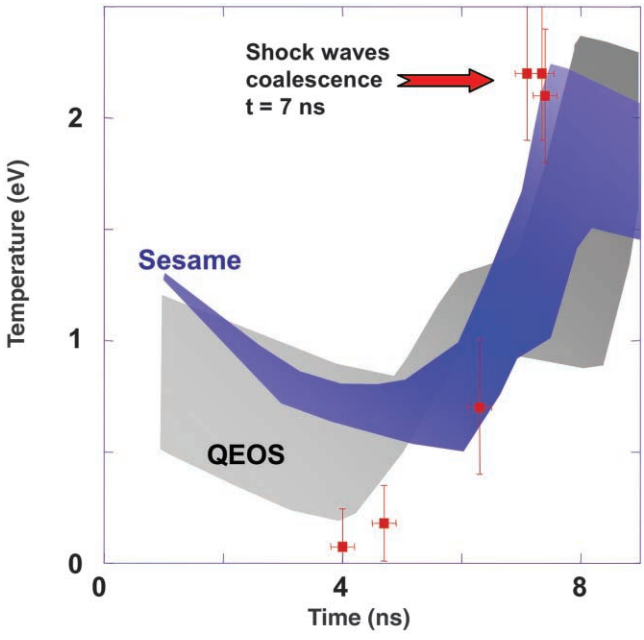

Fig. 3. The temperature of the shocked LiH as a function of time from x-ray Thomson scattering measurements and from radiation-hydrodynamic modeling using different EOS models. The range of temperatures for each model accounts for LiOH surface impurities (lower bounds) to no impurities (upper bounds). The experiments and calculations demonstrate efficient heating by shock coalescence, with small differences in shock timing resolved by the short K-α x-ray pulses. Error bars result mainly from noise in the experimental data.

mons. This feature has further allowed testing of radiation-hydrodynamic calculations with different EOS models for shock-compressed matter. This technique is opportune for inertial confinement fusion experiments that will achieve extreme densities, for example, on the National Ignition Facility (*25*).

Lastly, the K-α x-ray source used in this study provides the same number of x-ray photons on target as projected for future x-ray free electron laser facilities (*26*, *27*). This indicates that x-ray Thomson scattering experiments on dense matter will soon be accessible for high-repetition measurements of thermodynamic properties with 20- to 200-fs temporal resolution.

References and Notes

1. H. C. Connolly Jr., S. G. Love, *Science* **280**, 62 (1998).
2. T. Guillot, *Science* **286**, 72 (1999).
3. N. C. Holmes, M. Ross, W. J. Nellis, *Phys. Rev. B* **52**, 15835 (1995).
4. G. W. Collins *et al.*, *Science* **281**, 1178 (1998).
5. M. D. Knudson, D. L. Hanson, J. E. Bailey, C. A. Hall, J. R. Asay, *Phys. Rev. Lett.* **87**, 225501 (2001).
6. C. P. McKay, W. J. Borucki, *Science* **276**, 390 (1997).
7. J. D. Lindl *et al.*, *Phys. Plasmas* **11**, 339 (2004).
8. O. L. Landen *et al.*, *Rev. Sci. Instrum.* **72**, 627 (2001).
9. S. H. Glenzer *et al.*, *Phys. Rev. Lett.* **98**, 065002 (2007).
10. R. M. More, K. H. Warren, D. A. Young, G. B. Zimmerman, *Phys. Fluids* **31**, 3059 (1988).
11. S. Crockett, *Los Alamos National Laboratory Report No. LA-UR-06-8403* (Los Alamos National Laboratory, Los Alamos, NM, 2006).
12. B. C. Stuart *et al.*, in report no. UCRL-CONF-221530 (Conference on Lasers and Electro-Optics, IEEE/LEOS, Lasers and Electro-Optics Society and the Optical Society, Long Beach, CA, 21 to 26 May 2006), pp. 56–68.
13. J. J. MacFarlane, I. E. Golovkin, P. R. Woodruff, *J. Quant. Spectrosc. Radiat. Transfer* **99**, 381 (2006).
14. H. Chen *et al.*, *Phys. Rev. E* **76**, 056402 (2007).
15. L. Tonks, I. Langmuir, *Phys. Rev.* **33**, 195 (1929).
16. D. Bohm, E. P. Gross, *Phys. Rev.* **75**, 1851 (1949).
17. G. Gregori, A. Ravasio, A. Höll, S. H. Glenzer, S. J. Rose, *High Energy Density Phys.* **3**, 99 (2007).
18. Materials and methods are available as supporting material on *Science* Online.
19. J. Sheffield, *Plasma Scattering of Electromagnetic Radiation* (Academic Press, New York, 1975).
20. S. Ichimaru, *Rev. Mod. Phys.* **54**, 1017 (1982).
21. D. A. Lieberman, *Phys. Rev. B* **20**, 4798 (1979).
22. T. Ogitsu, E. Schwegler, F. Gygi, G. Galli, *Phys. Rev. Lett.* **91**, 175502 (2003).
23. W. Yu, C. Jin, A. Kohlmeyer, *J. Phys. Condens. Matter* **19**, 086209 (2007).
24. Y. Wang, R. Ahuja, B. Johansson, *Phys. Status Solidi* **235**, 470 (2003).
25. E. Moses, C. R. Wuest, *Fusion Sci. Tech. (Paris)* **47**, 314 (2005).
26. R. Akre *et al.*, *Phys. Rev. Spec. Top. Accelerators Beams* **11**, 030703 (2008).
27. W. Ackermann *et al.*, *Nat. Photonics* **1**, 336 (2007).

28. This work was performed under the auspices of the U.S. Department of Energy (DOE) by Lawrence Livermore National Laboratory under contract DE-AC52-07NA27344. This work was further supported by a DOE grant, the NA-16 Intermediate Facility Initiative, grant 08-ERI-002, grant 08-LW-004, and the Lawrence Scholar Program fellowship.

Supporting Online Material

www.sciencemag.org/cgi/content/full/322/5898/69/DC1
Materials and Methods
Figs. S1 to S4
References

6 June 2008; accepted 27 August 2008
10.1126/science.1161466

Time Reversal and Negative Refraction

J. B. Pendry

Time reversal and negative refraction have been shown to be intimately linked processes. We propose a scheme that exploits transitions between positive and negative frequencies to mimic negative refraction at an interface and hence to make a negatively refracting lens. The theory applies equally to electromagnetic and acoustic waves. We also propose an experimental realization, and under ideal circumstances this lens can exhibit subwavelength resolution, limited only by the strength of the time-reversed signal.

In a time-reversal experiment, a wave might strike a surface where it is reflected into a new state such that its phase evolves backward in time (*1*, *2*). As a result, a wave originally diverging from a source now converges back onto that source. In contrast, a wave striking a negatively refracting medium (*3*, *4*) is transmitted into the medium, where its phase evolves backward in space (Fig. 1), and the wave converges to a focus inside the medium. There is an appealing symmetry between the two processes, provoking a deeper inquiry into their relationship.

Let us examine the similarities between the two processes. Negative refraction implies that, as a pulse of waves moves forward, the phase evolves in the opposite direction. In other words, the group and phase velocities are oppositely directed

$$\frac{\omega}{k}\frac{d\omega}{dk} < 0 \qquad (1)$$

and hence moving into the negatively refracting medium begins the process of phase reversal (here, ω is the frequency and k is the wave vector).

Sometimes the same medium can host both positively and negatively refracting states. This may happen in certain chiral media (*5*), where the spin of the photon dictates positive or negative refraction, or in graphene (*6*, *7*), where the pseudospin of an electron close to the Fermi energy controls the phase evolution. Such media are designated as "self-conjugate."

Self conjugation forges the link between time reversal and negative refraction. Consider a wave of the form

$$\mathbf{E} = E_0\,\hat{\mathbf{e}}_0 \exp(i\mathbf{k}\cdot\mathbf{r} - i\omega t) \qquad (2)$$

where $\mathbf{E}$ is the electric component of the field, E_0 is a constant, $\hat{\mathbf{e}}_0$ is a unit vector defining the polarization, $\boldsymbol{r}$ is a position vector, and t is time. Now shift the frequency down by an amount $\delta\omega = 2\omega$ (here, $\mathbf{E}'$ is the shifted electric field)

$$\mathbf{E}' = E_0\,\hat{\mathbf{e}}_0 \exp(i\mathbf{k}\cdot\mathbf{r} + i\omega t) \qquad (3)$$

Reversing frequency has the same effect as reversing time (Fig. 2). The same figure shows that, if negative frequencies are included, any linearly dispersing medium can be regarded as self-

Department of Physics, The Blackett Laboratory, Imperial College London, London SW7 2AZ, UK. E-mail: j.pendry@imperial.ac.uk

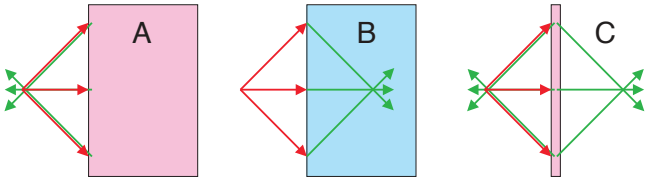

Fig. 1. **(A)** Medium (A) time-reverses a wave winding the phase backward in time to refocus on the source. **(B)** Medium (B) is negatively refracting and reverses the spatial evolution of the phase refocusing at some point inside the medium. **(C)** A thin sheet, (C), of time-reversing material produces negative frequency waves on both sides of the sheet: It both time-reverses and negatively refracts.

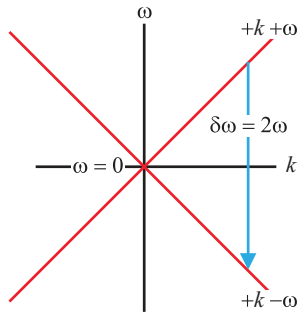

Fig. 2. Dispersion of a wave in a medium with constant velocity $\omega = ck$ (where c is the velocity of light). Both positive and negative frequencies are displayed. Time reversal can be understood as a vertical transition between positive and negative frequencies.

conjugate and contains a negatively dispersing band. Of course, negative refraction is never seen at an interface between ordinary media, because a positive frequency band has to refract into another positive frequency band or a negative frequency into another negative frequency. Both cases imply a positive angle of refraction. This is always true of passive systems.

The link between negative refraction and time reversal has been remarked on before in (*8*), where a phase-conjugating interface between two regions of space was postulated as a particular mathematical construction—one of many possible. Apparently independently of the earlier work, the analogy was carried further in (*9*), where it was pointed out that this particular interface supported surface resonances of the same character as those appearing at interfaces with negatively refracting materials. Somewhat later in (*10*), a practical realization of this mathematical scheme was proposed, but only a partial realization. Whereas the scheme is effective for the far field, it does not reproduce the same boundary conditions for evanescent states and therefore supports no surface modes. In fact, a realization of the boundary condition had already been implemented in (*11*), but again only effective for the far field.

Now consider a possible physical realization of the present approach. By making the interface time-dependent, more interesting things can happen. Consider the simplest case where a thin sheet of dielectric separates two regions of otherwise empty space, and let the permittivity uniformly pulsate at a frequency of 2ω. This parametric oscillation will induce transitions between positive and negative frequencies in a manner familiar to four-wave mixing experiments. There is an important difference in our configuration: If the dielectric sheet is much thinner than the wavelength, there is no momentum conservation normal to the sheet; only parallel momentum is conserved [scattering from a thin sheet has also been considered (*12*)]. Thus, the pulsating sheet generates two waves that are shown in Fig. 1C: (i) a conventional time-reversed wave that returns to the source on the same side of the sheet and (ii) another with opposite momentum normal to the sheet exiting on the far side to form an image in the manner of a medium with a refractive index $n = -1$.

Our configuration is an alternative to the Veselago lens, except that this version focuses only the far field and, like other schemes (*8*–*11*), is subject to wavelength limitations on resolution. It lacks the extraordinary property of a true $n = -1$ material of subwavelength resolution. This limitation can be overcome by the addition of further components to the system.

Figure 3 shows a system containing two time-reversing sheets separated by a distance d. Waves are reversed by the first sheet and again by the second, returning to "positive frequency" on emerging from the system.

More formally, transmission and reflection coefficients (T and R) are defined for the sheets that are assumed to be identical. Furthermore, if the sheets are very thin

$$T = R \tag{4}$$

This result can easily be understood by noting that transmitted and reflected waves are sourced on the same set of currents and charges. Because the sources are two-dimensional (2D), they are mirror symmetrical about the plane and hence give rise to the same transmitted and reflected fields.

The component of the wave vector perpendicular to the sheets is given by

$$k_z = +\sqrt{\omega^2/c_0^2 - k_x^2 - k_y^2} \tag{5}$$

when k_z is real, and by

$$k_z = +i\sqrt{k_x^2 + k_y^2 - \omega^2/c_0^2} \tag{6}$$

when k_z is imaginary.

The transmitted wave between the two sheets can be written in the case of real k_z (where R is a constant, $\|$ denotes the component of a vector parallel to the plane of the sheet, and d is defined in Fig. 3

$$\mathbf{E} = E_0\hat{\mathbf{e}}\, Re^{i\mathbf{k}_\parallel\cdot\mathbf{r}_\parallel} \times \begin{bmatrix} +(1 + R^2 + \cdots)e^{(-ik_z z + i\omega t)} \\ +(R + R^3 + \cdots)e^{(-ik_z z - i\omega t)} \end{bmatrix} = E_0\hat{\mathbf{e}}Re^{i\mathbf{k}_\parallel\cdot\mathbf{r}_\parallel} \times \begin{bmatrix} +(1-R^2)^{-1}e^{(-ik_z z + i\omega t)} \\ +R(1-R^2)^{-1}e^{(-ik_z z - i\omega t)} \end{bmatrix}, 0 < z < d \tag{7}$$

Note the careful choice of signs in the exponents dictated by the requirement that each set of waves must carry flux away from the last surface of interaction. At each reflection and transmission, the frequency is reversed. See the supporting online material (SOM) for further discussion of this point.

A slightly different result follows when k_z is imaginary

$$\mathbf{E} = E_0\hat{\mathbf{e}}\, Re^{i\mathbf{k}_\parallel\cdot\mathbf{r}_\parallel} \times \begin{bmatrix} +(1 + R^2e^{2ik_z d} + \cdots)e^{(+ik_z z + i\omega t)} \\ +(R + R^3e^{2ik_z d} + \cdots)e^{(-ik_z(z-2d) - i\omega t)} \end{bmatrix} = E_0\hat{\mathbf{e}}Re^{i\mathbf{k}_\parallel\cdot\mathbf{r}_\parallel} \times \begin{bmatrix} +(1 - R^2e^{2ik_z d})^{-1}e^{(+ik_z z + i\omega t)} \\ +R(1 - R^2e^{2ik_z d})^{-1}e^{(-ik_z(z-2d) - i\omega t)} \end{bmatrix}, 0 < z < d \tag{8}$$

Finally, the waves are allowed to emerge from the end of the cavity. For real k_z

$$\mathbf{E} = E_0\hat{\mathbf{e}}\,\frac{R^2e^{i\mathbf{k}_\parallel\cdot\mathbf{r}_\parallel + ik_z(z-2d) - i\omega t}}{1 - R^2}, d < z \tag{9}$$

For imaginary k_z

$$\mathbf{E} = E_0\hat{\mathbf{e}}\,\frac{R^2e^{i\mathbf{k}_\parallel\cdot\mathbf{r}_\parallel + ik_z z - i\omega t}}{1 - R^2e^{2ik_z d}}, d < z \tag{10}$$

Because the sheets are connected to a source of power, there is no longer a requirement that energy is conserved, so (at least in theory) the limit of very large transmission and reflection coefficients could be envisaged

$$\lim_{R\to\infty}\mathbf{E} = -E_0\hat{\mathbf{e}}e^{i\mathbf{k}_\parallel\cdot\mathbf{r}_\parallel + ik_z(z-2d) - i\omega t}, d < z \tag{11}$$

It is assumed that Eq. 4 is true, and the limit is independent of whether k_z is real or imaginary. In the same limit, it can be shown that the sheets do not scatter waves back into the region $z < 0$.

The interpretation of Eq. 11 is that fields are translated along the axis normal to the sheets by a distance $2d$. In other words, objects between $-d < z < 0$ appear as images between $d < z < 2d$. Furthermore, according to Eq. 11, all Fourier components of the image that satisfy

$$|R| >> \left|e^{ik_z d}\right| \tag{12}$$

contribute their due weight to the image, and in the limit $R \to \infty$ the image tends to perfection.

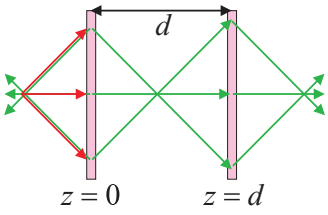

Fig. 3. Two thin sheets of time-reversing material produce a focusing effect very similar to a negatively refracting lens. The system is capable of subwavelength resolution.

Unlike the perfect lens based on negative refraction (*13*), loss is not an issue in this instance because the fields are translated through loss-less vacuum. The issue here is whether a time-reversing sheet can be found sufficiently powerful to give the resolution, Δ, required

$$\Delta \approx 1/k_{\parallel \max} \approx d/\ln R \qquad (13)$$

A scheme for subwavelength resolution was also proposed in (*9*) but, as noted above, this scheme depended on the existence of surface states derived from a mathematically postulated boundary for which no physical realization has so far been suggested.

Although our discussion has been in terms of electromagnetic waves, the same principles apply to any waves and particularly to acoustic waves, where time-reversal studies are also well developed (*14*).

Our original discussion (illustrated in Fig. 2) assumes a single-step transition from +ω to –ω. Such processes occur but are very weak. At optical frequencies, perhaps the best system for the realization of these ideas is a four-wave mixing experiment: One of two counterpropagating pump beams of the same frequency as the signal writes a hologram. The second pump beam then reads the hologram to produce a time-reversed signal. In other words, there is a two-step process in which there first occurs a transition $+\omega \rightarrow 0$ and then a second transition $0 \rightarrow -\omega$. This process has much in common with the recent proposal for a subwavelength focusing device (*15*), except that in our scheme the system writes its own hologram.

As a generalization of the analogy, any positively refracting medium can have the sign of its refraction reversed by coating the surface with a phase-reversing sheet. This leads to the possibility of curved lenses that can magnify an object (*16*).

In principle, our new lens can be realized if the hologram is written in a thin sheet of nonlinear material. In practice, such a hologram would be very weak, and instead, 3D holograms are written if a strong output is desired. As a consequence of the 3D nature of the hologram, the second phase-reversed beam (shown on the right of Fig. 1C) is not seen, but if the left-hand surface of the medium is half silver (Fig. 4), reflection of the phase-reversed beam will generate an image

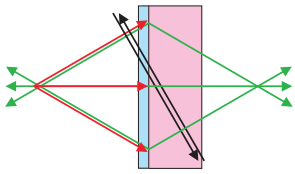

Fig. 4. In a four-wave mixing experiment, two counterpropagating waves first create a hologram and then diffract off the hologram to form a phase-reversed beam. A half-silvered mirror reflects the reversed beam to form an image on the far side of the system.

to the right of the system reproducing the effect predicted in Fig. 1C and mimicking the Veselago negatively refracting lens. However, the 3D nature of the hologram precludes any subwavelength resolution.

Creating a 2D hologram and attaining the ideal shown in Fig. 3 will be a challenge. Enhancing the nonlinearity of existing media—possibly through the use of plasmonic or metamaterial layers to enhance the local fields (*17*)—may offer a route to realizing a 2D version and hence subwavelength resolution. Further discussion of the practicalities of a four-wave mixing scheme can be found in the SOM.

References and Notes

1. J. P. Woerdman, *Opt. Commun.* **2**, 212 (1970).
2. P. Yeh, *Introduction to Photorefractive Nonlinear Optics* (Wiley, New York, 1993).
3. V. G. Veselago, *Sov. Phys. Usp.* **10**, 509 (1968).
4. J. B. Pendry, *Contemp. Phys.* **45**, 191 (2004).
5. J. B. Pendry, *Science* **306**, 1353 (2004).
6. K. Kobayashi, *J. Phys. Condens. Matter* **18**, 3703 (2006).
7. V. V. Cheianov, V. Fal'ko, B. L. Altshuler, *Science* **315**, 1252 (2007).
8. M. Nieto-Vesperinas, E. Wolf, *J. Opt. Soc. Am. A* **2**, 1429 (1985).
9. S. Maslovski, S. Tretyakov, *J. Appl. Phys.* **94**, 4241 (2003).
10. O. Malyuskin, V. Fusco, A. G. Schuchinsky, *IEEE Trans. Antenn. Propag.* **54**, 1399 (2006).
11. C. A. Allen, K. M. K. H. Leong, T. Itoh, *IEEE Int. Microwave Theory Tech. Symp. Dig.* **3**, 1875 (2003).
12. M. Wubs, A. Lagendijk, *Phys. Rev. E Stat. Nonlin. Soft Matter Phys.* **65**, 046612 (2002).
13. J. B. Pendry, *Phys. Rev. Lett.* **85**, 3966 (2000).
14. S. Yon, M. Tanter, M. Fink, *J. Acoust. Soc. Am.* **113**, 1533 (2003).
15. R. Merlin, *Science* **317**, 927 (2007); published online 11 July 2007 (10.1126/science.1143884).
16. J. B. Pendry, S. A. Ramakrishna, *J. Phys. Condens. Matter* **15**, 6345 (2003).
17. J. B. Pendry, A. J. Holden, D. J. Robbins, W. J. Stewart, *IEEE Trans. Microwave Theory Tech.* **47**, 2075 (1999).

18. I thank the Engineering and Physical Sciences Research Council for a Senior Fellowship, M. Damsen for educating me in various aspects of four-wave mixing, S. Maier for discussions on plasmonic enhancements of fields, and A. Lagendijk for comments on the manuscript.

Supporting Online Material

www.sciencemag.org/cgi/content/full/1162087/DC1
SOM Text
Figs. S1 to S6

20 June 2008; accepted 20 August 2008
Published online 28 August 2008;
10.1126/science.1162087
Include this information when citing this paper.

Surface-Modified Carbon Nanotubes Catalyze Oxidative Dehydrogenation of *n*-Butane

Jian Zhang, Xi Liu, Raoul Blume, Aihua Zhang, Robert Schlögl, Dang Sheng Su*

Butenes and butadiene, which are useful intermediates for the synthesis of polymers and other compounds, are synthesized traditionally by oxidative dehydrogenation (ODH) of *n*-butane over complex metal oxides. Such catalysts require high O_2/butane ratios to maintain the activity, which leads to unwanted product oxidation. We show that carbon nanotubes with modified surface functionality efficiently catalyze the oxidative dehydrogenation of *n*-butane to butenes, especially butadiene. For low O_2/butane ratios, a high selectivity to alkenes was achieved for periods as long as 100 hours. This process is mildly catalyzed by ketonic C=O groups and occurs via a combination of parallel and sequential oxidation steps. A small amount of phosphorus greatly improved the selectivity by suppressing the combustion of hydrocarbons.

Transition metal oxides have been widely used as catalysts for the conversion of butane to C_4 alkenes, important industrial precursors for producing synthetic rubbers, plastics, and a number of industrially important chemicals. Despite a great deal of research, alkene selectivity in the current butane-to-butadiene process is severely limited (*1*). One important reason is that the unsaturated products are much more readily oxidized to CO_2 than is the starting alkane. The chemical complexity of polyvalent metal oxides, although found to be necessary for catalytic activity, impedes satisfactory selectivity through isolation of active sites (*2*–*6*). For this reason, the origin of the catalytic activity is debated, and there is as yet no generally accepted picture of the reaction mechanism (*7*, *8*).

Carbon materials have been reported to catalyze the oxidative dehydrogenation (ODH) of an aromatic molecule, ethylbenzene. However, conventional carbons, in particular activated carbon, underwent unavoidable deactivations

Surface-Modified Carbon Nanotubes Catalyze Oxidative Dehydrogenation of n-Butane

Jian Zhang, *et al.*

Science **322**, 73 (2008);
DOI: 10.1126/science.1161916

Science (print ISSN 0036-8075; online ISSN 1095-9203) is published weekly, except the last week in December, by the American Association for the Advancement of Science, 1200 New York Avenue NW, Washington, DC 20005.

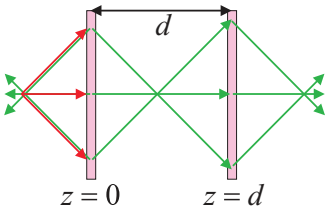

Fig. 3. Two thin sheets of time-reversing material produce a focusing effect very similar to a negatively refracting lens. The system is capable of subwavelength resolution.

Unlike the perfect lens based on negative refraction (*13*), loss is not an issue in this instance because the fields are translated through loss-less vacuum. The issue here is whether a time-reversing sheet can be found sufficiently powerful to give the resolution, Δ, required

$$\Delta \approx 1/k_{\parallel \max} \approx d/\ln R \qquad (13)$$

A scheme for subwavelength resolution was also proposed in (*9*) but, as noted above, this scheme depended on the existence of surface states derived from a mathematically postulated boundary for which no physical realization has so far been suggested.

Although our discussion has been in terms of electromagnetic waves, the same principles apply to any waves and particularly to acoustic waves, where time-reversal studies are also well developed (*14*).

Our original discussion (illustrated in Fig. 2) assumes a single-step transition from +ω to –ω. Such processes occur but are very weak. At optical frequencies, perhaps the best system for the realization of these ideas is a four-wave mixing experiment: One of two counterpropagating pump beams of the same frequency as the signal writes a hologram. The second pump beam then reads the hologram to produce a time-reversed signal. In other words, there is a two-step process in which there first occurs a transition $+\omega \rightarrow 0$ and then a second transition $0 \rightarrow -\omega$. This process has much in common with the recent proposal for a subwavelength focusing device (*15*), except that in our scheme the system writes its own hologram.

As a generalization of the analogy, any positively refracting medium can have the sign of its refraction reversed by coating the surface with a phase-reversing sheet. This leads to the possibility of curved lenses that can magnify an object (*16*).

In principle, our new lens can be realized if the hologram is written in a thin sheet of nonlinear material. In practice, such a hologram would be very weak, and instead, 3D holograms are written if a strong output is desired. As a consequence of the 3D nature of the hologram, the second phase-reversed beam (shown on the right of Fig. 1C) is not seen, but if the left-hand surface of the medium is half silver (Fig. 4), reflection of the phase-reversed beam will generate an image

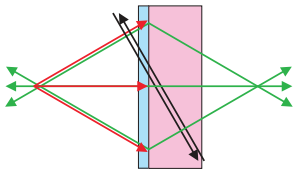

Fig. 4. In a four-wave mixing experiment, two counterpropagating waves first create a hologram and then diffract off the hologram to form a phase-reversed beam. A half-silvered mirror reflects the reversed beam to form an image on the far side of the system.

to the right of the system reproducing the effect predicted in Fig. 1C and mimicking the Veselago negatively refracting lens. However, the 3D nature of the hologram precludes any subwavelength resolution.

Creating a 2D hologram and attaining the ideal shown in Fig. 3 will be a challenge. Enhancing the nonlinearity of existing media—possibly through the use of plasmonic or metamaterial layers to enhance the local fields (*17*)—may offer a route to realizing a 2D version and hence subwavelength resolution. Further discussion of the practicalities of a four-wave mixing scheme can be found in the SOM.

References and Notes

1. J. P. Woerdman, *Opt. Commun.* **2**, 212 (1970).
2. P. Yeh, *Introduction to Photorefractive Nonlinear Optics* (Wiley, New York, 1993).
3. V. G. Veselago, *Sov. Phys. Usp.* **10**, 509 (1968).
4. J. B. Pendry, *Contemp. Phys.* **45**, 191 (2004).
5. J. B. Pendry, *Science* **306**, 1353 (2004).
6. K. Kobayashi, *J. Phys. Condens. Matter* **18**, 3703 (2006).
7. V. V. Cheianov, V. Fal'ko, B. L. Altshuler, *Science* **315**, 1252 (2007).
8. M. Nieto-Vesperinas, E. Wolf, *J. Opt. Soc. Am. A* **2**, 1429 (1985).
9. S. Maslovski, S. Tretyakov, *J. Appl. Phys.* **94**, 4241 (2003).
10. O. Malyuskin, V. Fusco, A. G. Schuchinsky, *IEEE Trans. Antenn. Propag.* **54**, 1399 (2006).
11. C. A. Allen, K. M. K. H. Leong, T. Itoh, *IEEE Int. Microwave Theory Tech. Symp. Dig.* **3**, 1875 (2003).
12. M. Wubs, A. Lagendijk, *Phys. Rev. E Stat. Nonlin. Soft Matter Phys.* **65**, 046612 (2002).
13. J. B. Pendry, *Phys. Rev. Lett.* **85**, 3966 (2000).
14. S. Yon, M. Tanter, M. Fink, *J. Acoust. Soc. Am.* **113**, 1533 (2003).
15. R. Merlin, *Science* **317**, 927 (2007); published online 11 July 2007 (10.1126/science.1143884).
16. J. B. Pendry, S. A. Ramakrishna, *J. Phys. Condens. Matter* **15**, 6345 (2003).
17. J. B. Pendry, A. J. Holden, D. J. Robbins, W. J. Stewart, *IEEE Trans. Microwave Theory Tech.* **47**, 2075 (1999).

18. I thank the Engineering and Physical Sciences Research Council for a Senior Fellowship, M. Damsen for educating me in various aspects of four-wave mixing, S. Maier for discussions on plasmonic enhancements of fields, and A. Lagendijk for comments on the manuscript.

Supporting Online Material

www.sciencemag.org/cgi/content/full/1162087/DC1
SOM Text
Figs. S1 to S6

20 June 2008; accepted 20 August 2008
Published online 28 August 2008;
10.1126/science.1162087
Include this information when citing this paper.

Surface-Modified Carbon Nanotubes Catalyze Oxidative Dehydrogenation of *n*-Butane

Jian Zhang, Xi Liu, Raoul Blume, Aihua Zhang, Robert Schlögl, Dang Sheng Su*

Butenes and butadiene, which are useful intermediates for the synthesis of polymers and other compounds, are synthesized traditionally by oxidative dehydrogenation (ODH) of *n*-butane over complex metal oxides. Such catalysts require high O_2/butane ratios to maintain the activity, which leads to unwanted product oxidation. We show that carbon nanotubes with modified surface functionality efficiently catalyze the oxidative dehydrogenation of *n*-butane to butenes, especially butadiene. For low O_2/butane ratios, a high selectivity to alkenes was achieved for periods as long as 100 hours. This process is mildly catalyzed by ketonic C=O groups and occurs via a combination of parallel and sequential oxidation steps. A small amount of phosphorus greatly improved the selectivity by suppressing the combustion of hydrocarbons.

Transition metal oxides have been widely used as catalysts for the conversion of butane to C_4 alkenes, important industrial precursors for producing synthetic rubbers, plastics, and a number of industrially important chemicals. Despite a great deal of research, alkene selectivity in the current butane-to-butadiene process is severely limited (*1*). One important reason is that the unsaturated products are much more readily oxidized to CO_2 than is the starting alkane. The chemical complexity of polyvalent metal oxides, although found to be necessary for catalytic activity, impedes satisfactory selectivity through isolation of active sites (*2*–*6*). For this reason, the origin of the catalytic activity is debated, and there is as yet no generally accepted picture of the reaction mechanism (*7*, *8*).

Carbon materials have been reported to catalyze the oxidative dehydrogenation (ODH) of an aromatic molecule, ethylbenzene. However, conventional carbons, in particular activated carbon, underwent unavoidable deactivations

due to coking or combustion (*9*–*12*). Recently, it was shown that only well-nanostructured carbons are stable and coke-free catalysts for styrene synthesis (*12*, *13*). Activation of C–H bonds in the ethyl group is considered to be coordinated by the ketonic carbonyl (C=O) group. Ethylbenzene has an aromatic moiety that enables relatively facile activation. Here, we report on surface-modified carbon nanotubes (CNTs) as a high-performance catalyst for the ODH of the much less active butane. Relative to metal-based catalysts, CNTs displayed an enhanced selectivity to C_4 alkenes, especially butadiene.

We conducted the reaction at 400° or 450°C with an O_2/butane ratio of 2.0. The product mixture contained only 1-butene, 2-butene, butadiene, CO_2, CO, and residual reactants; the resulting carbon balance was 100 ± 3% (fig. S1A) (*14*). In a blank experiment without catalyst, the alkene yield was as low as 0.9%. Over pristine CNTs, 88.9% of the converted butane was burnt, yielding 1.6% alkenes (Fig. 1A). Considering the intensive stability of CNTs in O_2 (fig. S1B) (*14*), we conclude that the CO_2 during the reaction mainly originated from the oxidation of the hydrocarbon feedstock and not from burning of the carbon catalysts. Neither washing CNTs in HCl solution nor loading with acidic nitro group could enhance the selectivity to alkene (fig. S2) (*14*).

We then functionalized surfaces of pristine CNTs with oxygen-containing groups by refluxing and oxidizing them in concentrated HNO_3 (*15*). With the resulting oCNTs as catalyst, we observed an improved yield of 6.7% alkenes. The alkene yield was further enhanced to 13.8% after the oCNTs catalyst was additionally modified by passivating defects with phosphorus [P-oCNTs, 0.5 ± 0.1 weight percent (wt %) P]. The increase in alkene selectivity is partially explained in Fig. 1B, which compares the catalytic performance of oCNTs and P-oCNTs for three individual reactions: (i) ODH of butane, (ii) ODH of 1-butene, and (iii) combustion of butadiene. The passivation apparently suppresses the activation and deep oxidation of the alkene substrates.

A survey of recent literature showed that the P-oCNTs catalyst is as selective as the best V/MgO catalyst developed during the past 20 years (fig. S3A) (*14*). To compare the present reaction conditions to those previously used, we synthesized and evaluated two V/MgO samples. At the same conversion of butane, the $Mg_3V_2O_8$ and $Mg_3V_2O_7$ samples were less selective than P-oCNTs (fig. S3B) (*14*); in particular, relative to $Mg_3V_2O_7$, P-oCNTs gave twice the selectivity to butadiene (16.2%).

Safety can be a challenge when mixing hydrocarbons with oxidants. One solution is to operate the reaction under anaerobic conditions. After we reduced the O_2/butane ratio from 2.0 to 0.5, the P-oCNTs sample still exhibited outstanding stability. During a reaction lasting 100 hours, the butane and oxygen conversion remained almost unchanged, and the alkene selectivity stayed above 53% (Fig. 1C). To the best of our knowledge, the oxidative stability of P-oCNTs far exceeds those of metal oxide catalysts, which only work well with excess oxygen (O_2/butane ≥ 2), a condition necessary to prevent severe deactivation due to coke deposition.

In Fig. 1D, we show the ODH activity of oCNTs and P-oCNTs as a function of residence time. These results demonstrate that the overall reaction comprises a combination of parallel and sequential oxidation steps. The alkene selectivity at zero residence time was not unity (*16*), indicating that direct butane combustion occurred in parallel with the ODH reactions (i.e., butane to butenes, butane to butadiene). Two reaction pathways to butadiene were identified. Selectivity toward butadiene remained finite at the zero residence time, evidencing a primary ODH of butane to butadiene; it increased with the residence time as the selectivity of butenes deceased, revealing a secondary ODH of butenes to butadiene.

The effect of phosphorus as a promoter was studied by kinetic measurements. The initial rate

Fritz Haber Institute of the Max Planck Society, Faradayweg 4-6, D-14195 Berlin, Germany.

*To whom correspondence should be addressed. E-mail: dangsheng@fhi-berlin.mpg.de

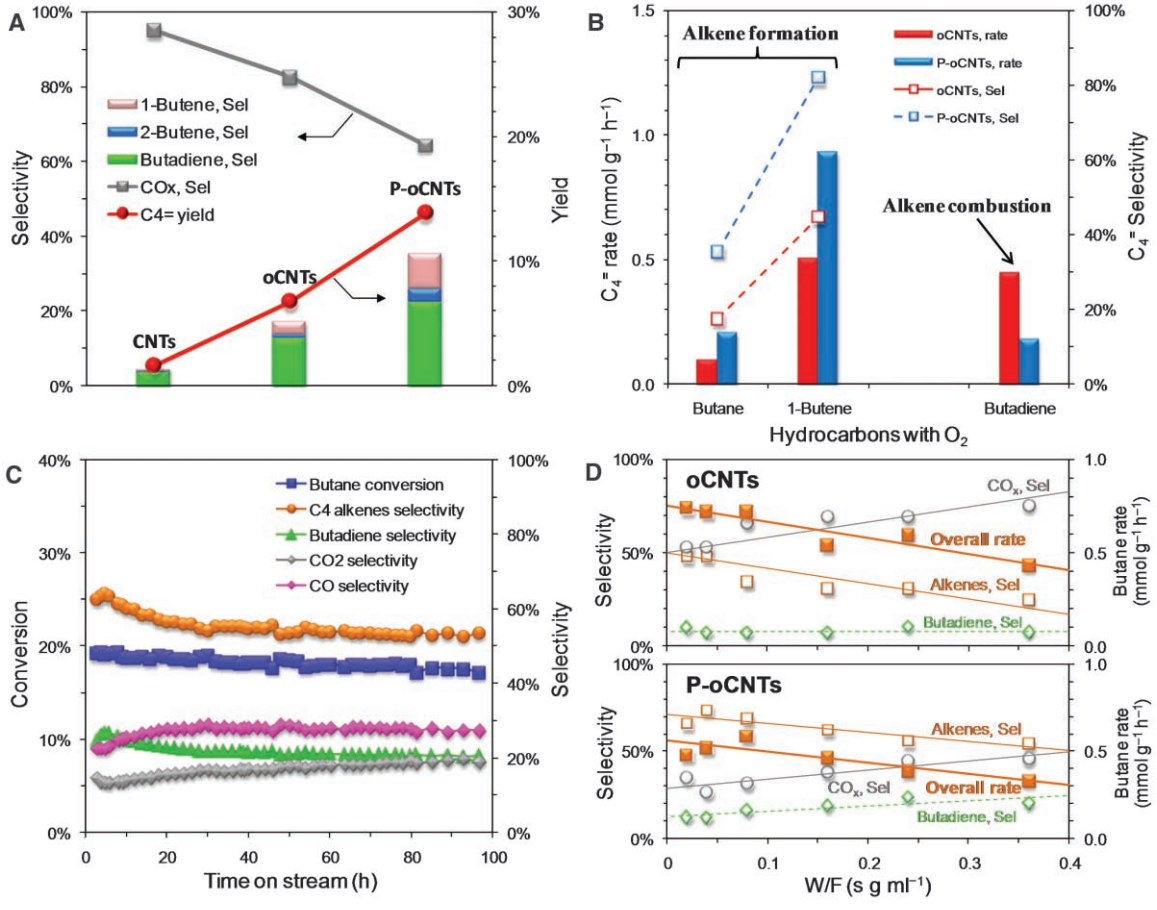

Fig. 1. ODH activities of various carbon nanotubes. (**A**) Performance of various CNTs for ODH of butane under oxygen-rich conditions: 0.18 g, 0.67% butane, O_2/butane = 2, 15 ml min^{-1}, 400°C. (**B**) Performance of modified CNTs in ODH reactions of butane and 1-butene and in combustion of butadiene: 0.18 g, 0.67% C_4 hydrocarbon, O_2/butane = 2, 15 ml min^{-1}, 400°C. (**C**) Stability of P-oCNTs catalyst for ODH of butane over 100 hours: 0.18 g, 2.7% butane, O_2/butane = 0.5, 10 ml min^{-1}, 450°C. (**D**) Dependence of product selectivity and reaction rate on residence time (*W/F*) in ODH reaction of butane: 0.005 to 0.09 g, 2.7% butane, O_2/butane = 0.5, 10 ml min^{-1}, 450°C. Helium was used as balance gas in all experiments.

constants for primary reactions were quantified as the residence time approached zero (*16*). After the modification with P, three important changes happened at the initial state: (i) The overall rate of converted butane decreased from 0.75 to 0.56 mmol g^{-1} $hour^{-1}$; (ii) the combustion of butane was reduced by as much as a factor of 2.3; and (iii) the formation rate of alkenes kept nearly unchanged at 0.38 to 0.40 mmol g^{-1} $hour^{-1}$. Therefore, P increased the selectivity by suppressing the combustion rate, rather than enhancing the formation rate of alkenes.

One of the key concerns in identifying and describing metal-free catalysis is the suspected influence of metal impurities in the catalyst. Commercial CNTs were prepared on supported metal catalysts, which inevitably remain as metal contaminants. Post-treatment by refluxing in strong acid effectively removed the residual metals to a great extent. X-ray fluorescence spectrometry revealed that the residual metals in the tested CNTs were very low (table S1) (*14*). The highest value of residual Fe was still as low as 0.09 wt %, as confirmed by energy-dispersive x-ray analysis (around 0.1 wt %). Furthermore, there was no signal of Fe or other metals in the surface layer at the limit of detection by synchrotron-excited x-ray photoelectron spectroscopy (XPS) (Fig. 2A). This difference suggests that if there is residual metal, it must be embedded in the carbon and not exposed to the reactants. This explanation is supported by the high-resolution transmission electron microscopy (HRTEM) image in Fig. 2B, which shows a catalyst particle encapsulated inside the CNTs. To fully exclude the role of Fe in the reaction, we deliberately added Fe to oCNTs in fractions ranging from 0.05 to 0.5 wt %. As shown in Fig. 2C, both the butane conversion and selectivity to C_4 alkenes gradually decreased with the increasing Fe content. Furthermore, there was no correlation of alkene selectivity with the residual metal content (fig. S4A) (*14*). We prepared a sample with 5% Fe phosphate in oCNTs; this sample also exhibited performance inferior to that of P-oCNTs without Fe (fig. S4B) (*14*). We can thus conclude that the reactivity originated exclusively from metal-free active sites on CNTs and that the residual metals played no positive role.

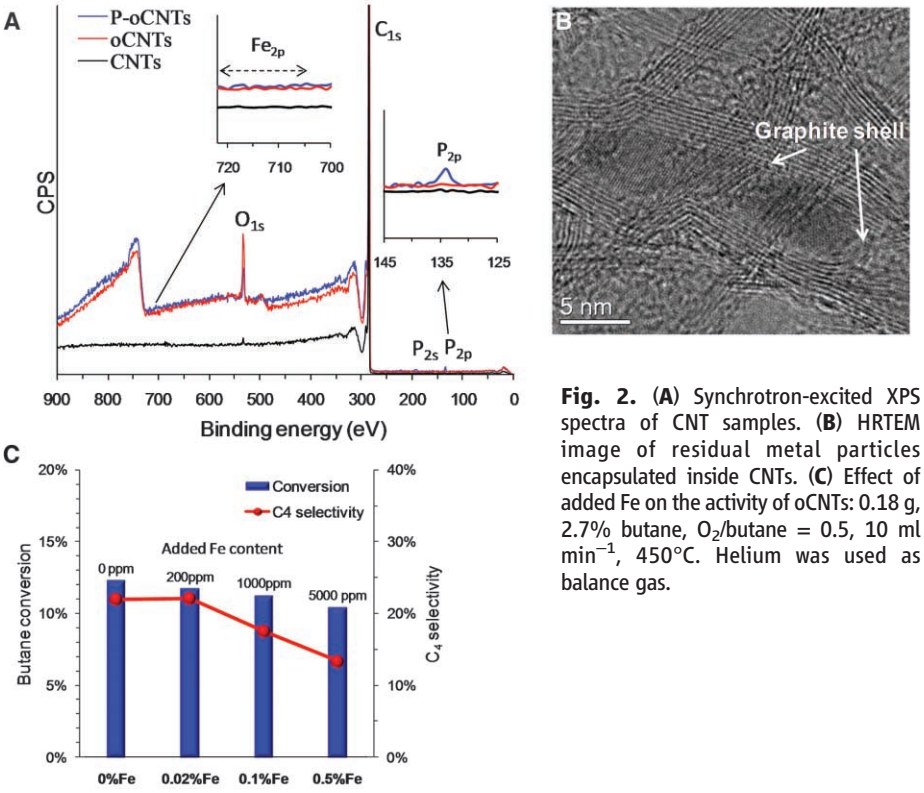

Fig. 2. (**A**) Synchrotron-excited XPS spectra of CNT samples. (**B**) HRTEM image of residual metal particles encapsulated inside CNTs. (**C**) Effect of added Fe on the activity of oCNTs: 0.18 g, 2.7% butane, O_2/butane = 0.5, 10 ml min^{-1}, 450°C. Helium was used as balance gas.

To elucidate the structure-activity relation, we studied the morphological features by TEM with elemental mapping. Figure 3A gives an overview elemental map from a typical area. Both P and O are dispersed throughout the sample without aggregation. After an ODH reaction that ran for more than 800 min, the morphology of the CNTs remained intact and no evidence for their combustion was identified (Fig. 3B), as expected from the thermal stability data (fig. S1B) (*14*). Some areas of the outer and inner walls of the CNTs were covered by thin layers of phosphorus, which obviously differs from fullerenoid carbon species on pristine CNTs originating from condensation of hydrocarbon fragments (fig. S5) (*14*). Most of the surface of the CNTs did not give rise to carbon deposition, which is one advantage of this metal-free catalyst.

We also monitored the working surface of CNTs with near-ambient XPS (*17*). The best P-oCNTs catalyst was heated in vacuum to 350°C; at this temperature, the less stable groups (anhydride, carboxyl, ester, and nitro) would already have desorbed from the surface (fig. S6) (*14*). We identified two contributions from ketonic C=O groups (531.2 ± 0.2 eV) and from C–O groups (533.1 ± 0.2 eV) (i.e., ether and hydroxyl) (*15*, *18*). Relative amounts of C–O and C=O are represented in Fig. 3C by the ratio

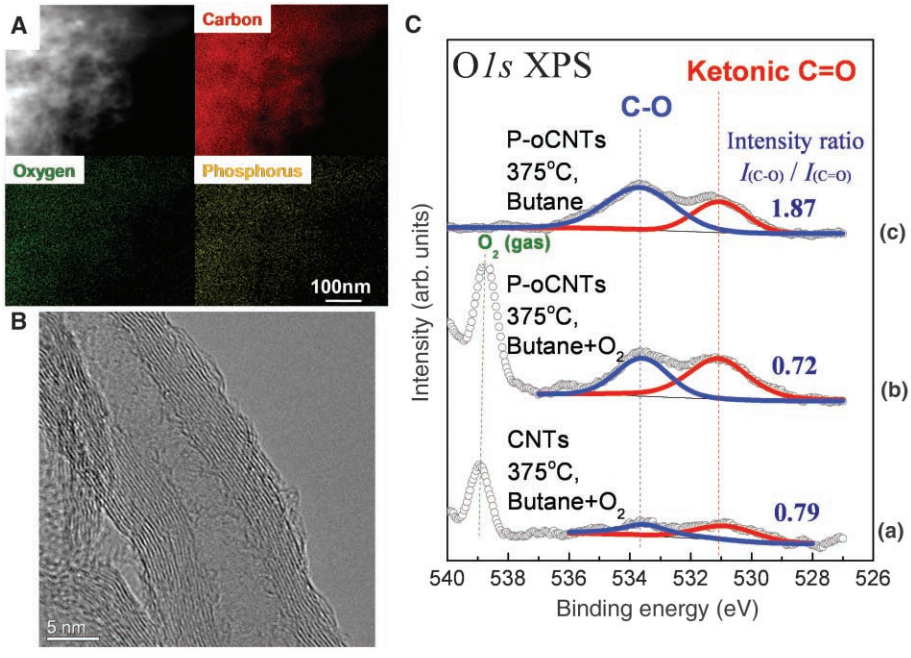

Fig. 3. (**A**) Elemental maps and (**B**) HRTEM image of the used P-oCNTs in Fig. 1A. (**C**) In situ O1*s* XPS spectra of working catalysts taken at 350° to 375°C: (a) CNTs: butane + O_2 (1:1), 0.25 mbar; (b) P-oCNTs: butane + O_2 (1:1), 0.25 mbar; (c) P-oCNTs: butane, 0.125 mbar.

of their intensities, $I_{(C-O)}/I_{(C=O)}$. Under ODH conditions (butane + O_2, 1:1, 0.25 atm, 350° to 375°C), $I_{(C-O)}/I_{(C=O)}$ values ranged from 0.72 to 0.80. However, after switching off O_2, the $I_{(C-O)}/I_{(C=O)}$ value sharply increased to 1.87 (Fig. 3C) and the activity went to almost zero. This finding indicates that ketonic C=O groups are a critical ingredient of the active sites, whereas C–O groups constitute inactive intermediates or adsorbates.

Figure 4A summarizes our proposed mechanism for the CNTs-catalyzed butane oxidation. For this purpose, surface oxygen species are classified into electrophilic (superoxide O_2^-, peroxide O_2^{2-}) and nucleophilic (O^{2-}) types (*19*). Electrophilic oxygen species are electron-deficient and attack the electron-rich C=C bonds in alkenes, leading to the rupture of the carbon skeleton and subsequent combustion. Pristine CNTs were produced from chemical vapor deposition of unsaturated hydrocarbons, resulting in a number of structural defects and terminal carbon fragments. Below 600°C, these defect sites or edges of graphene have been reported to convert O_2 molecules to electrophilic oxygen species (*20*) and thus cause low selectivity to alkenes.

More controlled oxidation of carbon surfaces can be carried out in liquid-phase oxidants (*21*). After refluxing in HNO_3, defect sites were functionalized by O^{2-} anions into various functional groups. For example, ketonic C=O, a nucleophilic species with high electron density, preferentially reacts with electron-poor saturated bonds. However, at the reaction temperature, desorption of less stable groups results in new graphitic defects that subsequently generate new electrophilic oxygen sites, thus partially limiting the selectivity to alkenes on oCNTs. The addition of phosphate reacting with these defects suppresses the formation of electrophilic oxygen species (*22*). Thus, P-oCNTs displayed a lower overall activity but a much better selectivity.

We used density functional theory (DFT) calculations with the CASTEP code and the Perdew-Burke-Ernzerhof generalized gradient approximation (*23*, *24*) to study the ODH reaction over ketonic C=O groups. These calculations are independent of the precise mechanism and the transition state of each elementary step. We used the graphitic zigzag edge as a model to anchor the ketonic C=O groups (Fig. 4B). Conversion of butane is energetically controlled by the abstraction of the first H atom, which was predicted to be mildly endothermic at 0.92 eV. To convert butane into 1- or 2-butene, two C=O sites would ultimately be needed, and each one returns a single electron to the surrounding graphene as the reservoir. The remaining H atoms combine with surrounding oxygen to water, thereby closing the primary ODH cycle. The enthalpy of formation of water compensates for the endothermic dehydrogenation of butane. As a consequence, the calculated free energies for formation of 1- and 2-butenes were −0.88 eV and −1.03 eV, respectively. Another pathway to regenerate active sites is that H atoms recombine into H_2 molecules. However, as expected, such a direct dehydrogenation reaction is energetically unfavorable, because energy barriers are as high as 1.45 to 1.60 eV.

The DFT calculation also provides insights into the reaction pathways to butadiene. Butadiene may directly form from butane as primary product with an overall energy of −1.97 eV. However, the need for neighboring C=O sites to accommodate four H atoms in one elementary step does not seem to be pronounced, accounting for a much lower rate than the secondary ODH from butenes (Fig. 1D). It is more likely that C=O primarily activates butenes (rather than butane) to butadiene. The energy for the abstraction of the first H from butenes ($\Delta E_{butenes,1H}$), 0.25 to 0.40 eV, is much lower than that from butane ($\Delta E_{butane,1H}$), 0.92 eV. In this way, we can understand the influence of residence time. Because the residence time is long enough for the butenes produced to diffuse and react with the surrounding C=O sites, butadiene will be primarily generated from the secondary ODH, as demonstrated by the prevailing fraction of butadiene in C_4 alkenes in an integral reaction, 63 to 74% (Fig. 1A).

Our work contains some implications for catalysis in general. It is possible to imitate heterogeneously the concepts of homogeneous metal-free catalysis. The function of oxygen heteroatoms in molecular catalysts is reproduced by defects of bent graphitic sheets. The catalytic principle of site isolation can be realized by electronic localization of charges at the defect sites corresponding to molecular analogs of double bonds. The operation mode of ODH reactions can be studied on metal-free catalysts with greater precision than in metal oxide systems. There is neither lattice nor structural oxygen, but only oxygen at active sites. The present catalysts are free of polyvalent metal sites with complex electronic and spin structures, allowing for a facile theoretical treatment. Finally, the application of a heterogeneous CNTs catalyst is attractive because of favorable management of energy over a good thermal and electronic conductor.

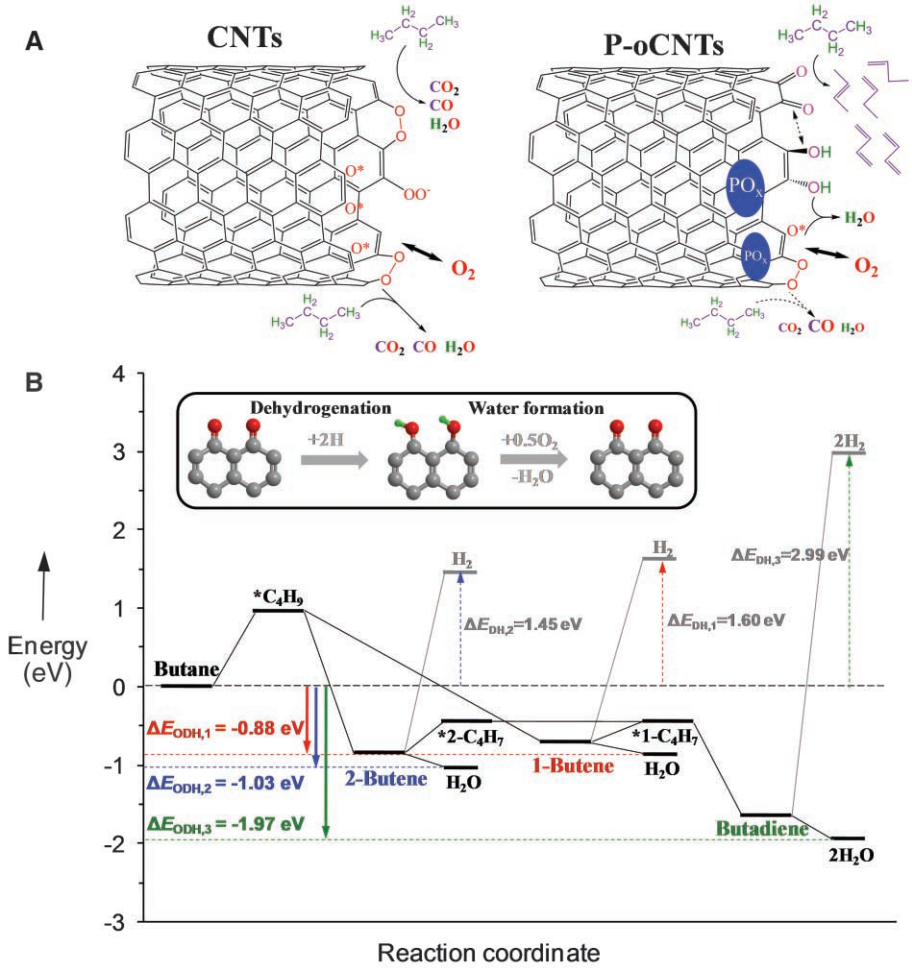

Fig. 4. (**A**) Schematic reaction and (**B**) energy steps of butane oxidation on pristine and P-modified CNTs.

References and Notes

1. F. Cavani, F. Trifirò, *Appl. Catal. A* **133**, 219 (1995).
2. R. Grabowski, *Catal. Rev.* **48**, 199 (2006).
3. K. D. Chen, A. T. Bell, E. Iglesia, *J. Catal.* **209**, 35 (2002).
4. G. I. Panov, K. A. Dubkov, E. V. Starokon, *Catal. Today* **117**, 148 (2006).
5. A. Miyakoshi, A. Ueno, M. Ichikawa, *Appl. Catal. A* **219**, 249 (2001).
6. L. B.-Tapia, I. H. Pérez, P. Schacht, I. R. Córdova, G. G. Aguilar-Ríos, *J. Catal.* **107–108**, 371 (2005).
7. E. V. Kondratenko, M. Cherian, M. Baerns, *Catal. Today* **99**, 59 (2005).

8. C. Resini, T. Montanari, G. Busca, J.-M. Jehng, I. E. Wachs, *Catal. Today* **99**, 105 (2005).
9. T. G. Alkhazov, E. A. Ismailov, A. Yu, A. I. Kozharov, *Kinet. Katal.* **19**, 611 (1978).
10. M. S. Kane, L. C. Kao, R. K. Mariwala, D. F. Hilscher, H. C. Foley, *Ind. Eng. Chem. Res.* **35**, 3319 (1996).
11. M. F. R. Pereira, J. J. M. Órfão, J. L. Figueiredo, *Appl. Catal. A* **218**, 307 (2001).
12. J. Zhang *et al.*, *Angew. Chem. Int. Ed.* **46**, 7319 (2007).
13. G. Mestl, N. I. Maksimova, N. Keller, V. V. Roddatis, R. Schlögl, *Angew. Chem. Int. Ed.* **40**, 2066 (2001).
14. See supporting material on *Science* Online.
15. J.-H. Zhou *et al.*, *Carbon* **9**, 1379 (2007).
16. K. D. Chen, E. Iglesia, A. T. Bell, *J. Phys. Chem. B* **105**, 646 (2001).
17. M. Salmeron, R. Schlögl, *Surf. Sci. Rep.* **63**, 169 (2008).
18. T. I. T. Okpalugo, P. Papakonstantinou, H. Murphy, J. McLaughlin, N. M. D. Brown, *Carbon* **43**, 153 (2005).
19. L. M. Madeira, M. F. Portela, *Catal. Rev.* **44**, 247 (2002).
20. F. Atamny *et al.*, *Mol. Phys.* **76**, 851 (1992).
21. M. L. Toebes, J. M. P. van Heeswijk, J. H. Bitter, A. J. van Dillen, K. P. de Jong, *Carbon* **42**, 307 (2004).
22. A. M. Puziy, O. I. Poddubnaya, A. M. Ziatdinov, *Appl. Surf. Sci.* **252**, 8036 (2006).
23. S. J. Clark *et al.*, *Z. Kristallogr.* **220**, 567 (2005).
24. J. P. Perdew, K. Burke, M. Ernzerhof, *Phys. Rev. Lett.* **77**, 3865 (1996).

25. We thank the Max Planck Society; U. Wild, A. Klein-Hoffmann, and J. Thielemann for technical assistance; Berliner Elektronenspeicherring-Gesellschaft für Synchrotronstrahlung for support of in situ XPS measurements; and M. A Smith for helpful discussions. Supported by the CANAPE project of the 6th Framework Programme of European Commission and the ENERCHEM project of the Max Planck Society.

Supporting Online Material

www.sciencemag.org/cgi/content/full/322/5898/73/DC1
Materials and Methods
Figs. S1 to S6
Table S1
References

17 June 2008; accepted 21 August 2008
10.1126/science.1161916

Merging Photoredox Catalysis with Organocatalysis: The Direct Asymmetric Alkylation of Aldehydes

David A. Nicewicz and David W. C. MacMillan*

Photoredox catalysis and organocatalysis represent two powerful fields of molecule activation that have found widespread application in the areas of inorganic and organic chemistry, respectively. We merged these two catalysis fields to solve problems in asymmetric chemical synthesis. Specifically, the enantioselective intermolecular α-alkylation of aldehydes has been accomplished using an interwoven activation pathway that combines both the photoredox catalyst $Ru(bpy)_3Cl_2$ (where bpy is 2,2′-bipyridine) and an imidazolidinone organocatalyst. This broadly applicable, yet previously elusive, alkylation reaction is now highly enantioselective and operationally trivial.

Nature's ability to convert solar energy to chemical energy in photosynthesis has inspired the development of a host of photoredox systems in efforts to mimic this process. Arguably the most studied one-electron photoredox catalyst has been $Ru(bpy)_3^{2+}$ (where bpy is 2,2′-bipyridine): an inorganic complex that has facilitated important advances in the areas of energy storage, hydrogen and oxygen evolution from water, and methane production from carbon dioxide (*1*, *2*). Given its proven ability to mediate electron transfer, it is surprising that $Ru(bpy)_3^{2+}$ has not found a substantial application in organic synthesis, wherein a large number of fundamental reactions rely on the generation and exploitation of radicals or single-electron intermediates (*3*).

Over the past decade, the field of organocatalysis has grown at a dramatic pace, providing more than 130 chemical reactions that rapidly facilitate enantioselective C–C, C–O, C–N, and C–halogen bond formation (*4*, *5*). Whereas a broad range of reaction types have recently succumbed to this mode of catalysis (including aldol, Friedel-Crafts, and cycloadditions), it is important to consider that nearly all organocatalytic bond constructions are restricted to two-electron pathways, wherein the highest occupied molecular orbital of an electron-rich substrate reacts with the lowest unoccupied molecular orbital of an electron-deficient partner. Recently, however, our laboratory introduced the concept of organo–singly occupied molecular orbital (SOMO) catalysis, a one-electron mode of activation that has enabled the development of several useful transformations (*6*–*10*).

Given the widespread success of both electron transfer catalysis and organocatalysis, we recently questioned whether it might be possible to merge these two powerful areas, with the goal of solving long-standing, yet elusive problems in chemical synthesis. More specifically, as a blueprint for reaction invention, we hoped to exploit the lessons of photoredox enzymatic catalysis (*11*), wherein a series of consecutive low-barrier, open-shell steps are energetically preferred to high-barrier, two-electron pathways. On this basis, we hypothesized that the enantioselective catalytic α-alkylation of aldehydes (*12*–*15*), a widely sought yet elusive transformation, might be brought to fruition via the marriage of inorganic electron transfer and organic catalysis (Fig. 1).

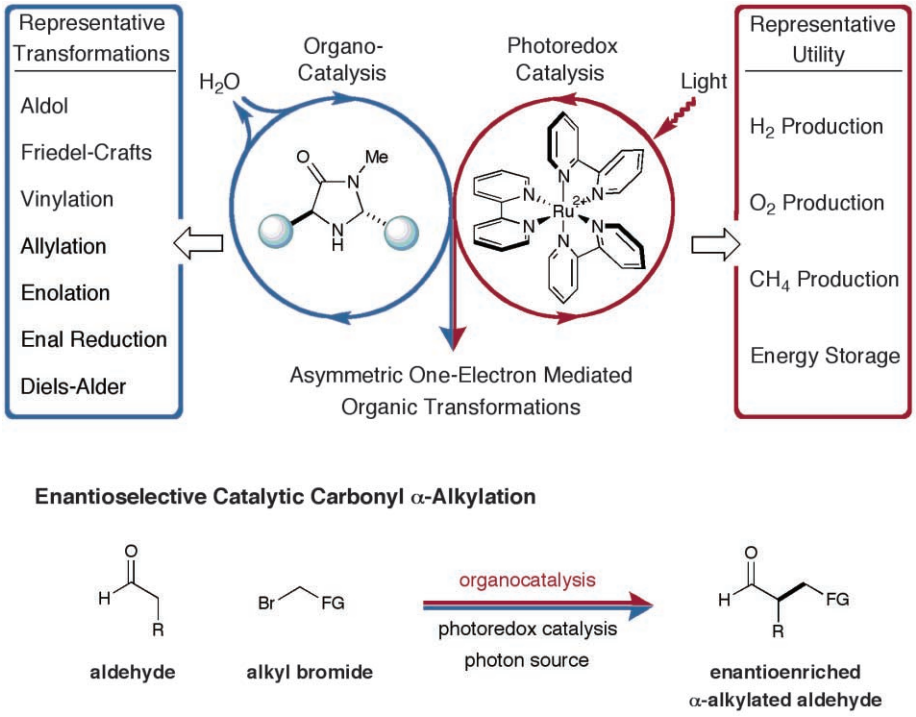

Fig. 1. Merging amine catalysis and organometallic photoredox catalysis to enable asymmetric organic transformations. Me, methyl; R, generic organic substituent; FG, electron-withdrawing functional group.

Contribution from Merck Center for Catalysis, Department of Chemistry, Princeton University, Princeton, NJ 08544, USA.

*To whom correspondence should be addressed. E-mail: dmacmill@princeton.edu

Merging Photoredox Catalysis with Organocatalysis: The Direct Asymmetric Alkylation of Aldehydes

David A. Nicewicz, *et al.*

Science **322**, 77 (2008);
DOI: 10.1126/science.1161976

Science (print ISSN 0036-8075; online ISSN 1095-9203) is published weekly, except the last week in December, by the American Association for the Advancement of Science, 1200 New York Avenue NW, Washington, DC 20005.

8. C. Resini, T. Montanari, G. Busca, J.-M. Jehng, I. E. Wachs, *Catal. Today* **99**, 105 (2005).
9. T. G. Alkhazov, E. A. Ismailov, A. Yu, A. I. Kozharov, *Kinet. Katal.* **19**, 611 (1978).
10. M. S. Kane, L. C. Kao, R. K. Mariwala, D. F. Hilscher, H. C. Foley, *Ind. Eng. Chem. Res.* **35**, 3319 (1996).
11. M. F. R. Pereira, J. J. M. Órfão, J. L. Figueiredo, *Appl. Catal. A* **218**, 307 (2001).
12. J. Zhang *et al.*, *Angew. Chem. Int. Ed.* **46**, 7319 (2007).
13. G. Mestl, N. I. Maksimova, N. Keller, V. V. Roddatis, R. Schlögl, *Angew. Chem. Int. Ed.* **40**, 2066 (2001).
14. See supporting material on *Science* Online.
15. J.-H. Zhou *et al.*, *Carbon* **9**, 1379 (2007).
16. K. D. Chen, E. Iglesia, A. T. Bell, *J. Phys. Chem. B* **105**, 646 (2001).
17. M. Salmeron, R. Schlögl, *Surf. Sci. Rep.* **63**, 169 (2008).
18. T. I. T. Okpalugo, P. Papakonstantinou, H. Murphy, J. McLaughlin, N. M. D. Brown, *Carbon* **43**, 153 (2005).
19. L. M. Madeira, M. F. Portela, *Catal. Rev.* **44**, 247 (2002).
20. F. Atamny *et al.*, *Mol. Phys.* **76**, 851 (1992).
21. M. L. Toebes, J. M. P. van Heeswijk, J. H. Bitter, A. J. van Dillen, K. P. de Jong, *Carbon* **42**, 307 (2004).
22. A. M. Puziy, O. I. Poddubnaya, A. M. Ziatdinov, *Appl. Surf. Sci.* **252**, 8036 (2006).
23. S. J. Clark *et al.*, *Z. Kristallogr.* **220**, 567 (2005).
24. J. P. Perdew, K. Burke, M. Ernzerhof, *Phys. Rev. Lett.* **77**, 3865 (1996).

25. We thank the Max Planck Society; U. Wild, A. Klein-Hoffmann, and J. Thielemann for technical assistance; Berliner Elektronenspeicherring-Gesellschaft für Synchrotronstrahlung for support of in situ XPS measurements; and M. A Smith for helpful discussions. Supported by the CANAPE project of the 6th Framework Programme of European Commission and the ENERCHEM project of the Max Planck Society.

Supporting Online Material

www.sciencemag.org/cgi/content/full/322/5898/73/DC1
Materials and Methods
Figs. S1 to S6
Table S1
References

17 June 2008; accepted 21 August 2008
10.1126/science.1161916

Merging Photoredox Catalysis with Organocatalysis: The Direct Asymmetric Alkylation of Aldehydes

David A. Nicewicz and David W. C. MacMillan*

Photoredox catalysis and organocatalysis represent two powerful fields of molecule activation that have found widespread application in the areas of inorganic and organic chemistry, respectively. We merged these two catalysis fields to solve problems in asymmetric chemical synthesis. Specifically, the enantioselective intermolecular α-alkylation of aldehydes has been accomplished using an interwoven activation pathway that combines both the photoredox catalyst $Ru(bpy)_3Cl_2$ (where bpy is 2,2′-bipyridine) and an imidazolidinone organocatalyst. This broadly applicable, yet previously elusive, alkylation reaction is now highly enantioselective and operationally trivial.

Nature's ability to convert solar energy to chemical energy in photosynthesis has inspired the development of a host of photoredox systems in efforts to mimic this process. Arguably the most studied one-electron photoredox catalyst has been $Ru(bpy)_3^{2+}$ (where bpy is 2,2′-bipyridine): an inorganic complex that has facilitated important advances in the areas of energy storage, hydrogen and oxygen evolution from water, and methane production from carbon dioxide (*1*, *2*). Given its proven ability to mediate electron transfer, it is surprising that $Ru(bpy)_3^{2+}$ has not found a substantial application in organic synthesis, wherein a large number of fundamental reactions rely on the generation and exploitation of radicals or single-electron intermediates (*3*).

Over the past decade, the field of organocatalysis has grown at a dramatic pace, providing more than 130 chemical reactions that rapidly facilitate enantioselective C–C, C–O, C–N, and C–halogen bond formation (*4*, *5*). Whereas a broad range of reaction types have recently succumbed to this mode of catalysis (including aldol, Friedel-Crafts, and cycloadditions), it is important to consider that nearly all organocatalytic bond constructions are restricted to two-electron pathways, wherein the highest occupied molecular orbital of an electron-rich substrate reacts with the lowest unoccupied molecular orbital of an electron-deficient partner. Recently, however, our laboratory introduced the concept of organo–singly occupied molecular orbital (SOMO) catalysis, a one-electron mode of activation that has enabled the development of several useful transformations (*6*–*10*).

Given the widespread success of both electron transfer catalysis and organocatalysis, we recently questioned whether it might be possible to merge these two powerful areas, with the goal of solving long-standing, yet elusive problems in chemical synthesis. More specifically, as a blueprint for reaction invention, we hoped to exploit the lessons of photoredox enzymatic catalysis (*11*), wherein a series of consecutive low-barrier, open-shell steps are energetically preferred to high-barrier, two-electron pathways. On this basis, we hypothesized that the enantioselective catalytic α-alkylation of aldehydes (*12*–*15*), a widely sought yet elusive transformation, might be brought to fruition via the marriage of inorganic electron transfer and organic catalysis (Fig. 1).

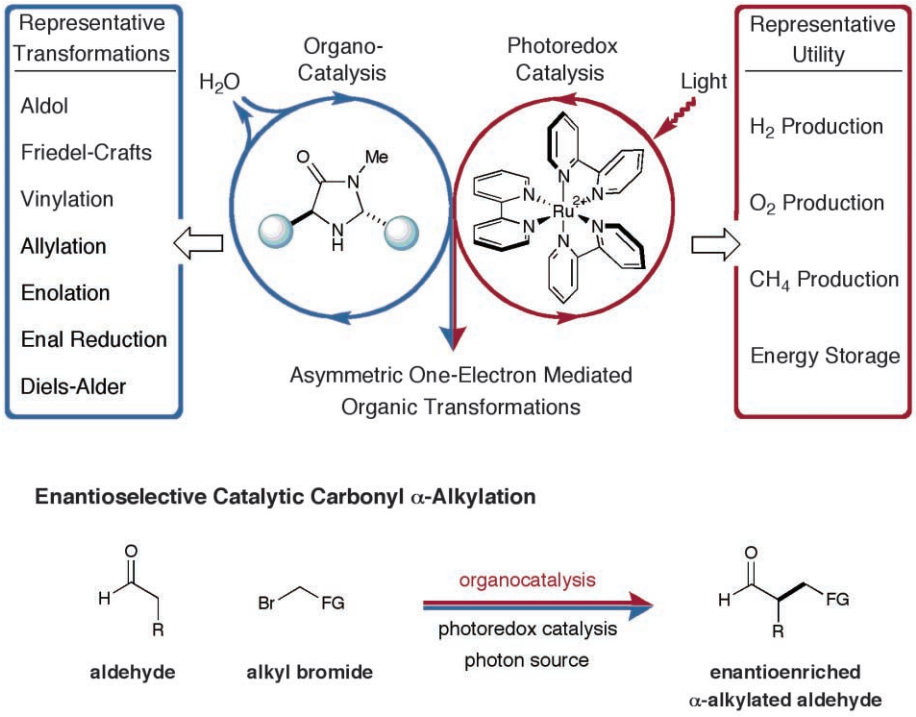

Fig. 1. Merging amine catalysis and organometallic photoredox catalysis to enable asymmetric organic transformations. Me, methyl; R, generic organic substituent; FG, electron-withdrawing functional group.

Contribution from Merck Center for Catalysis, Department of Chemistry, Princeton University, Princeton, NJ 08544, USA.

*To whom correspondence should be addressed. E-mail: dmacmill@princeton.edu

We proposed that two interwoven catalytic cycles might be engineered to simultaneously generate an electron-rich enamine from the condensation of an aldehyde and an amine catalyst and an electron-deficient alkyl radical via reduction of an alkyl bromide with a Ru photoredox catalyst (Fig. 2). Given that electron-deficient radicals are known to rapidly combine with π-rich olefins to forge even the most elusive C–C bonds (*16*, *17*), we hoped that this dual-catalysis mechanism would successfully converge to enable the direct coupling of aldehydes with α-bromo ketones or esters. As a critical design element, we presumed that the use of a suitable chiral amine catalyst would induce high enantioselectivity. Moreover, we recognized that the interaction of a SOMOphilic enamine with an electron-deficient radical is the converse mechanism to our previously described SOMO activation studies. As such, a complementary array of catalytic bond constructions should be possible.

A detailed description of our dual-catalysis aldehyde alkylation is presented in Fig. 2. It has long been established that $Ru(bpy)_3^{2+}$ (**1**) will readily accept a photon from a variety of light sources to populate the $*Ru(bpy)_3^{2+}$ (**2**) metal-to-ligand charge transfer (MLCT) excited state (*1*, *2*). Although $*Ru(bpy)_3^{2+}$ (**2**) can function as a reductant or an oxidant, we postulated that this high-energy intermediate would efficiently remove a single electron from a sacrificial quantity of enamine, to initiate our first catalytic cycle and provide the electron-rich $Ru(bpy)_3^{+}$ (**3**). Given that $Ru(bpy)_3^{+}$ (**3**) has been shown to be a potent reductant [–1.33 V versus saturated calomel electrode (SCE) in CH_3CN] (*18*), we anticipated that single-electron transfer (SET) to the α-bromocarbonyl substrate **4** would rapidly furnish the electron-deficient alkyl radical **5** while returning $Ru(bpy)_3^{2+}$ (**1**) to the catalytic cycle ($E_{1/2}$ for phenacyl bromide = –0.49 V versus SCE in CH_3CN, where $E_{1/2}$ is the half reduction potential) (*19*–*22*). As a central design consideration, we recognized that the redox potentials of $Ru(bpy)_3^{2+}$ can be readily fine-tuned by ligand modification (*1*).

Concurrent with this photoredox pathway, the organocatalytic cycle would begin with condensation of the imidazolidinone catalyst **6** and the aldehyde substrate **7** to form enamine **8**. At this stage, we expected the two catalytic cycles to intersect via the addition of the SOMOphilic enamine **8** to the electron-deficient alkyl radical **5**, thereby achieving the key alkylation step. This coupling event would concomitantly produce an electron-rich α-amino radical **9**, a single-electron species that has a low barrier to oxidation (–0.92 to –1.12 V versus SCE in CH_3CN) (*23*). Once again, convergence of our catalytic cycles should ensure SET from α-amino radical **9** to the $*Ru(bpy)_3^{2+}$ (**2**) excited state to produce the iminium ion **10** and regenerate the active reductant, $Ru(bpy)_3^{+}$ (**3**)—a step that would close the photoredox cycle (*24*). Hydrolysis of the resulting iminium **10** would reconstitute the amine catalyst **6** while delivering the requisite enantioenriched α-alkyl aldehyde product.

From the outset, we understood that the utility of this alkylation reaction would rely on the identification of an amine catalyst that could generically enforce high levels of enantiocontrol in the coupling of the pivotal π-rich enamine with a diverse array of electron-deficient radicals. On the basis of density functional theory (DFT) calculations (*25*, *26*), we proposed that the imidazolidinone catalyst **6** should selectively form an enamine **8** (DFT-**8**), that projects the 2π electron system away from the bulky *tert*-butyl group, whereas the electron-rich olefin will selectively populate an (*E*)-configuration to minimize nonbonding interactions with the imidazolidinone ring (Fig. 2). In terms of enantiofacial discrimination, the calculated DFT-**8** structure also reveals that the methyl group on the catalyst system will effectively shield the *Re* face of the enamine, leaving the *Si* face exposed for enantioselective radical addition. We have found that the trans methyl, *tert*-butyl 2,5-disubstituted imidazolidinone **6** is an excellent enamine catalyst for transformations performed at room temperature. Specifically, catalyst **6** provides excellent levels of kinetic enantiocontrol yet does not readily participate in enamine formation with the 2,2′-disubstituted aldehyde-alkylation adduct, a step that would erode product enantiopurity via epimerization.

This new asymmetric alkylation protocol was first examined using octanal and bromo diethylmalonate as the coupling partners, along with a catalyst combination of $Ru(bpy)_3Cl_2$ (**1**) and imidazolidinone **6**, and a 15-W fluorescent light source (Table 1) (*27*). To our great delight, preliminary studies revealed the successful execution of our dual-cycle design ideals to provide (*R*)-2-malonyloctanal with excellent levels of enantiocontrol and reaction efficiency [entry 1, 93% yield, 90% enantiomeric excess (ee)]. Experiments that probe the scope of the aldehyde component in this new alkylation reaction are summarized in Table 1 (entries 1 to 6). Chemical functionalities that are often prone to either oxidation or reduction (e.g., olefins, esters, carbamates, and arenes) were found to be inert to these mild redox conditions (entries 2 to 5, 66 to 92% yield, 90 to 95% ee). Moreover, the steric demand of the α-formyl substituent has little impact on the efficiency and enantioinduction of the alkylation process (entries 1 and 4, substituent is *n*-hexyl versus cyclohexyl, 83 to 93% yield, 90 to 95% ee), a point that is underscored by the successful use of adamantyl acetaldehyde (entry 6, 63% yield, 93% ee).

A broad array of electron-deficient α-bromo carbonyls can effectively serve as alkylating agents

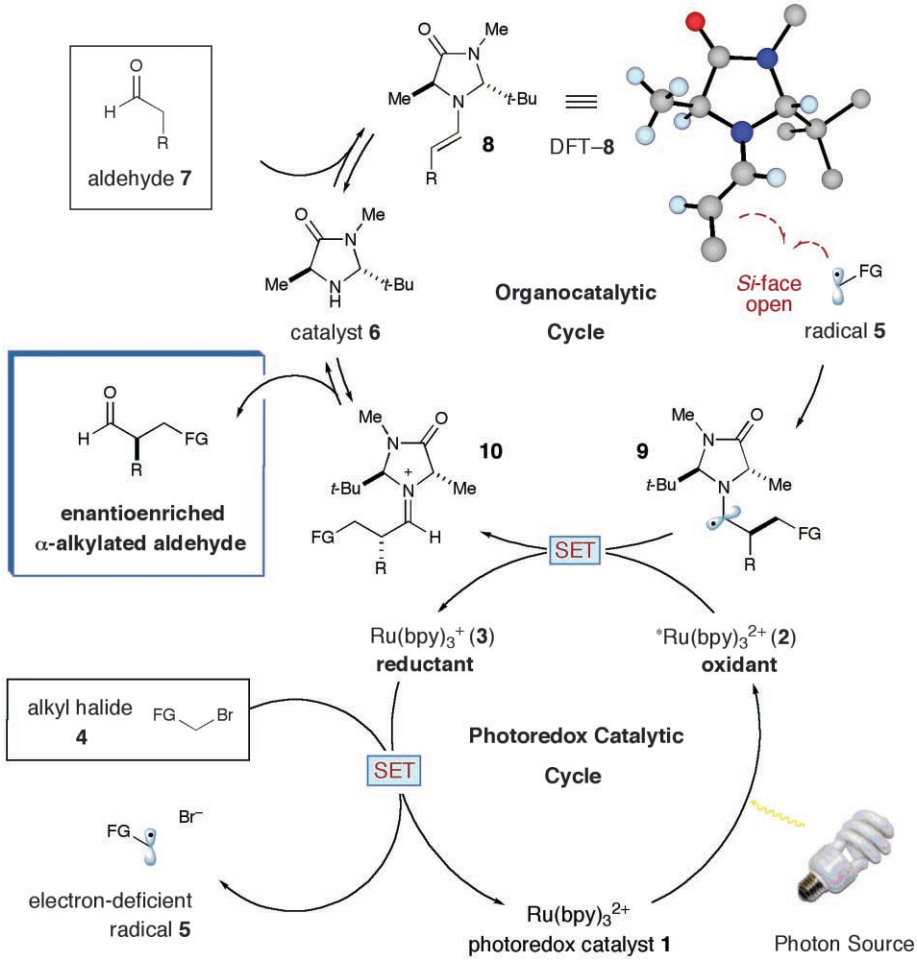

Fig. 2. Merging photoredox catalysis with organocatalysis. Proposed mechanism. *t*-Bu, *tert*-butyl.

Table 1. Survey of the bromide and aldehyde scope in the direct α-alkylation of aldehydes. Y, any organic substituent (alkyl, aryl, alkenyl, alkynyl, etc.); DMF, *N*,*N*′-dimethylformamide; Tf, triflate; Me, methyl; Et, ethyl; Hex, hexyl; Ph, phenyl; *t*-Bu, *tert*-butyl; Boc, *tert*-butyl carbamoyl.

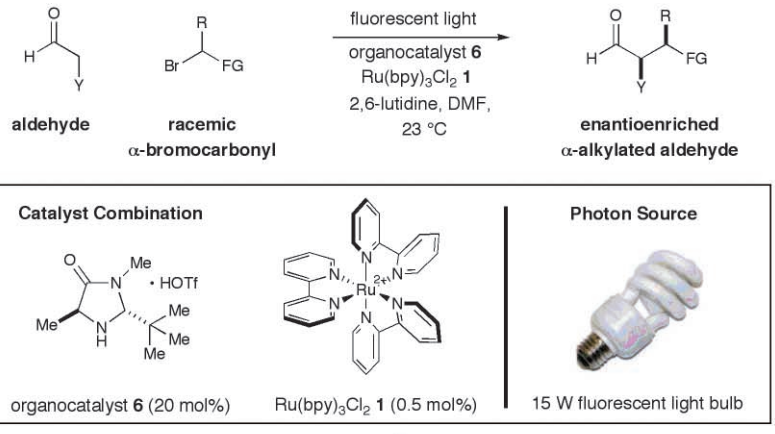

entry	aldehyde	product*
1	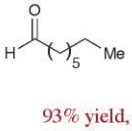	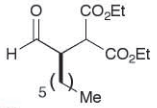 93% yield, 90% ee
2	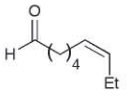	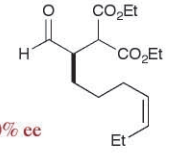 86% yield, 90% ee
3	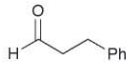	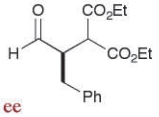 92% yield, 90% ee
4	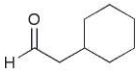	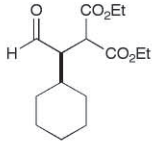 83% yield, 95% ee
5	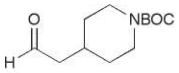	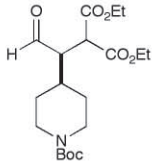 66% yield, 91% ee
6		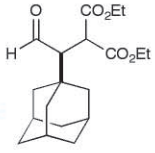 63% yield†, 93% ee

entry	α-bromocarbonyl	product‡
7	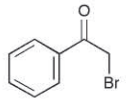	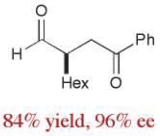 84% yield, 96% ee
8	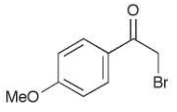	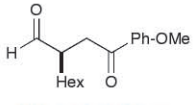 87% yield, 96% ee
9	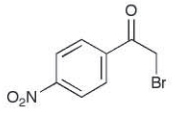	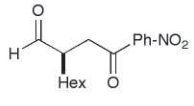 84% yield, 95% ee
10	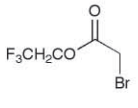	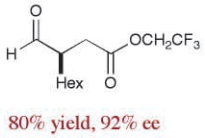 80% yield, 92% ee
11	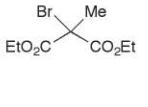	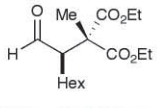 80% yield, 88% ee
12	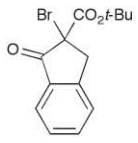	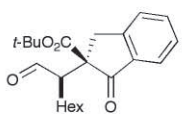 70% yield, 5:1 dr, 99% ee

*Reactions performed with diethyl bromomalonate. †40 mole percent of organocatalyst **6** was employed. ‡Reactions performed with octanal.

in this tandem catalysis manifold (Table 1, entries 7 to 12). For example, bromoacetophenone systems of diverse electronic orientation (*p*-OMe, *p*-NO_2, *p*-H) provide almost identical selectivity and efficiency profiles (entries 7 to 9; 84 to 87% yield, 95 to 96% ee). Whereas α-bromo esters are readily tolerated ($BrCH_2CO_2Et$, 53% yield, 94% ee), we have found that superior yields are obtained with markedly electron-deficient carbonyls such as the trifluoroethyl ester (80% yield, 92% ee). As a testament to the versatility and power of one-electron mediated pathways, we have found that tertiary bromo-substituted alkylating agents can be readily employed to forge all-carbon quaternary centers, (entries 11 and 12, ≥70% yield, 88 to 99% ee). Moreover, racemic α-bromo radical precursors can be employed to generate quaternary stereocenters with appreciable levels of diastereocontrol (entry 12, 5:1 diastereomeric ratio), illustrating the capacity of the pivotal enamine intermediate to differentiate the enantiotopic faces of a trisubstituted carbon-centered radical. The sense of asymmetric induction observed in all cases (Table 1) is consistent with selective addition of the electron-deficient radical to the *Si* face of the enamine **8**, in complete accord with the calculated structure DFT-**8**.

With respect to operational convenience, it is important to consider that this alkylation protocol does not require any heating or cooling, all of the components employed in this study (substrates, catalysts, and solvents) are commercially available and inexpensive, and a simple household 15-W fluorescent light bulb can be employed as a suitable light source. A 2-g alkylation was readily accomplished using the outlined procedure (entry 7).

We have conducted a series of control experiments and luminescence quenching studies to test the validity of our proposed dual-cycle pathway and gain further insight into the photonic requirements for metal-mediated redox catalysis. The control experiments were performed using octanal with α-bromoacetophenone or diethyl bromomalonate in the presence of various catalyst combinations and a 15-W fluorescent light source (unless otherwise stated). Several observations are of note: Rigorous exclusion of light failed to produce even trace quantities of the coupling adduct. Moreover, removal of $Ru(bpy)_3^{2+}$ from our standard protocol resulted in <10% alkylation product over an extended timeframe (24 hours). High levels of reaction efficiency (>80%) can be obtained in the absence of $Ru(bpy)_3^{2+}$ if a high-energy UV irradiation source (300 to 350 nm) is employed in a photobox environment. In this specific case, we assume that a monocyclic catalysis mechanism is operable wherein the α-bromocarbonyl is converted to the requisite electron-deficient radical via photolytic bond homolysis (as opposed to catalytic SET reduction). Execution of our standard reaction with a light source specifically tuned to the $Ru(bpy)_3^{2+}$ MLCT absorption band (465 ± 20 nm full width

at half maximum, 500 mW) resulted in a dramatic acceleration in overall rate (90 min) as compared with the use of a typical household 15-W fluorescent bulb (6 hours), which operates with a wide spectral window (~400 to 700 nm). The use of the same 465-nm photon source in the absence of $Ru(bpy)_3^{2+}$ resulted in only trace product formation (<5%) (*28*). These experiments provide strong evidence of the participation of the $*Ru(bpy)_3^{2+}$ (**2**) excited state in the catalytic cycle.

With respect to our luminescence quenching studies, it has long been established that certain electron-deficient C–Br bonds can quench the emission intensity of $*Ru(bpy)_3^{2+}$ by SET (*29*). However, we did not observe a decrease in $*Ru(bpy)_3^{2+}$ luminescence in the presence of α-bromoacetophenone or diethyl bromomalonate, a result that negates the possibility that $*Ru(bpy)_3^{2+}$ (**2**) is participating as a reductant in our tandem catalysis sequence. In contrast, enamine **8** (pregenerated in stoichiometric quantities) does decrease the $*Ru(bpy)_3^{2+}$ emission intensity with a small but significant Stern-Volmer constant of 10 M^{-1} (see fig. S1) (*30*). These observations collectively support our mechanistic proposal that the $*Ru(bpy)_3^{2+}$ (**2**) excited state behaves as an oxidant in our photoredox cycle.

We have also gained circumstantial evidence that enamine **8** is the organocatalytic intermediate that participates in the key bond-forming step. More specifically, exposure of 2-phenylcyclopropyl acetaldehyde to our standard reaction protocol resulted in clean conversion (83% yield) to the corresponding alkylation product (see supporting online material). Failure of this radical clock substrate to undergo cyclopropyl ring opening clearly indicates that a 3π electron SOMO activated intermediate is not operative in the organocatalytic cycle.

References and Notes

1. K. Kalyanasundaram, *Coord. Chem. Rev.* **46**, 159 (1982).
2. A. Juris *et al.*, *Coord. Chem. Rev.* **84**, 85 (1988).
3. P. Renaud, M. P. Sibi, Eds., *Radicals in Organic Synthesis* (Wiley-VCH, Weinheim, Germany, 2001).
4. A. Berkessel, H. Gröger, Eds., *Asymmetric Organocatalysis: From Biomimetic Concepts to Applications in Asymmetric Synthesis* (Wiley-VCH, Weinheim, Germany, 2005).
5. P. I. Dalko, Ed., *Enantioselective Organocatalysis: Reactions and Experimental Procedures* (Wiley-VCH, Weinheim, Germany, 2007).
6. T. D. Beeson, A. Mastracchio, J. B. Hong, K. Ashton, D. W. C. MacMillan, *Science* **316**, 582 (2007); published online 28 March 2007 (10.1126/science. 1142696).
7. H. Jang, J. B. Hong, D. W. C. MacMillan, *J. Am. Chem. Soc.* **129**, 7004 (2007).
8. H. Kim, D. W. C. MacMillan, *J. Am. Chem. Soc.* **130**, 398 (2008).
9. A SOMO activation mechanism has also been reported for the α-oxidation of aldehydes (*10*).
10. M. Sibi, M. Hasegawa, *J. Am. Chem. Soc.* **129**, 4124 (2007).
11. H. B. Gray, J. R. Winkler, *Annu. Rev. Biochem.* **65**, 537 (1996).
12. An intramolecular α-formyl alkylation has been reported (*13*).
13. N. Vignola, B. List, *J. Am. Chem. Soc.* **126**, 450 (2004).
14. For a catalytic enantioselective alkylation of racemic α-bromoesters, see (*15*).
15. X. Dai, N. A. Strotman, G. C. Fu, *J. Am. Chem. Soc.* **130**, 3302 (2008).
16. P. Renaud, S. Schubert, **1990**, *Synlett* 624 (1990).
17. G. A. Russell, K. Wang, *J. Org. Chem.* **56**, 3475 (1991).
18. C. R. Bock *et al.*, *J. Am. Chem. Soc.* **101**, 4815 (1979).
19. Value was corrected from the $Ag/Ag^+ClO_4^-$ electrode (*20*).
20. D. D. Tanner, H. K. Singh, *J. Org. Chem.* **51**, 5182 (1986).
21. $Ru(bpy)_3^+$ has previously been shown to reduce phenacyl bromide (*22*).
22. S. Fukuzumi, S. Mochizuki, T. Tanaka, *J. Phys. Chem.* **94**, 722 (1990).
23. D. D. M. Wayner, J. J. Dannenberg, D. Griller, *Chem. Phys. Lett.* **131**, 189 (1986).
24. The possibility of direct one-electron reduction of the α-bromocarbonyl by the α-amino radical as a propagation step cannot be excluded.
25. DFT calculations were performed with the use of B3LYP/6-311+G(2d,2p)//B3LYP/6-31G(d).
26. A conformer that positions the enamine olefin toward the *tert*-butyl group was also found to be energetically relevant in these calculations. Because of the pseudo C_2-symmetric nature of catalyst **6**, this enamine conformer also exists with the *Si* face open and the *Re* face blocked in a manner similar to DFT–**8**.
27. Materials and methods are available as supporting material on *Science* Online.
28. No rate enhancement was observed in the absence of $Ru(bpy)_3^{2+}$ with additive bpy or Bu_4NCl.
29. S. Oishi, N. Furuta, *Chem. Lett.* **7**, 45 (1978).
30. None of the remaining reaction components (aldehyde, amine catalyst, 2,6-lutidine, or 2,6-lutidinium bromide) quenched $*Ru(bpy)_3^{2+}$.

31. We thank S. Bernhard for his assistance in performing quenching experiments, as well as many insightful discussions. Additionally, we thank T. J. Rainey for performing DFT calculations. Financial support was provided by the NIH General Medical Sciences (grant R01 GM078201-01-01) and gifts from Merck, Amgen, and Bristol-Myers Squibb. D.A.N. is grateful for a NIH National Service Research Award fellowship (F32GM076816).

Supporting Online Material

www.sciencemag.org/cgi/content/full/1161976/DC1
Materials and Methods
Figs. S1 to S3
References

18 June 2008; accepted 8 August 2008
Published online 4 September 2008;
10.1126/science.1161976
Include this information when citing this paper.

Temperature-Induced Hydrophobic-Hydrophilic Transition Observed by Water Adsorption

Hai-Jing Wang, Xue-Kui Xi, Alfred Kleinhammes, Yue Wu*

The properties of nanoconfined and interfacial water in the proximity of hydrophobic surfaces play a pivotal role in a variety of important phenomena such as protein folding. Water inside single-walled carbon nanotubes (SWNTs) can provide an ideal system for investigating such nanoconfined interfacial water on hydrophobic surfaces, provided that the nanotubes can be opened without introducing excess defects. Here, we report a hydrophobic-hydrophilic transition upon cooling from 22°C to 8°C via the observation of water adsorption isotherms in SWNTs measured by nuclear magnetic resonance. A considerable slowdown in molecular reorientation of such adsorbed water was also detected. The observed transition demonstrates that the structure of interfacial water could depend sensitively on temperature, which could lead to intriguing temperature dependences involving interfacial water on hydrophobic surfaces.

Water in the immediate vicinity of hydrophobic surfaces plays a crucial role in various important phenomena such as the folding and activity of proteins (*1*, *2*), but experimental signatures of these water layers have proven difficult to obtain. One possibility is that the structures and dynamics of nanoconfined interfacial water could possess distinctive temperature dependences (analogous perhaps to the anomalous density maximum manifested by bulk water at 4°C). A temperature dependence in the properties of interfacial water could be important for various processes, such as the cold denaturation of proteins (*2*).

Single-walled carbon nanotubes (SWNTs) provide a model system for investigating the properties of nanoconfined interfacial water (*3*–*9*). Because each nanotube with diameter of 1.4 nm can only accommodate one layer of water molecules on their inside surface (*5*), the behavior of adsorbed water inside such SWNTs could provide important insight into the properties of nanoconfined interfacial water. A previous theoretical study showed that water could fill the interior of carbon nanotubes through favorable structural effects on the local excess chemical potential (*3*). This result implies that water could be adsorbed inside SWNTs below saturated vapor pressure, as demonstrated by previous studies (*10*, *11*). However, in those studies, the defect density and principal adsorption sites (PAS), known to alter water adsorption isotherms in activated carbon (*12*), were likely too high to reveal the intrinsic adsorption properties of SWNTs. Water

Department of Physics and Astronomy, University of North Carolina, Chapel Hill, NC 27599–3255, USA.

*To whom correspondence should be addressed. E-mail: yuewu@physics.unc.edu

Temperature-Induced Hydrophobic-Hydrophilic Transition Observed by Water Adsorption

Hai-Jing Wang, *et al.*

Science **322**, 80 (2008);
DOI: 10.1126/science.1162412

Science (print ISSN 0036-8075; online ISSN 1095-9203) is published weekly, except the last week in December, by the American Association for the Advancement of Science, 1200 New York Avenue NW, Washington, DC 20005.

at half maximum, 500 mW) resulted in a dramatic acceleration in overall rate (90 min) as compared with the use of a typical household 15-W fluorescent bulb (6 hours), which operates with a wide spectral window (~400 to 700 nm). The use of the same 465-nm photon source in the absence of $Ru(bpy)_3^{2+}$ resulted in only trace product formation (<5%) (*28*). These experiments provide strong evidence of the participation of the $*Ru(bpy)_3^{2+}$ (**2**) excited state in the catalytic cycle.

With respect to our luminescence quenching studies, it has long been established that certain electron-deficient C–Br bonds can quench the emission intensity of $*Ru(bpy)_3^{2+}$ by SET (*29*). However, we did not observe a decrease in $*Ru(bpy)_3^{2+}$ luminescence in the presence of α-bromoacetophenone or diethyl bromomalonate, a result that negates the possibility that $*Ru(bpy)_3^{2+}$ (**2**) is participating as a reductant in our tandem catalysis sequence. In contrast, enamine **8** (pregenerated in stoichiometric quantities) does decrease the $*Ru(bpy)_3^{2+}$ emission intensity with a small but significant Stern-Volmer constant of 10 M^{-1} (see fig. S1) (*30*). These observations collectively support our mechanistic proposal that the $*Ru(bpy)_3^{2+}$ (**2**) excited state behaves as an oxidant in our photoredox cycle.

We have also gained circumstantial evidence that enamine **8** is the organocatalytic intermediate that participates in the key bond-forming step. More specifically, exposure of 2-phenylcyclopropyl acetaldehyde to our standard reaction protocol resulted in clean conversion (83% yield) to the corresponding alkylation product (see supporting online material). Failure of this radical clock substrate to undergo cyclopropyl ring opening clearly indicates that a 3π electron SOMO activated intermediate is not operative in the organocatalytic cycle.

References and Notes

1. K. Kalyanasundaram, *Coord. Chem. Rev.* **46**, 159 (1982).
2. A. Juris *et al.*, *Coord. Chem. Rev.* **84**, 85 (1988).
3. P. Renaud, M. P. Sibi, Eds., *Radicals in Organic Synthesis* (Wiley-VCH, Weinheim, Germany, 2001).
4. A. Berkessel, H. Gröger, Eds., *Asymmetric Organocatalysis: From Biomimetic Concepts to Applications in Asymmetric Synthesis* (Wiley-VCH, Weinheim, Germany, 2005).
5. P. I. Dalko, Ed., *Enantioselective Organocatalysis: Reactions and Experimental Procedures* (Wiley-VCH, Weinheim, Germany, 2007).
6. T. D. Beeson, A. Mastracchio, J. B. Hong, K. Ashton, D. W. C. MacMillan, *Science* **316**, 582 (2007); published online 28 March 2007 (10.1126/science. 1142696).
7. H. Jang, J. B. Hong, D. W. C. MacMillan, *J. Am. Chem. Soc.* **129**, 7004 (2007).
8. H. Kim, D. W. C. MacMillan, *J. Am. Chem. Soc.* **130**, 398 (2008).
9. A SOMO activation mechanism has also been reported for the α-oxidation of aldehydes (*10*).
10. M. Sibi, M. Hasegawa, *J. Am. Chem. Soc.* **129**, 4124 (2007).
11. H. B. Gray, J. R. Winkler, *Annu. Rev. Biochem.* **65**, 537 (1996).
12. An intramolecular α-formyl alkylation has been reported (*13*).
13. N. Vignola, B. List, *J. Am. Chem. Soc.* **126**, 450 (2004).
14. For a catalytic enantioselective alkylation of racemic α-bromoesters, see (*15*).
15. X. Dai, N. A. Strotman, G. C. Fu, *J. Am. Chem. Soc.* **130**, 3302 (2008).
16. P. Renaud, S. Schubert, **1990**, *Synlett* 624 (1990).
17. G. A. Russell, K. Wang, *J. Org. Chem.* **56**, 3475 (1991).
18. C. R. Bock *et al.*, *J. Am. Chem. Soc.* **101**, 4815 (1979).
19. Value was corrected from the $Ag/Ag^+ClO_4^-$ electrode (*20*).
20. D. D. Tanner, H. K. Singh, *J. Org. Chem.* **51**, 5182 (1986).
21. $Ru(bpy)_3^+$ has previously been shown to reduce phenacyl bromide (*22*).
22. S. Fukuzumi, S. Mochizuki, T. Tanaka, *J. Phys. Chem.* **94**, 722 (1990).
23. D. D. M. Wayner, J. J. Dannenberg, D. Griller, *Chem. Phys. Lett.* **131**, 189 (1986).
24. The possibility of direct one-electron reduction of the α-bromocarbonyl by the α-amino radical as a propagation step cannot be excluded.
25. DFT calculations were performed with the use of B3LYP/6-311+G(2d,2p)//B3LYP/6-31G(d).
26. A conformer that positions the enamine olefin toward the *tert*-butyl group was also found to be energetically relevant in these calculations. Because of the pseudo C_2-symmetric nature of catalyst **6**, this enamine conformer also exists with the *Si* face open and the *Re* face blocked in a manner similar to DFT–**8**.
27. Materials and methods are available as supporting material on *Science* Online.
28. No rate enhancement was observed in the absence of $Ru(bpy)_3^{2+}$ with additive bpy or Bu_4NCl.
29. S. Oishi, N. Furuta, *Chem. Lett.* **7**, 45 (1978).
30. None of the remaining reaction components (aldehyde, amine catalyst, 2,6-lutidine, or 2,6-lutidinium bromide) quenched $*Ru(bpy)_3^{2+}$.

31. We thank S. Bernhard for his assistance in performing quenching experiments, as well as many insightful discussions. Additionally, we thank T. J. Rainey for performing DFT calculations. Financial support was provided by the NIH General Medical Sciences (grant R01 GM078201-01-01) and gifts from Merck, Amgen, and Bristol-Myers Squibb. D.A.N. is grateful for a NIH National Service Research Award fellowship (F32GM076816).

Supporting Online Material

www.sciencemag.org/cgi/content/full/1161976/DC1
Materials and Methods
Figs. S1 to S3
References

18 June 2008; accepted 8 August 2008
Published online 4 September 2008;
10.1126/science.1161976
Include this information when citing this paper.

Temperature-Induced Hydrophobic-Hydrophilic Transition Observed by Water Adsorption

Hai-Jing Wang, Xue-Kui Xi, Alfred Kleinhammes, Yue Wu*

The properties of nanoconfined and interfacial water in the proximity of hydrophobic surfaces play a pivotal role in a variety of important phenomena such as protein folding. Water inside single-walled carbon nanotubes (SWNTs) can provide an ideal system for investigating such nanoconfined interfacial water on hydrophobic surfaces, provided that the nanotubes can be opened without introducing excess defects. Here, we report a hydrophobic-hydrophilic transition upon cooling from 22°C to 8°C via the observation of water adsorption isotherms in SWNTs measured by nuclear magnetic resonance. A considerable slowdown in molecular reorientation of such adsorbed water was also detected. The observed transition demonstrates that the structure of interfacial water could depend sensitively on temperature, which could lead to intriguing temperature dependences involving interfacial water on hydrophobic surfaces.

Water in the immediate vicinity of hydrophobic surfaces plays a crucial role in various important phenomena such as the folding and activity of proteins (*1*, *2*), but experimental signatures of these water layers have proven difficult to obtain. One possibility is that the structures and dynamics of nanoconfined interfacial water could possess distinctive temperature dependences (analogous perhaps to the anomalous density maximum manifested by bulk water at 4°C). A temperature dependence in the properties of interfacial water could be important for various processes, such as the cold denaturation of proteins (*2*).

Single-walled carbon nanotubes (SWNTs) provide a model system for investigating the properties of nanoconfined interfacial water (*3*–*9*). Because each nanotube with diameter of 1.4 nm can only accommodate one layer of water molecules on their inside surface (*5*), the behavior of adsorbed water inside such SWNTs could provide important insight into the properties of nanoconfined interfacial water. A previous theoretical study showed that water could fill the interior of carbon nanotubes through favorable structural effects on the local excess chemical potential (*3*). This result implies that water could be adsorbed inside SWNTs below saturated vapor pressure, as demonstrated by previous studies (*10*, *11*). However, in those studies, the defect density and principal adsorption sites (PAS), known to alter water adsorption isotherms in activated carbon (*12*), were likely too high to reveal the intrinsic adsorption properties of SWNTs. Water

Department of Physics and Astronomy, University of North Carolina, Chapel Hill, NC 27599–3255, USA.

*To whom correspondence should be addressed. E-mail: yuewu@physics.unc.edu

adsorption isotherms in SWNTs depend on both the interaction with the surface and the structure of adsorbed water, which could depend on temperature. Here, we report a hydrophobic-hydrophilic transition upon cooling from 22.1°C to 8.0°C, revealed by water adsorption isotherms on the inside surface of low-defect SWNTs. Strong evidence is provided for the formation of monolayer water inside SWNTs at 8.0°C. Nuclear magnetic resonance (NMR) studies of the dynamics of reorientation of nanoconfined water molecules are shown to be much slower than in bulk water. In addition to various important biological processes, this new phenomenon could also shed light on the intrinsic adsorption mechanism of water in nanoporous carbon (*12*, *13*).

We synthesized SWNTs by laser ablation using 0.6 weight percent (each) Ni/Co as catalysts. The raw material was purified by refluxing in 20% H_2O_2 solution at 100°C for 12 hours and rinsing in CS_2 and then in methanol. The purified SWNTs were then annealed at 800°C. The tube diameter of 1.4 nm was determined from the Raman spectrum. Details of the sample preparation were described previously (*14*). The transmission electron microscope (TEM) image of the SWNTs is shown in fig. S1 (*15*). SWNTs after annealing usually have end caps that prevent the guest molecules from being adsorbed inside. Several techniques can be used to open the ends of SWNTs. In our previous study, etching by strong acids was used to cut tubes into short segments (*10*, *16*, *17*). Although this method is effective for opening tubes, it introduces a considerable amount of defect sites and functional groups acting as PAS that could have a strong influence on the water adsorption behavior. The high defect density in cut SWNTs could obscure the intrinsic adsorption behavior of SWNTs (*10*).

To reduce the influence of PAS and to reveal the intrinsic adsorption behavior, a much gentler method was adopted here to remove end caps (*18*). The SWNTs were heated at around 350°C in a thermogravimetric analyzer under air flow for more than 20 min until a weight loss of about 3% was reached. The ^{1}H NMR spectrum of ethane (fig. S2) (*15*) adsorbed in such treated SWNTs shows clear signatures of opened SWNTs (*16*, *17*). Water adsorption isotherms were measured by ^{1}H NMR at 0.8 T (34 MHz ^{1}H NMR frequency) equipped with an in situ water loading system with controlled vapor pressure and temperature. The ^{1}H NMR signal of vapor is negligible because of its low pressure (~2 kPa); no bulk water is condensed outside SWNTs below the saturated vapor pressure (P_0). Furthermore, water molecules are too large to access the interstitial sites of 1.4-nm diameter SWNTs bundles (*16*). Thus, the ^{1}H NMR signal is associated predominantly with the water adsorbed inside the SWNTs (*11*). The water content is calibrated by ethane ^{1}H NMR spectra as described in details elsewhere (*10*, *16*).

The amount of adsorbed water measured by ^{1}H NMR versus the relative pressure P/P_0 at 8.0°C, 18.4°C, and 22.1°C is shown in Fig. 1A. All three isotherms differ substantially from the S-shaped type V isotherm as observed in activated carbon and defective cut SWNTs, where adsorption increases slowly at low relative pressure but increases sharply above $P/P_0 = 0.5$, quickly reaching the level of saturation (*10*). Such an S-shaped adsorption isotherm in activated carbon is often attributed to PAS (*12*). Figure 1A shows that this ubiquitous sharp increase in the isotherms of activated carbon near $P/P_0 = 0.5$ is absent in low-defect SWNTs. The isotherm at 22.1°C exhibits a concave pattern as a type III isotherm, typical for clean hydrophobic surfaces with surface-water interactions weaker than water-water interactions (*19*). Interestingly, the isotherm at 8.0°C exhibits a convex pattern, a type II isotherm observed on hydrophilic surfaces (*20*). The isotherm at 18.4°C shows a linear pattern, which is a transitional pattern between the hydrophilic isotherm at 8.0°C and the hydrophobic isotherm at 22.1°C.

The water content was about 15 mmol/g when the relative pressure first reached the saturated pressure of $P/P_0 = 1$. This value is in good agreement with the calculated adsorption capacity of 13 mmol/g when SWNTs are supposed to be completely filled with water. This estimate is made by assuming that the van der Waals diameter of (10, 10) SWNTs is 0.99 nm (*5*) and the density of water is comparable to those at the hydrophobic interface, about 0.9 g/cm^3 (*21*). Further exposure at $P/P_0 = 1$ will lead to further increase of adsorption caused by condensation outside SWNTs.

More insight can be gained by analyzing the isotherm at 8.0°C with the Dubinin-Radushkevitch-Kaganer equation (*19*). It describes monolayer adsorption, given by

$$\log_{10} x = \log_{10} x_m - D[\log_{10} P_0/P)]^2 \quad (1)$$

where x is the adsorbed water content, x_m is the monolayer capacity, and D is a constant related to the temperature. A logarithmic plot of the adsorbed water versus $[\log_{10}(P_0/P)]^2$ is shown in Fig. 1C. Using the linear fit of data below the pressure of condensation and extrapolating to $[\log_{10}(P_0/P)]^2 = 0$, the monolayer capacity x_m is evaluated to be 8.7 ± 0.4 mmol/g. This value agrees well with the calculated value of 9.5 mmol/g for monolayer coverage of the inner surface of SWNTs. The monolayer water forms a tubular structure under the confinement of nanotubes, as illustrated in Fig. 1B (*22*). The convex shape of the water adsorption isotherm at 8.0°C and its upward turn at $P/P_0 \approx 0.8$ are also evidences of molecular layering on the adsorbed surface (*23*). This layering effect is commonly seen in liquid films (above the triple point temperature of the bulk liquid) of simple hydrocarbons and inert gases on graphite.

Water adsorption is a process of balancing the chemical potential of the confined water and the vapor. When water is confined in SWNTs, the energy loss from the breaking of hydrogen bonding (~20 kJ/mol) will not be completely compensated by the van der Waals interaction (<15 kJ/mol) (*24*). However, the local excess chemical potential is dominated not by the aver-

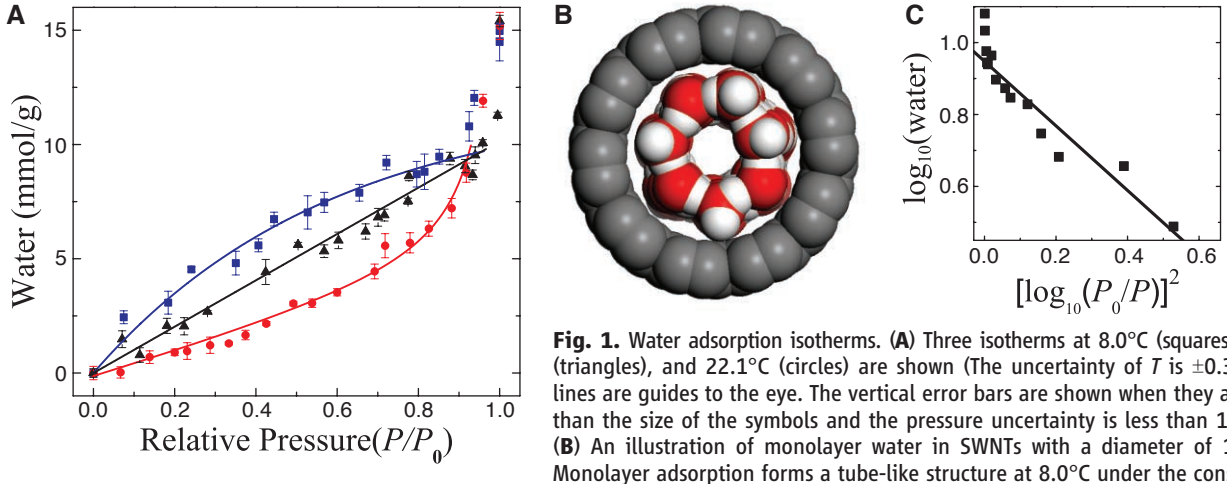

Fig. 1. Water adsorption isotherms. (**A**) Three isotherms at 8.0°C (squares), 18.4°C (triangles), and 22.1°C (circles) are shown (The uncertainty of T is ±0.3°C). The lines are guides to the eye. The vertical error bars are shown when they are larger than the size of the symbols and the pressure uncertainty is less than 1% of P_0. (**B**) An illustration of monolayer water in SWNTs with a diameter of 1.36 nm. Monolayer adsorption forms a tube-like structure at 8.0°C under the constraint of SWNTs. (**C**) A logarithmic plot of water content versus $[\log_{10}(P_0/P)]^2$ for the isotherm at 8.0°C, following the Dubbin-Radushkevitch-Kaganer equation.

age binding energy but by the low binding energy part, as determined by

$$\exp(\beta\mu^{ex}) = \langle\exp(\beta u)\rangle = \int p_{bind}(u)\exp(\beta u)du \quad (2)$$

where $\beta = 1/k_BT$, $p_{bind}(u)$ is the probability distribution of binding energy u ($u < 0$), and μ^{ex} is the local excess chemical potential defined as the difference between the chemical potential of water and that of an ideal gas under the same condition (*3*).

At 8.0°C, water adsorption proceeds so as to form a monolayer. The binding energy for adsorbed water with an ordered water nanotube structure, as predicted theoretically (*25*, *26*), is expected to be distributed more sharply than in bulk water. States of low binding energy are less frequently occupied. The chemical potential could be lower than that of saturated vapor. Thus, substantial adsorption could happen even at low relative pressure at 8.0°C, as shown in Fig. 1A. At 22.1°C, the adsorbed water in SWNTs could possess a variety of local structures and a broader distribution in binding energy. More states could be located in the low binding energy region, leading to higher chemical potential and an unfavorable condition for adsorption. Thus, much less water was adsorbed in SWNTs at 22.1°C than at 8.0°C.

To investigate the dynamics of adsorbed water molecules, the correlation time of molecular motion was estimated with ^{1}H spin-lattice relaxation time (T_1) and transverse relaxation time (T_2). The ^{1}H T_1 in water is determined by interaction fluctuations induced by molecular motions characterized by a correlation time τ. Assuming that the intramolecular proton-proton dipolar interaction of water molecules dominates the relaxation process, T_1 is given by (*27*)

$$\left(\frac{1}{T_1}\right) = \frac{3\gamma^4\hbar^2}{10r^6}\left(\frac{\tau}{1+\omega_0^2\tau^2} + \frac{4\tau}{1+4\omega_0^2\tau^2}\right) \quad (3)$$

where γ is the gyromagnetic ratio of proton, $2\pi\hbar$ is the Planck constant, r is the distance between the two hydrogen atoms in a water molecule, and $\omega_0/2\pi$ is the Larmor frequency (34 MHz at 0.8 T). A quantitative relation between T_2 and τ can also be established (*28*).

$$\left(\frac{1}{T_2}\right) = \frac{3\gamma^4\hbar^2}{20r^6} \times \left(3\tau + \frac{5\tau}{1+\omega_0^2\tau^2} + \frac{2\tau}{1+4\omega_0^2\tau^2}\right) \quad (4)$$

Figure 2C plots the theoretical values of T_1 and T_2 versus τ. The measured T_1 values versus pressure at 8.0°C and 18.4°C are shown in Fig. 2A. The T_1 at 8.0°C is shorter than that of 18.4°C at the same relative pressure until the saturated pressure is reached, where T_1 values at both temperatures converge to the same value. At 8.0°C, T_1 decreases slowly with increasing pressure up to $P/P_0 = 1.0$. At 18.4°C, however, T_1 decreases slowly with increasing pressure below $P/P_0 = 0.8$ but decreases rapidly with pressure above $P/P_0 = 0.8$.

Similarly, at 8.0°C, T_2 (Fig. 2B) increases slowly with pressure up to $P/P_0 = 1.0$, whereas at 18.4°C, T_2 increases very slowly below $P/P_0 = 0.8$ but increases sharply above $P/P_0 = 0.8$. T_2 is longer at 8.0°C than at 18.4°C at low relative pressure and becomes comparable at saturated pressure. This measurement reveals that T_2 is much shorter than T_1. Also, T_2 increases while T_1 decreases with either increasing relative pressure or decreasing temperature. Thus, the measured T_1 values are situated to the right of the T_1 minimum (slow-motion limit), as illustrated in Fig. 2C by the data at $P/P_0 = 0.75$. The measured T_2 values at $P/P_0 = 0.75$ are shorter than theoretical predictions, as plotted in Fig. 2C. The theoretical prediction of T_2 considers only intramolecular dipolar interaction and underestimates the relaxation rate $1/T_2$, which also depends on the intermolecular dipolar interactions. The molecular motions under confinement are anisotropic, and the intermolecular dipolar interaction cannot be easily averaged to zero (*29*, *30*).

The correlation time changes from 132 ns when T_1 is 7 ms (18.4°C, $P/P_0 = 0.75$) to 46 ns when T_1 is 3 ms (8.0°C, $P/P_0 = 0.75$). They are several orders of magnitude longer than 3.5 ps of bulk water at 20°C (on the left edge of Fig. 2C). The correlation time at 8.0°C is shorter than that at 18.4°C at low relative pressure, and the amount of adsorbed water at a given relative pressure below $P/P_0 = 0.9$ is different at these two temperatures. The structure and density of adsorbed water are also expected to be different and could lead to the observed difference in the correlation time. The correlation time at these two temperatures did become the same at $P/P_0 = 1.0$ (26 ns), where the amount of water became comparable. This suggests that the structure is similar at these two temperatures when the SWNTs are filled with water.

Because the intramolecular dipolar interaction dominates the spin-lattice relaxation, the long correlation time τ suggests that there is a substantial slowdown in molecular reorientation. The slowdown of certain dynamics of water in proximity to small hydrophobic groups has been shown previously (*31*). Here, we show a similar slowdown of water reorientation in proximity to an extended nonpolar surface.

Although the hydrophobic effect is widely known to be temperature dependent, our observation demonstrates that such temperature dependence could cause a qualitative change, as manifested by the hydrophobic-hydrophilic transition. At lower temperatures, well-defined layered structures of nanoconfined water on hydrophobic surfaces lead to a narrower probability distribution of the binding energy, making adsorption favorable in terms of the free energy. When such ordered structure is weakened at higher temperature, the distribution of the binding energy broadens, making adsorption unfavorable.

The hydrophobicity should not be considered as an absolute property of a surface under nanoconfinement without considering the structure of interfacial water. The correlation time of water reorientation in SWNTs is determined to be on the order of 10 to 100 ns. This result shows that the dynamics of water reorientation is hin-

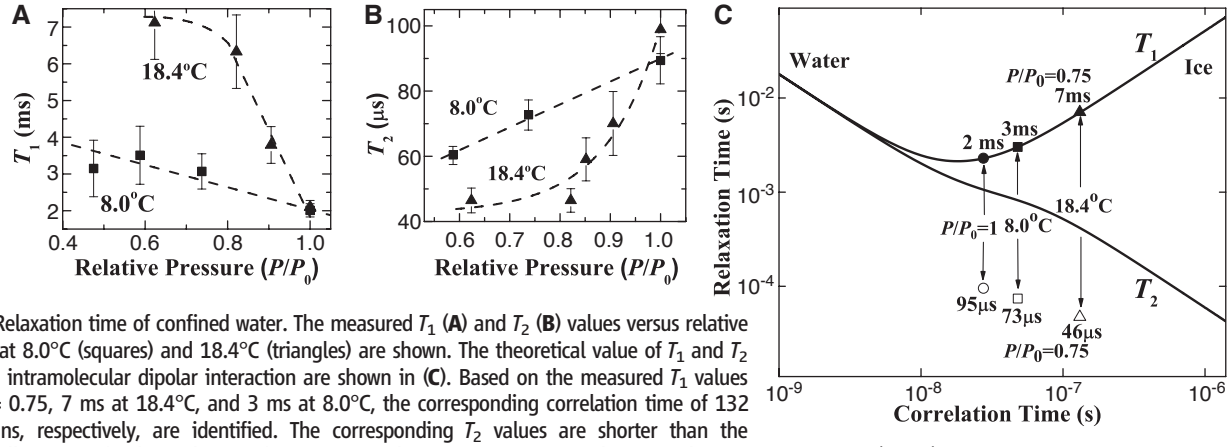

Fig. 2. Relaxation time of confined water. The measured T_1 (**A**) and T_2 (**B**) values versus relative pressure at 8.0°C (squares) and 18.4°C (triangles) are shown. The theoretical value of T_1 and T_2 based on intramolecular dipolar interaction are shown in (**C**). Based on the measured T_1 values at $P/P_0 = 0.75$, 7 ms at 18.4°C, and 3 ms at 8.0°C, the corresponding correlation time of 132 and 46 ns, respectively, are identified. The corresponding T_2 values are shorter than the theoretically expected values. The correlation time at these two temperatures becomes the same at $P/P_0 = 1$ (26 ns).

dered compared with bulk water, consistent with the dynamics of water molecules in proximity to small hydrophobic groups (*31*). The confined and interfacial water are prevalent in biological systems, such as the water in ion channels and in proximity to proteins. The affinity change due to temperature-induced structural change of water could be relevant to various phenomena, including in biological systems, such as the cold denaturation of proteins (*2*).

References and Notes

1. D. Chandler, *Nature* **437**, 640 (2005).
2. C. J. Tsai, J. V. Maizel, R. Nussinov, *Crit. Rev. Biochem. Mol. Biol.* **37**, 55 (2002).
3. G. Hummer, J. C. Rasaiah, J. P. Noworyta, *Nature* **414**, 188 (2001).
4. K. Koga, G. T. Gao, H. Tanaka, X. C. Zeng, *Physica A* **314**, 462 (2002).
5. R. J. Mashl, S. Joseph, N. R. Aluru, E. Jakobsson, *Nano Lett.* **3**, 589 (2003).
6. A. I. Kolesnikov *et al.*, *Phys. Rev. Lett.* **93**, 035503 (2004).
7. Y. Maniwa *et al.*, *Chem. Phys. Lett.* **401**, 534 (2005).
8. A. Striolo *et al.*, *Adsorption* **11**, 397 (2005).
9. J. K. Holt *et al.*, *Science* **312**, 1034 (2006).
10. S. H. Mao, A. Kleinhammes, Y. Wu, *Chem. Phys. Lett.* **421**, 513 (2006).
11. Q. Chen *et al.*, *Nano Lett.* **8**, 1902 (2008).
12. R. S. Vartapetyan, A. M. Voloshchuk, *Usp. Khim.* **64**, 1055 (1995).
13. T. Ohba, H. Kanoh, K. Kaneko, *J. Am. Chem. Soc.* **126**, 1560 (2004).
14. X. P. Tang *et al.*, *Science* **288**, 492 (2000).
15. Materials and methods are available as supporting material on *Science* Online.
16. A. Kleinhammes *et al.*, *Phys. Rev. B* **68**, 075418 (2003).
17. H. Z. Geng *et al.*, *Chem. Phys. Lett.* **399**, 109 (2004).
18. Y. Maniwa *et al.*, *Nat. Mater.* **6**, 135 (2007).
19. S. J. Gregg, K. S. W. Sing, *Adsorption, Surface Area, and Porosity* (Academic Press, London, New York, ed. 2, 1982).
20. J. Pires, M. L. Pinto, A. Carvalho, M. B. de Carvalho, *Adsorption* **9**, 303 (2003).
21. T. R. Jensen *et al.*, *Phys. Rev. Lett.* **90**, 086101 (2003).
22. O. Byl *et al.*, *J. Am. Chem. Soc.* **128**, 12090 (2006).
23. D. Beaglehole, H. K. Christenson, *J. Phys. Chem.* **96**, 3395 (1992).
24. G. R. Birkett, D. D. Do, *J. Phys. Chem. C* **111**, 5735 (2007).
25. T. Kurita, S. Okada, A. Oshiyama, *Phys. Rev. B* **75**, 205424 (2007).
26. D. Takaiwa, I. Hatano, K. Koga, H. Tanaka, *Proc. Natl. Acad. Sci. U.S.A.* **105**, 39 (2008).
27. A. Abragam, *The Principles of Nuclear Magnetism* (Clarendon Press, Oxford, 1961).
28. R. Kubo, K. Tomita, *J. Phys. Soc. Jpn.* **9**, 888 (1954).
29. J. P. Korb, S. Xu, J. Jonas, *J. Chem. Phys.* **98**, 2411 (1993).
30. J. Baugh *et al.*, *Science* **294**, 1505 (2001).
31. Y. L. A. Rezus, H. J. Bakker, *Phys. Rev. Lett.* **99**, 148301 (2007).

32. This work was supported by NSF under contract DMR 0513915. We thank O. Zhou for help in SWNTs synthesis.

Supporting Online Material

www.sciencemag.org/cgi/content/full/322/5898/80/DC1
Figs. S1 and S2

26 June 2008; accepted 19 August 2008
10.1126/science.1162412

Atmospheric CO_2 and Climate on Millennial Time Scales During the Last Glacial Period

Jinho Ahn* and Edward J. Brook

Reconstructions of ancient atmospheric carbon dioxide (CO_2) variations help us better understand how the global carbon cycle and climate are linked. We compared CO_2 variations on millennial time scales between 20,000 and 90,000 years ago with an Antarctic temperature proxy and records of abrupt climate change in the Northern Hemisphere. CO_2 concentration and Antarctic temperature were positively correlated over millennial-scale climate cycles, implying a strong connection to Southern Ocean processes. Evidence from marine sediment proxies indicates that CO_2 concentration rose most rapidly when North Atlantic Deep Water shoaled and stratification in the Southern Ocean was reduced. These increases in CO_2 concentration occurred during stadial (cold) periods in the Northern Hemisphere, several thousand years before abrupt warming events in Greenland.

The last glacial period was characterized by abrupt climate and environmental changes on millennial time scales. Prominent examples include abrupt warming and cooling in Greenland ice core records (Dansgaard-Oeschger, or DO, events) (*1*, *2*) and abrupt iceberg discharges in the North Atlantic (Heinrich, or H, events) (*3*), the latter appearing to predate the longest and largest DO events (Fig. 1A). Age synchronization between Greenland and Antarctic ice cores through atmospheric CH_4 variations reveals that Antarctic and Greenlandic temperature are linked, but not in phase (*4*, *5*) (Fig. 1, A, B, and D). Antarctic warming started before warming in Greenland for most of the large millennial events in the records, and Antarctic temperatures began to decline when Greenland rapidly warmed. Model and ice core studies suggest that this link is maintained by changes in meridional overturning circulation (*6*, *7*).

In contrast to the interhemispheric climate link, the relation between atmospheric CO_2 and climate, in the glacial period [~20 to 120 thousand years ago (ka)], has not been as well documented because of scatter in data sets (*8*) and/or chronological uncertainties (*9*). Understanding CO_2 variability is important, however, because of the direct role of CO_2 as a greenhouse gas and the probable influence of changes in ocean circulation on past atmospheric CO_2 concentrations. Here, we provide high-resolution atmospheric CO_2 data from the Byrd ice core (*10*), with a chronology well synchronized with the Greenland ice cores via CH_4 correlation (*4*). The data cover the period of 20 to 90 ka (Fig. 1C), including previously published results for 47 to 65 ka (*11*). We also measured CH_4 in 36 samples from Byrd to better constrain the chronology of the 67- to 87-ka time period [the time of DO-19, 20, and 21 and Antarctic events A5 to A7 (*4*)] (Fig. 1D). Rapid increases in CH_4 concentration are essentially synchronous with abrupt warming in Greenland within decades (*12*–*14*). With CH_4 and CO_2 data from the same core, and in many cases from the same samples, we could directly study the phasing between CO_2 and Greenland temperature variations, circumventing uncertainties due to age differences between ice and gas in ice core records (*12*–*14*).

We call attention to two distinct features of atmospheric CO_2 variations associated with climate changes in the Northern and Southern Hemispheres. First, CO_2 variation is strongly correlated with $\delta^{18}O_{ice}$ in the Byrd core, a proxy for site temperature, but whereas CO_2 remained relatively stable for about 1 to 2 ka after reaching maximum levels associated with peaks in Antarctic warming, Antarctic temperature dropped rapidly (Fig. 1, B and C, and fig. S1). In contrast to the slow decline of CO_2 relative to Antarctic cooling, the onsets of CO_2 increases are generally synchronous with Antarctic warming within data and age uncertainties (fig. S1).

Second, an increase in CO_2 predates, by 2 to 5 ka, the abrupt warming in Greenland associated with DO events, 8, 12, 14, 17, 20 and 21, the largest and longest abrupt events in the Greenland record over this time period (Figs. 1, A and C, and 2) (DO-19 may be an exception, but the timing of the onset of CO_2 rise is difficult to determine). The CO_2 increase slowed just after the abrupt warming of those events. We do not resolve any similar CO_2 variability associated with the shorter DO climate oscillations in the 37- to 65-ka period (DO-9, 11, 13, 15) with the current data set, but small variations associated with the shorter DO cycles cannot be excluded. Between 19 and 37 ka, there are some variations that may be associated with DO events 2 to 7, particularly a CO_2 peak at ~28 ka, which may be related to DO-4 and the stadial period preceding it. Higher-resolution data will be needed to further understand this variability.

Models of millennial-scale CO_2 variations suggest that changes in North Atlantic Deep

Department of Geosciences, Oregon State University, Corvallis, OR 97331–5506, USA.

*To whom correspondence should be addressed. E-mail: jinhoahn@gmail.com

Atmospheric CO2 and Climate on Millennial Time Scales During the Last Glacial Period

Jinho Ahn, *et al.*

Science **322**, 83 (2008);
DOI: 10.1126/science.1160832

Science (print ISSN 0036-8075; online ISSN 1095-9203) is published weekly, except the last week in December, by the American Association for the Advancement of Science, 1200 New York Avenue NW, Washington, DC 20005.

dered compared with bulk water, consistent with the dynamics of water molecules in proximity to small hydrophobic groups (*31*). The confined and interfacial water are prevalent in biological systems, such as the water in ion channels and in proximity to proteins. The affinity change due to temperature-induced structural change of water could be relevant to various phenomena, including in biological systems, such as the cold denaturation of proteins (*2*).

References and Notes

1. D. Chandler, *Nature* **437**, 640 (2005).
2. C. J. Tsai, J. V. Maizel, R. Nussinov, *Crit. Rev. Biochem. Mol. Biol.* **37**, 55 (2002).
3. G. Hummer, J. C. Rasaiah, J. P. Noworyta, *Nature* **414**, 188 (2001).
4. K. Koga, G. T. Gao, H. Tanaka, X. C. Zeng, *Physica A* **314**, 462 (2002).
5. R. J. Mashl, S. Joseph, N. R. Aluru, E. Jakobsson, *Nano Lett.* **3**, 589 (2003).
6. A. I. Kolesnikov *et al.*, *Phys. Rev. Lett.* **93**, 035503 (2004).
7. Y. Maniwa *et al.*, *Chem. Phys. Lett.* **401**, 534 (2005).
8. A. Striolo *et al.*, *Adsorption* **11**, 397 (2005).
9. J. K. Holt *et al.*, *Science* **312**, 1034 (2006).
10. S. H. Mao, A. Kleinhammes, Y. Wu, *Chem. Phys. Lett.* **421**, 513 (2006).
11. Q. Chen *et al.*, *Nano Lett.* **8**, 1902 (2008).
12. R. S. Vartapetyan, A. M. Voloshchuk, *Usp. Khim.* **64**, 1055 (1995).
13. T. Ohba, H. Kanoh, K. Kaneko, *J. Am. Chem. Soc.* **126**, 1560 (2004).
14. X. P. Tang *et al.*, *Science* **288**, 492 (2000).
15. Materials and methods are available as supporting material on *Science* Online.
16. A. Kleinhammes *et al.*, *Phys. Rev. B* **68**, 075418 (2003).
17. H. Z. Geng *et al.*, *Chem. Phys. Lett.* **399**, 109 (2004).
18. Y. Maniwa *et al.*, *Nat. Mater.* **6**, 135 (2007).
19. S. J. Gregg, K. S. W. Sing, *Adsorption, Surface Area, and Porosity* (Academic Press, London, New York, ed. 2, 1982).
20. J. Pires, M. L. Pinto, A. Carvalho, M. B. de Carvalho, *Adsorption* **9**, 303 (2003).
21. T. R. Jensen *et al.*, *Phys. Rev. Lett.* **90**, 086101 (2003).
22. O. Byl *et al.*, *J. Am. Chem. Soc.* **128**, 12090 (2006).
23. D. Beaglehole, H. K. Christenson, *J. Phys. Chem.* **96**, 3395 (1992).
24. G. R. Birkett, D. D. Do, *J. Phys. Chem. C* **111**, 5735 (2007).
25. T. Kurita, S. Okada, A. Oshiyama, *Phys. Rev. B* **75**, 205424 (2007).
26. D. Takaiwa, I. Hatano, K. Koga, H. Tanaka, *Proc. Natl. Acad. Sci. U.S.A.* **105**, 39 (2008).
27. A. Abragam, *The Principles of Nuclear Magnetism* (Clarendon Press, Oxford, 1961).
28. R. Kubo, K. Tomita, *J. Phys. Soc. Jpn.* **9**, 888 (1954).
29. J. P. Korb, S. Xu, J. Jonas, *J. Chem. Phys.* **98**, 2411 (1993).
30. J. Baugh *et al.*, *Science* **294**, 1505 (2001).
31. Y. L. A. Rezus, H. J. Bakker, *Phys. Rev. Lett.* **99**, 148301 (2007).

32. This work was supported by NSF under contract DMR 0513915. We thank O. Zhou for help in SWNTs synthesis.

Supporting Online Material

www.sciencemag.org/cgi/content/full/322/5898/80/DC1
Figs. S1 and S2

26 June 2008; accepted 19 August 2008
10.1126/science.1162412

Atmospheric CO_2 and Climate on Millennial Time Scales During the Last Glacial Period

Jinho Ahn* and Edward J. Brook

Reconstructions of ancient atmospheric carbon dioxide (CO_2) variations help us better understand how the global carbon cycle and climate are linked. We compared CO_2 variations on millennial time scales between 20,000 and 90,000 years ago with an Antarctic temperature proxy and records of abrupt climate change in the Northern Hemisphere. CO_2 concentration and Antarctic temperature were positively correlated over millennial-scale climate cycles, implying a strong connection to Southern Ocean processes. Evidence from marine sediment proxies indicates that CO_2 concentration rose most rapidly when North Atlantic Deep Water shoaled and stratification in the Southern Ocean was reduced. These increases in CO_2 concentration occurred during stadial (cold) periods in the Northern Hemisphere, several thousand years before abrupt warming events in Greenland.

The last glacial period was characterized by abrupt climate and environmental changes on millennial time scales. Prominent examples include abrupt warming and cooling in Greenland ice core records (Dansgaard-Oeschger, or DO, events) (*1*, *2*) and abrupt iceberg discharges in the North Atlantic (Heinrich, or H, events) (*3*), the latter appearing to predate the longest and largest DO events (Fig. 1A). Age synchronization between Greenland and Antarctic ice cores through atmospheric CH_4 variations reveals that Antarctic and Greenlandic temperature are linked, but not in phase (*4*, *5*) (Fig. 1, A, B, and D). Antarctic warming started before warming in Greenland for most of the large millennial events in the records, and Antarctic temperatures began to decline when Greenland rapidly warmed. Model and ice core studies suggest that this link is maintained by changes in meridional overturning circulation (*6*, *7*).

In contrast to the interhemispheric climate link, the relation between atmospheric CO_2 and climate, in the glacial period [~20 to 120 thousand years ago (ka)], has not been as well documented because of scatter in data sets (*8*) and/or chronological uncertainties (*9*). Understanding CO_2 variability is important, however, because of the direct role of CO_2 as a greenhouse gas and the probable influence of changes in ocean circulation on past atmospheric CO_2 concentrations. Here, we provide high-resolution atmospheric CO_2 data from the Byrd ice core (*10*), with a chronology well synchronized with the Greenland ice cores via CH_4 correlation (*4*). The data cover the period of 20 to 90 ka (Fig. 1C), including previously published results for 47 to 65 ka (*11*). We also measured CH_4 in 36 samples from Byrd to better constrain the chronology of the 67- to 87-ka time period [the time of DO-19, 20, and 21 and Antarctic events A5 to A7 (*4*)] (Fig. 1D). Rapid increases in CH_4 concentration are essentially synchronous with abrupt warming in Greenland within decades (*12*–*14*). With CH_4 and CO_2 data from the same core, and in many cases from the same samples, we could directly study the phasing between CO_2 and Greenland temperature variations, circumventing uncertainties due to age differences between ice and gas in ice core records (*12*–*14*).

We call attention to two distinct features of atmospheric CO_2 variations associated with climate changes in the Northern and Southern Hemispheres. First, CO_2 variation is strongly correlated with $\delta^{18}O_{ice}$ in the Byrd core, a proxy for site temperature, but whereas CO_2 remained relatively stable for about 1 to 2 ka after reaching maximum levels associated with peaks in Antarctic warming, Antarctic temperature dropped rapidly (Fig. 1, B and C, and fig. S1). In contrast to the slow decline of CO_2 relative to Antarctic cooling, the onsets of CO_2 increases are generally synchronous with Antarctic warming within data and age uncertainties (fig. S1).

Second, an increase in CO_2 predates, by 2 to 5 ka, the abrupt warming in Greenland associated with DO events, 8, 12, 14, 17, 20 and 21, the largest and longest abrupt events in the Greenland record over this time period (Figs. 1, A and C, and 2) (DO-19 may be an exception, but the timing of the onset of CO_2 rise is difficult to determine). The CO_2 increase slowed just after the abrupt warming of those events. We do not resolve any similar CO_2 variability associated with the shorter DO climate oscillations in the 37- to 65-ka period (DO-9, 11, 13, 15) with the current data set, but small variations associated with the shorter DO cycles cannot be excluded. Between 19 and 37 ka, there are some variations that may be associated with DO events 2 to 7, particularly a CO_2 peak at ~28 ka, which may be related to DO-4 and the stadial period preceding it. Higher-resolution data will be needed to further understand this variability.

Models of millennial-scale CO_2 variations suggest that changes in North Atlantic Deep

Department of Geosciences, Oregon State University, Corvallis, OR 97331–5506, USA.

*To whom correspondence should be addressed. E-mail: jinhoahn@gmail.com

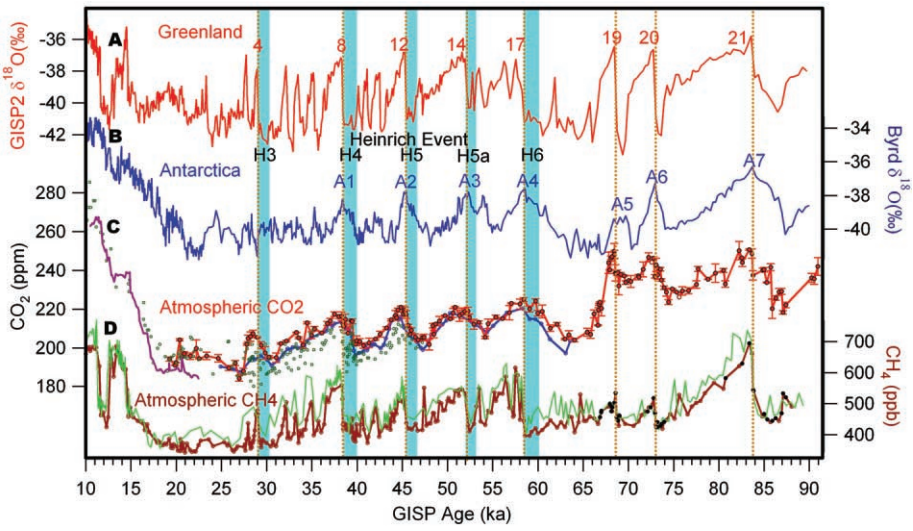

Fig. 1. Atmospheric CO_2 composition and climate during the last glacial period. (**A**) Greenlandic temperature proxy, $\delta^{18}O_{ice}$ (*2*). Red numbers denote DO events. (**B**) Byrd Station, Antarctica temperature proxy, $\delta^{18}O_{ice}$ (*4*). A1 to A7, Antarctic warming events (*4*). (**C**) Atmospheric CO_2 concentrations. Red dots [this study and early results for 47 to 65 ka (*11*) at Oregon State University] and green circles (*8*) (results from University of Bern) are from Byrd ice cores. Red dots are averages of replicates, and red open circles at ~73 and 76 ka are single data [this study and (*11*)]. The chronology used for Byrd CO_2 is described in (*10*). Blue line is from Taylor Dome ice core (*9*) on the GISP2 time scale (*11*). Purple line is from EPICA Dome C (*27*). (**D**) CH_4 concentrations from Greenland (green) (*4*) and Byrd ice cores (brown) [(*4*) and this study]. Black dots, new measurements for this study. Vertical blue bars, timing of Heinrich events (H3 to H6) (*25*, *26*). Brown dotted lines, abrupt warming in Greenland.

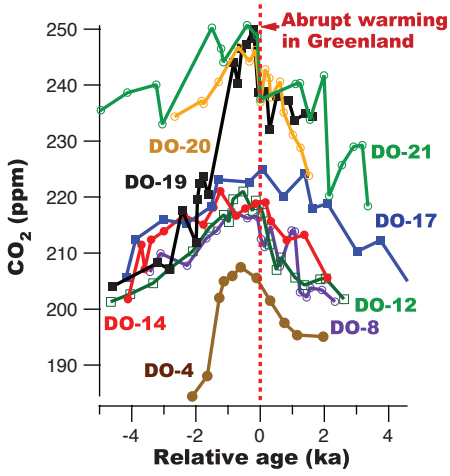

Fig. 2. Atmospheric CO_2 variations relative to abrupt warming in Greenland. The sequence of Byrd CO_2 variations [this study and (*11*)] associated with each DO event is numbered. Red dotted line indicates the timing of the abrupt warming in Greenland defined by the rapid rise in CH_4 concentration in the Byrd ice core.

Water (NADW) formation can affect atmospheric CO_2 concentration through both physical and biological processes in the ocean and terrestrial biosphere. Comparing model results is difficult because of differences in boundary conditions, amount and duration of freshwater forcing, and treatment of the terrestrial biosphere and other relevant processes. Model results suggest that several different mechanisms may relate changes in NADW to changes in atmospheric CO_2 concentration, including increases in Southern Ocean sea surface temperatures and decreased salinity in the North Atlantic (*15*), and reduced Southern Ocean stratification and release of CO_2 (*16*). Climate-induced changes in the terrestrial biosphere caused by changes in ocean circulation may also affect the atmospheric CO_2 (*17*, *18*), but the magnitude of this effect is not yet clear.

To explore the possible link between ocean circulation and CO_2, we compared our data with the benthic foraminiferal $\delta^{13}C$ from Iberian margin sediments at depth of 3146 m, using $\delta^{13}C$ as a proxy for the balance between northern source and southern source deep waters at this site (*19*) (Fig. 3C). We also used bulk sediment $\delta^{15}N$ from the Chile margin in intermediate depths as a proxy for input of the Subantarctic Mode Water to this region (*20*). Following (*20*), we interpreted this proxy as an indicator of the reduction of stratification in the Southern Ocean (Fig. 3D), which may result from changes in NADW. The two data sets are inversely correlated (note the reverse scale of the $\delta^{13}C$) in most time intervals, implying that shoaling NADW is linked to reduction of stratification in the Southern Ocean. The rate of change of CO_2 concentration peaks when these proxies indicate a maximum in NADW shoaling and reduction of stratification in the Southern Ocean (Fig. 3, B to D), implying CO_2 release to the atmosphere during maxima in Southern Ocean destratification, as suggested in model experiments (*16*). At around 19 to 37 ka, the correlations among the two marine proxies and the rate of change of CO_2 are not as clear as they are in the 37- to 91-ka time period. Other, perhaps longer-term processes may have controlled atmospheric CO_2 during this time period. Alternatively, the geochemical proxies plotted in Fig. 3 may not directly reflect millennial change in ocean circulation as climate approached the last glacial maximum. Models of long-term glacial-interglacial CO_2 variations indicate that destratification in the Southern Ocean should cause CO_2 to increase (*21*, *22*), although it is not clear if these model results are directly applicable to millennial-scale variations. Other mechanisms that may contribute to glacial-interglacial cycles and may be important on millennial time scales include changes in CO_2 outgassing due to variations in sea ice extent (*23*) and changes in iron fertilization (*24*) in the Southern Ocean.

Heinrich events are associated with the cold periods before major DO events, and one scenario that could explain CO_2 variations is that large freshwater fluxes associated with Heinrich events cause changes in ocean circulation and release of CO_2 to the atmosphere through mechanisms discussed above (*15*, *16*). However, based on existing age constraints (*3*, *25*, *26*), H events 3, 4, 5, 5a, and 6 appear to have occurred 0 to 3 ka after CO_2 started to rise (Fig. 1 and fig. S2). Unfortunately, precise comparison of CO_2 and all of the H events is prevented by chronological uncertainties. In some cases the relative timing of H events and events in the ice core record can be constrained via correlations between temperature proxies in marine records and ice core data, and identification of ash layers (*3*, *25*, *26*). For example, the abrupt warming at DO-15 (defined by the rapid rise in CH_4 concentration, fig. S2) has a correlative feature in North Atlantic sediment records (*26*) and occurred before H5a, whereas the CO_2 rise associated with A3 started during or before DO-15, and therefore also before H-5a. However, for other H events, the timing of the associated CO_2 rise cannot be precisely determined in this way given the current time resolution of the ice core records.

The data also indicate abrupt increases in CO_2 concentration of ~10 parts per million (ppm) at the times of abrupt warming associated with DO-19, 20, and 21 (Figs. 1 and 2). The magnitude of these jumps is similar to those during the last Termination (*27*), when the CO_2 level and temperature are similar to those of DO-19, 20, and 21 (65 to 90 ka). During the intervening period (20 to 65 ka), this type of variability is not as apparent in our record. The origin of these brief periods of elevated CO_2 is not clear, but may be related to increases in sea surface temperature in the Northern Hemisphere or release of CO_2 from the terrestrial biosphere by respiration, associated with abrupt warming in Greenland.

Another notable feature is the rapid decrease in CO_2 concentration of ~43 ppm at ~68 ka [Greenland Ice Sheet Project 2 (GISP2) time scale] after DO-19 (Figs. 1C and 4). The magnitude of the CO_2 drop is about half the total CO_2

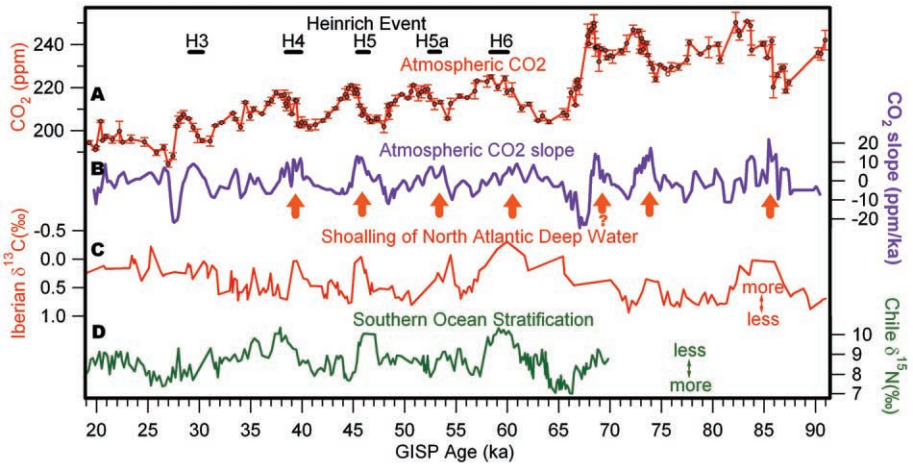

Fig. 3. Atmospheric CO_2 and change in ocean circulation. (**A**) Atmospheric CO_2 concentrations from the Antarctic Byrd ice core [this study and (*11*)], measured at Oregon State University (table S1). (**B**) Derivative of the Byrd CO_2 concentrations shown in (A). Nine-point running mean of the first derivative is calculated from data interpolated to 100-year spacing. (**C**) Benthic foraminifera (*Cibicidoides* wuellerstorfi) $\delta^{13}C$ from the Iberian margin sediment core (*19*). Ages are synchronized by correlation between planktonic foraminifera from the same sediment core and Greenland $\delta^{18}O_{ice}$ (*19*). (**D**) Bulk sediment $\delta^{15}N$ from the Chile Margin as a proxy for the reduction of the Southern Ocean stratification (*20*). Ages are synchronized by benthic foraminifera $\delta^{18}O$ correlation with that from Iberian margin (*20*). Orange arrows show the positive correlation between CO_2 derivative and reduced stratification in the Southern Ocean or shoaling NADW. The arrow with a question mark indicates an unclear correlation due to lack of resolution in the $\delta^{13}C$ record. Horizontal black bars, timing of Heinrich events (H3 to H6) (*25*, *26*).

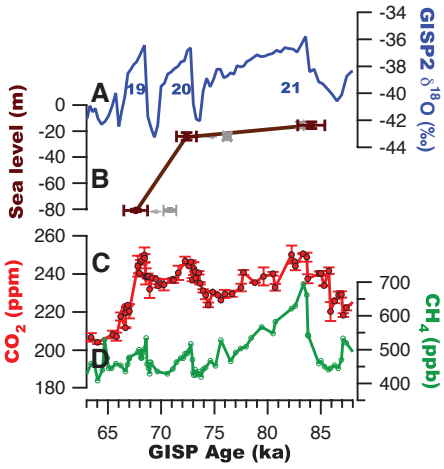

Fig. 4. Comparison of the rapid drop in CO_2 concentration with coral sea-level proxy. (**A**) Greenland temperature proxy (*2*). Blue numbers denote DO events. (**B**) Coral sea-level records (*33*). Original U-Th absolute ages (*33*) (gray dots) are adjusted to the GISP2 time scale (brown dots) by means of the correlations between Sanbao speleothem $\delta^{18}O$ (*34*) and GISP2 $\delta^{18}O_{ice}$ (*2*). The sea-level age uncertainties on the GISP2 time scale were calculated with age uncertainties from coral U-Th (±0.3 to 0.6 ka) and speleothem U-Th (±0.5 to 0.65 ka), and correlations between GISP2 and speleothem $\delta^{18}O$ (±0.5 to 1.0 ka) and between GISP2 $\delta^{18}O_{ice}$ and Byrd CO_2 records (±0.3 to 0.5 ka). (**C**) Atmospheric CO_2 concentration from Byrd ice core [this study and (*11*)]. (**D**) Atmospheric CH_4 concentration from Byrd ice core [(*4*) and this study].

variations during long-term glacial-interglacial cycles. The fastest rate of decrease during the event is ~11 ppm/ka, but the true value could have been even larger. A similar decrease of ~40 ppm at this time is also observed in low-resolution Vostok (*28*) and Dome Fuji records (*29*). A large sea-level drop appears to predate the CO_2 decline (Fig. 4). It is notable that a rapid increase of dust flux occurred in the equatorial Pacific and Antarctica at around the same time (*30*, *31*).

Our results support the idea that atmospheric CO_2 concentration is controlled by oceanic processes, especially those associated with proxies for the reduction of stratification in the Southern Ocean, but also affected by the Northern Hemisphere climate. Reductions in overturning circulation in the Northern Hemisphere appear to be associated with increases in atmospheric CO_2. On the basis of these data, if global warming causes a decrease in the overturning circulation (*32*), we might expect a positive feedback from additional CO_2 emissions to the atmosphere. However, the application of those observations to the future carbon cycle should be done cautiously because of differences between glacial and interglacial climate boundary conditions (*17*). It is likely that higher-resolution records of CO_2 will reveal more details about precise timing between Antarctic and Greenlandic temperature and atmospheric CO_2.

References and Notes

1. W. Dansgaard *et al.*, *Nature* **364**, 218 (1993).
2. P. M. Grootes, M. Stuiver, J. W. C. White, S. J. Johnsen, J. Jouzel, *Nature* **366**, 552 (1993).
3. G. Bond *et al.*, *Nature* **365**, 143 (1993).
4. T. Blunier, E. J. Brook, *Science* **291**, 109 (2001).
5. EPICA Community Members, *Nature* **444**, 195 (2006).
6. A. Ganopolski, S. Rahmstorf, *Nature* **409**, 153 (2001).
7. T. F. Stocker, S. J. Johnsen, *Paleoceanography* **18**, 10.1029/2003PA000920 (2003).
8. B. Stauffer *et al.*, *Nature* **392**, 59 (1998).
9. A. Indermühle, E. Monnin, B. Stauffer, T. F. Stocker, M. Wahlen, *Geophys. Res. Lett.* **27**, 735 (2000).
10. Materials and methods are available as supporting material on *Science* Online.
11. J. Ahn, E. J. Brook, *Geophys. Res. Lett.* **34**, L10703 10.1029/2007GL029551 (2007).
12. J. Severinghaus, A. Grachev, M. Spencer, R. Alley, E. J. Brook, *Geophys. Res. Abstr.* **5** (suppl.), 04455 (2003); available at www.cosis.net/abstracts/EAE03/04455/EAE03-J-04455.pdf.
13. C. Huber *et al.*, *Earth Planet. Sci. Lett.* **243**, 504 (2006).
14. A. Grachev, E. J. Brook, *Geophys. Res. Lett.* **34**, L20703, 10.1029/2007GL029799 (2007).
15. O. Marchal, T. F. Stocker, F. Joos, *Paleoceanography* **13**, 225 (1998).
16. A. Schmittner, E. J. Brook, J. Ahn, in *Ocean Circulation: Mechanisms and Impacts*, A. Schmittner, J. Chiang, S. Hemming, Eds. (AGU Geophysical Monograph Series, American Geophysical Union, Washington, DC, 2007), vol. 173, pp. 315–334.
17. P. Köhler, F. Joos, S. Gerber, R. Knutti, *Clim. Dyn.* **25**, 689 (2005).
18. L. Menviel, A. Timmermann, A. Mouchet, O. Timm, *Paleoceanography* **23**, 10.1029/2007PA001445 (2008).
19. N. J. Shackleton, M. A. Hall, E. Vincent, *Paleoceanography* **15**, 565 (2000).
20. R. Robinson, A. Mix, P. Martinez, *Quat. Sci. Rev.* **26**, 201 (2007).
21. A. J. Watson, A. C. N. Garabato, *Tellus* **58B**, 73 (2006).
22. J. R. Toggweiler, J. L. Russell, S. R. Carson, *Paleoceanography* **21**, 10.1029/2005PA001154 (2006).
23. B. B. Stephens, R. F. Keeling, *Nature* **404**, 171 (2000).
24. R. Röthlisberger *et al.*, *Geophys. Res. Lett.* **31**, 10.1029/2004GL020338 (2004).
25. M. Sarnthein *et al.*, in *The Northern North Atlantic: A Changing Environment*, P. Schäfer, M. Schlüter, W. Ritzrau, J. Thiede, Eds. (Springer, New York, 2001), pp. 365–410.
26. H. Rashid, R. Hesse, D. J. W. Piper, *Paleoceanography* **18**, 10.1029/2003PA000913 (2003).
27. E. Monnin *et al.*, *Science* **291**, 112 (2001).
28. J. R. Petit *et al.*, *Nature* **399**, 429 (1999).
29. K. Kawamura *et al.*, *Nature* **448**, 912 (2007).
30. G. Winckler, R. F. Anderson, M. Q. Fleisher, D. McGee, N. Mahowald, *Science* **320**, 93 (2008).
31. F. Lambert *et al.*, *Nature* **452**, 616 (2008).
32. IPCC, *Climate Change: The Physical Science Basis. Contribution of Working Group I to the Fourth Assessment Report of the Intergovernmental Panel on Climate Change*, S. Solomon *et al.*, Eds. (Cambridge Univ. Press, New York, 2007).
33. K. B. Cutler *et al.*, *Earth Planet. Sci. Lett.* **206**, 253 (2003).
34. Y. Wang *et al.*, *Nature* **451**, 1090 (2008).

35. We thank K. Howell, Q. Ouada, J. Lee, and L. Mitchell for assistance in gas chromatographic analysis; the staff of the National Ice Core Lab for ice sampling and curation; and S. Terhune for invaluable technical assistance. We also thank P. Clark, A. Schmittner, A. Mix, N. Pisias, and J. Stoner (Oregon State University) for helpful discussions. Financial support was provided by the Gary Comer Science and Education Foundation, and NSF grants OPP 0337891 and ATM 0602395.

Supporting Online Material

www.sciencemag.org/cgi/content/full/1160832/DC1
Materials and Methods
Figs. S1 and S2
Table S1
References

22 May 2008; accepted 2 September 2008
Published online 11 September 2008;
10.1126/science.1160832
Include this information when citing this paper.

Rates of Molecular Evolution Are Linked to Life History in Flowering Plants

Stephen A. Smith, *et al.*

Science **322**, 86 (2008);
DOI: 10.1126/science.1163197

Science (print ISSN 0036-8075; online ISSN 1095-9203) is published weekly, except the last week in December, by the American Association for the Advancement of Science, 1200 New York Avenue NW, Washington, DC 20005.

Rates of Molecular Evolution Are Linked to Life History in Flowering Plants

Stephen A. Smith* and Michael J. Donoghue

Variable rates of molecular evolution have been documented across the tree of life, but the cause of this observed variation within and among clades remains uncertain. In plants, it has been suggested that life history traits are correlated with the rate of molecular evolution, but previous studies have yielded conflicting results. Exceptionally large phylogenies of five major angiosperm clades demonstrate that rates of molecular evolution are consistently low in trees and shrubs, with relatively long generation times, as compared with related herbaceous plants, which generally have shorter generation times. Herbs show much higher rates of molecular change but also much higher variance in rates. Correlates of life history attributes have long been of interest to biologists, and our results demonstrate how changes in the rate of molecular evolution that are linked to life history traits can affect measurements of the tempo of evolution as well as our ability to identify and conserve biodiversity.

Variation in the rate of molecular evolution has been attributed to a number of factors, including differences in body size, metabolic rate, DNA repair, and generation time (e.g., *1*–*4*). In plants, differences in rates of molecular evolution have been noted between annuals and perennials (*5*) and between woody and herbaceous species (*6*, *7*). These differences have been presumed to reflect differences in generation time (the time from seed germination to the production of fruits/seeds). However, in plants the relationship between life history and the average length of time before a nucleotide is copied either through replication or repair [nucleotide generation time (*1*)] is complicated by the fact that somatic mutations can accumulate during growth and can be transmitted through gametes (*8*, *9*). Variation in breeding system and/or seed-banking by annual plants (*9*) may also affect the ability to detect a correlation between molecular rate and generation time.

Previous studies have been inconclusive with respect to the extent and the correlates of rate heterogeneity in plants (*5*, *7*, *9*, *10*). Studies focused on individual smaller clades, or on single gene regions, have yielded results of uncertain generality (*7*), whereas broader phylogenetic studies have suffered from limited taxon sampling and, hence, comparisons among very distant relatives (*11*). Some tests have failed to account for phylogenetic relatedness (*9*).

We assembled molecular sequence data for five major branches within the flowering plants: three clades of asterids (Apiales, Dipsacales, and Primulales), one clade of rosids (Moraceae/Urticaceae), and one of monocotyledons (Commelinidae). We used group-to-group profile alignments (*12*) that take advantage of previously recognized clades within the groups analyzed (*13*) and yield denser data matrices (containing less missing data) than those produced using other strategies (*14*). Specifically, we identified alignable clusters of homologous gene regions, which were then concatenated with profile alignment (*13*). To minimize missing data, only phylogenetically informative clusters (with at least four taxa) were used. The gene regions varied among the five matrices but in each case included markers from the chloroplast, nuclear, and mitochondrial genomes (figs. S1 and S2 and table S2). The average gene region in our analyses contained 305 species; the smallest contained 10 species. This process resulted in an Apiales matrix of 1593 species by 9522 sites (>15 megabases); for Dipsacales, it was 366 by 11374 (>4 megabases); for Primulales, 529 by 11505 (>6 megabases); for Moraceae/Urticaceae, 457 by 7820 (>3.5 megabases); and for Commelinidae, 4657 by 22391 sites (>104 megabases).

Phylogenetic trees (Fig. 1) were inferred under maximum-likelihood (ML) with RAxML (vers.7.0.0) (*15*), with gene regions treated as separate partitions (*13*). We conducted 100 rapid bootstrap analyses, using every 10th bootstrap tree as a starting tree for a full ML search, and chose the tree with the highest likelihood score; owing to the size of the Commelinidae matrix, only a single ML search was conducted. For all clades but Commelinidae, we used nonparametric rate smoothing (*16*) to set branch lengths proportional to time; we used the PATHd8 method (*17*) for the exceptionally large commelinid analysis. Published studies were used to calibrate each phylogeny, using multiple calibration points to limit the impact of clade-specific rate heterogeneity (*13*, *18*–*21*). For Apiales and Primulales, we separately calibrated the major subclades identified in previous analyses, which also accommodated the fact that our analyses included some taxa not represented in previous studies.

Ancestral states of the life history trait "trees/shrubs" versus "herbs" (a proxy for generation time) (*6*, *7*, *22*) were inferred with ML methods (Fig. 1) (*13*); palms (Arecaceae, Commelinidae), which do not produce true wood (secondary xylem), were scored as trees/shrubs. For each branch on each phylogeny, we calculated the number of substitutions per nucleotide site per million years using branch lengths estimated from the dated molecular trees. Branch calculations were binned on the basis of inferred life history to produce box plots for each clade (Fig. 1). Outliers (values >1.5 times beyond the first and third quartiles) were excluded as artifacts of divergence-time estimation (e.g., those with zero or near-zero branch lengths). Within each major clade, we noted that trees/shrubs were consistently evolving more slowly than related herbaceous plants. Median rates of nucleotide divergence were 2.7 to 10 times as high in herbs as in trees/shrubs; herbs also showed higher ranges and variances (Fig. 1). None of the tree/shrub lineages examined here showed high rates of molecular evolution, but some herbaceous lineages were inferred to have low evolutionary rates, in the range characteristic of trees/shrubs. This asymmetry in variance may reflect the fact that, although most trees/shrubs are not able to reproduce within the first few years (*23*, *24*), as most herbs can, some herbs take as long as trees to flower. Consistent with the view that generation time influences the rate of molecular evolution within the Commelinidae (Fig. 1), the longer-lived bromeliads [which take up to 18 years to reproduce (*25*)] have remarkably short branches, with even fewer substitutions per site per million years than palms (0.00059 and 0.0014, respectively). Other factors, such as population size, breeding system, and seed-banking, may also relate to the observed asymmetry; for example, the rate of fixation of mutations by selection increases in large populations. Although we do not dismiss these variables in explaining the observed variance, they are less clearly correlated with the life history distinction than is generation time [e.g., (*26*)].

To explore whether the difference in rates of molecular evolution has remained constant over time, we compared substitutions per site per million years through 10-million-year segments for each dated phylogeny (Fig. 2) (*13*). We found that the trend in rate heterogeneity holds through time, with some noteworthy exceptions in the earliest time periods. For example, woody Dipsacales are estimated to have a high rate of evolution before the herbaceous habit is inferred to have evolved in this lineage (Fig. 2B). Fossil data might help to distinguish whether these results are best explained by incorrect reconstructions (i.e., perhaps the first Dipsacales were herbaceous), by faster evolution of woody lineages during earlier times (e.g., due to warmer climate in the early Tertiary), or by the extinction of early woody lineages.

Because these comparisons do not directly take into account phylogenetic relationships or examine the effects of evolutionary change from one life history state to the other, we calculated branch length contrasts (*27*) around each inferred evolutionary shift in life history (Fig. 3) (*13*). Specifically, we calculated the average accumulation of molecular changes from each branch tip to the shared ancestor of a tree/shrub clade and

Department of Ecology and Evolutionary Biology, 21 Sachem Street, Post Office Box 208105, Yale University, New Haven, CT 06520–8105, USA.

*To whom correspondence should be addressed. E-mail: stephen.smith@yale.edu

compared this to the average accumulation in its herbaceous sister clade. We started from the most nested clades and worked toward the root, excising any nested contrasts from the more inclusive calculations to avoid measuring any node more than once. We omitted contrasts containing only one tree/shrub or one herb branch to lessen the impact of incorrectly estimating singleton branches (branch lengths were averaged in clades with two or more species).

Of the 13 contrasts identified using these criteria (Table 1 and Fig. 3), 12 showed a slower rate of molecular evolution in trees/shrubs than in herbs (sign test, $P = 0.00342$). On average, herbs evolve 2.5 times as fast as trees/shrubs. A maximum rate difference of 4.75 times was found between *Dorstenia* (Moraceae) and its tree/shrub sister clade. The single exception occurred within *Sambucus* (Dipsacales), where the tree/shrub species showed a slightly higher rate than the herbs (0.0075 and 0.0061, respectively). This case involved the smallest

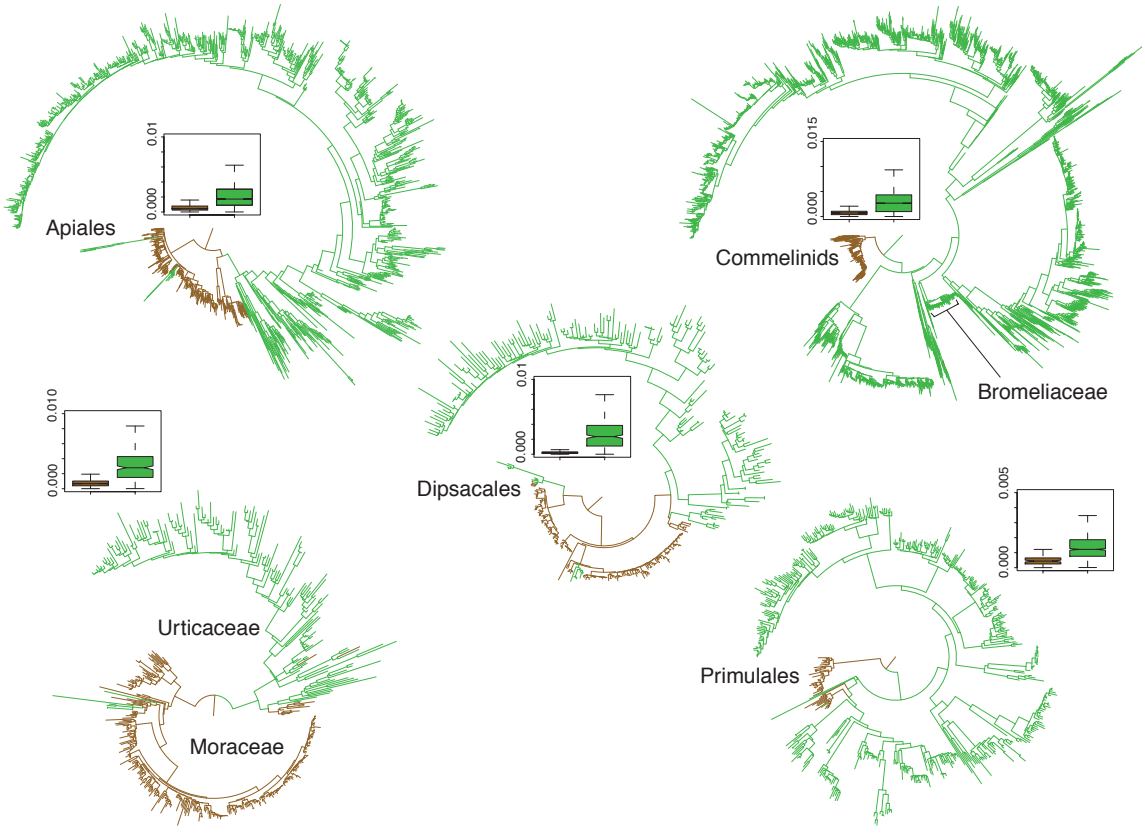

Fig. 1. Phylogenies of five angiosperm clades with branch lengths proportional to substitutions per site. Branch colors represent inferred life history states (brown for trees/shrubs; green for herbs). Box plots show substitutions per site per million years for the inferred life history categories; centerline represents the median, hinges mark the first and third quartiles, whiskers extend to the lowest and highest nonoutlier. Outliers (not shown) have values >1.5 times beyond the first or third quartiles.

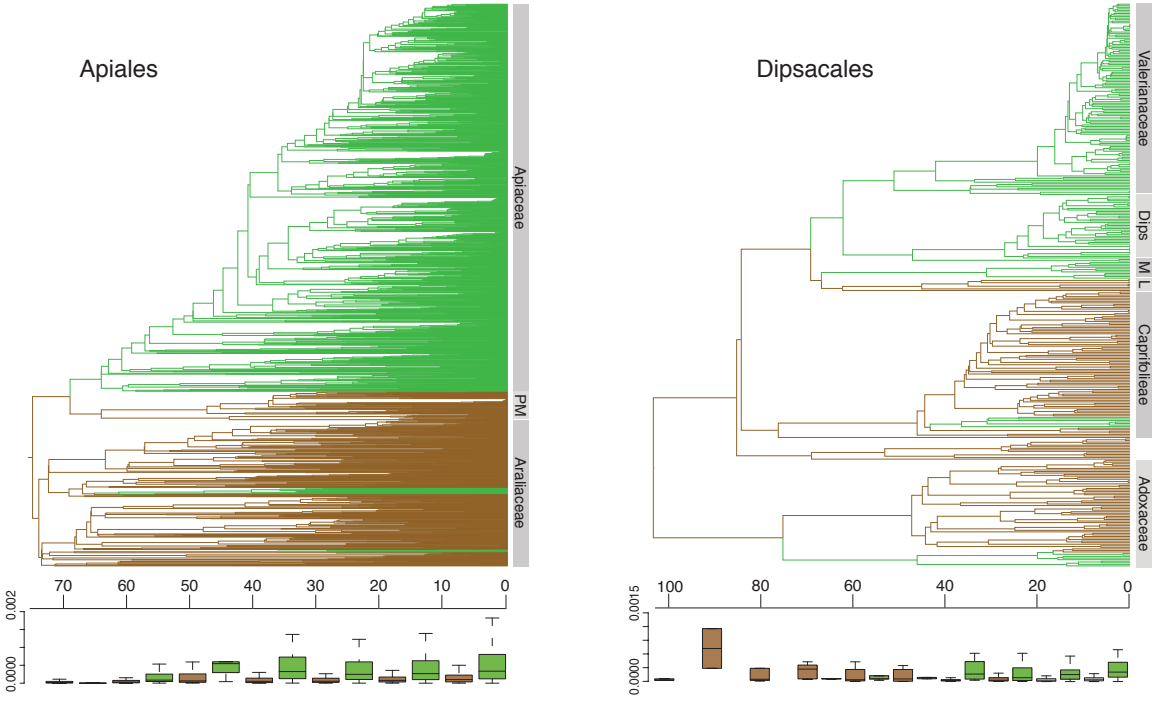

Fig. 2. Dated phylogenies for Apiales and Dipsacales with substitutions per site per million years plotted for 10-million-year intervals through the life of the clade. Branch colors represent inferred life history states (brown for trees/shrubs; green for herbs). Box plots as in Fig. 1. PM, Pittosporaceae and Myodocarpaceae; Dips, Dipsacaceae; M, Morinaceae; L, Linnaceae.

numbers of species (three shrubby species versus three herbs) and also presented the greatest difficulty in assigning life history states (the herbaceous species are subshrubby and the woody species mature rapidly). As such uncertainties are inherent in large comparative analyses, we explored whether alternative phylogenetic hypotheses (*13*) affected the results for the smallest clade examined here, the Dipsacales, as well as the effect of scoring all *Sambucus* species as trees/shrubs. These alternatives (Table 1 and Fig. 3) yielded a similarly strong historical correlation ($P = 0.00049$), as did the exclusion of these contrasts altogether ($P = 0.00195$).

On the basis of our trees and broader phylogenetic studies of angiosperms [reviewed in (*28*); see also (*29*)], the likely direction of evolution of plant habit was from trees/shrubs to the herbaceous condition in Apiales, Dipsacales, and Primulales, and with less certainly in Moraceae/Urticaceae. The palms (Arecaceae) within the Commelinidae present the one clear instance in our sample of the evolution of trees/shrubs from herbaceous ancestors (*30*). From our comparisons and a broader analysis of monocotyledons (*11*), the shift to the tree/shrub habit in palms was associated with a marked decrease in the rate of molecular evolution (palms evolve 2.7 times as slow as their sister commelinids), as predicted by the hypothesis that generation time drives the rate of molecular evolution.

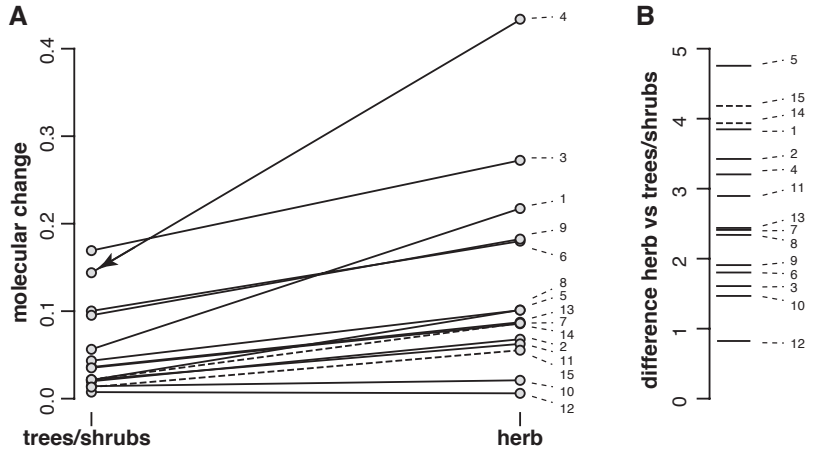

Fig. 3. Branch-length contrasts for trees/shrubs versus herbs. (**A**) Lines are drawn between the accumulated average molecular branch lengths for each tree/shrub clade and its sister herbaceous clade (numbers correspond to those in Table 1). All evolutionary shifts were inferred to be from trees/shrubs to herbs except for the evolution of palms within monocotyledons (arrowhead in contrast 4). Contrasts 1 to 13 were used in an initial sign test ($P = 0.00342$). Alternative contrasts within the Dipsacales (14 and 15) are marked by dotted lines and were substituted for 11 to 13 in one test ($P = 0.00049$); contrasts 11 to 15 were omitted in a third test ($P = 0.00195$). (**B**) Magnitude of change between each tree/shrub clade and its herbaceous sister clades; values above 1 show higher rates of molecular evolution in herbs than in trees/shrubs.

Table 1. Branch length contrasts 1 to 13 derive from the trees in Fig. 1 [see (*13*) for more exact locations of the nodes in question]. Plants in the first taxon in each pair of representative taxa are trees/shrubs; plants in the second are herbs. Within Dipsacales, we explored alternative contrasts, substituting contrasts 14 and 15 for 11 to 13 in one test and omitting contrasts 11 to 15 in another.

Major clade		Representative taxa	Trees/shrubs	Herbs	Difference
Apiales	1	*Astrotricha–Hydrocotyle*	0.0564	0.2173	3.8538
	2	*Aralia–Panax*	0.0198	0.0679	3.4224
	3	Pittosporaceae–Apiaceae	0.1692	0.2724	1.6097
Commelinidae	4	Arecales–remaining Commelinidae	0.1363	0.4350	3.1915
Moraceae–Urticaceae	5	*Brosimum–Dorstenia*	0.0213	0.1013	4.7527
	6	Moraceae–Urticaceae	0.1002	0.1800	1.7967
	7	*Cecropia/Coussapoa–Boehmeria*	0.0361	0.0873	2.4169
Primulales	8	*Ardisia*–sister Myrsinaceae	0.0433	0.1011	2.3330
	9	Theophrastaceae–Myrsinaceae/Primulaceae	0.0953	0.1824	1.9138
Dipsacales	10	*Symphoricarpos–Triosteum*	0.0142	0.0210	1.4747
	11	Linnaeeae–Morinaceae	0.0217	0.0626	2.8912
	12	Woody *Sambucus*–herbaceous *Sambucus*	0.0075	0.0061	0.8130
	13	*Viburnum–Adoxa*	0.0352	0.0856	2.4304
	14	Linnaeeae–Morinaceae/Dipsacaceae/Valerianaceae	0.0219	0.0863	3.9432
	15	"Woody" *Sambucus–Adoxa*	0.0133	0.0554	4.1783

Differences in rates of evolution associated with generation time may be reflected most clearly in synonymous substitutions within coding sequences (*31*). We analyzed 1208 commelinid *rbcL* sequences, pruning species lacking an *rbcL* sequence in GenBank from our Commelinidae phylogeny and using RAxML to estimate branch lengths for several partitions of the data (Table 2) (*13*). As expected, estimated amino acid branch lengths showed the least difference in rate between life history classes (2.1 times as fast as in herbs), with first and second nucleotide positions being next smallest (3.2 times as fast). The rate difference in the full Commelinidae data set (all species, all genes) fell between these two values (2.7 times as fast in herbs). The third positions showed the greatest difference in rate (4.98 times as fast in herbs). These findings are similar to those based on a much smaller sample of *rbcL* sequences from grasses and palms (*11*).

Our findings highlight the need for the methods used to date phylogenies to address the form of clade-dependent heterogeneity documented here. A rate of nucleotide substitution obtained from an herbaceous group cannot be used to calibrate a clade of trees/shrubs, or vice versa, without confounding age estimates. Likewise, relaxed clock methods [e.g., (*32*)] are likely to estimate that slowly evolving groups are younger, and that rapidly evolving groups are older, than their true ages. It may be possible to avoid mixing clades with very different life histories in designing dating studies. Otherwise, as we have attempted here, the use of multiple calibration points spanning clades that differ in life history may help alleviate this problem. Also, as shown here for Commelinidae, the use of amino acid sequences (or the removal of third sites) may be useful. Bayesian models that do not assume an autocorrelated rate of molecular evolution [e.g., (*33*)] are promising, but current methods are incapable of analyzing large data sets.

We hope that our results will also focus new attention on the extent to which molecular and morphological evolution are coupled [see (*34*, *35*)]. Are rates of morphological evolution also slower in trees/shrubs than in herbs [e.g., (*36*)]? Until this question is addressed, we urge caution in assuming that morphological change scales with molecular change and in using molecular branch lengths alone to assess "feature diversity" and design conservation strategies [e.g., (*37*)]. A related issue is the likely success of "barcoding" methods

Table 2. Branch length contrast estimates for different partitions of *rbcL* sequences from Commelinidae.

Estimate data	Palms	Rest of Commelinidae	Difference
Third sites	0.0369	0.1842	4.9872
First, second, and third sites	0.0331	0.1284	3.8808
First and second sites	0.0313	0.1007	3.2180
Amino acids	0.0464	0.0993	2.1379
All genes/species	0.1363	0.4350	3.1915

for identifying plant species from short DNA sequences [reviewed in (*33*)]. We predict that the chloroplast genes proposed as universal barcode loci will be most successful in resolving herbaceous species and may be incapable of confidently distinguishing closely related woody species.

Finally, our studies underscore the need for better and more accessible information on the underlying drivers of rates of molecular evolution. In addition to data on generation times, we need better knowledge of effective population sizes. Past analyses (e.g., in mammals) have assumed that larger, longer-lived organisms have smaller population sizes, but this may be reversed in plants, where tropical trees often appear to have large population sizes (*31*). Our analyses imply that somatic mutation has not counteracted the influence of generation time on rates of evolution, but more data are needed on the rate and fate of such mutations (*8*). In any event, our analyses demonstrate a general pattern that must now be taken into account in evolutionary studies and whose existence demands the elaboration of a cohesive causal explanation.

References and Notes

1. A. P. Martin, S. R. Palumbi, *Proc. Natl. Acad. Sci. U.S.A.* **90**, 4087 (1993).
2. A. O. Mooers, P. H. Harvey, *Mol. Phylogenet. Evol.* **3**, 344 (1994).
3. L. Bromham, A. Rambaut, P. H. Harvey, *J. Mol. Evol.* **43**, 610 (1996).
4. J. F. Gillooly, A. P. Allen, G. B. West, J. H. Brown, *Proc. Natl. Acad. Sci. U.S.A.* **102**, 140 (2005).
5. K. Andreasen, B. G. Baldwin, *Mol. Biol. Evol.* **18**, 936 (2001).
6. J. Laroche, P. Li, L. Maggia, J. Bousquet, *Proc. Natl. Acad. Sci. U.S.A.* **94**, 5722 (1997).
7. K. M. Kay, J. B. Whittall, S. A. Hodges, *BMC Evol. Biol.* **6**, 36 (2006).
8. E. J. Klekowski, P. J. Godfrey, *Nature* **340**, 389 (1989).
9. C. A. Whittle, M. O. Johnston, *J. Mol. Evol.* **56**, 223 (2003).
10. K. Andreasen, *Conserv. Genet.* **6**, 399 (2005).
11. B. S. Gaut, B. R. Morton, B. C. McCaig, M. T. Clegg, *Proc. Natl. Acad. Sci. U.S.A.* **93**, 10274 (1996).
12. R. C. Edgar, *Nucleic Acids Res.* **32**, 1792 (2004).
13. Materials and methods are available as supporting material on *Science* Online.
14. M. M. McMahon, M. J. Sanderson, *Syst. Biol.* **55**, 818 (2006).
15. A. Stamatakis, *Bioinformatics* **22**, 2688 (2006).
16. M. J. Sanderson, *Mol. Biol. Evol.* **14**, 1218 (1997).
17. T. Britton, C. L. Anderson, D. Jacquet, S. Lundqvist, K. Bremer, *Syst. Biol.* **56**, 741 (2007).
18. K. Bremer, E. M. Friis, B. Bremer, *Syst. Biol.* **53**, 496 (2004).
19. C. D. Bell, M. J. Donoghue, *Am. J. Bot.* **92**, 284 (2005).
20. N. J. C. Zerega, W. L. Clement, S. L. Datwyler, G. D. Weiblen, *Mol. Phylogenet. Evol.* **37**, 402 (2005).
21. T. Janssen, K. Bremer, *Bot. J. Linn. Soc.* **146**, 385 (2004).
22. J. Bousquet, S. H. Strauss, A. H. Doerksen, R. A. Price, *Proc. Natl. Acad. Sci. U.S.A.* **89**, 7844 (1992).
23. R. J. Petit, A. Hampe, *Annu. Rev. Ecol. Evol. Syst.* **37**, 187 (2006).
24. M. Verdú, *Evol. Int. J. Org. Evol.* **56**, 1352 (2002).
25. P. Hietz, J. Ausserer, G. Schindler, *J. Trop. Ecol.* **18**, 177 (2002).
26. S. S. Renner, R. E. Ricklefs, *Evol. Int. J. Org. Evol.* **82**, 596 (1995).
27. T. J. Davies, V. Savolainen, *Evol. Int. J. Org. Evol.* **60**, 476 (2006).
28. D. E. Soltis, P. S. Soltis, P. K. Endress, M. W. Chase, *Phylogeny and Evolution of Angiosperms* (Sinaur Associates, Sunderland, MA, 2005).
29. P. F. Stevens, Angiosperm Phylogeny Website, www.mobot.org/MOBOT/research/APweb (2008).
30. M. W. Chase *et al.*, *Aliso* **22**, 63 (2006).
31. T. Ohta, *Proc. Natl. Acad. Sci. U.S.A.* **90**, 10676 (1993).
32. M. J. Sanderson, *Mol. Biol. Evol.* **19**, 101 (2002).
33. A. J. Drummond, S. Y. W. Ho, M. J. Phillips, A. Rambaut, *PLoS Biol.* **4**, e88 (2006).
34. R. Lahaye, *Proc. Natl. Acad. Sci. U.S.A.* **105**, 2923 (2008).
35. T. G. Barraclough, V. Savolainen, *Evol. Int. J. Org. Evol.* **55**, 677 (2001).
36. E. W. Sinnott, *Am. Nat.* **50**, 466 (1916).
37. F. Forest *et al.*, *Nature* **445**, 757 (2007).

38. We thank D. Tank, J. Beaulieu, S. Stearns, D. Weinreich, C. Dunn, and E. Edwards for helpful discussions. Funded by the NSF through the Cyberinfrastructure for Phylogenetic Research (EF-0331654) and the angiosperm Assembling the Tree of Life (EF-0431258) projects.

Supporting Online Material

www.sciencemag.org/cgi/content/full/322/5898/86/DC1
Materials and Methods
Fig. S1 to S8
Tables S1 and S2
References

14 July 2008; accepted 5 September 2008
10.1126/science.1163197

Chemokine Signaling Controls Endodermal Migration During Zebrafish Gastrulation

Sreelaja Nair and Thomas F. Schilling*

Directed cell movements during gastrulation establish the germ layers of the vertebrate embryo and coordinate their contributions to different tissues and organs. Anterior migration of the mesoderm and endoderm has largely been interpreted to result from epiboly and convergent-extension movements that drive body elongation. We show that the chemokine Cxcl12b and its receptor Cxcr4a restrict anterior migration of the endoderm during zebrafish gastrulation, thereby coordinating its movements with those of the mesoderm. Depletion of either gene product causes disruption of integrin-dependent cell adhesion, resulting in separation of the endoderm from the mesoderm; the endoderm then migrates farther anteriorly than it normally would, resulting in bilateral duplication of endodermal organs. This process may have relevance to human gastrointestinal bifurcations and other organ defects.

A crucial feature of vertebrate embryogenesis is the coordinated morphogenesis of germ layers (endoderm, mesoderm, and ectoderm) during gastrulation (*1*). Interactions between the endoderm and mesoderm specify organ locations and symmetries (*2*). Defects in the endoderm alter the morphogenesis of mesodermal organs (e.g., heart, kidneys, and blood), whereas mesodermal defects disrupt the locations of the liver and pancreas (*2*–*5*). Morphogenesis is regulated by Wnt (*6*) and Nodal signaling (*7*) when cells are intermingled in a bipotential "mesendoderm" (*8*). However, relatively little is known about germ layer–specific pathways that establish organ rudiments. In zebrafish, mesendodermal organ progenitors involute at the gastrula margin (blastopore) and move anteriorly toward the animal pole (future head) while converging toward the midline (convergent extension).

The chemokine receptor CXCR4 controls directional migration in many contexts and is expressed in the endoderm. It is up-regulated by the endodermal determinants Mixer and Sox17β (*9*–*13*) and is required for gastrointestinal vascularization (*14*). Of the two closely related zebrafish Cxcr4s, Cxcr4b regulates the migration of many cell types (*12*, *15*–*18*), but no roles have been reported for Cxcr4a during embryogenesis.

Zebrafish embryos deficient in Cxcr4a or Cxcl12b, generated by injection with antisense morpholino oligonucleotides (MO), appeared morphologically normal (Fig. 1, A to C, and fig. S1). However, analysis of *Tg(gutGFP)*^{s854} transgenic embryos in which the entire gut fluoresces [(*19*); GFP, green fluorescent protein] revealed duplications of endodermal organs at 56 hours post-fertilization (hpf) (Fig. 1, D to F, and fig. S2), including the pancreas (normally on the right; fig. S3, A to F) and liver (normally

Department of Developmental and Cell Biology, University of California, Irvine, CA 92697, USA.

*To whom correspondence should be addressed. E-mail: tschilli@uci.edu

Chemokine Signaling Controls Endodermal Migration During Zebrafish Gastrulation

Sreelaja Nair, *et al.*

Science **322**, 89 (2008);
DOI: 10.1126/science.1160038

Science (print ISSN 0036-8075; online ISSN 1095-9203) is published weekly, except the last week in December, by the American Association for the Advancement of Science, 1200 New York Avenue NW, Washington, DC 20005.

Table 2. Branch length contrast estimates for different partitions of *rbcL* sequences from Commelinidae.

Estimate data	Palms	Rest of Commelinidae	Difference
Third sites	0.0369	0.1842	4.9872
First, second, and third sites	0.0331	0.1284	3.8808
First and second sites	0.0313	0.1007	3.2180
Amino acids	0.0464	0.0993	2.1379
All genes/species	0.1363	0.4350	3.1915

for identifying plant species from short DNA sequences [reviewed in (*33*)]. We predict that the chloroplast genes proposed as universal barcode loci will be most successful in resolving herbaceous species and may be incapable of confidently distinguishing closely related woody species.

Finally, our studies underscore the need for better and more accessible information on the underlying drivers of rates of molecular evolution. In addition to data on generation times, we need better knowledge of effective population sizes. Past analyses (e.g., in mammals) have assumed that larger, longer-lived organisms have smaller population sizes, but this may be reversed in plants, where tropical trees often appear to have large population sizes (*31*). Our analyses imply that somatic mutation has not counteracted the influence of generation time on rates of evolution, but more data are needed on the rate and fate of such mutations (*8*). In any event, our analyses demonstrate a general pattern that must now be taken into account in evolutionary studies and whose existence demands the elaboration of a cohesive causal explanation.

References and Notes

1. A. P. Martin, S. R. Palumbi, *Proc. Natl. Acad. Sci. U.S.A.* **90**, 4087 (1993).
2. A. O. Mooers, P. H. Harvey, *Mol. Phylogenet. Evol.* **3**, 344 (1994).
3. L. Bromham, A. Rambaut, P. H. Harvey, *J. Mol. Evol.* **43**, 610 (1996).
4. J. F. Gillooly, A. P. Allen, G. B. West, J. H. Brown, *Proc. Natl. Acad. Sci. U.S.A.* **102**, 140 (2005).
5. K. Andreasen, B. G. Baldwin, *Mol. Biol. Evol.* **18**, 936 (2001).
6. J. Laroche, P. Li, L. Maggia, J. Bousquet, *Proc. Natl. Acad. Sci. U.S.A.* **94**, 5722 (1997).
7. K. M. Kay, J. B. Whittall, S. A. Hodges, *BMC Evol. Biol.* **6**, 36 (2006).
8. E. J. Klekowski, P. J. Godfrey, *Nature* **340**, 389 (1989).
9. C. A. Whittle, M. O. Johnston, *J. Mol. Evol.* **56**, 223 (2003).
10. K. Andreasen, *Conserv. Genet.* **6**, 399 (2005).
11. B. S. Gaut, B. R. Morton, B. C. McCaig, M. T. Clegg, *Proc. Natl. Acad. Sci. U.S.A.* **93**, 10274 (1996).
12. R. C. Edgar, *Nucleic Acids Res.* **32**, 1792 (2004).
13. Materials and methods are available as supporting material on *Science* Online.
14. M. M. McMahon, M. J. Sanderson, *Syst. Biol.* **55**, 818 (2006).
15. A. Stamatakis, *Bioinformatics* **22**, 2688 (2006).
16. M. J. Sanderson, *Mol. Biol. Evol.* **14**, 1218 (1997).
17. T. Britton, C. L. Anderson, D. Jacquet, S. Lundqvist, K. Bremer, *Syst. Biol.* **56**, 741 (2007).
18. K. Bremer, E. M. Friis, B. Bremer, *Syst. Biol.* **53**, 496 (2004).
19. C. D. Bell, M. J. Donoghue, *Am. J. Bot.* **92**, 284 (2005).
20. N. J. C. Zerega, W. L. Clement, S. L. Datwyler, G. D. Weiblen, *Mol. Phylogenet. Evol.* **37**, 402 (2005).
21. T. Janssen, K. Bremer, *Bot. J. Linn. Soc.* **146**, 385 (2004).
22. J. Bousquet, S. H. Strauss, A. H. Doerksen, R. A. Price, *Proc. Natl. Acad. Sci. U.S.A.* **89**, 7844 (1992).
23. R. J. Petit, A. Hampe, *Annu. Rev. Ecol. Evol. Syst.* **37**, 187 (2006).
24. M. Verdú, *Evol. Int. J. Org. Evol.* **56**, 1352 (2002).
25. P. Hietz, J. Ausserer, G. Schindler, *J. Trop. Ecol.* **18**, 177 (2002).
26. S. S. Renner, R. E. Ricklefs, *Evol. Int. J. Org. Evol.* **82**, 596 (1995).
27. T. J. Davies, V. Savolainen, *Evol. Int. J. Org. Evol.* **60**, 476 (2006).
28. D. E. Soltis, P. S. Soltis, P. K. Endress, M. W. Chase, *Phylogeny and Evolution of Angiosperms* (Sinaur Associates, Sunderland, MA, 2005).
29. P. F. Stevens, Angiosperm Phylogeny Website, www.mobot.org/MOBOT/research/APweb (2008).
30. M. W. Chase *et al.*, *Aliso* **22**, 63 (2006).
31. T. Ohta, *Proc. Natl. Acad. Sci. U.S.A.* **90**, 10676 (1993).
32. M. J. Sanderson, *Mol. Biol. Evol.* **19**, 101 (2002).
33. A. J. Drummond, S. Y. W. Ho, M. J. Phillips, A. Rambaut, *PLoS Biol.* **4**, e88 (2006).
34. R. Lahaye, *Proc. Natl. Acad. Sci. U.S.A.* **105**, 2923 (2008).
35. T. G. Barraclough, V. Savolainen, *Evol. Int. J. Org. Evol.* **55**, 677 (2001).
36. E. W. Sinnott, *Am. Nat.* **50**, 466 (1916).
37. F. Forest *et al.*, *Nature* **445**, 757 (2007).

38. We thank D. Tank, J. Beaulieu, S. Stearns, D. Weinreich, C. Dunn, and E. Edwards for helpful discussions. Funded by the NSF through the Cyberinfrastructure for Phylogenetic Research (EF-0331654) and the angiosperm Assembling the Tree of Life (EF-0431258) projects.

Supporting Online Material

www.sciencemag.org/cgi/content/full/322/5898/86/DC1
Materials and Methods
Fig. S1 to S8
Tables S1 and S2
References

14 July 2008; accepted 5 September 2008
10.1126/science.1163197

Chemokine Signaling Controls Endodermal Migration During Zebrafish Gastrulation

Sreelaja Nair and Thomas F. Schilling*

Directed cell movements during gastrulation establish the germ layers of the vertebrate embryo and coordinate their contributions to different tissues and organs. Anterior migration of the mesoderm and endoderm has largely been interpreted to result from epiboly and convergent-extension movements that drive body elongation. We show that the chemokine Cxcl12b and its receptor Cxcr4a restrict anterior migration of the endoderm during zebrafish gastrulation, thereby coordinating its movements with those of the mesoderm. Depletion of either gene product causes disruption of integrin-dependent cell adhesion, resulting in separation of the endoderm from the mesoderm; the endoderm then migrates farther anteriorly than it normally would, resulting in bilateral duplication of endodermal organs. This process may have relevance to human gastrointestinal bifurcations and other organ defects.

A crucial feature of vertebrate embryogenesis is the coordinated morphogenesis of germ layers (endoderm, mesoderm, and ectoderm) during gastrulation (*1*). Interactions between the endoderm and mesoderm specify organ locations and symmetries (*2*). Defects in the endoderm alter the morphogenesis of mesodermal organs (e.g., heart, kidneys, and blood), whereas mesodermal defects disrupt the locations of the liver and pancreas (*2*–*5*). Morphogenesis is regulated by Wnt (*6*) and Nodal signaling (*7*) when cells are intermingled in a bipotential "mesendoderm" (*8*). However, relatively little is known about germ layer–specific pathways that establish organ rudiments. In zebrafish, mesendodermal organ progenitors involute at the gastrula margin (blastopore) and move anteriorly toward the animal pole (future head) while converging toward the midline (convergent extension).

The chemokine receptor CXCR4 controls directional migration in many contexts and is expressed in the endoderm. It is up-regulated by the endodermal determinants Mixer and Sox17β (*9*–*13*) and is required for gastrointestinal vascularization (*14*). Of the two closely related zebrafish Cxcr4s, Cxcr4b regulates the migration of many cell types (*12*, *15*–*18*), but no roles have been reported for Cxcr4a during embryogenesis.

Zebrafish embryos deficient in Cxcr4a or Cxcl12b, generated by injection with antisense morpholino oligonucleotides (MO), appeared morphologically normal (Fig. 1, A to C, and fig. S1). However, analysis of *Tg(gutGFP)*^{s854} transgenic embryos in which the entire gut fluoresces [(*19*); GFP, green fluorescent protein] revealed duplications of endodermal organs at 56 hours post-fertilization (hpf) (Fig. 1, D to F, and fig. S2), including the pancreas (normally on the right; fig. S3, A to F) and liver (normally

Department of Developmental and Cell Biology, University of California, Irvine, CA 92697, USA.

*To whom correspondence should be addressed. E-mail: tschilli@uci.edu

on the left; fig. S3, A to C and G to I), a phenotype we call "viscera bifida" (*cxcl12b*MO, 78%, *n* = 23; *cxcr4a*MO, 68%, *n* = 37). At 26 hpf, the intestine was also split bilaterally (Fig. 1, G to I; *12b*MO, 78%, *n* = 18; *4a*MO, 76%, *n* = 34), as revealed by *foxa2* expression, whereas the floor plate of the neural tube was unaffected (Fig. 1, H and I). No defects were detected in the mesoderm or ectoderm (fig. S3, J to O, and fig. S4).

During gastrulation, *cxcl12b* is expressed in mesoderm (Fig. 2, A, C, and E, and fig. S5, A and B), whereas *cxcr4a* is expressed in endoderm (Fig. 2, B, D, and F, and fig. S5, E and F), and both require Nodal signaling (fig. S5, C, D, G, and H), suggesting that chemokine signaling regulates endoderm-mesoderm interactions. At the onset of gastrulation (6 hpf), *sox32*$^{+}$ endodermal cells appeared normal in number but were displaced slightly anteriorly in *cxc12b* (83%, *n* = 82) and *cxcr4a* (74%, *n* = 62) morphants (Fig. 1, J to L). Displacement became more pronounced by 8 hpf, as revealed by *foxa2* expression (Fig. 1, M to O; *12b*MO, 88%, *n* = 34; *4a*MO, 85%, *n* = 55). In controls, the trailing edge of *foxa2*$^{+}$ cells was 50 to 100 μm from the margin, whereas in morphants this gap was larger by a factor of >3 (178 to 275 μm dorsally, 170 to 310 μm laterally, 186 to 340 μm ventrally) (Fig. 1P). The leading edge was also displaced up to 100 μm, particularly ventrally. Displacement was not due to precocious endodermal internalization (fig. S6), which suggests a later requirement for chemokine signaling in restricting endodermal movements anteriorly, toward the animal pole. We refer to this as endodermal tethering.

Despite displacement of the endoderm, the mesoderm was unaffected, as assayed by *no tail* (*ntl*) at 6 hpf (Fig. 1, J to L), *tbx16* in paraxial mesoderm at 8 hpf (fig. S4, A to C), and *hand2* in lateral plate mesoderm at 11 hpf (LPM; fig. S4, D to F). Our results reveal an early distinction between endodermal and mesodermal cell behaviors before they separate from the mesendoderm, thereby implicating the Cxcl12b-Cxcr4a system as among the earliest known signals in endodermal morphogenesis.

If Cxcl12b in mesoderm binds Cxcr4a in endodermal cells to restrict (tether) their movements, Cxcr4a should be required cell-autonomously in the endoderm. To test this, we transplanted endoderm-targeted *cxcr4a* morphant cells into wild-type hosts (Fig. 2, G to L). As an internal control, these cells were cotransplanted with wild-type endoderm into the same locations (Fig. 2, G, I, and K) in unlabeled hosts at 4 hpf, and cell distributions were compared 4 hours later (Fig. 2, H, J, and L). *cxcr4a* morphant endodermal cells moved, on average, 200 μm farther anteriorly than did controls (Fig. 2M), demonstrating a cell-autonomous requirement.

How does Cxcl2b-Cxcr4a signaling regulate endoderm migration? Because *cxcl12b* is maternally deposited and localized to the mesoderm, from which endodermal cells separate during gastrulation, it seems unlikely to act as a chemoattractant here. However, increasing evidence suggests that chemokine signaling modulates ex-

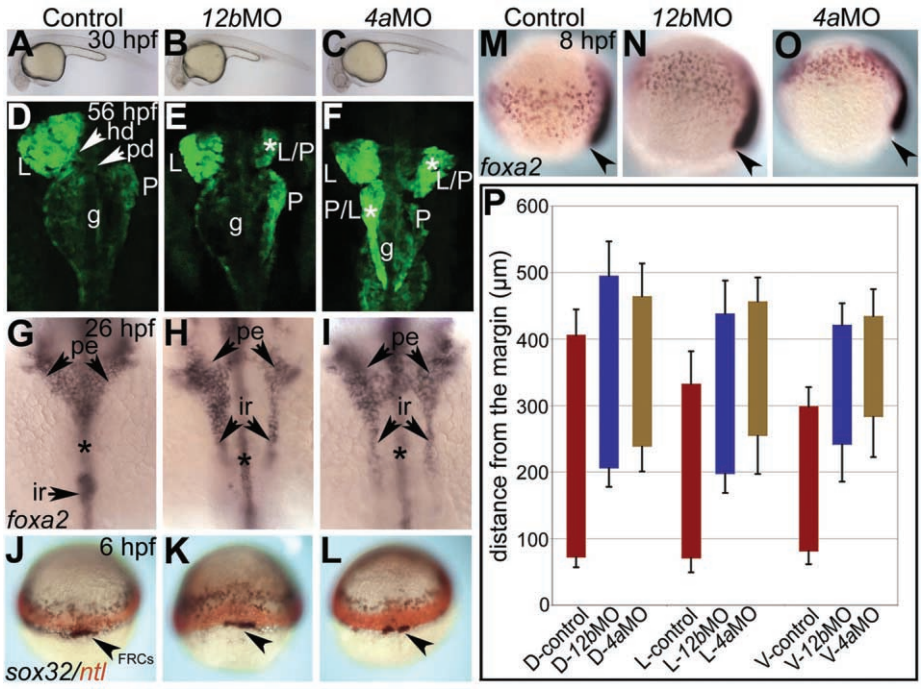

Fig. 1. *cxcl12b* and *cxcr4a* are required for endodermal morphogenesis. (**A** to **C**) Bright-field images, live embryos, 30 hpf; (A) control, (B) *cxcl12b* morphant, (C) *cxcr4a* morphant. (**D** to **L**) Dorsal views, anterior to the top. [(D) to (F)] *Tg(gutGFP)*^{s854}, 56 hpf, reveals duplicated liver (L) and pancreas (P) (asterisks) in confocal projections of *cxcl12b* (E) and *cxcr4a* (F) morphants. g, gut; hd, hepatic duct; pd, pancreatic duct. [(G) to (I)] *foxa2*, 26 hpf; the intestinal rod (ir) bifurcates, but not the floor plate (asterisks); pe, pharyngeal endoderm. [(J) to (L)] Double in situ hybridizations for *sox32* (endoderm, blue) and *ntl* (mesoderm, red), 6 hpf; *sox32*$^{+}$ cells, but not *ntl*$^{+}$ or *sox32*$^{+}$ forerunner cells (FRCs, arrowheads), move anteriorly (toward the animal pole and away from the margin). (**M** to **O**) *foxa2*, 8 hpf; lateral view. Morphant endoderm moves anteriorly (arrowheads indicate margin). (**P**) Quantitation of displacement of *foxa2*$^{+}$ cells at dorsal (D), lateral (L, 90° from D), and ventral (V, 180° from D) positions, 8 hpf. Controls, red bars; *cxcl12b* morphants, blue bars; *cxcr4a* morphants, gold bars.

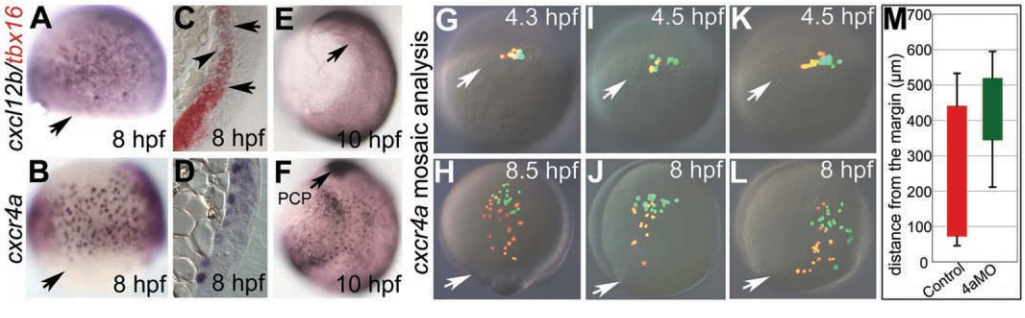

Fig. 2. Mesoderm expresses *cxcl12b* and endoderm requires *cxcr4a* cell-autonomously. (**A** to **F**) Whole-mount in situ hybridizations, dorsal right [except (C) and (D), transverse sections of gastrulae]. (A) *cxcl12b* in mesoderm, 8 hpf; arrow indicates margin. (B) *cxcr4a* in endoderm. (C) Double in situ hybridizations for *cxcl12b* (blue) and *tbx16* (red), 8 hpf, confirms coexpression in region indicated by arrows, but not in endoderm (arrowhead). (D) Endodermal *cxcr4a* expression. (E) *cxcl12b* in lateral mesoderm (arrow), 10 hpf. (F) *cxcr4a* in endoderm and prechordal plate (PCP, arrow), 10 hpf. (**G** to **L**) *cxcr4a* morphant (green; fluorescein) and control cells (red; rhodamine) grafted into unlabeled hosts, lateral views at 4.3 to 4.5 hpf [(G), (I), (K)] and 8 to 8.5 hpf [(H), (J), (L)]. (**M**) Average leading and trailing positions of control (red bar) and cxcr*4a* morphant (green bar) transplanted cells (*n* = 7).

tracellular matrix (ECM) proteins [e.g., fibronectin (FN), laminin] and their receptors (integrins), which are required for gastrulation (*20*–*24*). FN in ECM binds secreted CXCL12 and presents it to CXCR4, causing its redistribution to leading edges of migrating cells (*25*). Of several *fn*s in zebrafish, *fn1* is expressed by mesoderm during gastrulation (*26*). Thus, FN in the mesodermal ECM might bind and present Cxcl12b to Cxcr4a-expressing endoderm, sensitizing it to chemokines. CXCR4 activation by CXCL12 also enhances integrin-dependent adhesion of renal carcinoma and small-cell lung cancer cells to FN (*22*, *27*). Thus, we considered both FNs and integrins as potential downstream effectors during endoderm migration.

If this is correct, interfering with FN-integrin interactions should also disrupt endoderm migration. To test this, we treated gastrulating zebrafish embryos with RGD peptides (containing the tripeptide motif Arg-Gly-Asp), which bind integrins and block signaling (*28*). This caused anterior displacement of the endoderm at 8 hpf, similar to *cxcl12b* and *cxcr4a* morphants (Fig. 3, A and B; 40%, $n = 52$), and delayed convergence of endoderm toward the midline (fig. S7, A to F; 55%, $n = 20$). In contrast, convergence of LPM, which is required for gut morphogenesis (*5*), was unaffected (fig. S7, G and H), as in morphants (fig. S4, D to F). RGD peptide treatments of transgenic *Tg(gutGFP)*^{s854} embryos caused viscera bifida (Fig. 3, C and D; 42%, $n = 65$) or situs inversus (fig. S7, I and J; 14%, $n = 64$), even when applied at mid- to late gastrula stages (viscera bifida, 32%, $n = 22$; situs inversus, 18%, $n = 22$), indicating that integrin-dependent interactions are essential throughout gastrulation.

These results argue against the presentation of FN-bound Cxcl12b to Cxcr4a and instead suggest that chemokines control ECM-integrin–dependent adhesive interactions of the endoderm. To test this, we conducted in vitro cell adhesion assays to determine the ability of *cxcr4a* morphant endodermal cells to adhere to FN-coated surfaces. Relative to controls, the number of morphant cells that remained attached was reduced by one-third; adhesion was rescued by coinjection of *integrin beta 1b* (*itgb1b*) mRNA (Fig. 3E), which confirmed that chemokine signaling directly regulates adhesion of endoderm to FN.

Molecular interactions between CXCL12 and CXCR4 up-regulate levels of integrin α and β mRNAs in renal carcinoma cells to enhance their adhesion to FN (*22*). Thus, Cxcl12b-Cxcr4a signaling in the endoderm may similarly regulate integrin levels. Of the integrin βs expressed in zebrafish, *itgb1b* is expressed maternally and ubiquitously during gastrulation (*29*). Quantitative real-time polymerase chain reaction (qPCR) revealed a reduction in *itgb1b* mRNA levels in whole embryos and in *cxcr4a*MO endoderm (fig. S7K); this finding suggests that the link between chemokines and integrins is, at least in part, a transcriptional one.

If endodermal defects in *cxcl12b-cxcr4a* morphants reflect disruption of ECM-integrin signaling, injecting *itgb1b* mRNA into morphants should rescue these defects. *itgb1b* mRNA injected into *cxcl12b* and *cxcr4a* morphants rescued intestinal bifurcations in a dose-dependent manner (Fig. 3, F to K), either unilaterally (50 to 75 pg; Fig. 3, I and J) or completely (100 pg; Fig. 3K and table S1). Taken together, our results suggest that Cxcl12b-Cxcr4a interactions promote integrin-mediated adhesion to tether the endoderm to the mesoderm during gastrulation.

Cell adhesion is a key regulator of gastrulation movements. E-cadherin mediates epiboly and anterior migration of prechordal mesoderm (*30*), integrin-αB allows mesendodermal cells to

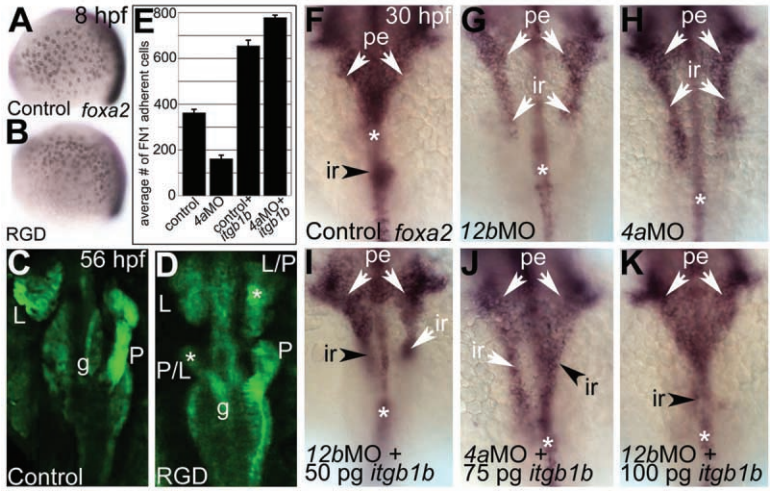

Fig. 3. FN-integrin–mediated cell adhesion restricts anterior migration of endoderm. (**A** and **B**) Whole-mount in situ hybridizations for *foxa2*, 8 hpf; lateral view, dorsal (right). *foxa2*$^{+}$ cells move anteriorly in RGD-treated embryos. (**C** and **D**) *Tg(gutGFP)*^{s854}, 56 hpf; liver (L) and pancreas (P) duplications (asterisks) in RGD-treated embryos. (**E**) Reduced adhesion of *cxcr4a* morphant endoderm to a FN1-coated surface, and rescue by *itgb1b* overexpression ($P = 0.003$ and 0.0003, respectively). (**F** to **K**) *foxa2*, 30 hpf; dorsal views, anterior to the top, showing expression in pharyngeal endoderm (pe), floor plate (asterisk), and intestinal rod (ir, arrowhead), which bifurcates in morphants (white arrows). Injection of 50 pg (I), 75 pg (J), and 100 pg (K) of *itgb1b* mRNA rescues the intestine partially [arrowheads, (I) and (J)] or completely [arrowhead, (K)].

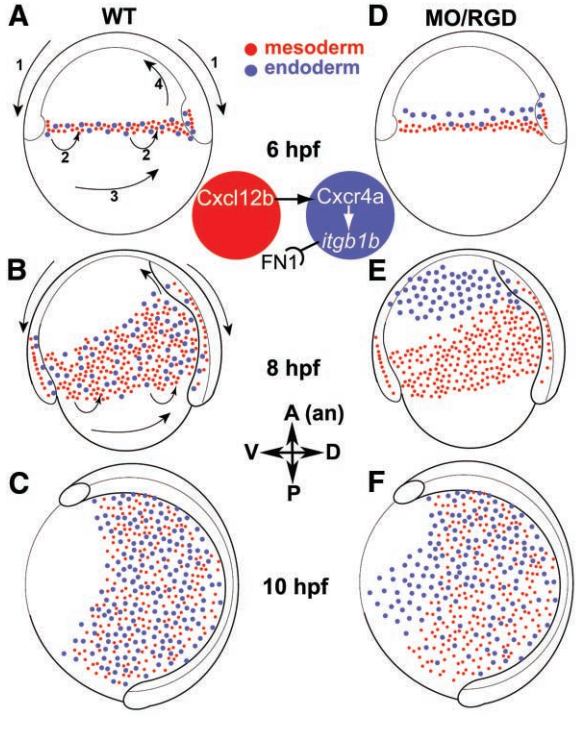

Fig. 4. A chemokine-mediated tether model for endodermal morphogenesis. Diagrams of a wild-type (WT) gastrula at 6, 8, and 10 hpf, and *cxcl12b*/*cxcr4a* morphants or RGD-treated (MO/RGD) embryos, lateral view, animal pole (top), dorsal (right). Endoderm, blue; mesoderm, red. Arrows: epiboly (1), involution (2), convergent extension (3), and anterior migration (4). (**A**) At onset of gastrulation, *cxcl12b*$^{+}$ mesoderm tethers *cxcr4a*$^{+}$ endoderm, which coordinates mesendoderm migration. (**B** and **C**) By the end of gastrulation, midline convergence clears ventral cells. (**D**) In morphants or RGD-treated embryos, endoderm released from this tether migrates anteriorly. (**E** and **F**) Displaced endoderm in anterior and ventral positions does not reach the midline [ectopic ventral blue dots in (F)], leading to organ duplication. Enlarged cells at center depict a molecular model in which Cxcl12b from mesoderm signals through Cxcr4a in endoderm to up-regulate *itgb1b* expression, which binds FN1 in the mesodermal extracellular matrix.

crawl on FN along the blastocoel roof (*31*), and *fn1* controls migration of myocardial progenitors toward the midline (*26*, *32*)—a process that also requires another chemokine, *apelin* (*33*, *34*). However, gut defects have generally been interpreted as secondary to defects in mesoderm migration. In contrast, our studies reveal an earlier requirement for ECM-integrin interactions directly in endoderm migration.

We have shown that endoderm migration toward the anterior is genetically separable from other gastrulation movements (*35*). We propose that chemokine-dependent expression of integrin tethers the endoderm to the mesoderm, and that loss of this tether releases the endoderm to move anteriorly (Fig. 4); a secondary result is viscera bifida, because endodermal cells on either side [presumably containing organ progenitors (*8*)] have farther to converge dorsally and do not reach the midline in time to fuse. Viscera bifida–like syndromes in humans, including intestinal cysts and ectopic pancreatic or liver tissue, are relatively common and are not associated with spina bifida (ectoderm) (*36*), and defects in the CXCL12-CXCR4 signaling pathway may be an underlying cause.

For zebrafish endodermal cells, regulation of migration by controlling adhesion reconciles the recent observation that involuted endodermal cells initially move via a "random walk" rather than the directed migration displayed by the mesoderm (*37*). Classically, chemokines are cytokines that induce chemotaxis in responding cells; CXCL12-CXCR4 interactions control homing of hematopoietic stem cells to the bone marrow, as well as migration of germ cells, neuronal progenitors, and several metastatic cancers (*15*–*18*, *27*). In some of these cases, however, there is evidence for a system more like the tether described here, where receptor-expressing cells are confined to a territory defined by ligand-expressing cells. Thus, chemokine-dependent changes in adhesion to the ECM may influence cell migration rates and directionality in many developmental and disease contexts.

References and Notes

1. L. Solnica-Krezel, *Curr. Biol.* **15**, R213 (2005).
2. D. J. Roberts, *Dev. Dyn.* **219**, 109 (2000).
3. J. Alexander *et al.*, *Dev. Biol.* **215**, 343 (1999).
4. F. Biemar *et al.*, *Dev. Biol.* **230**, 189 (2001).
5. E. A. Ober *et al.*, *Nature* **442**, 688 (2006).
6. R. Keller, *Science* **298**, 1950 (2002).
7. A. F. Schier, *Annu. Rev. Cell Dev. Biol.* **19**, 589 (2003).
8. R. M. Warga, C. Nusslein-Volhard, *Development* **126**, 827 (1999).
9. S. W. Chong *et al.*, *Mech. Dev.* **109**, 347 (2001).
10. K. Dickinson *et al.*, *Dev. Dyn.* **235**, 368 (2006).
11. A. Fukui *et al.*, *Biochem. Biophys. Res. Commun.* **354**, 472 (2007).
12. K. E. McGrath *et al.*, *Dev. Biol.* **213**, 442 (1999).
13. F. Yusuf *et al.*, *Anat. Embryol.* **210**, 35 (2005).
14. K. Tachibana *et al.*, *Nature* **393**, 591 (1998).
15. N. B. David *et al.*, *Proc. Natl. Acad. Sci. U.S.A.* **99**, 16297 (2002).
16. H. Knaut *et al.*, *Neuron* **47**, 653 (2005).
17. Q. Li *et al.*, *J. Neurosci.* **25**, 1711 (2005).
18. E. Raz, *Curr. Opin. Cell Biol.* **16**, 169 (2004).
19. H. A. Field *et al.*, *Dev. Biol.* **253**, 279 (2003).
20. T. N. Hartmann *et al.*, *Oncogene* **24**, 4462 (2005).
21. J. E. Howard *et al.*, *Mech. Dev.* **38**, 109 (1992).
22. J. Jones *et al.*, *Exp. Cell Res.* **313**, 4051 (2007).
23. F. M. Watt, K. J. Hodivala, *Curr. Biol.* **4**, 270 (1994).
24. R. Winklbauer, R. E. Keller, *Dev. Biol.* **177**, 413 (1996).
25. A. J. Pelletier *et al.*, *Blood* **96**, 2682 (2000).
26. L. A. Trinh, D. Y. Stainier, *Dev. Cell* **6**, 371 (2004).
27. J. Juarez, L. Bendall, *Histol. Histopathol.* **19**, 299 (2004).
28. E. Ruoslahti, *Annu. Rev. Cell Dev. Biol.* **12**, 697 (1996).
29. A. P. Mould *et al.*, *BMC Cell Biol.* **7**, 24 (2006).
30. J. A. Montero *et al.*, *Development* **132**, 1187 (2005).
31. R. Winklbauer *et al.*, *Int. J. Dev. Biol.* **40**, 305 (1996).
32. T. Sakaguchi *et al.*, *Development* **133**, 4063 (2006).
33. I. C. Scott *et al.*, *Dev. Cell* **12**, 403 (2007).
34. X. X. Zeng *et al.*, *Dev. Cell* **12**, 391 (2007).
35. R. Keller *et al.*, *Differentiation* **71**, 171 (2003).
36. R. E. Stevenson *et al.*, *Human Malformations and Related Anomalies* (Oxford Univ. Press, New York, 1993).
37. G. Pezeron *et al.*, *Curr. Biol.* **18**, 276 (2008).

38. We thank E. Raz for *cxcl12b* and *cxcr4a* constructs; our laboratory colleagues, especially S. Piloto for help with qPCR and T. Hoffman for help with itgb1b constructs; and I. Blitz for reviewing the manuscript. Supported by NIH grants R01NS41353 and R01DE13828.

Supporting Online Material

www.sciencemag.org/cgi/content/full/1160038/DC1
Materials and Methods
Figs. S1 to S7
Table S1
References

5 May 2008; accepted 13 August 2008
Published online 21 August 2008;
10.1126/science.1160038
Include this information when citing this paper.

Molecular Architecture of the "Stressosome," a Signal Integration and Transduction Hub

Jon Marles-Wright,[1]* Tim Grant,[2]* Olivier Delumeau,[1]† Gijs van Duinen,[2]‡ Susan J. Firbank,[1] Peter J. Lewis,[3] James W. Murray,[1]§ Joseph A. Newman,[1] Maureen B. Quin,[1] Paul R. Race,[1] Alexis Rohou,[2] Willem Tichelaar,[2]‖ Marin van Heel,[2]¶ Richard J. Lewis[1]¶

A commonly used strategy by microorganisms to survive multiple stresses involves a signal transduction cascade that increases the expression of stress-responsive genes. Stress signals can be integrated by a multiprotein signaling hub that responds to various signals to effect a single outcome. We obtained a medium-resolution cryo–electron microscopy reconstruction of the 1.8-megadalton "stressosome" from *Bacillus subtilis*. Fitting known crystal structures of components into this reconstruction gave a pseudoatomic structure, which had a virus capsid–like core with sensory extensions. We suggest that the different sensory extensions respond to different signals, whereas the conserved domains in the core integrate the varied signals. The architecture of the stressosome provides the potential for cooperativity, suggesting that the response could be tuned dependent on the magnitude of chemophysical insult.

Microorganisms experiencing a fluctuating environment commonly exhibit a short-lived, reversible response that allows survival and recovery of the cell (*1*). In Gram-positive bacteria such as *Bacillus subtilis*, one such signaling cascade ultimately leads to the activation of the general stress sigma factor, σ^B (fig. S1), and enhanced transcription of its large regulon to provide a global response to the imposed stress (*2*, *3*). The stressosome is the signaling hub that integrates multiple physical stress signals (*4*–*7*) and orchestrates a single signaling outcome: the activation of σ^B. The stressosome is found in many microbial phyla, including representatives of the Methanomicrobiales branch of the Euryarchaea and, within Bacteria, the Proteobacteria, the Firmicutes, the Actinobacteria, the Cyanobacteria, and the *Bacteroides* and *Deinococcus* groups (*8*). The downstream chromosomal organization in these organisms points to the involvement of stressosome orthologs in regulating aerotaxis, a variety of two-component signaling systems, and the biosynthesis of secondary messenger signaling molecules. Thus, the stressosome appears to have evolved to provide a common solution to the problem of signal integration.

In *Bacillus*, the stressosome is a ~1.8 MD supramolecular complex comprising multiple copies of the regulator of sigma B proteins: RsbS, RsbR, and four paralogs of RsbR (*7*, *9*–*13*). The C-terminal domain of RsbR and its paralogs is conserved and is similar in sequence to RsbS. By contrast, the N-terminal domains of the RsbR paralogs show high sequence variability, suggesting that they function as sensors, whereas the C-terminal domains integrate the various signals. A third protein, RsbT, interacts with RsbR:RsbS complexes (*9*) to transmit integrated environmental signals into the σ^B activation pathway. The ability of stressosomes to integrate multiple inputs to effect a single output represents a departure from the more common one- and two-component signaling systems in prokaryotes (*14*). These systems typically convert a single signal into a single outcome, usually the transcriptional modulation of small regulons in response to specific metabolic changes (*15*). The activity of the stressosome can be reconstituted both in vitro and in vivo by complexes consisting

Molecular Architecture of the "Stressosome," a Signal Integration and Transduction Hub

Jon Marles-Wright, *et al.*

Science **322**, 92 (2008);
DOI: 10.1126/science.1159572

Science (print ISSN 0036-8075; online ISSN 1095-9203) is published weekly, except the last week in December, by the American Association for the Advancement of Science, 1200 New York Avenue NW, Washington, DC 20005.

crawl on FN along the blastocoel roof (*31*), and *fn1* controls migration of myocardial progenitors toward the midline (*26*, *32*)—a process that also requires another chemokine, *apelin* (*33*, *34*). However, gut defects have generally been interpreted as secondary to defects in mesoderm migration. In contrast, our studies reveal an earlier requirement for ECM-integrin interactions directly in endoderm migration.

We have shown that endoderm migration toward the anterior is genetically separable from other gastrulation movements (*35*). We propose that chemokine-dependent expression of integrin tethers the endoderm to the mesoderm, and that loss of this tether releases the endoderm to move anteriorly (Fig. 4); a secondary result is viscera bifida, because endodermal cells on either side [presumably containing organ progenitors (*8*)] have farther to converge dorsally and do not reach the midline in time to fuse. Viscera bifida–like syndromes in humans, including intestinal cysts and ectopic pancreatic or liver tissue, are relatively common and are not associated with spina bifida (ectoderm) (*36*), and defects in the CXCL12-CXCR4 signaling pathway may be an underlying cause.

For zebrafish endodermal cells, regulation of migration by controlling adhesion reconciles the recent observation that involuted endodermal cells initially move via a "random walk" rather than the directed migration displayed by the mesoderm (*37*). Classically, chemokines are cytokines that induce chemotaxis in responding cells; CXCL12-CXCR4 interactions control homing of hematopoietic stem cells to the bone marrow, as well as migration of germ cells, neuronal progenitors, and several metastatic cancers (*15*–*18*, *27*). In some of these cases, however, there is evidence for a system more like the tether described here, where receptor-expressing cells are confined to a territory defined by ligand-expressing cells. Thus, chemokine-dependent changes in adhesion to the ECM may influence cell migration rates and directionality in many developmental and disease contexts.

References and Notes

1. L. Solnica-Krezel, *Curr. Biol.* **15**, R213 (2005).
2. D. J. Roberts, *Dev. Dyn.* **219**, 109 (2000).
3. J. Alexander *et al.*, *Dev. Biol.* **215**, 343 (1999).
4. F. Biemar *et al.*, *Dev. Biol.* **230**, 189 (2001).
5. E. A. Ober *et al.*, *Nature* **442**, 688 (2006).
6. R. Keller, *Science* **298**, 1950 (2002).
7. A. F. Schier, *Annu. Rev. Cell Dev. Biol.* **19**, 589 (2003).
8. R. M. Warga, C. Nusslein-Volhard, *Development* **126**, 827 (1999).
9. S. W. Chong *et al.*, *Mech. Dev.* **109**, 347 (2001).
10. K. Dickinson *et al.*, *Dev. Dyn.* **235**, 368 (2006).
11. A. Fukui *et al.*, *Biochem. Biophys. Res. Commun.* **354**, 472 (2007).
12. K. E. McGrath *et al.*, *Dev. Biol.* **213**, 442 (1999).
13. F. Yusuf *et al.*, *Anat. Embryol.* **210**, 35 (2005).
14. K. Tachibana *et al.*, *Nature* **393**, 591 (1998).
15. N. B. David *et al.*, *Proc. Natl. Acad. Sci. U.S.A.* **99**, 16297 (2002).
16. H. Knaut *et al.*, *Neuron* **47**, 653 (2005).
17. Q. Li *et al.*, *J. Neurosci.* **25**, 1711 (2005).
18. E. Raz, *Curr. Opin. Cell Biol.* **16**, 169 (2004).
19. H. A. Field *et al.*, *Dev. Biol.* **253**, 279 (2003).
20. T. N. Hartmann *et al.*, *Oncogene* **24**, 4462 (2005).
21. J. E. Howard *et al.*, *Mech. Dev.* **38**, 109 (1992).
22. J. Jones *et al.*, *Exp. Cell Res.* **313**, 4051 (2007).
23. F. M. Watt, K. J. Hodivala, *Curr. Biol.* **4**, 270 (1994).
24. R. Winklbauer, R. E. Keller, *Dev. Biol.* **177**, 413 (1996).
25. A. J. Pelletier *et al.*, *Blood* **96**, 2682 (2000).
26. L. A. Trinh, D. Y. Stainier, *Dev. Cell* **6**, 371 (2004).
27. J. Juarez, L. Bendall, *Histol. Histopathol.* **19**, 299 (2004).
28. E. Ruoslahti, *Annu. Rev. Cell Dev. Biol.* **12**, 697 (1996).
29. A. P. Mould *et al.*, *BMC Cell Biol.* **7**, 24 (2006).
30. J. A. Montero *et al.*, *Development* **132**, 1187 (2005).
31. R. Winklbauer *et al.*, *Int. J. Dev. Biol.* **40**, 305 (1996).
32. T. Sakaguchi *et al.*, *Development* **133**, 4063 (2006).
33. I. C. Scott *et al.*, *Dev. Cell* **12**, 403 (2007).
34. X. X. Zeng *et al.*, *Dev. Cell* **12**, 391 (2007).
35. R. Keller *et al.*, *Differentiation* **71**, 171 (2003).
36. R. E. Stevenson *et al.*, *Human Malformations and Related Anomalies* (Oxford Univ. Press, New York, 1993).
37. G. Pezeron *et al.*, *Curr. Biol.* **18**, 276 (2008).

38. We thank E. Raz for *cxcl12b* and *cxcr4a* constructs; our laboratory colleagues, especially S. Piloto for help with qPCR and T. Hoffman for help with itgb1b constructs; and I. Blitz for reviewing the manuscript. Supported by NIH grants R01NS41353 and R01DE13828.

Supporting Online Material

www.sciencemag.org/cgi/content/full/1160038/DC1
Materials and Methods
Figs. S1 to S7
Table S1
References

5 May 2008; accepted 13 August 2008
Published online 21 August 2008;
10.1126/science.1160038
Include this information when citing this paper.

Molecular Architecture of the "Stressosome," a Signal Integration and Transduction Hub

Jon Marles-Wright,[1]* Tim Grant,[2]* Olivier Delumeau,[1]† Gijs van Duinen,[2]‡ Susan J. Firbank,[1] Peter J. Lewis,[3] James W. Murray,[1]§ Joseph A. Newman,[1] Maureen B. Quin,[1] Paul R. Race,[1] Alexis Rohou,[2] Willem Tichelaar,[2]‖ Marin van Heel,[2]¶ Richard J. Lewis[1]¶

A commonly used strategy by microorganisms to survive multiple stresses involves a signal transduction cascade that increases the expression of stress-responsive genes. Stress signals can be integrated by a multiprotein signaling hub that responds to various signals to effect a single outcome. We obtained a medium-resolution cryo–electron microscopy reconstruction of the 1.8-megadalton "stressosome" from *Bacillus subtilis*. Fitting known crystal structures of components into this reconstruction gave a pseudoatomic structure, which had a virus capsid–like core with sensory extensions. We suggest that the different sensory extensions respond to different signals, whereas the conserved domains in the core integrate the varied signals. The architecture of the stressosome provides the potential for cooperativity, suggesting that the response could be tuned dependent on the magnitude of chemophysical insult.

Microorganisms experiencing a fluctuating environment commonly exhibit a short-lived, reversible response that allows survival and recovery of the cell (*1*). In Gram-positive bacteria such as *Bacillus subtilis*, one such signaling cascade ultimately leads to the activation of the general stress sigma factor, σ^B (fig. S1), and enhanced transcription of its large regulon to provide a global response to the imposed stress (*2*, *3*). The stressosome is the signaling hub that integrates multiple physical stress signals (*4*–*7*) and orchestrates a single signaling outcome: the activation of σ^B. The stressosome is found in many microbial phyla, including representatives of the Methanomicrobiales branch of the Euryarchaea and, within Bacteria, the Proteobacteria, the Firmicutes, the Actinobacteria, the Cyanobacteria, and the *Bacteroides* and *Deinococcus* groups (*8*). The downstream chromosomal organization in these organisms points to the involvement of stressosome orthologs in regulating aerotaxis, a variety of two-component signaling systems, and the biosynthesis of secondary messenger signaling molecules. Thus, the stressosome appears to have evolved to provide a common solution to the problem of signal integration.

In *Bacillus*, the stressosome is a ~1.8 MD supramolecular complex comprising multiple copies of the regulator of sigma B proteins: RsbS, RsbR, and four paralogs of RsbR (*7*, *9*–*13*). The C-terminal domain of RsbR and its paralogs is conserved and is similar in sequence to RsbS. By contrast, the N-terminal domains of the RsbR paralogs show high sequence variability, suggesting that they function as sensors, whereas the C-terminal domains integrate the various signals. A third protein, RsbT, interacts with RsbR:RsbS complexes (*9*) to transmit integrated environmental signals into the σ^B activation pathway. The ability of stressosomes to integrate multiple inputs to effect a single output represents a departure from the more common one- and two-component signaling systems in prokaryotes (*14*). These systems typically convert a single signal into a single outcome, usually the transcriptional modulation of small regulons in response to specific metabolic changes (*15*). The activity of the stressosome can be reconstituted both in vitro and in vivo by complexes consisting

solely of RsbS and RsbR (*9*, *10*, *16*–*19*); thus, to gain insight into the organization of the stressosome, we have determined by single-particle cryo–electron microscopy (EM) reconstruction the three-dimensional structures of the complex of the C-terminal domain of RsbR with RsbS ($RsbR_{146-274}$:RsbS), the RsbR:RsbS binary complex, and the ternary RsbR:RsbS:RsbT complex to 6.5, 8.0, and 8.3 Å, respectively (*20*).

We first generated a stressosome core structure from $RsbR_{146-274}$:RsbS. The reconstruction reveals that the core of the complex, with a radius of 90 Å, displays an approximate icosahedral symmetry (Fig. 1A and fig. S2A), though it is an order of magnitude smaller than that of most icosahedral viruses. We then investigated stressosomes comprising full-length RsbR with RsbS (RsbR:RsbS). This structure displays an unusual mixed symmetry with the same pseudo-icosahedral symmetric core supporting 20 protruding "turrets." The arrangement of RsbR N-terminal domains is consistent only with D_2 point-group symmetry (Fig. 1B and fig. S2B). The mismatch of symmetry, though unusual, has been observed previously in the packaging of nucleic acid portal translocases at the vertices of icosahedral bacteriophages (*21*) and in multicomponent proteasome-type complexes (*22*). The radius of the RsbR:RsbS complex is 150 Å; the increase of 60 Å is due to the presence of the N-terminal domains of RsbR that form the turrets that protrude from the core. Finally, we solved the structure of the RsbR:RsbS:RsbT complex. In the absence of environmental stress, the RsbT kinase is believed to be sequestered by the stressosome (*9*) and in our reconstruction, electron density corresponding to RsbT is located above the core RsbS regions, thus occupying spaces between the sensory turrets (Fig. 1C and fig. S2C).

These medium-resolution stressosome reconstructions can be interpreted at higher resolution from the known structures of N-RsbR (*19*), the RsbT homolog SpoIIAB (*23*), and the RsbS ortholog from *Moorella thermoacetica* (*Mt*RsbS), which we have determined by x-ray crystallography and present here (*20*) (table S1). The $RsbR_{146-274}$:RsbS stressosome core can be constructed with icosahedral symmetry operators to build the entire 60-chain structure after fitting a single *Mt*RsbS molecule in the molecular envelope of the cryo-EM reconstruction (Figs. 1A and 2A). In the structure, the 20 projections were fitted with the dimeric N-RsbR domain (thus, there are 40 copies of RsbR) and corresponding regions of the core assigned as the C terminus of RsbR (Fig. 1B). The N-terminal domains of RsbR are found at two of the three positions at each three-fold and thus obey D_2 point-group symmetry. This fitting enabled us to discriminate between RsbR and RsbS STAS (sulfate transporter and anti-sigma factor) domains in the $RsbR_{146-274}$:RsbS stressosome core (Fig. 1A), assuming that the coexpressed $RsbR_{146-274}$:RsbS and RsbR:RsbS complexes assemble identically. To complete the interpretation of the RsbR:RsbS:RsbT reconstruction, we positioned a copy of the RsbT homolog and fitted it in density above each of the 20 copies of RsbS (Fig. 2B). The density corresponding to the N-RsbR domains in Fig. 1, B and C, appears different. However, these domains are relatively flexible in comparison to the rigid core, and their positions may be affected by the presence of RsbT in the ternary complex.

The RsbR and RsbS C-terminal helices project into an area of density at the two-fold axis of the

[1]Institute for Cell and Molecular Biosciences, Newcastle University, Newcastle-upon-Tyne NE2 4HH, UK. [2]Faculty of Natural Sciences, Division of Molecular Biosciences, Imperial College London, London SW7 2AZ, UK. [3]School of Environmental and Life Sciences, University of Newcastle, Callaghan, Newcastle, NSW 2308, Australia.

*These authors contributed equally to this work.
†Present address: Laboratoire de Génétique Microbienne, Domaine de Vilvert, Institut de la Recherche Agronomique INRA, 78350 Jouy-en-Josas, France.
‡Present address: FEI Europe, Achtseweg Noord 5, 5651 GG Eindhoven, Netherlands.
§Present address: Faculty of Natural Sciences, Division of Molecular Biosciences, Imperial College London, London SW7 2AZ, UK.
‖Present address: European Molecular Biology Laboratory, Meyerhofstrasse 1, 69117 Heidelberg, Germany.
¶To whom correspondence should be addressed. E-mail: r.lewis@ncl.ac.uk and m.vanheel@imperial.ac.uk

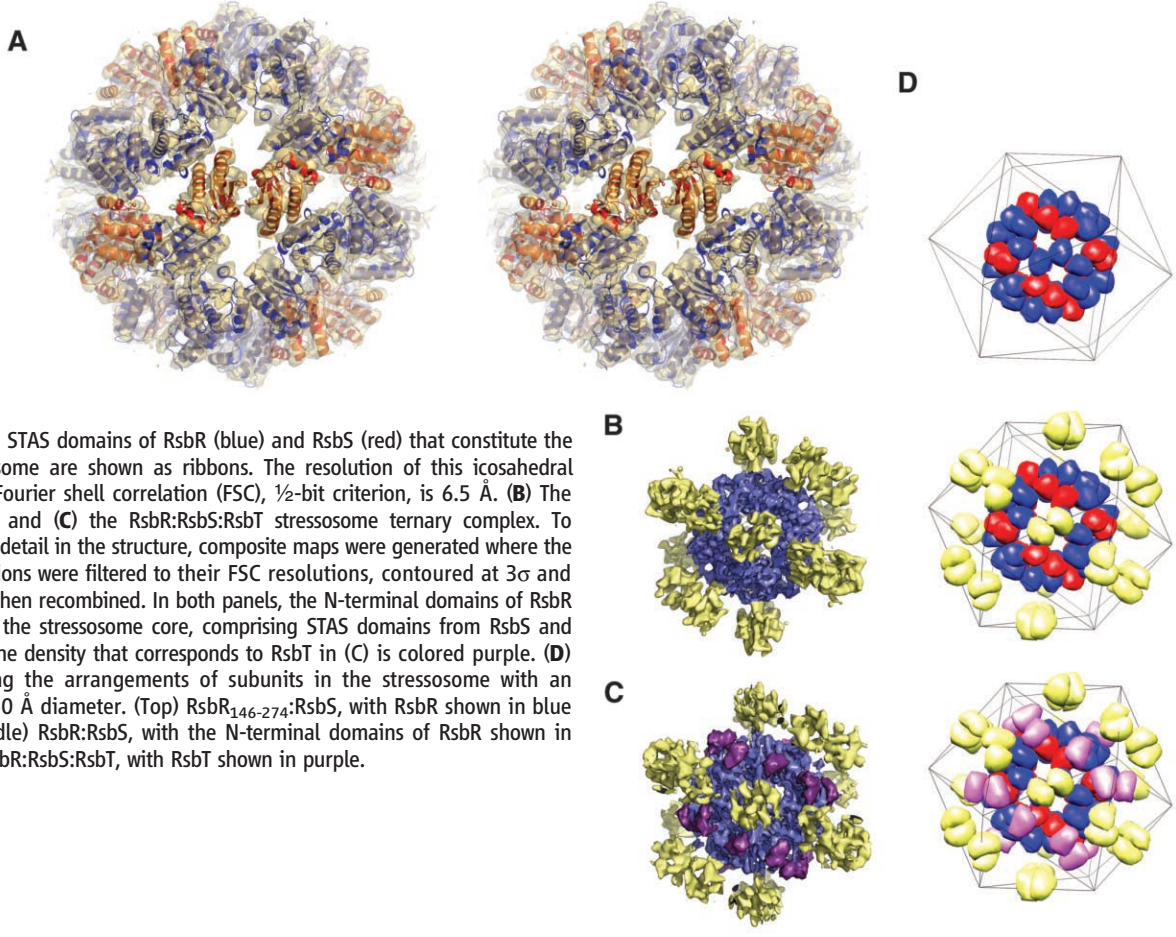

Fig. 1. Cryo-EM envelopes of stressosome structures. The cryo-EM envelopes of the three stressosome reconstructions shown in surface representation. (**A**) The final experimental EM-derived icosahedral molecular envelope of the $RsbR_{146-274}$:RsbS core is shown in stereo as a gold semi-transparent surface, with the map contoured at 3.0σ, and the STAS domains of RsbR (blue) and RsbS (red) that constitute the scaffold of the stressosome are shown as ribbons. The resolution of this icosahedral reconstruction, by the Fourier shell correlation (FSC), ½-bit criterion, is 6.5 Å. (**B**) The RsbR:RsbS stressosome and (**C**) the RsbR:RsbS:RsbT stressosome ternary complex. To demonstrate clearly the detail in the structure, composite maps were generated where the core and peripheral regions were filtered to their FSC resolutions, contoured at 3σ and 1.5σ, respectively, and then recombined. In both panels, the N-terminal domains of RsbR are colored yellow and the stressosome core, comprising STAS domains from RsbS and RsbR, is colored blue. The density that corresponds to RsbT in (C) is colored purple. (**D**) "Bean" models showing the arrangements of subunits in the stressosome with an icosahedral mesh of 150 Å diameter. (Top) $RsbR_{146-274}$:RsbS, with RsbR shown in blue and RsbS in red; (middle) RsbR:RsbS, with the N-terminal domains of RsbR shown in yellow; and (bottom) RsbR:RsbS:RsbT, with RsbT shown in purple.

core of the stressosome that may act as a pivot to propagate the structural changes that are brought about by the activation of the N-terminal signaling domains in the stressosome. The domains in the stressosome are arranged such that the serine and threonine residues in RsbR (Thr^{171} and Thr^{205}) and RsbS (Ser^{59}), which are phosphorylated by RsbT (*24*, *25*), are solvent accessible. Upon receipt of a stress signal, RsbT phosphorylates the stressosome and then disassociates to activate its alternative binding partner, the phosphatase RsbU (*9*, *26*, *27*); this stimulation is a prerequisite of σ^B activation (*17*) (fig. S1). Each of the 20 copies of RsbS, in the RsbR:RsbS:RsbT structure, is in close proximity to a copy of RsbT such that the adenosine 5′-triphosphate (ATP) lid of RsbT is positioned above Ser^{59} of RsbS, poised to catalyze phosphoryl transfer (Figs. 1C and 2B). In our structures, the phosphorylatable residues in RsbR are sterically hindered from forming a stable interaction with RsbT, indicating that some movements must occur in the stressosome to phosphorylate RsbR.

To link our structural studies of the stressosome with the cell biology of *Bacillus*, we have visualized stressosome formation using immunofluorescence and assessed σ^B activation in vivo with a reporter gene fusion. Using RsbR-specific antibodies, we determined the location and distribution of the complexes in live cells, before and after the imposition of stress. In cells that had not been subjected to environmental stress, ~20 bright foci per cell were observed in the cytoplasm directly adjacent to the nucleoids (Fig. 3, A and B). Each focus is predicted to correspond to a single stressosome. These foci maintained the same subcellular localization pattern over a 120-min period after induction of environmental stress. Thus, stressosomes are highly robust complexes that exist before stress induction and do not dissociate after their activation by RsbT-dependent phosphorylation. This is illustrated in Fig. 3C, which shows cells 20 min after stress induction when σ^B activity is maximal (*6*, *10*, *13*, *26*–*28*). No foci are seen in an *rsbR*-null mutant strain of *B. subtilis*, BSK5 (Fig. 3, D and E), the construction of which does not affect the expression of the downstream gene products in the *rsb* operon (*29*). Hence, the number of foci per cell is consistent with the cellular concentration of the Rsb proteins (*13*, *28*), given the multimeric organization of the stressosome. The distribution of the stressosomes throughout the cell is compatible with the requirement of the cell to sample its entire environment for physical insults.

The sequestration of multiple copies of RsbT by the stressosome suggests a mechanism of activation whereby the release of a single RsbT molecule reduces the affinity of neighboring ones so that multiple copies of RsbT are released in a cooperative manner. We used a σ^B-dependent *ctc-lacZ* reporter gene fusion to quantify σ^B activity as a function of the concentration of ethanol and NaCl. Both these stimuli induce the σ^B response and represent independent agonists of the σ^B pathway that are likely to enter the cell by different routes. The σ^B response in these two experiments was sigmoidal (Fig. 4, A and B), indicating that the response to environmental stress is complex and cooperative in at least one point in the σ^B pathway. The multisubunit stressosome is a logical point where the cooperative stage of the response, the release of RsbT by the stressosome, could commence. By contrast, when azide was used to induce the nutritional stress σ^B pathway, which is independent of the stressosome, the σ^B response was hyperbolic (Fig. 4C), confirming that the sigmoidal effect we observed is specific to the environmental stress signaling pathway. Presumably, the stressosome oligomer has evolved to provide cooperativity because small, diffusible complexes containing RsbT and its antagonist would provide a less finely controlled response to physical stress.

The structures presented are consistent with biochemical, biophysical, and cell biology data. The calculated mass of the RsbR:RsbS complex is 1.5 MD, consistent with measurements made by sedimentation velocity (*9*). When RsbT is bound, the mass of the stressosome increases to 1.8 MD. The distance between the end of the N-terminal domain of RsbR and the beginning of the C-terminal domain of RsbR is 30 Å, consistent with a 13-residue α-helical linker between the two domains that is absent in the crystallographic models; this structure is modeled in Fig. 2C. Small differences that are seen between the turrets in the RsbR:RsbS and RsbR:RsbS:RsbT maps are due to the inherent flexibility of the structures. That RsbT is bound above RsbS agrees with the knowledge that RsbT phosphorylates RsbS, in the RsbR:RsbS complex, more rapidly than it phosphorylates RsbR in vitro (*9*). The requirement for the correct interaction between RsbS and RsbT is crucial for signaling the stress response; *rsbS*-null mutant strains exhibit a small-cell phenotype indicative of severely compromised growth, and the mutation of Ser^{59} to Asp in RsbS—which mimics phosphorylation—is lethal, presumably as a result of constitutive σ^B activity (*16*). Point mutations in *rsbS* that also give rise to increased σ^B activity (*17*) map to regions involved in RsbT binding in our RsbR:RsbS:RsbT model (Fig. 2B).

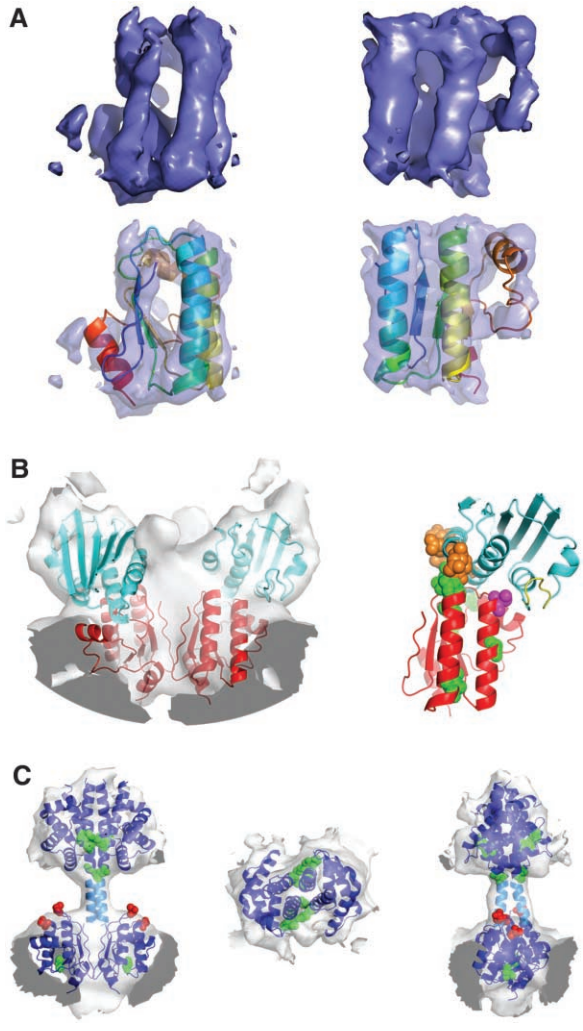

Fig. 2. The quasi-atomic structure of the stressosome. (**A**) Two orthogonal views of the secondary-structure fit of a single RsbS STAS domain in the icosahedral reconstruction of the $RsbR_{146-274}$:RsbS. (Top) The electron density map contoured at 3.0σ (to emphasize α helices); (bottom) the map shown as a semitransparent surface with RsbS fitted and shown as a cartoon continuously color-ramped from N terminus (blue) to C terminus (red). The experimental map is displayed as a semitransparent surface at 3.0σ (to emphasize the α helices). (**B**) Orthogonal views of the interactions between RsbS (red) and RsbT (cyan) in the stressosome. (Left) The final RsbR:RsbS:RsbT EM envelope is shown as a semitransparent surface contoured at 1.5σ. (Right) A view of a single molecule of RsbT poised above a single copy of RsbS to catalyze phosphorylation of Ser^{59} (magenta spheres) on receipt of stress. The residues known to be affected in the binding of RsbT to RsbS, or that are defective in signaling, are shown as spheres and colored green in RsbS and orange in RsbT (*29*). The peptide backbone of the ATP lid in RsbT is colored yellow. (**C**) Cartoon views of the sensory extensions of RsbR (blue) in the RsbR:RsbS complex that protrude from the core of the stressosome. The models for the N-terminal globin domain and C-terminal STAS domains are shown with an idealized helix illustrating the neck region (shown in cyan). Mutations that affect the activity of RsbR are shown as spheres and colored green, and phosphorylatable threonine residues are shown as red spheres (*17*, *19*). The experimental map is shown as a semitransparent surface at 1.5σ.

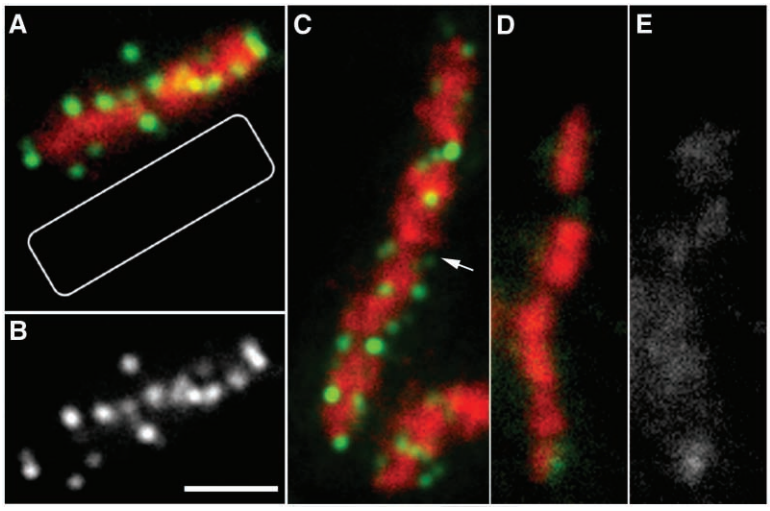

Fig. 3. Immunolocalization of stressosomes. (**A**) Pseudocolored image of stressosomes (green) and DNA (red) before induction of stress. A cartoon representation of the *Bacillus* (below) reveals the boundary of the cell. This cell contains two nucleoids. (**B**) The stressosomes immunolocalized with RsbR-specific antibodies from (A) are shown in monochrome. (**C**) A pseudocoloured image of a pair of cells 20 min after the induction of stress when σ^B activity is maximal, with stressosomes shown in green and DNA in red. The arrow indicates the position of the division septum between the two cells. (**D**) As in (C) but in the *rsbR*-null mutant strain, BSK5, with the green channel levels raised to show a faint background staining but no localization of stressosomes. (**E**) Monochrome version of (D). Scale bar, 2 μm.

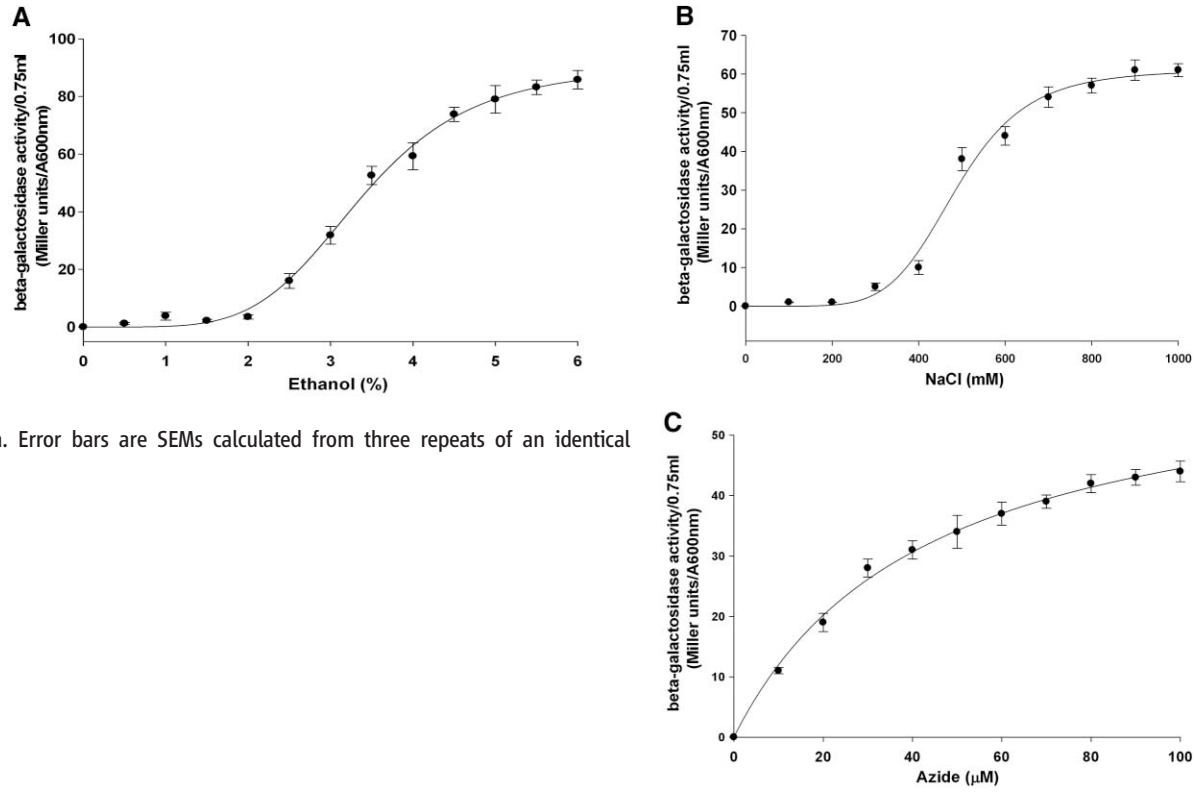

Fig. 4. Response of *B. subtilis* to stress. Plots of differential β-galactosidase activity versus inducer concentration for ethanol (**A**), sodium chloride (**B**), and sodium azide (**C**). All data were collected and analyzed as described in the supporting online material. Data were fitted to either a three-parameter Hill equation or a single rectangular hyperbola. Error bars are SEMs calculated from three repeats of an identical experiment.

In addition, mutations in RsbT that abrogate binding to RsbR:RsbS complexes are concentrated at the RsbT interface to RsbS (*30*, *31*). Thus, the structural model of the RsbR:RsbS:RsbT complex provides a molecular explanation of all the phenotypes of stress-associated mutants described previously (*16*, *17*, *30*, *31*).

Our results suggest a model for stressosome activation. Although no activating signal is known for RsbR, structures of the N-terminal domain of the light-responsive RsbR paralog YtvA have been reported recently (*32*). These show that upon activation by light, there are movements of helices at the C-terminal end of this domain, analogous to that of N-RsbR. This movement, in the context of the stressosome ternary complex that we describe, could allow transmission of the stress signals to RsbT, resulting in conformational changes to allow the phosphorylation of RsbS and RsbR by RsbT. Potentially, activation of the sensory domains is communicated to the stressosome core domains and is propagated via the C-terminal helices of the N-terminal domains to neighboring chains to allow optimal positioning of RsbT at the RsbS phosphorylation site. Phosphorylation ensues, RsbT is released to activate RsbU, and hence the large σ^B regulon is transcribed to protect the cell from the imposed stress. That the N-terminal domains of RsbR are not in direct contact with RsbT indicates that the stressosome is a dynamic complex. Other structures are required to fully elucidate all steps in the pathway leading to activation of the stressosome and to determine the precise role of the phosphorylation of RsbR (*9*, *10*, *33*). The structure of the stressosome reveals that the sensory domains are, however, ideally located to interact with trigger cues that range in size from photons of ultraviolet light to macromolecules. The sequestration of multiple copies of RsbT in a single structure, until the arrival of a single stress signal, may allow allosteric control over the activation of σ^B.

References and Notes

1. G. Storz, R. Hengge-Aronis, *Bacterial Stress Responses* (American Society for Microbiology, Washington, DC, 2000).
2. C. W. Price *et al.*, *Mol. Microbiol.* **41**, 757 (2001).

3. A. Petersohn *et al.*, *J. Bacteriol.* **183**, 5617 (2001).
4. M. Avila-Perez, K. J. Hellingwerf, R. Kort, *J. Bacteriol.* **188**, 6411 (2006).
5. A. K. Benson, W. G. Haldenwang, *J. Bacteriol.* **175**, 1929 (1993).
6. S. A. Boylan, A. R. Redfield, M. S. Brody, C. W. Price, *J. Bacteriol.* **175**, 7931 (1993).
7. T. A. Gaidenko, T. J. Kim, A. L. Weigel, M. S. Brody, C. W. Price, *J. Bacteriol.* **188**, 6387 (2006).
8. J. Pané-Farré, R. J. Lewis, J. Stülke, *J. Mol. Microbiol. Biotechnol.* **9**, 65 (2005).
9. C. C. Chen, R. J. Lewis, R. Harris, M. D. Yudkin, O. Delumeau, *Mol. Microbiol.* **49**, 1657 (2003).
10. T. J. Kim, T. A. Gaidenko, C. W. Price, *J. Mol. Biol.* **341**, 135 (2004).
11. S. Akbar *et al.*, *J. Bacteriol.* **183**, 1329 (2001).
12. O. Delumeau, C. C. Chen, J. W. Murray, M. D. Yudkin, R. J. Lewis, *J. Bacteriol.* **188**, 7885 (2006).
13. A. Dufour, U. Voelker, A. Voelker, W. G. Haldenwang, *J. Bacteriol.* **178**, 3701 (1996).
14. L. E. Ulrich, E. V. Koonin, I. B. Zhulin, *Trends Microbiol.* **13**, 52 (2005).
15. T. Mascher, J. D. Helmann, G. Unden, *Microbiol. Mol. Biol. Rev.* **70**, 910 (2006).
16. C. M. Kang, M. S. Brody, S. Akbar, X. Yang, C. W. Price, *J. Bacteriol.* **178**, 3846 (1996).
17. A. Reeves, W. G. Haldenwang, *J. Bacteriol.* **189**, 1531 (2007).
18. T. J. Kim, T. A. Gaidenko, C. W. Price, *J. Bacteriol.* **186**, 6124 (2004).
19. J. W. Murray, O. Delumeau, R. J. Lewis, *Proc. Natl. Acad. Sci. U.S.A.* **102**, 17320 (2005).
20. Materials and Methods are available as supporting material on *Science* Online.
21. P. Dube, P. Tavares, R. Lurz, M. van Heel, *EMBO J.* **12**, 1303 (1993).
22. F. Beuron *et al.*, *J. Struct. Biol.* **123**, 248 (1998).
23. S. Masuda *et al.*, *J. Mol. Biol.* **340**, 941 (2004).
24. T. A. Gaidenko, X. Yang, Y. M. Lee, C. W. Price, *J. Mol. Biol.* **288**, 29 (1999).
25. S. Zhang, W. G. Haldenwang, *J. Bacteriol.* **185**, 5714 (2003).
26. C. M. Kang, K. Vijay, C. W. Price, *Mol. Microbiol.* **30**, 189 (1998).
27. O. Delumeau *et al.*, *J. Biol. Chem.* **279**, 40927 (2004).
28. O. Delumeau, R. J. Lewis, M. D. Yudkin, *J. Bacteriol.* **184**, 5583 (2002).
29. S. Kuo, S. Zhang, R. L. Woodbury, W. G. Haldenwang, *Microbiology* **150**, 4125 (2004).
30. S. W. Hardwick *et al.*, *J. Biol. Chem.* **282**, 11562 (2007).
31. R. L. Woodbury, T. Luo, L. Grant, W. G. Haldenwang, *J. Bacteriol.* **186**, 2789 (2004).
32. A. Möglich, K. Moffat, *J. Mol. Biol.* **373**, 112 (2007).
33. C. C. Chen, M. D. Yudkin, O. Delumeau, *J. Bacteriol.* **186**, 6830 (2004).

34. This work was supported by the Biotechnology and Biological Sciences Research Council (BBSRC), Newcastle University (UK), Australian Research Council, University of Newcastle (Australia) by grants from the European Union (NOE, Contract LSHG-CT-2004-502828), and the Dutch Ministry of Economic Affairs ("Cyttron", BSIK 03036). The electron microscopes used for this work were purchased with financial support from the BBSRC, Glaxo Wellcome, and SmithKline Beecham. We are grateful to M. Schatz (Image Science, Berlin, Germany) for IMAGIC software support and to W. Haldenwang for strain BSK5. We thank R. Harris, H. Gilbert, M. Embley, and N. Robinson for advice and useful comments on the manuscript and E. Lowe for help with curve fitting. We are grateful for access to the Diamond synchrotron light source and its beamline scientists for help during data collection. Coordinates and structure factors for *Mt*RsbS are deposited in the Protein Databank with the accession number 2VY9. Electron microscopy–derived molecular envelopes are deposited in the Electron Microscopy Database at the Macromolecular Structure Database Group with the following accession numbers: $RsbR_{(146-274)}$:RsbS, 1558; RsbR:RsbS, 1555; and RsbR:RsbS:RsbT 1556.

Supporting Online Material

www.sciencemag.org/cgi/content/full/322/5898/92/DC1
Materials and Methods
SOM Text
Figs. S1 to S8
Table S1
References
Movie S1

24 April 2008; accepted 10 September 2008
10.1126/science.1159572

Internally Generated Reactivation of Single Neurons in Human Hippocampus During Free Recall

Hagar Gelbard-Sagiv,[1] Roy Mukamel,[2] Michal Harel,[1] Rafael Malach,[1] Itzhak Fried[2,3]*

The emergence of memory, a trace of things past, into human consciousness is one of the greatest mysteries of the human mind. Whereas the neuronal basis of recognition memory can be probed experimentally in human and nonhuman primates, the study of free recall requires that the mind declare the occurrence of a recalled memory (an event intrinsic to the organism and invisible to an observer). Here, we report the activity of single neurons in the human hippocampus and surrounding areas when subjects first view cinematic episodes consisting of audiovisual sequences and again later when they freely recall these episodes. A subset of these neurons exhibited selective firing, which often persisted throughout and following specific episodes for as long as 12 seconds. Verbal reports of memories of these specific episodes at the time of free recall were preceded by selective reactivation of the same hippocampal and entorhinal cortex neurons. We suggest that this reactivation is an internally generated neuronal correlate for the subjective experience of spontaneous emergence of human recollection.

The human hippocampus and its associated structures in the medial temporal lobe (MTL) transform present experience into future conscious recollections (*1*–*4*). Human MTL neurons respond in a highly specific manner to complex stimulus features (*5*), to complex stimulus categories (*5*, *6*), to individual persons or landmarks (*7*–*9*), and to previously seen and novel stimuli (*5*, *10*, *11*). These responses have been demonstrated for stationary stimuli and are usually brief, often lasting between 300 and 600 ms following stimulus onset, and rarely persist beyond 1 to 2 s (*8*). However, the human experience is seldom that of stationary stimuli; rather, we live and operate in a constantly changing environment. In this environment, we encounter complex stimuli constituting episodes, series of variant multimodal representations linked in temporal succession. It is such temporally sequenced information that is processed by the human MTL (*12*, *13*) and later becomes available for conscious recollection. For this reason, we set out to examine how neurons in the MTL respond to cinematic sequences depicting specific episodes, and, later, when these episodes spontaneously come to mind in the absence of external stimuli, in a free-recall situation that can be reported by individual subjects.

Subjects were patients with pharmacologically intractable epilepsy implanted with depth electrodes to localize the focus of seizure onset. For each patient, the placement of the depth

[1]Department of Neurobiology, Weizmann Institute of Science, Rehovot, 76100, Israel. [2]Department of Neurosurgery, David Geffen School of Medicine, and Semel Institute for Neuroscience and Human Behavior, University of California Los Angeles, Los Angeles, CA 90095, USA. [3]Functional Neurosurgery Unit, Tel Aviv Medical Center and Sackler School of Medicine, Tel Aviv University, Tel Aviv, 64239, Israel.

*To whom correspondence should be addressed. E-mail: ifried@mednet.ucla.edu

Fig. 1. A single-unit in the right entorhinal cortex was activated during viewing and recall of an episode from the TV series *The Simpsons*. (**A**) Cell responses to a selection of 48 different episodes (movie clips) presented to the patient in three different viewing sessions (parts 1 to 3). For each clip, the corresponding raster plots (six trials, order of trials is from top to bottom) and post–stimulus time histogram (500-ms bins) are given. Vertical dashed lines indicate clip onset and offset (5 s apart); 5-s blank periods were presented occasionally within groups of successive clips and were used to calculate the baseline firing rate, denoted by a gray horizontal line. Red boxes indicate sustained responses. (**B**) Trial-by-trial response of the neuron. Order of clips is for the purpose of illustration; more intervening clips separated successive *Simpsons* clips in the actual experiment. Spike raster plot and instantaneous firing rate (spike train convolved with a Gaussian of the full width at half maximum of 1200 ms) are displayed together. (**C**) Free-recall session that followed the third viewing session (part 3). (Bottom) Sound amplitude of patient voice; (top) a spike raster plot and instantaneous firing rate; gray dashed line denotes the average firing rate during the recall session + 3 SD; numbered dots denote onset time of verbal report of recall events, corresponding to clip numbers in (A). Note the distinct elevation of firing rate just before the patient reported the recall of the *Simpsons* clip (red arrow). (**D**) A 50-s window around the *Simpsons* recall event [blue area in (C)]. Patient's words are below the bottom panel. Note that the cell's firing rate rose significantly above baseline 1500 ms before onset of verbal report of the *Simpsons* clip and returned to baseline after more than 10 s.

Internally Generated Reactivation of Single Neurons in Human Hippocampus During Free Recall

Hagar Gelbard-Sagiv, *et al.*

Science **322**, 96 (2008);
DOI: 10.1126/science.1164685

3. A. Petersohn *et al.*, *J. Bacteriol.* **183**, 5617 (2001).
4. M. Avila-Perez, K. J. Hellingwerf, R. Kort, *J. Bacteriol.* **188**, 6411 (2006).
5. A. K. Benson, W. G. Haldenwang, *J. Bacteriol.* **175**, 1929 (1993).
6. S. A. Boylan, A. R. Redfield, M. S. Brody, C. W. Price, *J. Bacteriol.* **175**, 7931 (1993).
7. T. A. Gaidenko, T. J. Kim, A. L. Weigel, M. S. Brody, C. W. Price, *J. Bacteriol.* **188**, 6387 (2006).
8. J. Pané-Farré, R. J. Lewis, J. Stülke, *J. Mol. Microbiol. Biotechnol.* **9**, 65 (2005).
9. C. C. Chen, R. J. Lewis, R. Harris, M. D. Yudkin, O. Delumeau, *Mol. Microbiol.* **49**, 1657 (2003).
10. T. J. Kim, T. A. Gaidenko, C. W. Price, *J. Mol. Biol.* **341**, 135 (2004).
11. S. Akbar *et al.*, *J. Bacteriol.* **183**, 1329 (2001).
12. O. Delumeau, C. C. Chen, J. W. Murray, M. D. Yudkin, R. J. Lewis, *J. Bacteriol.* **188**, 7885 (2006).
13. A. Dufour, U. Voelker, A. Voelker, W. G. Haldenwang, *J. Bacteriol.* **178**, 3701 (1996).
14. L. E. Ulrich, E. V. Koonin, I. B. Zhulin, *Trends Microbiol.* **13**, 52 (2005).
15. T. Mascher, J. D. Helmann, G. Unden, *Microbiol. Mol. Biol. Rev.* **70**, 910 (2006).
16. C. M. Kang, M. S. Brody, S. Akbar, X. Yang, C. W. Price, *J. Bacteriol.* **178**, 3846 (1996).
17. A. Reeves, W. G. Haldenwang, *J. Bacteriol.* **189**, 1531 (2007).
18. T. J. Kim, T. A. Gaidenko, C. W. Price, *J. Bacteriol.* **186**, 6124 (2004).
19. J. W. Murray, O. Delumeau, R. J. Lewis, *Proc. Natl. Acad. Sci. U.S.A.* **102**, 17320 (2005).
20. Materials and Methods are available as supporting material on *Science* Online.
21. P. Dube, P. Tavares, R. Lurz, M. van Heel, *EMBO J.* **12**, 1303 (1993).
22. F. Beuron *et al.*, *J. Struct. Biol.* **123**, 248 (1998).
23. S. Masuda *et al.*, *J. Mol. Biol.* **340**, 941 (2004).
24. T. A. Gaidenko, X. Yang, Y. M. Lee, C. W. Price, *J. Mol. Biol.* **288**, 29 (1999).
25. S. Zhang, W. G. Haldenwang, *J. Bacteriol.* **185**, 5714 (2003).
26. C. M. Kang, K. Vijay, C. W. Price, *Mol. Microbiol.* **30**, 189 (1998).
27. O. Delumeau *et al.*, *J. Biol. Chem.* **279**, 40927 (2004).
28. O. Delumeau, R. J. Lewis, M. D. Yudkin, *J. Bacteriol.* **184**, 5583 (2002).
29. S. Kuo, S. Zhang, R. L. Woodbury, W. G. Haldenwang, *Microbiology* **150**, 4125 (2004).
30. S. W. Hardwick *et al.*, *J. Biol. Chem.* **282**, 11562 (2007).
31. R. L. Woodbury, T. Luo, L. Grant, W. G. Haldenwang, *J. Bacteriol.* **186**, 2789 (2004).
32. A. Möglich, K. Moffat, *J. Mol. Biol.* **373**, 112 (2007).
33. C. C. Chen, M. D. Yudkin, O. Delumeau, *J. Bacteriol.* **186**, 6830 (2004).

34. This work was supported by the Biotechnology and Biological Sciences Research Council (BBSRC), Newcastle University (UK), Australian Research Council, University of Newcastle (Australia) by grants from the European Union (NOE, Contract LSHG-CT-2004-502828), and the Dutch Ministry of Economic Affairs ("Cyttron", BSIK 03036). The electron microscopes used for this work were purchased with financial support from the BBSRC, Glaxo Wellcome, and SmithKline Beecham. We are grateful to M. Schatz (Image Science, Berlin, Germany) for IMAGIC software support and to W. Haldenwang for strain BSK5. We thank R. Harris, H. Gilbert, M. Embley, and N. Robinson for advice and useful comments on the manuscript and E. Lowe for help with curve fitting. We are grateful for access to the Diamond synchrotron light source and its beamline scientists for help during data collection. Coordinates and structure factors for *Mt*RsbS are deposited in the Protein Databank with the accession number 2VY9. Electron microscopy–derived molecular envelopes are deposited in the Electron Microscopy Database at the Macromolecular Structure Database Group with the following accession numbers: $RsbR_{(146-274)}$:RsbS, 1558; RsbR:RsbS, 1555; and RsbR:RsbS:RsbT 1556.

Supporting Online Material

www.sciencemag.org/cgi/content/full/322/5898/92/DC1
Materials and Methods
SOM Text
Figs. S1 to S8
Table S1
References
Movie S1

24 April 2008; accepted 10 September 2008
10.1126/science.1159572

Internally Generated Reactivation of Single Neurons in Human Hippocampus During Free Recall

Hagar Gelbard-Sagiv,[1] Roy Mukamel,[2] Michal Harel,[1] Rafael Malach,[1] Itzhak Fried[2,3]*

The emergence of memory, a trace of things past, into human consciousness is one of the greatest mysteries of the human mind. Whereas the neuronal basis of recognition memory can be probed experimentally in human and nonhuman primates, the study of free recall requires that the mind declare the occurrence of a recalled memory (an event intrinsic to the organism and invisible to an observer). Here, we report the activity of single neurons in the human hippocampus and surrounding areas when subjects first view cinematic episodes consisting of audiovisual sequences and again later when they freely recall these episodes. A subset of these neurons exhibited selective firing, which often persisted throughout and following specific episodes for as long as 12 seconds. Verbal reports of memories of these specific episodes at the time of free recall were preceded by selective reactivation of the same hippocampal and entorhinal cortex neurons. We suggest that this reactivation is an internally generated neuronal correlate for the subjective experience of spontaneous emergence of human recollection.

The human hippocampus and its associated structures in the medial temporal lobe (MTL) transform present experience into future conscious recollections (*1*–*4*). Human MTL neurons respond in a highly specific manner to complex stimulus features (*5*), to complex stimulus categories (*5*, *6*), to individual persons or landmarks (*7*–*9*), and to previously seen and novel stimuli (*5*, *10*, *11*). These responses have been demonstrated for stationary stimuli and are usually brief, often lasting between 300 and 600 ms following stimulus onset, and rarely persist beyond 1 to 2 s (*8*). However, the human experience is seldom that of stationary stimuli; rather, we live and operate in a constantly changing environment. In this environment, we encounter complex stimuli constituting episodes, series of variant multimodal representations linked in temporal succession. It is such temporally sequenced information that is processed by the human MTL (*12*, *13*) and later becomes available for conscious recollection. For this reason, we set out to examine how neurons in the MTL respond to cinematic sequences depicting specific episodes, and, later, when these episodes spontaneously come to mind in the absence of external stimuli, in a free-recall situation that can be reported by individual subjects.

Subjects were patients with pharmacologically intractable epilepsy implanted with depth electrodes to localize the focus of seizure onset. For each patient, the placement of the depth

[1]Department of Neurobiology, Weizmann Institute of Science, Rehovot, 76100, Israel. [2]Department of Neurosurgery, David Geffen School of Medicine, and Semel Institute for Neuroscience and Human Behavior, University of California Los Angeles, Los Angeles, CA 90095, USA. [3]Functional Neurosurgery Unit, Tel Aviv Medical Center and Sackler School of Medicine, Tel Aviv University, Tel Aviv, 64239, Israel.

*To whom correspondence should be addressed. E-mail: ifried@mednet.ucla.edu

Fig. 1. A single-unit in the right entorhinal cortex was activated during viewing and recall of an episode from the TV series *The Simpsons*. (**A**) Cell responses to a selection of 48 different episodes (movie clips) presented to the patient in three different viewing sessions (parts 1 to 3). For each clip, the corresponding raster plots (six trials, order of trials is from top to bottom) and post–stimulus time histogram (500-ms bins) are given. Vertical dashed lines indicate clip onset and offset (5 s apart); 5-s blank periods were presented occasionally within groups of successive clips and were used to calculate the baseline firing rate, denoted by a gray horizontal line. Red boxes indicate sustained responses. (**B**) Trial-by-trial response of the neuron. Order of clips is for the purpose of illustration; more intervening clips separated successive *Simpsons* clips in the actual experiment. Spike raster plot and instantaneous firing rate (spike train convolved with a Gaussian of the full width at half maximum of 1200 ms) are displayed together. (**C**) Free-recall session that followed the third viewing session (part 3). (Bottom) Sound amplitude of patient voice; (top) a spike raster plot and instantaneous firing rate; gray dashed line denotes the average firing rate during the recall session + 3 SD; numbered dots denote onset time of verbal report of recall events, corresponding to clip numbers in (A). Note the distinct elevation of firing rate just before the patient reported the recall of the *Simpsons* clip (red arrow). (**D**) A 50-s window around the *Simpsons* recall event [blue area in (C)]. Patient's words are below the bottom panel. Note that the cell's firing rate rose significantly above baseline 1500 ms before onset of verbal report of the *Simpsons* clip and returned to baseline after more than 10 s.

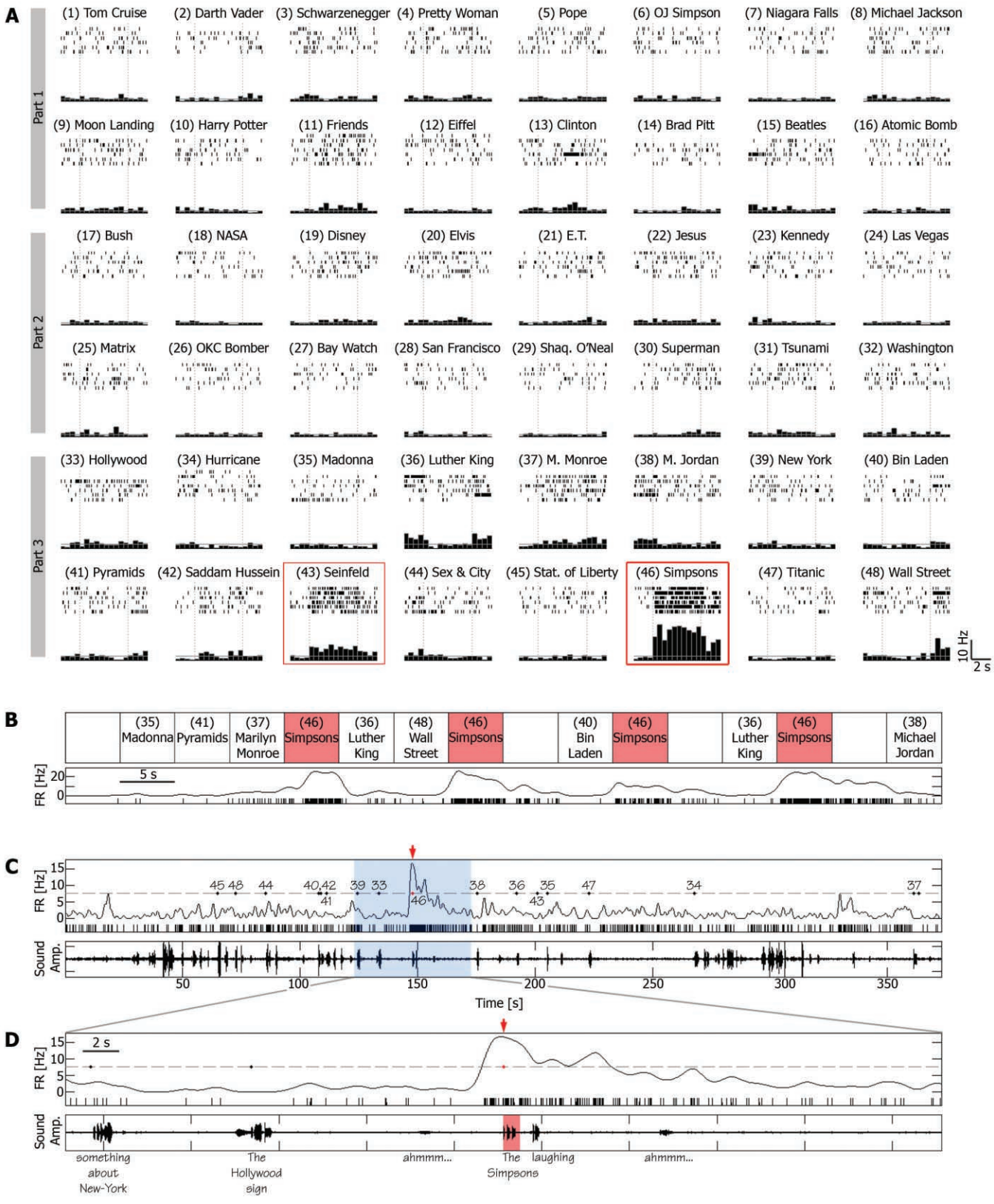

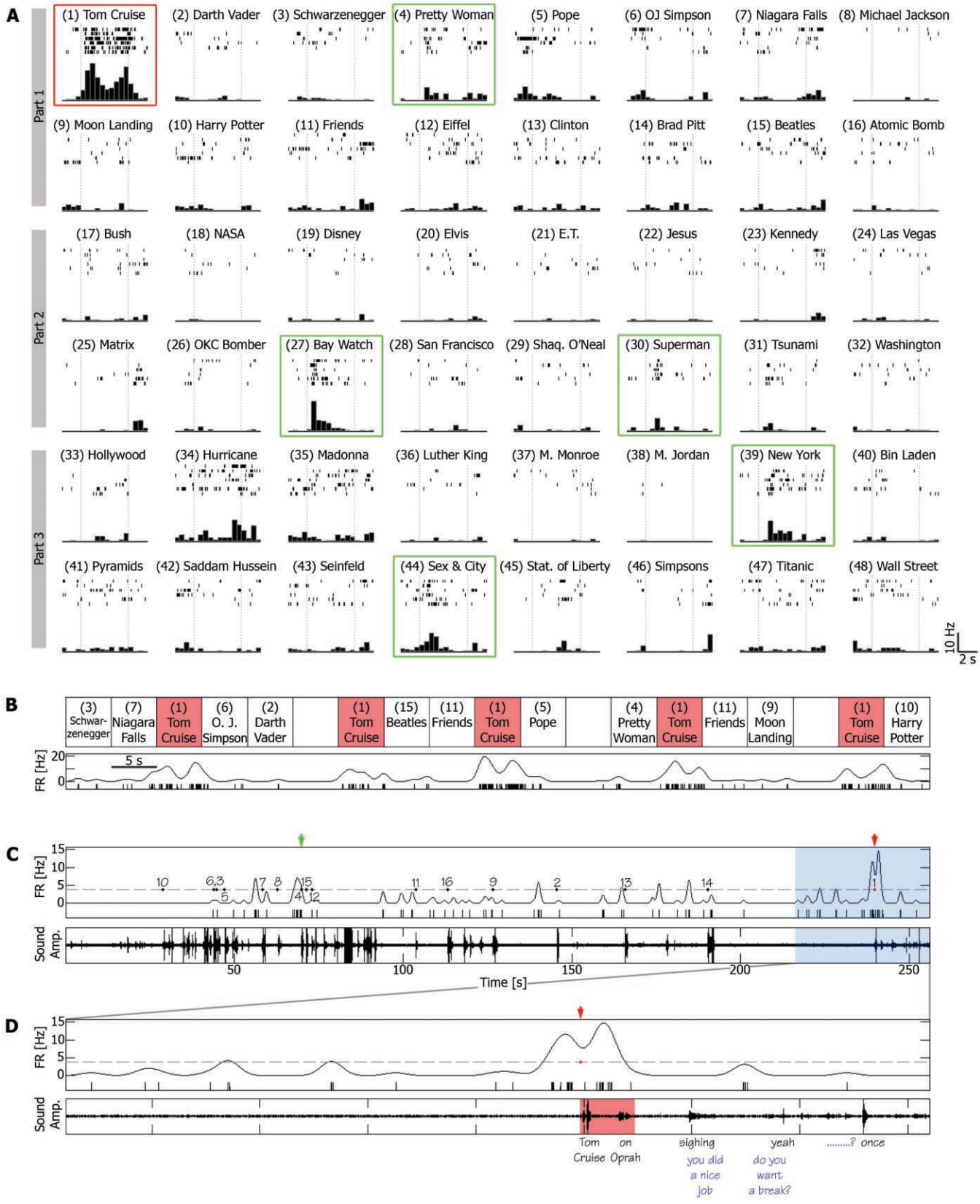

Fig. 2. A single-unit in the left anterior hippocampus is activated during viewing and recall of an episode (conventions as in Fig. 1). (**A** and **B**) Note the sustained elevation of firing rate during the episode depicting actor Tom Cruise during an interview on the *Oprah Winfrey Show* (red box). Note also the transient responses to various clips (green boxes). (**C** and **D**) Free-recall session that followed the first viewing session (part 1). Note that the burst of spikes that accompanied the recall of the Tom Cruise clip began 1500 ms before onset of verbal report ("Tom Cruise … on Oprah"). Blue words indicate experimenter's speech.

electrodes was determined exclusively by clinical criteria (*14*, *15*). Patients first participated in a viewing session in which they viewed a series of audiovisual clips lasting 5 to 10 s each. Each clip depicted an "episode" featuring famous people, characters, or animals engaged in activity, or landmarks described from various views, and was presented 5 to 10 times in a pseudorandomized order (*15*). After the viewing session, patients performed an intervening task (1 to 5 min) (*15*), after which they were asked to freely recall the clips they had seen and to verbally report immediately when a specific clip "came to mind" (free-recall session). Patients spontaneously recalled a mean of 83.2% (±5% SEM) of the clips presented.

Thirteen patients participated in a total of 43 viewing and recall sessions. We recorded from a total of 857 units (441 single units and 416 multi units) (*15*) in the MTL and the medial frontal cortex (table S1). A unit was considered responsive to a specific clip if it showed a consistent elevated pattern of firing in all trials of that clip. Overall, the majority of recorded neurons, 475 units (54.9%), showed a significant response to one or more of the clips, i.e., consistently increased firing rate in at least one 500-ms segment of clip presentation (*15*). There were no differences in proportion of responsive units among the various regions sampled in this study [$P > 0.05$, $\chi^2(5) = 7.6$] (table S1). Of the responsive units, 46 (9.7%) showed a sustained response to at least one clip, i.e., a significant elevation of firing rate through most of the clip duration (although not necessarily at a fixed level) (*15*). Of these 46 cells, 44 were in MTL and only 2 in medial frontal lobe [$P < 0.03$, $\chi^2(1) = 5.2$] (table S1, fig. S1). Twenty of these cells maintained their elevated firing rate at least 1 s beyond clip offset, and in some cases, up to 5 s beyond clip offset. Responses observed were as long as 12 s and were usually attenuated only by the onset of the next clip.

For example, a single unit in the right entorhinal cortex of a patient, presented with a selection of 48 different clips, responded in a sustained manner to an episode from the animated television (TV) series *The Simpsons* (Fig. 1A). Each time this clip was shown, the firing rate was elevated to an average of 15.57 Hz, compared with 2.11 and 2.23 Hz during other clips and blank periods, respectively ($P < 10^{-9}$, two-sample t test). The response persisted for the entire 5-s duration of the clip, continued in some of the trials up to 5 s after clip offset, and appeared to be silenced only by the onset of a different clip (Fig. 1B and movie S1a).

The neuron did not respond exclusively to this *Simpsons* episode. Even within the limited selection of 48 clips, there was a considerably weaker, yet significant, response to another clip, an episode from the TV situational comedy (sitcom) *Seinfeld*. Of the 46 units with sustained responses, a unit responded in a sustained manner to an average of 1.4 ± 0.1 SEM clips (or an average of 5.7% ± 0.5 SEM of clips presented). For another example, see fig. S2.

In a second example, a neuron in left anterior hippocampus responded with elevated firing rate throughout a single clip from a choice of 48 clips—that of the actor Tom Cruise during an interview (Fig. 2, A and B, and movie S2a). Note that this cell also exhibited shorter, transient (*15*) neuronal responses to other clips, i.e., consistent elevation of firing rate above baseline only during particular segments of the clip (green boxes in Fig. 2A), possibly reflecting the preference of the cell to a specific feature of the clip or to an episode within the clip. Additional examples are shown in figs. S3 and S4. Overall, responsive units significantly responded in a sustained or transient manner to an average of

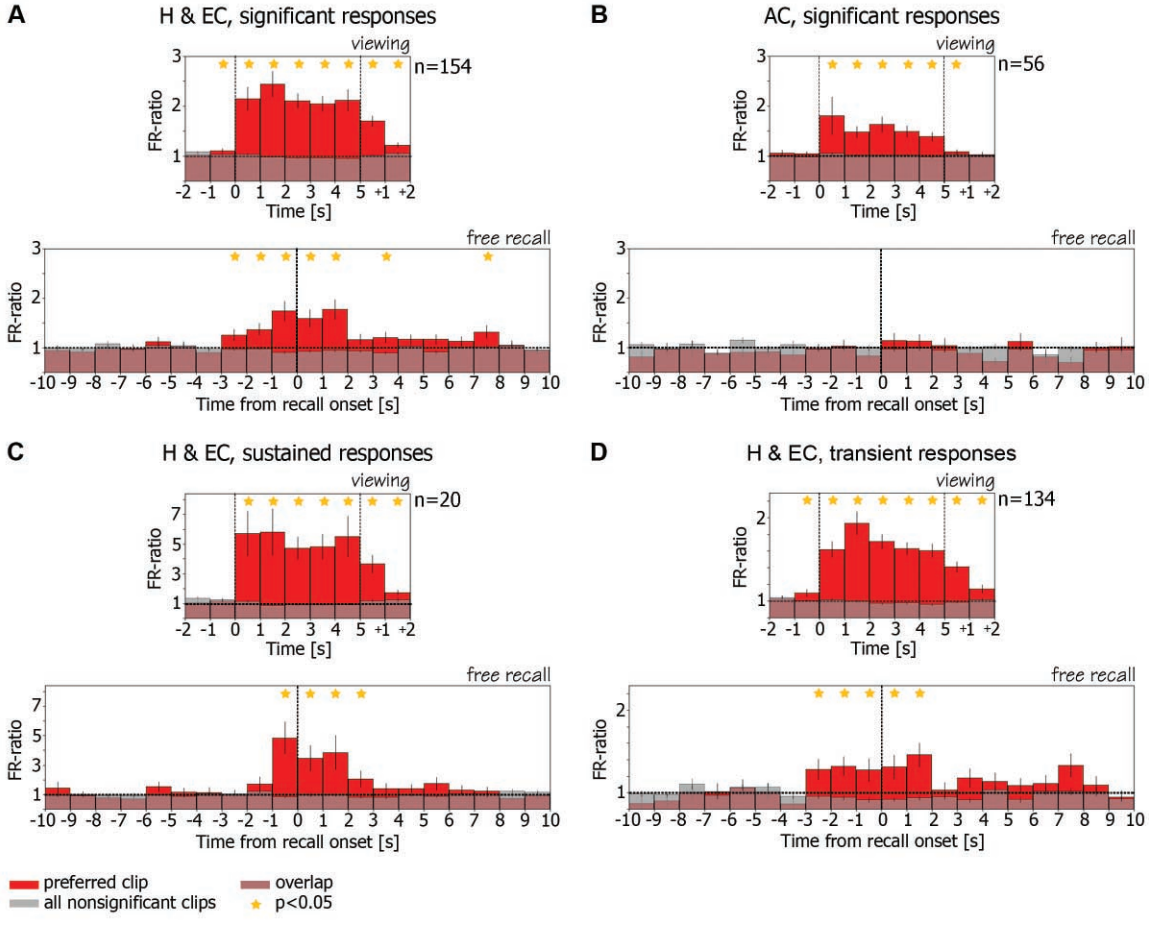

Fig. 3. Average FR ratio histograms during viewing and during free recall. (**A**) (Top) Ratio of firing rate during viewing of clips to baseline firing rate is averaged across all responsive hippocampal and entorhinal cortex cells ($n = 154$). Vertical dashed lines denote clip onset and offset. Cells increased their firing rate significantly above baseline during and following viewing of their preferred clip (*15*) (red bars). Note small elevation before clip onset, probably attributable to anticipatory effect. These cells remained at baseline firing rate (FR ratio = 1) during viewing of other clips (*15*) (gray bars). (Bottom) FR ratio during recall events is averaged across the same cells from the top panel. Traces were aligned on the onset time of the verbal report of recall (zero time, vertical dashed line). Note that the same cells increased their firing rate significantly above baseline in the 3 s before onset of verbal report of their preferred clips (red bars) and maintained this elevated firing rate in the ensuing 2 s. However, these cells remained at baseline during recall of clips that did not elicit significant responses during viewing (gray bars). Stars denote statistical significance of $P < 0.05$ (t test) (*15*). (**B**) Same as (A) but for cells from anterior cingulate ($n = 56$). Note that, in contrast to hippocampal and entorhinal cortex cells, although these cells exhibited selectivity during viewing (top), this selectivity was not maintained during free recall (bottom). (**C** and **D**) are the same as (A) but for sustained and transient responses separately.

17.7% ± 0.7 SEM of the clips presented (or 4.0 ± 0.2 SEM clips) (fig. S5).

We next examined the neuronal firing at the time of free recall when no external representation of the stimulus was present, no external cue was provided, and no external constraint was placed on the recall process. We found that the neurons that responded during viewing of a particular clip also responded during recall of that clip, with a robust elevation of firing rate for several seconds that could be detected during a single recall trial. This is illustrated for the entorhinal cortex neuron that responded selectively during viewing of a 5-s video clip from the cartoon *The Simpsons* (Fig. 1, A and B); when all 16 clips were freely recalled, the maximal firing rate was obtained in conjunction with recall of *The Simpsons* episode (Fig. 1C). The unit's firing rate rose to more than 3 SD above baseline (*15*) about 1500 ms before onset of the verbal report of recall, peaked about 100 ms before verbal report onset, but returned to baseline only after 10 s or more (see also movie S1b). Similar examples are illustrated in Fig. 2 and movie S2b, and in figures S6 to S10.

This recurrence of selective activity during recall was not an isolated observation found in a few neurons, but was also evident when the population of responsive units was examined as a whole. We calculated the average ratio of firing rate during viewing of clips to baseline firing rate (FR ratio) (*15*), for all responsive entorhinal cortex and hippocampal units (Fig. 3A, top). The FR ratio during viewing of the "preferred clip" (*15*) (red bars) is compared with the average FR ratio across all other clips with nonsignificant responses in the same viewing session (gray bars). The composite graph shows a marked elevation of the ratio following onset of the preferred clip, during viewing and, notably, also 3 s after clip offset. The FR ratio histogram for the recall is then shown in the bottom of Fig. 3A, averaged across the same units with respect to the onset time of verbal report of recall (*15*). During recall of the preferred clip (red), the averaged firing rate of the neurons increased significantly above baseline in the 3 s before onset of verbal report of recall and remained significantly above baseline in the ensuing 2 s ($P < 0.05$, Student's t test) (*15*). These neurons remained at baseline firing during recall of clips that did not elicit significant responses during viewing (gray). This recurrence during free recall of the same selective neuronal responses present during viewing was found in the population of hippocampal and entorhinal units but not in medial frontal units (compare bottom panels of Fig. 3, A and B). These frontal units exhibited a significant selective increase in firing rate during viewing, but not during recall (Fig. 3B, top and bottom, respectively). This episode-specific reactivation phenomenon was weak in amygdala and absent from parahippocampal gyrus (fig. S11), but was particularly striking for hippocampal and entorhinal neurons with sustained responses (Fig. 3C). We also noted reactivation of inhibitory responses, but because of the low baseline firing rate, these inhibitory responses were evident only at the population level (fig. S12). This phenomenon was most prominent in entorhinal cortex cells. For further details, see supporting online text.

In conclusion, we report here that a subset of neurons in the human hippocampus and entorhinal cortex exhibited highly reliable and specific responses during viewing of video episodes. These responses persisted throughout an episode or appeared during specific segments. The same neurons showed an increased firing rate again with free conscious recall, before the verbal report, when the sequence of physical sensory stimuli was absent and no external cues were provided. This recurrence during recall of specific past neuronal activity was not observed in medial frontal cortex sites. However, it is possible that top-down early recall signals do originate in other frontal or temporal lobe regions not sampled in this study (*16*–*20*).

Could the findings reported here be attributed to the neurological pathology of the patients? Although these results should be viewed with caution, such interpretation is unlikely for various reasons. Epileptic activity is characterized by highly correlated activity in large groups of neighboring neurons. The neuronal responses reported here were extremely sparse and seen selectively in individual neurons out of dozens of nonresponsive neurons that were recorded in their immediate vicinity. Furthermore, only 27% of the units were recorded from within the epileptogenic seizure foci. No significant difference was detected when these units were excluded from the analysis (see supporting online text for more details).

The responses to episodes observed here were often remarkably selective and relatively sparse; yet it is clear, even by a simple statistical reasoning, that these neurons must display selective responses to multiple other clips that have not been presented, as only a minute fraction of the vast set of possible episodes was tested in our study (*9*). Whether multiple clips to which a neuron responds may be related by some abstract association rule is not clear at present. However, some intriguing examples in our data suggest that such rules may exist (see supporting online text and figs. S2, S9, and S13 to S15). It is also important to exercise caution in claims as to what exact aspect of the clips the cell responded to. The critical point, however, is that the same selective responses recur during free recall.

Several neuroimaging studies show that brain activity present during the learning of information, as indirectly measured by the BOLD signal, is reinstated during cued or free recall (*21*–*24*), although spatiotemporal limits of fMRI restrict the possible conclusions. Selective increases in single-unit activation during mental imagery of stationary stimuli have been reported (*25*). However, unlike the situation in our study, subjects were cued by an external, content-specific, sensory stimulus.

The sparse neuronal responses arising from a very low baseline to robust firing during a specific episode are reminiscent of the responses of hippocampal place cells in rodents (*26*), in which a cell responds whenever the animal is in a particular place in the environment. Internally generated replay of previous firing sequences by hippocampal neurons has been reported in rodents, mostly during sleep and rest states after locomotion (*27*–*29*), but also during the awake state (*30*, *31*) and at decision points of a spatial memory task (*32*), where it might be predictive of the animal's future choice (*33*). However, the relation of such replay in rodents to recall of past navigation events has been merely conjectural. Our results from conscious human patients, who can spontaneously declare their memories, now directly link free recall and neuronal replay in hippocampus and entorhinal cortex. The hippocampal and entorhinal machinery used in spatial navigation in rodents may have been preserved in humans but put to a more elaborate and abstract use (*5*, *34*–*36*).

References and Notes

1. W. B. Scoville, B. Milner, *J. Neurol. Neurosurg. Psychiatry* **20**, 11 (1957).
2. L. R. Squire, C. E. Stark, R. E. Clark, *Annu. Rev. Neurosci.* **27**, 279 (2004).
3. H. Eichenbaum, *Neuron* **44**, 109 (2004).
4. M. Moscovitch, L. Nadel, G. Winocur, A. Gilboa, R. S. Rosenbaum, *Curr. Opin. Neurobiol.* **16**, 179 (2006).
5. I. Fried, K. A. MacDonald, C. L. Wilson, *Neuron* **18**, 753 (1997).
6. G. Kreiman, C. Koch, I. Fried, *Nat. Neurosci.* **3**, 946 (2000).
7. G. Heit, M. E. Smith, E. Halgren, *Nature* **333**, 773 (1988).
8. R. Q. Quiroga, L. Reddy, G. Kreiman, C. Koch, I. Fried, *Nature* **435**, 1102 (2005).
9. R. Q. Quiroga, G. Kreiman, C. Koch, I. Fried, *Trends Cogn. Sci.* **12**, 87 (2008).
10. U. Rutishauser, A. N. Mamelak, E. M. Schuman, *Neuron* **49**, 805 (2006).
11. I. V. Viskontas, B. J. Knowlton, P. N. Steinmetz, I. Fried, *J. Cogn. Neurosci.* **18**, 1654 (2006).
12. N. J. Fortin, K. L. Agster, H. B. Eichenbaum, *Nat. Neurosci.* **5**, 458 (2002).
13. J. E. Lisman, *Neuron* **22**, 233 (1999).
14. I. Fried *et al.*, *J. Neurosurg.* **91**, 697 (1999).
15. Materials and methods are available as supporting material on *Science* Online.
16. Y. Miyashita, *Science* **306**, 435 (2004).
17. R. N. Henson, M. D. Rugg, T. Shallice, R. J. Dolan, *J. Cogn. Neurosci.* **12**, 913 (2000).
18. G. A. Ojemann, J. Schoenfield-McNeill, D. P. Corina, *Nat. Neurosci.* **5**, 64 (2002).
19. S. M. Polyn, M. J. Kahana, *Trends Cogn. Sci.* **12**, 24 (2008).
20. D. L. Schacter, *Philos. Trans. R. Soc. Lond. B Biol. Sci.* **352**, 1689 (1997).
21. S. M. Polyn, V. S. Natu, J. D. Cohen, K. A. Norman, *Science* **310**, 1963 (2005).
22. L. Nyberg, R. Habib, A. R. McIntosh, E. Tulving, *Proc. Natl. Acad. Sci. U.S.A.* **97**, 11120 (2000).
23. M. E. Wheeler, S. E. Petersen, R. L. Buckner, *Proc. Natl. Acad. Sci. U.S.A.* **97**, 11125 (2000).
24. I. Kahn, L. Davachi, A. D. Wagner, *J. Neurosci.* **24**, 4172 (2004).
25. G. Kreiman, C. Koch, I. Fried, *Nature* **408**, 357 (2000).
26. J. O'Keefe, J. Dostrovsky, *Brain Res.* **34**, 171 (1971).
27. M. A. Wilson, B. L. McNaughton, *Science* **265**, 676 (1994).
28. W. E. Skaggs, B. L. McNaughton, *Science* **271**, 1870 (1996).
29. A. K. Lee, M. A. Wilson, *Neuron* **36**, 1183 (2002).
30. K. Diba, G. Buzsáki, *Nat. Neurosci.* **10**, 1241 (2007).
31. D. J. Foster, M. A. Wilson, *Nature* **440**, 680 (2006).
32. A. Johnson, A. D. Redish, *J. Neurosci.* **27**, 12176 (2007).
33. E. Pastalkova, V. Itskov, A. Amarasingham, G. Buzsáki, *Science* **321**, 1322 (2008).
34. J. O'Keefe, L. Nadel, *The Hippocampus as a Cognitive Map* (Oxford Univ. Press, Oxford, 1978), pp. 380–410.

35. E. R. Wood, P. A. Dudchenko, H. Eichenbaum, *Nature* **397**, 613 (1999).
36. C. M. Bird, N. Burgess, *Nat. Rev. Neurosci.* **9**, 182 (2008).
37. We thank the patients for their cooperation and participation in this study. We also thank E. Ho, B. Scott, E. Behnke, R. Kadivar, T. Fields, A. Postolova, K. Laird, C. Wilson, R. Quian-Quiroga, A. Kraskov, F. Mormann, and M. Cerf for assistance with data acquisition; B. Salaz and I. Wainwright for administrative help; and I. Kahn, Y. Nir, G. Buzsáki, E. Pastalkova, and S. Gilaie-Dotan for discussions and comments on this manuscript. This work was supported by NINDS (to I. Fried), Israel Science Foundation (to R. Malach), Binational United States–Israel grant (to I. Fried and R. Malach), and Human Frontier Science Program Organization (HFSPO) fellowship (to R. Mukamel).

Supporting Online Material
www.sciencemag.org/cgi/content/full/1164685/DC1
Materials and Methods
Figs. S1 to S15
Table S1
References
Movies S1 and S2

14 August 2008; accepted 28 August 2008
Published online 4 September 2008;
10.1126/science.1164685
Include this information when citing this paper.

A Physical Map of the 1-Gigabase Bread Wheat Chromosome 3B

Etienne Paux,[1] Pierre Sourdille,[1] Jérôme Salse,[1] Cyrille Saintenac,[1] Frédéric Choulet,[1] Philippe Leroy,[1] Abraham Korol,[2] Monika Michalak,[3] Shahryar Kianian,[3] Wolfgang Spielmeyer,[4] Evans Lagudah,[4] Daryl Somers,[5] Andrzej Kilian,[6] Michael Alaux,[7] Sonia Vautrin,[8] Hélène Bergès,[8] Kellye Eversole,[9] Rudi Appels,[10] Jan Safar,[11] Hana Simkova,[11] Jaroslav Dolezel,[11] Michel Bernard,[1] Catherine Feuillet[1]

As the staple food for 35% of the world's population, wheat is one of the most important crop species. To date, sequence-based tools to accelerate wheat improvement are lacking. As part of the international effort to sequence the 17–billion–base-pair hexaploid bread wheat genome ($2n = 6x = 42$ chromosomes), we constructed a bacterial artificial chromosome (BAC)–based integrated physical map of the largest chromosome, 3B, that alone is 995 megabases. A chromosome-specific BAC library was used to assemble 82% of the chromosome into 1036 contigs that were anchored with 1443 molecular markers, providing a major resource for genetic and genomic studies. This physical map establishes a template for the remaining wheat chromosomes and demonstrates the feasibility of constructing physical maps in large, complex, polyploid genomes with a chromosome-based approach.

Among plants providing food for humans and animals, one of the oldest and most widespread is wheat (*Triticum aestivum* L.). Despite its socioeconomic importance and the challenges that agriculture is facing today (*1*), wheat genomics and its application to crop improvement are lagging behind those of most other important crops. The wheat genome has always been viewed as impossible to sequence because of its large amount of repetitive sequences (>80%) and its size of 17 Gb, which is five times larger than the human genome. The largest wheat chromosome (3B) alone is more than twice the size of the entire 370-Mb rice genome (*2*), whereas the entire maize genome (2.6 Gb) is about the size of three wheat chromosomes (table S1). Further complicating the challenge, bread wheat is a relatively recent hexaploid ($2n = 6x = 42$) containing three homoeologous A, B, and D genomes of related progenitor species, meiotic recombination is not distributed homogeneously along the chromosomes, and intervarietal polymorphism is very low.

Genome sequencing is the foundation for understanding the molecular basis of phenotypic variation, accelerating breeding, and improving the exploitation of genetic diversity to develop new crop varieties with increased yield and improved resistance to biotic and abiotic stresses. These new varieties will be critical for meeting the challenges of the 21st century, such as climatic changes, modifications of diets, human population growth, and the increased demand for biofuels. Physical maps are essential for high-quality sequence assembly regardless of the sequencing strategy used [such as bacterial artificial chromosome (BAC)–by–BAC or whole-genome shotgun strategies], and they will remain pivotal for de novo sequencing even with the advent of short-read technologies (*3*). As the foundation for genome sequencing, physical maps have been established for a dozen plants species so far, including cereals such as maize, rice, and sorghum (*4*–*6*). Recently, the development of new genomic resources for analyzing wheat paved the way for physically mapping and ultimately sequencing a species for which this was unthinkable a few years ago.

A physical map with 10-fold coverage of the 17-Gb bread wheat genome would require more than 1.4 million BAC clones to be fingerprinted, assembled into contigs, and anchored to genetic maps. Although whole-genome BAC libraries are available and fingerprinting millions of BAC clones is technically feasible with high-information-content fingerprinting (HICF) (*7*), assembly to accurately depict individual chromosomes and the anchoring of homoeologous BAC contigs onto genetic maps remains daunting. To address these issues, we used a chromosome-based approach (*8*) to construct a physical map of the largest hexaploid wheat chromosome (3B) and, to compensate for the inherent limits of the wheat genome (the lack of recombination and polymorphism), we deployed a combination of genetic mapping strategies for anchoring the physical map.

Fingerprinting and contig assembly were performed with BAC clones originating from sorted 3B wheat chromosomes of Chinese Spring (*9*), the reference cultivar chosen for genome sequencing by the International Wheat Genome Sequencing Consortium because of its previous use for cytogenetic studies and the availability of a set of aneuploid lines (*10*). 67,968 3B BAC clones were fingerprinted with a modified (*11*) HICF SNaPshot protocol (*7*), and a total of 56,952 high-quality fingerprints (84%) was obtained. A first automated assembly (*11*) resulted in a final build of 1991 contigs with an average size of 482 kb for a total length of 960 Mb (table S2). One hundred ninety-seven contigs were larger than 1 Mb; the largest was 3852 kb in size. A minimal tiling path (MTP) consisting of 7440 overlapping BAC clones was defined for further analyses. After the preliminary automated assembly, contigs were merged manually (*11*), resulting in a final assembly of 1036 contigs with an average size of 783 kb (table S2) covering 811 Mb (~82%) of the estimated 995 Mb (*12*) constituting chromosome 3B.

Contig assembly was validated through BAC library screening with markers derived from BAC-end sequences (BESs) (*13*) and by genetic mapping (*11*). Out of 421 markers derived from BESs, 369 (88%) correctly identified the BAC clones belonging to computationally identified contigs. Conversely, 35 markers originating from the same contigs mapped to the same genetic

[1]Institut National de la Recherche Agronomique, Université Blaise Pascal (INRA-UBP), UMR 1095, Genetics Diversity and Ecophysiology of Cereals, Clermont-Ferrand, France. [2]Institute of Evolution, University of Haifa, Haifa, Israel. [3]Department of Plant Sciences, North Dakota State University, Fargo, ND, USA. [4]Commonwealth Scientific and Industrial Research Organization Plant Industry, Canberra, Australia. [5]Agriculture and Agri-Food Canada, Cereal Research Centre, Winnipeg, Canada. [6]Diversity Arrays Technology, Yarralumla, Canberra, Australia. [7]INRA–Unité de Recherches en Génomique-Info, Versailles, France. [8]INRA–Centre National de Ressources Génomiques Végétales, Toulouse, France. [9]International Wheat Genome Sequencing Consortium, Eversole Associates, Bethesda, MD, USA. [10]Centre for Comparative Genomics, Murdoch University, Perth, Australia. [11]Laboratory of Molecular Cytogenetics and Cytometry, Institute of Experimental Botany, Olomouc, Czech Republic.

A Physical Map of the 1-Gigabase Bread Wheat Chromosome 3B

Etienne Paux, *et al.*

Science **322**, 101 (2008);
DOI: 10.1126/science.1161847

Science (print ISSN 0036-8075; online ISSN 1095-9203) is published weekly, except the last week in December, by the American Association for the Advancement of Science, 1200 New York Avenue NW, Washington, DC 20005.

35. E. R. Wood, P. A. Dudchenko, H. Eichenbaum, *Nature* **397**, 613 (1999).
36. C. M. Bird, N. Burgess, *Nat. Rev. Neurosci.* **9**, 182 (2008).
37. We thank the patients for their cooperation and participation in this study. We also thank E. Ho, B. Scott, E. Behnke, R. Kadivar, T. Fields, A. Postolova, K. Laird, C. Wilson, R. Quian-Quiroga, A. Kraskov, F. Mormann, and M. Cerf for assistance with data acquisition; B. Salaz and I. Wainwright for administrative help; and I. Kahn, Y. Nir, G. Buzsáki, E. Pastalkova, and S. Gilaie-Dotan for discussions and comments on this manuscript. This work was supported by NINDS (to I. Fried), Israel Science Foundation (to R. Malach), Binational United States–Israel grant (to I. Fried and R. Malach), and Human Frontier Science Program Organization (HFSPO) fellowship (to R. Mukamel).

Supporting Online Material
www.sciencemag.org/cgi/content/full/1164685/DC1
Materials and Methods
Figs. S1 to S15
Table S1
References
Movies S1 and S2

14 August 2008; accepted 28 August 2008
Published online 4 September 2008;
10.1126/science.1164685
Include this information when citing this paper.

A Physical Map of the 1-Gigabase Bread Wheat Chromosome 3B

Etienne Paux,[1] Pierre Sourdille,[1] Jérôme Salse,[1] Cyrille Saintenac,[1] Frédéric Choulet,[1] Philippe Leroy,[1] Abraham Korol,[2] Monika Michalak,[3] Shahryar Kianian,[3] Wolfgang Spielmeyer,[4] Evans Lagudah,[4] Daryl Somers,[5] Andrzej Kilian,[6] Michael Alaux,[7] Sonia Vautrin,[8] Hélène Bergès,[8] Kellye Eversole,[9] Rudi Appels,[10] Jan Safar,[11] Hana Simkova,[11] Jaroslav Dolezel,[11] Michel Bernard,[1] Catherine Feuillet[1]

As the staple food for 35% of the world's population, wheat is one of the most important crop species. To date, sequence-based tools to accelerate wheat improvement are lacking. As part of the international effort to sequence the 17–billion–base-pair hexaploid bread wheat genome ($2n = 6x = 42$ chromosomes), we constructed a bacterial artificial chromosome (BAC)–based integrated physical map of the largest chromosome, 3B, that alone is 995 megabases. A chromosome-specific BAC library was used to assemble 82% of the chromosome into 1036 contigs that were anchored with 1443 molecular markers, providing a major resource for genetic and genomic studies. This physical map establishes a template for the remaining wheat chromosomes and demonstrates the feasibility of constructing physical maps in large, complex, polyploid genomes with a chromosome-based approach.

Among plants providing food for humans and animals, one of the oldest and most widespread is wheat (*Triticum aestivum* L.). Despite its socioeconomic importance and the challenges that agriculture is facing today (*1*), wheat genomics and its application to crop improvement are lagging behind those of most other important crops. The wheat genome has always been viewed as impossible to sequence because of its large amount of repetitive sequences (>80%) and its size of 17 Gb, which is five times larger than the human genome. The largest wheat chromosome (3B) alone is more than twice the size of the entire 370-Mb rice genome (*2*), whereas the entire maize genome (2.6 Gb) is about the size of three wheat chromosomes (table S1). Further complicating the challenge, bread wheat is a relatively recent hexaploid ($2n = 6x = 42$) containing three homoeologous A, B, and D genomes of related progenitor species, meiotic recombination is not distributed homogeneously along the chromosomes, and intervarietal polymorphism is very low.

Genome sequencing is the foundation for understanding the molecular basis of phenotypic variation, accelerating breeding, and improving the exploitation of genetic diversity to develop new crop varieties with increased yield and improved resistance to biotic and abiotic stresses. These new varieties will be critical for meeting the challenges of the 21st century, such as climatic changes, modifications of diets, human population growth, and the increased demand for biofuels. Physical maps are essential for high-quality sequence assembly regardless of the sequencing strategy used [such as bacterial artificial chromosome (BAC)–by–BAC or whole-genome shotgun strategies], and they will remain pivotal for de novo sequencing even with the advent of short-read technologies (*3*). As the foundation for genome sequencing, physical maps have been established for a dozen plants species so far, including cereals such as maize, rice, and sorghum (*4*–*6*). Recently, the development of new genomic resources for analyzing wheat paved the way for physically mapping and ultimately sequencing a species for which this was unthinkable a few years ago.

A physical map with 10-fold coverage of the 17-Gb bread wheat genome would require more than 1.4 million BAC clones to be fingerprinted, assembled into contigs, and anchored to genetic maps. Although whole-genome BAC libraries are available and fingerprinting millions of BAC clones is technically feasible with high-information-content fingerprinting (HICF) (*7*), assembly to accurately depict individual chromosomes and the anchoring of homoeologous BAC contigs onto genetic maps remains daunting. To address these issues, we used a chromosome-based approach (*8*) to construct a physical map of the largest hexaploid wheat chromosome (3B) and, to compensate for the inherent limits of the wheat genome (the lack of recombination and polymorphism), we deployed a combination of genetic mapping strategies for anchoring the physical map.

Fingerprinting and contig assembly were performed with BAC clones originating from sorted 3B wheat chromosomes of Chinese Spring (*9*), the reference cultivar chosen for genome sequencing by the International Wheat Genome Sequencing Consortium because of its previous use for cytogenetic studies and the availability of a set of aneuploid lines (*10*). 67,968 3B BAC clones were fingerprinted with a modified (*11*) HICF SNaPshot protocol (*7*), and a total of 56,952 high-quality fingerprints (84%) was obtained. A first automated assembly (*11*) resulted in a final build of 1991 contigs with an average size of 482 kb for a total length of 960 Mb (table S2). One hundred ninety-seven contigs were larger than 1 Mb; the largest was 3852 kb in size. A minimal tiling path (MTP) consisting of 7440 overlapping BAC clones was defined for further analyses. After the preliminary automated assembly, contigs were merged manually (*11*), resulting in a final assembly of 1036 contigs with an average size of 783 kb (table S2) covering 811 Mb (~82%) of the estimated 995 Mb (*12*) constituting chromosome 3B.

Contig assembly was validated through BAC library screening with markers derived from BAC-end sequences (BESs) (*13*) and by genetic mapping (*11*). Out of 421 markers derived from BESs, 369 (88%) correctly identified the BAC clones belonging to computationally identified contigs. Conversely, 35 markers originating from the same contigs mapped to the same genetic

[1]Institut National de la Recherche Agronomique, Université Blaise Pascal (INRA-UBP), UMR 1095, Genetics Diversity and Ecophysiology of Cereals, Clermont-Ferrand, France. [2]Institute of Evolution, University of Haifa, Haifa, Israel. [3]Department of Plant Sciences, North Dakota State University, Fargo, ND, USA. [4]Commonwealth Scientific and Industrial Research Organization Plant Industry, Canberra, Australia. [5]Agriculture and Agri-Food Canada, Cereal Research Centre, Winnipeg, Canada. [6]Diversity Arrays Technology, Yarralumla, Canberra, Australia. [7]INRA–Unité de Recherches en Génomique-Info, Versailles, France. [8]INRA–Centre National de Ressources Génomiques Végétales, Toulouse, France. [9]International Wheat Genome Sequencing Consortium, Eversole Associates, Bethesda, MD, USA. [10]Centre for Comparative Genomics, Murdoch University, Perth, Australia. [11]Laboratory of Molecular Cytogenetics and Cytometry, Institute of Experimental Botany, Olomouc, Czech Republic.

locus. The wheat genome has a high content of long terminal repeat retrotransposons (> 67%) (*13*) and a large number of tandemly repeated sequences, which may result in the misassembly of BAC clones. A statistical analysis (*11*) indicated that less than 10% of the fragments were randomly shared between any two nonoverlapping BAC clones. We calculated that approximately 58% overlap between fingerprints was required for automated assembly (fig. S1), and therefore with the high stringency (Sulston score = le = 75) used for the assembly (*11*), the repeated sequences did not affect the quality of the contig build.

The physical map was anchored with 685 microsatellites [simple sequence repeats (SSRs)], some of which were designed from the BESs, as well as expressed sequence tag (EST) markers (table S3) previously mapped to chromosome 3B (*14*) and identified on the basis of their synteny with rice chromosome 1. In total, 291 SSR markers were anchored to 203 contigs representing 219 Mb, and 394 ESTs were anchored to 250 individual contigs representing 283 Mb (Fig. 1 and table S3). Four hundred seventy-two additional contigs representing 452 Mb were then anchored with 711 insertion site–based polymorphism (ISBP) markers derived from 19,400 BESs (*13*) (Fig. 1 and table S3). We also tested the multiplexed and genomewide Diversity Arrays Technology (DArT) (*15*) by hybridizing a wheat array composed of 5000 DArT markers with three-dimensional pools of the MTP (*11*). Thirty-five DArTs were unambiguously assigned and anchored to 25 individual contigs (19 Mb) (table S3).

In total, 1443 molecular markers were linked to 680 BAC contigs representing 611 Mb and 75% of the 3B physical map. The longer contigs were anchored more easily (fig. S2), and more than 80% of contigs longer than 900 kb were anchored. Very few contigs (50, <80 Mb) were anchored with all marker types, and most (463 out of 680) were anchored by a single marker type (Fig. 1). This indicates that the different classes of markers cover different regions of the genome and should be used in combination to ensure optimal representation of the chromosome.

The anchored physical map can expedite map-based cloning, but its full value is achieved by determining the relative contig order along the chromosome and producing an integrated physical map. To integrate the 3B physical map, we used deletion mapping [in which the absence of two genetic sites in the same deletion line (that is, one of many lines containing small deletions in specific sites along the chromosome) is a measure of the maximal distance between them] and meiotic mapping (in which the relative order of markers is determined on the basis of recombination). This combined approach was necessary because in wheat, the resolution of meiotic mapping is limited by both the nonhomogeneous distribution of recombination events along the chromosome arms (for example, on chromosome 3B, 42% of the physical map length is represented by only 2.2% of the genetic map length in the centromeric regions) and the low level of polymorphism in the cultivated pool.

Deletion mapping resulted in the integration of 599 contigs (556 Mb, ~56% of the chromosome) in 16 physical intervals along chromosome 3B (table S3). To assess whether our physical map accurately depicts 3B, we systematically compared the total size of the contigs present in the 16 intervals defined by genetic deletions (so-called deletion bins) with the size of the genetic deletion as estimated cytologically from the chromosomes in the corresponding deletion line stocks (*16*) (table S3). Coverage within the bins ranged from 33 to 99%, with an average of 56% (fig. S3). The most terminal bin on the short arm (bin 3BS3-0.87-1.00) was only 10% covered and had a smaller average contig size (630 kb) than other bins (957 kb), suggesting that the telomeric and heterochromatic region of the short arm may be underrepresented in our BAC library.

We tested high-resolution radiation hybrid (RH) mapping, which relies on lines carrying specific radiation-induced chromosomal fragments in nonhomoeologous backgrounds (*17*) and measures the distance between genetic sites as the frequency with which they remain together after fragmentation. A panel of 184 RH lines developed for chromosome 3B (*11*) was tested with 65 ISBP markers (table S5) and indicated a resolution of about 263 kb per break. In addition, with a limited set of critical RH lines, we were able to order 35 loci (32 contigs) previously assigned to 3BL7-0.63-1.00 (table S5). We are in the process of increasing the number of RH lines for mapping all the contigs along chromosome 3B.

Further integration of the 3B physical map was achieved through meiotic mapping with a reference genetic map developed from an F_2 population (CsRe) derived from a cross between Chinese Spring (Cs) and the French cultivar Renan (Re). Because the physical contigs originate from Chinese Spring, anchoring them to the CsRe genetic map guarantees high accuracy in ordering. Because BAC libraries are available for both cultivars, this physical map also provides an efficient platform for single-nucleotide polymorphism discovery. To date, 102 SSR and ISBP markers have been mapped with 376 F_2 individuals of the CsRe population (*11*). Eighty-nine of them were anchored to contigs, permitting the integration of 75 individual contigs (77 Mb) to the genetic map, of which 80% (60/75) were ordered. Using the same criteria as the IBM Neighbors map of maize (*18*), we also established a 3B neighbor map (*11*) containing 636 SSR, restriction fragment length polymorphism, sequence tagged site (STS), DArT, and ISBP markers (table S6). In total, 213 contigs were anchored on this map, providing 225 Mb of sequence information for map-based cloning. A Gbrowse interface displaying the integrated chromosome 3B physical map is available at http://urgi.versailles.inra.fr/projects/Triticum/eng/index.php.

We also aligned the wheat 3B physical map against the rice genome using the genic sequences (ESTs/STSs) present on the 75 contigs integrated to the CsRe genetic map (*11*). Twenty-seven contigs carried 49 ESTs/STSs with homology to 56 orthologous rice genes, including 14 contigs located in the terminal part of the short arm of chromosome 3B, which is collinear with rice chromosome 1S (table S7). In this region, we identified four inversions as well as noncol-

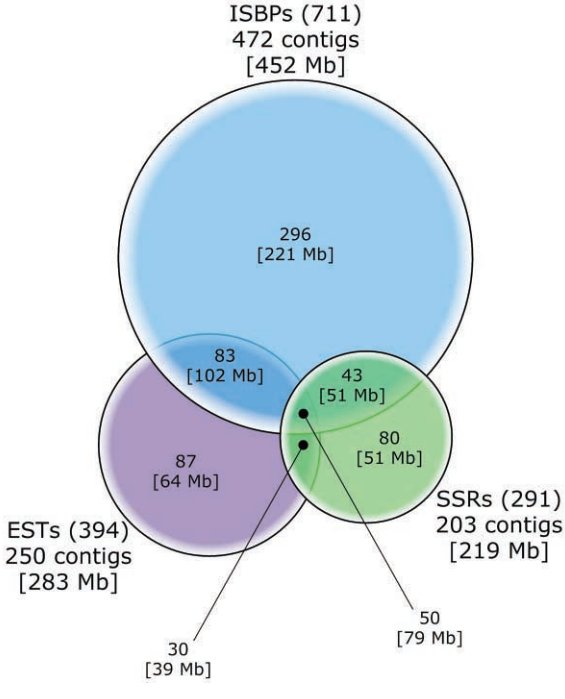

Fig. 1. Relative contribution of ISBP, EST, and SSR markers for anchoring the 3B physical map. Markers found in BAC contigs are indicated in parentheses after the marker type. The numbers of contigs anchored, as well as their physical size (in brackets), are provided for each marker type. The Venn diagram illustrates the relative contribution of each marker type, with the number and total size of contigs anchored by one or more types of markers.

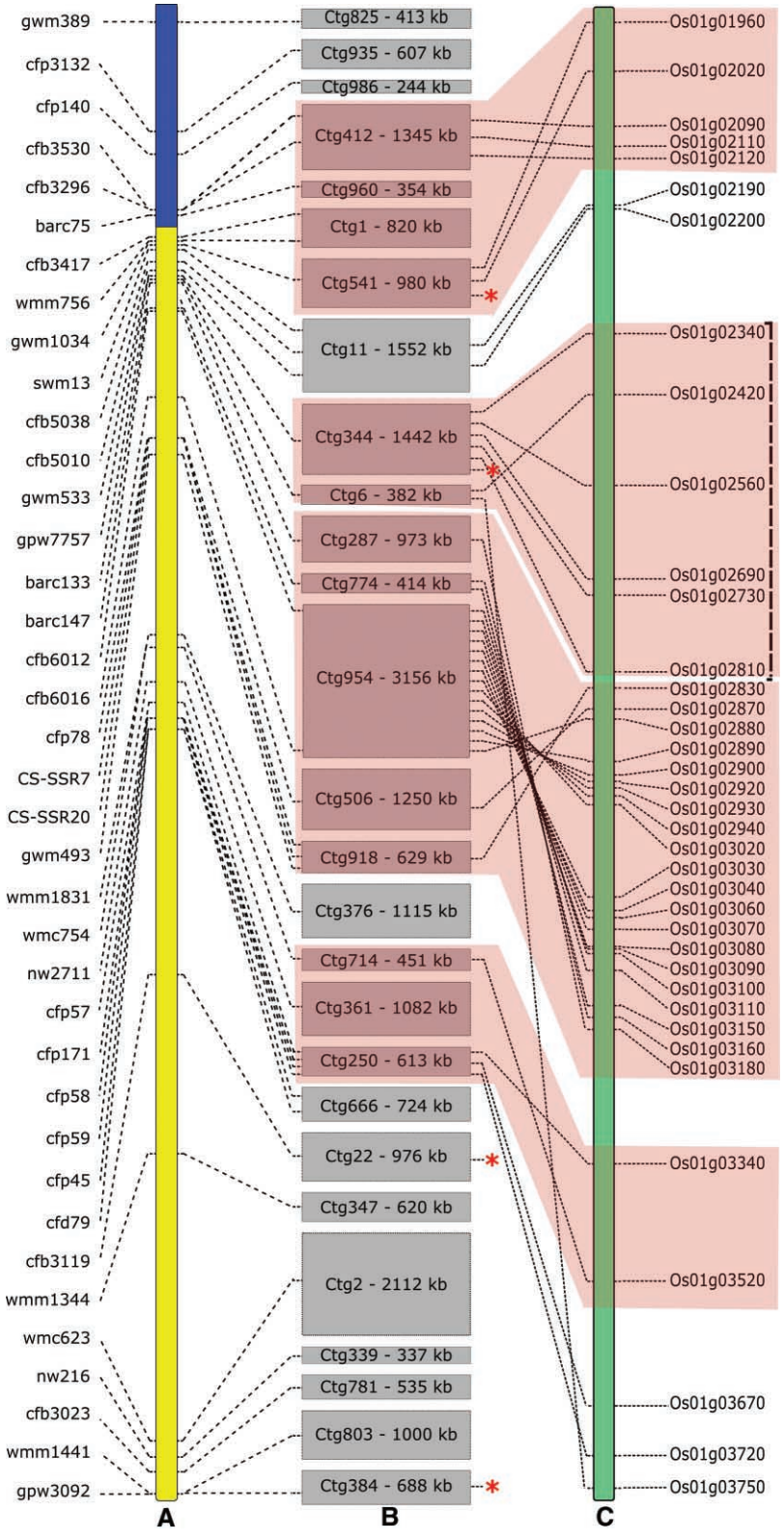

Fig. 2. Integrated physical map at the telomeric end of chromosome 3BS and colinearity with rice. (**A**) Genetic map of wheat chromosome 3B. The blue and yellow sectors represent the two distal deletion bins 3BS3-0.87-1.00 and 3BS8-0.78-0.87, respectively. (**B**) BAC contigs integrated to the genetic map. The names and sizes of the 27 contigs are displayed in gray boxes, the sizes of which reflect the relative contig sizes. (**C**) Rice chromosome 1. Each line represents the relationship between an EST located in a wheat BAC contig and the orthologous rice gene. The red sectors indicate rearrangements between the two chromosomes. The four red asterisks designate wheat ESTs for which rice orthologs were found on noncollinear regions or chromosomes other than chromosome 1. The vertical dashed bracket represents a region containing more than 30 kinase-related genes in rice.

linear genes (Fig. 2). This confirms, with a higher degree of resolution, rearrangements observed by deletion mapping between the two most conserved wheat and rice chromosomes (*19*) and suggests that many local rearrangements have occurred in globally collinear regions since the divergence of wheat and rice more than 50 million years ago. This result also indicates that predicting gene order from sequenced genomes that are not closely related so as to order the physical maps of other genomes requires great caution.

To date, less than a dozen wheat genes have been isolated through map-based cloning. About 40 genes and quantitative trait loci (QTLs) have been identified on chromosome 3B (http://wheat.pw.usda.gov/GG2/maps.shtml) and none have been cloned. Seventeen contigs representing 16.8 Mb are anchored with markers flanking or cosegregating with 16 of these genes and QTLs on our physical map (table S8). With an average contig size of 783 kb, the chromosome 3B physical map allows one to land on any target locus, in a single step, provided that recombination is compatible with fine mapping of the target gene. This has been carried out for the stem rust resistance gene *Sr2* (*20*) and the QTL *Fhb1* conferring resistance to Fusarium head blight (*21*) (table S8). The 3B physical map also provides the foundation for sequencing and in-depth studies of the wheat genome composition and organization. Sequencing and annotation are under way for 13 BAC contigs of 800 kb to 3.2 Mb, originating from different regions of chromosome 3B. These large sequenced regions will also aid in SSR and ISBP marker development. Finally, a 15-fold coverage physical map is under way for future chromosome 3B sequencing, which is envisaged for the near future.

By establishing a physical map of the largest wheat chromosome, we demonstrate that the chromosome-based approach is feasible and suitable for the construction of the hexaploid wheat genome physical map. With this physical map, the structure of agronomically important target loci can be defined in a single step and marker development can be accelerated (*22*), opening up new possibilities for accessing regions important for yield, disease resistance, and trait improvement in wheat. An international collaborative effort is under way now to exploit this new resource and, using the same strategy, projects have begun for the 20 remaining chromosomes (table S1; www.ueb.cas.cz/Olomouc1/LMCC/Resources/resources.html#chrs and www.wheatgenome.org/projects.php), opening the way to future sequencing of the wheat genome.

Finally, although chromosome sorting has so far been applied only to a few other cereals [barley, durum wheat, and rye (*8*)], important legumes (pea and bean), and trees (Norway spruce) (*23*), this work exemplifies its broader potential for other complex nonmodel genomes heretofore considered impossible to sequence

despite their socioeconomic importance. Until now, the selection of genomes for sequencing has been determined on the basis of genome simplicity and not agronomic relevance, with serious consequences for crop improvement and food security [for example, by neglecting wheat or choosing the diploid of cotton, *Gossypium raimondii*, to sequence first rather than focusing on the economically important tetraploid *G. hirsutum* (*24*)]. Our work may pave the way for a major change in how the next genomes for de novo sequencing are selected, thereby accelerating improvements in economically important crop species.

References and Notes

1. B. Wollenweber *et al.*, *Curr. Opin. Plant Biol.* **8**, 337 (2005).
2. T. Itoh *et al.*, *Genome Res.* **17**, 175 (2007).
3. R. L. Warren *et al.*, *Genome Res.* **16**, 768 (2006).
4. M. Chen *et al.*, *Plant Cell* **14**, 537 (2002).
5. P. E. Klein *et al.*, *Genome Res.* **10**, 789 (2000).
6. F. Wei *et al.*, *PLoS Genet.* **3**, e123 (2007).
7. M. C. Luo *et al.*, *Genomics* **82**, 378 (2003).
8. J. Dolezel *et al.*, *Chromosome Res.* **15**, 51 (2007).
9. J. Safar *et al.*, *Plant J.* **39**, 960 (2004).
10. T. R. Endo, B. S. Gill, *J. Hered.* **87**, 295 (1996).
11. Materials and methods are available as supporting material on *Science* Online.
12. B. S. Gill *et al.*, *Genome* **34**, 830 (1991).
13. E. Paux *et al.*, *Plant J.* **48**, 463 (2006).
14. J. D. Munkvold *et al.*, *Genetics* **168**, 639 (2004).
15. M. Akbari *et al.*, *Theor. Appl. Genet.* **113**, 1409 (2006).
16. M. Dilbirligi *et al.*, *Genetics* **166**, 461 (2004).
17. K. G. Hossain *et al.*, *Genetics* **168**, 415 (2004).
18. K. C. Cone *et al.*, *Plant Physiol.* **130**, 1598 (2002).
19. M. La Rota, M. E. Sorrells, *Funct. Integr. Genomics* **4**, 34 (2004).
20. R. Kota *et al.*, *Theor. Appl. Genet.* **112**, 492 (2006).
21. S. Liu *et al.*, *Funct. Integr. Genomics* **6**, 83 (2006).
22. M. D. McNeil *et al.*, *Mol. Breed.* **22**, 15 (2008).
23. J. Dolezel *et al.*, *Chromosome Res.* **12**, 77 (2004).
24. Z. J. Chen *et al.*, *Plant Physiol.* **145**, 1303 (2007).

25. We thank D. Boyer, K. Paux, and members of the GENTYANE platform for technical assistance; M. Ganal (Trait Genetics), P. Jack (RAGT), and F. Azanza (Syngenta) for providing SSR markers and genotyping data; the support of F. Legeai and D. Steinbach from Unité de Recherche en Génomique-Info in establishing the Gbrowse display of the integrated physical map; A. Kumar (Choudhury Charan Singh University Meerut), O. Riera-Lizarazu (Oregon State University), and Y. Gu (U.S. Department of Agriculture–Agricultural Research Service) for significant contributions to the RH mapping work; and F. Quetier (Agence Nationale de la Recherche) for support and discussions. Supported by the Agence Nationale de la Recherche (grant ANR-05-BLANC-0258-01) and the INRA.

Supporting Online Material

www.sciencemag.org/cgi/content/full/322/5898/101/DC1
Materials and Methods
Figs. S1 to S3
Tables S1 to S8
References

16 June 2008; accepted 10 September 2008
10.1126/science.1161847

High-Quality Binary Protein Interaction Map of the Yeast Interactome Network

Haiyuan Yu,[1,2]* Pascal Braun,[1,2]* Muhammed A. Yıldırım,[1,2,3]* Irma Lemmens,[4] Kavitha Venkatesan,[1,2] Julie Sahalie,[1,2] Tomoko Hirozane-Kishikawa,[1,2] Fana Gebreab,[1,2] Na Li,[1,2] Nicolas Simonis,[1,2] Tong Hao,[1,2] Jean-François Rual,[1,2] Amélie Dricot,[1,2] Alexei Vazquez,[5] Ryan R. Murray,[1,2] Christophe Simon,[1,2] Leah Tardivo,[1,2] Stanley Tam,[1,2] Nenad Svrzikapa,[1,2] Changyu Fan,[1,2] Anne-Sophie de Smet,[4] Adriana Motyl,[6] Michael E. Hudson,[6] Juyong Park,[1,7] Xiaofeng Xin,[8] Michael E. Cusick,[1,2] Troy Moore,[9] Charlie Boone,[8] Michael Snyder,[6] Frederick P. Roth,[1,10] Albert-László Barabási,[1,7] Jan Tavernier,[4] David E. Hill,[1,2] Marc Vidal[1,2]†

Current yeast interactome network maps contain several hundred molecular complexes with limited and somewhat controversial representation of direct binary interactions. We carried out a comparative quality assessment of current yeast interactome data sets, demonstrating that high-throughput yeast two-hybrid (Y2H) screening provides high-quality binary interaction information. Because a large fraction of the yeast binary interactome remains to be mapped, we developed an empirically controlled mapping framework to produce a "second-generation" high-quality, high-throughput Y2H data set covering ~20% of all yeast binary interactions. Both Y2H and affinity purification followed by mass spectrometry (AP/MS) data are of equally high quality but of a fundamentally different and complementary nature, resulting in networks with different topological and biological properties. Compared to co-complex interactome models, this binary map is enriched for transient signaling interactions and intercomplex connections with a highly significant clustering between essential proteins. Rather than correlating with essentiality, protein connectivity correlates with genetic pleiotropy.

A crucial step toward understanding cellular systems properties is mapping networks of physical DNA-, RNA-, and protein-protein interactions, the "interactome network," of an organism of interest as completely and accurately as possible. One approach consists in systematically testing all pairwise combinations of predicted proteins to derive the "binary" interactome. Early attempts at binary interactome mapping used high-throughput yeast two-hybrid (Y2H) screening, in which a protein interaction reconstitutes a transcription factor that activates expression of reporter genes. High-throughput Y2H maps have been generated for *Saccharomyces cerevisiae* (*1*–*3*), *Caenorhabditis elegans* (*4*–*6*), *Drosophila melanogaster* (*7*), and humans (*8*–*10*). An alternative approach consists in generating "co-complex" interactome maps, achievable by high-throughput coaffinity purification followed by mass spectrometry (AP/MS) to identify proteins bound to tagged baits, as done for *Escherichia coli* (*11*, *12*), *S. cerevisiae* (*13*–*16*), and humans (*17*).

To investigate fundamental questions of interactome network structure and function, it is necessary to understand how the size and quality of currently available maps, including thorough evaluation of differences between binary and co-complex maps, might have affected conclusions about global and local properties of interactome networks (*18*, *19*). Here, we address these issues using the yeast *S. cerevisiae* as a model system.

First, we compared the quality of existing high-throughput binary and co-complex data sets to information obtained from curating low-throughput experiments described in the literature (Fig. 1A). For binary interactions, we examined (i) the subset found by Uetz *et al.* in a proteome-scale all-by-all screen ("Uetz-screen"), excluding the pairs found in a focused, potentially biased experiment involving only 193 baits ("Uetz-array") (*2*); and (ii) the Ito *et al.* interactions found three times or more ("Ito-core"), independently from those found one or two times ("Ito-noncore"), a distinction recommended by the authors but seldom applied in the literature (*3*). For co-complex associations, we investigated two high-throughput AP/MS data sets referred to as "Gavin" (*15*) and "Krogan" (*16*). For literature-curated interactions, we considered only those curated from two or more publications ("LC-multiple") (*20*), which we judged of higher quality than those curated from a single publication.

To experimentally compare the quality of these data sets, we selected a representative sample of ~200 protein interaction pairs from each one and tested them by means of two independent interaction assays, Y2H and a yellow fluorescent protein complementation assay (PCA) (*21*) [Supporting Online Material (SOM) I]. In PCA, bait and prey proteins are fused to nonfluorescent fragments of yellow fluorescent protein that, when brought in close proximity by interacting proteins, reconstitute a fluorescent protein in mammalian cells. In con-

High-Quality Binary Protein Interaction Map of the Yeast Interactome Network

Haiyuan Yu, *et al.*

Science **322**, 104 (2008);
DOI: 10.1126/science.1158684

Science (print ISSN 0036-8075; online ISSN 1095-9203) is published weekly, except the last week in December, by the American Association for the Advancement of Science, 1200 New York Avenue NW, Washington, DC 20005.

despite their socioeconomic importance. Until now, the selection of genomes for sequencing has been determined on the basis of genome simplicity and not agronomic relevance, with serious consequences for crop improvement and food security [for example, by neglecting wheat or choosing the diploid of cotton, *Gossypium raimondii*, to sequence first rather than focusing on the economically important tetraploid *G. hirsutum* (*24*)]. Our work may pave the way for a major change in how the next genomes for de novo sequencing are selected, thereby accelerating improvements in economically important crop species.

References and Notes

1. B. Wollenweber *et al.*, *Curr. Opin. Plant Biol.* **8**, 337 (2005).
2. T. Itoh *et al.*, *Genome Res.* **17**, 175 (2007).
3. R. L. Warren *et al.*, *Genome Res.* **16**, 768 (2006).
4. M. Chen *et al.*, *Plant Cell* **14**, 537 (2002).
5. P. E. Klein *et al.*, *Genome Res.* **10**, 789 (2000).
6. F. Wei *et al.*, *PLoS Genet.* **3**, e123 (2007).
7. M. C. Luo *et al.*, *Genomics* **82**, 378 (2003).
8. J. Dolezel *et al.*, *Chromosome Res.* **15**, 51 (2007).
9. J. Safar *et al.*, *Plant J.* **39**, 960 (2004).
10. T. R. Endo, B. S. Gill, *J. Hered.* **87**, 295 (1996).
11. Materials and methods are available as supporting material on *Science* Online.
12. B. S. Gill *et al.*, *Genome* **34**, 830 (1991).
13. E. Paux *et al.*, *Plant J.* **48**, 463 (2006).
14. J. D. Munkvold *et al.*, *Genetics* **168**, 639 (2004).
15. M. Akbari *et al.*, *Theor. Appl. Genet.* **113**, 1409 (2006).
16. M. Dilbirligi *et al.*, *Genetics* **166**, 461 (2004).
17. K. G. Hossain *et al.*, *Genetics* **168**, 415 (2004).
18. K. C. Cone *et al.*, *Plant Physiol.* **130**, 1598 (2002).
19. M. La Rota, M. E. Sorrells, *Funct. Integr. Genomics* **4**, 34 (2004).
20. R. Kota *et al.*, *Theor. Appl. Genet.* **112**, 492 (2006).
21. S. Liu *et al.*, *Funct. Integr. Genomics* **6**, 83 (2006).
22. M. D. McNeil *et al.*, *Mol. Breed.* **22**, 15 (2008).
23. J. Dolezel *et al.*, *Chromosome Res.* **12**, 77 (2004).
24. Z. J. Chen *et al.*, *Plant Physiol.* **145**, 1303 (2007).

25. We thank D. Boyer, K. Paux, and members of the GENTYANE platform for technical assistance; M. Ganal (Trait Genetics), P. Jack (RAGT), and F. Azanza (Syngenta) for providing SSR markers and genotyping data; the support of F. Legeai and D. Steinbach from Unité de Recherche en Génomique-Info in establishing the Gbrowse display of the integrated physical map; A. Kumar (Choudhury Charan Singh University Meerut), O. Riera-Lizarazu (Oregon State University), and Y. Gu (U.S. Department of Agriculture–Agricultural Research Service) for significant contributions to the RH mapping work; and F. Quetier (Agence Nationale de la Recherche) for support and discussions. Supported by the Agence Nationale de la Recherche (grant ANR-05-BLANC-0258-01) and the INRA.

Supporting Online Material

www.sciencemag.org/cgi/content/full/322/5898/101/DC1
Materials and Methods
Figs. S1 to S3
Tables S1 to S8
References

16 June 2008; accepted 10 September 2008
10.1126/science.1161847

High-Quality Binary Protein Interaction Map of the Yeast Interactome Network

Haiyuan Yu,[1,2]* Pascal Braun,[1,2]* Muhammed A. Yıldırım,[1,2,3]* Irma Lemmens,[4] Kavitha Venkatesan,[1,2] Julie Sahalie,[1,2] Tomoko Hirozane-Kishikawa,[1,2] Fana Gebreab,[1,2] Na Li,[1,2] Nicolas Simonis,[1,2] Tong Hao,[1,2] Jean-François Rual,[1,2] Amélie Dricot,[1,2] Alexei Vazquez,[5] Ryan R. Murray,[1,2] Christophe Simon,[1,2] Leah Tardivo,[1,2] Stanley Tam,[1,2] Nenad Svrzikapa,[1,2] Changyu Fan,[1,2] Anne-Sophie de Smet,[4] Adriana Motyl,[6] Michael E. Hudson,[6] Juyong Park,[1,7] Xiaofeng Xin,[8] Michael E. Cusick,[1,2] Troy Moore,[9] Charlie Boone,[8] Michael Snyder,[6] Frederick P. Roth,[1,10] Albert-László Barabási,[1,7] Jan Tavernier,[4] David E. Hill,[1,2] Marc Vidal[1,2]†

Current yeast interactome network maps contain several hundred molecular complexes with limited and somewhat controversial representation of direct binary interactions. We carried out a comparative quality assessment of current yeast interactome data sets, demonstrating that high-throughput yeast two-hybrid (Y2H) screening provides high-quality binary interaction information. Because a large fraction of the yeast binary interactome remains to be mapped, we developed an empirically controlled mapping framework to produce a "second-generation" high-quality, high-throughput Y2H data set covering ~20% of all yeast binary interactions. Both Y2H and affinity purification followed by mass spectrometry (AP/MS) data are of equally high quality but of a fundamentally different and complementary nature, resulting in networks with different topological and biological properties. Compared to co-complex interactome models, this binary map is enriched for transient signaling interactions and intercomplex connections with a highly significant clustering between essential proteins. Rather than correlating with essentiality, protein connectivity correlates with genetic pleiotropy.

A crucial step toward understanding cellular systems properties is mapping networks of physical DNA-, RNA-, and protein-protein interactions, the "interactome network," of an organism of interest as completely and accurately as possible. One approach consists in systematically testing all pairwise combinations of predicted proteins to derive the "binary" interactome. Early attempts at binary interactome mapping used high-throughput yeast two-hybrid (Y2H) screening, in which a protein interaction reconstitutes a transcription factor that activates expression of reporter genes. High-throughput Y2H maps have been generated for *Saccharomyces cerevisiae* (*1*–*3*), *Caenorhabditis elegans* (*4*–*6*), *Drosophila melanogaster* (*7*), and humans (*8*–*10*). An alternative approach consists in generating "co-complex" interactome maps, achievable by high-throughput coaffinity purification followed by mass spectrometry (AP/MS) to identify proteins bound to tagged baits, as done for *Escherichia coli* (*11*, *12*), *S. cerevisiae* (*13*–*16*), and humans (*17*).

To investigate fundamental questions of interactome network structure and function, it is necessary to understand how the size and quality of currently available maps, including thorough evaluation of differences between binary and co-complex maps, might have affected conclusions about global and local properties of interactome networks (*18*, *19*). Here, we address these issues using the yeast *S. cerevisiae* as a model system.

First, we compared the quality of existing high-throughput binary and co-complex data sets to information obtained from curating low-throughput experiments described in the literature (Fig. 1A). For binary interactions, we examined (i) the subset found by Uetz *et al.* in a proteome-scale all-by-all screen ("Uetz-screen"), excluding the pairs found in a focused, potentially biased experiment involving only 193 baits ("Uetz-array") (*2*); and (ii) the Ito *et al.* interactions found three times or more ("Ito-core"), independently from those found one or two times ("Ito-noncore"), a distinction recommended by the authors but seldom applied in the literature (*3*). For co-complex associations, we investigated two high-throughput AP/MS data sets referred to as "Gavin" (*15*) and "Krogan" (*16*). For literature-curated interactions, we considered only those curated from two or more publications ("LC-multiple") (*20*), which we judged of higher quality than those curated from a single publication.

To experimentally compare the quality of these data sets, we selected a representative sample of ~200 protein interaction pairs from each one and tested them by means of two independent interaction assays, Y2H and a yellow fluorescent protein complementation assay (PCA) (*21*) [Supporting Online Material (SOM) I]. In PCA, bait and prey proteins are fused to nonfluorescent fragments of yellow fluorescent protein that, when brought in close proximity by interacting proteins, reconstitute a fluorescent protein in mammalian cells. In con-

trast, reconstitution of a transcription factor in Y2H experiments takes place in the nucleus of yeast cells. In terms of assay designs, Y2H and PCA can be considered as orthogonal assays and can be used to validate each other's results.

No single assay is expected to detect 100% of genuine interactions, and the actual fraction of positives detected is inherently linked to the stringency at which the assay is implemented. To identify the optimal scoring condition of each assay, we selected a set of ~100 well-documented yeast protein-protein interaction pairs ["positive reference set" (PRS)] and a set of ~100 random pairs ["random reference set" (RRS)] (Fig. 1B; SOM II). Because RRS pairs were picked uniformly from the 14×10^6 possible pairings of proteins within our yeast ORFeome collection (*22*) (excluding those reported as interacting), these pairs are extremely unlikely to be interacting.

Sampled pairs from binary Uetz-screen and Ito-core data sets tested positive at levels as high as those of the positive-control PRS, demonstrating their high quality (Fig. 1C). A sample of literature-curated LC-multiple interactions tested slightly lower with Y2H, while being indistinguishable by PCA (Fig. 1C), demonstrating that high-throughput Y2H data sets can be comparable in quality to literature-curated information. In marked contrast, sampled pairs from Ito-noncore tested positive at levels similar to those of the negative-control RRS, confirming the low quality of this particular data set (Fig. 1C).

Sampled pairs from Gavin and Krogan high-throughput AP/MS data sets tested poorly in our two binary interaction assays (Fig. 1C), albeit at levels similar to those of Munich Information Center for Protein Sequences (MIPS) complexes, a widely used "gold standard" (*23*). This observation demonstrates that, at least for detecting binary interactions, Y2H performs better than AP/MS.

Our experimental data quality assessment shows that binary Uetz-screen, Ito-core, and LC-multiple data sets are of high quality, whereas Ito-noncore should not be used. AP/MS data sets, although of intrinsically good quality (*15*, *16*), should be used cautiously when binary interaction information is needed.

Our experimental results contrast markedly with computational analyses that suggested that high-throughput Y2H data sets contain more false-positives than literature-curated or high-throughput AP/MS data sets (*24*, *25*). In computational analyses, the quality of a data set is often determined by the fraction of interactions also present in a predefined gold standard set (*24*). Generally, MIPS complexes have been considered as gold standard, with all proteins constituting a given complex modeled as interacting with each other. Such modeling results in limited and biased sampling issues against binary interactions because not all

A

Reference	Uetz *et al.* (*2*)		Ito *et al.* (*3*)		Gavin *et al.* (*15*)	Krogan *et al.* (*16*)	Reguly *et al.* (*20*)
Dataset name	Uetz-screen	Uetz-array	Ito-core	Ito-noncore	Gavin	Krogan	LC-multiple
Number of reported interactions	682	281	843	3632	6942	7123	2925
	Binary				Co-complex		Literature

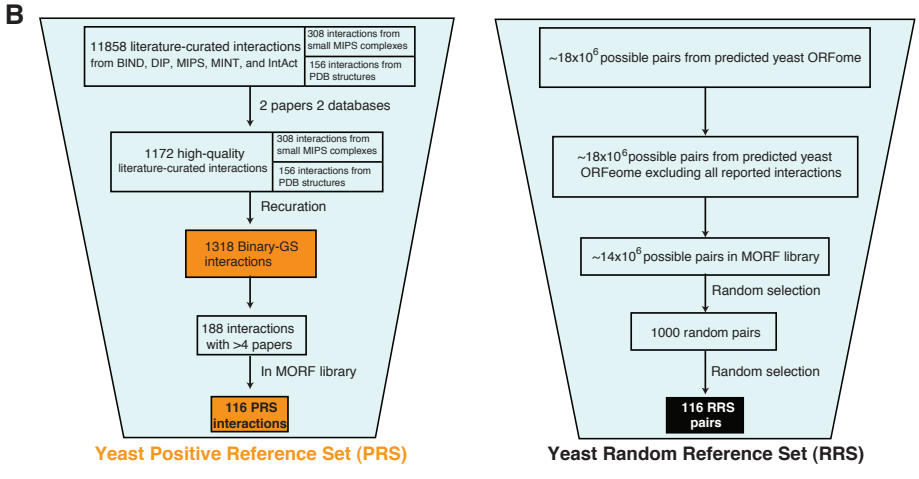

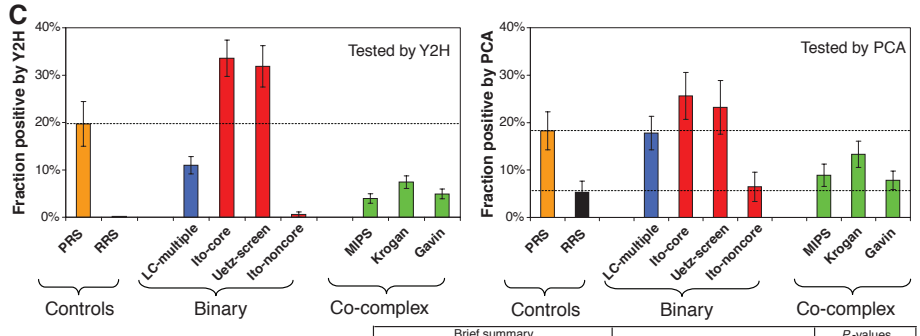

Brief summary (For detecting binary interactions)	Representative datasets	*P*-values Y2H	*P*-values PCA
1. Y2H is comparable to LC-multiple	Uetz-screen ≥ LC-multiple	$P<10^{-16}$	$P=0.1$
2. Ito-noncore is of extremely low quality	Ito-noncore ≈ RRS	$P=0.9$	$P=0.2$
3. Y2H performs better than AP/MS	Uetz-screen > Krogan	$P<10^{-30}$	$P<10^{-3}$
4. Y2H performs better than MIPS	Uetz-screen > MIPS	$P<10^{-41}$	$P<10^{-5}$

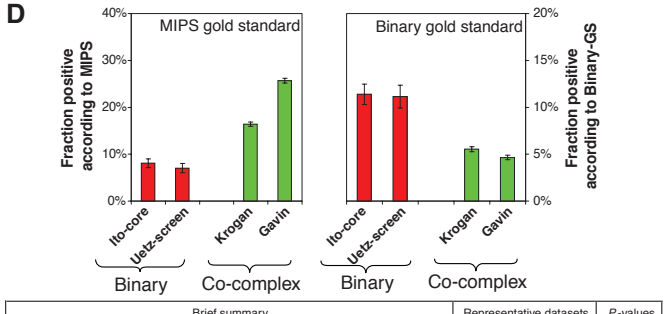

Brief summary	Representative datasets	*P*-values
1. AP/MS performs well at detecting co-complex associations according to MIPS	Uetz-screen < Krogan	$P<10^{-12}$
2. Y2H performs well at detecting binary interactions according to Binary-GS	Uetz-screen > Krogan	$P<10^{-5}$

Fig. 1. Evaluation of *S. cerevisiae* protein-protein interaction data sets. (**A**) Number of interactions reported in various large-scale *S. cerevisiae* protein-protein interaction data sets. (**B**) Schema of pipeline used to assemble binary positive and random reference sets. (**C**) Fraction of a random sample of interactions from each data set confirmed by Y2H and PCA. (**D**) Fraction of positive interactions in each data set calculated with MIPS and Binary-GS. Error bars indicate SE.

[1]Center for Cancer Systems Biology (CCSB), Dana-Farber Cancer Institute, Boston, MA 02115, USA. [2]Department of Cancer Biology, Dana-Farber Cancer Institute, and Department of Genetics, Harvard Medical School, Boston, MA 02115, USA. [3]School of Engineering and Applied Sciences, Harvard University, Cambridge, MA 02138, USA. [4]Department of Medical Protein Research, VIB, and Department of Biochemistry, Faculty of Medicine and Health Sciences, Ghent University, 9000 Ghent, Belgium. [5]The Simons Center for Systems Biology, Institute for Advanced Studies, Princeton, NJ 08540, USA. [6]Department of Molecular, Cellular, and Developmental Biology, Yale University, New Haven, CT 06620, USA. [7]Center for Complex Network Research and Departments of Physics, Biology, and Computer Science, Northeastern University, Boston, MA 02115, USA. [8]Banting and Best Department of Medical Research and Department of Medical Genetics and Microbiology, Terrence Donnelly Centre for Cellular and Biomolecular Research, University of Toronto, Toronto, ON M5S 3E1, Canada. [9]Open Biosystems, Huntsville, AL 35806, USA. [10]Department of Biological Chemistry and Molecular Pharmacology, Harvard Medical School, Boston, MA 02115, USA.

*These authors contributed equally to this work.
†To whom correspondence should be addressed. E-mail: marc_vidal@dfci.harvard.edu

proteins in a complex contact each other directly (fig. S1), and not all direct physical interactions occur within complexes (fig. S2 and SOM III). Hence, although MIPS complexes are appropriate for benchmarking co-complex membership data sets, they are not appropriate for binary interaction data sets. This distinction is corroborated by the poor experimental confirmation rate of pairs from MIPS complexes with binary assays (Fig. 1C).

To computationally reexamine the quality of existing yeast interactome data sets, we assembled a binary gold standard set ("Binary-GS") of 1318 high-confidence physical binary interactions (Fig. 1B and SOM III). Binary-GS includes direct physical interactions within well-established complexes, as well as conditional interactions (e.g., dependent on posttranslational modifications), and thus represents well-documented direct physical interactions in the yeast interactome (*26*). When measured against Binary-GS, the quality of high-throughput Y2H data sets (with the exception of Ito-noncore) was substantially better (SOM IV and V) than that of high-throughput AP/MS data sets (Fig. 1D). Our results demonstrate the distinct nature of binary and co-complex data. Generally, Y2H data sets contain high-quality direct binary interactions, whereas AP/MS co-complex data sets are composed of direct interactions mixed with preponderant indirect associations (SOM VI).

The proteome-wide binary data sets, Uetz-screen and Ito-core, contain 682 and 843 interactions, respectively (*2*, *3*). The overlap between these two data sets appears low (*3*, *24*): 19% of Uetz-screen and 15% of Ito-core interactions were detected in the other data set. Given our demonstration of high quality for these data sets (Fig. 1, C and D), we conclude that the small overlap stems primarily from low sensitivity (i.e., many false-negatives) rather than from low specificity (i.e., many false-positives, as previously suggested).

Several factors might affect sensitivity. First, the space of pairwise protein combinations actually tested in each data set might have been considerably different. We refer to the fraction of all possible pairs tested in a given screen as the "completeness." For example, missing 10% of open reading frames (ORFs) in each mapping project could reduce the common tested space down to 66% [(0.9 × 0.9) × (0.9 × 0.9)] of all possible pairwise combinations. Second, different protein interaction assays or even different versions of the same assay detect different subsets of pairs out of all possible interactions, which explains partly the limited overlap between data sets obtained with different Y2H versions. For any assay, the "assay sensitivity" is estimated as the fraction of PRS interactions detected, which for our Y2H assay was determined empirically to be ~20% (Fig. 1C). Finally, when screening tens if not hundreds of millions of protein pairs in any tested space, that search space might need to be sampled multiple times to report all or nearly all interactions detectable by the assay used. The fraction of all theoretically detectable interactions by a particular assay found in a given experiment is its "sampling sensitivity." These three parameters fully account for the seemingly small overlap between Ito-core and Uetz-screen (SOM VII), demonstrating that a large fraction of the *S. cerevisiae* binary interactome remains to be mapped. Therefore, we carried out a new proteome-scale yeast high-throughput Y2H screen (fig. S3).

We used 5796 Gateway-cloned ORFs available in the yeast movable ORF (MORF) collection (*22*). After subcloning these ORFs into Y2H vectors and removing autoactivators (*27*, *28*), our search space became 3917 DB-Xs against 5246 AD-Ys, representing a completeness of 77% (Fig. 2A and SOM VI), comparable to that of recent AP/MS data sets (*15*) (~78%; SOM VI).

To address sampling sensitivity, we determined what fraction of all detectable interactions is found in each pass after eight trials in a search space of 658 DB-X and 1249 AD-Y ORFs. A single trial identified about 60% of all possible interactions that can be detected with our high-throughput Y2H, whereas three to five repeats were required to obtain 80 to 90% (Fig. 2B and SOM VI). Consequently, we screened the whole search space three times independently to yield an estimated sampling sensitivity of 85% (Fig. 2B). In total, ~88,000 colonies were selected, of which 21,432 scored positive upon more detailed phenotyping (SOM I). After identifying all putative interaction pairs by sequencing, phenotypically retesting them with fresh cultures from archival stocks, and eliminating de novo autoactivators (*28*), we obtained a final data set, "CCSB-YI1," of 1809 interactions among 1278 proteins, which can be downloaded from our Web site (http://interactome.dfci.harvard.edu/S_cerevisiae).

To validate the overall quality of CCSB-YI1, we tested 94 randomly chosen interactions by PCA and mammalian protein-protein interaction trap (MAPPIT; SOM I) (*21*, *29*). MAPPIT takes place at the mammalian cell membrane and measures interactions via activation of signal transducer and activator of transcription 3 (STAT3)–dependent reporter expression. Using both PCA and MAPPIT, we found that the confirmation rate of CCSB-YI1 was similar to those of Ito-core and Uetz-screen (Fig. 1C). The precision [i.e., fraction of true positives in the data set (*30*)] of CCSB-YI1 is estimated at 94 to 100% (Fig. 2C, fig. S4, and SOM VI). Additionally, the performance of our high-throughput Y2H approach was confirmed via a larger RRS of 1000 random pairs (*30*) (Fig. 1B), none of which tested positive (SOM II).

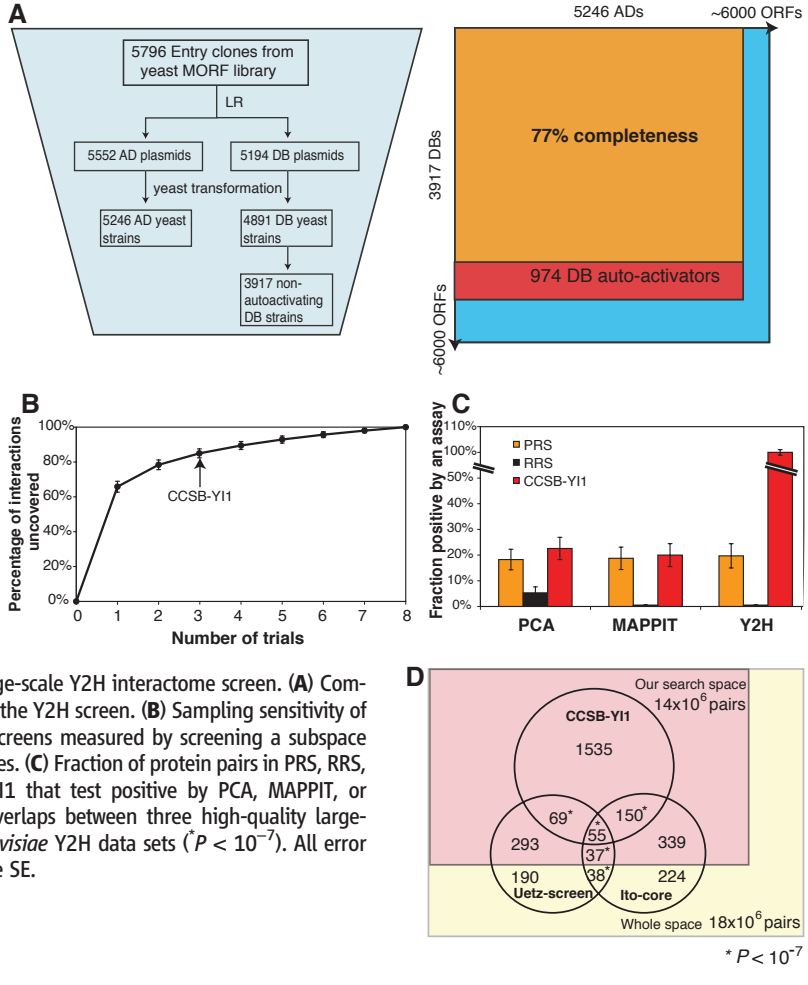

Fig. 2. Large-scale Y2H interactome screen. (**A**) Completeness of the Y2H screen. (**B**) Sampling sensitivity of CCSB Y2H screens measured by screening a subspace multiple times. (**C**) Fraction of protein pairs in PRS, RRS, and CCSB-YI1 that test positive by PCA, MAPPIT, or Y2H. (**D**) Overlaps between three high-quality large-scale *S. cerevisiae* Y2H data sets ($^*P < 10^{-7}$). All error bars indicate SE.

The overlaps of Uetz-screen (27%) and Ito-core (35%) with CCSB-YI1 (Fig. 2D) can be explained by the completeness, assay sensitivity, and sampling sensitivity of the three experiments (SOM VII) and agree well with the results of the pairwise confirmation of those two data sets (Fig. 1C). Similar principles apply to other large-scale experiments such as AP/MS, likely accounting for the low overlap between Krogan and Gavin (~25%; fig. S5B).

Factoring in completeness, precision, and assay and sampling sensitivity, we estimated that the yeast binary interactome consists of ~18,000 ± 4500 interactions (SOM VI), experimentally validating previous computational estimates of 17,000

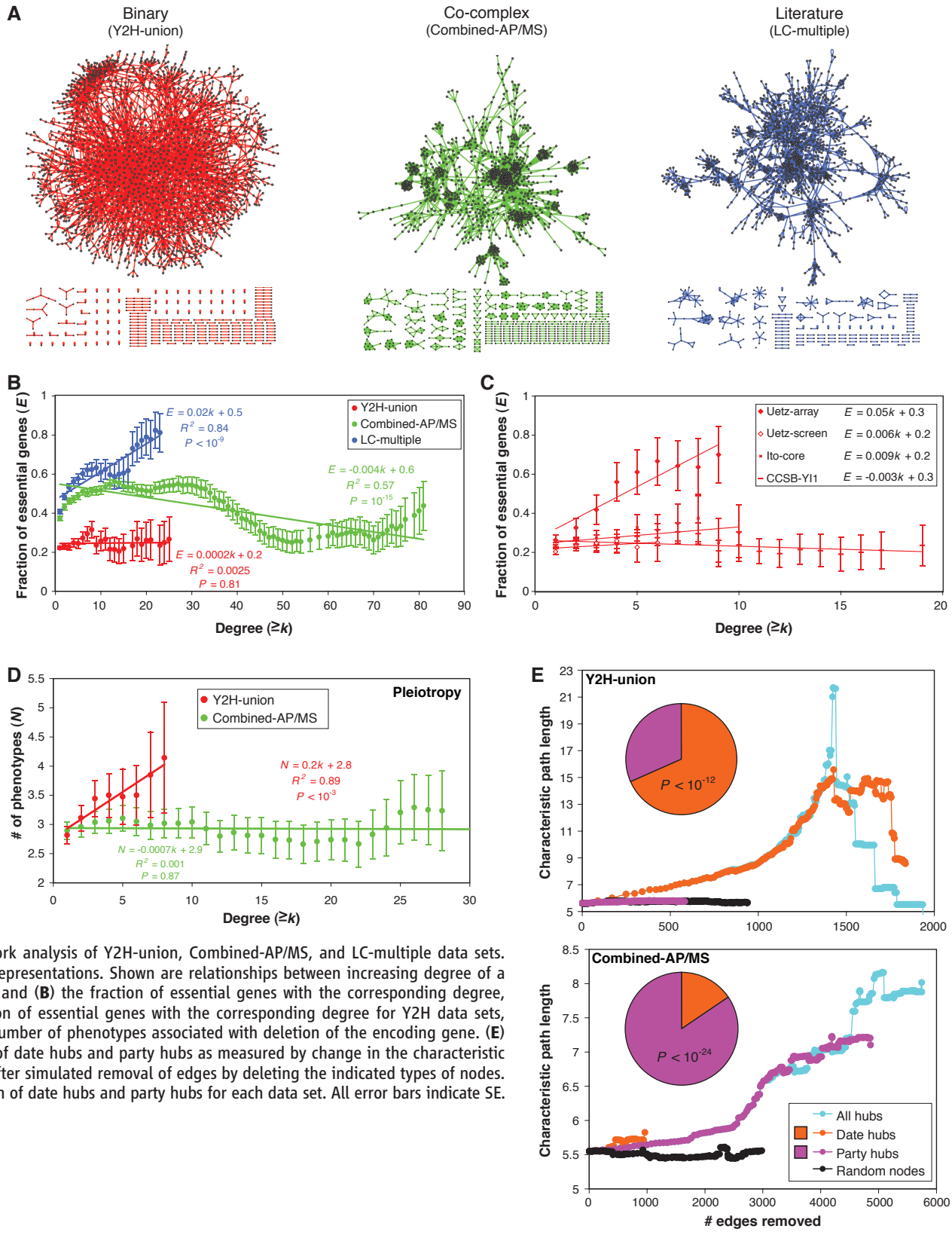

Fig. 3. Network analysis of Y2H-union, Combined-AP/MS, and LC-multiple data sets. (**A**) Network representations. Shown are relationships between increasing degree of a gene product and (**B**) the fraction of essential genes with the corresponding degree, (**C**) the fraction of essential genes with the corresponding degree for Y2H data sets, and (**D**) the number of phenotypes associated with deletion of the encoding gene. (**E**) Contribution of date hubs and party hubs as measured by change in the characteristic path length after simulated removal of edges by deleting the indicated types of nodes. (Inset) Fraction of date hubs and party hubs for each data set. All error bars indicate SE.

to 25,000 interactions (*31*, *32*). To obtain a more comprehensive map of the binary yeast interactome, we combined the three available high-quality proteome-scale Y2H data sets (SOM VII). The union of Uetz-screen, Ito-core, and CCSB-YI1, "Y2H-union," contains 2930 binary interactions among 2018 proteins, which, according to our empirical estimate of the interactome size, represents ~20% of the whole yeast binary interactome (Fig. 3A).

We reexamined global topological features of this new yeast interactome network, facing lower risk of overinterpreting properties due to limited sampling and various biases in the data (*18*). To contrast topological properties of the binary Y2H-union network with that of the co-complex network, we used an integrated AP/MS data set (*33*), which was generated by combining raw high-throughput AP/MS data (*15*, *16*). This "Combined-AP/MS" data set, composed of 9070 co-complex membership associations between 1622 proteins, attempts to model binary interactions from co-complex data (Fig. 3A).

As found previously for other macromolecular networks, the connectivity or "degree" distribution of all three data sets is best approximated by a power-law (*34*) (fig. S6 and SOM VIII). Highly connected proteins, or "hubs," are reportedly more likely encoded by essential genes than less-connected proteins (*35*). Surprisingly, Y2H-union lacked any correlation between degree and essentiality (Fig. 3B). This discrepancy might stem from biases in the data sets available at the time of the original observation: interactions reported in Uetz *et al*. (Uetz-array and Uetz-screen) and literature-curated interactions. Although Uetz-array is of high quality (fig. S7), its experimental design could negatively influence network analyses. Most hub proteins in Uetz-array were found as baits (fig. S8), and the percentage of essential proteins in the 193 bait proteins is twice as high (34.7%) as that of all protein-encoding ORFs in the yeast genome (18.4%), explaining the high correlation between degree and essentiality (Fig. 3C). Likewise, literature-curated interactions seem prone to sociological and other inspection biases (SOM VII). Thus, we refrain hereinafter from using LC-multiple in our further topological and biological analyses. No significant correlation between degree of connectedness and essentiality was observed in any of the three proteome-wide high-throughput binary data sets currently available (i.e., Ito-core, Uetz-screen, and CCSB-YI1; Fig. 3C), as well as in new versions of our *C. elegans* and human interactome maps (fig. S9 and SOM IX).

Hub proteins instead relate to pleiotropy, the number of phenotypes observed as a consequence of gene knockout (SOM I). There was a significant correlation in Y2H-union between connectivity and the number of phenotypes observed in global phenotypic profiling analyses of yeast genes (*36*) (Fig. 3D). Thus, the number of binary physical interactions mediated by a protein seems to better correlate with the number of cellular processes in which it participates than with its essentiality. The correlation between degree and number of phenotypes is not observed in Combined-AP/MS, likely because co-complex associations reflect the size of protein complexes more than the number of processes they might be involved in.

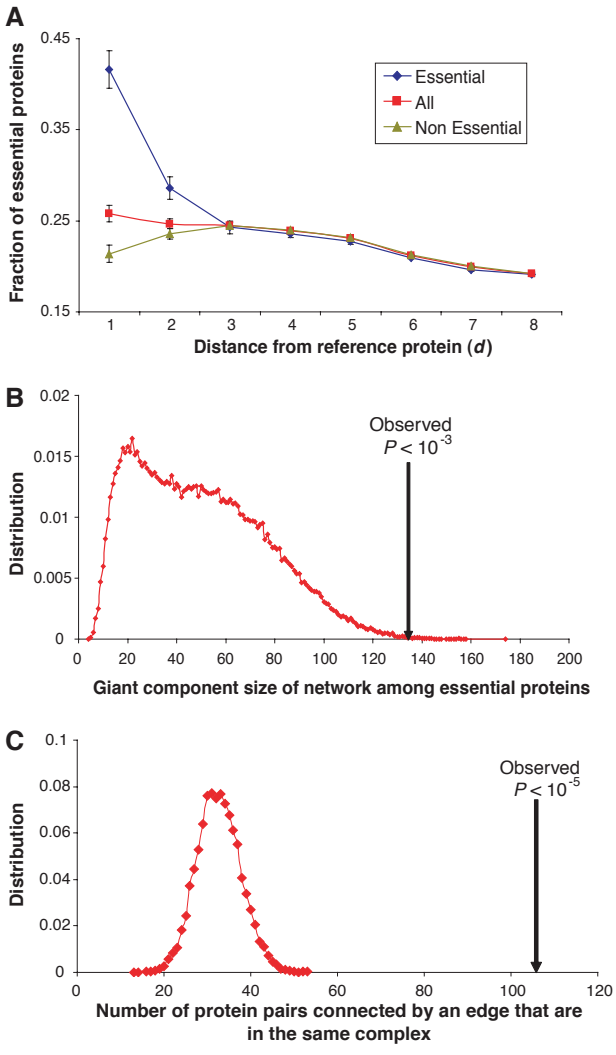

Fig. 4. Clustering of essential proteins. (**A**) Average fraction of essential proteins among proteins whose distance is equal to *d* from a protein selected from essential, nonessential, and all proteins. (**B**) Giant component size of network formed by essential proteins (arrow) compared to 100,000 random networks of same topological properties. (**C**) The number of interacting essential proteins that are also found in the same complex compared to 10,000 random selections of proteins of the same number as essential proteins (SOM IX).

We confirmed the concept of modularity in the yeast interactome network, whereby date hubs that dynamically interact with their partners appear particularly central to global connectivity, whereas static party hubs appear to function locally in specific biological modules (*37*). The proportion of date and party hubs is substantially different between Y2H-union and Combined-AP/MS (Fig. 3E). There are significantly more date hubs in the binary network, whereas party hubs are prevalent in the co-complex network. In the binary network, date hubs are crucial to the topological integrity of the network, whereas party hubs have minimal effects. However, in the co-complex network, date and party hubs affect the topological integrity of the network equally, likely because most hubs in Combined-AP/MS reside in large stable complexes, whereas hubs in Y2H-union preferentially connect diverse cellular processes.

Surprisingly, essential proteins strongly tended to interact with each other (Fig. 4A and SOM IX). By concentrating on the subnetwork formed by interactions mediated by and among essential proteins (fig. S10), we found a giant component whose size is much larger than expected by chance (Fig. 4B). To better understand the clustering of essential proteins, we examined the interacting essential protein pairs that are also reported to be in the same complex; we found 106 interacting essential protein pairs, a number greater than expected by chance (Fig. 4C and SOM IX).

We investigated the overall relationships between Y2H-union and Gene Ontology (GO) attributes (*38*), phenotypic and expression profiling similarities (*39*), and transcriptional regulatory networks (*40*). Both Y2H-union and Combined-AP/MS show significant enrichment (all $P < 10^{-10}$) for functionally similar pairs in all three GO branches (Fig. 5A) (*41*). There is also significant enrichment of positive correlations of phenotypic profiles (*36*) between interacting pairs in both data sets (Fig. 5B and fig. S11). Such interactions, when supported by strong phenotypic information, constitute likely possibilities of functional relationships. Lastly, both data sets are significant-

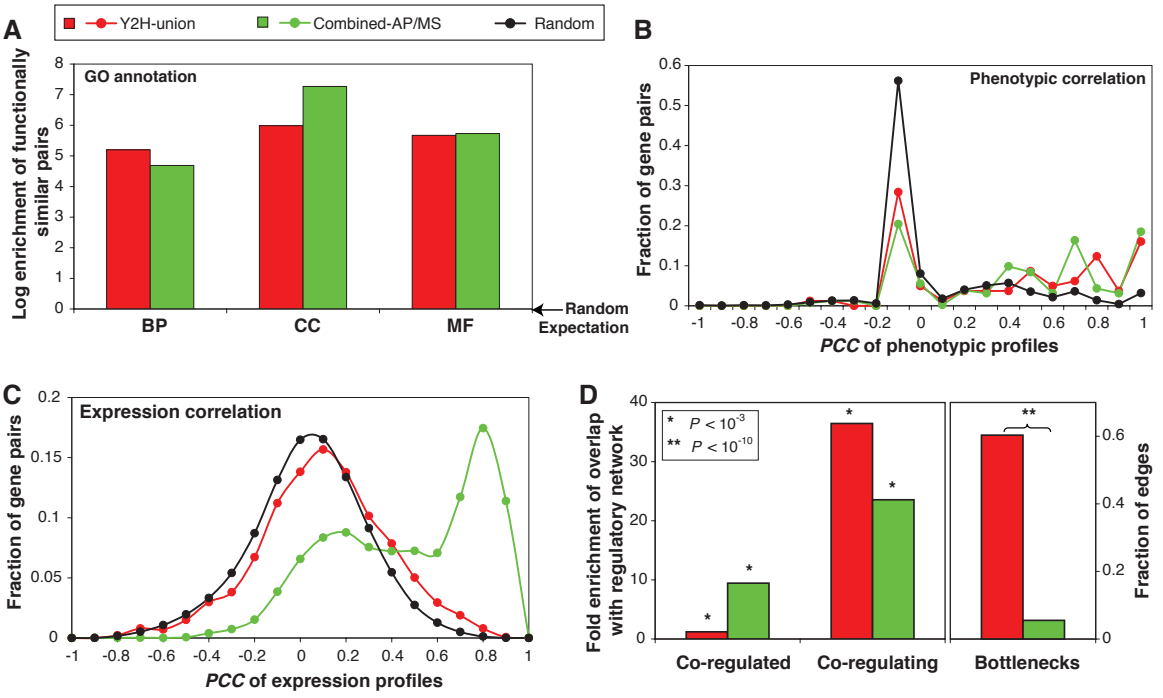

Fig. 5. Biological features of yeast interactome data sets. (**A**) Enrichment of interacting protein pairs (relative to random) that share GO annotations in the biological process, cellular component, and molecular function branches of GO ontology. (**B**) Pearson correlation coefficient (PCC) of phenotypic profiles between interacting pairs in different data sets. (**C**) Coexpression correlation between interacting pairs. (**D**) (Left) Enrichment of interacting proteins as targets of a common TF (co-regulated), and enrichment of interacting TFs in a common MIM (co-regulating) (*$P < 10^{-3}$). (Right) Fraction of bottlenecks from each data set in the combined network (SOM XI). Top 10% of edges with the highest betweenness are defined as "bottlenecks" (*45*).

ly enriched with pairs coexpressed across many conditions (fig. S12), although Combined-AP/MS shows higher enrichment (Fig. 5C), agreeing well with the different nature of the two assays: AP/MS aims at detecting stable complexes, whereas Y2H tends to detect more transient and condition-specific protein interactions. This observation is further supported by enrichment of kinase-substrate pairs in Y2H-union (SOM X and fig. S13).

To explore the mechanisms underlying coexpression of interacting protein pairs, we combined transcriptional regulatory networks with interactome network information (*40*). Interacting proteins in both networks tended to be co-regulated by common transcription factors (TFs; Fig. 5D). Similar to what we observed in the coexpression correlation analysis (Fig. 5C), the enrichment of interacting pairs in Combined-AP/MS was significantly higher than that of Y2H-union. Notably, we observed a significant enrichment of protein-protein interactions between TFs involved in a common "multi-input motif" (*42*, *43*) (MIM, where multiple TFs co-regulate a given set of genes; Fig. 5D and SOM X). The fraction of co-regulating TF pairs is much higher in the binary interactome than in the co-complex network, suggesting that various TFs function together to form transient complexes to differentially regulate transcriptional targets (*44*).

These observations suggest that our binary interactome data set is enriched in transient or condition-specific interactions linking different subcellular processes and molecular machines. To further explore this possibility, we calculated "edge-betweenness" for each interaction in a merged network of all available interactions (SOM XI), measuring the number of shortest paths between all protein pairs that traverse a given edge. The higher edge-betweenness of interactions from Y2H-union shows the tendency of Y2H to detect key interactions outside of complexes significantly more often than AP/MS (Fig. 5D). Several examples of such complex-to-complex connectivity are evident in a complete map of MIPS complexes connected by Y2H interactions (fig. S14).

Overall, we infer that Y2H interrogates a different subspace within the whole interactome than does AP/MS, and Y2H interactions represent key connections between different complexes and pathways. Y2H and AP/MS provide orthogonal information about the interactome and are both vital to obtaining a complete picture of cellular protein-protein interaction networks.

References and Notes

1. M. Fromont-Racine, J. C. Rain, P. Legrain, *Nat. Genet.* **16**, 277 (1997).
2. P. Uetz *et al.*, *Nature* **403**, 623 (2000).
3. T. Ito *et al.*, *Proc. Natl. Acad. Sci. U.S.A.* **98**, 4569 (2001).
4. A. J. Walhout *et al.*, *Science* **287**, 116 (2000).
5. J. Reboul *et al.*, *Nat. Genet.* **34**, 35 (2003).
6. S. Li *et al.*, *Science* **303**, 540 (2004).
7. L. Giot *et al.*, *Science* **302**, 1727 (2003).
8. F. Colland *et al.*, *Genome Res.* **14**, 1324 (2004).
9. J. F. Rual *et al.*, *Nature* **437**, 1173 (2005).
10. U. Stelzl *et al.*, *Cell* **122**, 957 (2005).
11. G. Butland *et al.*, *Nature* **433**, 531 (2005).
12. M. Arifuzzaman *et al.*, *Genome Res.* **16**, 686 (2006).
13. A. C. Gavin *et al.*, *Nature* **415**, 141 (2002).
14. Y. Ho *et al.*, *Nature* **415**, 180 (2002).
15. A. C. Gavin *et al.*, *Nature* **440**, 631 (2006).
16. N. J. Krogan *et al.*, *Nature* **440**, 637 (2006).
17. R. M. Ewing *et al.*, *Mol. Syst. Biol.* **3**, 89 (2007).
18. J. D. Han, D. Dupuy, N. Bertin, M. E. Cusick, M. Vidal, *Nat. Biotechnol.* **23**, 839 (2005).
19. D. Scholtens, M. Vidal, R. Gentleman, *Bioinformatics* **21**, 3548 (2005).
20. T. Reguly *et al.*, *J. Biol.* **5**, 11 (2006).
21. I. Remy, S. W. Michnick, *Methods Mol. Biol.* **261**, 411 (2004).
22. D. M. Gelperin *et al.*, *Genes Dev.* **19**, 2816 (2005).
23. H. W. Mewes *et al.*, *Nucleic Acids Res.* **34**, D169 (2006).
24. C. von Mering *et al.*, *Nature* **417**, 399 (2002).
25. J. S. Bader, A. Chaudhuri, J. M. Rothberg, J. Chant, *Nat. Biotechnol.* **22**, 78 (2004).
26. H. Yu *et al.*, *Genome Res.* **14**, 1107 (2004).
27. P. O. Vidalain, M. Boxem, H. Ge, S. Li, M. Vidal, *Methods* **32**, 363 (2004).
28. A. J. Walhout, M. Vidal, *Genome Res.* **9**, 1128 (1999).
29. S. Eyckerman *et al.*, *Nat. Cell Biol.* **3**, 1114 (2001).
30. R. Jansen, M. Gerstein, *Curr. Opin. Microbiol.* **7**, 535 (2004).
31. A. Grigoriev, *Nucleic Acids Res.* **31**, 4157 (2003).
32. R. Jansen *et al.*, *Science* **302**, 449 (2003).
33. S. R. Collins *et al.*, *Mol. Cell. Proteomics* **6**, 439 (2007).
34. A. L. Barabási, R. Albert, *Science* **286**, 509 (1999).
35. H. Jeong, S. P. Mason, A. L. Barabasi, Z. N. Oltvai, *Nature* **411**, 41 (2001).
36. A. M. Dudley, D. M. Janse, A. Tanay, R. Shamir, G. M. Church, *Mol. Syst. Biol.* **1**, 0001 (2005).
37. J. D. Han *et al.*, *Nature* **430**, 88 (2004).
38. Gene Ontology Consortium, *Nucleic Acids Res.* **36**, D440 (2008).
39. M. Vidal, *Cell* **104**, 333 (2001).
40. H. Yu, M. Gerstein, *Proc. Natl. Acad. Sci. U.S.A.* **103**, 14724 (2006).
41. H. Yu, R. Jansen, G. Stolovitzky, M. Gerstein, *Bioinformatics* **23**, 2163 (2007).
42. T. I. Lee *et al.*, *Science* **298**, 799 (2002).
43. R. Milo *et al.*, *Science* **298**, 824 (2002).
44. N. M. Luscombe *et al.*, *Nature* **431**, 308 (2004).
45. H. Yu, P. M. Kim, E. Sprecher, V. Trifonov, M. Gerstein, *PLOS Comput. Biol.* **3**, e59 (2007).

46. Supported by funds from the W. M. Keck Foundation (M.V. and F.P.R.); by Institute Sponsored Research funds from the Dana-Farber Cancer Institute Strategic Initiative (M.V. and CCSB); by NIH grant R01-HG001715 (M.V. and F.P.R.); by NIH grants U01-A1070499-01 and U56-CA113004 (A.-L.B.); by grant GOA12051401 from the University of Ghent and grant FWO-V G.0031.06 from the Fund for Scientific Research Flanders (J.T.); by a grant from the National Cancer Institute of Canada

(C.B.); and by NIH grant HG003224 (F.P.R.). I.L. is a postdoctoral fellow with the Fonds Wetenschappelijk Onderzoek–Vlanderen. M.V. is a "Chercheur Qualifié Honoraire" from the Fonds de la Recherche Scientifique (FRS-FNRS, French Community of Belgium). We thank members of our laboratories for helpful discussions and Agencourt Biosciences for sequencing assistance. All data sets can be downloaded from our Web site (http://interactome.dfci.harvard.edu/S_cerevisiae).

Supporting Online Material
www.sciencemag.org/cgi/content/full/1158684/DC1
SOM Text
Figs. S1 to S35
Tables S1 to S5
References

4 April 2008; accepted 1 August 2008
Published online 21 August 2008;
10.1126/science.1158684
Include this information when citing this paper.

Ceramide Biogenesis Is Required for Radiation-Induced Apoptosis in the Germ Line of *C. elegans*

Xinzhu Deng,[1] Xianglei Yin,[1] Richard Allan,[1] Diane D. Lu,[1] Carine W. Maurer,[2] Adriana Haimovitz-Friedman,[3] Zvi Fuks,[3] Shai Shaham,[2] Richard Kolesnick[1]*

Ceramide engagement in apoptotic pathways has been a topic of controversy. To address this controversy, we tested *loss-of-function (lf)* mutants of conserved genes of sphingolipid metabolism in *Caenorhabditis elegans*. Although somatic (developmental) apoptosis was unaffected, ionizing radiation–induced apoptosis of germ cells was obliterated upon inactivation of ceramide synthase and restored upon microinjection of long-chain natural ceramide. Radiation-induced increase in the concentration of ceramide localized to mitochondria and was required for BH3-domain protein EGL-1–mediated displacement of CED-4 (an APAF-1–like protein) from the CED-9 (a Bcl-2 family member)/CED-4 complex, an obligate step in activation of the CED-3 caspase. These studies define CEP-1 (the worm homolog of the tumor suppressor p53)–mediated accumulation of EGL-1 and ceramide synthase–mediated generation of ceramide through parallel pathways that integrate at mitochondrial membranes to regulate stress-induced apoptosis.

Although studies that use genetic deficiency in ceramide production support it as essential for apoptosis in diverse models (*1*), many have questioned whether ceramide functions as a bona fide transducer of apoptotic signals (*2*). One reason for skepticism is that, despite delineation of a number of ceramide-activated proteins, no single protein has been identified as mediator of ceramide-induced apoptosis. Recent studies have suggested an alternate mode of ceramide action, based on its capacity to self-associate and locally rearrange membrane bilayers into ceramide-rich macrodomains (1 to 5 μm in diameter), which are sites of protein concentration and oligomerization (*3*). Ceramide may thus mediate apoptosis through its ability to reconfigure membranes, coordinating protein complexation at critical junctures of signaling cascades.

To establish the role of ceramide definitively, we used a model of radiation-induced apoptosis in *Caenorhabditis elegans* germ cells (*4*). Germline stem cells, located at the distal gonad tip, divide incessantly throughout adult life, with daughter cells arresting in meiotic prophase. Upon exiting prophase, germ cells become sensitive to radiation-induced apoptosis, detected morphologically just proximal to the bend of the gonadal arm (*5*). This apoptotic pathway is antagonized by the ABL-1 tyrosine kinase, requiring sequentially the cell cycle checkpoint genes *rad-5*, *hus-1*, and *mrt-2*; the *C. elegans* p53 homolog *cep-1*; and the genes making up the conserved apoptotic machinery, the caspase *ced-3*, the apoptotic protease activating factor 1–like protein *ced-4*, the Bcl-2 protein *ced-9*, and the BH3-domain protein *egl-1*. This pathway differs from apoptotic somatic cell death, which is not subject to upstream checkpoint regulation via the CEP-1 pathway (*5*, *6*).

We identified conserved genes that regulate *C. elegans* sphingolipid intermediary metabolism and tested deletion alleles (Table 1 and table S1). Screening for mutants resistant to radiation-induced germ cell apoptosis revealed apoptosis suppression in only deletion mutants of *hyl-1* and *lagr-1*, two of the three ceramide synthase (CS) genes (Fig. 1A). CS gene products regulate de novo ceramide biosynthesis, acylating sphinganine to form dihydroceramide that is subsequently converted to ceramide by a desaturase (*7*). CSs contain six to seven putative transmembrane domains and a Lag1p motif [which confers enzyme activity (*8*)], regions conserved in the *C. elegans* orthologs. The deleted CS sequences in *hyl-1(ok976)* and *lagr-1(gk327)* result in frameshifts that disrupt the Lag1p motifs (fig. S1A). We detected a ~1.6-kb *hyl-1* transcript in wild-type (WT) worms and a smaller ~1.35-kb transcript in *hyl-1(ok976)*, whereas we observed a ~1.4-kb *lagr-1* transcript in WT worms and a ~1.25-kb transcript in *lagr-1(gk327)* (fig. S1B). In contrast, a deletion mutant of the third *C. elegans* CS (*9*, *10*), *hyl-2(ok1766)*, lacking a 1626-base pair fragment of the *hyl-2* gene locus that eliminates exons 2 to 5 corresponding to 74% of the coding sequence, displayed no defect in germ cell death (fig. S1C).

In N2 WT strain young adults, apoptotic germ cells gradually increased in abundance with age from a baseline of 0.7 ± 0.1 to 1.8 ± 0.2 corpses per distal gonad arm over 48 hours. Exposure to a 120-gray (Gy) ionizing radiation dose increased germ cell apoptosis to 5.2 ± 0.3 cells 36 to 48 hours after treatment. In contrast, in *hyl-1 (ok976)* and *lagr-1(gk327)* animals, age-dependent and radiation-induced germ cell apoptosis were nearly abolished (Fig. 1A). Similar effects were observed in the *lagr-1(gk327);hyl-1(ok976)* double mutant (Fig. 1B). The rate of germ cell corpse removal was unaffected in CS mutants, excluding the possibility that defective corpse engulfment elevated corpse numbers (table S2). In contrast, *loss-of-function (lf)* mutations of *hyl-1* or *lagr-1* did not affect developmental somatic cell death, nor did the *lf hyl-2(ok1766)* mutation (table S3). These studies indicate a requirement for two *C. elegans* CS genes for radiation-induced germline apoptosis.

To confirm ceramide as critical for germline apoptosis, we injected C_{16}-ceramide into gonads of young adult WT worms. C_{16}-ceramide is the predominant ceramide species in apoptosis induction by diverse stresses in multiple organisms (*11*) and in low abundance in *C. elegans* (*12*, *13*). C_{16}-ceramide microinjection resulted in time- and dose-dependent increases in germ cell apoptosis (Fig. 1C), with a median effective dose of ~0.05 μM gonadal ceramide. Peak effect occurred at ~0.1 μM gonadal ceramide at 36 hours (6.6 ± 0.8 versus 1.5 ± 0.4 cell corpses per distal gonad arm, $P < 0.0001$), qualitatively and quantitatively mimicking the 120-Gy effect in WT worms. In contrast, C_{16}-dihydroceramide, which differs from C_{16}-ceramide in a trans double bond at sphingoid base position four to five, was without effect (0.71 ± 0.28 cell corpses per distal gonad arm at ~1 μM), indicating specificity for ceramide in apoptosis induction. Furthermore, C_{16}-ceramide microinjection into *lagr-1(gk327);hyl-1(ok976)* animals (~1 μM gonadal ceramide) resulted in a 5.7-fold increase in germ cell apoptosis (from 0.60 ± 0.17 to 3.43 ± 0.88, $P < 0.0001$) (Fig. 1D). Note that the baseline level of apoptosis in *lagr-1(gk327);hyl-1(ok976)* was less than one-half that in WT worms. Moreover, ~0.005 μM gonadal ceramide, a concentration without impact on germ cell apoptosis, completely restored radiation (120 Gy)–induced apoptosis, an effect inhibitable in a *lf ced-3* background (Fig. 1E). C_{16}-ceramide's ability to bypass the genetic defect and restore the radiation-response pheno-

[1]Laboratory of Signal Transduction, Memorial Sloan-Kettering Cancer Center (MSKCC), New York, NY 10021, USA. [2]Laboratory of Developmental Genetics, Rockefeller University, New York, NY, 10021, USA. [3]Department of Radiation Oncology, Memorial Sloan-Kettering Cancer Center, New York, NY 10021, USA.

*To whom correspondence should be addressed. E-mail: r-kolesnick@ski.mskcc.org

Ceramide Biogenesis Is Required for Radiation-Induced Apoptosis in the Germ Line of C. elegans

Xinzhu Deng, *et al.*

Science **322**, 110 (2008);
DOI: 10.1126/science.1158111

Science (print ISSN 0036-8075; online ISSN 1095-9203) is published weekly, except the last week in December, by the American Association for the Advancement of Science, 1200 New York Avenue NW, Washington, DC 20005.

(C.B.); and by NIH grant HG003224 (F.P.R.). I.L. is a postdoctoral fellow with the Fonds Wetenschappelijk Onderzoek–Vlanderen. M.V. is a "Chercheur Qualifié Honoraire" from the Fonds de la Recherche Scientifique (FRS-FNRS, French Community of Belgium). We thank members of our laboratories for helpful discussions and Agencourt Biosciences for sequencing assistance. All data sets can be downloaded from our Web site (http://interactome.dfci.harvard.edu/S_cerevisiae).

Supporting Online Material
www.sciencemag.org/cgi/content/full/1158684/DC1
SOM Text
Figs. S1 to S35
Tables S1 to S5
References

4 April 2008; accepted 1 August 2008
Published online 21 August 2008;
10.1126/science.1158684
Include this information when citing this paper.

Ceramide Biogenesis Is Required for Radiation-Induced Apoptosis in the Germ Line of *C. elegans*

Xinzhu Deng,[1] Xianglei Yin,[1] Richard Allan,[1] Diane D. Lu,[1] Carine W. Maurer,[2] Adriana Haimovitz-Friedman,[3] Zvi Fuks,[3] Shai Shaham,[2] Richard Kolesnick[1]*

Ceramide engagement in apoptotic pathways has been a topic of controversy. To address this controversy, we tested *loss-of-function (lf)* mutants of conserved genes of sphingolipid metabolism in *Caenorhabditis elegans*. Although somatic (developmental) apoptosis was unaffected, ionizing radiation–induced apoptosis of germ cells was obliterated upon inactivation of ceramide synthase and restored upon microinjection of long-chain natural ceramide. Radiation-induced increase in the concentration of ceramide localized to mitochondria and was required for BH3-domain protein EGL-1–mediated displacement of CED-4 (an APAF-1–like protein) from the CED-9 (a Bcl-2 family member)/CED-4 complex, an obligate step in activation of the CED-3 caspase. These studies define CEP-1 (the worm homolog of the tumor suppressor p53)–mediated accumulation of EGL-1 and ceramide synthase–mediated generation of ceramide through parallel pathways that integrate at mitochondrial membranes to regulate stress-induced apoptosis.

Although studies that use genetic deficiency in ceramide production support it as essential for apoptosis in diverse models (*1*), many have questioned whether ceramide functions as a bona fide transducer of apoptotic signals (*2*). One reason for skepticism is that, despite delineation of a number of ceramide-activated proteins, no single protein has been identified as mediator of ceramide-induced apoptosis. Recent studies have suggested an alternate mode of ceramide action, based on its capacity to self-associate and locally rearrange membrane bilayers into ceramide-rich macrodomains (1 to 5 μm in diameter), which are sites of protein concentration and oligomerization (*3*). Ceramide may thus mediate apoptosis through its ability to reconfigure membranes, coordinating protein complexation at critical junctures of signaling cascades.

To establish the role of ceramide definitively, we used a model of radiation-induced apoptosis in *Caenorhabditis elegans* germ cells (*4*). Germline stem cells, located at the distal gonad tip, divide incessantly throughout adult life, with daughter cells arresting in meiotic prophase. Upon exiting prophase, germ cells become sensitive to radiation-induced apoptosis, detected morphologically just proximal to the bend of the gonadal arm (*5*). This apoptotic pathway is antagonized by the ABL-1 tyrosine kinase, requiring sequentially the cell cycle checkpoint genes *rad-5*, *hus-1*, and *mrt-2*; the *C. elegans* p53 homolog *cep-1*; and the genes making up the conserved apoptotic machinery, the caspase *ced-3*, the apoptotic protease activating factor 1–like protein *ced-4*, the Bcl-2 protein *ced-9*, and the BH3-domain protein *egl-1*. This pathway differs from apoptotic somatic cell death, which is not subject to upstream checkpoint regulation via the CEP-1 pathway (*5*, *6*).

We identified conserved genes that regulate *C. elegans* sphingolipid intermediary metabolism and tested deletion alleles (Table 1 and table S1). Screening for mutants resistant to radiation-induced germ cell apoptosis revealed apoptosis suppression in only deletion mutants of *hyl-1* and *lagr-1*, two of the three ceramide synthase (CS) genes (Fig. 1A). CS gene products regulate de novo ceramide biosynthesis, acylating sphinganine to form dihydroceramide that is subsequently converted to ceramide by a desaturase (*7*). CSs contain six to seven putative transmembrane domains and a Lag1p motif [which confers enzyme activity (*8*)], regions conserved in the *C. elegans* orthologs. The deleted CS sequences in *hyl-1(ok976)* and *lagr-1(gk327)* result in frameshifts that disrupt the Lag1p motifs (fig. S1A). We detected a ~1.6-kb *hyl-1* transcript in wild-type (WT) worms and a smaller ~1.35-kb transcript in *hyl-1(ok976)*, whereas we observed a ~1.4-kb *lagr-1* transcript in WT worms and a ~1.25-kb transcript in *lagr-1(gk327)* (fig. S1B). In contrast, a deletion mutant of the third *C. elegans* CS (*9*, *10*), *hyl-2(ok1766)*, lacking a 1626-base pair fragment of the *hyl-2* gene locus that eliminates exons 2 to 5 corresponding to 74% of the coding sequence, displayed no defect in germ cell death (fig. S1C).

In N2 WT strain young adults, apoptotic germ cells gradually increased in abundance with age from a baseline of 0.7 ± 0.1 to 1.8 ± 0.2 corpses per distal gonad arm over 48 hours. Exposure to a 120-gray (Gy) ionizing radiation dose increased germ cell apoptosis to 5.2 ± 0.3 cells 36 to 48 hours after treatment. In contrast, in *hyl-1 (ok976)* and *lagr-1(gk327)* animals, age-dependent and radiation-induced germ cell apoptosis were nearly abolished (Fig. 1A). Similar effects were observed in the *lagr-1(gk327);hyl-1(ok976)* double mutant (Fig. 1B). The rate of germ cell corpse removal was unaffected in CS mutants, excluding the possibility that defective corpse engulfment elevated corpse numbers (table S2). In contrast, *loss-of-function (lf)* mutations of *hyl-1* or *lagr-1* did not affect developmental somatic cell death, nor did the *lf hyl-2(ok1766)* mutation (table S3). These studies indicate a requirement for two *C. elegans* CS genes for radiation-induced germline apoptosis.

To confirm ceramide as critical for germline apoptosis, we injected C_{16}-ceramide into gonads of young adult WT worms. C_{16}-ceramide is the predominant ceramide species in apoptosis induction by diverse stresses in multiple organisms (*11*) and in low abundance in *C. elegans* (*12*, *13*). C_{16}-ceramide microinjection resulted in time- and dose-dependent increases in germ cell apoptosis (Fig. 1C), with a median effective dose of ~0.05 μM gonadal ceramide. Peak effect occurred at ~0.1 μM gonadal ceramide at 36 hours (6.6 ± 0.8 versus 1.5 ± 0.4 cell corpses per distal gonad arm, $P < 0.0001$), qualitatively and quantitatively mimicking the 120-Gy effect in WT worms. In contrast, C_{16}-dihydroceramide, which differs from C_{16}-ceramide in a trans double bond at sphingoid base position four to five, was without effect (0.71 ± 0.28 cell corpses per distal gonad arm at ~1 μM), indicating specificity for ceramide in apoptosis induction. Furthermore, C_{16}-ceramide microinjection into *lagr-1(gk327);hyl-1(ok976)* animals (~1 μM gonadal ceramide) resulted in a 5.7-fold increase in germ cell apoptosis (from 0.60 ± 0.17 to 3.43 ± 0.88, $P < 0.0001$) (Fig. 1D). Note that the baseline level of apoptosis in *lagr-1(gk327);hyl-1(ok976)* was less than one-half that in WT worms. Moreover, ~0.005 μM gonadal ceramide, a concentration without impact on germ cell apoptosis, completely restored radiation (120 Gy)–induced apoptosis, an effect inhibitable in a *lf ced-3* background (Fig. 1E). C_{16}-ceramide's ability to bypass the genetic defect and restore the radiation-response pheno-

[1]Laboratory of Signal Transduction, Memorial Sloan-Kettering Cancer Center (MSKCC), New York, NY 10021, USA. [2]Laboratory of Developmental Genetics, Rockefeller University, New York, NY, 10021, USA. [3]Department of Radiation Oncology, Memorial Sloan-Kettering Cancer Center, New York, NY 10021, USA.

*To whom correspondence should be addressed. E-mail: r-kolesnick@ski.mskcc.org

type is strong evidence that *hyl-1* and *lagr-1* represent legitimate *C. elegans* CS genes. Animals with *sphk-1(ok1097)*, a null allele of sphingosine kinase (SPHK), which prevents conversion of ceramide to its anti-apoptotic derivative sphingosine 1-phosphate (S1P) (*14*), displayed high baseline germ cell death and were hypersensitive to radiation-induced germ cell apoptosis (fig. S2, A and B), inhibitable (by 85 ± 9%) in a *lagr-1(gk327);sphk-1(ok1097)* double mutant. Collectively, these studies identify ceramide as a critical effector of radiation-induced germ cell apoptosis, although they do not define its mode of engaging the apoptotic pathway.

Inactivation of the *C. elegans* ABL-1 ortholog in the *lf* mutant *abl-1(ok171)* (or by RNA interference) increases baseline and post-radiation germ cell apoptosis, modeling radiation hypersensitivity

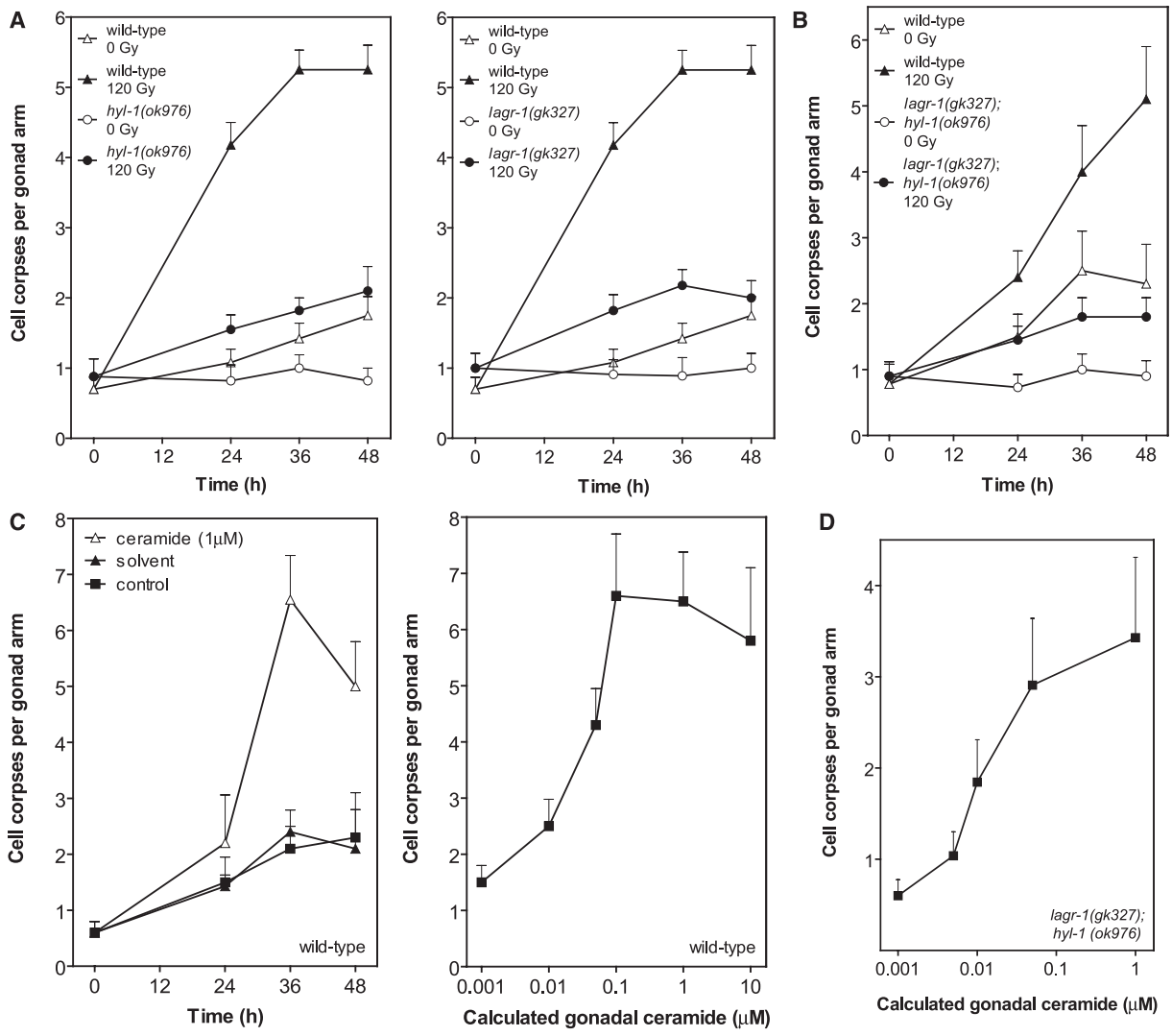

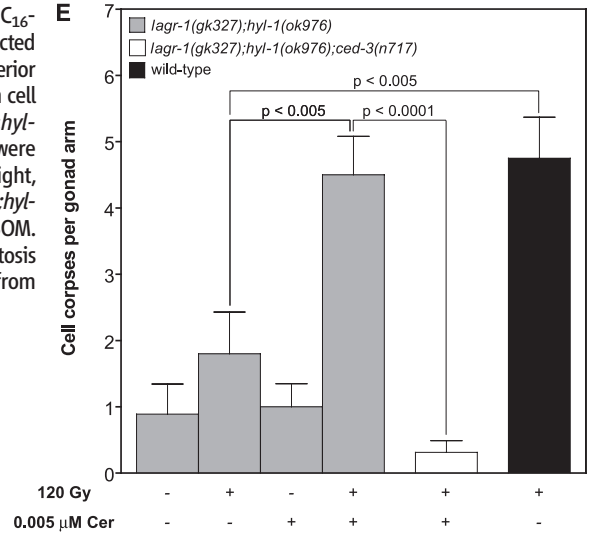

Fig. 1. *lf hyl-1* and *lagr-1* prevent radiation-induced germ cell apoptosis, reversible by C_{16}-ceramide. WT and mutant worms were synchronized at 20°C and irradiated (**A**, **B**, and **E**) or injected with C_{16}-ceramide into the posterior gonad (**C** to **E**) at 24 hours after the L4 stage. The posterior gonad distal arm was scored for cell corpses under Nomarski optics. Time dependence of germ cell corpse induction in *hyl-1(ok976)* (left) and *lagr-1(gk327)* (right) (A) and in *lagr-1(gk327);hyl-1(ok976)* (B) after 120 Gy is shown. WT data are identical in (A), left and right; these panels were separated for clarity. C_{16}-ceramide microinjection induces time- (left) and dose-dependent (right, at 36 hours) germ cell apoptosis in WT worms (C) and dose-dependent apoptosis in *lagr-1(gk327);hyl-1(ok976)* at 36 hours (D). Gonadal ceramide concentration was calculated as described in the SOM. (E) Sublethal C_{16}-ceramide microinjection restores radiation (120 Gy)-induced germ cell apoptosis to *lagr-1(gk327);hyl-1(ok976)*. Data (mean ± SEM, represented by error bars) are collated from ≥15 worms per group in (A) to (E).

phenotypes (*15*). To order CS action relative to ABL-1, we generated *hyl-1(ok976);abl-1(ok171)* and *lagr-1(gk327);abl-1(ok171)* and a triple mutant *lagr-1(gk327);hyl-1(ok976);abl-1(ok171). lf hyl-1* or *lagr-1* in an *abl-1(ok171)* genetic background prevented the time-dependent increase in physiologic germ cell apoptosis and completely blocked radiation-induced apoptosis (Fig. 2A, left). Similarly, *lagr-1(gk327);hyl-1(ok976);abl-1(ok171)* displayed inhibition of baseline and radiation-induced germ cell apoptosis (Fig. 2A, right). Thus, increased germ cell apoptosis in irradiated *abl-1(ok171)* depends on the CS genes *hyl-1* and *lagr-1*.

In *C. elegans*, DNA damage activates the p53 homolog CEP-1, which is required for transcriptional up-regulation of the BH3-only proteins, EGL-1 and CED-13, that in turn activate the core apoptotic machinery (CED-9, CED-4, and CED-3) (*6*, *16*). Exposure of *hyl-1(ok976)* and *lagr-1 (gk327)* to 120 Gy increased *egl-1* transcripts

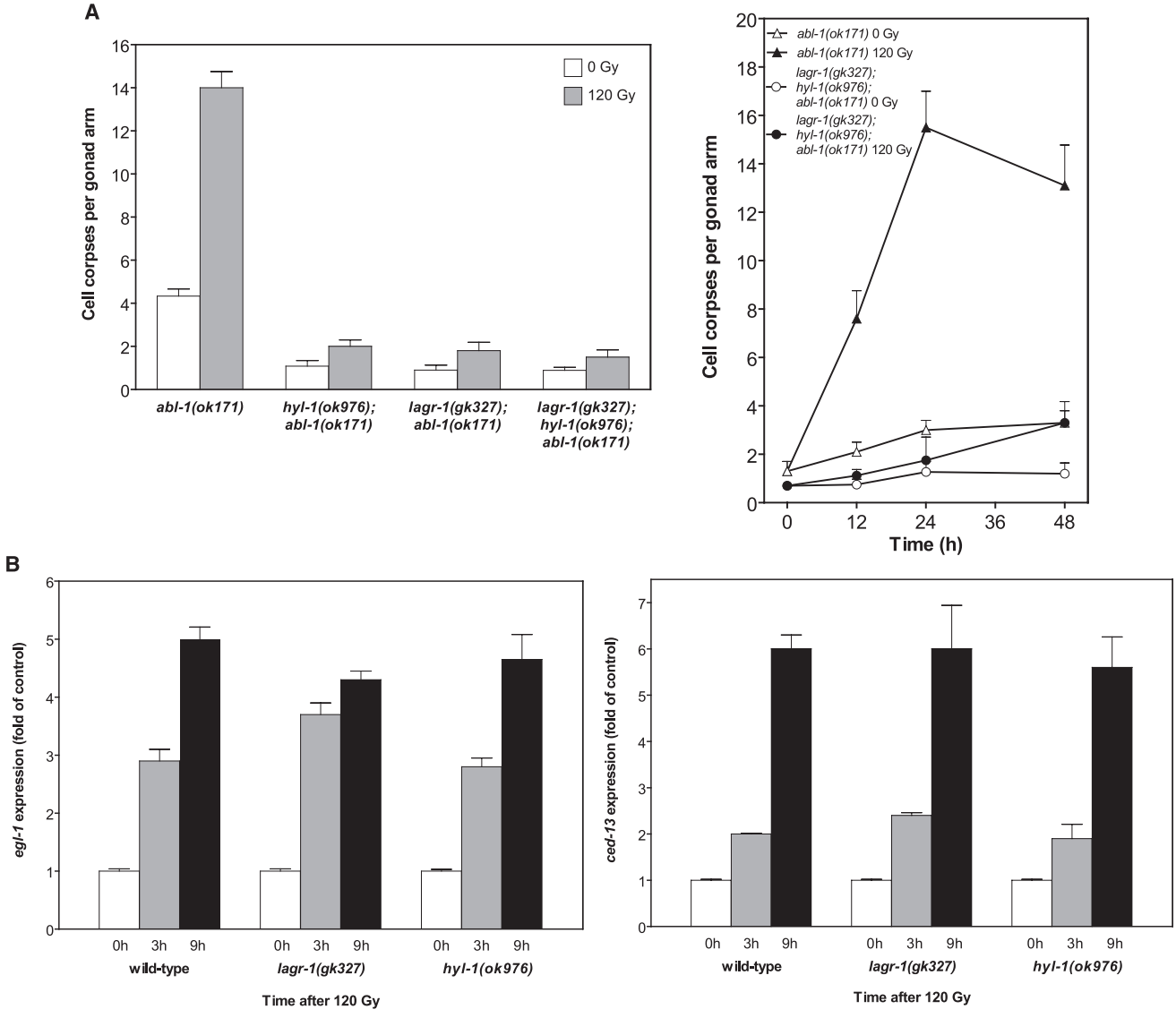

Fig. 2. Role of ceramide in CEP-1/p53–mediated germ cell apoptosis. (**A**) *hyl-1* and *lagr-1* are epistatic to *abl-1* in germ cell apoptosis. Germ cell apoptosis was scored in *abl-1(ok171), hyl-1(ok976);abl-1(ok171), lagr-1(gk327);abl-1(ok171)*, and *lagr-1(gk327);hyl-1(ok976);abl-1(ok171)* at 36 hours (left) and in *lagr-1(gk327);hyl-1(ok976);abl-1(ok171)* at the indicated times after exposure to 120 Gy (right). Data (mean ± SEM, represented by error bars) are collated from 10 to 15 worms per group. (**B**) *hyl-1* and *lagr-1* deletions do not affect 120-Gy–induced p53-mediated *egl-1* (left) and *ced-13* (right) up-regulation measured by reverse transcription polymerase chain reaction. Data (mean ± SEM) are compiled from three experiments. (**C**) Baseline EGL-1 is required for C_{16}-ceramide (~1 μM gonadal ceramide)–induced germ cell apoptosis. Studies were performed as in Fig. 1B. Data (mean ± SEM) are collated from ≥15 worms per group.

four- to fivefold at 9 hours after irradiation (Fig. 2B, left), whereas *ced-13* expression was enhanced five- to sixfold (Fig. 2B, right)—levels comparable to those detected in irradiated WT worms. Thus, the loss of CS did not affect CEP-1 activation upon irradiation, suggesting that ceramide and CEP-1 might function in parallel, coordinately conferring radiation-induced germ cell death.

We reasoned that in contrast to radiation-induced germ cell apoptosis, which apparently requires increased abundance of both BH3-only proteins and ceramide, C_{16}-ceramide provided exogenously might act independent of p53-mediated *egl-1* expression by maximizing the effect of baseline EGL-1. In fact, microinjected C_{16}-ceramide partially restored germ cell death in *cep-1(gk138)* from 0.4 ± 0.13 to 2.5 ± 0.32 corpses per distal gonad arm (Fig. 2C) ($P < 0.001$). As C_{16}-ceramide

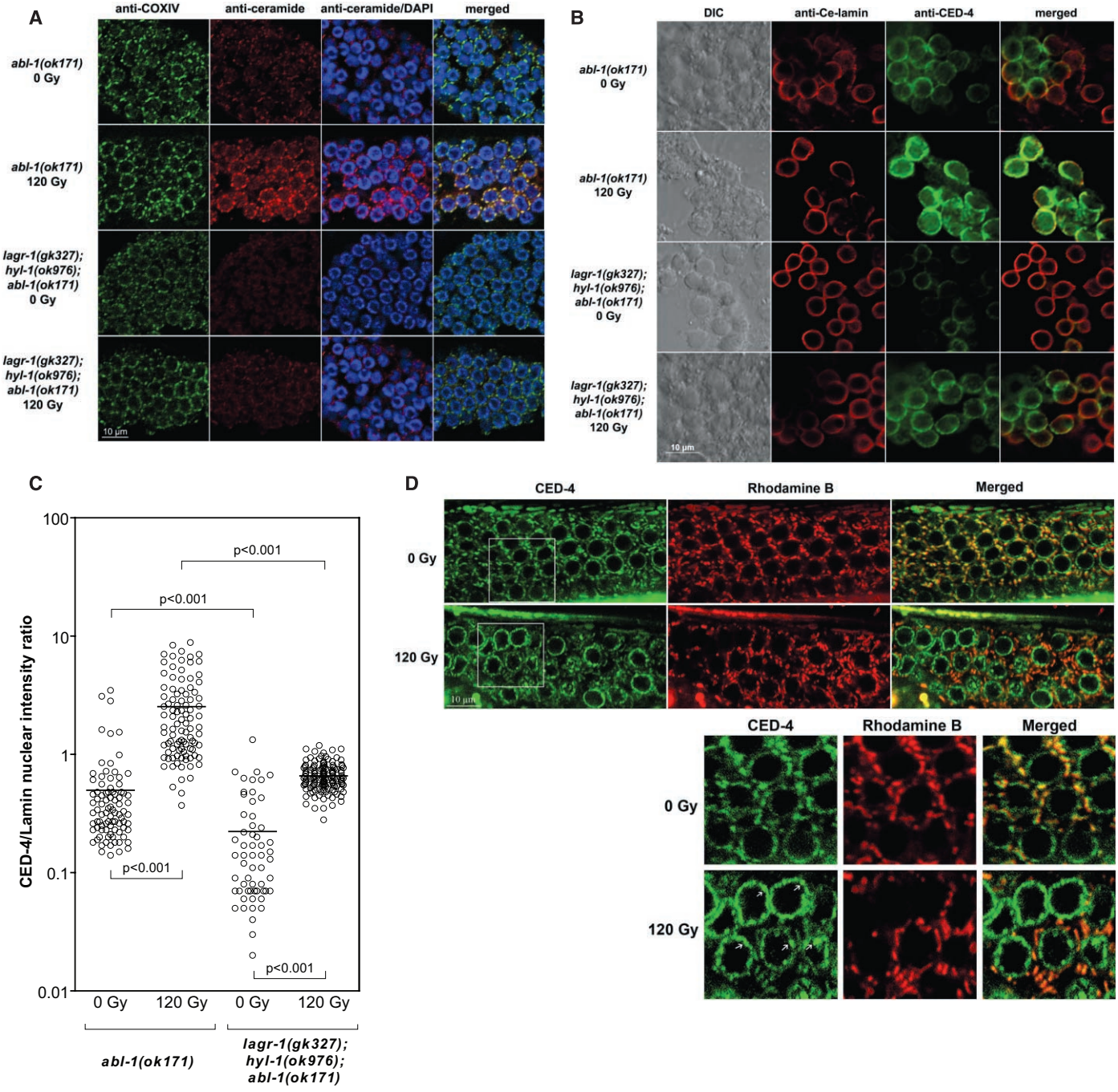

Fig. 3. Mitochondrial ceramide mediates CED-4 displacement. (**A**) Gonads were dissected from young adult *abl-1(ok171)* and *lagr-1(gk327);hyl-1(ok976);abl-1(ok171)* at 24 hours after 120 Gy and stained with anti–COX-IV antibody (green), anti-ceramide antibody (red), and 4′,6′-diamidino-2-phenylindole (blue). (**B** and **C**) Germ cells were released from gonads of young adult *abl-1(ok171)* and *lagr-1(gk327);hyl-1(ok976);abl-1(ok171)* at 24 hours after 120 Gy and stained with anti–Ce-lamin (red) and anti–CED-4 (green). CED-4/lamin intensity in individual germ cell nuclei (circles) was measured using Metamorph software. Horizontal bars indicate means from ≥50 nuclei per group. In *lagr-1(gk327);hyl-1(ok976);abl-1(ok171)*, the baseline CED-4/lamin ratio is reduced by 63%, and the post-radiation fold and absolute change are reduced by 40% and 78%, respectively, as compared with *abl-1(ok171)* animals. (**D**) L1 larvae of *opls219*, cultured in Rhodamine B–containing plates until the young adult stage, were exposed to 120 Gy, and GFP (CED-4) and Rhodamine B (mitochondria) signals were imaged at 36 hours post-irradiation. Images represent single confocal planes from the distal gonad of *opls219* (upper panels). Boxed insets (lower panels) were enlarged 1.75 times to ease the observation of colocalized CED-4/Rhodamine B mitochondrial yellow signal (top right bottom panel) pre-irradiation and green nuclear CED-4 platformlike structures post-irradiation (white arrows in bottom left lower panel).

Table 1. Role of *C. elegans* orthologs of sphingolipid metabolism in radiation-induced apoptosis. The family of sphingolipids and associated metabolic enzymes involved in ceramide intermediary metabolism, conserved from yeast to humans is shown on at left. Thick arrows designate the de novo ceramide synthetic pathway. Enzymes listed in bold indicate *C. elegans* enzymes for which *lf* alleles were screened for germ cell apoptosis at 36 hours post–120 Gy (shown at right). Apoptosis inhibition (+) was interpreted relative to WT-irradiated controls. Asterisks indicate hypersensitivity to radiation-induced apoptosis. At least 20 worms were counted per allele. SPT, serine palmitoyltransferase; 3-KSR, 3-ketosphinganine reductase; CerS, ceramide synthase; DES, dihydoceramide desaturase; CerK, ceramide kinase; SMase, sphingomyelinase; CDase, ceramidase; SphK, sphingosine kinase; S1PPL, S1P lyase.

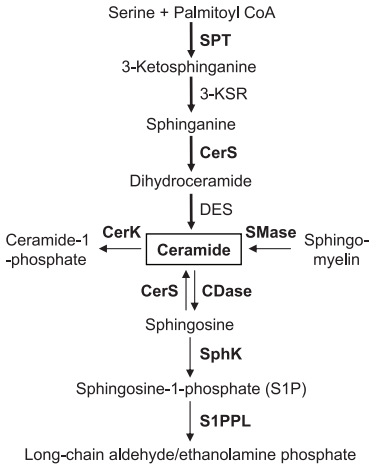

Mammalian gene product	*C. elegans* orthologous gene(s)	Sequence name	Alleles	Apoptosis inhibition
SPT 1	*sptl-1*	C23H3.4	*ok1693*	–
SPT 2	*sptl-3*	T22G5.5	*ok1927*	–
CerS	*hyl-1*	C09G4.1	*ok976*	+
	hyl-2	K02G10.6	*ok1766*	–
	lagr-1	Y6B3B.10	*gk327* *gk331*	+ +
Acid CDase		F27E5.1	*ok564*	–
SphK-1	*ok1097*	C34C6.5a,b	*ok1097*	–*
S1PPL 1	*tag-38*	B0222.4	*tm470*	–
CerK		T10B11.2	*ok1252*	–
Acid SMase	*asm-1*	B0252.2	*kk-1*	–
	asm-2	ZK455.4	*ok183*	–
	asm-3	W03G1.7a,b	*tm2384*	–
Neutral SMase		T27F6.6	*tm2178*	–

is inactive in the *lf egl-1* mutant *egl-1(n1084n3082)* (Fig. 2C), it appears that there is a requirement for at least a baseline level of BH3-only proteins for ceramide-induced apoptosis. Consistent with this notion, C_{16}-ceramide administration did not increase *egl-1* and *ced-13* transcription (1.2 ± 0.1– and 0.8 ± 0.1–fold of control, respectively, at 5 hours). Furthermore, inactivating the core apoptotic machinery in *lf ced-3(n717)* and *ced-4(n1162)* or in gain-of-function *ced-9(n1950)* animals, which abolish radiation-induced germline apoptosis, similarly abolished C_{16}-ceramide-induced death (Fig. 2C). Collectively, these data indicate that ceramide acts in conjunction with BH3-only proteins upstream of the mitochondrial commitment step of apoptosis in the *C. elegans* germ line.

As these studies point to a mitochondrial site of ceramide action, we devised an immune histochemical approach to evaluate whether ceramide might increase in the mitochondria of *C. elegans* germ cells. We took advantage of the increased frequency of germ cell apoptosis in *abl-1(ok171)*, anticipating a maximized ceramide signal upon irradiation in this strain. Gonads from unirradiated or irradiated worms were dissected, opened by freeze-cracking (*17*), and then stained with MID15B4, a specific anti-ceramide antibody [see the supporting online material (SOM)]. Mitochondria were localized with an antibody to the mitochondrial marker protein OxPhos Complex IV subunit I (COX-IV) or by Rhodamine B staining (*18*). COX-IV staining (green) before and after irradiation displayed a prominent perinuclear distribution reminiscent of mitochondrial topography in some mammalian cell systems (Fig. 3A) (*19*, *20*). Ceramide staining (red) displayed a similar profile and at baseline was faint, increasing 2.4-fold at 24 hours post-irradiation (Fig. 3A and fig. S3) ($P < 0.0001$). Merging the two signals (red and green) revealed that ceramide accumulation was distinctively mitochondrial (yellow). Radiation-induced ceramide accumulation was abrogated in *lagr1(gk327);hyl-1(ok976);abl-1(ok171)* animals (Fig. 3A). Similarly, ceramide increase was abrogated in irradiated *lagr-1(gk327);hyl-1(ok976)* as compared with WT animals (1.2- versus 3.9-fold of unirradiated controls, respectively). These results define ionizing radiation-induced ceramide accumulation in the *C. elegans* germ line as mitochondrial in origin, mediated via the classic ceramide biosynthetic pathway.

We examined whether mitochondrial ceramide accumulation was required for CED-4 redistribution to nuclear membranes. In nonapoptotic somatic cells, CED-4 is sequestered to mitochondria by binding CED-9. When displaced by EGL-1, CED-4 targets nuclear membranes and activates caspase CED-3, necessary for the effector phase of apoptosis (*21*–*24*). For these studies, *abl-1(ok171)* and *lagr-1(gk327);hyl-1(ok976);abl-1(ok171)* animals were exposed to 120 Gy, and germ cells were released from gonads and stained with antibodies against *C. elegans* CED-4 and Ce-lamin, a nuclear membrane marker. CED-4 and Ce-lamin colocalization by confocal microscopy (yellow merged signal) served as readout for nuclear CED-4 redistribution. After irradiation nuclear CED-4 staining intensity increased 4.3-fold from 0.59 ± 0.03 to 2.53 ± 0.42 arbitrary fluorescence units in *abl-1(ok171)* (Fig. 3, B and C) ($P < 0.001$). Consistent with reduced germ cell apoptosis (Fig. 2A), nuclear CED-4 staining is significantly reduced in *lagr-1(gk327);hyl-1(ok976);abl-1(ok171)* (Fig. 3, B and C) [$P <$ 0.001 versus *abl-1(ok171)*]. Specifically, baseline CED-4 intensity at the nuclear membrane is lower in *lagr-1(gk327);hyl-1(ok976);abl-1(ok171)* than in *abl-1(ok171)*, increasing post-irradiation only to the control level of unirradiated *abl-1(ok171)* worms (Fig. 3C), an effect probably of biologic relevance as the biophysical effects of ceramide on membrane structure are concentration-dependent (*1*, *3*).

We also used *opls219* worms, a strain expressing a CED-4::GFP fusion protein (where GFP is green fluorescent protein), which permits in vivo detection of CED-4 trafficking (*25*). *opls219* worms were cultured on plates containing Rhodamine B to stain mitochondria (red). Merged images detect mitochondrial CED-4 as a yellow signal (red and green overlay), whereas nonmitochondrial CED-4 appears green. Although a low-intensity green CED-4 signal was detected in nuclear membranes of unirradiated germ cells, the large majority of CED-4 was present in mitochondria before irradiation. At 36 hours postradiation, the CED-4 signal was markedly reduced in mitochondria, relocalizing primarily to nuclear membranes as bright green platform-like structures (arrows in lower left panel in bottom of Fig. 3D). In eight worms, overall reduction in CED-4 mitochondrial colocalization upon irradiation was ~50% ($P < 0.0001$), abrogated in *lagr-1(gk327);opls219* (fig. S4). Consistent with the anti–CED-4 antibody staining (Fig. 3B), the loss of mitochondrial CED-4 signal in *opls219* was accompanied by a twofold increase in nuclear CED-4 signal, blocked entirely in *lagr-1(gk327);opls219* (to 0.9 ± 0.1 fold of control). These results indicate that mitochondrial ceramide contributes substantively to CED-4 displacement from mitochondrial membranes during radiation-induced germ cell apoptosis.

Our data indicate that the ceramide synthetic pathway is required for radiation-induced apoptosis of *C. elegans* germ cells. The most parsimonious molecular ordering suggests that CS (as well as its enzymatic product ceramide) functions on a pathway that is parallel to the CEP-1/p53–EGL-1 system. The coordinated function of these two pathways occurs at the mitochondrial commitment step of the apoptotic process. We hypothesize that ceramide may recompartmentalize the mitochondrial outer membrane, yielding a permissive microenvironment for EGL-1–mediated displacement of CED-4, the trigger for the effector stage of the apoptotic process.

References and Notes

1. E. Gulbins, P. L. Li, *Am. J. Physiol. Regul. Integr. Comp. Physiol.* **290**, R11 (2006).
2. K. Hofmann, V. M. Dixit, *Trends Biochem. Sci.* **23**, 374 (1998).
3. F. M. Goni, A. Alonso, *Biochim. Biophys. Acta* **1758**, 1902 (2006).
4. Materials and methods are available as supporting material on *Science* Online.
5. A. Gartner, S. Milstein, S. Ahmed, J. Hodgkin, M. O. Hengartner, *Mol. Cell* **5**, 435 (2000).
6. E. R. Hofmann *et al.*, *Curr. Biol.* **12**, 1908 (2002).
7. L. Geeraert, G. P. Mannaerts, P. P. van Veldhoven, *Biochem. J.* **327**, 125 (1997).
8. S. Spassieva *et al.*, *J. Biol. Chem.* **281**, 33931 (2006).
9. That *hyl-1* and *hyl-2* encode ceramide syntheses is clearly shown by their ability to restore growth to nearly

WT levels when expressed in Lag1/Lac1 double yeast mutants (*10*).
10. J.-C. Martinou, H. Riezman, personal communication.
11. Y. Pewzner-Jung, S. Ben-Dor, A. H. Futerman, *J. Biol. Chem.* **281**, 25001 (2006).
12. A small amount of C16:0:0 ceramide with a C17 sphingosine base (2% of the amount of the most abundant species C22:0:1) can be detected in *C. elegans* extracts (*13*).
13. H. Riezman, personal communication.
14. T. A. Taha *et al.*, *FASEB J.* **20**, 482 (2006).
15. X. Deng *et al.*, *Nat. Genet.* **36**, 906 (2004).
16. B. Schumacher *et al.*, *Cell Death Differ.* **12**, 153 (2005).
17. J. S. Duerr, in *Worm Book* (The *C. elegans* Research Community, WormBook, 2007), www.wormbook.org.
18. A. M. Labrousse, M. D. Zappaterra, D. A. Rube, A. M. van der Bliek, *Mol. Cell* **4**, 815 (1999).
19. K. De Vos *et al.*, *J. Biol. Chem.* **273**, 9673 (1998).
20. L. del Peso, V. M. Gonzalez, N. Inohara, R. E. Ellis, G. Nunez, *J. Biol. Chem.* **275**, 27205 (2000).
21. B. Conradt, H. R. Horvitz, *Cell* **93**, 519 (1998).
22. W. D. Fairlie *et al.*, *Cell Death Differ.* **13**, 426 (2006).
23. F. Chen *et al.*, *Science* **287**, 1485 (2000).
24. N. Yan *et al.*, *Mol. Cell* **15**, 999 (2004).
25. Y. Zermati *et al.*, *Mol. Cell* **28**, 624 (2007).
26. We thank Caenorhabditis Genetics Center and National BioResource Project-Japan for the strains provided; H. R. Horwitz for the anti–CED-4 antibody; Y. Gruenbaum for the anti–Ce-lamin-antibody; M. O. Hengartner for the strain opls219; and S. Davidor, D. Chau, H. Lee, J. Mesicek, and the Molecular Cytology and Genomics Core Laboratory of MSKCC for the technical assistance. This work was supported by grants CA85704 (R.K.), CA105125-03 (A.H.-F.), and 2R01HD42680-06 (S.S.).

Supporting Online Material
www.sciencemag.org/cgi/content/full/322/5898/110/DC1
Materials and Methods
Figs. S1 to S5
Tables S1 to S3
References

20 March 2008; accepted 9 September 2008
10.1126/science.1158111

Lacking Control Increases Illusory Pattern Perception

Jennifer A. Whitson[1]* and Adam D. Galinsky[2]

We present six experiments that tested whether lacking control increases illusory pattern perception, which we define as the identification of a coherent and meaningful interrelationship among a set of random or unrelated stimuli. Participants who lacked control were more likely to perceive a variety of illusory patterns, including seeing images in noise, forming illusory correlations in stock market information, perceiving conspiracies, and developing superstitions. Additionally, we demonstrated that increased pattern perception has a motivational basis by measuring the need for structure directly and showing that the causal link between lack of control and illusory pattern perception is reduced by affirming the self. Although these many disparate forms of pattern perception are typically discussed as separate phenomena, the current results suggest that there is a common motive underlying them.

The desire to combat uncertainty and maintain control has long been considered a primary and fundamental motivating force in human life (*1*–*3*) and one of the most important variables governing psychological well-being and physical health (*4*–*6*). For example, when individuals can control, or even just perceive that they can control, the duration of painful shocks, they show lower arousal (*7*); similarly, learning details about a painful medical procedure can reduce anxiety and even lead to shorter recovery time (*8*). In contrast, lacking control is an unsettling and aversive state, activating the amygdala, which indicates a fear response (*9*). It is not surprising, then, that individuals actively try to reestablish control when it disappears or is taken away (*10*).

We propose that when individuals are unable to gain a sense of control objectively, they will try to gain it perceptually. Faced with a lack of control, people will turn to pattern perception, the identification of a coherent and meaningful interrelationship among a set of stimuli. Through pattern perception, individuals can make sense of events and develop predictions for the future (*11*–*13*). For instance, spontaneous causal attributions (identifying a cause-and-effect pattern in a sequence of events) are best predicted by unexpected events rather than negative ones, suggesting that a major determinant of sense-making behavior is whether an individual lacks control (*14*, *15*). Indeed, researchers have designated "desire for control as a motivational force behind the attribution process" (*16*).

Related to our theoretical framework, research has found that current needs can shape and even bias perceptual processes. For example, children of lower economic status overestimate the size of coins as compared with the wealthy (*17*), and hungry individuals are more likely to see food in ambiguous images (*18*). This research has established that specific needs alter the perception of stimuli directly relevant to those needs. The current research explores a much broader phenomenon: whether lacking control creates a tendency to see patterns more generally.

Because these feelings of control are so essential for psychological well-being, our main hypothesis is that lacking control will lead to illusory pattern perception, which we define as the identification of a coherent and meaningful interrelationship among a set of random or unrelated stimuli (such as the tendency to perceive false correlations, see imaginary figures, form superstitious rituals, and embrace conspiracy beliefs, among others). In fact, a high desire for control has been associated with distortions of objective reality (*19*), and studies have found that lacking control produces attributional biases to restore feelings of control (*16*). We suggest that a lack of control provokes seeing and seeking patterns because pattern perception is a compensatory mechanism designed to restore feelings of control. Conspiracy beliefs are one example of how this process might work: They have been described as giving "causes and motives to events that are more rationally seen as accidents . . . [in order to] bring the disturbing vagaries of reality under . . . control" (*20*).

There are a number of findings that circumstantially support our specific hypothesis that lacking control leads to illusory pattern perception. Such disparate groups as preindustrial fisherman, skydivers, baseball players, and first-year MBA students have all displayed a connection between a lack of control and perceiving illusory patterns in one's environment. Tribes of the Trobriand islands who fish in the deep sea, where sudden storms and unmapped waters are constant concerns, have far more rituals associated with fishing than do those who fish in shallow waters (*21*). Parachute jumpers are more likely to see a nonexistent figure in a picture of visual noise just before a jump than at an earlier time (*22*). Baseball players create rituals in direct proportion to the capriciousness of their position (for example, pitchers are particularly likely to see connections between the shirt they wear and success) (*23*). First-year MBA students are more susceptible to conspiratorial perceptions than are second-year students (*24*). Even on a national level, when times are economically uncertain, superstitions increase (*25*). These anthropological observations and correlational studies all provide suggestive but nonconclusive evidence that lacking control leads to the perception of illusory patterns.

To test whether a lack of control directly increases illusory pattern perception, we conducted six experiments that used multiple methods to induce a lack of control and measured illusory pattern perception by using a variety of stimuli. Our definition of pattern perception, both illusory and accurate, encompasses a range of phenomena that were previously studied independently. Despite their surface disparities, seeing figures in noise, forming illusory correlations, creating superstitious rituals, and perceiving conspiracy beliefs all represent the same underlying process: the identification of a coherent and meaningful interrelationship among a set of random or unrelated stimuli.

In the first experiment, we sought to establish that lacking control creates a need to see patterns. We manipulated lack of control by using a concept-identification paradigm specifically created to re-

[1]Department of Management, The University of Texas at Austin, Austin, TX 78712, USA. [2]Department of Management and Organizations, Northwestern University, Evanston, IL 60208, USA.

*To whom correspondence should be addressed. E-mail: jennifer.whitson@mccombs.utexas.edu

Lacking Control Increases Illusory Pattern Perception

Jennifer A. Whitson, *et al.*

Science **322**, 115 (2008);
DOI: 10.1126/science.1159845

Science (print ISSN 0036-8075; online ISSN 1095-9203) is published weekly, except the last week in December, by the American Association for the Advancement of Science, 1200 New York Avenue NW, Washington, DC 20005.

WT levels when expressed in Lag1/Lac1 double yeast mutants (*10*).
10. J.-C. Martinou, H. Riezman, personal communication.
11. Y. Pewzner-Jung, S. Ben-Dor, A. H. Futerman, *J. Biol. Chem.* **281**, 25001 (2006).
12. A small amount of C16:0:0 ceramide with a C17 sphingosine base (2% of the amount of the most abundant species C22:0:1) can be detected in *C. elegans* extracts (*13*).
13. H. Riezman, personal communication.
14. T. A. Taha *et al.*, *FASEB J.* **20**, 482 (2006).
15. X. Deng *et al.*, *Nat. Genet.* **36**, 906 (2004).
16. B. Schumacher *et al.*, *Cell Death Differ.* **12**, 153 (2005).
17. J. S. Duerr, in *Worm Book* (The *C. elegans* Research Community, WormBook, 2007), www.wormbook.org.
18. A. M. Labrousse, M. D. Zappaterra, D. A. Rube, A. M. van der Bliek, *Mol. Cell* **4**, 815 (1999).
19. K. De Vos *et al.*, *J. Biol. Chem.* **273**, 9673 (1998).
20. L. del Peso, V. M. Gonzalez, N. Inohara, R. E. Ellis, G. Nunez, *J. Biol. Chem.* **275**, 27205 (2000).
21. B. Conradt, H. R. Horvitz, *Cell* **93**, 519 (1998).
22. W. D. Fairlie *et al.*, *Cell Death Differ.* **13**, 426 (2006).
23. F. Chen *et al.*, *Science* **287**, 1485 (2000).
24. N. Yan *et al.*, *Mol. Cell* **15**, 999 (2004).
25. Y. Zermati *et al.*, *Mol. Cell* **28**, 624 (2007).
26. We thank Caenorhabditis Genetics Center and National BioResource Project-Japan for the strains provided; H. R. Horwitz for the anti–CED-4 antibody; Y. Gruenbaum for the anti–Ce-lamin-antibody; M. O. Hengartner for the strain opls219; and S. Davidor, D. Chau, H. Lee, J. Mesicek, and the Molecular Cytology and Genomics Core Laboratory of MSKCC for the technical assistance. This work was supported by grants CA85704 (R.K.), CA105125-03 (A.H.-F.), and 2R01HD42680-06 (S.S.).

Supporting Online Material
www.sciencemag.org/cgi/content/full/322/5898/110/DC1
Materials and Methods
Figs. S1 to S5
Tables S1 to S3
References

20 March 2008; accepted 9 September 2008
10.1126/science.1158111

Lacking Control Increases Illusory Pattern Perception

Jennifer A. Whitson[1]* and Adam D. Galinsky[2]

We present six experiments that tested whether lacking control increases illusory pattern perception, which we define as the identification of a coherent and meaningful interrelationship among a set of random or unrelated stimuli. Participants who lacked control were more likely to perceive a variety of illusory patterns, including seeing images in noise, forming illusory correlations in stock market information, perceiving conspiracies, and developing superstitions. Additionally, we demonstrated that increased pattern perception has a motivational basis by measuring the need for structure directly and showing that the causal link between lack of control and illusory pattern perception is reduced by affirming the self. Although these many disparate forms of pattern perception are typically discussed as separate phenomena, the current results suggest that there is a common motive underlying them.

The desire to combat uncertainty and maintain control has long been considered a primary and fundamental motivating force in human life (*1*–*3*) and one of the most important variables governing psychological well-being and physical health (*4*–*6*). For example, when individuals can control, or even just perceive that they can control, the duration of painful shocks, they show lower arousal (*7*); similarly, learning details about a painful medical procedure can reduce anxiety and even lead to shorter recovery time (*8*). In contrast, lacking control is an unsettling and aversive state, activating the amygdala, which indicates a fear response (*9*). It is not surprising, then, that individuals actively try to reestablish control when it disappears or is taken away (*10*).

We propose that when individuals are unable to gain a sense of control objectively, they will try to gain it perceptually. Faced with a lack of control, people will turn to pattern perception, the identification of a coherent and meaningful interrelationship among a set of stimuli. Through pattern perception, individuals can make sense of events and develop predictions for the future (*11*–*13*). For instance, spontaneous causal attributions (identifying a cause-and-effect pattern in a sequence of events) are best predicted by unexpected events rather than negative ones, suggesting that a major determinant of sense-making behavior is whether an individual lacks control (*14*, *15*). Indeed, researchers have designated "desire for control as a motivational force behind the attribution process" (*16*).

Related to our theoretical framework, research has found that current needs can shape and even bias perceptual processes. For example, children of lower economic status overestimate the size of coins as compared with the wealthy (*17*), and hungry individuals are more likely to see food in ambiguous images (*18*). This research has established that specific needs alter the perception of stimuli directly relevant to those needs. The current research explores a much broader phenomenon: whether lacking control creates a tendency to see patterns more generally.

Because these feelings of control are so essential for psychological well-being, our main hypothesis is that lacking control will lead to illusory pattern perception, which we define as the identification of a coherent and meaningful interrelationship among a set of random or unrelated stimuli (such as the tendency to perceive false correlations, see imaginary figures, form superstitious rituals, and embrace conspiracy beliefs, among others). In fact, a high desire for control has been associated with distortions of objective reality (*19*), and studies have found that lacking control produces attributional biases to restore feelings of control (*16*). We suggest that a lack of control provokes seeing and seeking patterns because pattern perception is a compensatory mechanism designed to restore feelings of control. Conspiracy beliefs are one example of how this process might work: They have been described as giving "causes and motives to events that are more rationally seen as accidents . . . [in order to] bring the disturbing vagaries of reality under . . . control" (*20*).

There are a number of findings that circumstantially support our specific hypothesis that lacking control leads to illusory pattern perception. Such disparate groups as preindustrial fisherman, skydivers, baseball players, and first-year MBA students have all displayed a connection between a lack of control and perceiving illusory patterns in one's environment. Tribes of the Trobriand islands who fish in the deep sea, where sudden storms and unmapped waters are constant concerns, have far more rituals associated with fishing than do those who fish in shallow waters (*21*). Parachute jumpers are more likely to see a nonexistent figure in a picture of visual noise just before a jump than at an earlier time (*22*). Baseball players create rituals in direct proportion to the capriciousness of their position (for example, pitchers are particularly likely to see connections between the shirt they wear and success) (*23*). First-year MBA students are more susceptible to conspiratorial perceptions than are second-year students (*24*). Even on a national level, when times are economically uncertain, superstitions increase (*25*). These anthropological observations and correlational studies all provide suggestive but nonconclusive evidence that lacking control leads to the perception of illusory patterns.

To test whether a lack of control directly increases illusory pattern perception, we conducted six experiments that used multiple methods to induce a lack of control and measured illusory pattern perception by using a variety of stimuli. Our definition of pattern perception, both illusory and accurate, encompasses a range of phenomena that were previously studied independently. Despite their surface disparities, seeing figures in noise, forming illusory correlations, creating superstitious rituals, and perceiving conspiracy beliefs all represent the same underlying process: the identification of a coherent and meaningful interrelationship among a set of random or unrelated stimuli.

In the first experiment, we sought to establish that lacking control creates a need to see patterns. We manipulated lack of control by using a concept-identification paradigm specifically created to re-

[1]Department of Management, The University of Texas at Austin, Austin, TX 78712, USA. [2]Department of Management and Organizations, Northwestern University, Evanston, IL 60208, USA.

*To whom correspondence should be addressed. E-mail: jennifer.whitson@mccombs.utexas.edu

duce a sense of control (*26*–*28*). Consistent with this paradigm, participants in the lack-of-control condition received random performance feedback that was not contingent on their responses. Baseline participants identified concepts without feedback. We measured the individuals' need to perceive patterns using the Personal Need for Structure Scale, which assesses the need to "structure the world into a simplified, more manageable form" (*29*).

Participants lacking control in the concept identification task [Personal Need for Structure Scale mean (M) = 44.9, SD = 6.3] showed an increase in their personal need for structure as compared with those in the baseline condition [M = 38.2, SD = 10.7; Student's t test, $t(27) = 2.11$, $P = 0.045$]. Having established that a lack of control increases the need to see structure and patterns, we next tested whether it increases the perception of illusory patterns.

Experiment 2 manipulated lack of control using the same concept-identification task from the previous experiment and then measured visual pattern perception with a modified version of the snowy pictures task (*30*). Twelve of the 24 pictures were from the original task and contained a grainy embedded image that was difficult but possible to perceive. The other 12 pictures were manipulated using software to eliminate any traces of the embedded image. Participants were asked to identify whether there was an image or not and, if so, what it was.

In the 12 pictures in which an image did exist, almost all participants perceived an image [overall M = 11.4, SD = 1.1; $t(34) = 0.57$, $P = 0.57$]. However, in pictures that lacked an image, participants in the lack-of-control condition (M = 5.16, SD = 3.5) saw marginally more images than did participants in the baseline condition [M = 3.47, SD = 2.0; $t(34) = 1.76$, $P = 0.09$]. Participants who lacked control were more likely to perceive images where none existed.

In the third experiment, we manipulated lack of control by having participants vividly recall an experience in which they lacked or had full control over a situation. They next responded to three scenarios that tapped into superstitious beliefs; each scenario described an outcome that was preceded by a potentially unrelated behavior (such as knocking on wood before an important meeting and then getting one's idea approved). The participants were asked whether they thought the behavior was related to the outcome and how worried they were about performing that behavior in the future. Those who recalled an experience in which they lacked control (M = 4.92, SD = 2.5) perceived a greater connection between the two events than did those who recalled having control [M = 3.5, SD = 1.8; $t(39) = 2.03$, $P = 0.05$] and were more worried about performing similar behaviors in the future [M = 5.95, SD = 2.6 versus M = 4.12, SD = 2.3;, $t(39) = 2.42$, $P = 0.02$]. This experiment establishes that the mere recollection of an experience involving a lack of control increases superstitious perceptions.

To demonstrate that threat, independent of lacking control, is not the driving force behind illusory pattern perception, we conducted a fourth experiment in which all participants recalled a situation "in which something threatening happened," but we manipulated whether they had or lacked control in the situation. Our dependent measures were visual pattern perception and an additional type of pattern perception, conspiracy perceptions. Because the altered snowy pictures in the second experiment may have contained trace images of the original image, we measured illusory pattern perception by creating 10 pictures that each contained a random scattering of black dots on a white background, resembling noise on a television set. We also measured conspiracy perceptions to rule out the possibility that the above findings are simply the result of increased heuristic processing: The perception of conspiracies is not a simplifying process but a complex integration of data that is cognitively effortful. In each of our conspiracy scenarios, the situation was ambiguous as to whether there was a coordinated effort among a set of individuals to produce an outcome; participants were asked how connected they thought the individuals' behavior was to the outcome.

Even though all participants recalled a threatening situation, our manipulation of control still had the predicted effects. Lacking control (M = 2.92, SD = 2.5) led participants to see more images in the visual static than did those in the control condition [M = 0.92, SD = 2.0; $t(23) = 2.18$, $P = 0.04$]. In addition, participants who lacked control (M = 4.42, SD = 1.1) perceived a significantly greater likelihood of conspiracy than did control participants [M = 3.50, SD = 1.0; $t(23) = 2.19$, $P = 0.04$]. Two raters that were blind to the conditions and hypotheses coded the situations the participants recalled (*31*), and we found no differences between conditions in the level of threat expressed [$t(23) = 1.1$, $P = 0.30$]. Lack of control, and not threat alone, appears to produce illusory pattern perception.

We next tested the relationship between lack of control and illusory pattern perception in a financial domain, the stock market, by using a standard illusory correlation paradigm, which assesses whether two uncorrelated sets of information are perceived as related (that is, whether a pattern is seen that does not exist). We manipulated control by describing the stock market environment as either volatile or stable. In the volatile condition, participants read that the stock market was volatile and uncertain and were given a headline that said, "Rough Seas Ahead for Investors." In the stable condition, participants read that the stock market was stable and predictable and were given a headline that said, "Smooth Sailing Ahead for Investors."

Participants then read 24 statements about the financial performance of two companies. Each statement contained either positive or negative performance information. The ratio of positive to negative statements was constant across the companies, but the amount of information seen about each company was different: company A had 16 positive and 8 negative statements, whereas company B had 8 positive and 4 negative statements. Participants were then given a choice to invest in either company A or B and were asked to report the number of negative statements that they remembered referring to companies A and B.

The presentation of the financial performance statements was designed to be consistent with the typical illusory correlation paradigm. Using this paradigm, researchers typically find that participants perceive a correlation between the infrequent behaviors and the group with less information, overestimating the number of times the two rare events occurred together, even though the information they are given distributes the positive and negative behaviors in equal proportion between the two groups. Because people typically over-associate the infrequent information with the infrequent group (that is, they perceive a correlation), we predicted that market volatility would increase the association between negative information and company B.

Market volatility affected investment decisions: Only 25% chose to invest in company B during a volatile market as compared with 58% during a stable market [χ^2 test, $\chi^2(1) = 4.94$, $P = 0.03$]. The volatile market condition also led to a stronger association between the negative information and company B: Participants overestimated the frequency of negative statements about company B in the volatile market (M = 5.0, SD = 1.5) but accurately perceived the amount of negative statements in the stable market [M = 3.9, SD = 1.7; $t(42) = 2.40$, $P = 0.02$]. The degree that participants overestimated the frequency of negative statements about company B mediated the effect of market volatility on investment decisions: when market volatility and frequency of negative statements simultaneously predicted investment decisions, market volatility was no longer a significant predictor ($P = .169$), but frequency of negative statements did predict investment decision ($P = .009$; Sobel test, $z = 1.78$, $P = 0.07$). These analyses demonstrate that participants formed illusory correlations: participants overestimated the infrequent type of information (negative) with the infrequently presented group (company B), and this illusory connection between negative statements and company B drove their investment decisions.

If the perception of illusory patterns is a compensatory mechanism induced by the distressing experience of lacking control, then an intervention that ameliorates this aversive state should break the link between lacking control and illusory pattern perception. Numerous studies have shown that letting individuals contemplate and affirm their important values is an effective method for reducing a variety of psychologically aversive states, including learned helplessness, dissonance, attributional biases, and persistent rumination (*32*–*34*). Because (i) self-affirmation reduces reactivity to threats and eliminates compensatory responses and (ii) lacking control is such a psychologically aversive and distressing state, we predicted that self-affirmation would reduce the tendency for individuals who lack control to perceive illusory patterns.

To test whether self-affirmations would reduce illusory pattern perception, we used the recall task from experiment 3 to manipulate lack of control and measured illusory pattern perception by using experiment 2's snowy pictures task and

conspiracy scenarios similar to those used in experiment 4 (*35*). The experiment had three conditions: lack of control without self-affirmation, lack of control against self-affirmation, and baseline (no recall task). After completing the recall task but before reading and responding to the snowy pictures and the conspiracy scenarios, participants completed a standard self-affirmation procedure (*34*). They were asked to complete a scale focused on a value they had indicated at the beginning of the experiment to be either most important (self-affirmation) or least important (no self-affirmation) to them.

To analyze the data, we conducted contrast tests that compared the lack of control/no self-affirmation condition with the self-affirmation and baseline conditions. Similar to effects found in Experiment 2 on the snowy pictures task, participants who lacked control and received no opportunity for self-affirmation ($M = 5.44$, SD = 3.6) saw more patterns when none existed than did those in the self-affirmation condition ($M = 3.24$, SD = 2.6) and the baseline condition [$M = 3.47$, SD = 3.3; $t(47) = 2.21$, $P = 0.03$]. Additionally, participants who lacked control without self-affirmation ($M = 4.76$, SD = 0.87) perceived a significantly greater likelihood of conspiracy than did those in the self-affirmation ($M = 4.18$, SD = 0.83) and baseline conditions [$M = 4.20$, SD = 1.10; $t(47) = 2.08$, $P = 0.04$] (*36*). Lacking control without an opportunity to self-affirm led participants to see images that did not exist and to perceive conspiracies. However, participants who experienced a lack of control but then had the opportunity to self-affirm resembled participants in the baseline condition. This experiment shows that a lack of control creates a need to perceive patterns in one's environment, even when the patterns perceived are illusory.

These six experiments demonstrate that lacking control motivates pattern perception: Experiencing a loss of control led participants to desire more structure and to perceive illusory patterns. The need to be and feel in control is so strong that individuals will produce a pattern from noise to return the world to a predictable state.

We acknowledge that the studies did not involve large sample sizes, but given the large effects required to achieve significance, combined with the consistent pattern across the studies, we feel our hypothesis has been effectively supported.

The focus of the current research was on illusory pattern perception. Because nearly all participants correctly identified an image in the snowy pictures when one was present, we were not able to address whether a lack of control also increases accuracy in detecting real patterns, ones that do in fact exist. If so, a lack of control would seem to increase positive identifications, both false and accurate. Future research should employ tasks with greater variance in participants' ability to detect actual patterns to test this idea more systematically. It should also explore whether increased pattern perception exists not just in the identification of more patterns but also in shorter latencies to perceive them.

Illusory pattern perception may not be entirely maladaptive. If pattern perception helps an individual regain a sense of control, the very act of perceiving a pattern, even an illusory one, may be enough to soothe this aversive state, decreasing depression and learned helplessness, creating confidence, and increasing agency. Although it is certainly preferable to accurately perceive one's environment, illusory pattern perception itself may be at times adaptive by allowing an individual to psychologically engage with rather than withdraw from their environment.

The current research offers insights into how illusory pattern perception driven by a lack of control may be overcome. When individuals were made to feel psychologically secure after lacking control, they were less prone to the perception of illusory patterns. Indeed, the beneficial effects of this sense of security are tapped into by psychotherapy, which attempts to give clients a sense of control over their lives to reduce the obsessive-compulsive tendencies or sinister attributions engendered by seeing too much meaning and intentions in others' innocuous behaviors. Collectively, the six experiments highlight the importance of having versus lacking control and hold promise for preventing futile pursuits born of the perception of illusory patterns.

References and Notes

1. H. H. Kelley, *Attribution in Social Interaction* (General Learning Press, Morristown, NJ, 1971).
2. R. White, *Psychol. Rev.* **66**, 297 (1959).
3. R. deCharms, *Personal Causation* (Academic Press, New York, 1969).
4. D. C. Glass, J. E. Singer, *Am. Sci.* **60**, 457 (1972).
5. D. C. Klein, E. Fencil-Morse, M. E. P. Seligman, *J. Pers. Soc. Psychol.* **33**, 508 (1976).
6. S. Cohen, *Behavior, Health, and Environmental Stress* (Plenum Press, New York, 1986).
7. D. C. Glass, J. E. Singer, H. S. Leonard, D. Krantz, S. Cohen, H. Cummings, *J. Pers.* **41**, 577 (1973).
8. A. Luck, S. Pearson, G. Maddern, P. Hewett, *Lancet* **354**, 2032 (1999).
9. P. J. Whalen, *Curr. Dir. Psychol. Sci.* **7**, 177 (1998).
10. J. W. Brehm, *A Theory of Psychological Reactance* (Academic Press, New York, 1966).
11. T. A. Pyszczynski, J. Greenberg, *J. Pers. Soc. Psychol.* **40**, 31 (1981).
12. R. Hastie, *J. Pers. Soc. Psychol.* **46**, 44 (1984).
13. E. G. Clary, A. Tesser, *Pers. Soc. Psychol. Bull.* **9**, 609 (1983).
14. S. Kanazawa, *Pers. Soc. Psychol. Bull.* **18**, 659 (1992).
15. B. Weiner, *Psychol. Bull.* **97**, 74 (1985).
16. T. S. Pittman, N. L. Pittman, *J. Pers. Soc. Psychol.* **39**, 377 (1980).
17. J. S. Bruner, C. C. Goodman, *J. Abnorm. Soc. Psychol.* **42**, 33 (1947).
18. R. Levine, I. Chein, G. Murphy, *J. Psychol.* **13**, 283 (1942).
19. J. M. Burger, L. T. Hemans, *J. Pers.* **56**, 531 (1988).
20. D. Pipes, *Conspiracy: How the Paranoid Style Flourishes and Where It Comes From* (Free Press, New York, 1997).
21. B. Malinowski, R. Redfield, *Magic, Science and Religion, and Other Essays* (Beacon Press, Boston, 1948).
22. P. Simonov, M. Frolov, V. Evtushenko, E. Sviridov, *Aviat. Space Environ. Med.* **48**, 856 (1977).
23. G. Gmelch, *Trans Action* **9**, 39 (1971).
24. R. M. Kramer, *Motiv. Emot.* **18**, 199 (1994).
25. S. M. Sales, *J. Pers. Soc. Psychol.* **28**, 44 (1973).
26. N. L. Pittman, T. S. Pittman, *J. Pers. Soc. Psychol.* **37**, 39 (1979).
27. A pretest experiment found that this manipulation did not affect self-esteem {lacking control condition ($M = 5.33$, SD = 1.4) versus the baseline condition [$M = 5.15$, SD = 0.90; $t(26) = 0.38$, $P = 0.70$]}.
28. Materials and methods are available as supporting material on *Science* Online.
29. S. L. Neuberg, J. T. Newsom, *J. Pers. Soc. Psychol.* **65**, 113 (1993).
30. R. B. Ekstrom, J. W. French, H. H. Harman, D. Dermen, *Manual for Kit of Factor-Referenced Cognitive Tests* (Educational Testing Service, Princeton, NJ, 1976).
31. The two raters independently coded each situation for "How much did the person experience or feel threat in the situation?" using a 7-point scale with anchors 1 (very little) and 7 (very much). Because inter-rater reliability was acceptable ($\alpha = .71$), we averaged the coders' ratings.
32. C. M. Steele, T. J. Liu, *J. Pers. Soc. Psychol.* **45**, 5 (1983).
33. T. J. Liu, C. M. Steele, *J. Pers. Soc. Psychol.* **51**, 531 (1986).
34. S. L. Koole, K. Smeets, A. van Knippenberg, A. Dijksterhuis, *J. Pers. Soc. Psychol.* **77**, 111 (1999).
35. Because the conspiracy and superstition scenarios used in the previous experiments were written from a first-person perspective, it may be that illusory pattern perception in social domains only occurs when the self is affected by or implicated in the pattern. To test this possible boundary condition, we altered the conspiracy scenarios used in experiment 6 to be from a third-person perspective (other-focused) and manipulated the lack of control by using the recall task from experiments 3 and 6. We submitted conspiratorial perceptions to a 2 (control: control, lacking control) by 2 (scenario focus: self, other) analysis of variance (ANOVA). The analyses revealed a main effect of lacking control ($F_{1,82} = 9.96$, $P = 0.002$) and no interaction between scenario focus and lacking control ($F_{1,82} = 0.001$, $P = 0.98$). Separate analyses showed that the effect of lacking control significantly increased the perception of conspiracies in both the other-focused scenarios [$M_{\text{lack of control}} = 4.76$, SD = 0.76; $M_{\text{control}} = 4.18$, SD = 0.78; $t(43) = 2.49$, $P = 0.02$] and the self-focused scenarios [$M_{\text{lack of control}} = 4.87$, SD = 0.85; $M_{\text{control}} = 4.30$, SD = 0.95; $t(39) = 2.01$, $P = 0.05$], demonstrating that illusory pattern perception increased regardless of whether the self was affected by the possible conspiracy.
36. Focused contrasts are the preferred analysis with three levels of a single experimental factor when researchers have a hypothesis that one condition will be different from the other two conditions (*37*). For the interested reader, we report the omnibus ANOVA testing the overall variance among the conditions: for snowy pictures, $F_{1,47} = 2.49$, $P = .09$; for conspiracy, $F_{1,47} = 2.17$, $P = .13$.
37. R. Rosenthal, R. L. Rosnov, *Essentials of Behavioral Research: Methods and Data Analysis* (McGraw-Hill, New York, 3rd ed., 2008).

38. This work benefited from the generous financial support of the Dean's office of the Kellogg School of Management. We thank C. Appleton, K. Dover-Taylor, L. Howland, and A. Marfia for research help. The research was based in part on the doctoral dissertation submitted by J.W. to Northwestern University and has benefited from the comments of the committee members W. Gardner, V. Medvec, and K. Murnighan. We also thank L. Egan, Z. Kinias, G. Ku, K. Liljenquist, L. Nordgren, N. Sivanathan, C. Wang, and C. Zhong for their helpful comments.

Supporting Online Material

www.sciencemag.org/cgi/content/full/322/5898/115/DC1
Materials and Methods
References

30 April 2008; Accepted 10 September 2008
10.1126/science.1159845

New Products Focus: PCR/RT-PCR

Applied Biosystems
For information 800-327-3002
www.appliedbiosystems.com

MicroRNA Products

The TaqMan MicroRNA MegaPlex products consist of three new molecular tools designed to streamline the workflow for microRNA (miRNA) analysis, address the needs of researchers working with minute amounts of RNA, and provide broad, up-to-date coverage of known miRNAs expressed in biological samples from humans, mice, and rats. The Megaplex RT Primers consist of high-complexity pools of novel stem-looped reverse transcriptase (RT) primers that reduce the number of RT reactions needed to profile miRNA expression. The MegaPlex PreAmp Primers enable preamplification of starting RNA material when sensitivity is of the utmost importance. Incorporation of preamplification reduces the total RNA input needed to perform an analysis to as little as one nanogram. The TaqMan MicroRNA Arrays are microfluidics cards containing TaqMan MicroRNA Assays that enable rapid and reproducible generation of real-time PCR data for hundreds of miRNA targets in parallel.

PCR Boosting Reagent

PCRboost is a reagent that enhances end-point and reverse-transcription polymerase chain reaction (PCR) fivefold or more during amplification of genomic DNA or RNA templates. It can improve amplification of challenging samples, including trace or degraded samples, long fragments, and low-copy transcripts. PCRboost requires no changes to the user's PCR protocol, but can simply be used to replace the water in the reaction.

Biomatrica
For information 858-550-0308
www.biomatrica.com

Pipetting Tips

Polymerase chain reaction and Sterile CyBi-TipsTrays are available for all purity specifications for use with bacteria and cell cultures as well as nucleic acids. CyBio guarantees precise results at the highest stage. The pipetting tips were designed and developed with great care according to precise specifications to ensure consistent high quality.

CyBio
For information +49-36-41-351-0
www.cybio-ag.com

Electronic Dispensers

The electronic Repeater stream and Xstream hand dispensers are designed for accelerating processes and saving time on long-series pipetting. When used with Combitips Plus tips, the Repeater stream is suitable for all standard pipetting and dispensing applications, while the Repeater Xstream can also perform titrations, sequential dispensing, and aspiration of supernatants. The instruments' increased volume selection provides the flexibility needed for research as well as routine tasks. Their smooth handling reduces the fatigue associated with repetitive work. The nine sizes of Combitips Plus allow a wide dispensing range of up to 112 different volumes. The large volumes allow longer series dispensing without stopping for a refill.

Eppendorf
For information 800-645-3050
www.eppendorf.com

Genomic DNA

The OmniPrep kit isolates high-quality genomic DNA from many different species and tissue types, including animal, plant, bacteria, yeast, fungi, whole blood, and cells in culture. DNA can be isolated from samples high in polysaccharides or other contaminants difficult to remove from the preparations. The kit features a rapid precipitation technique with unique reagents that isolate genomic DNA free from proteins and RNA. Genomic DNA can be isolated in 20 to 40 minutes, depending on the tissue sample type used. The resulting genomic DNA is visualized on an agarose gel as a large single band, demonstrating the high quality and minimal shearing of the technique.

G-Biosciences/Genotech
For information 314-991-6034
www.GBiosciences.com

Gene Expression Arrays

The Roche NimbleGen Sequence Capture 385K Custom Arrays save time and money compared with polymerase chain reaction methods by capturing up to 5Mb of targeted regions from full complexity genomic DNA. Captured fragments are well suited for high throughput sequencing on instruments such as the 454 Genome Sequencer FLX system. The Capture Arrays incorporate built-in control probes and can be tailored to capture target genomic regions or thousands of exons in parallel. The NimbleGen HD2 12-plex arrays for gene expression analysis enable the user to hybridize 12 independent samples on a single slide. These multiplex arrays offer a cost-effective approach to gene expression analysis, without compromising information content or data quality. These arrays are available in a broad range of whole-genome designs or can be custom designed for experimental goals and genomes of interest.

Roche Nimblegen
For information 608-218-7600
www.nimblegen.com

Electronically submit your new product description or product literature information! Go to **www.sciencemag.org/products/newproducts.dtl** for more information.

Newly offered instrumentation, apparatus, and laboratory materials of interest to researchers in all disciplines in academic, industrial, and governmental organizations are featured in this space. Emphasis is given to purpose, chief characteristics, and availabilty of products and materials. Endorsement by *Science* or AAAS of any products or materials mentioned is not implied. Additional information may be obtained from the manufacturer or supplier.

POSITIONS OPEN

UNIVERSITY of VIRGINIA

ASSISTANT PROFESSOR DEVELOPMENTAL BIOLOGIST
Department of Biology
University of Virginia, Charlottesville, Virginia

The Department of Biology at the University of Virginia invites applications for a tenure-track Assistant Professor appointment beginning August 25, 2009. Applications are invited from outstanding individuals studying fundamental aspects of developmental biology at the molecular, cellular, evolutionary, organismal, or systems level.

The Department of Biology at the University of Virginia **(website: http://www.virginia.edu/biology/)** spans a broad range of interests including cell and developmental biology, morphogenesis, neurobiology, biological timing, and evolutionary biology. The successful candidate is expected to establish a vigorous, independent, and externally funded research program, interact with one or more existing departmental strengths, and contribute to undergraduate and graduate instruction and training in developmental biology. A generous startup package and excellent research facilities are available.

Developmental biology has been identified by the University of Virginia as a key area for the future. As part of this focus a University-wide Morphogenesis and Regenerative Medicine Institute **(website: http://www.morphogenesis.virginia.edu/index.htm)** was established that contains a wide group of interactive and energetic investigators. There is also an interschool graduate Program in Molecular, Cell and Developmental Biology **(website: http://healthsystem.virginia.edu/internet/bims_cdb).**

The successful candidate will have the opportunity to participate in these programs.

To apply, please submit a candidate profile, cover letter, curriculum vitae, a statement of current and future research interests, a statement of teaching experience and goals, and the contact information for three references through Jobs at UVA **(website: https://jobs.virginia.edu);** posting number 0602723.

Inquiries about the position may be e-mailed to **e-mail: biosearch@virginia.edu.**

Review of applications by the Search Committee will begin November 1, 2008; however, the position will remain open until filled.

Women and members of underrepresented groups are encouraged to apply. The University of Virginia is an Equal Opportunity/Affirmative Action Employer.

SCIENTIFIC ECOLOGICAL ANTHROPOLOGIST

The University of California, Santa Barbara, Department of Anthropology, Integrative Anthropological Sciences (IAS), seeks a Scientific Ecological Anthropologist for tenure-track position at **ASSISTANT PROFESSOR** level. Possible specializations include human ecology, behavioral or evolutionary ecology, cooperation and common pool resources, indigenous resource management, dual inheritance theory, ethnobiology, subsistence economics, nutritional ecology, reproductive ecology, life history theory, ecological genetics, demography, and epidemiology. Applications should be postmarked by November 14, 2008. For more details see **website: http://www.anth.ucsb.edu.**

The Biology Department at Missouri State University anticipates an August 2009 opening for an **ASSISTANT PROFESSOR** with a specialty in genetics. For a full position description and to apply online see **website: http://www.missouristate. edu/academicopenings.** Letter of application, curriculum vitae, statement of teaching experience and interests, research plan, and names and addresses for three to five references can be uploaded electronically. For additional information contact: **John Heywood, Department of Biology, Missouri State University, Springfield, MO 65897.** *Employment will require a criminal background check at University expense. An Equal Opportunity/Affirmative Action Institution.*

POSITIONS OPEN

EMORY | OXFORD COLLEGE

OXFORD COLLEGE of EMORY UNIVERSITY
Department of Biology

The Department of Biology at Oxford College of Emory University seeks a tenure-track **ASSISTANT PROFESSOR** to begin August 2009. Oxford College **(website: http://www.oxford.emory.edu),** located 38 miles east of Atlanta, is a two-year, liberal arts, fully residential college of Emory University, ranked in the 90th percentile on the National Survey of Student Engagement (NSSE). A Ph.D. or expectation of degree completion this academic year with expertise in cellular and molecular biology is required, along with demonstrated teaching experience. The successful candidate will teach lecture and laboratory courses in introductory cell biology and genetics and sophomore-level genetics and molecular biology. Engagement in scholarly activities is expected and opportunities exist to mentor student research in a liberal arts intensive environment. The Division of Natural Science and Mathematics of Oxford College is in the planning stages of a new state-of-the-art science facility that will encourage student-faculty collaboration, provide an environment for innovative teaching, and be a model of sustainability. Applicants must submit a letter of application, curriculum vitae, statement of teaching philosophy, transcripts, and three reference letters to: **Dr. Nitya Jacob, Chair, Biology Search, Oxford College of Emory University, 100 Hamill Street, Oxford, GA 30054.** Review of applications will begin on November 1, 2008. *Affirmative Action/Equal Opportunity Employer.*

FACULTY POSITIONS in ENVIRONMENTAL CHEMISTRY
University of California, San Diego

The Department of Chemistry and Biochemistry of the University of California San Diego **(website: http://www-chem.ucsd.edu)** seeks applications for two tenure-track faculty positions in environmental chemistry. Candidates with a strong interdisciplinary focus are especially encouraged to apply. Candidates must have a Ph.D. with a substantial record of research accomplishment and an innovative research and teaching plan. Research projects related to multiphase complex systems such as aerosols are of particular interest, and topics could include, but are not limited to, heterogeneous reaction processes, interfacial chemistry, health effects studies of air pollution, cloud/fog reactions, and development of new atmospheric measurement and modeling tools. The successful candidate will be expected to teach environmental chemistry courses at both the graduate and undergraduate levels. Salary is commensurate with qualifications and based on University of California pay scale. Applicants are asked to submit a cover letter, curriculum vitae, research proposal, samples of published research, and a statement of their teaching experience online at **website: http://www.chem.ucsd.edu/recruit/index.cfm?addno=5-121.** Applicants are welcome to include in their cover letters a personal statement summarizing their contributions to diversity. Please arrange for three reference letters to be mailed to: **Chair, Environmental Search Committee 5-121, Department of Chemistry and Biochemistry, University of California, San Diego, 9500 Gilman Drive, Mail Code 0332, La Jolla, CA 92093-0332.** The deadline for applications is December 1, 2008, but until the positions are filled, all applications received will be assured full consideration. *UCSD is an Equal Opportunity/Affirmative Action Employer with a strong institutional commitment to the achievement of diversity.*

WAYNE STATE UNIVERSITY

Biology Faculty Positions

The Department of Biological Sciences at Wayne State University anticipates multiple tenure-track openings for new faculty, subject to administrative approval. Rank will be dependent upon qualifications. Preference will be given to candidates who use innovative approaches to study complex biological problems that complement existing research programs.

Cell Biologist. Areas of interest include, but are not limited to, neurobiology, lipids and signal transduction, RNA biology, and organelle biogenesis and function.

Developmental Biologist. We are particularly interested in individuals taking a systems approach to the analysis of developmental problems, including but not limited to epigenetics and developmental plasticity, gastrulation/neurulation in a vertebrate model system, and plant development.

Microbiologist. Areas of interest include, but are not limited to, bacteriology, virology, immunology, host-pathogen interactions, and infectious disease processes.

Wayne State University is a large, comprehensive, nationally ranked research institution that offers state-of-the-art research facilities and generous start-up packages. Applicants must have a Ph.D. degree, postdoctoral experience and an outstanding record of research achievement. Successful applicants are expected to establish and maintain vigorous, externally funded research programs and to participate in graduate and undergraduate education. All positions will officially be posted on-line at **jobs.wayne.edu** by mid October. Only those application materials that are submitted to this site will be considered. In addition to an online application that includes cover letter and curriculum vitae, applicants must submit a 2-page statement of their research plans and have three letters of reference sent to: **Chair, Faculty Search Committee, Department of Biological Sciences, Wayne State University, 5047 Gullen Mall, Detroit, MI 48202**. Review of applications will begin immediately and the search will remain open until the positions have been filled. Applications will be considered only when all materials have been received.

Wayne State University is an Affirmative Action/Equal Opportunity Employer. Women and members of minority groups are especially encouraged to apply.

Associate Research Scientist

University of Iowa
Department of Biology
LABORATORY OF
DR. BERND FRITZSCH
317 BIOLOGY BUILDING

The Department of Biology is seeking a highly qualified individual for an Associate Research Scientist to head the laboratory of the Departmental DEO, **Dr. Bernd Fritzsch**. The individual will conduct NIH funded research to further molecular understanding of neurosensory development of the ear and incorporate these insights into proper design of tissue culture experiments aimed toward regenerating hair cells. This research is conducted in collaboration with local, national and international colleagues and requires appropriate personality skills to deal with a multiethnic, multicultural laboratory. The University of Iowa ranks in the top 25 of public research universities and is located in a culturally and ethnically diverse community.

To apply for this position requisition number **56043**, please go to **Jobs@uiowa**; **http://jobs.uiowa.edu/**. Salary range: $47,652 to commensurate with experience. See: **http://www.biology.uiowa.edu/faculty_info.php?ID=1503** for description of the lab's research.

The University of Iowa is an Affirmative Action/Equal Opportunity Employer. Women and minority candidates are encouraged to apply.

Faculty Position in Chemical Biology

The Life Sciences Institute (LSI) at the University of Michigan invites applications for a position at the rank of Assistant or Associate Professor in the field of chemical biology. Chemical biology is broadly defined and the successful applicant will use chemical methods to address an important biological question.

The LSI is a scientific enterprise at the University of Michigan dedicated to opening new scientific paths by blending diverse research talents in a state-of-the-art collaborative physical space (**www.lsi.umich.edu**). The LSI is currently home to 29 interactive faculty in the areas of cell biology, genetics, bioinformatics, structural biology, signaling, and chemistry.

Candidates are expected to develop an internationally recognized program of scholarly research and to excel in teaching at undergraduate and graduate levels. The positions will remain open until filled but preference will be given to applicants who have submitted all requested materials prior to **October 31, 2008**. Applicants should send the following (in PDF format): a curriculum vitae, copies of up to three reprints, a one- to two-page summary of research plans, and arrange to have three letters of reference (also in PDF format) sent directly to: **lsichembio@umich.edu**.

The University of Michigan is supportive of the needs of dual career couples and is a non-discriminatory, Affirmative Action Employer. Women and minorities are encouraged to apply.

life sciences institute

University of Pittsburgh
Center for Vaccine Research

The Center for Vaccine Research (CVR) of the University of Pittsburgh is seeking outstanding scientists involved in emerging pathogens and biodefense research for several tenure and tenure-track positions at the Assistant, Associate, or Professor levels. Established investigators with expertise or interest in pathogenesis or immunology of infectious diseases, with special emphasis on Category A, B or C pathogens (BLS3) are strongly encouraged to apply. Appointments are available in the School of Medicine, the Graduate School of Public Health, or one of the other schools of the health sciences.

The CVR is housed in the new, state-of-the-art, 300,000 sq. ft. Biomedical Research Tower-3 (BST3), which is located on the main campus of the University of Pittsburgh—one of the nation's leading research institutions. The CVR is composed of two components—the Vaccine Research Lab (VRL) and the Regional Biocontainment Lab (RBL), offering comprehensive BSL2 and BSL3 laboratory and animal facilities.

Applicants must demonstrate academic accomplishments that meet the standards for a tenure-track appointment, including an advanced degree (MD, PhD, or equivalent). Successful candidates will have a sound publication record, be active contributors to the vaccine research field, and have a demonstrated ability to obtain extramural research funding. Salary, rank, and academic appointment will be commensurate with qualifications and experience.

Review of applications will begin immediately and continue until all positions are filled. Interested individuals should submit a letter of application, curriculum vitae, a statement of research accomplishments and goals, and the names, mailing addresses, e-mail addresses and telephone numbers of three professional references. Electronic applications are preferred and should be sent to **CVRInfo@pitt.edu** (subject line: CVR Faculty Search). Applications submitted by mail should be sent to: **CVR Search Committee, c/o Donald S. Burke, MD, Director, Center for Vaccine Research, University of Pittsburgh, 9014 Biomedical Science Tower 3, 3501 Fifth Avenue, Pittsburgh, PA 15261.**

Inquiries: e-mail CVRInfo@pitt.edu or telephone 412-624-4480.

For more information about the CVR, please visit our web site at **http://www.cvr.pitt.edu**

The University of Pittsburgh is an equal opportunity, affirmative action employer. Women and minority candidates are strongly encouraged to apply.

NIAID

NATIONAL INSTITUTE OF ALLERGY AND INFECTIOUS DISEASES

NIAID Clinical Research Transition Program

The NIAID Clinical Research Transition Program was initiated in 2006 to provide opportunities for physicians to gain clinical and translational research experience in association with a NIAID Division of Intramural Research (DIR) laboratory. The program aims to increase the pool of well-trained clinical investigators who are competitive for clinical tenure-track positions.

One to three candidates per year will be selected for 2-3-year appointments. Applicants must have an M.D. or M.D./Ph.D. degree, be board eligible or board certified in a subspecialty (or equivalent), and qualify for credentialing by the NIH Clinical Center. Applicants should identify a DIR lab chief who will agree to host the applicant's research. Information about DIR labs and contact information for lab chiefs is available at **http://www3.niaid.nih.gov/about/organization/dir/default.htm**

Applications will be evaluated by a search committee composed of NIAID DIR principal investigators with clinical research interests. Competitive candidates will be asked to present their research accomplishments and plans to the search committee.

Participants will receive independent resources, staff, and be paired with the NIAID senior clinical investigator who will serve as a clinical research mentor. At completion of the 2nd year, participants will be encouraged to apply for available tenure-track or staff clinician positions at NIH or elsewhere.

Interested candidates may contact **Dr. Karyl Barron**, **Deputy Director**, **DIR**, **NIAID**, at 301-402-2208 or via e-mail (kbarron@nih.gov) for additional information or assistance in identifying an appropriate host lab.

To apply for the program, send your CV-Bib, an outline of your proposed research program (no more than two pages) and a letter of support from the accepting NIAID lab chief by **October 31, 2008** via e-mail to Ms. Wanda Jackson at NIAID.DIR.Search@niaid.nih.gov. In addition, three letters of recommendation must be sent to Chair, NIAID Clinical Transition Program Search Committee, c/o Ms. Wanda Jackson at NIAID.DIR.Search@niaid.nih.gov or 10 Center Drive MSC 1356, Building 10, Rm. 4A-26, Bethesda, Maryland 20892-1356. E-mail is preferred. Please note search #024 when sending materials.

Further information about working at NIAID is available on our website at:
http://healthresearch.niaid.nih.gov/crtp

Department of Health and Human Services
National Institutes of Health
National Institute of Allergy and Infectious Diseases

Proud to be Equal Opportunity Employers

Consortium *for* Conservation Medicine

The CCM announces 7 New Positions in Emerging Infectious Disease Ecology

The Consortium for Conservation Medicine, based at Wildlife Trust in New York City, is ramping up its research program in infectious disease ecology and seeks outstanding candidates for seven positions.

Five Postdoctoral Positions

1. **Vector-borne disease modeler** to study the dynamics of Chikungunya and other vector-borne diseases. Excellent spatial statistical and modeling skills required.
2. **Emerging Disease 'Hotspots' modeler** to extend the research recently published in *Nature* **451:**990-3, 2008. Strong statistical, GIS/spatial analysis, and database skills required.
3. **Ecologist/Modeler** to study the dynamics of viral pathogens in peri-domestic and wild animals in Bangladesh. A strong background in statistics is required.
4. **Ecologist or Veterinarian** to run field programs surveying wildlife in Bangladesh and India for our new program on pathogen discovery.
5. **Avian Influenza Ecologist/Modeler** to study the dynamics and spread of H5N1 avian influenza in China and globally.

Two Staff Positions at CCM HQ

1. **Program Coordinator**, who will be a recent graduate (bachelor's or master's level) in the biological sciences. Responsibilities include grants management, operational logistics for research programs, and international meeting coordination. International travel is required.
2. **Program Assistant**, who will be a bachelor's degree level candidate, to manage office functions in New York. Candidate must have excellent organizational and communication skills.

Further details can be found at **www.conservationmedicine.org**. All positions are based in New York and require some international travel. Review of applications will begin **October 15, 2008** and continue until positions are filled. Candidates should submit a full *Curriculum Vitae*, names and email addresses of 2 academic referees, and a cover letter by email to **jobs@conservationmedicine.org** stating clearly the position of interest and career goals.

FACULTY POSITIONS DEPARTMENT OF PHYSICS THE UNIVERSITY OF TEXAS AT AUSTIN

The Department of Physics at The University of Texas at Austin is seeking candidates for tenure-track assistant professorship positions in physics starting in September 2009. In special cases, appointments at more senior levels will be considered. Successful candidates will assume full teaching responsibilities for undergraduate and graduate courses in the Department of Physics and are also expected to conduct vigorous research programs. Research areas of current highest priority for the Department are Biophysics Experiment and Fundamental Theory/Cosmology. Outstanding candidates in other areas of departmental focus will also be considered. Excellent English language communication skills are required. Applicants must have a Ph.D. (or equivalent) and a demonstrated potential for excellence in teaching and research.

Interested applicants should send a curriculum vitae, a list of publications, a statement of research interests, a research plan, and should arrange for at least five letters of recommendation to be sent to: **Prof. John T. Markert, Chair, Department of Physics, The University of Texas at Austin, 1 University Station C1600, Austin, TX 78712-0264**. Review of completed applications will begin in **October, 2008**.

The University of Texas at Austin is an Equal Opportunity/Affirmative Action Employer.

Medical College of Wisconsin

TENURE-TRACK FACULTY POSITION

DEPARTMENT OF BIOCHEMISTRY

The Department of Biochemistry welcomes candidates for a tenure-track position at the Assistant or Associate Professor level. We seek investigators using **structural biological approaches**, particularly **X-ray crystallography**, to develop a competitive, independent research program that complements existing institutional strengths in cancer and cardiovascular and infectious diseases. Applicants must have a doctoral degree (Ph.D. and/or M.D.), over two years of postdoctoral training, a strong publication record, and the potential to obtain extramural funding. Competitive salary support, start-up funds, and new laboratory space will be provided.

The Medical College of Wisconsin (**www.mcw.edu**) is the largest private research institution in Wisconsin, conducting over $130 million annually in funded research, and over the past few years has been among the fastest growing research-oriented medical schools in the United States for NIH funding. The Department of Biochemistry is home to state-of-the-art X-ray and NMR facilities. The College is conveniently located 90 minutes from the Advanced Photon Source at Argonne National Laboratory. The Medical College is also home to nine federally designated Centers of Biomedical Research, including a National Biomedical Electron Paramagnetic Resonance Center. Shared facilities are available for proteomics, imaging, molecular biology, and mouse genetics. The College is located in suburban Milwaukee and is 8 miles west of Lake Michigan with easy access to surrounding communities, lakes, and parks. For more information visit the departmental website at **www.mcw.edu/biochemistry**.

Applications should include a cover letter, curriculum vitae, statement of research interests, copies of key publications, and three reference letters. Review of applicants will begin on **October 31, 2008**. For full consideration applications should be received by **November 30, 2008**. Send application materials and reference letters electronically in pdf format to **pmalkowski@mcw.edu** or by regular mail to: **Dr. Jung-Ja Kim, Search Committee Chair, Department of Biochemistry, Medical College of Wisconsin, 8701 Watertown Plank Road, Milwaukee, WI 53226.**

EOE M/F/D/V
(www.mcw.edu/hr)

Faculty Position Molecular Biology Sloan-Kettering Institute

The Molecular Biology Program of the Sloan-Kettering Institute, Memorial Sloan-Kettering Cancer Center (www.ski.edu), has initiated a faculty search at the Assistant Member level (equivalent to Assistant Professor). We are interested in outstanding individuals who have demonstrated records of significant accomplishment and the potential to make noteworthy contributions to the biological sciences as independent investigators. Successful applicants will have research interests that move the Program into exciting new areas that complement and enhance our existing strengths in the areas of maintenance of genomic integrity, regulation of the cell cycle, and regulation of gene expression. Faculty will be eligible to hold appointments in the Gerstner Sloan-Kettering Graduate School of Biomedical Sciences, the Weill Cornell Graduate School of Medical Sciences, as well as the Tri-Institutional MD/PhD Training Program.

Candidates should e-mail their application in PDF format to: **molbio@mskcc.org** by **November 15, 2008**. The application should include a CV, description of past and proposed research (3-7 pp), and copies of three representative publications. Candidates should arrange to have three signed letters of reference sent in PDF format to: **molbio@mskcc.org**. The letters should arrive by **November 15, 2008** and should be addressed to **Dr. Kenneth Marians, c/o Julie Kwan, Box 135, Memorial Sloan-Kettering Cancer Center, 1275 York Avenue, New York, New York 10065**. Inquiries may be sent to Ms. Kwan at **molbio@mskcc.org** or to Dr. Kenneth Marians, Chair, Molecular Biology Program at **kmarians@sloankettering.edu**. Memorial Sloan-Kettering Cancer Center is an Equal Opportunity Employer. Smoke-free environment.

Memorial Sloan-Kettering Cancer Center
www.mskcc.org

EMBL

Australian Government
National Health and Medical Research Council

Applications are invited from suitably qualified scientists wishing to develop their research programme as a group leader at EMBL. In accordance with Australia's associate membership of EMBL, funding from NHMRC is available to support one research group located at one of the five EMBL sites in Europe for a maximum period of five years. The position will then be continued for a further four years at an Australian institution. To be eligible for NHMRC support applicants must be working in a field relevant to human health.

Group Leader

5 years in Europe and 4 years in Australia

EMBL Site: The group's location is dependent on the successful candidate's preferences and the proposed research programme. Options available include Heidelberg (Germany) and the EMBL Outstations in Hinxton (UK), Grenoble (France), Hamburg (Germany) and Monterotondo (Italy).

Australian Site: The group leader's location in Australia is dependent on the location of the Australian institution which satisfies Australia's National Health and Medical Research Council (NHMRC) and EMBL that the standard of the proposed programme of research is sufficient to compete for funding from Australian research funding agencies. As such, there are research institutions meeting this requirement in every Australian state or territory.

EMBL is an international research organisation offering a highly collaborative, uniquely international culture. It fosters top quality, interdisciplinary research by promoting a vibrant environment consisting of young independent research groups composed of outstanding graduate students and postdoctoral fellows. The scientific programme of EMBL emphasises experimental analysis at multiple levels of biological organisation, from the molecule to the organism, as well as computational biology, bioinformatics and systems biology. In addition to exciting colleagues, the laboratory provides excellent shared facilities for a variety of advanced experimental approaches. High-level expertise is also available in computational biology, diverse aspects of experimental molecular biology as well as physics, biophysics, chemical biology and instrument development.

The successful candidate will lead a research group for a period of five years at the selected EMBL site in Europe and will participate in the collegial culture of EMBL. Following the term in Europe, the candidate will continue as a group leader at an Australian institution. The successful applicant will need to select and finalise arrangements with an approved Australian institution prior to the commencement of placement in Europe. The candidate will also participate in a programme of linking activities with the Australian institution while in Europe.

Commencing date in Europe: from mid-2009

EMBL is an inclusive, equal opportunity employer offering attractive conditions and benefits appropriate to an international research organisation.

Further information about EMBL can be obtained at **www.embl.org** and on the position from:
- EMBL Director General, Iain Mattaj (dg-office@embl.org) or
- NHMRC Executive Director, Research Investment Branch, Elim Papadakis (elim.papadakis@nhmrc.gov.au).

To apply, please email a CV, including a summary of present and future research interests and three reference letters quoting ref. no. S/08/007 in the subject line, to:
application@embl.de

Closing date: 21 November 2008

www.embl.org

THE UNIVERSITY of TENNESSEE KNOXVILLE

ASSISTANT PROFESSOR: The Biochemistry, Cellular and Molecular Biology (BCMB) Department at the University of Tennessee, Knoxville seeks to fill a tenure-track faculty position at the assistant professor level to begin August 1, 2009 in the following area:

COMPUTATIONAL MOLECULAR BIOPHYSICS

The research associated with the appointment will be performed in the Center for Molecular Biophysics at Oak Ridge National Laboratory (ORNL). There is particular interest in candidates with expertise in the physical modeling and simulation of the dynamics of biological systems, complementing neutron experiments. Particularly strong interactions are expected with research undertaken at the new Spallation Neutron Source and the National Leadership Supercomputing Centre, both at ORNL, and with the ORNL Life, Computational and Physical Sciences programs. The successful candidate will also benefit from interactions with strong research groups within UTK. The successful applicant will be expected to develop a first-class, externally funded research program, to provide state-of-the-art training for graduate students and postdoctoral researchers, and to contribute to the teaching mission of the BCMB department at both the undergraduate and graduate levels. Required qualifications include a Ph.D. and postdoctoral experience in relevant areas of computational molecular biophysics, evidence of significant scientific productivity, and a commitment to an integrated program of teaching and research. The university welcomes and honors people of all races, creeds, cultures, and sexual orientations, and values intellectual curiosity, pursuit of knowledge, and academic freedom and integrity.

Interested candidates should send a cover letter, a resume, a description of research experience and of the proposed research program, and arrange for three letters of reference to be sent to: **Jeremy C. Smith, Chair, Faculty Search Committee, BCMB Department, M407 WLS, University of Tennessee, Knoxville, TN 37996-0840**. This is an extended search and review of applications will begin on **October 1, 2008** and continue until the position is filled.

The University of Tennessee is an EEO/AA/Title VI/Title IX/Section 504/ADA/ADEA institution in the provision of its education and employment programs and services. All qualified applicants will receive equal consideration for employment without regard to race, color, national origin, religion, sex, pregnancy, marital status, sexual orientation, age, physical or mental disability, or covered veteran status.

Assistant Professor

Stony Brook University's Department of Neurobiology and Behavior is continuing a major initiative in Neuroscience with recruitment of a tenure-track faculty member at the Assistant Professor level in 2009. Outstanding scientists in all fields of neuroscience will be considered, but those engaged in molecular approaches are especially encouraged to apply.

Required: Applicants must have a Ph.D. or equivalent degree, and postdoctoral experience. Successful candidates will join an active and diverse group of neuroscientists at Stony Brook University and its affiliated institutions, and will also participate in the Department's research mission and in undergraduate, graduate, and medical school teaching. Exceptional packages include state-funded salary and benefits, newly renovated lab space, and generous start-up funding. Review of applications starts immediately and will continue until the position is filled.

For full position description or to apply online visit *www.stonybrook.edu/jobs* (REF: F-4034-08-08-F) or send a C.V., a statement of research interests, and contact information for three references to:
Gary G. Matthews, Chair, Faculty Search Committee, Department of Neurobiology and Behavior, Life Sciences Building
Stony Brook University, SUNY
Stony Brook, NY 11794-5230

Equal Opportunity/Affirmative Action Employer

STONY BROOK

NC STATE UNIVERSITY

Governor Robert W. Scott Distinguished Professorship Department of Chemistry

The Department of Chemistry at North Carolina State University invites nominations and applications to fill the Governor Robert W. Scott Distinguished Professorship in chemistry. Preliminary inquiries are also encouraged. This position is one component of a major growth plan at the University with emphasis on interdisciplinary research related to life sciences and energy. The successful candidate must have a nationally and internationally recognized research program and be able to provide dynamic leadership in his or her area of research. All candidates are expected to have strong interest and ability in teaching at both the undergraduate and graduate levels. Formal requirements include a PhD in chemistry or in a related scientific field plus an established track record of accomplishments appropriate for appointment as a tenured full-professor in chemistry.

Candidates should submit an electronic copy of their curriculum vitae along with other material describing future directions of their research at: **http://jobs.ncsu.edu** under position number **07-48-0821**. Nominations and all inquiries should be sent to the Chemistry Department Chair **Morteza_Khaledi@ncsu.edu**. After a preliminary review, candidates will be contacted and asked to request letters of recommendation. However, if a candidate prefers, letters of recommendation may also be sent at the time of application and mailed to the **Governor Scott Search Committee Chair, Department of Chemistry, North Carolina State University, Raleigh, NC 27695-8204**. The review of applicants will begin on **November 1, 2008** and will continue until candidates are selected.

We welcome the opportunity to work with candidates to identify suitable employment opportunities for spouses or partners. AA/EOE. In addition, NC State welcomes all persons without regard to sexual orientation. Persons with disabilities requiring accommodations in the application and interview process please call (919) 515-3148.

BCM Baylor College of Medicine

Faculty Positions in Bacteriology and Tumor Virology

The Department of Molecular Virology and Microbiology at Baylor College of Medicine invites applications for two tenure/tenure-track faculty positions at the rank of Assistant or Associate Professor. Successful candidates will have demonstrated research productivity and will be expected to maintain an independent and innovative, funded research program and to participate in graduate training. This is an opportunity to join a strong, interactive department at Baylor College of Medicine in the rich scientific setting of the renowned Texas Medical Center. Current research interests of our departmental faculty focus on viral and bacterial gene expression, microbial pathogenesis, viral oncology, RNA and DNA viruses of human diseases, the human microbiome, vaccine development and evaluation, and microbial genomics and proteomics. Outstanding core facilities are available, including BSL-2 and new BSL-3/3E containment facilities for handling infectious agents and infected small animals. Multidisciplinary research centers, including the Dan L. Duncan Cancer Center and the Center for AIDS Research, facilitate collaborations. Candidates in the following areas are invited to apply:

- **Bacterial Pathogenesis** — Applicants with an interest in emerging infectious disease or biodefense bacterial pathogens and expertise in host–pathogen interactions or host responses to infection are particularly encouraged to apply. Email: **BCM-MVM-facultypos4@bcm.edu**.
- **Tumor Virology** — Applicants with an interest in viruses and cancer are sought. Applicants with expertise in HIV-associated malignancy research are particularly encouraged to apply. Email: **BCM-MVM-facultypos5@bcm.edu**.

Applicants should submit a curriculum vitae, a statement of research experience, a summary of future plans, and names of three references by **November 1, 2008** to: **Dr. Janet S. Butel, Faculty Recruitment Committee, Department of Molecular Virology and Microbiology, Mail Stop: BCM385, Baylor College of Medicine, Houston, TX 77030**. E-submission preferred using the email address listed for each position.

Baylor College of Medicine is an Equal Opportunity, Affirmative Action and Equal Access Employer.

Did you know... our company is seeking you?

BD, a leading global medical technology company with operations in over 50 countries, is instrumental in combatting some of the world's most pressing diseases.

BD Biosciences, a segment of BD, is one of the largest businesses supporting the Life Sciences today, focused on bringing innovative tools, systems, and solutions to researchers and clinicians. The BD Biosciences European Headquarters, located in Erembodegem near Brussels, Belgium at the heart of Europe, regroup essential European functions such as European Marketing, Scientific Support, and a Flow Cytometry Training and Education Center.

Anne-Louise
RA/QA Specialist

We are currently looking for:

European Application Specialist – Bioimaging

As a European Application Specialist – Bioimaging, you will be providing application and software support to BD Biosciences' current and potential customers in the bioimaging area across Europe. In this role, you will be working closely with our Application Consultants and Sales Specialists to organize and provide instrument- and software related trainings on the BD Pathway™ bioimaging platform. You will also actively participate in developing a European Bioimaging Training Center at the Erembodegem site.

European Flow Cytometry Instrument Trainer

As a European Flow Cytometry Instrument Trainer, you will be responsible for providing training on high-end flow cytometry (cell sorting) instrumentation to both external and internal customers. In this role, you will be designing and conducting appropriate training programs at the European level, as well as providing assistance to the countries in the development of local trainings.

Scientific Support Specialist(s) – German language

As a European Scientific Support Specialist – Flow Cytometry, you will be part of a multicultural team where you will use your scientific knowledge to help scientists solve complex problems all over Europe, Middle East, and Africa. In this role you will provide product support to customers via phone and email and use the product knowledge you gain at BD Biosciences to actively contribute to education programs. You will also participate in building and maintaining a European contact database and provide technical content for our Expert Solution Database.

Key Account Manager – Bioimaging

As a European Key Account Manager – Bioimaging, you will be responsible for direct sales of BD Pathway Bioimager High Content Imaging instruments and their associated reagents in a European sales territory that includes several countries. The sales territory will be centred on Belgium and the Netherlands. You will be fully accountable for the territory sales objectives and the tactical environment required to achieve these objectives in collaboration with the local sales organizations. You will also work closely with the Bioimaging applications team based in Erembodegem and Basel, plus interact regularly with BD Bioimaging, Rockville, USA.

BD

Helping all people live healthy lives

BD offers a stimulating working environment, a very competitive compensation and benefits package, and strong leadership commitment to individual development and learning.

For further information, please log on to www.bdbeurope.com and click on "Careers". To apply, please send your resume and motivational letter to HR_BDB@europe.bd.com

Washington University in St. Louis

DEAN, FACULTY OF ARTS & SCIENCES

Washington University in St. Louis seeks nominations and applications for the position of Dean of the Faculty of Arts & Sciences.

Washington University ranks among premier universities and is nationally and internationally acclaimed for its excellence in research, teaching, and service to society. Arts & Sciences is the intellectual hub of teaching and scholarship at Washington University, incorporating more than 45 departments, programs, and centers, 40 buildings, approximately 370 tenured and tenure-track faculty, and more than 5,000 students.

The Dean oversees academic and financial planning, departmental budgets, faculty salaries, faculty appointments, tenure decisions, and administration of the three component parts of the Faculty of Arts & Sciences: The College, The Graduate School, and University College. The Dean will manage an estimated budget for 2008-09 of more than $230 million, including $40-50 million in sponsored research.

The successful candidate will have a record of exceptional scholarship and teaching, as well as substantial administrative experience in a complex environment.

The review of credentials will begin immediately and will continue until the position is filled. For full consideration, please submit an application and accompanying materials before October 24, 2008. Nominations, inquiries and expressions of interest should be forwarded, in confidence and preferably electronically, to:

storbeck / pimentel
executive search consultants

Shelly Weiss Storbeck, Managing Partner
Lori A. Cunningham, Associated Consultant
Storbeck/Pimentel & Associates, LLC
1400 North Providence Road, Suite 6000
Media, PA 19063
484/927-4069 (phone); 610/565-2939 (fax)
l.cunningham@storbeckpimentel.com (preferred)

For more information about Washington University in St. Louis, please consult its website, **www.wustl.edu**.

Washington University is an equal opportunity, affirmative action institution and encourages applications from, and nominations of, women and minority candidates.

Westfalian
Wilhelms-University
Muenster, Germany

The Medical Faculty of the Westfalian Wilhelms-University (Westfälische Wilhelms-Universität Muenster) invites applications for a tenured position as

University Professor (W3) for Neuroinflammation

The future holder of the position must fully represent the subject with regard to research and teaching. Clinical work will cover the field of neurodegenerative diseases with the exception of primary vascular dementia.

Candidates should have an excellent research record in the field of molecular mechanisms of inflammation related to neurodegeneration. As part of the position, an associate professorship, research and clinical (ambulatory, stationary) units will be generated. Candidates are expected to participate in collaborative research programs of the Medical Faculty, such as the "Interdisciplinary Clinical Research Centre" (IZKF), the "Collaborative Research Centres" (Sonderforschungsbereiche) SFB-TRR58, SFB-TRR3, SFB 293, SFB 492, SFB 629, and the Max-Planck-Institute of Molecular Biomedicine.

The position is tenure track, will be initially filled for 5 years, and converted to tenure based upon evaluation.

Prerequisite for the application are the license to practice medicine in Germany, an advanced medical qualification in the field of Neurology, including excellent scientific achievements as a junior professor, from a postdoctoral lecture qualification (habilitation), as a research scientist at a school of higher education/university, at non-university institutes, industry, administration, or other fields of society within or outside Germany.

Applications of women are specifically invited. In the case of equal qualifications, competence, and specific achievements, women will be considered on preferential terms within the framework of the legal possibilities.
Handicapped candidates with equivalent qualifications will be given preference.

According to a resolution by the Conference of the German Ministers for Science and Education of November 19, 1999, professors with clinical tasks will principally be employed on the basis of individually negotiable contracts (exceptions are possible, if applicants are already employed as life time professor of the salary group C3/W2). The clinical duties affiliated with this professorship will be laid down in a separate contract with the Universitätsklinikum.

Documents in support of an application, enclosing CV, scientific career, structured catalogue of publications, acquired third-party funds and reprints of the six most important publications should be submitted to the **Dean of the Faculty of Medicine, University of Muenster, Domagkstrasse 3, 48129 Muenster, Germany,** by **October 24th 2008.** References:
http://campus.uni-muenster.de/fileadmin/dekanat/Merkblatt_Berufungen_Ms.pdf

---

Argonne NATIONAL LABORATORY

The Argonne Named Postdoctoral Fellowship Program

The Director's Office initiated these special postdoctoral fellowships at Argonne, to be awarded internationally on an annual basis to outstanding doctoral scientists and engineers who are at early points in promising careers. The fellowships are named after scientific and technical luminaries who have been associated with Argonne and its predecessors, and the University of Chicago, since the 1940's.

Candidates for these fellowships must display superb ability in scientific or engineering research, and must show definite promise of becoming outstanding leaders in the research they pursue. Fellowships are awarded for a two-year term, with a possible renewal for a third year, and carry a stipend of $76,000 per annum with an additional allocation of up to $20,000 per annum for research support and travel.

Requirements for applying for an Argonne Named Postdoctoral Fellowship:

The following documents must be sent via e-mail to: Named-Postdoc@anl.gov by November 5, 2008. In the subject line please include the name of the candidate.

- Nomination memo (≤ 2 pages) from ANL sponsor
- Research proposal (≤ 2 pages)
- Three letters of recommendation from other than Argonne staff
- CV
- Graduate School and Undergraduate Transcripts

The sponsor could be someone who is already familiar with your research work and accomplishments through previous collaborations of professional societies. If you have not yet identified an ANL sponsor, visit the detailed websites of the various Research Programs and Research Divisions at www.anl.gov

All correspondence should be addressed to Argonne Named Postdoctoral Fellowship Program. One application is sufficient to be considered for all named fellowships. For additional details, visit the Argonne web site at http://www.dep.anl.gov/postdocs/ Argonne is an equal opportunity employer and we value diversity in our workforce.

Argonne is a U.S. Department of Energy laboratory managed by UChicago Argonne, LLC

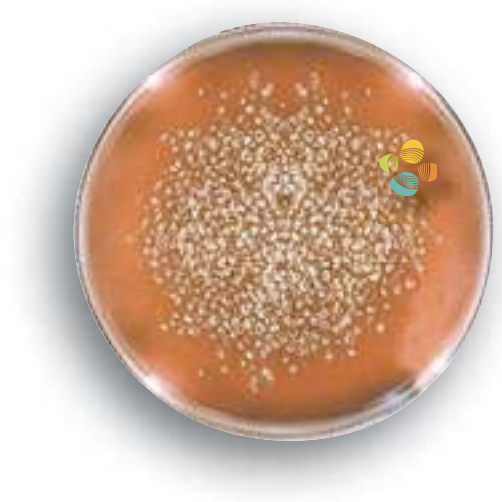

Faculty Positions

Bioscience and Bioengineering

Very attractive base salaries plus benefits

Make a major scientific discovery.

FACULTY POSITIONS IN BIOSCIENCES AND BIOENGINEERING

Professors, Associate Professors, Assistant Professors

The King Abdullah University of Science and Technology (KAUST) in Saudi Arabia will provide exceptional research facilities and all the benefits of an independent, merit-based institution with one of the world's largest university endowments. KAUST is an international graduate-level research university dedicated to inspiring a new age of scientific achievement and becoming a major contributor to global collaborative research. A university where education, administration and the recruitment of both staff and students are based on merit, without regard to race, religion or gender.

We are looking for recognized and promising academics with fundamental research interests in plant and microbial sciences. Your research may provide a base for new renewable technologies, bioenergy, sustainable agriculture and water conservation. Ideally you will use and develop one or more of these technical areas as part of your research:

- High throughput DNA sequencing for non-model plants and microbes
- High throughput analysis of mRNA and small regulatory RNAs
- Data management for genomic, proteomic and transcriptomic datasets
- Proteomic technologies applied to non-model plants and microbes
- Metabolic enzyme engineering for bulk feedstock and biotransformation
- Synthetic Biology tools for genetic systems assembly and analysis
- Microscopy-based approaches to cellular structure-function relationships
- Biophysical approaches for analysis and engineering of biological systems

The overall originality and promise of your work will be more important than your specialist area. You will enjoy opportunities to pursue innovative research, and take advantage of world-class facilities in genomics, proteomics, imaging, structural biology, nanotechnology and computation. You will have a PhD in a biological science or related scientific or bioengineering discipline, along with evidence of the ability to pursue independent research, and an existing track record of publications in high-profile international journals. KAUST has a strong commitment to graduate education. You will have the opportunity to teach new graduate courses, and to lead teams of graduate students in Master's and PhD research.

KAUST opens in September 2009 at Thuwal on the Red Sea, 80 km north of Jeddah, and welcomes exceptional researchers, faculty and students from around the world. KAUST will offer very attractive base salaries and a wide range of benefits. To find out more about KAUST, go to www.kaust.edu.sa.

The University of Cambridge

As part of an Academic Excellence Alliance agreement, a committee from the Faculty of the School of Biological Sciences at the University of Cambridge will conduct the search, and nominate top applicants for roles at KAUST. KAUST will make all recruiting decisions, appointment offers, explanations of employment benefits and will be the faculty's employer.

For more information about the positions and the KAUST Academic Excellence Alliance with the University of Cambridge, see www.kaust-aea.cam.ac.uk .

To apply, send your CV, statements of research, an outline of potential teaching interests, and the contact details of at least three referees, by email to the Search Committee at info@kaust-aea.cam.ac.uk. Applications will be reviewed immediately.

Closing date for the first round of applications: October 31 2008. Applications will be accepted until July 2009, or until all ten positions have been filled.

Enquiries: info@kaust-aea.cam.ac.uk

KAUST

UNIVERSITY OF CAMBRIDGE

FACULTY OF MEDICINE
GREAT MINDS FOR A GREAT FUTURE
University of Toronto

DEPARTMENT OF LABORATORY MEDICINE AND PATHOBIOLOGY
ACADEMIC POSITION IN MICROBIAL PATHOGENESIS

The Department of Laboratory Medicine and Pathobiology, Faculty of Medicine, University of Toronto (**www.lmp.facmed.utoronto.ca**) is seeking applicants for one full-time tenure-stream faculty position at the rank of Assistant Professor available July 1, 2009 or at a mutually agreeable date. The position comes with a faculty salary commensurate with the applicant's experience and training. The successful applicant will be provided with a start-up package and space to establish a strong independent research program. We are particularly interested in dynamic individuals working in the areas of molecular and biochemical mechanisms of microbial disease, including virology.

Candidates must have a PhD, have completed significant postdoctoral training, and have an established track record of high quality innovative research. Exceptional candidates with established funded research programs and a rank of Associate or Full Professor may be considered as well. Teaching experience at the undergraduate and graduate level is an asset.

The successful candidate is expected to participate actively in graduate and undergraduate teaching programs, maintain a well-funded, independent research program and interact with other investigators on the University campus and at the major affiliated teaching hospitals. The University of Toronto is the fourth largest research entity in North America, with a large vibrant community of investigators carrying out excellent innovative research on the pathogenesis of microbial disease. The interaction of basic scientists with clinicians at the teaching hospitals and also at the Public Health Laboratories provides for outstanding opportunities for transformative research.

Applicants should submit a **hard copy** of **curriculum vitae, description of their research accomplishments, the focus of their planned research program and the names of three referees by December 23, 2008** or until the position is filled, to the **Chair, Academic Search Committee, Department of Laboratory Medicine and Pathobiology, Faculty of Medicine, University of Toronto, Room 110, 100 College Street, Toronto, Ontario, Canada, M5G 1L5**.

The University of Toronto is strongly committed to diversity within its community and especially welcomes applications from visible minority group members, women, Aboriginal persons, persons with disabilities, members of sexual minority groups and others who may contribute to the further diversification of ideas. All qualified candidates are encouraged to apply. However, Canadians and permanent residents will be given priority.

Children's Hospital Boston — Harvard Medical School

Assistant Professor
Division of Genetics
Department of Medicine

Applications are invited for a tenure-track Assistant/Associate Professor position in the Division of Genetics in the Department of Medicine at Children's Hospital Boston. We are seeking an outstanding MD and/or MD/PhD scientist who will establish a vigorous basic science or translational research program with relevance to developmental biology and developmental disorders of childhood. The successful candidate will have modern laboratory space located in the newly opened Center for Life Science Building. Joint appointments in the Program in Genomics at Children's Hospital and the Broad Institute of MIT and Harvard may be available for appropriate applicants. The Division resides within a very strong research community in genetics, developmental biology and related disciplines throughout the Harvard Longwood Medical Area and the investigator will hold both Children's Hospital Boston and Harvard Medical School faculty appointments.

Candidate should submit a current CV, a 2- to 3-page description of research interests and future directions, and three to five reference letters. Materials should be sent via e-mail by **December 1, 2008** to: **geneticssearch@childrens.harvard.edu**. Please contact **Andrea McDonald** at **617-355-2449** with questions. We particularly encourage applications from women and minority candidates.

Equal Opportunity/Affirmative Action Employer.

University of Michigan
CENTER FOR
stem cell biology

The Life Sciences Institute and the University of Michigan Medical School invite applications for tenure track **ASSISTANT PROFESSOR** positions. We are seeking outstanding scholars, with Ph.D., M.D. or equivalent degrees and relevant postdoctoral experience, who show exceptional potential to develop an independent research program that will address fundamental issues in any aspect of stem cell biology. Applicants who have already established successful independent research programs will be considered for tenured **ASSOCIATE PROFESSOR** or **PROFESSOR** positions.

Applicants should send a curriculum vitae, copies of up to three reprints, a one- to two-page summary of research plans, and arrange to have three letters of reference sent directly by **October 31, 2008** to: **Stem Cell Search Committee, c/o Rebecca Fritts, Life Sciences Institute, University of Michigan, 210 Washtenaw Avenue, Ann Arbor, Michigan, 48109-2216**.

The University of Michigan is an Affirmative Action/ Equal Opportunity Employer.

The University of Texas at Austin

Eukaryotic Molecular Biology Positions
The Institute for Cellular and Molecular Biology

The Institute for Cellular and Molecular Biology, Alan Lambowitz, Director, invites applications for two tenure-track/tenured positions in eukaryotic molecular biology. Academic appointments at the level of Assistant, Associate, or Full Professor will be in an appropriate academic unit in the College of Natural Sciences. Candidates should have an outstanding record of research productivity and a research plan that utilizes molecular and biochemical approaches to address important problems in eukaryotic molecular biology. Areas of particular interest include but are not limited to chromatin structure, regulation of gene expression, microRNAs and RNA interference, DNA damage responses, and cell cycle control.

Building on a strong existing faculty, the Institute has recruited more than 50 new faculty members over the past ten years (see www.icmb.utexas.edu). In addition to it's highly interactive and interdisciplinary research environment, the Institute provides administrative and financial support for the Graduate Program in Cell and Molecular Biology and state-of-the-art core facilities including DNA sequencing, mass spectrometry, electron and confocal microscopy, DNA microarrays, robotics, and mouse genetic engineering. A recently instituted MD-PhD program with the UT Medical Branch and the new Dell Pediatrics Research Institute further enhance the environment for basic Biomedical Research.

Austin is located in the Texas hill country and is widely recognized as one of America's most beautiful and livable cities.

Please apply on-line at http://www.icmb.utexas.edu/apply/between Sept. 1 and Nov. 1, 2008.

The University of Texas at Austin is an Equal Opportunity Employer. Qualified women and minorities are encouraged to apply; a background check will be conducted on applicant selected.

Assistant Professorships in Systems Biology at Harvard University

Harvard University has a large and growing systems biology community composed of faculty, fellows, and trainees, housed at several locations across the Boston area. This year, faculty positions are available in four locations. Applications for positions at the rank of assistant professor (tenure track) are especially encouraged, but exceptional candidates for associate professor (untenured) positions may also be considered.

1. The **FAS Center for Systems Biology** (**http://sysbio.harvard.edu/csb/**) on the Cambridge campus has two positions available and is particularly interested to hire in the field of microbial evolution and ecology and the field of physical properties of biological systems, but will consider outstanding candidates in other fields. Each new faculty member will hold an academic appointment in a participating department, such as Molecular and Cellular Biology or Organismic and Evolutionary Biology. Access to Harvard facilities including the Center's own Core Resource, the Center for Nanoscale Systems, the Center for Brain Science, and the Broad Institute will provide opportunities for collaborative research and technology development.

2. The **MGH Center for Systems Biology** (**http://csb.mgh.harvard.edu/**) has one position available. This position is a joint appointment with the Department of Systems Biology at Harvard Medical School. The candidate will work in close proximity to MD and PhD scientists with strong research programs in human disease. He/she will have the opportunity to establish collaborations with MGH clinicians, and with researchers and technology programs at the Broad Institute. Areas of special interest include: how disease-causing mutations perturb cellular networks to yield disease phenotypes; identification of network nodes that may be novel drug targets; epigenetics and disease; gene–environment interactions; using computational methods, quantitation, statistics, modeling and analysis of large data sets to understand mechanisms of complex disease, and to translate this understanding into new diagnostic methods, treatments, or prevention strategies. Expertise at analyzing (and/or generating) large data sets to investigate biological pathways and networks, using model organism or human samples, would be especially welcome.

3. The **Department of Systems Biology at Harvard Medical School** (**http://sysbio.med.harvard.edu/**) has two positions available. Special interests include systematic, quantitative and/or theoretical approaches to the following biological areas: variation in gene expression and function (such as variation in transcriptional control, translational control, protein degradation or protein modification); proteomics, particularly mass spectrometry; human genetics and population genetics; pharmacology, physiology and metabolism.

4. The **Harvard Institute for Biologically Inspired Engineering** (**http://hibie.harvard.edu/**). This position is a joint appointment with the Department of Systems Biology at Harvard Medical School. The special focus of this recruitment is Synthetic Biology, i.e. using genetic engineering and nanotechnology to build programmable self assembling materials, biological factories or integrated multifunctional living microdevices. The successful candidate will become a member of a new interdisciplinary research institute composed of experimentalists, theoreticians and clinicians from Harvard University, its affiliated hospitals, and other academic institutions in the Boston/Cambridge area. The Institute's central focus is research and advanced technology development and translation in the field of biologically inspired engineering.

Applications are due by **December 1, 2008**. Please submit a curriculum vitae, research proposal (≤5 pages), summary of previous research accomplishments (≤2 pages), and PDFs of ≤3 publications to **http://www.lsdiv.harvard.edu/csb/facultysearch/**. All files must be submitted electronically in PDF or Word format. During the application process you will be asked to give the e-mail addresses of at least three colleagues who have agreed to write letters of recommendation for you. You will also need to state which position you are interested in, or whether you are interested in more than one.

Applications from, or nominations of, women and minority candidates are encouraged. Harvard University and the Massachusetts General Hospital are Affirmative Action/Equal Opportunity Employers.

IOWA STATE UNIVERSITY

Where you can become your best.

College of Agriculture and Life Sciences
Department of Natural Resource Ecology and Management

Chair, Department of Natural Resource Ecology and Management

Iowa State University, one of the nation's leading land-grant universities, is seeking a visionary leader for its Department of Natural Resource Ecology and Management (NREM). The NREM Department was formed on July 1, 2002, through the merger of the Animal Ecology and Forestry departments. This unit reflects a diversity of disciplines, including ecology and other biological sciences, social science, economics, sustainable resource management and utilization, and human dimensions, and has strategically developed interdisciplinary programs that attract many students. The department has over 350 students enrolled in the department's undergraduate and graduate programs. The department has 32 faculty members. A description of the department's mission, programs, faculty and facilities is available at **http://www.nrem.iastate.edu/**.

This is a 12-month appointment with starting date to be negotiated. The successful candidate will provide visionary leadership to serve the needs of students and stakeholders and to fulfill the university's land-grant mission; demonstrate effective leadership abilities including skills in organization, budgeting and communications; stimulate and facilitate excellence in all aspects of the department's teaching, research, extension, outreach and service programs, assist the department in obtaining resources through extramural funding; have appropriate experience to qualify for the rank of professor and tenure; and have an earned doctorate in a discipline relevant to the subject areas of the department. For a complete job description, go to **www.iastatejobs.com** - vacancy **ID: 080782**.

All interested, qualified persons must apply for this position through the ISU Jobs website at **www.iastatejobs.com**. Applications will be accepted immediately with a deadline of **December 1, 2008** or until the position is filled. Please direct questions to **Dr. Paul Lasley, Chair, NREM Chair Search Committee at 515/294-2506. Email: plasley@iastate.edu**.

Iowa State University is an Affirmative Action/Equal Opportunity Employer.

Assistant Professor, Vertebrate Conservation Biology (Terrestrial Emphasis)

Department of Wildlife, Fish, and Conservation Biology,
University of California, Davis

We are recruiting a Vertebrate Conservation Biologist (terrestrial emphasis) at the tenure track **ASSISTANT PROFESSOR** level, with the possibility of an appointment in the California Agricultural Experiment Station. Candidates must have the ability to develop a vigorous, extramurally funded research program that addresses questions relevant to the conservation of vertebrates in California's diverse terrestrial environments, and to teach courses in vertebrate conservation biology. Qualifications include Ph.D. in relevant discipline, and evidence of potential for accomplishment in research, teaching, and service.

Information and applications: **https://secure.caes.ucdavis.edu/Recruitment/**. Inquiries: **Professor Dirk Van Vuren, Committee Chair, (530) 752-4181, email: dhvanvuren@ucdavis.edu**. The position will remain open until filled but to ensure consideration, applications should be received by **19 December 2008**.

UC Davis is an Affirmative Action/Equal Employment Opportunity Employer and is dedicated to recruiting a diverse faculty community. We welcome all qualified applicants to apply, including women, minorities, veterans, and individuals with disabilities.

PRESIDENT OF THE SANTA FE INSTITUTE

The Santa Fe Institute (SFI) is seeking a President who can be an effective leader of this unique institution. The successful candidate must be a compelling representative for the broad, transdisciplinary research program carried out at SFI.

Nominations and applications for this position are invited, and should be sent to: Charles F. Stevens, Chair, Presidential Search Committee, Santa Fe Institute, MS202S, 1399 Hyde Park Road, Santa Fe, NM 87501

SFI is an equal opportunity employer
http://www.santafe.edu

UMKC

UNIVERSITY OF MISSOURI-KANSAS CITY
SCHOOL OF BIOLOGICAL SCIENCES

Professor and Head
Division of Cell Biology and Biophysics

Applications are invited for the Head of the Division of Cell Biology and Biophysics at the School of Biological Sciences, University of Missouri-Kansas City. The successful candidate should have a proven record of sustained externally funded research, scholarly activity, and leadership potential. The candidate will be expected to participate in graduate and/or undergraduate teaching, faculty mentorship, and work closely with the Dean on decision-making matters pertaining to the growth, development and direction of the School. The School of Biological Sciences is positioning itself to become a regional leader in the areas of structural biology and molecular cell biology and welcomes applications from qualified candidates in these research areas; however, outstanding scientists from all areas of basic life sciences research are encouraged to apply. The successful candidate will receive a competitive 12-month salary, renovated research space, a start-up package commensurate with rank, and the availability of excellent research support facilities within the School of Biological Sciences. Candidates should have a Ph.D. degree and currently be in a tenured academic position at the rank of Professor.

To apply, please submit electronically (MS Word or pdf) a CV, a statement of present and future research interests, and the names and addresses of 3 references to: **Ms Micaela Escareno (escarenom@umkc.edu)**. All materials will be handled with strict confidentiality. The position will remain open until filled.

UMKC is an Affirmative Action/Equal Opportunity Employer. Women, minorities, veterans, and individuals with disabilities are encouraged to apply.

London **Research** Institute
Clare Hall Laboratories

CANCER RESEARCH UK
LONDON RESEARCH INSTITUTE
LINCOLN'S INN FIELDS
CLARE HALL

Research Group Leaders

The London Research Institute (LRI) is Cancer Research UK's flagship research institute, focusing on the analysis of fundamental biological processes related to cancer. LRI encourages pursuit of ambitious and longer term research programmes at the highest level.

LRI scientists are funded directly through the Institute's core grant from Cancer Research UK, Europe's largest independent cancer research organisation, as part of its comprehensive portfolio of basic, applied and clinical research. The Institute's international staff work in 50 research groups, housed in well-supported laboratories at Lincoln's Inn Fields in central London, and at **Clare Hall** in Hertfordshire.

We are seeking innovative scientists to establish independent research programmes at the LRI **Clare Hall Laboratories** and to contribute to the Institute's vibrant scientific programme. LRI Group Leaders receive generous Institute core funding for personnel (research fellows, graduate students and technical support), laboratory consumables, and access to the Institute's scientific core facilities, backed by a substantial laboratory space and equipment package. Junior appointments are initially for seven years, with consideration for promotion in the sixth year. Suitably experienced applicants may be appointed at a senior level.

For 2008 recruitment, we are interested in scientists interested in addressing fundamental questions in the area of:

Genome Integrity and Cell Cycle

Including but not limited to

Gene expression mechanisms; DNA repair mechanisms and regulation; Mammalian cell cycle.

Outstanding candidates working in any area of basic cancer biology which complements the interests of the Institute will also be considered favourably: our primary criterion for appointment will be the quality of the scientist.

Informal enquiries may be made by e-mail to john.diffley@cancer.org.uk

---

For information about the London Research Institute, its staff, and their research interests visits
www.london-research-institute.co.uk

Applications should be submitted electronically to Dr Ava Yeo at the address below and must include:

1. Complete CV
2. Past and current research interests (approx 500 words)
3. Future research proposals (1000-1500 words)

At the time the application is submitted
three referees should be instructed to submit letters of recommendation to:

Dr Ava Yeo, Director of Operations, London Research Institute, 44 Lincoln's Inn Fields, London WC2A 3PX, UK.
E-mail: ava.yeo@cancer.org.uk; Confidential Fax (references only): (44)-20-7269-3585

Applications should be received by 14th November 2008

Charity no: 1089464

Monterey Bay Aquarium Research Institute

2009 POSTDOCTORAL FELLOWSHIPS

Founded in 1987 and supported by the David and Lucile Packard Foundation, The Monterey Bay Aquarium Research Institute (MBARI) is a non-profit oceanographic research institute, dedicated to the development of state-of-the-art instrumentation, systems, and methods for scientific research in the oceans. MBARI's research center includes science and engineering laboratories, as well as an operations facility to support our research vessels and oceanographic equipment, including remotely operated and autonomous underwater vehicles. Located in Moss Landing, California, the heart of the nation's largest marine sanctuary, MBARI places a balanced emphasis on science and engineering, with established programs in marine robotics, ocean physics, chemistry, geology, and biology, as well as information management and ocean instrumentation research and development.

MBARI invites applications each year for several postdoctoral fellowships in the fields of biological, chemical, and physical oceanography, marine geology, and ocean engineering. Fellowships may require occasional trips to sea. Awards are typically for two years.

Candidates must be awarded their Ph.D. degree prior to commencing the two-year appointment between September 2009 and March 2010.

Applicants are encouraged to communicate with potential research sponsors at MBARI for guidance on project feasibility, relevance to ongoing MBARI research, and resource availability.
(http://www.mbari.org/about/researchers.html)

Application deadline: Thursday, December 11, 2008

Selected candidates will be contacted in early March 2009.

Application requirements:
1. Curriculum vitae
2. At least three professional letters of recommendation
3. Succinct statement of the applicant's doctoral research
4. Potential research goals at MBARI
5. Supplemental Information online form
(http://www.mbari.org/oed/jobs/forms/postdoc_form.htm)

Competitive compensation and benefits package.

MBARI considers all applicants for employment without regard to race, color, religion, sex, national origin, disability, or veteran status.

Address your application materials to:
MBARI, Human Resources
Job code: Postdocs-2009
7700 Sandholdt Road, Moss Landing, CA 95039-9644

Submit by e-mail to jobs_postdocs@mbari.org (preferred),
by mail, or fax to (831) 775-1620.

M B A R I

EOE • MBARI Welcomes Diversity

Boston University College of Health & Rehabilitation Sciences: Sargent College
Department of Health Sciences

BOSTON UNIVERSITY

Tenure-Track Position in Computational Physiology/Neurobiology

The Dept. of Health Sciences at Boston University is searching for a tenure-track faculty member at the Assistant Professor level in the areas of Bioinformatics, Computational Biology, or Systems Biology relevant to Physiology/Neurobiology. In exceptional cases candidates at the Associate or Full Professor level will be considered. The department has undergraduate programs in human physiology, health science, and nutrition, and a graduate program in physiology and neurobiology. Faculty have active research in muscle biology, cytoskeletal signaling, and neurobiology. Opportunities for collaborations exist in other research programs at Boston University, and through interdisciplinary programs in bioinformatics, systems biology, and experimental and computational neuroscience. Applicants should have a doctorate in physiology, cell biology, neurobiology, or a related field, and post-doctoral training, a strong scholarly record with research funding, or potential for funding and a commitment to further develop departmental undergraduate and graduate programs.

Please submit a letter of application, C.V., statement of research plans and names of three individuals who can provide letters of reference to: **D. Charland, Assist. to the Search Committee, Dept. of Health Sciences, Boston University, 635 Commonwealth Avenue, 4th floor, Boston, MA 02215**.

Boston University is an Equal Opportunity/ Affirmative Action Employer.

Columbia University

Department of Biological Sciences

TENURE-TRACK FACULTY POSITION

The Department of Biological Sciences at Columbia University invites applications for a tenure-track faculty position at the assistant professor level. We are especially interested in new investigators and those early in their independent careers. We are seeking highly accomplished individuals with innovative research records and future plans, who will complement the current strengths and collegial atmosphere of the Department. Our Department has a long history of leadership in modern biology and a broad multidisciplinary focus (see http://www.columbia.edu/cu/biology/). We are located on the main campus of Columbia University, surrounded by other basic science and engineering departments, and have strong ties to our Medical School. We expect that the successful candidate will develop a vigorous research program and also participate in undergraduate and graduate teaching.

Send CV, statement of research goals, and three letters of reference **by November 17, 2008,** to:

academicjobs.columbia.edu/applicants/Central?quickFind=50780

Columbia University is an equal opportunity/affirmative action employer.

DEPAUW UNIVERSITY

Ecologist

Tenure-track position beginning August 2009. Rank and salary commensurate with experience. Ph.D. preferred, ABD considered. Commitment to undergraduate teaching in liberal arts setting essential. Teaching responsibilities include: general education and introductory biology, advanced ecology and environmental biology. Successful candidate expected to develop a research program involving undergraduates; preference may be given to those with field research programs adaptable to local systems. Preference for individuals whose expertise complements that of existing faculty members. For information about department, visit **http://www.depauw.edu/acad/biology/**. DePauw has exceptional faculty development programs including pre-tenure leave and internal grants (see **http://www.depauw.edu/admin/acadaffairs/facdev/**). Submit letter of application, curriculum vitae, three letters of recommendation, transcripts, statements of teaching philosophy and research interests, and evidence of teaching effectiveness to: **Ecology Search Committee, Department of Biology, DePauw University, Greencastle, IN 46135**. Review of applications begins October 15, 2008 and continues until position is filled.

DePauw University is an Equal Opportunity Employer. Women and members of under-represented groups are encouraged to apply.

London **Research** Institute
Lincoln's Inn Fields Laboratories

CANCER RESEARCH UK
LONDON RESEARCH INSTITUTE
LINCOLN'S INN FIELDS
CLARE HALL

Research Group Leaders

The London Research Institute (LRI) is Cancer Research UK's flagship research institute, focusing on the analysis of fundamental biological processes related to cancer. LRI encourages pursuit of ambitious and longer term research programmes at the highest level.

LRI scientists are funded directly through the Institute's core grant from Cancer Research UK, Europe's largest independent cancer research organisation, as part of its comprehensive portfolio of basic, applied and clinical research. The Institute's international staff work in 50 research groups, housed in well-supported laboratories at **Lincoln's Inn Fields** in central London, and at Clare Hall in Hertfordshire.

We are seeking innovative scientists to establish independent research programmes at the LRI **Lincoln's Inn Fields** Laboratories and to contribute to the Institute's vibrant scientific programme. LRI Group Leaders receive generous Institute core funding for personnel (research fellows, graduate students and technical support), laboratory consumables, and access to the Institute's scientific core facilities, backed by a substantial laboratory space and equipment package. Junior appointments are initially for seven years, with consideration for promotion in the sixth year. Suitably experienced applicants may be appointed at a senior level.

For 2008 recruitment, we are interested in scientists interested in addressing fundamental questions in the areas of:

Biology of Tissues and Tumours

including but not limited to

Tumour-host interactions; Oncogenes and tumour suppression; Cancer models.

Cell Regulatory Mechanisms

including but not limited to

Signal transduction mechanisms; Chromosome biology; Gene expression; Molecular cell biology.

Outstanding candidates working in any area of basic cancer biology which complements the interests of the Institute will also be considered favourably: our primary criterion for appointment will be the quality of the scientist.

Informal enquiries may be made by e-mail to
david.horowicz@cancer.org.uk, julian.downward@cancer.org.uk, richard.treisman@cancer.org.uk

For information about the London Research Institute, its staff, and their research interests visit
www.london-research-institute.co.uk

Applications should be submitted electronically to Dr Ava Yeo at the address below and must include:

1. Complete CV
2. Past and current research interests (approx 500 words)
3. Future research proposals (1000-1500 words)

At the time the application is submitted three referees should be instructed to submit letters of recommendation to:

Dr Ava Yeo, Director of Operations, London Research Institute
44 Lincoln's Inn Fields, London WC2A 3PX, UK.
E-mail: ava.yeo@cancer.org.uk; Confidential Fax (references only): (44)-20-7269-3585

Applications should be received by 14th November 2008

Charity no: 1089464

Faculty Position
Assistant or Associate Professor of Medicinal Chemistry

The Division of Medicinal and Natural Products Chemistry of the College of Pharmacy at the University of Texas at Austin invites applications for a tenure-track Assistant or Associate Professor. Appointment as Associate Professor requires demonstrated sustained extramural grant support and research, and scholarship achievements that are consistent with appointment to rank at a research-intensive university. The successful applicant for the Assistant Professor position will be expected to establish a vigorous externally funded research program in any area of modern medicinal or bioorganic chemistry. In addition to performing cutting edge research, the successful applicant will be expected to teach in the Pharm.D. program and develop graduate courses in the area of research expertise. Qualified candidates must have an earned Ph.D. in Medicinal Chemistry, Chemistry, Biochemistry, or the Biological Sciences, relevant postdoctoral experience, and be able to demonstrate effective teaching. The University of Texas at Austin is a leading tier one, research focused, state university and the College of Pharmacy offers an exciting and highly visible research environment with excellent opportunities for collaboration with faculty in the Department of Chemistry and Biochemistry and the Institute for Cellular and Molecular Biology. Additional information regarding UT College of Pharmacy can be located at: **http://www.utexas.edu/pharmacy/**. All positions offer a competitive salary and benefits package.

We welcome qualified applicants to submit application materials by **November 17, 2008**, however review of applications will begin immediately upon receipt and will continue until the position is filled. Applicants should submit electronically (preferred), a letter of application with a summary of research plans, curriculum vitae, and the names of 3 professional references to: **whitman@mail.utexas.edu**. Applicants should address all communication to:

Christian P. Whitman, Ph.D.
College of Pharmacy
1 University Station C0850
The University of Texas at Austin
Austin, Texas 78712

Women and minorities are encouraged to apply.
The University of Texas at Austin is an Affirmative Action, Equal Opportunity Employer.

UNIVERSITY of ROCHESTER MEDICAL CENTER

FACULTY POSITIONS CENTER FOR NEURAL DEVELOPMENT AND DISEASE

The Center for Neural Development and Disease at the University of Rochester School of Medicine and Dentistry invites applications for tenure-track faculty positions at the Assistant, Associate, or Full Professor level. Candidates should employ genetic, molecular and/or physiological approaches to carry out vigorous and creative research on important problems in neural development and function in health and disease. Successful applicants will join a dynamic, interdepartmental group of investigators whose research spans a broad area of molecular and cellular neuroscience.

Interested candidates should submit a cover letter, CV, and statement of research interests to **cnddsearch@urmc.rochester.edu**. Please also arrange for three letters of reference to be sent to this address.

The University of Rochester is an Equal Opportunity Employer, has a strong commitment to diversity and actively encourages applications from candidates from groups underrepresented in higher education.

CHAIR
Department of Basic Science
NYU College Of Dentistry

The New York University College of Dentistry (NYUCD) is seeking a strong academic leader to serve as Chair of Basic Science. The College has undergone extensive renovation and currently has 28,000 square feet of research space, which it is currently planning to dramatically increase over the next 3-5 years. The College is located on 1st Avenue within the medical complex that includes the College of Dentistry, School of Medicine, affiliated hospitals and several vibrant research institutes.

The Department of Basic Science consists of 24 full-time faculty members and an additional 12 part-time and adjunct members. Research strengths of the department include cancer, infectious diseases, oral-systemic disease linkages, and tissue engineering. The department is also responsible for the teaching of the basic science courses to DDS, Post-graduate and Graduate students. The chair will oversee the teaching, research and future growth of the department.

This is a full time tenured position at the rank of Associate or Full Professor. Candidates must possess a PhD, DDS, MD degree or a combination thereof, have outstanding administrative experience and be a distinguished researcher with an international reputation and a strong track record of research funding.

NYUCD has demonstrated an entrepreneurial philosophy in its recruitment of academic leaders with respect to professional packages, in addition to offering competitive salaries and benefits.

Please submit a CV and a statement of interests and goals to **Dr. Daniel Malamud, Chair of the Basic Science Chair Search committee, Department of Basic Science, NYU College of Dentistry, 345 East 24th Street, Room 917S, New York, NY, 10010-4086** or via e-mail to **daniel.malamud@nyu.edu**.

NEW YORK UNIVERSITY

NYU is an Equal Opportunity/Affirmative Action Employer.

Vice-Chair for Research/Open Rank

The Department of Anesthesiology, University of Texas Health Science Center at San Antonio, Texas (UTHSCSA) invites nominations and applications for the position of Vice-Chair for Research (VCR). As the chief research officer for the department, the VCR is responsible for implementation of the research vision, the overall management of departmental research activities, and the administration of sponsored research. The VCR will engage in multidisciplinary collaboration within UTHSCSA—a Clinical and Translational Science Award (CTSA) grantee—and its affiliated institutions.

Qualifications for this position include an M.D., M.D.-Ph.D., or Ph.D. degree in an appropriate field of study. The successful candidate will have a national/international reputation as a distinguished scientist with an outstanding record of research accomplishments; a proven track record of directing a research enterprise; outstanding communication skills as evidenced by an ability to mentor junior faculty, scientists, residents, and students. The candidate must be a critical and strategic thinker and a visionary leader who can develop and enhance the research enterprise; and one who can demonstrate expertise in crafting interdisciplinary proposals and negotiating multi-faceted awards. One or more currently funded NIH grant(s) and experience in translational research is highly desirable. Given the excellent research infrastructure in neurobiology at UTHSCSA, research experience in pain medicine would be a plus.

For more information, please visit our website at **www.anesthesia.uthscsa.com**. To apply or nominate a candidate for the position of Vice-Chair for Research, Department of Anesthesiology, U.T. Health Science Center at San Antonio, please submit a current CV, supporting documents, and names and addresses of five references to: **J. Jeffrey Andrews, M.D, Chair, Department of Anesthesiology – MSC 7838, U.T. Health Science Center at San Antonio, 7703 Floyd Curl Drive, San Antonio, TX 78229.**

All faculty appointments are designated as security sensitive positions. The University of Texas Health Science Center at San Antonio is an Equal Employment Opportunity/Affirmative Action Employer.

COLUMBIA UNIVERSITY
IN THE CITY OF NEW YORK

Neuroscience Faculty Recruitment

The Department of Neuroscience at Columbia University Medical Center, as part of a University-wide Neuroscience Initiative, is recruiting faculty concentrating on the analysis of neural circuitry through molecular, genetic, cellular electrophysiological and/or imaging approaches. We are particularly interested in individuals whose research program explores neural circuits in genetically tractable model systems and in the context of well-defined behaviors, synaptic connectivity, and/or development. We encourage applications for positions at the Assistant Professor level, but will also consider applications from more senior investigators for positions at the level of Associate or full Professor.

Columbia University currently has a world-renowned program in neurobiology and behavior, and the Neuroscience Initiative aims to enhance interactions between basic and clinical neurosciences and link the neurosciences to other scientific disciplines within the University. Faculty will be affiliated with the Department of Neuroscience and the Doctoral Program in Neurobiology and Behavior and there will be opportunities for strong ties with scientific departments and programs on the Morningside Heights campus.

Applications for this round of recruitment are requested by **November 14, 2008**. A CV, cover letter including statement of interests, and three letters of reference under separate cover should be e-mailed care of **David Leyden, dgl2102@columbia.edu**. In addition, please mail a hard copy of these documents to:

Chair, Neuroscience Search Committee
c/o: David Leyden
Columbia University
Hammer Health Sciences Center
Room 2-205G
701 West 168th Street
New York NY 10032

Columbia University takes affirmative action to ensure equal employment opportunity.

DEPAUW UNIVERSITY

Comparative Anatomist/Neurobiologist

Tenure-track position beginning August 2009. Rank and salary commensurate with experience. Ph.D. preferred, ABD considered. Commitment to undergraduate teaching in liberal arts setting essential. Teaching responsibilities include: general education and introductory biology, advanced courses in comparative anatomy, neurobiology and area of expertise. Successful candidate is expected to develop a research program involving undergraduate students. For information about department, visit **http://www.depauw.edu/acad/biology/**. DePauw has exceptional faculty development programs including pre-tenure leave and internal grants (see **http://www.depauw.edu/admin/acadaffairs/facdev/**). Submit letter of application, curriculum vitae, three letters of recommendation, transcripts, statements of teaching philosophy and research interests, and evidence of teaching effectiveness to: **Comparative Anatomy/Neurobiology Search Chair, Department of Biology, DePauw University, Greencastle, IN 46135**. Review of applications begins October 15, 2008 and continues until position is filled.

DePauw University is an Equal Opportunity Employer. Women and members of under-represented groups are encouraged to apply.

THE UNIVERSITY of TENNESSEE HEALTH SCIENCE CENTER

TWO ASSISTANT PROFESSOR POSITIONS
DEPARTMENT OF PHYSIOLOGY
MEMPHIS, TN

The Department of Physiology at The University of Tennessee Health Science Center (UTHSC) in Memphis invites outstanding scientists with Ph.D., M.D., or equivalent degrees for **two tenure-track faculty positions at the rank of assistant professor to begin July 1, 2009**. We are searching for creative scientists who have or will establish an extramurally funded research program and also excel at teaching medical, dental, and graduate students. UTHSC is the state's flagship academic health center with an annual budget of close to 400 million dollars, and the Department of Physiology is currently ranked seventh based on extramural funding by the American Physiological Society. While we will consider applicants in all areas of physiology, the Department has a particular interest in recruiting candidates with experience studying the interface between immunity and vascular biology, stem cell physiology, or innovative techniques in molecular physiology. The positions are part of the expansion of the department; significant new laboratory space, a substantial start up package, and a competitive salary with an additional incentive bonus will be offered.

Candidates should submit their Curriculum Vitae, a description of research interests/goals (not to exceed two pages) as a single PDF document, and arrange to have three letters of reference sent to: **Gabor Tigyi, M.D., Ph.D., Harriett Van Vleet Professor and Chair, Department of Physiology; E-Mail: PhysiologySearch@utmem.edu; Website: http://physio1.utmem.edu.**

Applicants should have their applications complete by **December 15, 2008**, as review will begin upon receipt of the application.

UTHSC is an Equal Opportunity Employer. The University of Tennessee is an EEO/AA/Title VI/Title IX/Section 504/ADA/ADEA institution in the provision of its education and employment programs and services.

NASA

Chief, Hydrospheric and Biospheric Sciences Laboratory

The NASA/Goddard Space Flight Center invites applications for the position of Chief of the Hydrospheric and Biospheric Sciences Laboratory, located in Greenbelt, Maryland. The Laboratory is part of the Earth Sciences Division in the Sciences and Exploration Directorate. The Chief of the Hydrospheric and Biospheric Sciences Laboratory is responsible for all the activities of the Laboratory whose mission is to conceive, develop, and implement cutting-edge observations from space to carry out a large range of basic and applied research dedicated to advancing knowledge and understanding of the Earth's oceanic, cryospheric, biospheric, and hydrospheric systems.

The laboratory chief is also responsible for encouraging mutually beneficial collaborative activities with other NASA organizations, with universities, other Government agencies, and private scientific institutions. The laboratory chief performs individual research and may act as a principal investigator, a co-investigator, and/or a project scientist on NASA missions, in addition to being the supervisor for personnel within the laboratory.

This search is targeted primarily to those with an advanced degree and extensive post-graduate experience in both scientific research and scientific management. The incumbent must be recognized as an authority in an area of hydrospheric or biospheric science that is relevant to the primary activities of the laboratory. Compensation for this position ranges from $115,317 to $149,000 per annum, including locality pay. Salary will be commensurate with the incumbent's experience.

Interested applicants are welcome to submit a curriculum vitae and a statement of career interest of approximately 1000 words to Ms. Emilie Rank, email: **emilie.j.rank@nasa.gov**. For more information about position requirements and application procedures, please call **Emilie Rank** at **(301) 614-5566**; and for scientific questions, please call **Dr. Franco Einaudi**, Director of the Earth Sciences Division at **(301) 614-5634**.

The Goddard Space Flight Center has and encourages a diverse workforce. Equal Opportunity Employer. U.S. citizenship required.

With a staff of 4400, we are one of the largest interdisciplinary research centres in Europe and are also a member of the Helmholtz Association of German National Research Centres. We work in the fields of "Health", "Energy and the Environment", and "Information". To assist us we have top-class super-computers at our disposal.

JÜLICH
FORSCHUNGSZENTRUM

www.fz-juelich.de

For our Institute of Neurosciences and Biophysics – Medicine (INB-3), we are seeking the following:

PHYSICISTS
ELECTRICAL/RF ENGINEERS
COMPUTER SCIENTISTS

A new 9.4T high-field MRI scanner is currently being installed in Jülich. This scanner will be capable of the **simultaneous** acquisition of MRI and PET data in human studies and is thus the first system worldwide to combine high-field MRI and PET. Additionally, the Institute houses state-of-the-art 1.5T, 3T and 4T human MRI scanners, a 3T hybrid MR-PET and a 9.4T animal MRI scanner. All of the scanners are based on the Siemens software and hardware platform.

The position offers you:
The opportunity to participate in the following projects:

- Development of new MRI sequences designed for brain imaging and neuroscientific applications targeting structural and functional MRI, e.g. ultra-fast MRI techniques, DTI, and contrast-enhanced, high-resolution imaging
- Development of new *in vivo* methods for quantitative MRI including image processing of quantitative data
- Development of new imaging methods for the *in vivo* quantification of other MR-active nuclei such as ^{23}Na and ^{17}O in the brain
- Development of RF coils and coil arrays for high-field MRI as well as hybrid MR-PET imaging.

Qualifications required:
Applicants should possess a PhD in physics or one of the above subjects; in depth experience and knowledge of MR imaging is indispensable. Cooperative teamwork as well as structured approaches to problem solving are essential requirements.

Candidates should preferably have:
Experience of object-oriented software design (C++), multivariate image analysis, digital signal processing, and computational electrodynamics would be extremely advantageous. Similarly, construction of radiofrequency coils for MRI applications or antenna design is highly desirable.

Further information at: www.fz-juelich.de/inb/inb-3/

The positions are initially for a fixed term of two years with possible extensions thereafter.

Salary and social benefits will conform to the provisions of the Collective Agreement for the German Civil Service (TVöD).

The implementation of equal opportunities is a cornerstone of our staff policy at Forschungszentrum Jülich; for this we have received the „TOTAL E-QUALITY" Award. Applications from women are therefore particularly welcome. We also welcome applications from disabled persons.

Candidates are requested to send full applications (letter of application, CV, copies of all certificates, representative publications, brief description of your research interests and also three letters of recommendation).

Please submit your application with the **reference number 085-086/2008** to:

Forschungszentrum Jülich GmbH
Geschäftsbereich Personal
- Personalentwicklung -
52425 Jülich - Germany

contact:
Mrs. Crützen
phone: +49 2461 61-2110

VICE PRESIDENT FOR RESEARCH AND VICE PROVOST

The University of Alabama invites applications for and nominations for the position of Vice President for Research and Vice Provost.

Responsibilities: The Vice President for Research and Vice Provost is responsible for providing leadership and advancing the research goals of the University and expanding the base of research funding from federal agencies, foundations, and the private sector. The Vice President oversees university-wide research enhancement and compliance activities including the formulation and promotion of research policies and guidelines, promotion and coordination of multidisciplinary research programs, development of research infrastructure, and oversight of technology transfer and economic development activities. The Vice President fosters research collaboration between and among faculty and students at UA and other institutions within the University of Alabama System and at other research universities in the state. The Vice President fosters collaborative research partnerships with the business community to expand the University's applied research capacity.

The Vice President for Research participates with the President, Provost and other vice presidents in the senior leadership of the University. The Vice President must maintain a close working relationship with the deans, associate deans for research, center directors and other faculty.

Qualifications:

- An earned doctorate from an accredited institution in an appropriate discipline;
- Extensive professional, academic, and administrative experience in all aspects of research and technology transfer in a complex organizational environment;
- Demonstrated success in proposing, negotiating, and acquiring externally funded research;
- Capacity to work with a diverse faculty in a wide range of disciplines and have the vision and administrative expertise to create and implement innovative research initiatives;
- Ability to maintain and expand positive relationships on the campus and within the University of Alabama System.

Applications: To apply for this position, go to **https://facultyjobs.ua.edu** and apply to requisition number 0800754. Attach your resume and names, addresses and phone numbers of five references to the online faculty application. Confidential nominations may be submitted by mail to:

Dr. Martha Powell, Chair
Vice President for Research Search Committee
Office of the Provost
Box 870117
The University of Alabama
Tuscaloosa, AL 35487

Inquiries concerning the position should be directed to Dr. Martha Powell at mpowell@biology.as.ua.edu.

For full consideration, applications should be received by November 3, 2008, but review of applications will continue until the position is filled. The starting date is negotiable and the salary and benefits are competitive.

The University is located on a beautiful 1,000 acre residential campus in Tuscaloosa a community of 100,000 in central Alabama. Tuscaloosa is conveniently located between Atlanta, New Orleans and the white sandy beaches of the Gulf coast and is only 45 minutes from metropolitan Birmingham. The area offers excellent climate, reasonable living costs, minimal urban congestion and abundant outdoor recreation. The Tuscaloosa community provides rich cultural, educational and athletic resources for a broad range of lifestyles.

The University of Alabama is an Affirmative Action/Equal Opportunity Employer. Applications from women and minorities are encouraged.

Crimson is
THE UNIVERSITY OF ALABAMA

Fellowship Opportunities

Postdoctoral Fellowship appointments at the Santa Fe Institute begin fall 2009. Appointed for up to three years, fellows pursue research questions of their own design, are encouraged to transcend disciplinary lines, and collaborate with SFI faculty, other Fellows, and researchers from around the world. Successful foreign applicants must acquire an acceptable visa.

The Santa Fe Institute is an affirmative action, equal opportunity employer. We are building a culturally diverse faculty and staff and strongly encourage applications from women, minorities, individuals with disabilities, and covered veterans.

TO APPLY: View the full position announcement and application instructions at www.santafe.edu/postdoc. Application is due by November 14, 2008. For further information, email postdocinfo@santafe.edu.

SANTA FE INSTITUTE

Do what you love. Love what you do.

Senior Research Cell Molecular Biologist

Abbott's Tumor Genomics group offers a unique scientific environment, including excellent collaborative opportunities with multiple groups involved in research in the areas of apoptosis, DNA repair, angiogenesis, siRNA-mediated gene silencing, and others. We offer access to outstanding core scientific support services and a significant amount of internal genomics, informatics and cancer biology expertise, and a network of external collaborations in several areas of basic research.

Seek a highly motivated PhD in Molecular/Cell Biology or related fields to initiate and lead research projects in cancer biomarker discovery.

Incumbent will analyze critical molecular components involved in intracellular signaling and drug inhibition of cancer cell function, leading to discovery of cancer biomarkers.

• Post-doctoral experience preferred • Strong experimental skills in cell biology including DNA and RNA work • Demonstrated experience in cancer research • Strong publication record required • Experience in genomics data mining and bioinformatics preferred

If you want to work with people who share a common desire to improve the quality of people's lives, we invite you to learn more about Abbott's exciting career opportunities and employment benefits. Please visit the career section of www.abbott.com and reference requisition #52665BR when applying.

www.abbott.com/careers

An EEO/AA employer, Abbott welcomes and encourages diversity in our workforce.

Abbott
A Promise for Life

WRIGHT STATE UNIVERSITY

Assistant Professor - Tenure Track
Department of Biochemistry and Molecular Biology
Wright State University Boonshoft School of Medicine and College of Science and Mathematics

The Department of Biochemistry and Molecular Biology invites applications from outstanding candidates for the position of Assistant Professor of biochemistry. This faculty position is part of the department's growth coinciding with the opening of the Matthew O. Diggs III Laboratory for Life Sciences. This is a tenure-track, nine-month appointment with a competitive startup package, the opportunity to occupy state of the art research space, and access to proteomic, genomic and NMR facilities. The department currently consists of 11 full-time faculty actively engaged in research in the areas of biochemistry, cell signaling and molecular genetics.

Applicants must have a Ph.D., M.D., or equivalent doctoral degree and at least two years of postdoctoral research experience. Applicants are expected to establish a funded, independent research program and participate in collaborative projects with current faculty. Candidates whose research employs biochemical approaches to human disease through studies of protein structure/function, protein:protein interactions and cellular signaling are encouraged to apply.

Please send a letter of application, curriculum vitae, a focused research plan, and three reference letters to: **Dr. Steven Berberich, Chair, Department of Biochemistry and Molecular Biology, Wright State University, 3640 Colonel Glenn Hwy, Dayton, OH 45435**. Review of applications will begin on **December 1, 2008** and continue until the position is filled. Please visit **http://www.med.wright.edu/bmb/** to learn more about the department, the university and the Dayton area.

Wright State University is an Equal Opportunity/Affirmative Action Employer. Candidates from groups underrepresented in academic science are strongly encouraged to apply.

KU THE UNIVERSITY OF KANSAS

DEPARTMENT OF MOLECULAR BIOSCIENCES

The Department of Molecular Biosciences at the University of Kansas seeks applications from outstanding individuals for a tenure-track ASSISTANT PROFESSOR position in the area of protein biochemistry. The successful applicant will have a strong background in applying chemical, physical and/or structural biological approaches to fundamental problems in biology. Preference will be given to candidates working in areas that enhance or complement existing departmental strengths. Important strengths include structure-function studies of enzymes and macromolecular assembly. Other existing areas of departmental strengths include signal transduction, cell and developmental biology, neurobiology, immunology, and pathogenesis (for details see **http://www.molecularbiosciences.ku.edu**). This appointment is expected to begin as early as August 18, 2009. Applicants must hold a Ph.D. or equivalent degree in biological or chemical sciences and have at least two years of post-doctoral research experience. For full job announcement visit: **http://www.clas.ku.edu/employment/**. Successful candidates will be expected to develop and maintain an active research program and contribute to the Department's teaching mission.

Interested applicants should send a cover letter, curriculum vitae, research plan, and statement of teaching philosophy to **ProteinBiochem@ku.edu**, preferably as a single PDF file. Applicants should also arrange to have three letters of reference sent to: **Linda Wiley, Administrative Associate, Protein Biochemistry Search, Dept. of Molecular Biosciences, Univ. of Kansas, 1200 Sunnyside Ave., Room 2034 Lawrence, KS 66045-7534**. To ensure full consideration, complete applications should be received by **November 1, 2008**.

EO/AA Employer.

Department of Health & Human Services
National Institutes of Health
National Institute of Dental and Craniofacial Research (NIDCR)

Tenured Senior Investigator

An expert is sought in the area of **Salivary Gland Biology and Physiology** to fill a tenured Senior Investigator position (Full Professor Equivalent) in the Molecular Physiology and Therapeutics Branch, Division of Intramural Research (DIR), National Institute of Dental and Craniofacial Research, NIH. The successful applicant will establish a strong research program that encompasses fundamental aspects of salivary gland biology and physiology, as well as translational research leading to clinically relevant studies. The mission of the DIR is to improve oral, dental and craniofacial health through research, research training, and the translation of discoveries to the public domain. The DIR accomplishes this mission by: 1) performing distinctive basic and clinical research that emphasizes high quality and relevance to health; 2) training the next generation of researchers in its laboratories and clinic, and 3) translating the results of its research through publications and technology transfer.

We are seeking an established senior scientist (Ph.D., D.D.S., M.D., or equivalent) with an outstanding track record in physiology (experience in salivary or other exocrine gland physiology/biology preferable), as evidenced by a strong publication record and successful funding. Research in the Branch is focused on bench-to-bedside efforts that involve acquiring basic understanding of salivary gland physiology and pathology for translation into clinically relevant studies and development of therapeutic strategies for the treatment of salivary gland dysfunction. The selected person will be expected to complement the ongoing research within the Branch and integrate with the NIDCR salivary gland research initiative, which includes efforts on pathophysiology of salivary glands and novel therapies, stem cell biology, and salivary gland morphogenesis.

Applicants should submit the following: current *curriculum vitae* with complete bibliography; names and addresses of five references; statement of research interests; and summary of proposed research plan.

Salary will be commensurate with qualifications and experience. More detailed information about the NIDCR Division of Intramural Research may be found at: **http://www.nidcr.nih.gov/Research/NIDCRLaboratories/OverviewDIR/**

Applications must be received by **December 6, 2008**. PDF versions of documents sent by electronic mail are strongly preferred. Materials should be sent to; Ms Marsha Greco, by email: **grecom@mail.nih.gov**; or by regular mail: NIDCR, 10 CENTER DR MSC-1190, Bldg. 10, Room 1N113, Bethesda, MD 20892-1190.

DHHS and NIH are Equal Opportunity Employers

CSIRO

Post Doctoral Fellowships 2008-09

CSIRO is Australia's national science organisation with over 6,500 staff located across the country. It is one of the largest and most diverse research organisations in the world, with its research delivering solutions for agribusiness, the environment, information and communication technologies, health, advanced materials and manufacturing, minerals and energy, services, transport and infrastructure.

The CSIRO Postdoctoral Fellowship Scheme provides the opportunity for postgraduates to undertake postdoctoral research projects within CSIRO for a period of three years. 20 postdoctoral positions are now being offered across a broad range of disciplines, as follows:

- Restoring Function: Vegetation Ecology and Genetics **(2008/1067)**
- Encapsulants for Organic Photovoltaics **(2008/1069)**
- Quantifying Nitrous Oxide Emission from Soil **(2008/1071)**
- Flow Synthesis of Histrionicotoxin Alkaloids **(2008/073)**
- Engineering Novel Fatty Acid Desaturases **(2008/1075)**
- RNA Silencing in Fungal Pathogenesis **(2007/1077)**
- Nutrients, Grazing and Global Plant Biodiversity **(2008/1079)**
- Climate Change: Planning for Biodiversity Persistence **(2008/1081)**
- Insitu Diffraction Studies into Inert Anodes **(2008/1083)**
- Chemiresistor Sensor Arrays **(2008/1085)**
- High Temperature Fuel Cell Electrochemistry **(2008/1068)**
- Mycobacterial Genomics and Aetiology of Crohn's Disease **(2008/1070)**
- Southern Ocean, Carbon Dioxide and Climate Change **(2008/1072)**
- Insitu Crystallisation Studies of Jarosite Minerals **(2008/1074)**
- Genetic and Demographic Modeling of Self-incompatibility **(2008/1076)**
- Modeling of Nonlinear Dynamic Drilling System **(2007/1078)**
- Brain Connectivity Atlas from MRI **(2008/1080)**
- Local Property Enhancement in Light Alloys **(2008/1082)**
- Insect Prospectors for Mineral Deposit Discovery **(2008/1084)**
- Biomarker Discovery in Alzheimer's Disease **(2008/1086)**

For further information, selection documentation and details on how to apply, visit **www.csiro.au/careers**

Alternatively contact CSIRO on 1300 301 509

hmaC089221

www.csiro.au

POSITIONS OPEN

TWO ASSISTANT PROFESSOR POSITIONS MARINE BIOLOGIST and CELL/MOLECULAR BIOLOGIST

The Department of Biology and Marine Biology at the University of North Carolina Wilmington (UNCW) invites applications for two tenure-track positions starting August 2009.

Marine Biologist. Candidates in any subdiscipline of marine biology are encouraged to apply.

Cell and Molecular Biologist. Candidates with research interests in the field of sensory biology are especially welcomed.

Duties for both positions include undergraduate and graduate teaching; the Cell and Molecular Biologist will contribute to the anatomy and physiology sequence. Contact **Dr. Steve Kinsey** for questions about the Marine Biologist position **(e-mail: kinseys@uncw.edu; telephone: 910-962-7398)** and **Dr. Ann Pabst (e-mail: pabsta@uncw.edu; telephone: 910-962-7266)** for questions about the Cell and Molecular Biologist position. For assistance with the online application process, contact **Ms. Tracie Chadwick (e-mail: chadwickt@uncw.edu; telephone: 910-962-3536).** For more information and to apply, please visit **website: http://consensus.uncw.edu.** *Equal Employment Opportunity/Affirmative Action Employer.*

MOLECULAR ENVIRONMENTAL PHYSIOLOGY

The Department of Biological Sciences at the University of Wisconsin, Milwaukee seeks applicants for a tenure-track position in molecular environmental physiology at the rank of **ASSISTANT PROFESSOR.** We seek candidates with research interests in the cellular and molecular mechanisms by which signaling pathways in the endocrine or nervous systems are disrupted by environmental chemicals. Candidates must have a Ph.D. and postdoctoral experience and will be expected to establish an independent, extramurally funded research program involving M.S. and Ph.D. students in an area of physiology/toxicology and eukaryotic molecular biology. Teaching responsibilities include participation in core biology courses and an advanced course in an area of specialization. To apply, please go to **website: http://www.jobs.uwm.edu/applicants/Central?quickFind=50597.** A completed application should include: cover letter, curriculum vitae, statement of research goals, statement of teaching interests, and letters of professional reference. Applicants should arrange to have three letters of reference sent as PDF attachments to the **Departmental Chair (e-mail: sandgren@uwm.edu)** or mailed to: **Molecular Environmental Physiologist Search, Department of Biological Sciences, University of Wisconsin-Milwaukee, P.O. Box 413, Milwaukee, WI 53201.** Screening of candidates will begin December 19, 2008, and continue until the position is filled. Appointment begins August 2009. *UWM is an Equal Opportunity/Affirmative Action Employer.*

FACULTY POSITION in CARIBBEAN MEDICAL SCHOOL

Saint James School of Medicine **(website: http://www.sjsm.org)** is hiring faculty with teaching experience in any of the basic medical science subjects for its campus in the Caribbean (Bonaire). Immediate need is in pathology, physiology, and physical diagnosis. Applicants must be M.D. and/or Ph.D. with teaching experience in medical schools. U.S. experience is desirable but not essential. Retired persons with experience in medical education are encouraged to apply. Excellent salary and benefits. *Applicant must be fluent in English and willing to relocate. Alien Registration Receipt Card (green card) holders are a plus.* Submit resume to **e-mail: career@sjsm.org** or mail to: **HRDS Inc., 1480 Renaissance Drive, Suite 300, Park Ridge, IL 60068 U.S.A.**

TWO CHEMISTRY FACULTY POSITIONS in the ENERGY for the FUTURE INITIATIVE University of California, Davis

The University of California (UC), Davis Department of Chemistry **(website: http://www.chem.ucdavis.edu/)** invites applications for two chemistry faculty positions associated with the UC Davis Energy for the Future Initiative targeting major energy issues facing California and the nation. The two positions are at the **ASSISTANT PROFESSOR** level. Online applications are available at **website: http://energy.ucdavis.edu.** This website also provides further information about the Energy for the Future Initiative, which brings a total of fourteen new faculty positions to the campus including a total of four positions in the Chemistry Department to be filled over a two-to-three year period.

The first position is in areas that focus on inorganic, materials, or solid state chemistry with fundamental research relevant to the broad field of energy. The second is in biological, inorganic, or physical chemistry, exploring fundamental energy-relevant chemistry, broadly defined in biological or bio-inspired synthetic systems. In conjunction with the campuswide Energy for the Future Initiative and UC Davis Energy Institute, these scientists will interact with colleagues in other energy-related disciplines. Competitive candidates will bring strong research programs in chemistry that are relevant to energy, as well as strong commitments to undergraduate and graduate teaching. A Ph.D. or equivalent degree in chemistry or related disciplines is required. The positions are open until filled; but to assure full consideration, online applications should be submitted no later than November 1, 2008, for a targeted start date of July 1, 2009.

The University of California is an Affirmative Action/Equal Opportunity Employer.

The Boise, Idaho VA Medical Center (MC), in association with the University of Washington, is recruiting for a full-time Board-certified **INFECTIOUS DISEASE PHYSICIAN** (M.D. or M.D.-equivalent) with strong research commitment to investigations of pathogenic mechanisms of Gram positive infections. The Boise VAMC is a Dean's Committee Hospital affiliated with the University of Washington, as well as Boise State University, the University of Idaho and Idaho State University, and has an excellent Residency Training Program in Primary Care Internal Medicine, Psychiatry and Family Practice. The incumbent will be appointed to the full-time faculty at the University of Washington at the **ASSISTANT or ASSOCIATE PROFESSOR** level in the physician/scientist pathway. University of Washington faculty engage in teaching, research, and service. Interested candidates should contact: **Dennis L. Stevens, Ph.D., M.D., Chief, Infectious Disease Section, 500 West Fort Street, Boise, ID 83702. Telephone: 208-422-1599; e-mail: dennis.stevens@va.gov.** This position is open until filled. *The Boise VAMC and the University of Washington are building a culturally diverse faculty and staff and strongly encourage applications from women, minority, individuals with disabilities, and covered veterans.*

ASSISTANT PROFESSOR, MOLECULAR FORENSIC SCIENCES. The Department of Entomology at Texas A&M University is conducting a search for a full-time, tenure-track position, 67 percent research, 33 percent teaching. The incumbent faculty member will have primary responsibility for developing an extramurally funded research program that leads to new knowledge in the forensic sciences as applicable to evidentiary analysis and interpretation resulting in novel discoveries, technologies, and applications in the area of DNA-based evidence. Research and leadership training of graduate and undergraduate students is expected for programmatic success. Other responsibilities include teaching two to three courses depending on need, supervising graduate research, and acting as a team member of the forensic science degree program. Successful candidate will have current interactions with the forensic science community. The full announcement and application instructions can be found at **website: http://insects.tamu.edu/jobs/assistantprofforensics.cfm.**

Closing date for applications is November 1, 2008. *Texas A&M University is an Equal Opportunity Employer and encourages applications from minority group members and women.*

Penn
University of Pennsylvania

The Department of Dermatology at the University of Pennsylvania's School of Medicine seeks candidates for an **ASSISTANT, ASSOCIATE and/or FULL PROFESSOR** position in the tenure track. Rank will be commensurate with experience. The successful applicant will have experience in the field of dermatology. Responsibilities include some patient care, as well as resident, fellow, and medical student education. Applicants must have an M.D. or M.D./Ph.D. degree and have demonstrated excellent qualifications in clinical care, education, and research. Board-certified in dermatology is required.

Current research interests in the Department include: differentiation, adhesion, embryological development, stem cells and signal transduction in epidermis and hair follicles; skin and hair follicle regeneration; gene therapy targeting the epidermis and hair follicle; microRNA function in the skin; basic studies of autoimmune blistering and rheumatologic diseases of skin, impetigo and staphylococcal scalded skin syndrome; proteases in skin physiology and pathophysiology; and basic pathophysiologic and immunologic studies of cutaneous T cell lymphoma.

The effective date of appointment will be on July 1, 2009. Please submit curriculum vitae, a cover letter, three reference names, and a statement of research interests to:

Sarah E. Millar, Ph.D.
Associate Professor, Departments of Dermatology and Cell and Developmental Biology
Director of Research, Department of Dermatology
University of Pennsylvania School of Medicine
M8D Stellar-Chance Laboratories
422 Curie Boulevard, M8D SCL
Philadelphia, PA 19104
E-mail: millars@mail.med.upenn.edu
Fax: 215-573-2033

The University of Pennsylvania is an Equal Opportunity, Affirmative Action Employer. Women and minority candidates are strongly encouraged to apply.

TWO POSITIONS, ASSISTANT/ASSOCIATE PROFESSOR

The University of Miami (UM) invites applications for two positions, a tenure-track Assistant and an Associate Professor to develop innovative experimental research programs in biological physics. The initiative is part of UM's current drive to develop novel research collaborations at the frontiers of physics, the life sciences, and medicine. The successful candidate(s) will develop a novel line of research within physics while helping the Department strengthen its connections to UM's research activities across the life and medical sciences. Candidates for the Assistant Professor position must have a Ph.D. in physics or a similar field, postdoctoral experience, a demonstrated record of research, and a strong commitment to quality undergraduate teaching in physics and its applications. Candidates for the Associate Professor position must have a Ph.D. in physics or similar field, postdoctoral experience, a demonstrated record of research and external funding as well as a strong commitment to quality undergraduate and graduate teaching in physics and its applications. The Physics Department is located within the University's highly attractive Coral Gables campus in the greater Miami area, and has wide-ranging research expertise as well as an established Ph.D. program. Applicants should arrange for curriculum vitae, a statement of research interests, and three letters of recommendation to reach the following address by December 15, 2008: **Prof. Neil Johnson, Search Committee Chair for Biological Physics, Department of Physics, University of Miami, P.O. Box 248046, Coral Gables, Fl 33124. E-mail: njohnson@physics.miami.edu.** *UM is a young and vibrant private Institution, and an Equal Opportunity/Affirmative Action Employer.*

University of Massachusetts Medical School

UMASS

Faculty Positions
Department of Neurobiology

The Department of Neurobiology, established as part of the unprecedented research expansion at the University of Massachusetts Medical School, has recently hired a group of outstanding faculty using invertebrate model systems to investigate the genetic and molecular mechanisms of brain function. This group is unique in that it crosses many boundaries in the use of invertebrate systems to study central and interrelated areas in neuroscience ranging from learning and memory, synapse plasticity, sensory transduction, glial cell biology and circadian rhythms. The new Department augments an already existing interdisciplinary Program in Neuroscience. The laboratories for the Department are housed on one floor of a new state-of-the-art, 340,000 sq ft research building.

We now solicit applications for additional tenure-track positions.
The Department seeks individuals of outstanding potential who are using invertebrate model systems, including C. elegans and Drosophila, as well as less conventional invertebrate species (e.g., Apis mellifera and Tribolium castaneum), to study the nervous system. Specific areas of emphasis include, but are not limited to, cellular and molecular neuroscience, developmental neuroscience, brain physiology, and behavior. The positions are highly competitive with regard to start-up funds, laboratory space, and salary. Rank will be commensurate with ability and experience.

Applicants should send a CV, statement of research interests, and names and addresses of three references to:

Dr. Vivian Budnik
Chair of Faculty Search Committee
Professor of Neurobiology
University of Massachusetts Medical School
364 Plantation Street
Worcester, MA 01605-2324

Visit Neurobiology at: **http://www.umassmed.edu/neurobiology/**

An Equal Opportunity/Affirmative Action Employer. Women and under-represented minorities are especially encouraged to apply.

Chair: Department of Biology
University of Maryland, College Park

We seek a distinguished senior scientist with a vigorous research program, commitment to excellence in graduate and undergraduate education, and broad vision, experience, and energy to chair the Department of Biology in the College of Chemical and Life Sciences at the University of Maryland. Biology is a broadly based and cohesive department with research strengths in cellular biophysics, developmental biology, ecology, evolutionary biology, genomics, and neurobiology. Faculty research laboratories are located in the new Bioscience Research Building and adjoining Biology-Psychology Building. The department is a key participant in undergraduate and graduate programs that span the College and campus. Recruitment of both senior and junior faculty is expected as part of an ambitious drive to enhance the life sciences. These efforts are focused in the College on ecological sustainability, genomics, host-pathogen interactions, nanoscience/biomaterials, and sensory neuroscience, and at the campus level on broad initiatives in areas such as climate, energy, health, and nanoscience. For more information please visit **www.chemlife.umd.edu**.

Apply electronically to **http://chemlife.umd.edu/biologychairsearch.html** with an application letter and the following: (1) curriculum vitae, (2) statement of research interests, (3) statement of academic vision and administrative experience, and (4) names, addresses, emails and phone numbers of at least four references. Review of credentials will continue until the position is filled. Review of applications will begin on **November 3, 2008**.

The University of Maryland, College Park is the flagship campus of the University System of Maryland and one of the most rapidly advancing public research universities in the country. Close proximity to Washington, Baltimore, and the Maryland Biotechnology Corridor facilitates interactions with an extraordinary range of major research institutions, including the NIH, FDA, Smithsonian Institution and the USDA.

The University of Maryland is an Equal Opportunity Affirmative Action Employer. Minorities and women are encouraged to apply.

John B. Pierce Laboratory / Yale School of Medicine / Yale University

THE JOHN B. PIERCE LABORATORY 1933

Systems Level Physiologist/ Neurophysiologist

The John B. Pierce Laboratory seeks a systems level physiologist or neurophysiologist conducting innovative research on hypothalamic regulatory mechanisms. The appointment will be made at the rank of Assistant Fellow or starting Associate Fellow. Co-appointment is anticipated at the equivalent rank of Assistant or Associate Professor at the Yale University School of Medicine. The successful candidate will join a multidisciplinary faculty with research interests that include the neural, behavioral, and physiological mechanisms of temperature sensitivity, fluid balance, food selection, reward, and metabolism. Now celebrating its 75th anniversary as a nonprofit laboratory dedicated to basic research in environmental physiology and health, the John B. Pierce Laboratory is an endowed institute, formally affiliated with Yale University since 1966, that makes both term and career appointments. Located immediately adjacent to the medical school campus, the Laboratory offers a unique, world-class collaborative research environment in which its faculty enjoys the added advantages of outstanding in-house technical, engineering, and design/build services, and independent business and administrative offices with exceptional grant support.

The Laboratory offers competitive salary, benefits, and start-up, as well as an outstanding work environment. Applicants should submit a CV, description of research interests, set of representative publications, and names of at least three references to: **scientificsearch@jbpierce.org**, or to: **Scientific Search, John B. Pierce Laboratory, Inc., 290 Congress Avenue, New Haven, CT 06519**. The search will begin on **October 1, 2008** and continue until the position is filled.

EOE/AA **www.jbpierce.org**

POSITIONS OPEN

UNIVERSITY of WISCONSIN
UWMILWAUKEE

BIOMATHEMATICS

The Department of Biological Sciences, University of Wisconsin, Milwaukee (UWM) invites applicants for a faculty position at the **ASSISTANT (TENURE-TRACK) or ASSOCIATE PROFESSOR** level. We are seeking outstanding candidates with a Ph.D. in biology or a related area with postdoctoral research experience. Applicants whose work has an aquatic focus, and with expertise in biometrics, bioinformatics, genomics, computational biology, ecological modeling, systems biology, or biological aspects of climate modeling, are preferred. The successful candidate will be expected to develop a vigorous, externally funded research program, take an active role in directing undergraduate and graduate education, and contribute to teaching in biomathematics and core biology courses. This position complements a second position in mathematical sciences and is part of a new interdisciplinary research initiative in aquatic biomathematics, involving our two Departments and the UWM Great Lakes Wisconsin Aquatic Technology and Environmental Research Institute. Potential applicants are encouraged to visit our **websites: http://www.uwm.edu/Dept/Biology, http://www.math.uwm.edu,** and **http://www.glwi.uwm.edu.** To apply, please go to **website: http://www.jobs.wmn.edu/applicants/Central?quickFind=50742.** A completed application should include: cover letter, curriculum vitae, statement of research goals, statement of teaching interests, and letters of professional reference. Applicants should arrange to have three letters of reference sent as PDF attachments to the **Departmental Chair (e-mail: sandgren@uwm.edu)** or mailed to **Biomathematics Search** at the following address: **Department of Biological Sciences, University of Wisconsin-Milwaukee, P.O. Box 413, Milwaukee, WI 53201.** Screening of candidates will begin November 19, 2008, and continue until the positions are filled. Appointments begin August 2009. *UWM is an Equal Opportunity/Affirmative Action Employer.*

RESEARCH ASSOCIATE (POSTDOCTORAL)
Protein Expression

A Research Associate position is available immediately for a highly motivated protein scientist at Fraunhofer USA Center for Molecular Biotechnology in Newark, Delaware. The Center focuses on the development of vaccines and therapeutics in plant-based protein production systems. The successful candidate will primarily be involved in developing strategies to optimize the expression of foreign proteins in plants, with an emphasis on protein synthesis, folding, processing, stability, and extractability. Qualified applicants will have extensive experience in molecular biology, bioinformatics, protein engineering, and protein biochemistry. Applicants with a Ph.D. in life sciences, including fields such as biology, molecular biology, biochemistry, or bioinformatics, are encouraged to apply. Applicants must have good organizational, record-keeping, and computer skills and must be able to work in a team environment. Fraunhofer USA offers a competitive salary and benefit package.

Interested candidates should send their curriculum vitae and cover letter referencing the position applying for along with contact information for three references to **e-mail: personnel@fraunhofer-cmb.org.** For more information and additional career opportunities, please visit our **website: http://www.fraunhofer-cmb.org.**

Equal Opportunity Employer.

POSTDOCTORAL FELLOW at UCLA

Position is available to study the role of gender factors in immune responses and autoimmune diseases (**Smith-Bouvier D. et al.,** *J. Exp. Medicine* **205:**1099, 2008). The project involves knowledge of gene inactivation, sex chromosome, and immunology in mouse and/or humans. Start date January to August 2009. Contact **e-mail: rrsingh@mednet.ucla.edu.**

POSITIONS OPEN

BIOLOGY FACULTY POSITIONS
University of South Florida

The Division of Integrative Biology/Department of Biology invites applications for two tenure-track faculty positions that will be part of a newly formed global change cluster in the School of Natural Sciences and Mathematics. A Ph.D. in biology or related field is required, and postdoctoral experience and evidence of an externally funded research program are desirable. Successful candidates for both positions will be expected to develop a strong externally funded research program, mentor graduate students, and teach undergraduate and graduate courses.

PLANT BIOLOGIST (ASSISTANT PROFESSOR level). We welcome candidates with research interests in any aspect of plant biology (including algae), from genes to ecosystems; especially those employing genetic tools.

SPATIAL ANALYSIS/ECOSYSTEMS (ASSISTANT/ASSOCIATE PROFESSOR level). We welcome candidates who focus on spatial analysis of ecological processes. Candidates already in tenure-track or tenured positions may be considered for the rank of Associate Professor.

Please submit the following: cover letter, curriculum vitae, statement of research and teaching interests, and three representative publications to: **Mary Parrish, Department of Biology, Division of Integrative Biology, University of South Florida, 4202 East Fowler Avenue, SCA110, Tampa, FL 33620.**

Also have three letters of recommendation in PDF sent to **e-mail: bioibsearches@cas.usf.edu.** Review of applications will begin on November 21, 2008. The position will be open until filled.

According to Florida law, applications and meetings regarding them are open to the public. *For ADA accommodations, please contact* ***Mary Parrish, telephone: 813-974-6210*** *at least five working days prior to need. USF is an Affirmative Action/Equal Employment Opportunity Institution.*

ASSISTANT PROFESSOR
Harvard University and Children's Hospital Boston

The Stem Cell Program at Children's Hospital Boston invites applications for an Assistant Professor position (tenure track). This position will be a joint appointment between Harvard University's newly established Department of Stem Cell and Regenerative Biology and the Stem Cell Program at Children's Hospital Boston. Both are affiliated with the Harvard Stem Cell Institute.

Candidates must hold a Ph.D. and/or M.D. Outstanding scientists with a demonstrated research interest in stem cells and regenerative biology/medicine will be given preference. This could include chromatin or transcriptional regulation, chemical biology, tissue regeneration, cancer, or disease models.

Applicants must submit an electronic copy of current curriculum vitae and a description of current and proposed research plans to **Leonard I. Zon, M.D., Director, Stem Cell Program at Children's Hospital Boston (e-mail: ckent@enders.tch.harvard.edu)** and should arrange to have three letters of recommendation mailed directly from the references to: **Search Committee, Leonard I. Zon, M.D., Stem Cell Program at Children's Hospital Boston, 300 Longwood Avenue, Karp 7.211, Boston, MA 02115.** Application review will continue until the position is filled. *Children's Hospital Boston and Harvard University are Equal Employment Opportunity Employers.*

Sonoma State University seeks a productive and dynamic **DIRECTOR** who will manage the 470-acre Fairfield Osborn Preserve and 3,670-acre Galbreath Wildlands Preserve. The successful candidate will support and develop environmental education, stewardship, outreach, research, and fundraising at the Preserves. Preferred start date: January 2009. Details at **website: http://www.sonoma.edu/es/employment/job_opportunities.html.**

POSITIONS OPEN

THE UNIVERSITY OF CHICAGO

The Physical and Biological Sciences Divisions in conjunction with the Computation Institute seek a **COMPUTATIONAL NEUROSCIENTIST** with a strong applied mathematics background. We seek an outstanding quantitative scientist who has demonstrated collaborative interactions with experimental neuroscientists. The candidate should complement our strengths in statistics, computation, and neuroscience. Candidates at all faculty levels will be considered. This position will likely be shared by two or more departments.

Applications should be submitted, preferably by e-mail, to **e-mail: compneurosearch@bsd.uchicago.edu,** or by regular mail to: **Chair, Computation Neuroscience Search Committee, c/o Jo DeGroot, Department of Neurobiology, 947 East 58th Street, Chicago, IL 60637.** Applications should include curriculum vitae, with a complete list of publications and a statement of research and teaching interests. Candidates should have three letters of recommendation sent to the same address. *The University of Chicago is an Equal Opportunity/Affirmative Action Employer.*

EVOLUTIONARY BIOLOGY or EVOLUTIONARY ECOLOGY ASSISTANT PROFESSOR
University of Michigan

The Department of Ecology and Evolutionary Biology at the University of Michigan invites applications for a tenure-track Assistant Professor position in evolutionary biology or its intersection with ecology. The position will have a university-year appointment. We seek outstanding individuals with research and teaching interests in any area of evolutionary biology or evolutionary ecology; including evolutionary and ecological genetics and genomics, population and quantitative genetics, phylogenetics of communities, evolutionary theory, phylogenetics, and evolution of morphology, function, and behavior. For further information, please see **website: http://www.eeb.lsa.umich.edu.**

To apply, please provide: complete curriculum vitae, statements of current and future research plans and teaching philosophy and experience, evidence of teaching excellence, copies of publications, and arrange to have three letters of recommendation sent to: **Evolutionary Biology Search Committee, Department of Ecology and Evolutionary Biology, 830 N. University, 2019-S Kraus Building, University of Michigan, Ann Arbor, MI 48109-1048** or to **e-mail: eebsearch@umich.edu.** Review of applications will begin on November 15, 2008, and continue until a suitable candidate is identified. *Women and minorities are encouraged to apply, and the University is supportive of the needs of dual-career couples. The University of Michigan is an Equal Opportunity/Affirmative Action Employer.*

POSTDOCTORAL POSITION

A Postdoctoral position is immediately available for a highly motivated individual to study genetic and epigenetic changes in breast cancer progression and metastasis. Current projects include (1) investigation of the functional role and therapeutic application of the PIK3CA gene in breast cancer and (2) investigation of novel genes in breast cancer metastasis. Competitive applicants should have obtained their Ph.D. not more than three years ago, have peer-reviewed publications, and be well-trained in cancer genetics, and molecular biology. Experience handling mice is preferred. Qualified candidates should send their curriculum vitae, including contact information for three references, to: **Guojun Wu, Ph.D., Karmanos Cancer Institute, Wayne State University, 4100 John R, Mail Code HW08AO, Detroit, MI 48082 U.S.A. E-mail: wugu@karmanos.org.**

POSITIONS OPEN

ASSISTANT/ASSOCIATE PROFESSOR of BIOMEDICAL SCIENCE

The Charles E. Schmidt College of Biomedical Science is seeking a tenure-track/tenured faculty member (position #980694) in the Department of Basic Science. The candidate will have a Ph.D., M.D. or equivalent degree and a demonstrated ability to conduct innovative research in biophysics and/or structural biology and experience in teaching general physiology. The faculty member will establish an externally funded research program that complements the research of current faculty and will teach in both college graduate programs and in the Medical Education Program of the regional campus of the University of Miami Miller School of Medicine (located at Florida Atlantic University) including facilitating small groups in a problem-based learning (PBL) curriculum. The position includes startup funds and a 12-month salary. Application materials must be submitted electronically including: cover letter, curriculum vitae, a one-page summary of research interests, a one-page statement of teaching experience and philosophy, and the names of three references to **website: https://jobs.fau.edu** by October 31, 2008. For information about the College, please see our **website: http://biomed.fau.edu/biomedical.** *Florida Atlantic University is an Equal Opportunity/Equal Access Institution.*

PLANT ECOLOGIST

The Department of Plant Biology at Michigan State University (MSU) invites applications for an **ASSISTANT PROFESSOR** (tenure track) who conducts research in any area of plant ecology. The successful applicant will contribute to undergraduate teaching, develop a graduate course in his or her area of expertise, participate in the Graduate Program in Ecology, Evolutionary Biology, and Behavior (**website: http://www.msu.edu/~eebb**), and maintain an externally funded research program. Applicants must have a Ph.D., and postdoctoral research experience is desirable. Applications should include curriculum vitae, a summary of research accomplishments and future research objectives, a brief description of teaching philosophy and goals, and three letters of reference. Information about the Department of Plant Biology can be found at **website: http://www.plantbiology.msu.edu.** Review of applications will begin November 17, 2008, and will continue until a suitable candidate is identified. Application materials can be sent electronically to **e-mail: ecology@msu.edu.** *MSU is an Affirmative Action, Equal Opportunity Employer. MSU is committed to achieving excellence through cultural diversity. The University actively encourages applications and/or nominations of women, persons of color, veterans, and persons with disabilities.*

POSTDOCTORAL RESEARCHER POSITIONS
Biochemistry and Physiology
Davis Heart and Lung Research Institute
The Ohio State University

We are seeking a Postdoctoral Researcher with biochemistry, molecular biology, or proteomics experience to study nitric oxide synthase and related enzymes and their posttranslational modifications in cardiovascular disease.

A position is also available for a Postdoctoral Researcher with experience in cardiac physiology to study free radical and nitric oxide formation and related mechanisms of post ischemic injury. Experience with isolated in vivo models desired.

Salary will be commensurate with experience. Please submit curriculum vitae and list of references to: **Jay L. Zweier, M.D., e-mail: jay.zweier@osumc.edu** for consideration. *OSU is an Equal Opportunity/Affirmative Action Employer.*

CHEMISTRY and BIOCHEMISTRY FACULTY POSITION
University of California, Los Angeles (UCLA)

The Department of Chemistry and Biochemistry at UCLA invites applications for a faculty position in all areas of chemistry, biochemistry, and chemical biology. The search is open to both junior and senior level candidates. Applicants are expected to have earned a Ph.D. degree in chemistry, biochemistry, or an allied field and to be strongly committed to both teaching and research. Successful applicants will show evidence of exceptional originality and promise, and aspire to establish a world-class research program in a stimulating environment that fosters collaboration and community. Candidates must give evidence of exceptional promise (for a junior appointment) or great distinction (for a senior appointment) in research and teaching. Applications should include curriculum vitae, a statement of research accomplishments and description of proposed research (not exceeding four pages), reprints of representative publications, and a list of professional references. Junior faculty applicants should arrange to have at least three letters of recommendation sent at the time of application. To assure consideration, all application materials should be received by November 15, 2008, and directed to:

Chair
Search Committee
Department of Chemistry and Biochemistry
University of California, Los Angeles
P.O. Box 951569
Los Angeles, CA 90095-1569

UCLA is an Equal Opportunity/Affirmative Action Employer. Women and minorities are encouraged to apply.

FACULTY POSITION in CHEMISTRY
University of California, Berkeley
Department of Chemistry

The Department of Chemistry at the University of California (UC), Berkeley invites applications for an **ASSISTANT PROFESSOR** faculty position beginning in the 2009 academic year. We will consider creative and energetic candidates who show extraordinary promise or accomplishment in research and teaching in any area of chemistry.

Applicants should send curriculum vitae and a proposed research program, and arrange to have three letters of recommendation sent to:

Chair, Faculty Recruitment Committee
Department of Chemistry
419 Latimer Hall
University of California
Berkeley, CA 94720-1460
or
e-mail: chemdept.recruit@berkeley.edu

or electronic submissions preferred via candidate self-registration at **website: http://chem-dept.berkeley.edu:80/sReg.php?i=56.**

The link above allows candidates to register and upload application material. Once application materials have been uploaded, candidates will be given a URL where their references may upload PDFs of their letters. Please refer references to the UC statement on confidentiality, **website: http://apo.chance.berkeley.edu/evalltr.html.** The deadline for receipt of application material is November 15, 2008. Application review will begin in the fall of 2008. *The University of California is an Equal Opportunity/Affirmative Action Employer.*

POSTDOCTORAL FELLOWSHIPS to study oocyte maturation (**Zhang et al.,** *Dev. Cell* **15:**386-400, 2008). We are equipped with in-laboratory facilities for time-lapse confocal imaging of both frog and mouse oocytes. Please send curriculum vitae, a brief statement of accomplishment/experience, and names of three references to: **Dr. Johné Liu, Ottawa Health Research Institute, 725 Parkdale Avenue, Ottawa, K1Y 4E9, Canada. E-mail: jliu@ohri.ca; website: http://www.ohri.ca/profiles/liu.asp.**

POSITIONS OPEN

ASSUMPTION COLLEGE

VERTEBRATE ANATOMIST

Assumption College invites applicants for a tenure-track position at the **ASSISTANT PROFESSOR** rank, starting August 2009. Primary teaching responsibility is mammalian anatomy, with shared responsibility for introductory biology courses. Our new science building includes dedicated space for student-faculty research. Ph.D. and a commitment to undergraduate teaching and research required. Postdoctoral research experience preferred. Applicants must be willing to contribute actively to the mission of the College as well as show respect for the Catholic and Assumptionist identity of Assumption College. Send curriculum vitae, statements of teaching philosophy and research interests, graduate and undergraduate transcripts, and three letters of recommendation to: **Steven Theroux (e-mail: stheroux@assumption.edu), Department of Natural Sciences, Assumption College, 500 Salisbury Street, Worcester, MA 01609-1296** by December 10, 2008 **(website: http://www.assumption.edu/programslNatSci).** *Assumption College, a Catholic liberal arts and professional studies college, was founded in 1904 by its sponsoring religious community, the Augustinians of the Assumption. Assumption College is a member of the Colleges of Worcester Consortium and an Affirmative Action Employer encouraging candidates who would enrich the College's diversity.*

TENURE-TRACK ASSISTANT PROFESSOR
Microbiology

The Department of Biological Sciences at Barnard College, Columbia University, seeks a full-time, tenure-track Assistant Professor (starting July 2009) to participate in undergraduate teaching and establish an active, externally funded research program that investigates any aspect of the biology of microbes. Before applying, please see **website: http://www.barnard.edu/biology/microjob.htm.**

Teaching responsibilities include advanced lecture and laboratory courses in microbial diversity, participation in the introductory biology sequence, and organization of a senior seminar in an area of interest to the successful candidate. Ph.D. and postdoctoral experience is required; teaching experience is desirable.

Applicants should send curriculum vitae, research and teaching statements, three representative publications, and three letters of recommendation to: **Microbiology Search Committee, Department Department Biological Sciences, Barnard College, 3009 Broadway, New York, NY 10027 (e-mail: biologyjob@barnard.edu).** Review of applications will begin November 1, 2008.

Barnard College is an Equal Opportunity Employer. Women and members of underrepresented minorities are encouraged to apply.

RESEARCH FACULTY POSITION

The Department of Urology at the University of Pittsburgh seeks tenure-track and nontenure-track faculty at all ranks in the area of prostate and urologic cancer. The successful candidate will also participate at the Prostate and Urologic Cancer Program of the University of Pittsburgh Cancer Institute. Candidates must possess a Ph.D. and/or M.D. degree with productive postdoctoral training in the area of cancer biology or related fields. Successful applicants will be expected to develop a vigorous research program with the potential for extramural funding. We offer competitive academic salary, fringe benefits, and state-of-the-art facilities for both basic and translational research. Positions available until filled. Applicants should send a letter describing their research interest, curriculum vitae, and the names of at least three persons from whom references can be obtained to: **Vinnette Sommariva, University of Pittsburgh School of Medicine, Department of Urology, Shadyside Medical Center, 5200 Centre Avenue, Suite G40, Pittsburgh, PA 15232.** *The University of Pittsburgh is an Affirmative Action, Equal Opportunity Employer.*

POSITIONS OPEN

FACULTY POSITION in COMPUTATIONAL BIOPHYSICS
Johns Hopkins University

The Thomas C. Jenkins Department of Biophysics seeks candidates for a tenured faculty position in computational biophysics. We are particularly interested in candidates with a background in physics and expertise in statistical thermodynamics, physical chemistry, and polymer physics, and with interests in the application of computational methods to the structure and function of biological macromolecules, their assemblies and regulatory interactions and networks.

Please send, by 15 December 2008, a cover letter, curriculum vitae, and a brief description of your research plans to: **Faculty Search Committee, T.C. Jenkins Department of Biophysics, Johns Hopkins University, 3400 N. Charles Street, Baltimore, MD 21218-2685; telephone: 410-516-7245.** Candidates should arrange for three letters of reference to be sent to the same address.

Johns Hopkins University is an Affirmative Action/Equal Opportunity Employer.

ANNOUNCEMENTS

U.S. POSTAL SERVICE

Statement required by the Act of 12 August 1970, Section 3685, Title 39, United States Code, showing the ownership, management, and circulation of:

1-9. *Science*, Publication No. 0036-8075, is published weekly on Friday, except the last week in December, at 1200 New York Ave., N.W., Washington, DC 20005. Date of filing: 26 September 2008. This is also the address of the publisher, the editor, and the managing editor, who are, respectively, Beth Rosner, Bruce Alberts, and Monica M. Bradford.

10. The owner is the American Association for the Advancement of Science, 1200 New York Ave., N.W., Washington, DC 20005. Stockholders: None.

11. Known bondholders, mortgages, and other security holders owning or holding 1 percent or more of total amount of bonds, mortgages, or other securities: None.

12. The purpose, function, and nonprofit status of this organization and the exempt status for federal income tax purposes have not changed during the preceding 12 months.

13-15. The average number of copies of each issue during the preceding 12 months is (A) Total number of copies printed: 132,394; (B) Paid circulation: 120,703; (1) Paid/Requested outside-county mail subscriptions stated on form 3541: 100,676; (2) Paid/Requested in-county subscriptions stated on form 3541: 0; (3) Sales through dealers and carriers, street vendors, counter sales: 20,008; (4) Other classes mailed through USPS: 19; (C) Total paid circulation: 120,703; (D) Free distribution: samples, complimentary, and other free copies: 10,824; (1) Outside-county as stated on form 3541: 2,427; (2) In-county as stated on form 3541: 0; (3) Other classes mailed through the USPS: 4; (E) Free distribution outside of mail: Carrier or other means: 8,393; (F) Total free distribution: 10,824; (G) Total distribution: 131,527; (H) Copies not distributed: 867; (I) Total: 132,394; (J) Percent paid and/or Requested Circulation: 91.8%.

Actual number of copies of single issue (9/12/2008) published nearest to filing date are (A) Total number of copies printed: 125,900; (B) Paid circulation: 119,443; (1) Paid/Requested outside-county mail subscriptions stated on form 3541: 99,836; (2) Paid/Requested in-county subscriptions stated on form 3541: 0; (3) Sales through dealers and carriers, street vendors, counter sales: 19,589; (4) Other classes mailed through USPS: 18; (C) Total paid circulation: 119,443; (D) Free distribution: Samples, complimentary, and other free copies: 5,714; (1) Outside-county as stated on form 3541: 2,444; (2) In-county as stated on form 3541: 0; (3) Other classes mailed through the USPS: 4; (E) Free distribution outside of mail: Carrier or other means: 3,266; (F) Total free distribution: 5,714; (G) Total distribution: 125,157; (H) Copies not distributed: 743; (I) Total: 125,900; (J) Percent paid and/or Requested Circulation: 95.4%.

I certify that the statements made above are correct and complete. (signed) Beth Rosner, Publisher.

POSITIONS OPEN

ASSISTANT PROFESSOR of ENVIRONMENTAL SCIENCE and POLICY, Clark University. The Department of International Development, Community, and Environment seeks to fill a tenure-track position in its Environmental Science and Policy Program. The candidate will teach undergraduate and graduate courses in such areas as: epidemiology, public health policy, environmental and community heath, and global health. A disciplinary or interdisciplinary doctoral degree with a focus on health and environment, a strong background in science, and a demonstrated interest in policy and social change are required.

For more information visit our **website: http://www.clarku.edu/idce.**

FACULTY POSITION in BIOCHEMISTRY
University of California, San Diego

The Department of Chemistry and Biochemistry of University of California, San Diego **(website: http://www-chem.ucsd.edu)** invites applications for a tenure-track faculty position in biochemistry. Candidates must have a Ph.D. and a demonstrated ability for creative research and teaching at the undergraduate and graduate levels. The Department will consider applicants who are researching significant biological problems using interdisciplinary methods, including but not limited to biochemical, biophysical, and computational techniques. Of particular interest are candidates whose research is focused on exploring how biological systems are influenced by the environment. Salary is commensurate with qualifications and based on University of California pay scale. Applicants are asked to submit materials online at **website: http://www-chem.ucsd.edu/recruit/index.cfm?addno=5-120.** Materials include a cover letter, curriculum vitae, research proposal, samples of published research, and a statement of teaching experience. Applicants are welcome to include in their cover letters a personal statement summarizing their contributions to diversity. Please arrange for three reference letters to be mailed to: **Chair, Biochemistry Search Committee 5-120, University of California, San Diego, Department of Chemistry and Biochemistry, La Jolla, CA 92093-0332.** The deadline for applications is December 1, 2008. Applications received after this deadline will be given full consideration if the position has not been filled. *UCSD is an Equal Opportunity/Affirmative Action Employer with a strong institutional commitment to the achievement of diversity.*

BULLARD FELLOWSHIPS in FOREST RESEARCH
Harvard University

Each year Harvard University awards a limited number of Bullard Fellowships to individuals in biological, social, physical, and political sciences to promote advanced study, research, or integration of subjects pertaining to forested ecosystems. The Fellowships, which include stipends up to $40,000, are intended to provide individuals in midcareer with an opportunity to utilize the resources and to interact with personnel in any department within Harvard University in order to develop their own scientific and professional growth. In recent years, Bullard Fellows have been associated with the Harvard Forest, Department of Organismic and Evolutionary Biology, and the J. F. Kennedy School of Government and have worked in areas of ecology, forest management, policy, and conservation. Fellowships are available for periods ranging from six months to one year after September 1. Applications from international scientists, women, and minorities are encouraged. Fellowships are not intended for graduate students or recent postdoctoral candidates. Information and application instructions are available on the Harvard Forest **website: http://harvardforest.fas.harvard.edu.** Annual deadline for applications is February 1.

POSITIONS OPEN

ENVIRONMENTAL RESEARCH ANALYST. Conduct research and analyze commercial land for potential development with emphasis on environmental effects including physical and health hazards. Analyze data to interpret correlations between commercial property development and environmental effects. Prepare reports to present to city, state, and federal authorities for permits. Conduct feasibility studies for development of physical plants. Review plans, designs, layout, and physical requirements for commercial sites and buildings. Required: Master of Science in chemical engineering, chemistry, or forestry. Equivalent of 40 hours per week. Job/interview site: Torrance, California. Send curriculum vitae to: **Person Realty Incorporated, 21641 S. Western Avenue, Suite C, Torrance, CA 90501.**

SHULL FELLOWSHIP at the Oak Ridge National Laboratory (ORNL): the Neutron Sciences Directorate of the ORNL invites applications for the Clifford G. Shull Fellowship. The Shull Fellowship provides an exciting opportunity to pursue research applying neutron scattering methods to forefront problems in physics, chemistry, biology, or materials science and engineering. Applications for Shull Fellowships commencing in 2009 are now being accepted. To receive full consideration applications must be submitted by December 12, 2008. For more information, and to apply, go to **website: http://jobs.ornl.gov/index.cfm.** *ORNL is an Equal Opportunity Employer, committed to workforce diversity. Applicants need not be U.S. citizens.*

MARKETPLACE